

STUDY OF THE ABILITY OF
CARBORANYLCARBOXYLATE LIGANDS TO
GENERATE POLYNUCLEAR COMPOUNDS.
POTENTIAL APPLICATIONS

Mònica Fontanet Cepeda

Per citar o enllaçar aquest document:
Para citar o enlazar este documento:
Use this url to cite or link to this publication:
<http://hdl.handle.net/10803/375906>



<http://creativecommons.org/licenses/by/4.0/deed.ca>

Aquesta obra està subjecta a una llicència Creative Commons Reconeixement

Esta obra está bajo una licencia Creative Commons Reconocimiento

This work is licensed under a Creative Commons Attribution licence



**STUDY OF THE ABILITY OF
CARBORANYLCARBOXYLATE LIGANDS TO
GENERATE POLYNUCLEAR COMPOUNDS.
POTENTIAL APPLICATIONS.**

Doctoral thesis

Mònica Fontanet Cepeda

2013

Programa de doctorat de Ciències Experimentals i Sostenibilitat

Supervised by: Dra. M. Isabel Romero García i Prof. Francesc Teixidor Bombardó

In candidacy for the degree of **Doctora per la Universitat de Girona**



Universitat de Girona
Departament de Química
Àrea de Química Inorgànica

La Dra. M.Isabel Romero García, professora titular del Departament de Química de la Universitat de Girona, i el Prof. Francesc Teixidor Bombardó, professor d'Investigació del Consejo Superior de Investigaciones Científicas a l'Institut de Ciència de Materials de Barcelona

DECLAREM:

Que aquest treball, titulat "Study of the ability of carboranylcarboxylate ligands to generate polynuclear compounds", que presenta Mònica Fontanet Cepeda per a l'obtenció del títol de doctora, ha estat realitzat sota la nostra direcció i que compleix els requeriments per poder optar a Menció Internacional.

I per a que així consti signem la present certificació

Dra. M.Isabel Romero García

Prof. Francesc Teixidor Bombardó

Girona, 19 de juliol de 2013.

The work performed in the present doctoral thesis has been possible thanks to the funding of:

- ❖ Departamento de Universidades, Investigación y Sociedad de la Información de la Generalidad de Cataluña through a FI predoctoral grant and a mobility grant.
- ❖ Ministerio de Economía y Competitividad (MINECO) through projects: CTQ2007-60476/PPQ and CTQ2010-21532-C02-01.
- ❖ Generalitat de Catalunya through project: 2009/SGR/00279.

*“A vegades sentim que el que fem és tan sols una gota en el mar,
però el mar seria menys si li faltés una gota”*

Teresa de Calcuta

*A la meua família, en especial
a la meua mare i al meu germà*

Agraïments

Arribats a aquest punt toca escriure la part que ser la més llegida de la tesi, donats els temps que corren es podria dir que és com el mur del facebook, allà on apareixen només les coses maques i els bons records, i així ho faré perquè de tot i tots em vull quedar amb lo millor i espero que vosaltres també ho feu de mi.

Primer de tot donar les gràcies a la Dra. Marisa Romero i a la Dra. Montse Rodríguez per deixar-me formar part del seu grup i per la formació que m'han donat durant tots aquest anys. De igual manera agrair al Prof. Francesc Teixidor per la co-direcció de la tesi i, juntament amb la Prof. Clara Viñas per acollir-me al seu grup i per tractar-me com una més. També volia agrair a la Dra. Rosario Nuñez i al Dr. José Giner per la seva ajuda en les meves estades a l'ICMAB.

Com no agrair a tots els tècnics, tant de la UdG com de l'ICMAB i UAB per la seva ajuda quan ho he necessitat així com a la Dra. Núria Aliaga per totes les mesures de magnetisme presentades a la tesi, als Dr. Eliseo Ruiz i Dr. Adrian Radu Popescu pels càlculs teòrics, al Dr. Pavel Matějček per els assajos de light scattering i al Dr. Fernando Bozoglian per les mesures d'oxidació d'aigua.

Per altre part donar les gràcies als que han sigut els meus companys durant aquest temps Isabel, Jordi, Mohamed, Maribel, Íngrid per tots els bons moments i l'ajuda rebuda, així com als companys de l'ICMAB: Anna i Anas varies, Marius L., Justo, Mireia, Jordi's, Jose, David, Radu, Patri, Adnana i especialment a en Pau i Ariadna per la introducció al món dels carborans, a l'Arantxa, pels bons consells, en Màrius T. per la seva alegria i per tots els bons records de congressos i sortides, a en Víctor per ser com és, a l'Albert per la seva ajuda sempre que l'he necessitat i sobretot en aquesta última fase de la tesi i, a l'Anna C. per convertir-se en una amiga.

Per part de l'UdG gràcies als companys d'altres grups, a en Plani i als Pep pels bons moments al despatx i fora, a les Cats (Anna, Lídia, Sandra, Magda, Ewelina i Mònica), als Lipssians i Lipssianes (Anna, Rafel, Imma, I-Teng, Marta, Cristina), al QBIS (especialment a l'Anna, Irene, Laura, Alícia, Isaac i Marc i a la Kristin), a les analítiques (especialment Ester, Dolors i Aida) i com no als químics físics i a en Fontrodona per tots els dinars, sopars, partits de bàsquet i J.O.D.E.T.E. i per tots els bons moments compartits així com per l'ajuda quan l'he necessitada.

I would also to thank to Prof. Janiak for the opportunity of taking part of the Bioanorganische Chemie und Katalyse group in the Heinrich-Heine Universität Düsseldorf for 4 month as well as all his colleagues and staff for making me feel part of the group during that short time and for all the explanations and help in my dairy work. At the same time I'd like to thank to all the Post-Doc and PhD students that I met there (Harold, Ishtvan, Gamall, Nader, Raquel, Antonio, Kika, Christina, Anna, Jamal, Bea, Kail, Hajo, Martin...) for the good moments and specially to Christian because, although maybe you will never read it, you were a really friend there and I will never forget some moments we lived together there. Germany was a really important time in my life and you all help to make it an unforgettable time.

Espero no deixar-me ningú de la UdG, ICMAB o de la Heinrich-Heine però si ho faig que sàpiga que encara que no estigui aquí, està present en els meus records.

Anant a un terreny més personal voldria agrair a en Xavi que em va donar suport i l'espenta que necessitava per començar la tesis. Així com a la família Viñoles perquè sempre seran part de la meva família i en especial a la Carme per tot lo viscut i a la Joana, perquè una abraçada seva val un món.

Canviant de vessant, vull agrair la Montse per totes les farres, les xerrades i per tots els bons moments viscuts, el fre de mà, el "cafè" després dels dinars UdG, les cervetes,...I a en Font per tot lo que m'he rigut amb ell amb aquell humor tan especial que molts cops la Montse m'havia d'explicar.

A l'Íngrid per la seva amistat i suport quan més ho vaig necessitar i per no deixar que m'enfonsés quan estava molt avall. Aprofitar per dir-te que, tot i que certes coses hagin passat factura a la nostra amistat me n'alegro d'haver-te conegut i que les coses et vagin bé i més amb en Jordi a qui, com a tu, aprecio molt i moltes gràcies per regalar-me una frase que mai oblidaré: si la vida no et somriu fes-li pessigolles.

En un paràgraf molt especial vull agrair simplement el formar part de la meva vida a la Raquel, la Laia, l'Ani, la Neus, en Toni i en Leandro. Perquè sense ells la meva vida no seria lo mateix i perquè me'ls estimo moltíssim encara que no els hi digui. In the same way, I'd like to thank to Isa for the motivation and help received in the last part of my thesis and for being a real friend.

No em puc deixar a tota la gent que m'ha acompanyat en tot aquest llarg viatge, a la gent de Gavà i rodalies i Girona i rodalies (Mònica, Carol, Juanjo, Gerard, Xènia, Jan,

Mònica R., Bea, Jose, Carlos, Dácil...) així com, people I met in Düsseldorf (Valerie, Anand, Victor, Ericka, Max, Björn, David ...) and the new people in my life (Toni, Liga, Ivonne, Sonia, Rocío, Pedro, Esteve,...) specially to Silvana and Albert who have become my weekends in enjoyable days, thanks for being here.

Arribats a aquest punt voldria agrair a la meva família tot el seu suport, a la meva mare i el meu germà, als meus tiets, la meva iaia i el meu iaio, que tot i que fa poquet ens va deixar segur que estaria molt content que la seva néta sigui doctora (tota la vida pensant que havia estudiat infermeria, ara pujaria de rang, :D) i, finalment a la meva cosina perquè sense ella no seria qui sóc ni estaria on estic i a en Luisma, així com a el nouvingut, l'Adri, amb el seu somriure que només veure'l m'alegra el dia.

L'últim paràgraf sol ser per una persona molt especial i en el meu cas no podia ser diferent. Vull donar-li les gràcies per ser com és, pel seu suport, per estar sempre allà, per aixecar-me quan estic avall i estar amb mi quan estic a dalt, per coneixem i entendre'm millor que ningú, perquè entre nosaltres no calen paraules, només mirades i per ser el pilar més fonamental en la meva vida vull agrair al meu germà, Andrés. Moltes gràcies.

Arribat a aquest punt i donat que em queda un full en blanc voldria afegir uns agraïments molt especials que vaig veure en una tesis. Espero l'autora no li sàpiga greu hagi copiat la seva idea així que, gireu la pàgina...



List of publications

❖ *A water soluble Mn(II) polymer with aqua metal bridges.* M. Fontanet, M. Rodríguez, I. Romero, X. Fontrodona, F. Teixidor, C. Viñas, N. Aliaga-Alcalde, P. Matejicek. *Dalton Trans.*, **2013**, 42, 7838-7841.

❖ *Design of Dinuclear Copper Species with Carboranylcarboxylate Ligands: Study of Their Steric and Electronic Effects.* M. Fontanet, A.-R. Popescu, X. Fontrodona, M. Rodríguez, I. Romero, F. Teixidor, C. Viñas, N. Aliaga-Alcalde, E. Ruiz. *Chem. Eur. J.*, **2011**, 17, 13217-13229.

Abbreviations

MOFs	Metal Organic Frameworks
ScOs	Organic Semiconductors
SMMs	Single-Molecule Magnets
<i>p</i> -CF ₃ -py	4-(Trifluoromethyl)pyridine
<i>p</i> -CH ₃ -py	4-Picoline
<i>o</i> -(CH ₃) ₂ -py	2,6-lutidine
pz	pyrazine
4,4'-bpy	4,4'-bipyridine
2,2'-bpy	2,2'-bipyridine
2,2'-bpm	2,2'-Bipyrimidine
THF	Tetrahydrofuran
NMR	Nuclear Magnetic Resonance
IR	Infra Red
UV-vis	Ultraviolet-visible spectroscopy
ESI-MS	Electrospray Ionization Mass Spectrometry
Cryo-TEM	Cryogenic Transmission. Electron Microscopy
DLS	Dynamic Light Scattering
SAXS	Small-Angle X-ray Scattering
WAXS	Wide Angle X-ray Scattering
<i>m/z</i>	mass-to-charge ratio
χ_M	magnetic susceptibility
emu	electric multiple unit
Oe	Oersted
J	Coupling constant
EPR	Electron Paramagnetic Resonance
TGA	Thermal Gravimetric Analysis

CV	Cyclic Voltammetric
TBAH	Tetra(n-butyl)ammonium
λ	Wavelength
ν	Frequency
Analysis calcd.	Analysis calculated
E	Potential
$E_{1/2}$	Half wave potential
E_{pa}	Anodic peak potential
E_{pc}	Cathodic peak potential
DFT	Density Functional Theory
ppm	parts per million
s	Singlet
br	Broad
eq	Equivalents
T	Temperature
ϵ	Extinction coefficient
carboxy	Carboxylate
CB	Carboranylcarboxylate
LMCT	Ligand to Metal Charge Transfer
MLCT	Metal to Ligand Charge Transfer
DPV	Differential pulse Voltammetry
GC	Gas Chromatography
GC-MS	Gas chromatography–mass spectrometry

Electronic supporting information

The material listed below can be found in the attached CD:

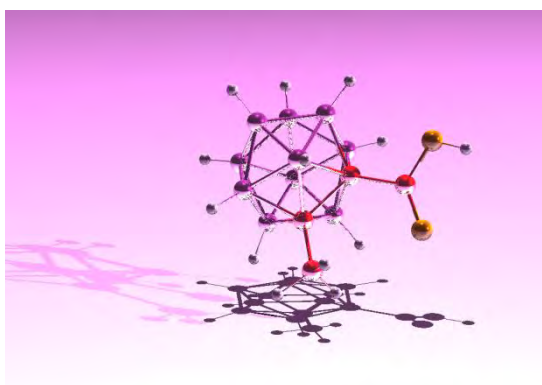
- ❖ Supporting information of Chapters III to VII
- ❖ pdf file of the PhD dissertation
- ❖ pdf files of the publications
- ❖ cif files for each crystal structure presented within this thesis

Chapter	Crystal Structure	Code
Chapter III	$[\text{Cu}_2(\text{L})_4(\text{THF})_2]$	A1
	$[\text{Cu}_2(\text{L})_4(\text{py})_2]$	A2
	$[\text{Cu}_2(\text{L})_4(\text{py})_2]$	A2'
	$[\text{Cu}_2(\text{L})_4(p\text{-CF}_3\text{-py})_2]$	A3
	$[\text{Cu}_2(\text{L})_4(p\text{-CH}_3\text{-py})_2]$	A4
	$[\text{Cu}(\text{L})_2(p\text{-CH}_3\text{-py})_2]$	A4'
	$[\text{Cu}_4(\text{L})_6(p\text{-CH}_3\text{-py})_4]$	A4''
	$[\text{Cu}(\text{L})(o\text{-(CH}_3)_2\text{-py})_2]$	A5
	$[\text{Cu}_2(\text{L})_4(\text{pz})_2]$	A6
	$[\text{Cu}(\text{L})(\text{EtOH})_2(4,4'\text{-bpy})_2]$	A8
Chapter IV	$[\text{Mn}(\mu\text{-H}_2\text{O})(\mu\text{-L})_2]_n \cdot (\text{H}_2\text{O})_n$	B1
	$[\text{Mn}_3(\text{H}_2\text{O})_4(\text{L})_6(\text{C}_4\text{H}_{10}\text{O})_2]$	B2
	$[\text{Mn}_2(\text{L})_4(\text{bpy})_2]$	B3'
	$[\text{Mn}(\text{L})_2(\text{bpy})_2]$	B4
	$[\text{Mn}(\text{L})_2(\text{bpm})]_n$	B5
Chapter V	$[\text{Fe}_3(\mu\text{-O})(\text{L})_6(\text{THF})_3]$	C1
	$[\text{Fe}_3(\mu\text{-O})(\text{L})_6(\text{py})_3]$	C2
	$[\text{Co}_2(\mu\text{-H}_2\text{O})(\text{L})_4(\text{THF})_4]$	C3
	$[\text{Co}_3(\mu\text{-H}_2\text{O})_2(\text{L})_6(\text{H}_2\text{O})_2(\text{C}_4\text{H}_{10}\text{O})_2]$	C4
Chapter VI	$[\text{Cu}_2(\text{L}')_4(\text{THF})_2]$	D1
	$[\text{Cu}_2(\text{L}')_4(\text{py})_2]$	D2
	$[\text{Cu}_2(\text{L}')_4(\text{py})_4]$	D2'
	$[\text{Cu}_2(\text{L}')_4(p\text{-CF}_3\text{-py})_2]$	D3
	$[\text{Cu}_2(\text{L}')_4(p\text{-CH}_3\text{-py})_2]$	D4
	$[\text{Cu}_2(\text{L}')_4(p\text{-CH}_3\text{-py})_4]$	D4'
	$[\text{Cu}(\text{L}')(o\text{-(CH}_3)_2\text{-py})_2]$	D5

Chapter	Crystal Structure	Code
Chapter VI	$[\text{Cu}(\text{L}')_4] \cdot (o\text{-(CH}_3)_2\text{-py)}$	D5'
	$[\text{Mn}(\text{H}_2\text{O})(\mu\text{-L}')_2]_n \cdot 2\text{H}_2\text{O}$	D6
	$[\text{Mn}(\text{L}')_2(\text{H}_2\text{O})_4]$	D6'
	$[\text{Mn}_2(\text{L}')_4(\text{bpy})_2]$	D7
	$[\text{Mn}(\text{L})_2(\text{bpy})_2]$	D8

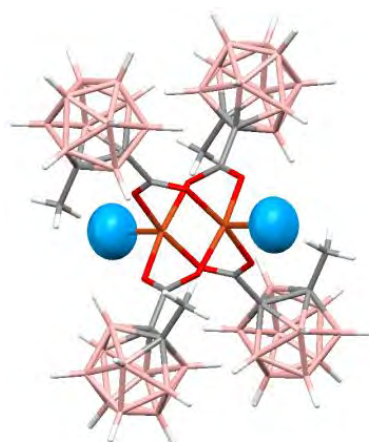
GRAPHICAL ABSTRACTS

CHAPTER I. General Introduction (pages 1-26)



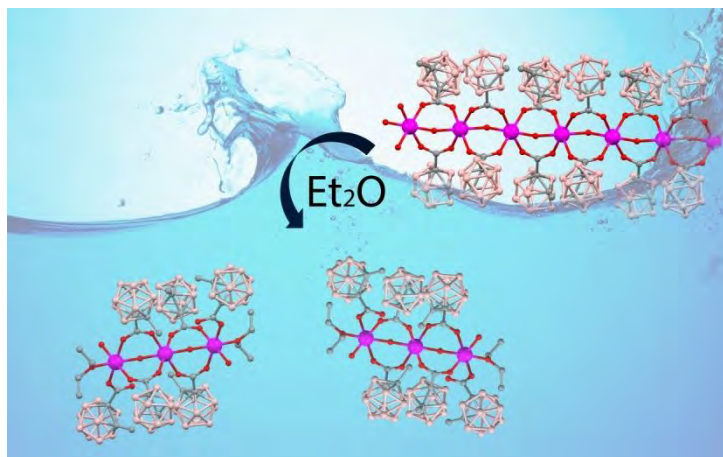
CHAPTER II. General objectives (pages 27-32)

CHAPTER III. Cu(II) complexes containing the carboranylcarboxylate ligand 1-CH₃-2-CO₂H-1,2-closo-C₂B₁₀H₁₀. Study of their steric and electronic effects (pages 33-72)



A series of new mononuclear and binuclear copper(II) compounds containing the 1-CH₃-2-CO₂H-1,2-closo-C₂B₁₀H₁₀ carborane ligand (LH) has been synthesized and fully characterized through analytical, spectroscopic (NMR, IR, UV-visible, ESI-MS) and magnetic techniques. X-ray structural analysis revealed for the binuclear compounds a paddle-wheel structure with the two copper (II) atoms holding together through four carboxylate bridges in syn-syn mode and square pyramidal geometry around each copper ion. The mononuclear complex obtained with the *o*-(CH₃)₂-py ligand presents a square-planar structure, in which the carboranylcarboxylate ligand adopts a monodentate coordination mode. Magnetic studies of the binuclear compounds have been carried out showing, in all cases, a strong antiferromagnetic coupling. Computational studies based on hybrid density functional methods have been used to study the magnetic properties of the complexes and also to evaluate their relative stability on the basis of the strength of the bond between each Cu(II) and the terminal ligand.

CHAPTER IV. Mn(II) complexes containing the carboranylcarboxylate ligand 1-CH₃-2-CO₂H-1,2-closo-C₂B₁₀H₁₀: a water soluble Mn(II) polymer with aqua metal bridges and its derivatives (pages 73-108)



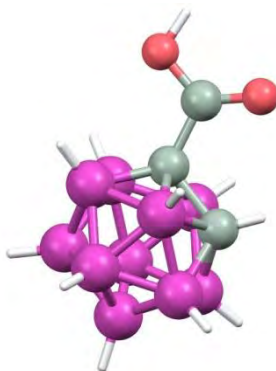
The first water soluble and crystallographically determined polynuclear Mn(II) complex has been synthesized utilizing the carboranylcarboxylate ligand, 1-CH₃-2-CO₂H-1,2-closo-C₂B₁₀H₁₀. It has been obtained in water with total atom economy and was fully characterized by analytical, spectroscopic (NMR, IR, UV-visible, ESI-MS), electrochemical, magnetic, microscopic (Cryo-TEM) and scattering (DLS, SAXS) techniques. Besides, its reactivity in coordinating solvents and with chelating ligand such as, 2,2'-bpy or 2,2'-bpm, has been studied leading to the formation of compounds with different nuclearities (mononuclear, binuclear, trinuclear and polymeric). The crystallographic structure of all of them has been obtained by X-Ray diffraction. DLS studies have demonstrated that the polymeric structure is preserved to a certain extent in water and the structure is broken in diethyl ether solution. The magnetic properties of the compounds studied show, in all cases, a weak antiferromagnetic coupling.

CHAPTER V. Study of the reactivity of the carboranylcarboxylate ligand 1-CH₃-2-CO₂H-1,2-closo-C₂B₁₀H₁₀ with Fe and Co (pages 109-136)



Four new polynuclear complexes containing the carboranylcarboxylate ligand, 1-CH₃-2-CO₂H-1,2-closo-C₂B₁₀H₁₀ and iron or cobalt atoms have been synthesized and thoroughly characterized by analytical and spectroscopic (NMR, IR, UV-visible) techniques. X-ray crystallographic structure of all complexes has been resolved showing trinuclear oxo-centred mixed valence carboxylate bridged complexes for iron ion and bi- and trinuclear complexes for cobalt ion, in which the metal ions are held together through two carboranylcarboxylate ligands and one aqua molecule.

CHAPTER VI. Cu(II) and Mn(II) complexes containing the carboranylcarboxylate ligand 1-CO₂H-1,2-closo-C₂B₁₀H₁₁ (pages 137-170)



A series of new mono- and polynuclear copper(II) and manganese(II) compounds containing the 1-CO₂H-1,2-closo-C₂B₁₀H₁₁ carborane ligand (L'H) has been synthesized and fully characterized through analytical, spectroscopic (NMR, IR, UV-visible) and electrochemical techniques. X-ray structural analysis has been performed on all compounds. A comparison of these compounds with the analogous containing the carboranylcarboxylate ligand [1-CH₃-2-CO₂-1,2-closo-C₂B₁₀H₁₁], LH, revealed in most cases a similarity in the structure of the compounds. However, some differences were found in these compounds arising from the presence of different substituents on the carboranylcarboxylate ligands. An evaluation of this behaviour is presented in this chapter.

CHAPTER VII. Catalytic activity of Mn(II) and Co(II) compound containing the carboranylcarboxylate ligand 1-CH₃-2-CO₂H-1,2-closo-C₂B₁₀H₁₀ (pages 171-194)



The reactivity of some of the new manganese (II) and cobalt(II) complexes synthesized in previous chapters has been tested with regard to the epoxidation of aromatic and aliphatic alkenes with peracetic acid as oxygen donor in dichloromethane. In general, manganese complexes show good catalytic activity, however, this activity is moderate for the binuclear cobalt complex [Co₂(μ-H₂O)(1-CH₃-2-CO₂-1,2-closo-C₂B₁₀H₁₀)₄(THF)₄] studied. Catalytic activity of polymeric manganese(II) complex [Mn(μ-H₂O)(1-CH₃-2-CO₂-1,2-closo-C₂B₁₀H₁₀)₂]_n·(H₂O)_n has been tested regarding the oxidation of water to molecular oxygen.

CHAPTER VIII. General results and discussion (pages 195-216)

CHAPTER IX. General conclusions (pages 217-226)

CHAPTER X. References (Chapters I and VIII) (pages 319-334)

TABLE OF CONTENTS

CHAPTER I. General Introduction (pages 1-26)

I.1. Historical background	5
I.2. Boranes and carboranes.....	5
I.3. <i>Closo</i>-carboranes.....	7
I.4. Chemical reactivity of <i>o</i>-carborane.....	8
1) Deprotonation of C-H vertexes and subsequent substitution	8
2) Substitution at boron by electrophilic reagents.....	9
3) Partial deboronation of the cluster by elimination of one B-H vertex using a base	9
4) Reduction reaction	11
I.5. Applications of the <i>o</i>-carboranes.....	11
I.6. Dihydrogen bonds.....	12
I.7. Characteristics and applications of carboxylate complexes	13
I.8. Oxidation catalysis	18
I.8.1. Epoxidation reaction.....	18
I.8.2. Water oxidation reaction.....	20
I.9. Molecular magnetism	21
I.9.1. Magnetization and magnetic susceptibility.....	21
I.9.2. Magnetic properties of polynuclear transition metal complexes	23
I.9.3. Binuclear copper(II) complexes	25
I.9.4. Manganese(II) complexes	26

CHAPTER II. General Objectives (pages 27-32)

CHAPTER III. Cu(II) complexes containing the carbonylcarboxylate ligand 1-CH₃-2-CO₂H-1,2-*closo*-C₂B₁₀H₁₀. Study of their steric and electronic effects. (pages 33-72)

III.1. Introduction.....	37
III.2. Objectives	39
III.3. Results and discussion.....	41

III.3.1.	Synthesis and characterization	41
III.3.2.	Electrochemical properties	48
III.3.3.	Spectroscopic properties	50
III.3.4.	Magnetic properties	55
III.3.5.	Electronic Structure Calculations	59
III.3.6.	Thermal decomposition	60
III.4.	Conclusions	62
III.5.	Experimental section.....	64
III.5.1.	Instrumentation and measurements.....	64
III.5.2.	Materials	65
III.5.3.	Preparations.....	66
III.6.	References	70

CHAPTER IV. Mn(II) complexes containing the carboranylcarboxylate ligand 1-CH₃-2-CO₂H-1,2-closo-C₂B₁₀H₁₀: a water soluble Mn(II) polymer with aqua metal bridges and its derivatives. (pages 73-108)

IV.1.	Introduction77
IV.2.	Objectives79
IV.3.	Results and discussion.....	80
IV.3.1.	Synthesis and structure	80
IV.3.2.	Electrochemical properties.....	90
IV.3.3.	Spectroscopic and microscopic properties.....	92
IV.3.4.	Magnetic properties	96
IV.4.	Conclusions	100
IV.5.	Experimental section.....	102
V.5.1.	Instrumentation and measurements.....	102
V.5.2.	Materials	103
V.5.3.	Preparations.....	104
IV.6.	References	106

CHAPTER V. Study of the reactivity of the carboranyl-carboxylate ligand 1-CH₃-2-CO₂H-1,2-closo-C₂B₁₀H₁₀ with Fe and Co. (pages 109-136)

V.1. Introduction	113
V.2. Objectives	115
V.3. Results and discussion	116
V.3.1. Synthesis and structure	116
V.3.1.1. Iron complexes	116
V.3.1.2. Cobalt complexes	121
V.3.2. Spectroscopic properties	127
V.4. Conclusions	130
V.5. Experimental section	131
V.5.1. Instrumentation and measurements.....	131
V.5.2. Materials	131
V.5.3. Preparations.....	131
V.6. References	134

CHAPTER VI. Cu(II) and Mn(II) complexes containing the carboranylcarboxylate ligand 1-CO₂H-1,2-closo-C₂B₁₀H₁₀. (pages 137-170)

VI.1. Introduction	141
VI.2. Objectives	142
VI.3. Results and discussion	143
VI.3.1. Synthesis and characterization of copper complexes	143
VI.3.2. Electrochemical properties.....	151
VI.3.3. Spectroscopic properties	152
VI.3.4. Synthesis and characterization of manganese complexes.....	153
VI.4. Conclusions	162
VI.5. Experimental section	164
VI.5.1. Instrumentation and measurements.....	164
VI.5.2. Materials	164
VI.5.3. Preparations.....	165

VI.6. References	169
-------------------------------	------------

CHAPTER VII. Catalytic activity of Mn(II) and Co(II) compound containing the carboranylcarboxylate ligand 1-CH₃-2-CO₂H-1,2-closo-C₂B₁₀H₁₀ (pages 171-194)

VII.1. Introduction	175
VII.2. Objectives	177
VII.3. Results and discussion.....	179
VII.3.1. Catalytic epoxidation of alkenes	179
VII.3.2. Water oxidation	186
VII.4. Conclusions	189
VII.5. Experimental section.....	191
VII.5.1. Instrumentation and measurements	191
VII.5.2. Materials	191
VII.5.3. Preparations	191
VII.5.4. Catalytic epoxidation.....	191
VII.5.5. Water oxidation	192
VII.6. References	193

CHAPTER VIII. General results and discussion (pages 195-216)

VIII.1. Cu(II) complexes.....	199
VIII.2. Mn(II) complexes	206
VIII.3. Fe (II) complexes	212
VIII.4. Co(II) complexes.....	214

CHAPTER IX. General conclusions (pages 217-226)

CHAPTER X. References (Chapters I and VIII) (pages 227-240)

Chapter I. General Introduction	231
Chapter VIII. General results and discussion.....	238

SUMMARY

Based on the experience of our group in the synthesis of metallic complexes with transition metals and their subsequent application in catalysis, in this thesis we present the synthesis and characterization of two different carboranylcarboxylate ligands and the study of their coordination chemistry towards different transition metals, as well as the performance of the synthesized complexes in oxidation reactions.

The first ligand synthesized was 1-CH₃-2-CO₂H-1,2-closo-C₂B₁₀H₁₀. In chapter III we described the coordination of this ligand to copper(II) affording a series of mono- and binuclear complexes which have been fully characterized and their main physical and chemical properties have been studied experimental and theoretically. We also pay attention to the magnetic behaviour of the binuclear complexes; these findings are corroborated by electronic-structure calculations. In chapter IV we described the coordination of this ligand to manganese(II), obtaining a new polymeric structure; the stability of this coordination polymer in solution was studied along with its reaction with chelating pyridyl ligands producing a series of mono-, bi-, tri- and polynuclear complexes that have been thoroughly characterized. We also studied the magnetic behaviour of the binuclear and polymeric compounds. Moreover, in chapter V we have also investigated the coordination of the carboranylcarboxylate ligand to iron(II) and cobalt (II) affording, in all cases, compounds of different nuclearity. These compounds have been fully characterized.

The second ligand synthesized was the 1-CO₂H-1,2-closo-C₂B₁₀H₁₁ in which the methyl group bonded to the carbon of the carborane cluster was replaced by a hydrogen atom. In Chapter VI we described the coordination of this new ligand to copper(II) and manganese(II) ions to study the structural and chemical differences between these two family of compounds containing different carboranylcarboxylate ligands.

Finally, in chapter VII, we have studied catalytic activity of some of the manganese(II) and cobalt(II) complexes with regard to the epoxidation of alkenes and the water oxidation.

RESUM

Basats en l'experiència del grup de recerca en la síntesi de compostos metàl·lics amb diferents metalls de transició i la seva posterior aplicació en catàlisi, en aquesta tesi es presenta la síntesi i caracterització de dos lligands diferents de tipus carboranilcarboxilat i l'estudi de la seva química de coordinació amb diferents metalls de transició, així com l'activitat dels complexos sintetitzats en reaccions d'oxidació.

El primer lligand sintetitzat va ser el 1-CH₃-2-CO₂H-1,2-closo-C₂B₁₀H₁₀. Al capítol III, es descriu la coordinació d'aquest lligand a l'ió coure(II) que condueix a una sèrie de complexos mono- i polinuclears els quals han estat caracteritzats exhaustivament mitjançant les diferents tècniques de caracterització; tanmateix les seves principals propietats físiques i químiques han sigut estudiades experimental i teòricament. També vam incidir en l'estudi del comportament magnètic dels complexos binuclears, els resultats dels quals van ser corroborats mitjançant estudis teòrics. Al capítol IV es descriu la coordinació d'aquest lligand a l'ió manganés(II), obtenint un nou compost polimèric del qual es va estudiar la seva estabilitat en dissolució així com la seva reactivitat davant de lligands de tipus piridil. Els compostos resultants varen ser estudiats i caracteritzats. Pel que fa al capítol V, s'ha estudiat la coordinació del lligand carboranilcarboxilat amb ferro(II) i cobalt(II) observant en tots els casos compostos de diferent nuclearitat que han sigut àmpliament caracteritzats.

El segon lligand sintetitzat va ser el lligand 1-CO₂H-1,2-closo-C₂B₁₀H₁₁ en el qual el grup metil unit al clúster del carborà va ser substituït per un àtom d'hidrogen. Al capítol VI, es descriu la coordinació d'aquest nou lligand als ions coure(II) i manganés(II) amb la finalitat d'estudiar les diferències estructurals i químiques entre aquests nous complexos sintetitzats i els seus anàlegs amb el lligand 1-CH₃-2-CO₂H-1,2-closo-C₂B₁₀H₁₀ contenint diferents lligands de tipus carboranilcarboxilat.

Finalment, al capítol VII, l'activitat catalítica d'alguns dels complexos de manganés(II) i cobalt(II) ha estat descrita respecte les reaccions d'epoxidació d'alquens i oxidació d'aigua.

RESUMEN

Basándonos en la experiencia del grupo de investigación en la síntesis de compuestos con diferentes metales de transición y su posterior aplicación en catálisis, en esta tesis se presenta la síntesis y caracterización de dos ligandos diferentes de tipo carboranilcarboxilato y el estudio de su química de coordinación con diferentes metales de transición, así como la actividad de los complejos sintetizados en reacciones de oxidación.

El primer ligando sintetizado fue el 1-CH₃-2-CO₂H-1,2-closo-C₂B₁₀H₁₀. En el capítulo III, se describe la coordinación de este ligando al ión cobre(II) dando lugar a una serie de complejos mono- y polinucleares, los cuales han sido caracterizados exhaustivamente mediante las diferentes técnicas de caracterización y cuyas principales propiedades físicas y químicas han sido estudiadas experimental y teóricamente. También hemos evaluado el comportamiento magnético de los complejos binucleares cuyos resultados han sido corroborados mediante estudios teóricos. En el capítulo IV se describe la coordinación de este ligando al ion manganeso(II), obteniendo un nuevo compuesto polimérico del cual se estudió su estabilidad en disolución así como su reactividad frente a diferentes ligandos de tipo piridílico. Los compuestos resultantes fueron estudiados y caracterizados. Por lo que respecta al capítulo V, se ha estudiado la coordinación del ligando carboranilcarboxilato con hierro(II) y cobalto(II), observando en todos los casos compuestos de diferentes nuclearidades que han sido ampliamente caracterizados.

El segundo ligando sintetizado fue el ligando 1-CO₂H-1,2-closo-C₂B₁₀H₁₁ en el cual el grupo metilo unido a uno de los carbonos del clúster del ligando carborano fue sustituido por un átomo de hidrógeno. En el capítulo VI se describe la coordinación de este nuevo ligando a los iones cobre(II) y manganeso(II) con la finalidad de estudiar las diferencias estructurales y químicas entre estas familias de compuestos conteniendo diferentes tipos de ligandos de tipo carboranilcarboxilato.

Finalmente, en el capítulo VII, se ha estudiado la actividad catalítica de algunos de los complejos de manganeso(II) y cobalto(II) respecto a las reacciones de epoxidación de alquenos y oxidación de agua.

CHAPTER I. General Introduction

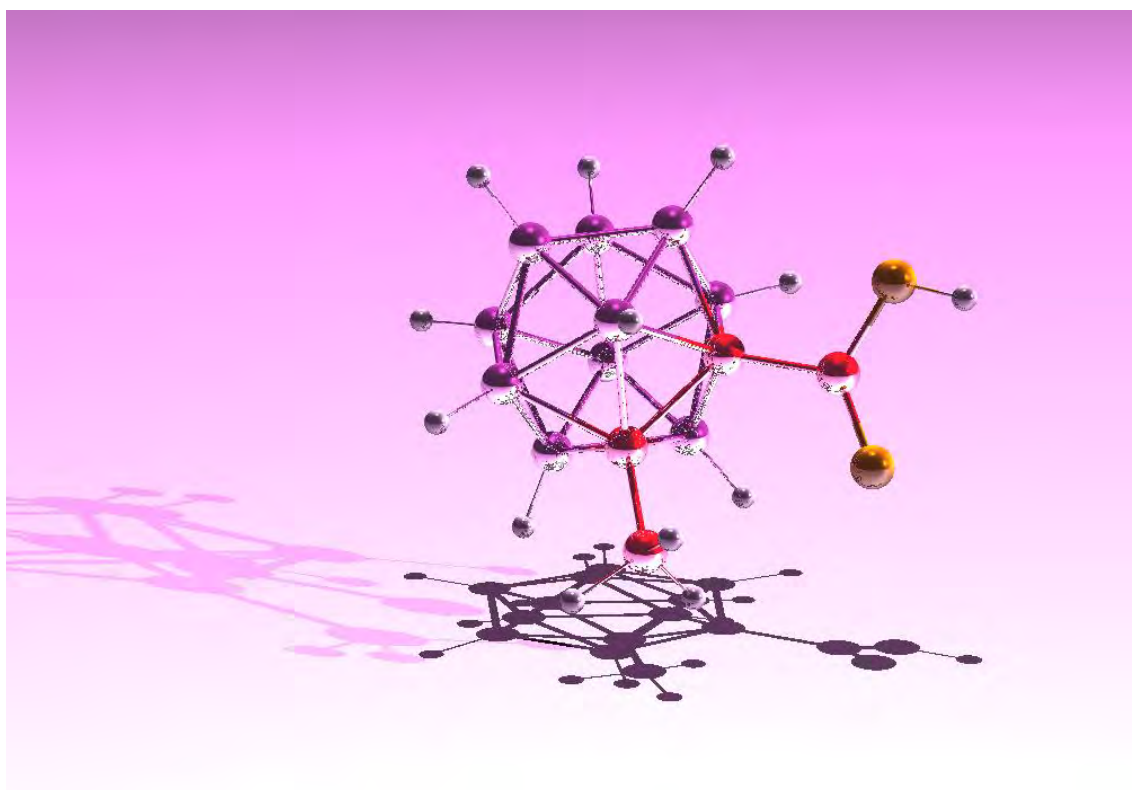


TABLE OF CONTENTS

CHAPTER I. General Introduction

I.1. Historical background.....	5
I.2. Boranes and carboranes	5
I.3. <i>Closo</i>-carboranes	7
I.4. Chemical reactivity of <i>o</i>-carborane	8
1) Deprotonation of C-H vertexes and subsequent substitution	8
2) Substitution at boron by electrophilic reagents	9
3) Partial deboronation of the cluster by elimination of one B-H vertex using a base	9
4) Reduction reaction	11
I.5. Applications of the <i>o</i>-carboranes	11
I.6. Dihydrogen bonds	12
I.7. Characteristics and applications of carboxylate complexes.....	13
I.8. Oxidation catalysis	18
I.8.1. Epoxidation reaction	18
I.8.2. Water oxidation reaction	20
I.9. Molecular magnetism.....	21
I.9.1. Magnetization and magnetic susceptibility	21
I.9.2. Magnetic properties of polynuclear transition metal complexes.....	23
I.9.3. Binuclear copper(II) complexes.....	25
I.9.4. Manganese(II) complexes	26

I.1. Historical background

Alfred Stock discovered and characterized most of the well-known boranes between 1912 and 1933.^[1] Beginning around 1930, H.I. Schlesinger and co-workers made countless important contributions to the development of borane chemistry.^[2] Stock was the first to prepare and characterize boron-hydrogen-bonded species although this work was expanded by Schlesinger and co-workers in 1942.^[2b] In 1946, immediately following the World War II, were initiated studies on the use of boranes as potential fuels for air-breathing engines. Hence, the discovery by Schlesinger and co-workers of practical methods of diborane synthesis and the development around 1950,^[3] at the General Electric Company, of pilot-plant procedures for the preparation of higher boranes from diborane, immeasurably aided the growth of borane chemistry. It should be emphasized the studies carried out by William Lipscomb on *“the structure of boranes illuminating problems of chemical bonding”*^[4] for which was awarded with the Nobel Prize in Chemistry in 1976.^[5]

In the latter part of 1957 a significant discovery in borane chemistry was made by Reaction Motors, Inc. by the synthesis of an extremely stable organoborane $(B_{10}H_{10}C_2H)CHCH_2$.^[6] The parent compound and its derivatives exhibited surprisingly high stability toward oxidation, hydrolysis and thermal decomposition. The name “carborane” has been used as the specific trivial name for the moiety $B_{10}H_{10}C_2H_2$ but it wasn't until April 28, 1959,^[7] this name was agreed upon as the trivial name for this moiety due to the name carborane was coined by an Olin-Mathieson group in early 1958^[8] for a series of compounds with general formula $B_nC_2H_{n+2}$ where n had values of 3, 4, 5 and 8. Finally, the term “carborane” was used both as a specific trivial name for $B_{10}H_{10}C_2H_2$ as well as a class name for the empirical series $B_nC_2H_{n+2}$.^[9] However, the subcommittee on boron nomenclature of the Inorganic Division of the American Chemical Society recommended the systematic name 1,2-dicarvaclovdodecaborane(12) for the original $B_{10}H_{10}C_2H_2$ isomer and the use of the trivial name “carborane” as a class name for boranes with a few skeletal carbon atoms.

I.2. Boranes and carboranes

Boron clusters chemistry is currently contemplate as a bridge between organic, inorganic and organometallic chemistry, with some theoretic chemistry, polymers and medicine influences. Boranes are neutral or anionic compounds with empirical formula $[B_nH_n]^x$. Their structure is based on triangular face polyhedral with a B-H unit in each vertex. There are a large number of boranes in which one or more of the boron vertexes have been substituted by heteroatoms such as C, P, Al or S giving rise to a variety of compounds called heteroboranes.

CHAPTER I

^[10] The most studied among them are the carboranes in which one or two of the boron atoms have been replaced by carbon atoms. The empiric formula of these compounds is: $[C_nB_mH_{n+m+p}]^x = [(CH)_n(BH)_mH_p]_x$, where n represents the number of C atoms within the vertices of the cluster, m is the number of B atoms within the cluster and p the number of bridging H (bridge H).

The electronic requirements of boranes were studied by Wade, Mingos, Rudolph and Williams and obey the classic Wade's rules.^[11] These electron-counting rules allow the prediction of the shape of the cluster structure taking into account the number of occupied vertices and the number of electron pairs required to form the cluster skeleton. Thus, being n the number of polyhedral vertexes (B atoms or different heteroatoms), if the number of electrons joining the cluster is $n+1$, the compound presents a *closo* structure; if it is $n+2$, the compound is *nido* and if it is $n+3$ the cluster is *arachno*. To make the skeletal electron counts is considered that each B-H unit gives two electrons to the cluster, from the boron atom; each C-H ó C-R unit contribute with three electrons from the carbon atom and each bridge hydrogen atom provides one electron to the cluster.

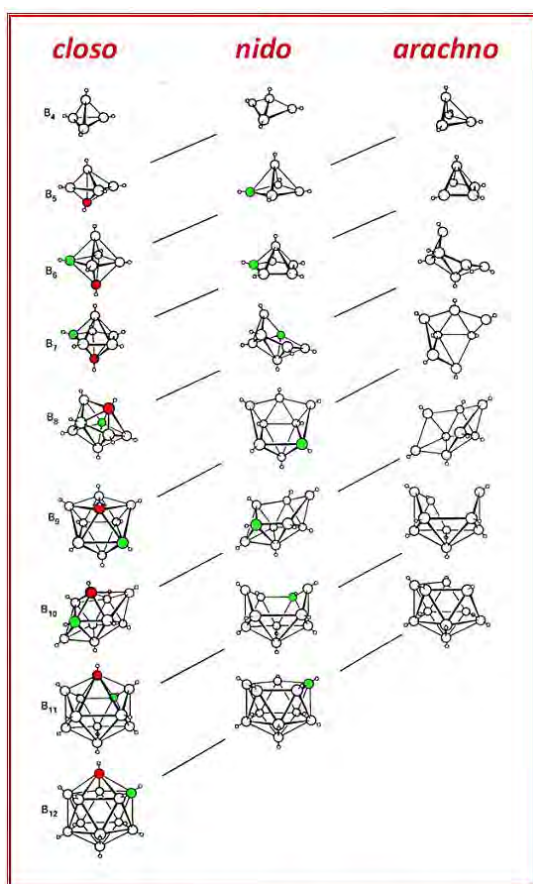


Figure 1. Structural relationship between *closo*, *nido* and *arachno* boranes and hetero-substituted boranes

Figure 1 shows the structural relationship between *closo*, *nido* and *arachno* boranes as well as hetero-substituted boranes.^[11b] The diagonal lines connect species that have the same number of skeletal electron pairs. Hydrogen atoms except those of the B-H framework have been omitted for clarity. Thus, when one vertex of the *closo* structure is removed (red atom in Figure 1), the *nido* is obtained and if a second vertex is removed of this structure (green vertex in Figure 1), the *arachno* cluster is obtained.

As can be observed, the boron clusters are electron deficient due to their peculiar molecular architecture and type of bond (3 centres-2 electrons),^[12] which provide to the cluster particular properties that cannot be found in their organic analogues.^[13]

The most studied boranes are the carboranes and among them, the more known are the

icosahedral clusters that possess two carbon atoms, named dicarba-*closo*-dodecaboranes, which corresponds to the empirical formula $C_2B_{10}H_{12}$.

1.3. *Closo*-carboranes

The dicarba-*closo*-dodecaboranes, *closo*- $C_2B_{10}R_{12}$, are the most studied of all the carboranes due to their high thermic stability^[13a, 14] and their high chemical resistance.^[10a, 10d] These properties are because of the electronic delocalization present in the structure.

Depending on the relative position of the carbon atoms in the cluster there are three isomers (Figure 2. : 1,2-dicarba-*closo*-dodecaborane (*o*-carborane), 1,7-dicarba-*closo*-dodecaborane (*m*-carborane) and 1,12-dicarba-*closo*-dodecaborane (*p*-carborane). The *o*-carborane is stable till temperatures around 460 °C, over this temperature it isomerizes becoming *m*-carborane and that one, between 600 and 700 °C, turns into *p*-carborane.^[10a, 15] As can be seen, the thermal isomerization process gives rise to the more stable isomer, which is the one with the carbon atoms opposite within the cluster.^[16]

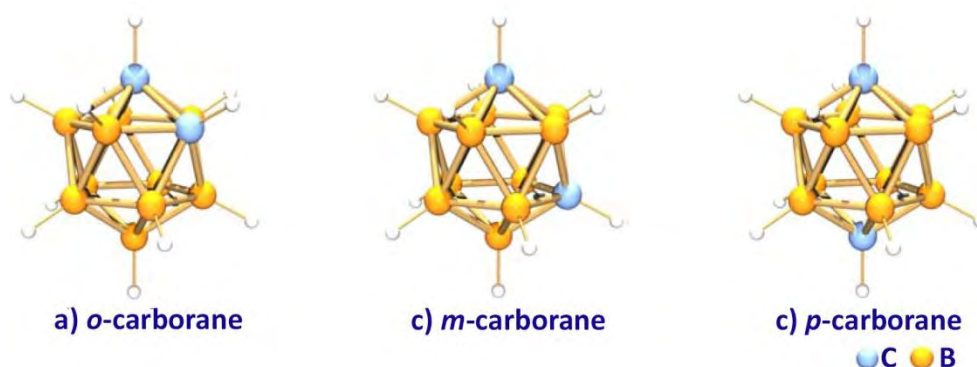


Figure 2. Positional isomers of the dicarba-*closo*-dodecaborane, *closo*- $C_2B_{10}H_{12}$

These dicarba-*closo*-dodecaborane compounds are really interesting due to their facility to change their behaviour according to the exo-cluster groups bond to the boron or carbon atoms.

The 1,2-dicarba-*closo*-dodecaborane, with the carbon atoms in adjacent position also known as *ortho*, has been the isomer used in this doctoral thesis (Figure 3).

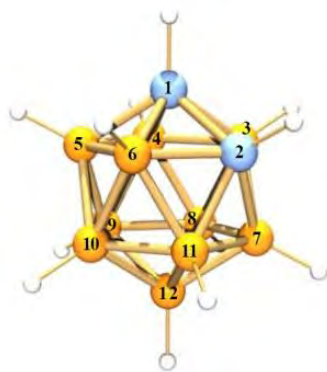


Figure 3. I.U.P.A.C numbering of the closo *o*-carborane cluster

I.4. Chemical reactivity of *o*-carborane

Although *o*-carborane shows high chemical stability in certain reaction conditions, it also exhibits a high synthetic versatility. Thus, the chemical reactivity of the *o*-carborane has been widely studied. The four most important reactions are: 1) deprotonation of C-H vertices and subsequent substitution; 2) substitution at boron by electrophilic reagents; 3) partial deboronation of the cluster by elimination of one B-H vertex using a base; 4) reduction reaction.

1) Deprotonation of C-H vertices and subsequent substitution

The hydrogen atoms bonded to the carbon atoms in the cluster are more acidic than those bonded to the boron atoms as a consequence of the polarity induced by the major electronegativity of the carbon atoms in comparison with the boron ones (2.5 and 2.0 respectively, according to Pauling scale). Actually, the hydrogen atoms bonded to the boron can be seen as hydride instead of protons. The relative acidity of these hydrogen atoms allows their easy substitution by alkaline and alkaline-earth metals, in the presence of strong bases such as *n*-BuLi or NaH, or Grignard reagents in organic solvents leading to the generation of C-metallated derivatives that, in turn, react with a wide variety of reagents to give C-substituted clusters having as substituents organic groups, heteroatoms or metals.^[16-17]

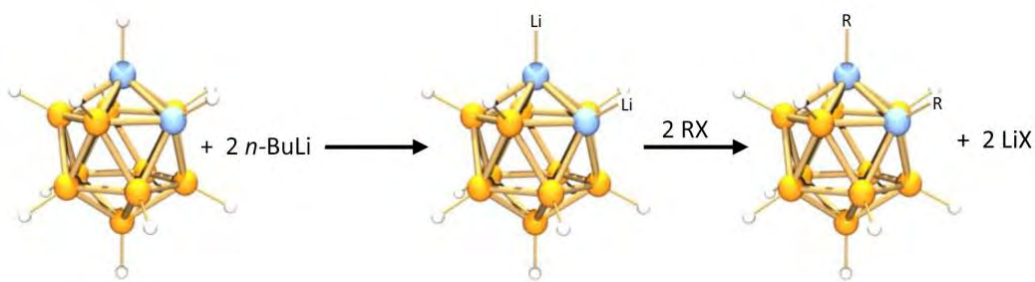


Figure 4. Obtaining of C-derivatives of the *o*-carborane

2) Substitution at boron by electrophilic reagents

The B-H hydrogen atoms in carboranes present low polarity due to the low electronegativity of boron, so that the BH hydrogen atoms exhibit almost no acidic character toward even the strongest proton acceptors, for instance, they are inert to the attack by organolithium and Grignard reagents. Nevertheless, the electron-delocalized of the *o*-carborane cage allow them to be attack by electrophiles.

Besides, the boron vertexes of the *o*-carborane present different reactivity depending on their relative position respect the carbon atoms (Figure 5). Consequently, the boron atoms bond directly to the carbon atoms (B3 and B6) present a higher positive charge density than the others so that, whereas the remaining eight BH vertexes can react with electrophiles, that two vertexes are susceptible to the attack of nucleophiles.

To functionalize them, usually an electrophilic substitution is performed on the vertexes located further from the carbon atoms due to these ones present the most negative electronic density. Thus, the B9 and B12 positions followed by B8 and B10 are the most susceptible to an electrophilic attack on the cluster and, for this reason, the halogenation in these positions is known from the 60s^[18] whilst the halogenation on the positions B3 and B6, directly bond to the carbon atoms, was not achieved until the past decade.^[19]

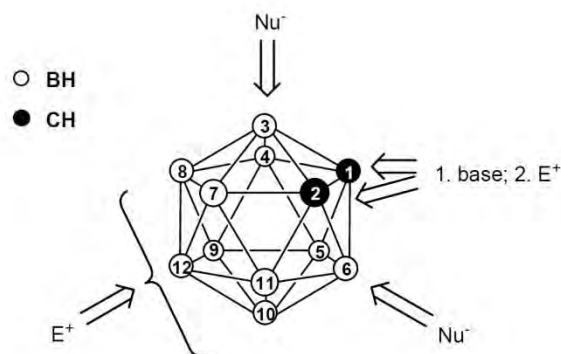


Figure 5. Reactivity of the different vertexes in the *o*-carborane. The susceptibility of the BH vertexes to a electrophilic attack decreases with their electronic density: B(9,12) > B(8,10) > B(4,5,7,11) >> B(3,6)

3) Partial deboronation of the cluster by elimination of one B-H vertex using a base

The partial deboronation of the 1,2-dicarba-*closo*-dodecaborane to 7,8- dicarba-*nido*-undecaborane(-1) by elimination of one B-H vertex was discovered by Hawthorne and co-workers at 1964.^[20] This partial deboronation of the cluster (Figure 6) implies the use of strong bases such as EtO^- or MeO^- , which can remove one boron atom of the cluster (B3 or B6 due to the higher positive charge density over them because of their direct bond to the carbon

CHAPTER I

atoms) and, consequently, lead to a eleven vertexes new cluster, the 7,8- dicarba-*nido*-undecaborane(-1), which contains nine vertexes occupied by boron atoms and two for carbon atoms.

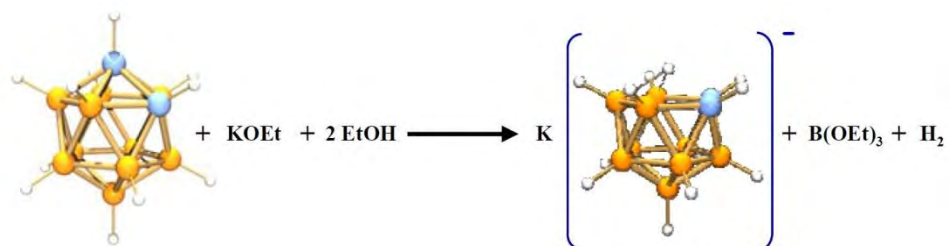


Figure 6. *O*-carborane partial deboronation reaction

The new cluster has the same number of hydrogen atoms that its precursor because the initial species has formally lost one B^+ fragment, so that the hydrogen atom previously bonded to the removed B^+ is now located in the open pentagonal face, C_2B_3 , as a bridge between B9-B10 and B10-B11 atoms (Figure 7). X-ray diffraction studies^[21] show that this H_{bridge} is stronger bonded to B10 than to B9 or B11 and that it maintains itself equidistant to these last two. Moreover, this H_{bridge} is enough acidic to be removed by a strong base leading to the dicarbollide dianion $[\text{C}_2\text{B}_9\text{H}_{11}]^{2-}$ (Figure 8).^[20, 22]

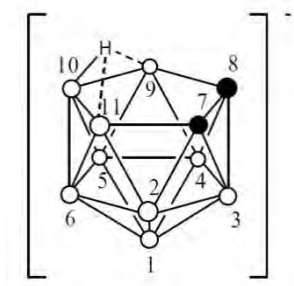


Figure 7. 7,8- dicarba-*nido*-undecaborane (-1) anion

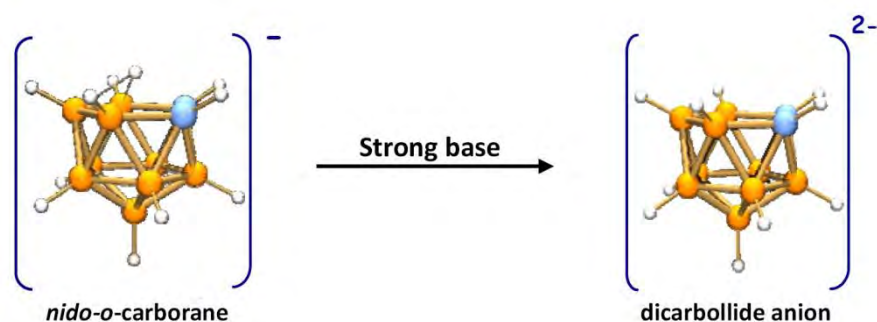


Figure 8. Diagram of the formation of the dicarbollide dianion

This carbollide anion is similar structurally and electronically to the cyclopentadienyl anion ($C_5H_5^-$) and by coordination to metals, it gives rise to the sandwich-type metallocarboranes.^[23]

4) Reduction reaction

The reduction reaction of the *o*-carborane was used for first time in 1963^[24] and consists of the opening of the polyhedral due to the addition of two electrons which break the C-C bond in the cluster to form the corresponding *nido* specie, remaining the initial vertexes. The reducing agents used in this reaction are alkaline metals being the Na and K the most common although, recently, reactions with Mg^[25] has been carried out, thus decreasing the threat of the reaction due to the use of Na or K.

In the reduction reaction is possible the obtaining of two isomers: the thermodynamic [μ -(9,10-CHR')-R-7-*nido*-CB₁₀H₁₀]⁻ and the kinetic, [7,9-*nido*-C₂B₁₀H₁₃]⁻ (Figure 9). The most studied of both is the kinetic isomer, which can be complexed by metals without any necessity of isolating.^[26]

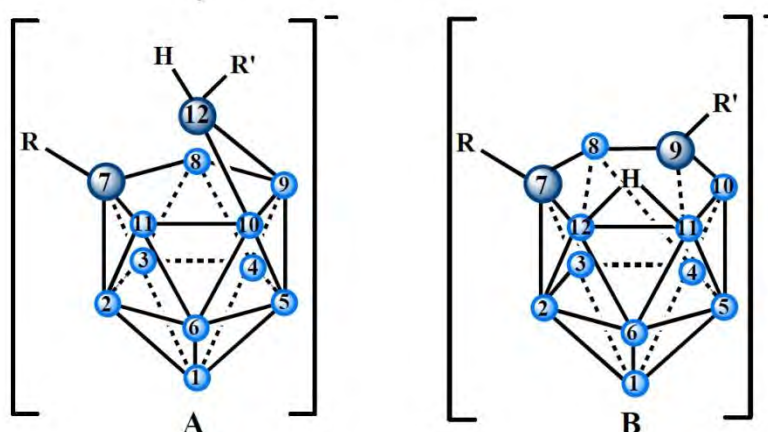


Figure 9. A) Thermodynamic and B) kinetic isomers of the *nido* type obtained by reduction of the *o*-carborane

The main interest of this reaction lies in the possibility of the cluster expansion obtaining 14 vertexes clusters, which are considered the most stable after the ones with 12 vertexes.^[27]

1.5. Applications of the *o*-carboranes

The 1,2-dicarba-closo-dodecaboranes, 1,2-closo-C₂B₁₀H₁₂, and its derivatives are clusters with structures that present uncommon characteristics such as low nucleophilicity, chemical inertness,^[10a, 10d] thermal stability,^[28] electron-withdrawing properties,^[29] and stability and low toxicity in biological systems^[30] that have stimulated the development of a wide range of potential applications based on a molecular approach for the preparation of materials^[31] such as, polymer synthesis,^[32] ceramic precursors,^[32] nonlinear optics,^[33] selective ion-exchange

sensors,^[34] microelectrodes^[35] and gold nanoparticles monolayers modification,^[36] as well as applications in catalysis,^[37] medicine and in wastewater treatment for nuclear power plants.

In the medicine field, the main use of the boron clusters is in the cancer treatment by electron capture therapy or BNCT (Boron Neutron Capture Therapy) which is based on the use of complexes with a large content of the ^{10}B isotope^[38] thus, looking for complexes with a large number of clusters which afford to have a molecule with a large number of boron atoms per molecule.^[13a, 39] Moreover, other applications of boron clusters are seen such as the use of iodinated boron clusters as contrast agents in the X-Ray technic^[40] or the use of cobalt metallacarboranes as proteins inhibitors.^[41]

Besides their use in medicine, the metallacarboranes can be applied in the treatment of wastewater of nuclear power plants^[42] due to their high selectivity in the extraction of metals such as Cs^+ , Sr^{+2} or Eu^{+3} , and as catalysts^[43] in such diverse reactions as alkene hydrogenation,^[37a, 44] hydrosilylation,^[45] cyclopropanation^[46] and polymerization of alkenes.^[47]

Finally, the rigid geometry and the relative ease of derivatization at the carbon vertexes of the carborane cluster^[48] allow the preparation of a wide number of compounds potentially useful as precursors of more complex materials.^[49] Furthermore, the use of carboranes in supramolecular chemistry is a topic that raises great interest for their particular properties^[50] that may induce unexpected behaviour in the supramolecular structures in which they are inserted.

1.6. Dihydrogen bonds

The hydrogen bond has gained wide attention in the last decades because they are an interesting bonding systems which have been studied from the theoretical point of view,^[51] throughout a biological point of view due to their implication in enzymatic catalysis,^[52] as well as for their study as tools for crystal engineering due to their application in building up of supramolecular structures.^[53] The conventional hydrogen bond is an analogous interaction $\text{H}\cdots\text{A}$ formed by a strongly polar group $\text{X}^{\delta-}-\text{H}^{\delta+}$ on one side, and atom $\text{A}^{\delta-}$ with a lone pair of electrons on the other side.^[54]

Unconventional hydrogen bonds (H-bond) are often a subject of investigation^[55] being known four different ones: those with unconventional donors (particularly C–H bonds),^[56] those with unconventional acceptors (π bonded systems or C-atoms),^[55a, 57] $\text{C}-\text{H}\cdots\text{C}$ or $\text{C}-\text{H}\cdots\pi$ bonds with unconventional donors and acceptors^[58] and dihydrogen bonds.^[59]

Focusing in the dihydrogen bonds, they are usually represented as $\text{E}-\text{H}^{\delta-}\cdots\delta^+\text{H}-\text{X}$, where E and X are more electropositive and electronegative than hydrogen, respectively.^[59b, 59c, 60] Usually, X-H is the typical proton-donating bond such as O-H or N-H and E designates a transition metal

or boron.^[59c, 61] One characteristic feature of the dihydrogen bonds are the H...H distance which are of less than 2.4 Å (sum of the Van der Waals radii).^[62] These interactions have been characterized structural and energetically by IR and NMR spectroscopy in solution,^[63] by X-ray or neutron diffraction in the solid state,^[64] and by theoretical calculations in the gas phase. Thus, with similar strength and directionality to conventional hydrogen bonding,^[65] these bonds can influence in the structure, reactivity and selectivity of compounds in gas and condensed phases, having a potential application in catalysis, crystal engineering and material chemistry.^[59b, 66] For example, in polyhydride complexes, an alteration in the quantum exchange couplings^[67] has been seen upon dihydrogen-bond formation.^[68]

These dihydrogen bonds have been also observed in compounds containing carboranes. Thus, dihydrogen bond type S-H...H-B, Si-H...H-C_c or C-H...H-C_c have been observed in metallocarboranes,^[69] which have an important role in the structure of the reported complexes. Moreover, other dihydrogen bonds have been observed such as C-H...H-Pt in a platinum complex with two carboranes cages,^[70] C-H...H-B in the solid-state structure of carboranes such as *o*-carboranyl alcohols bearing N-aromatic rings^[71] or 1-Ph-1,2-C₂B₁₀H₁₁^[70] (Figure 10). Finally, it has been recently reported by Teixidor and co-workers the role of the interactions C-H...H-B in establishing rotamer configurations in metallabis(dicarbollide) systems, observing also the presence of interactions B-H...H-B in these systems.^[72]

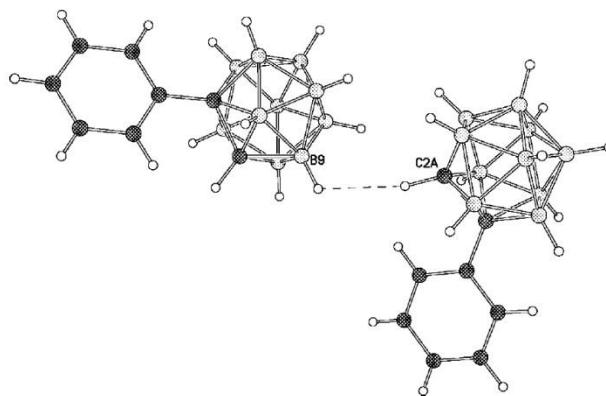


Figure 10.^[70] Interaction C-H...H-B in the solid-state structure of 1-Ph-1,2-C₂B₁₀H₁₁

I.7. Characteristics and applications of carboxylate complexes

Carboxylate anions exhibit a versatile coordination behaviour displaying distinct bonding modes toward metal cations such as monodentate, bidentate, chelate, and so on (Figure

11.).^[73] This property leads to the formation of a great variety of acetate complexes with different structural units such as mononuclear, binuclear or polynuclear.^[73d, 74]

The design and study of new coordination polymers and metal organic frameworks (MOFs)^[75] to generate supramolecular structures is receiving increasing attention due to the structural and chemical diversity of such species together with their attractive applications, among which are their uses as sensors, catalysts, or H₂-storage devices.^[76] The successful behaviour of these structures depends on the use of adequate building blocks whose coordination chemistry, and chemical and physical properties are well described. Thus, the use of carboxylate groups as a bridging ligands and rigid N-donor ligands as linkers is one of the most extensively studied association used for the design of these supramolecular architectures which possess interesting structures and topologies.^[77]

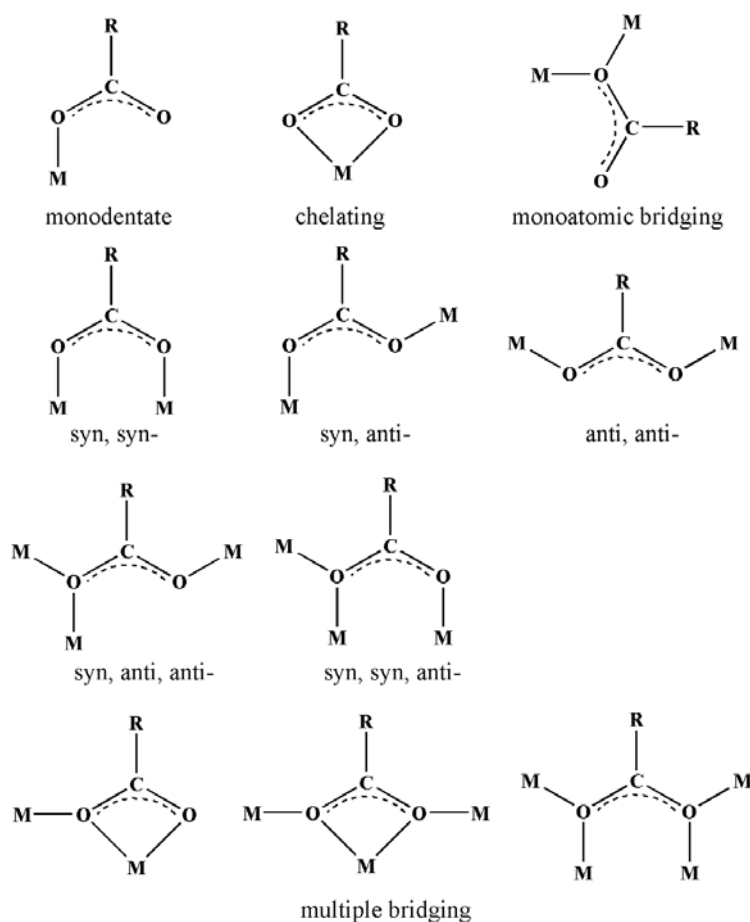


Figure 11. Coordination modes of the carboxylate anion.

Usually, when carboxylate ligands react with a copper (II) cation, binuclear tetracarboxylate copper (II) compounds, $[Cu_2(RCO_2)_4L_2]$, *paddle-wheel* type are obtained in which L is an apical ligand usually bond to metal through an oxygen or nitrogen atom.^[73a, 78]

Binuclear and polynuclear copper(II) carboxylates have received great interest in the studies of exchange-coupling interactions between adjacent metal centres,^[73c, 73d, 79] which are based on chemical and structural effects to control these interactions between paramagnetic centres through monoatomic and polyatomic bridges.^[80] With this aim, a large number of binuclear carboxylate copper(II) *paddle-wheel* adducts, have been reported in an effort to clarify the factors influencing the magnitude of the intramolecular magnetic exchange interaction between two Cu(II) ions.^[81]

Recently, molecular nanomagnets have been proposed as candidates for the manipulation and codification of qubits (quantum bits). Winpenny et al.^[82] have experimentally shown that the molecular spins of the clusters can be chemically bonded between them and that their coupling may be controlled using the suitable *linker*. Binuclear copper (II) compounds type paddle-wheel are promising candidates for the design of such materials.

On the other hand, copper complexes have been studied for many years for their special bioactive and biocatalytic functions.^[83] They constitute an important number of active sites in proteins and enzymes that catalyse many biological functions including oxygen transport and activation, electronic transfer and iron metabolism. Specifically, binuclear copper (II) compounds have been subject of extensive studies on the structure of the active centres of Type-3 binuclear copper enzymes as catechol oxidase,^[84] tyrosinase^[85] and hemocyanin.^[86] A characteristic of these Type-3 proteins is a binuclear antiferromagnetic coupled active centre. In particular, acetate copper compounds functionally act as the monooxygenase tyrosinase in the regioselectivity of the phenol to catechol *o*-hydroxylation as well as in the oxidation of catechol to *o*-benzoquinone.^[87]

Moreover, Cu(II) ion is one of the most common transition metals used in supramolecular chemistry due to its potential use in magnetic materials, having an important role both, in experimental and theoretical studies.^[88] However, its diverse and unpredictable coordination chemistry makes it difficult to incorporate such ions into designed assemblies with predetermined topology and connectivity. Despite this fact, numerous coordination polymers or metal-organic frameworks containing copper(II) and carboxylate ligands have been reported.^[89]

Apart from these applications, the research to design, characterize and apply organic semiconductors (ScOs) has increased in recent years.^[90] One of the most attractive characteristics of the organic semiconductors is the ability to modify their optical, electronic and morphological properties by chemical transformations as well as their direct use in liquid phase processes such as printer ink or spin coating which should allow deposit organic layers onto bulky and flexible substrates in an economic way. Most of the semiconductor species

CHAPTER I

known so far are from an organic nature, there are few examples of inorganic molecular semiconductors and those with hybrid nature mainly have organic composition. In this field, binuclear copper(II) complexes are also promising candidates.

For Mn (II), polynuclear manganese complexes are of great interest and represent an active area of coordination chemistry because of their rich biochemistry and by their remarkable magnetic properties. For instance, manganese complexes can be used as models to mimic the active site of metal-enzymes such as manganese superoxide dismutase,^[91] manganese ribonucleotide reductase,^[92] manganese peroxidase^[93] or photosystem II (PS II)^[94]. Actually, Umena and co-workers^[95] have recently reported the crystal structure of the oxygen-evolving centre in photosystem II in which water molecules are bonded to the Mn₄CaO₅ cluster.

Manganese carboxylate complexes with nitrogen donors ligands such as 2,2'-bpy or 1,10-phenantroline have been synthesised and study in order to mimic amino acid sites, obtaining polynuclear complexes of different nuclearities.^[96]

It is known that single-molecule magnets (SMMs) have attracted considerable attention in the last decade^[97] due to the significant progress they represent in the miniaturization of memory storage devices.^[98] In this field, polynuclear manganese carboxylate compounds have been widely studied^[99] being the most studies those containing twelve manganese atoms.^[100]

Apart from these applications polynuclear manganese complexes attract great interest owing to the supramolecular chemistry and crystal engineering due to their remarkable magnetochemical properties.^[101] Besides, the low cost and toxicity of these compounds are increasing their use in homogeneous catalysis^[102] such as oxidation catalysis.^[94c, 103]

Concerning iron complexes, polynuclear Fe(II) and Fe(III) ion complexes have been widely studied due to their importance in the active centres of some enzymes.^[104] Between them, carboxylate-bridged diiron(II) complexes have a great importance as models of active sites of carboxylate-bridged diiron metalloproteins such as monooxygenases.^[74f, 105] However, Fe(II) carboxylate ligands present strong tendency to form species of higher nuclearity,^[106] in particular, trinuclear oxo-centred iron carboxylate complexes have been known for long.^[107] Most of the M₃O clusters present the general formula [Fe^{III}₃O(O₂CR)₆L₃].nS or [Fe^{III}₂Fe^{II}O(O₂CR)₆L₃].nS in which L is a monodentate ligand and S is a solvent molecule of crystallization and have been broadly studied due to their interesting physical properties,^[74e, 108] their structural relevance to mimic the active sites of some metalloenzymes and ferritin^[106a, 109] as well as, their potential use in oxidation catalysis such as alkene epoxidation^[110] or oxidation of unsaturated lipids.^[111]

Besides, electron transfer reactions are one of the most studied processes in coordination chemistry.^[112] In this area, mixed-valence trinuclear complexes are broadly studied due to the

metal-metal interactions present in their cluster, especially, the intermolecular electron transfer process.^[74e, 113] The understanding of these processes is fundamental for the synthesis of new coordination clusters which can be precursors for clusters of higher nuclearity showing interesting magnetic properties that can act as new magnetic materials such as single molecule magnets (SMMs).^[114] SMMs are currently of great interest due to their potential applications in quantum computing, high-density information storage and biomedicine.^[115]

Finally, the use of cobalt as component in nanomaterials has a great interest due to its size as well as its electrical, magnetic, optical and catalytic properties.^[116] Focusing on cobalt(II) carboxylate compounds, they present a great number of structural motifs, among them there are four common different types (Figure 11).^[74g, 74h, 117] As can be observed in Figure 12, the type I compounds are structurally analogous to the above commented paddle-wheel copper(II) carboxylates, while type II, III and IV present bridging aqua molecules.

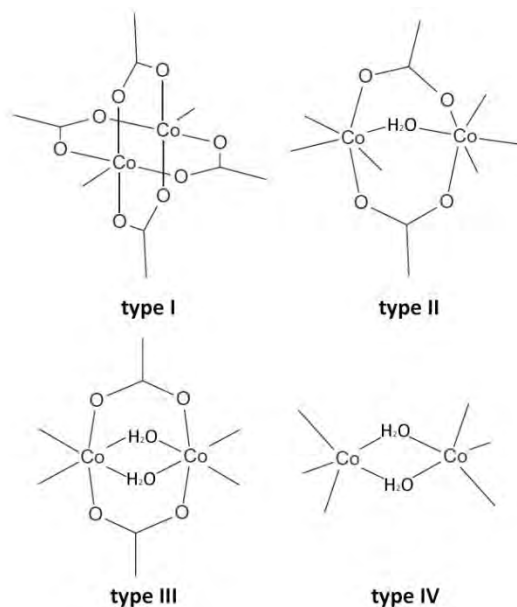


Figure 12.^[117d] Structural types of binuclear cobalt(II) carboxylates

Binuclear high-spin carboxylate-bridged cobalt(II) compounds are involved in many enzymatic but non-redox active processes,^[118] for example, they are analogous to metalloenzymes such as xylose glucose isomerase, aminopeptidase, hydroxylase or urease.^[119]

Furthermore, these carboxylate compounds have great interest as frameworks for building up supramolecular structures (MOF's) which are of great interest for applications in fields related to porous materials such as storage, separation and catalysis as well as in biomedical applications or their use as sensor materials.^[77, 120]

I.8. Oxidation catalysis

Metal-catalysed oxidation reactions are one of the most significant transfer reactions in chemistry and biology.^[121] In the chemical industry, the selective oxidation of raw materials has a great importance due to its application in the conversion of fossil hydrocarbons (olefins, alkanes and aromatics) to oxygenated derivatives avoiding the complete conversion to carbon dioxide.^[121a, 122] Examples of industrial processes include the gas phase oxidation of methanol to formaldehyde and the ethylene to ethylene oxide,^[123] as well as the liquid phase catalytic oxidation of propylene to produce propylene oxide.^[124]

Last decade, the use of catalytic oxidations in chemical industry was focused on the preparation of fine chemicals^[125] and, although selective oxidation used to be an obstacle in this area, it started to change with the introduction of an alcohol group in a drug precursor cleanly in the same manner as enzymes.

It is possible to find lots of enzymes in nature which can catalyse oxidation reaction in living organisms.^[126] For instance, multi-enzymatic systems in nature are able to perform mono-oxygenation reactions efficiently by introducing one oxygen atom of molecular oxygen within a defined substrate and eliminating the second oxygen atom from O₂ as a water molecule. For this reason, investigations based on the mimic of metalloenzyme-catalyzed oxidation have been carried out in the last three decades using metal complexes associated with different oxidants.^[121c] However, many difficulties have been found due to side reactions; one of the steps to improve these catalysis is the use of single oxygen atom donors such as PhIO, NaOCl or H₂O₂ being the last one the most desire due to the only secondary product obtained after the oxidation reaction is water.

I.8.1. Epoxidation reaction

Epoxides are important intermediates widely employed in organic synthesis.^[127] Thus, epoxidation is an important methodology for the synthesis of highly functionalized organic species. Moreover, many natural products possess epoxide units as essential structural moieties for their biological activities.^[128]

For these reasons, alkene epoxidation is an important field which has received considerable interest from academics and industry purposes. One of the most important class of epoxides are the enantiomerically pure ones which form versatile building blocks really useful in organic synthesis to obtain more elaborated chemical products in organic synthesis itself and in industrial production of bulk and fine chemicals.^[129] As commented above, epoxides are really important intermediates due to their easy transformation in several functionalized products,

for instance, by reduction, by rearrangements or by ring-opening reactions of epoxides with various nucleophiles can be formed ketones, allylic alcohols, diols, amino alcohols, polyethers and so on (Figure 13).^[130]

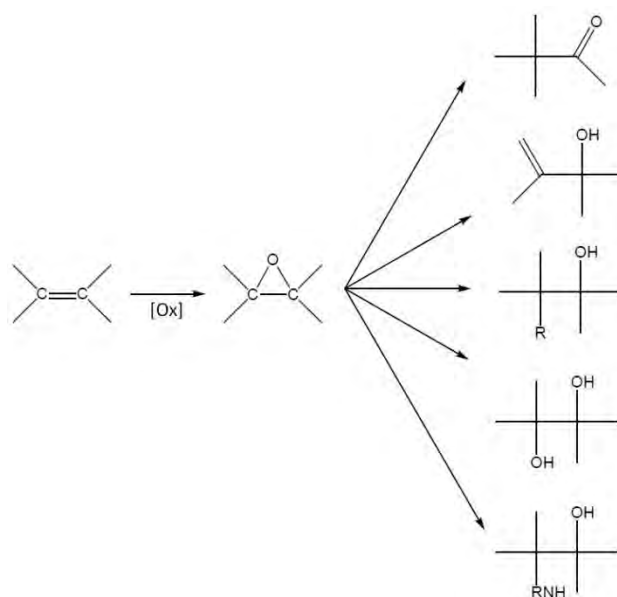


Figure 13. Alkene epoxidation and versatility of epoxides for further conversions.

As a result, the development of new methods for the direct synthesis of epoxides from low cost starting materials has received a steady interest in the last decades^[121] and, although a great number of methods have been developed, it is necessary new stable and available catalysts in order to understand the metal-mediated oxygen processes. With this objective, the selective olefin epoxidation is an important field of research in industry and academia.

For industrial purposes, manganese catalysts are preferable since manganese is a relatively non-toxic metal and presents superior selective values in alkene epoxidation reactions than other non-toxic metals such as iron. Moreover, manganese shows fewer side reactions than iron complexes. One of the most manganese catalysts studied in this reaction have been the manganese(III) complexes with Schiff-bases of N_2O_2 coordination spheres, called Salen complexes and derivatives.^[131] Many studies with these compounds have been reported making them genuine competitors of enzymes.^[103b, 130e, 132] The epoxidation of olefins catalysed by manganese Salen complexes are carried out using mostly PhIO or NaOCl as oxidant agent.^[132e]

In the last decade, Stack and co-workers reported a method based on a manganese complex containing $[CF_3SO_3]^-$ and bi-, tri- or tetradentate nitrogen ligands which used peracetic acid as oxidant, thus generating acetic acid as side product and being a good and “green” oxidising agent.^[103c, 133] It was seen that these systems performed higher activity, rapidity and efficiency

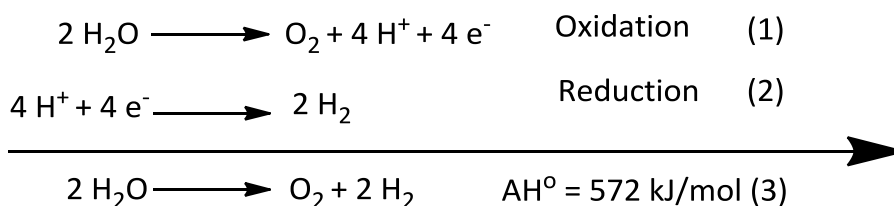
in alkene epoxidation reactions than those with Schiff base ligands, however, their stereoselectivity was poor. Therefore, closer studies show that trinuclear manganese complexes with the structure $[\text{Mn}_3(\text{L})_2(\text{OAc})_6]$, where L is a neutral bidentate nitrogen ligand, are highly efficient catalysts in the epoxidation of alkenes using peracetic acid.^[103d] In spite of this find, few studies of manganese complexes containing carboxylate groups as catalyst have been reported.

1.8.2. Water oxidation reaction

The research in the water oxidation reaction to molecular oxygen has received an increase interest in the last decade not only for its biological importance (to mimic the oxidation mechanism in the photosynthesis) but also for its significance in the development of artificial synthetic systems which can be used as power generators.^[134]

The energetic demand of our society is increasing sharply and, currently the major energy sources are derived from fossil fuels, some of which are rapidly dropping off,^[135] and their consumption produces CO_2 , contributing to the global warming.^[136] Thus, the necessity of find a carbon-free, sustainable, renewable and cost-effective energy source has been one of the most important challenges in the last years. Nowadays, hydrogen is considered a clean fuel, being an attractive energy carrier for further energy requirements.^[136-137] Moreover, it can be produced by splitting water into O_2 and H_2 using the abundant energy of sunlight.^[138]

Water splitting is a two-step process combining water oxidation (1) and hydrogen formation (proton reduction) (2):



It is noteworthy that although we are living on a planet dominated by the presence of water, in nature, there is only one oxidation reaction in which water is the substrate, its oxidation to molecular oxygen (reaction 1 above). This reaction is part of a complex sequence of reactions in the photosynthesis,^[139] and it takes place in the water oxidising complex (WOC) of Photosystem II (PSII) which comprises a Mn_4CaO_x cluster that is preserved in all oxygenic photosynthetic organisms (all cyanobacteria, algae and higher plants).^[140] The crystal structure of this cluster at an atomic resolution has been recently reported by Umena et al.,^[95, 141] and in this structure metal ions, one calcium and four manganese, are bridged by five oxygen atoms.

Four additional water molecules were also seen which were suggested as the substrates of water oxidation (Figure 14).

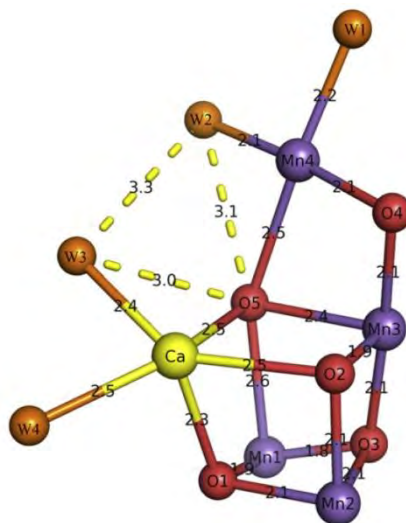


Figure 14.^[141] Structure of the Mn_4CaO_5 cluster determined at 1.9 Å resolution. The bond distances are shown in Å and hydrogen bonds are depicted as dashed lines.

In the last years, the development of catalysts for water oxidation has commanded considerable attention aimed at mimicking the WOC of PSII. So far, high catalytic activities have been achieved with mono- and binuclear ruthenium,^[142] iridium-,^[143] cobalt-,^[144] iron-,^[145] and manganese-based catalysts.^[142c, 146] However, complexes containing manganese ions have received particular attention not only motivated by the approach of modelling the reactivity of natural metalloenzymes but also because manganese is both low cost and environmentally friendly.^[94c, 147]

I.9. Molecular magnetism

I.9.1. Magnetization and magnetic susceptibility^[148]

The study of the magnetic properties of the metal transition complexes has received considerable attention since the 30's when Pauling postulated the existence of a relationship between the magnetic properties and the bond of the metal ion in the compound.

The paramagnetism is a property of substances which contain one or more unpaired electrons. These unpaired electrons can attract a magnetic field due to the electron's magnetic dipole moment so that, when a paramagnetic substance is exposed to a magnetic field H , that becomes magnetized with a magnetization M . The magnetic field inside the substance then is the sum of the external magnetic field and the magnetic field generated by itself and is called magnetic induction, B . In Gaussian units it is represented as:

CHAPTER I

$$B = H + 4\pi M$$

However, in SI units this relationship is given using the magnetic constant or permeability of free space, μ_0 , which is a measure of the amount of resistance encountered when forming a magnetic field in a classical vacuum with a value of $4\pi \times 10^{-7} \text{ H}\cdot\text{m}^{-1}$:

$$B = \mu_0 (H + M)$$

The units of B are G (Gauss) in Gaussian-cgs system and T (tesla) in SI units with a conversion of $1\text{G} = 10^{-4}\text{T}$.

Magnetization, M , is defined in classical mechanics as the variation of the internal energy of a sample when it is perturbed by a magnetic field:

$$M = -\frac{\partial E}{\partial H}$$

Nevertheless, following the quantum mechanics, a microscopic magnetization can be defined for each n discrete energy level:

$$\mu_n = -\frac{\partial E_n}{\partial H}$$

Thus, the global magnetization is the sum of the n microscopic magnetizations which, weighted following a thermic distribution (given for the Boltzmann distribution factors, P_n) among the different states, can be calculated as:

$$M = N \sum_n \mu_n P_n = N \frac{\sum_n (-\partial E / \partial H) \cdot e^{(-E_n/kT)}}{\sum_n e^{(-E_n/kT)}}$$

where k = Boltzmann constant, and N = Avogadro number.

It can be considered that inside the substrate each mol of compound presents a particular magnetization, M_M , which is originated by the difference in the population between levels with different magnetic quantum number and which is associated to the magnetic field H through the molar magnetic susceptibility χ_M by:

$$\chi_M = \frac{\partial M_M}{\partial H}$$

which units are $\text{emu}\cdot\text{mol}^{-1}\cdot\text{Oe}^{-1}$ in Gaussian-cgs units and $\text{m}^3\cdot\text{mol}^{-1}$ in SI units.

Considering the relationship between the molar magnetic susceptibility and the magnetization, the expression corresponding to χ_M can be written as:

$$X_M = \frac{N}{H} \cdot \frac{\sum_n (\partial E_n / \partial H) \cdot e^{(-E_n/kT)}}{\sum_n e^{(-E_n/kT)}}$$

In 1932, Van Vleck^[149] lead a simplification of the last expression supposing the magnetic susceptibility always independent of the magnetic field H , and expressing the energy of each level as a sequence of H powers, according to:

$$E_n = E_n^{(0)} + E_n^{(1)} H + E_n^{(2)} H^2 + \dots$$

where $E_n^{(0)}$ is the energy in the zero field, and $E_n^{(1)}$ and $E_n^{(2)}$ are the first- and second-order Zeeman terms.

Thus, the Van Vleck equation is:

$$X_M = N \cdot \frac{\sum_n [(E_n^{(1)})^2/kT - 2E_n^{(2)}] \cdot e^{(-E_n^{(0)}/kT)}}{\sum_n e^{(-E_n^{(0)}/kT)}}$$

This equation can be simplified to mononuclear or polynuclear complexes when their ions no present orbital contribution ($E_n^{(2)} = 0$):

$$X_M = \frac{Ng^2\mu_B^2}{3kT} \cdot \frac{\sum_S S(S+1)(2S+1) \cdot e^{(-E_S^{(0)}/kT)}}{\sum_S (2S+1) \cdot e^{(-E_S^{(0)}/kT)}} + N\alpha$$

where S is the total spin of each energy state $E_S^{(0)}$, μ_B is the Bohr magneton and g is the Landé factor.

1.9.2. Magnetic properties of polynuclear transition metal complexes

Polynuclear transition metals compounds containing diamagnetic bridges present some overlap between the metallic orbitals with unpaired electrons. It is known as superexchange mechanism and it consists in a strong magnetic coupling between two next-to-nearest neighbour metallic centres (cations) through a non-magnetic anion (bridge ligand) so that the ligand frontier orbitals are involved.

If we suppose a binuclear complex in which the metallic centres are paramagnetic with one unpaired electron each one and overlap between the two centres exists, two molecular orbitals will be generated with different spin. Then, two different distributions of the electrons are possible: both to the lower energy orbital leading to a resulting total spin $S_T=0$ (singlet) or one electron to each orbital leading to a total spin $S_T=1$ (triplet). Thus, when the ground state is the singlet, the coupling is antiferromagnetic, whilst when it is the triplet, the coupling is ferromagnetic. The difference in energy between the singlet and triplet states is known as the coupling constant J . (see Figure 15 for further details).

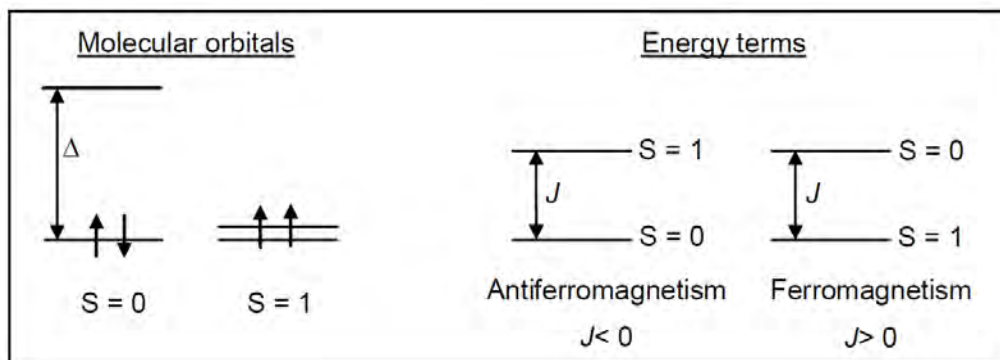


Figure 15. Different possible distributions of the electrons in a binuclear compound with paramagnetic metal centres.

The isotropic magnetic interaction between binuclear compounds with two ions A and B, with spins S_A and S_B can be described by the HDVV Hamiltonian, which was originally suggested by Heisenberg, Dirac and Van Vleck^[149-150]:

$$H = -JS_A S_B$$

where J is the coupling constant between A and B. As $S = S_A + S_B$, $S^2 = S_A^2 + S_B^2 + 2S_A S_B$ then, $S_A S_B = (S^2 - S_A^2 - S_B^2)/2$. Thus,

$$H = -\frac{J}{2}(S^2 - S_A^2 - S_B^2)$$

Being the exact quantum solution for this Hamiltonian:

$$E(S, S_A, S_B) = -\frac{J}{2} [S(S + 1) - S_A(S_A + 1) - S_B(S_B + 1)]$$

Making a change in the origin of the potential energy and considering $[S_A(S_A+1) - S_B(S_B+1)]$ as the zero, the energy for each value of S can be calculated as:

$$E(S) = -\frac{J}{2} [S(S + 1)]$$

An expression for χ_M as a function of the temperature could be found for any binuclear compound if the last expressions is applied to each spin of the system from $|S_A - S_B|$ to $|S_A + S_B|$ and is combined with the simplified Van Vleck equation.

However, to determinate the energies of the spin-states for trinuclear compounds, Kambe's method has to be used due to the no totally equivalence of the interacting anions. Thus, assuming as important the coupling between the nearest neighbour ions the Hamiltonian can be written as:

$$H = -2J(S_1 S_2 + S_2 S_3) = -2JS_2(S_1 + S_3)$$

I.9.3. Binuclear copper(II) complexes

Binuclear copper(II) complexes containing bridged ligands are constituted by two paramagnetic centres with an unpaired electron each one, that interact between them through the ligands leading to excited states of the molecule accessible by thermal energy ($\leq 1000 \text{ cm}^{-1}$). The resultant magnetic behaviour will be ferromagnetic if the ground state has total spin $S=1$ (unpaired electrons) or antiferromagnetic if the total spin $S=0$ (paired electrons), (see Figure 15 above).

When a magnetic field is present, the total spin state $S=1$ is unfolded in the corresponding sublevels with $M_S = -1, 0, +1$, as seen in Figure 16 for an antiferromagnetic system. If temperature is decreased, the population in the spin total level $S=0$ will be increased due to that level has lower energy.

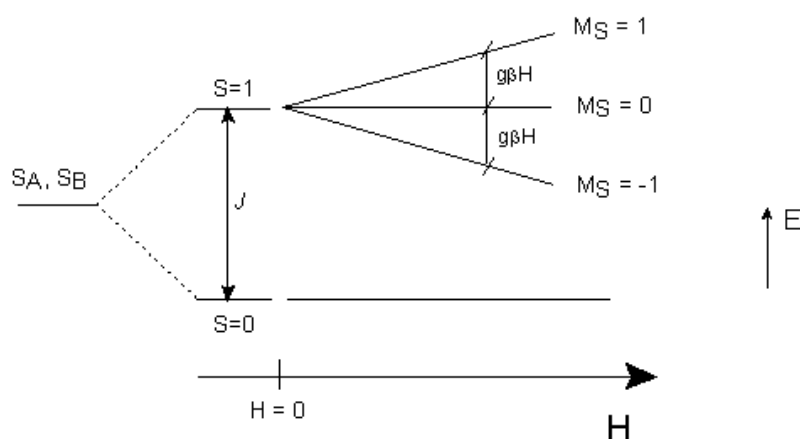


Figure 16. Split of the states in a system with $S_T = 1$ in the corresponding sublevels due to the magnetic field effect

Inside the *paddle-wheel* carboxylate copper(II) complexes, one of the most studied is the $[\text{Cu}_2(\text{OAc})_4(\text{H}_2\text{O})_2]$ having an antiferromagnetic behaviour with a J value of -296 cm^{-1} .^[151] Moreover, several magnetic studies changing the nature of the bridge molecules or the axial ligand has been reported.^[88a, 152] Computational studies of this compound has been also performed giving an idea about the parameters that affect the coupling between the two copper centres involved, such as the electron-withdrawing power of the ligands or the structure distortions among others.^[153] Thus, it has been established that as higher is the electron-withdrawing property of the carboxylate, stronger is the interaction between the metallic centres.^[88a, 151-154]

As seen in Figure 16, in a binuclear copper(II) complex the four possible energy states have, taking the $S=1$ state as the reference and $M_S=0$ ($E_{|1,0\rangle} = 0$), the corresponding energy values.^[150d]

$$E_{|1,-1\rangle} = -g\beta H$$

$$E_{|1,0\rangle} = 0$$

$$E_{|1,1\rangle} = g\beta H$$

$$E_{|0,0\rangle} = J$$

If these values are replaced in the Van Vleck equation, the Bleaney-Bowers^[151] equation is obtained which allows to calculate the magnetic susceptibility in binuclear copper(II) compounds :

$$\chi_M = \frac{2N_A \beta^2 g^2}{kT} [3 + \exp(-J/kT)]^{-1}$$

1.9.4. Manganese(II) complexes

Electronic and magnetic properties of polynuclear manganese(II) complexes bridged by organic or inorganic ligands have been widely studied. One of the most studied complexes are those containing carboxylates ligands^[155] which can adopt different coordination modes leading to several magnetic systems.^[156] The interest in these compounds leads to the fact that although they usually present weak antiferromagnetic coupling, depending on the distortion of the coordination polyhedron around the manganese(II) ion, ferromagnetic coupling is possible.^[157]

The simplified Van Vleck equation to calculate the magnetic susceptibility in binuclear manganese(II) compound where $S_A = S_B = 5/2$ is:

$$\chi_M = \frac{Ng^2 \mu_B^2}{kT} \cdot \frac{110e^{15x} + 60e^{10x} + 28e^{6x} + 10e^{3x} + 2e^x}{11e^{15x} + 9e^{10x} + 7e^{6x} + 5e^{3x} + 3e^x + 1}$$

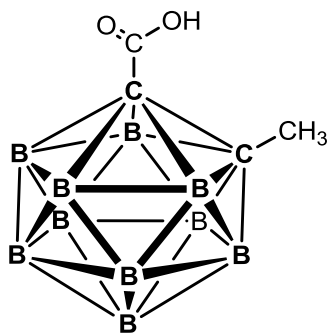
where $x = J/kT$.

CHAPTER II. General objectives

This thesis symbolized the introduction of a new research line to the existing ones in the research group and it has been developed centred in the study of coordination chemistry of two carboranylcarboxylate ligands with different metals of the first transition series, with the idea to generate different polynuclear compounds. These ligands present a fundamentally inorganic composition but simultaneously keep the properties and possibilities offered by organic molecules. In the previous chapter we have presented the important properties and possibilities offered by the carboxylate and acetate ligands, however, very few carboranylcarboxylate bridged metal (II) complexes have been previously synthesized, and their coordination chemistry, together with their physical and chemical properties, have remained mostly unexplored.

The ligands used in this work are the 1-CH₃-2-CO₂H-1,2-*closo*-C₂B₁₀H₁₀], LH and the [1-CO₂H-1,2-*closo*-C₂B₁₀H₁₀], L'H, showed in Chart 1.

a)



b)

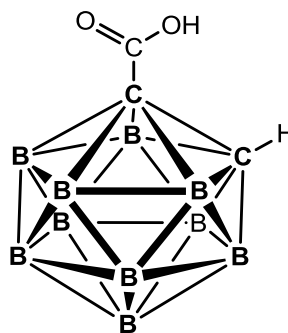


Chart 1. Ligands a) 1-CH₃-2-CO₂H-1,2-*closo*-C₂B₁₀H₁₀ (LH) and b) 1-CO₂H-1,2-*closo*-C₂B₁₀H₁₀ (L'H)

The main objectives of this thesis are:

❖ Copper complexes with carboranylcarboxylate ligands

- The synthesis of a new family of copper(II) complexes containing the carboranylcarboxylate ligands [1-CH₃-2-CO₂-1,2-*closo*-C₂B₁₀H₁₀]⁻ or [1-CO₂H-1,2-*closo*-C₂B₁₀H₁₀]⁻ and THF, water or pyridyl ligands (py, *p*-CF₃-py, *p*-CH₃-py, *o*-(CH₃)₂-py, pz, or 4,4'-bpy) as terminal ligands, as well as their full characterization through elemental analysis, structural, spectroscopic (NMR, IR, UV-visible, ESI-MS), electrochemical and magnetic techniques
- To study the stability of the synthesized complexes containing the ligand LH and THF or H₂O, against polypyridyl ligands through UV-visible spectra and magnetic studies while

employing electronic-structure calculations; also evaluating the electronic and steric effects of these ligands on the stability of the resulting compounds.

- To study the differences among the synthesized compounds containing carboranylcarboxylate ligand LH and the analogous μ -acetate to establish the structural and chemical differences such as their behaviour in nucleophilic solvents or their solubility.
- To establish structural and chemical differences between the synthesized compounds containing the ligand LH and the analogous ones containing the ligand L'H, where a hydrogen atom instead of a methyl group is present as a substituent on the carbon of the cluster.

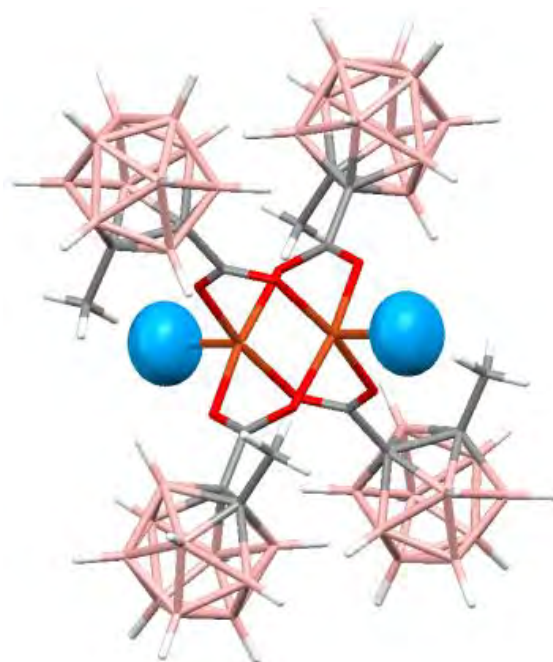
❖ Manganese complexes with carboranylcarboxylate ligands

- The synthesis and characterization of a series of new manganese(II) complexes containing the carboranylcarboxylate $[1\text{-CH}_3\text{-2-CO}_2\text{-1,2-closo-C}_2\text{B}_{10}\text{H}_{10}]^-$ or $[1\text{-CO}_2\text{-1,2-closo-C}_2\text{B}_{10}\text{H}_{10}]^-$ ligands and their full characterization by chemical analysis, structural, spectroscopic (NMR, IR, UV-visible, ESI-MS), electrochemical and magnetic techniques.
- To study the reactivity of the synthesized manganese complexes and the influence in their structure of the chelating polipyridyl ligands 2,2'-bpy and 2,2'-bpm and the full characterization of the resultant products through structural, analytical, spectroscopic, electrochemical and magnetic techniques.
- To establish structural and chemical similarities and differences between the synthesized manganese compounds due to the two different carboranylcarboxylate ligands used.
- To study the stability of a polynuclear manganese complex in solution through microscopic (Cryo-TEM), dynamic light scattering (DLS) and X-Ray scattering (SAXS and WAXS) techniques.
- To study the catalytic activity of the complexes containing the carboranylcarboxylate LH in two oxidation reactions: i) the epoxidation of representative terminal and internal double bonds of aliphatic and aromatic alkenes using commercial peracetic acid (32%) as oxidant, making a comparison with the acetate compound $\text{Mn}_3(\text{OAc})_6(\text{bpy})_2$; and ii) the water oxidation reaction.

❖ Iron and cobalt complexes with carboranylcarboxylate ligands

- The synthesis and full characterization through structural, analytical and spectroscopic techniques of a series of new polynuclear cobalt and iron(II) complexes containing the carboranylcarboxylate [1-CH₃-2-CO₂-1,2-*closo*-C₂B₁₀H₁₀]⁻ unit.
- To study the catalytic activity of a cobalt (II) complex in the epoxidation of representative terminal and internal double bonds of aliphatic and aromatic alkenes using commercial peracetic acid (32%) as oxidant.

CHAPTER III. Cu(II) complexes containing the carboranylcarboxylate ligand 1-CH₃-2-CO₂H-1,2-closo-C₂B₁₀H₁₀. Study of their steric and electronic effects.



A series of new mononuclear and binuclear copper(II) compounds containing the 1-CH₃-2-CO₂H-1,2-closo-C₂B₁₀H₁₀ carborane ligand (LH) has been synthesized and fully characterized through analytical, spectroscopic (NMR, IR, UV-visible, ESI-MS) and magnetic techniques. X-ray structural analysis revealed for the binuclear compounds a paddle-wheel structure with the two copper (II) atoms holding together through four carboxylate bridges in syn–syn mode and square pyramidal geometry around each copper ion. The mononuclear complex obtained with the *o*-(CH₃)₂-py ligand presents a square-planar structure, in which the carboranylcarboxylate ligand adopts a monodentate coordination mode. Magnetic studies of the binuclear compounds have been carried out showing, in all cases, a strong antiferromagnetic coupling. Computational studies based on hybrid density functional methods have been used to study the magnetic properties of the complexes and also to evaluate their relative stability on the basis of the strength of the bond between each Cu(II) and the terminal ligand.

TABLE OF CONTENTS

CHAPTER III. Cu(II) complexes containing the carbonylcarboxylate ligand 1-CH₃-2-CO₂H-1,2-closo-C₂B₁₀H₁₀. Study of their steric and electronic effects.

III.1.	Introduction	37
III.2.	Objectives.....	39
III.3.	Results and discussion	41
III.3.1.	Synthesis and characterization	41
III.3.2.	Electrochemical properties	48
III.3.3.	Spectroscopic properties.....	50
III.3.4.	Magnetic properties.....	55
III.3.5.	Electronic Structure Calculations	59
III.3.6.	Thermal decomposition	60
III.4.	Conclusions	62
III.5.	Experimental section	64
III.5.1.	Instrumentation and measurements	64
III.5.2.	Materials	65
III.5.3.	Preparations	66
III.6.	References.....	70

III.1. Introduction

Investigations of the design, characterization, and applications of organic semiconductor devices have attracted increasing attention in recent years.^[1] Particularly remarkable is the special relevance that these materials have as constituents of flat electroluminescent devices. This growing interest has attracted the attention of industry and thus has made possible their introduction into the commercial market. One of the features that make them attractive is the possibility of altering their optical, electronic, and morphological properties through chemical modification and also the fact that they can be applied to the direct use of liquid-phase processing such as ink printing or spin coating. This method should, in principle, allow the deposition of organic layers over flexible and large substrates in a cheap way.

Most of the semiconductor species known to date are of an organic nature, whereas inorganic molecular semiconductors are scarcely described and those of a hybrid nature are of a predominantly organic composition.

In recent years, molecular nanomagnets have been proposed as suitable candidates for qubit encoding and manipulation. Winpenny et al.^[2] experimentally demonstrated that molecular spin clusters can be chemically linked to each other and that the coupling between their spins can be tuned by choosing an adequate linker. Bimetallic Cu^{II} paddle-wheel moieties are promising candidates with regard to the design of single- and two-qubit gates in bipartite systems.

The assembling of complexes in two or three dimensions (metal–organic frameworks (MOFs))^[3] to generate supramolecular structures is receiving increasing attention due to the structural and chemical diversity of such species together with their attractive applications, among which are their use as sensors, catalysts, or H₂-storage devices.^[4] The successful behaviour of these structures depends on the use of adequate building blocks whose coordination chemistry, and chemical and physical properties are well described.

The 1,2-dicarba-closo-dodecaborane, 1,2-closo-C₂B₁₀H₁₂, and its derivatives are clusters with structures that present uncommon characteristics such as low nucleophilicity, chemical inertness,^[5] thermal stability,^[6] electron-withdrawing properties,^[7] and stability and low toxicity in biological systems^[8] that have stimulated the development of a wide range of potential applications based on a molecular approach for the preparation of materials.^[9] Moreover, the rigid geometry and the relative ease of derivatization at the carbon vertexes of the carborane cluster^[10] allow the preparation of a wide number of compounds potentially useful as precursors of more complex materials.^[11] Besides, the use of carboranes in supramolecular chemistry is a topic that raises great interest for their particular properties^[12]

CHAPTER III

that may induce unexpected behaviour in the supramolecular structures in which they are inserted.

In this chapter we aim to partially focus our investigations on molecules potentially applicable to these uses that present a fundamentally inorganic composition but that simultaneously keep the properties and possibilities offered by organic molecules.

III.2. Objectives

Very few carboranylcarboxylate bridged dicopper (II) complexes have been previously synthesized and their coordination chemistry, together with their physical and chemical properties, has remained mostly unexplored.

The main goal of this chapter was the synthesis, characterization and study of the main physical and chemical properties of new mono- and binuclear copper(II) complexes containing the ligand carboranylcarboxylate [1-CH₃-2-CO₂-1,2-*closo*-C₂B₁₀H₁₀].

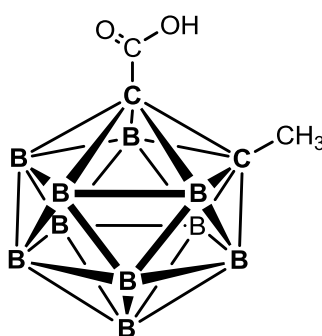


Chart 1. 1-CH₃-2-CO₂H-1,2-*closo*-C₂B₁₀H₁₀ ligand (LH)

First of all, binuclear Cu(II) starting materials complexes having water or THF molecules as terminal ligands were synthesized and fully characterized. Another goal was to study the performance of these starting materials with different pyridyl ligands and fully characterize the resulting complexes through structural, analytical and spectroscopic (IR, UV-visible, NMR) techniques, together with the study of the magnetic properties of the binuclear complexes.

We were also interested in studying the relative stability of the complexes and their magnetic properties employing electronic-structure calculations.

Finally, we have proposed to establish differences among the synthesized compounds and the analogous μ -acetate compounds regarding their behaviour in nucleophilic solvents or their solubility, as a consequence of the presence of the carboranylcarboxylate groups in these compounds.

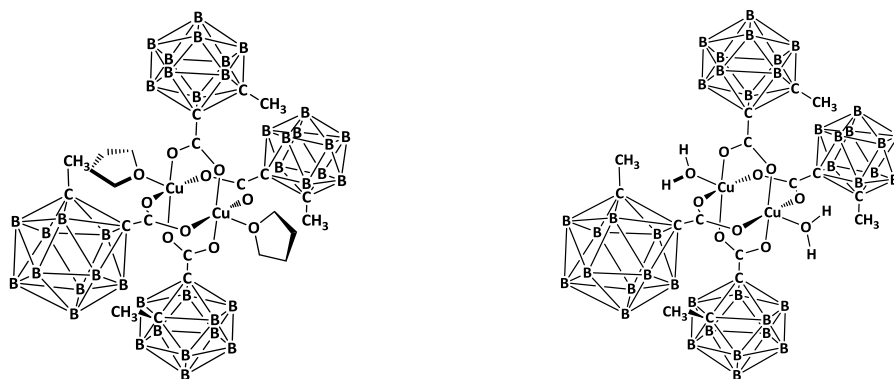
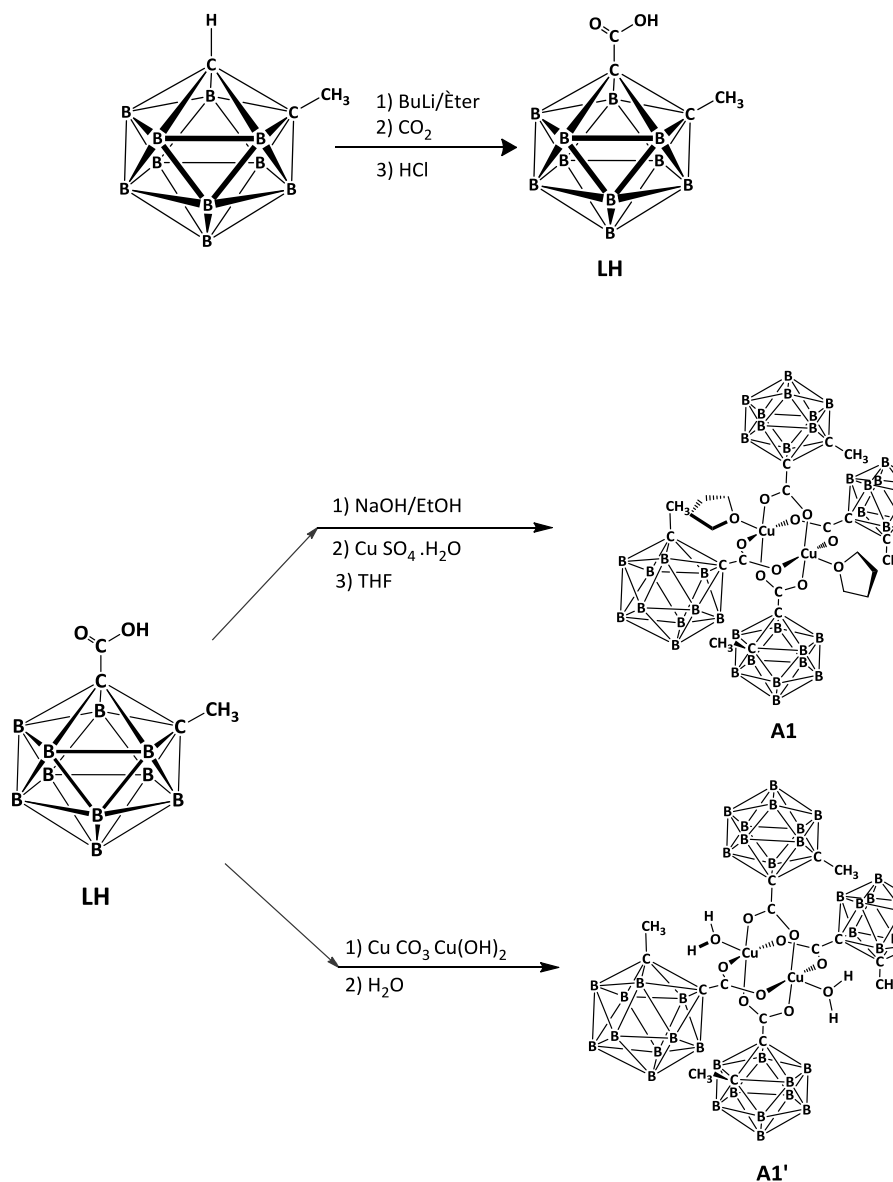


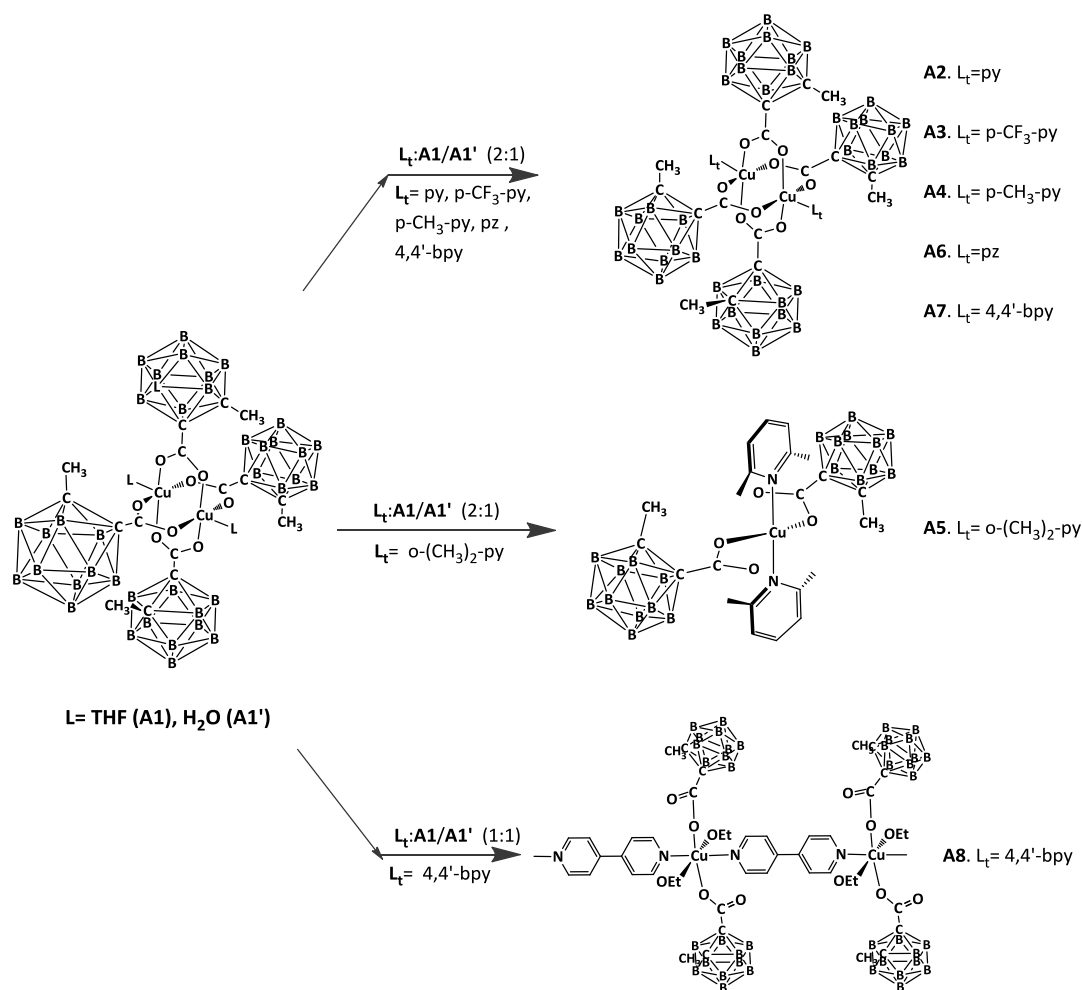
Chart 2. Binuclear compounds with the ligand carboranylcarboxylate [1-CH₃-2-CO₂-1,2-*closo*-C₂B₁₀H₁₀]⁻ and water or THF molecules as terminal ligands

III.3. Results and discussion

III.3.1. Synthesis and characterization

The synthetic strategy for the preparation of the ligand **LH** and the Cu(II) complexes **A1-A8**, containing the carboranylcarboxylate ligand 1-CH₃-2-CO₂H-1,2-*closo*-C₂B₁₀H₁₀ (**LH**) and different terminal ligands, **L_t**, is outlined in Scheme 1.





Scheme 1. Synthetic strategy for the preparation of LH and Cu(II) complexes **A1-A8**

The binuclear copper compound $[\text{Cu}_2(1\text{-CH}_3\text{-2-CO}_2\text{-1,2-closo-C}_2\text{B}_{10}\text{H}_{10})_4(\text{THF})_2]$, **A1**, was obtained by neutralization of carboranylcarboxylic acid, **LH**, with NaOH followed by reaction with CuSO_4 in ethanol/ H_2O and subsequent extraction in THF.^[13] Compound $[\text{Cu}_2(1\text{-CH}_3\text{-2-CO}_2\text{-1,2-closo-C}_2\text{B}_{10}\text{H}_{10})_4(\text{H}_2\text{O})_2]$, **A1'**, was obtained by reaction of a suspension of carborane ligand **LH** with CuCO_3 in water. This last synthesis is a new, easy and clean method to obtain the wanted starting material.

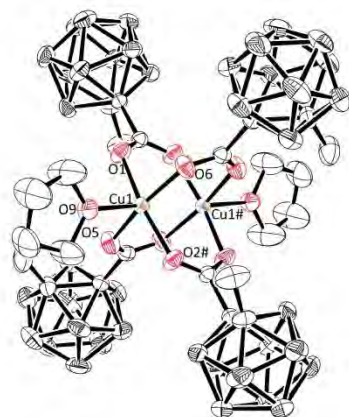
Compounds **A1** and **A1'** were used as starting materials that were subsequently reacted with different monodentate and bidentate nitrogen containing heterocyclic aromatic ligands, L_t ($L_t = \text{py, } p\text{-CF}_3\text{-py, } p\text{-CH}_3\text{-py, } o\text{-(CH}_3)_2\text{-py, pz, or } 4,4'\text{-bpy}$), with the aim to examine and study the electronic and steric effects of the terminal ligands on the stability of the binuclear copper core, and also to study and characterize the new compounds obtained. Both **A1** and **A1'** present the same reactivity with respect to the pyridylic ligands used in this chapter.

When the corresponding ligands L_t dissolved in CH_2Cl_2 are added to a solution of complex **A1** in CH_2Cl_2 (with a ligand:complex ratio of 2:1), blue-green solutions are formed that after slow

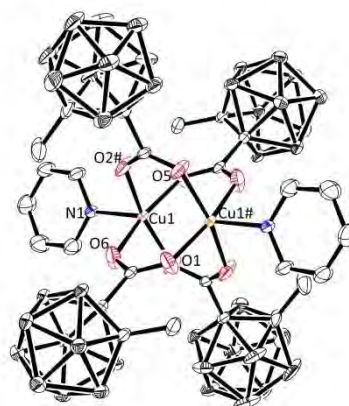
evaporation lead, in most cases, to the precipitation of binuclear complexes of general formula $[\text{Cu}_2(\text{L})_4(\text{L}_t)_2]$ as main products. In the case of the binuclear compounds **A2** and **A4**, obtained upon addition of pyridine and *p*-methylpyridine respectively, we have observed the parallel formation of other mononuclear and tetranuclear compounds in lower yield (complexes **A2'**, **A4'** and **A4''**, see experimental section and Figure S1 in the supporting information section). These compounds are obtained by manual separation from a mixture of compounds in crystalline form by separating crystals of different morphologies. In the case of the pyrazine complex **A6**, together with the binuclear compound we have obtained an insoluble compound not yet identified. Finally, the addition of 2,6-lutidine as axial L_t ligand leads to the exclusive formation of the mononuclear complex **A5** (Scheme 1). This diverse synthetic behaviour can be rationalized on the basis of the apical ligand basicity as it will be described below from spectrophotometrical experiments performed under an excess of L_t ligand and also from the electronic structure calculations.

However, when the terminal ligand 4,4'-bpy is used in a ratio ligand:complex of 1:1 an insoluble polymer, **A8**, is obtained (see experimental section and Scheme 1).

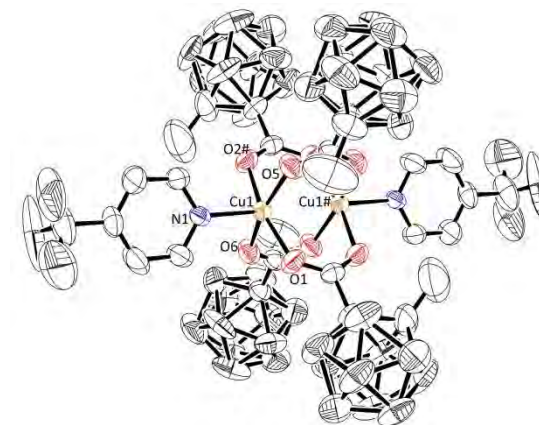
Crystallographic data and selected bond distances and angles for compounds **A1-A6** and **A8** are presented in Table S1 (see supporting information section) Table 1 and Table 2, respectively (the corresponding data for compounds **A2'**, **A4'** and **A4''** are gathered in the supporting information section, Table S2 and Table S3). ORTEP plots with the corresponding atom labels for the X-ray structures of all compounds are presented in Figure 2. and Figure S1.



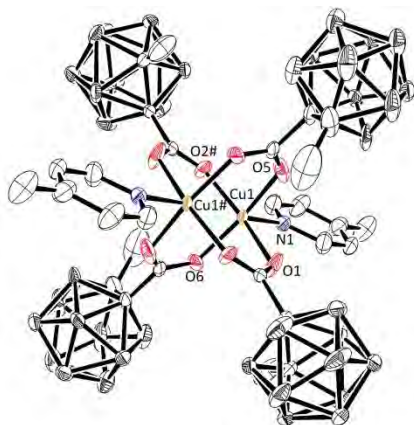
$[\text{Cu}_2(1\text{-CH}_3\text{-2-CO}_2\text{-1,2-closo-C}_2\text{B}_{10}\text{H}_{10})_4(\text{THF})_2]$, (**A1**)



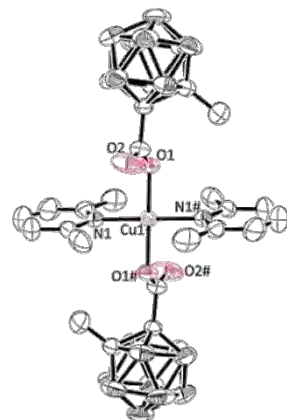
$[\text{Cu}_2(1\text{-CO}_2\text{-1,2-closo-C}_2\text{B}_{10}\text{H}_{10})_4(\text{py})_2]$, (**A2**)



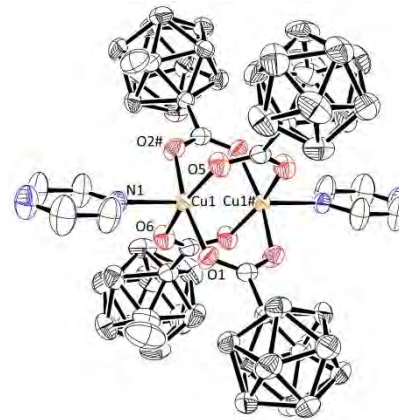
$[\text{Cu}_2(1\text{-CH}_3\text{-2-CO}_2\text{-1,2-closo-C}_2\text{B}_{10}\text{H}_{10})_4(p\text{-CF}_3\text{-Py})_2]$, (**A3**)



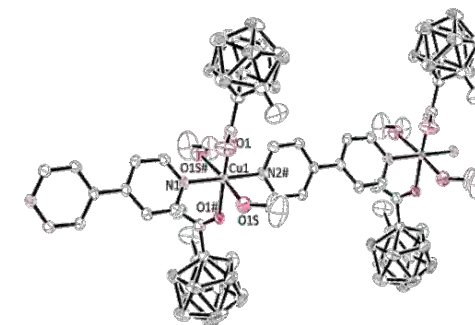
$[\text{Cu}_2(1\text{-CH}_3\text{-2-CO}_2\text{-1,2-closo-C}_2\text{B}_{10}\text{H}_{10})_4(p\text{-CH}_3\text{-Py})_2]$, (**A4**)



$[\text{Cu}(1\text{-CH}_3\text{-2-CO}_2\text{-1,2-closo-C}_2\text{B}_{10}\text{H}_{10})_2(o\text{-(CH}_3)_2\text{-py})_2]$, (**A5**)



$[\text{Cu}_2(1\text{-CH}_3\text{-2-CO}_2\text{-1,2-closo-C}_2\text{B}_{10}\text{H}_{10})_4(\text{pz})_2]$, (**A6**)



$[\text{Cu}(1\text{-CH}_3\text{-2-CO}_2\text{-1,2-closo-C}_2\text{B}_{10}\text{H}_{10})_2(\text{EtOH})_2(4,4'\text{-bpy})]$, (**A8**)

Figure 2. X-ray structures (ORTEP plots with ellipsoids at 40% probability level) and labelling scheme for complexes **A1- A6** and **A8**.

Table 1. Selected bond lengths (Å) and angles (°) for complexes **A1**, **A2**, **A3**, **A4**, **A6** and **A8**.

	A1	A2	A3	A4	A6	A8
Cu(1)-O(1)	1.956(2)	1.956(3)	1.965(3)	1.970(3)	1.964 (2)	1.975(2)
Cu(1)-O(2)#1	1.959(2)	1.953(3)	1.975(3)	1.964(3)	1.973(2)	
Cu(1)-O(1)#1						1.975(2)
Cu(1)-O(1s)						2.471(3)
Cu(1)-O(5)	1.972(2)	1.957(2)	1.971(3)	1.970(4)	1.965(2)	
Cu(1)-O(6)	1.973(2)	1.956(2)	1.965(3)	1.965(4)	1.963(2)	
Cu(1)-O(9)	2.114(2)					
Cu(1)-N(1)		2.104(3)	2.118(3)	2.104(4)	2.144(3)	1.999(3)
Cu(1)-N(2)#2						2.014(3)
Cu(1)-Cu(1)#1	2.672(2)	2.6937(9)	2.733(15)	2.7166(13)	2.7221(7)	
O(1)-Cu(1)-Y	167.20(7)	165.64(10)	165.23(12)	165.20(16)	165.73(9)	177.27(12)
O(1)-Cu(1)-O(1s)						90.26(10)
O(1)#1-Cu(1)-O(1s)						89.90(10)
O(1)-Cu(1)-O(5)	89.52(9)	89.09(13)	90.13(15)	88.65(19)	89.19(11)	
O(2) #1-Cu(1)-O(5)	88.50(9)	88.45(13)	87.74(15)	89.28(15)	89.71(11)	
O(1)-Cu(1)-O(6)	89.85(8)	89.60(13)	88.22(15)	88.5(2)	89.85(10)	
O(2)#-Cu(1)-O(6)	89.30(9)	89.24(14)	90.11(16)	89.79(16)	87.72(10)	
O(5)-Cu(1)-O(6)	167.30(6)	165.47(10)	165.14(13)	165.20(17)	165.71(10)	
O(1)-Cu(1)-X	98.44(8)	98.15(10)	96.22(14)	97.28(16)	97.48(10)	91.36(6)
Y-Cu(1)-X	94.31(9)	96.20(11)	98.53(14)	97.50(16)	96.72(10)	91.36(6)
N(1)-Cu(1)-O(1s)						86.75(8)
N(2)#2-Cu(1)- O(1s)						93.25(8)
O(1)-Cu(1)-N(2)#2						88.64(6)
O(1)#1-Cu(1)-N(2)#2						88.64(6)
N(1)-Cu(1)-N(2)#2						180.00(1)
O(5)-Cu(1)-X	93.69(12)	98.09(10)	95.37(14)	94.90(16)	100.19(10)	
O(6)-Cu(1)-X	98.94(11)	96.42(10)	99.49(14)	99.86(17)	94.07(10)	
O(1)-Cu(1)- Cu(1) #1	83.46(7)	83.48(8)	83.23(10)	84.56(12)	84.19(7)	
O(2)#-Cu(1)- Cu(1) #1	83.75(8)	82.18(8)	82.01(10)	80.64(11)	81.55(7)	
O(5)-Cu(1)-Cu(1) #1	82.83(11)	82.69(8)	82.76(11)	82.34(12)	82.89(8)	
O(6)-Cu(1)-Cu(1) #1	84.50(10)	82.78(8)	82.38(11)	82.94(12)	82.82(8)	
X-Cu(1)-Cu(1) #1	176.05(5)	178.19(8)	178.04(10)	176.66(11)	176.48(7)	

X= O(9), complex **A1**; X = N(1), complexes **A2-A6** and **A8**; Y= O(2) #1, complex **A1-A4** and **A6**; Y= O(1) #1 complex **A8**

Table 2. Selected bond lengths (Å) and angles (°) for complex **A5**.

	A5		A 5
Cu(1)-O(1)	1.9418(16)	O(1)#-Cu(1)-N(1)#	91.15(7)
Cu(1)-O(1)#	1.9418(16)	O(1)-Cu(1)-N(1)#	88.85(7)
Cu(1)-N(1)	2.0222(19)	O(1#)-Cu(1)-N(1)	88.85(7)
Cu(1)-N(1)#	2.0222(19)	O(1)-Cu(1)-N(1)	91.15(7)
O(1)#-Cu(1)-O(1)	180.00(10)	N(1) #-Cu(1)-N(1)	180.00(8)

Binuclear compounds **A1-A4** and **A6** display a similar structure with the two copper (II) atoms held together through four syn,syn $\eta^1: \eta^1: \mu^2$ -carboxylate bridges acting as equatorial ligands for each Cu(II) environment. The square pyramidal geometry around each metal ion is completed by the oxygen donor atom of a THF molecule in **A1**, a H₂O molecule in **A1'** and by the nitrogen donor atom of different pyridylic terminal ligands in **A2-A4** and **A6**. The overall geometry of the complexes corresponds to a binuclear paddle-wheel cage type structure.

The structures are centrosymmetric with the symmetry centre located between the two copper atoms. The Cu-O (carboxylic) bond distances are similar and comparable to other similar coordinated carboxylates,^[14] and are in the range 1.95-1.97 Å. For complex **A1**, the apical distance Cu-O_{THF} of 2.11 Å is longer than the basal distances, but it is within the range observed for other similar carboxylate structures with water as axial ligand.^[15] The apical Cu-L_t bond distances in the pyridyl complexes follow the trend L_t= pz > p-CF₃-py > p-CH₃-py \cong py, an order that could be related to the basic strength of the ligands. The Cu...Cu distances, in the range 2.67-2.73 Å, are similar to other carboranylcarboxylate compounds^[13] but somewhat longer than those of other centrosymmetric structures with water as apical ligand.^[16]

The distortion of the coordination polyhedron is evidenced by the trans O-Cu-O angles, which range from 165.1 to 167.3°. Also, each copper atom is displaced out of the mean plane towards the corresponding apical ligand (the bond angles involving the apical ligand, O-Cu-O/N, range from 94.3 to 100.2°, and the distances from each Cu atom to its mean basal plane vary between 0.214 and 0.253 Å for the set of binuclear complexes). For complexes **A2-A4** and **A6**, with N-pyridine molecules as apical ligands, this displacement is more pronounced than for complex **A1**, containing THF. The cis O-Cu-O angles around the copper atoms show slight differences with regard to the 90° ideal value and are in the range 88.5-90.1°.

The X-ray crystallography performed on the mononuclear complex **A2'** ([Cu(μ -CH₃COO)₂(py)₂(H₂O)]), Figure S1) reveals a five-coordinate Cu atom described as having a square pyramidal geometry, where the equatorial plane is occupied by two nitrogen atoms from the monodentate pyridine ligands and two oxygen atoms from the carboranylcarboxylate

ligands displaying a monodentate coordination mode. The oxygen atom O(5) from a water molecule is in the axial position. The two pyridine rings are markedly tilted with regard to the mean basal plane, 43.98° for pyN1 and 35.84° for pyN2. Compared to the ideal square pyramid, the angles between the axial and the basal positions show significant distortions with deviations from the theoretical value of 90° : O(5)-Cu(1)-O(3), 88.69° ; O(5)-Cu(1)-O(1), 98.41° ; O(5)-Cu(1)-N(1), 99.99° ; O(5)-Cu(1)-N(2), 90.67° , with the Cu metal centre placed at 0.152 \AA from the mean basal plane. The structural packing (see Figure S2f) shows that each water ligand of a given complex is involved in an intramolecular O-H...O hydrogen bonding with the O2 oxygen atom of the same molecule and with another oxygen atom (O4) from a neighbouring molecule, leading to a 2D double chain architecture. The analogous mononuclear complex **A4'** (see Figure S1b supporting information) displays similar square-pyramidal geometry, also with the p-methylpyridine ligands planes tilted (by 25.85° for CH₃-pyN1 and 56.58° for CH₃-pyN2) with regard to the mean basal plane.

The mononuclear complex **A5** shows a centrosymmetric square planar structure, where the copper atom is coordinated by two nitrogen atoms from the lutidine ligands and by two oxygen atoms from the two carboranylcarboxylate ligands that adopt a monodentate coordination. It is also of interest to discuss the packing structure of this mononuclear complex which is displayed in Figure 3. . Each O atom not coordinated of the carborane ligand forms two C-H...O hydrogen bonds: one intramolecular, involving the methyl group of one of the lutidine ligands, and another intermolecular, with one of the aromatic H atoms of a neighbouring molecule, leading to a 1D single zigzag architecture.

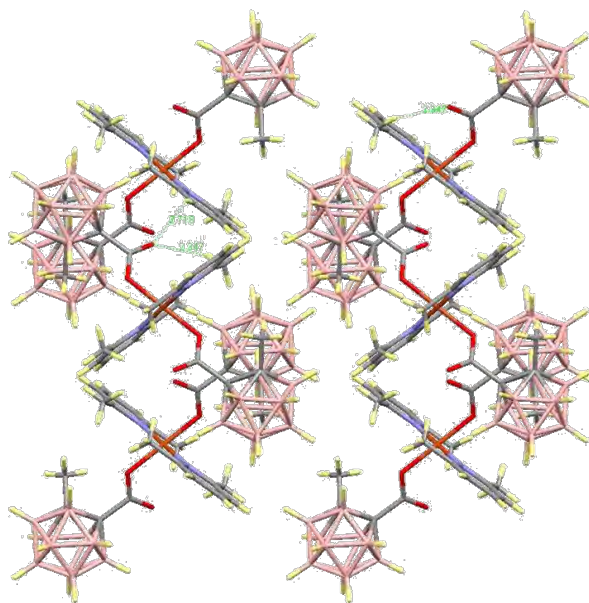


Figure 3. Packing diagram for the X-ray diffraction structure of complex **A5**.

Finally, the X-ray structure of complex **A8** discloses a polymer with a structure in which, each copper atom is coordinated by two carboxylate groups from two carboranylcarboxylate ligands that adopt a monodentate coordination mode, two ethanol molecules and two nitrogen atoms from different 4,4'-bipyridine ligands, showing an octahedral geometry (Figure 2.). The 4,4'-bpy ligand acts as linker, connecting the copper(II) centres leading a 1D polymer chain. Very few examples of copper (II) polymeric structures with carboxylate groups and 4,4'-bpy acting as linker has been found in the literature.^[17] The O(1)-Cu(1)-N(1) (91.36°), O(1)-Cu(1)-N(2)# (88.64°), O(1s)-Cu(1)-N(1) (86.75°) and O(1s)-Cu(1)-N(2)# (93.25°) bond angles produce significant differences in the coordination sphere with respect to regular octahedral coordination. The bond distances lengths are in the range observed for similar complexes described in the literature.^[17] It is worth mentioning that the two rings of 4,4'-bpy are not in the same plane, with a distortion between them of 21.30°. Besides, each O atom not coordinated of the carborane ligand forms one intramolecular C-H...O hydrogen bond (see Figure S2g), involving the coordinated ethanol molecule. It is interesting to observe the packing structure of this polymer in which the carboranylcarboxylate ligands of two adjacent 1D polymeric chains are alternated in the space filling the gaps between the Cu(II) ions provided for the 4,4'-bpy ligands (See Figure S2 at the Supporting information).

The collection of binuclear complexes presented here displays, as described above, structural parameters similar to the well-known, paddle-wheel copper acetate, $[\text{Cu}_2(\mu\text{-CH}_3\text{COO})_4(\text{H}_2\text{O})_2]$, and its derivatives. The reactivity of copper acetate with regard to the replacement of the apical H_2O or THF ligands by pyridyl ligands (as shown in Scheme 1 for **A1** and **A1'**) has been tested and it follows similar trends (see Figure S3 and Table S4 at the supporting information for the X-ray structure and the crystallographic data and selected bond distances and angles of the analogous *p*- CF_3 -py binuclear derivative, $[\text{Cu}_2(\mu\text{-CH}_3\text{COO})_4(\textit{p}\text{-CF}_3\text{-py})_2]$). However, the presence of the carboranylcarboxylate groups in **A1-A4** and **A6** induces particular electronic and structural properties that establish remarkable differences with the analogous μ -acetate compounds such as their behaviour in nucleophilic solvents (see below) or their solubility (complex **A1** is readily soluble in dichloromethane, diethyl ether or toluene, where copper acetate is completely insoluble).

III.3.2. Electrochemical properties

Complex **A1**, the analogous μ -acetate complex $[\text{Cu}_2(\mu\text{-CH}_3\text{COO})_4(\text{THF})_2]$ and the free carboranylcarboxylic ligand **LH** were studied by cyclic voltammetry (CV).

The CV of the free **LH** ligand is shown in Figure 4 (yellow line) and displays two redox processes centred at +1.04 and -0.56 V ($E_{\text{pc}} = +0.91\text{V}$, $E_{\text{pa}} = +1.17\text{V}$ for the former and $E_{\text{pc}} = -$

0,73V, $E_{pa} = -0.40V$ for the latter). On the other hand, the CV registered for both Cu complexes (also gathered in Figure 4.) display parallel electrochemical behaviour as expected from their analogous structures, however, slight differences are observed in the cathodic region between -0.2 and -1 V which probably arises from the presence of the carboranylcarboxylate ligand in **A1**.

For complex **A1** (blue line), two electrochemically irreversible redox waves appear at $E_{1/2} = -0.31 V$ ($E_{pc} = -0.53 V$, $E_{pa} = -0.09 V$) and $E_{1/2} = -0.52 V$ ($E_{pc} = -0.84 V$, $E_{pa} = -0.20 V$) that can be assigned respectively to Cu^{II}/Cu^I and Cu^I/Cu^0 redox pairs, together with other ligand-centred processes. A similar behaviour is observed for the copper acetate complex (Figure 4. , red line) where the corresponding Cu^{II}/Cu^I and Cu^I/Cu^0 redox couples appear respectively at $E_{1/2} = -0.25 V$ ($E_{pc} = -0.36 V$, $E_{pa} = -0.15 V$) and $E_{1/2} = -0.45 V$ ($E_{pc} = -0.65 V$, $E_{pa} = -0.25 V$), cathodically shifted with regard to complex **A1** in accordance with the higher electron-withdrawing character of the carboranylcarboxylate ligands relative to acetate. The reduction to Cu^0 should almost certainly involve the rupture of the binuclear structure in the compound and indeed, coulometry performed at a fixed potential of $E_{1,2} = -1.1 V$ for 3 minutes leads to the formation of a Cu^0 metallic deposit clearly visible on the working electrode surface.

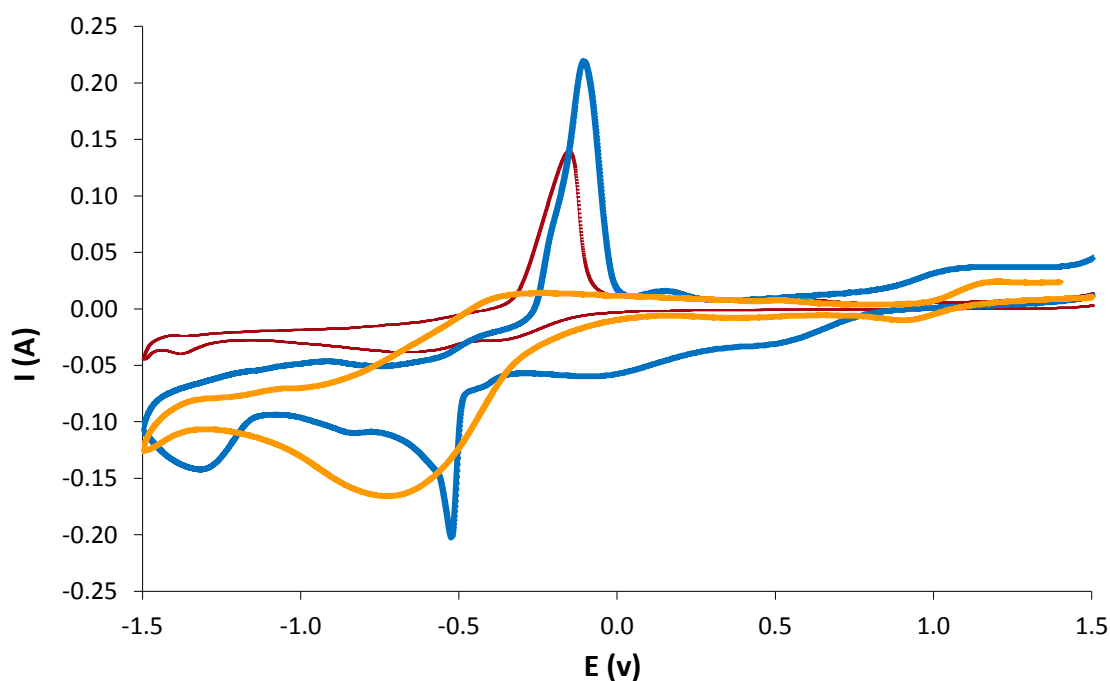


Figure 4. Cyclic voltammety recorded for complexes **A1** , (—), $[Cu_2(\mu-CH_3COO)_4(THF)_2]$, (—), and free carborane ligand, LH , (—) in acetonitrile.

III.3.3. Spectroscopic properties

The IR spectra of all complexes described display typical $\nu(\text{B-H})$ absorption at frequencies above 2590 cm^{-1} , characteristic of *closo* carborane derivatives,^[18] difference between the frequencies of the symmetric and antisymmetric stretches lies between the ranges quoted for bidentate bridging ligands.^[19] The $^1\text{H}\{^{11}\text{B}\}$ -, ^{11}B -, $^{11}\text{B}\{^1\text{H}\}$ - and $^{13}\text{C}\{^1\text{H}\}$ -NMR spectra of these compounds are in complete agreement with the solid structures confirmed by X-ray crystallography. It can be observed that the $^1\text{H}\{^{11}\text{B}\}$ - spectra exhibit resonances around $\delta = 2$ ppm attributed to the $\text{C}_c\text{-CH}_3$ protons and the resonances of the protons bonded to the B atoms appear as broad singlets over a wide chemical-shift range in the region from $\delta = 0$ to $+5$ ppm. The $^{11}\text{B}\{^1\text{H}\}$ -NMR resonances for all the complexes featured similar patterns in the range from $\delta = 2$ to -15 ppm that agree with a *closo* cluster.^[20]

The binuclear pyridyl compounds are stable in THF and CH_2Cl_2 solutions but are unstable in CH_3OH because a copper metallic mirror is observed after keeping the complex in CH_3OH solution for several hours. Figure 5. displays the appearance of a solution of complex **A3** (left) and $[\text{Cu}_2(\mu\text{-CH}_3\text{COO})_4(\text{THF})_2]$ (right) after keeping them at room temperature for 18 hours. The formation of a metallic copper mirror is clearly evidenced in the case of complex **A3** in sharp contrast with the analogous μ -acetate complex.

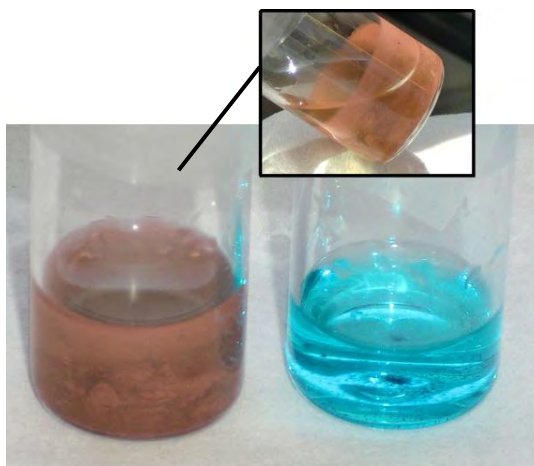


Figure 5. 1 mM solutions of complex **A3** (left vial) and $[\text{Cu}_2(\mu\text{-CH}_3\text{COO})_4(\text{p-CF}_3\text{-py})_2]$ (right vial) in methanol after 18 h of preparation in which the formation of a Cu^0 metallic mirror is observed only for the carboranylcarboxylate complex **A3**.

To know more about the stability of the *closo* cluster of the binuclear $[\text{Cu}_2(\text{L})_4(\text{L}_t)_2]$ complexes in methanol, the $^{11}\text{B}\{^1\text{H}\}$ NMR spectrum of a fresh solution of complex **A3** in methanol was run, initially observing its resonances at $\delta = -3.1$ (2B), -6.2 (4B) and -7.3 ppm (4B). A new $^{11}\text{B}\{^1\text{H}\}$ spectrum was run after 12 hours and it clearly displays the presence of two

compounds. The major resonances at $\delta = -1.5$ (1B), -5.5 (1B) and -9.3 ppm (8B) correspond to the free ligand **LH** and the resonances at $\delta = -15.7$, -16.8 , -18.6 , -33.2 and -35.7 ppm are characteristic of a *nido*-[7,8-C₂B₉H₁₀]⁻ species.^[20-21] An extra resonance at $\delta = +19.2$ ppm, not coupled to any H, was also present that is the consequence of the removed BH vertex. It is known for years that the partial degradation reaction on *o*-carborane derivatives is driven by a nucleophilic attack that can remove one of their BH units (B3 or B6), formally as BH²⁺, leaving *nido*-shaped [7,8-C₂B₉H₁₀]⁻ or [7,8-C₂B₉H₉]²⁻ anions. Several nucleophiles such as alkoxides,^[22] amines,^[23] fluorides^[24] or phosphanes^[25] have been used. According to the literature,^[26] the chemical shift for B(OCH₃)₃ appear at $\delta = +17.2$,^[27] 17.6,^[28] or 18.1 ppm.^[29] Having determined the fate of the extracted BH²⁺, we turned to the question of how the B(OCH₃)₃ was formed. Our explanation on why the partial degradation reaction of 1-CH₃-2-CO₂H-1,2-*closo*-C₂B₁₀H₁₀ ligand takes place is based on the fact that, once the complex is dissolved in CH₃OH, there is free *p*-CF₃-py ligand in the solution. Then, the pyridyl ligand^[30] establishes an acid-base equilibrium with methanol, and as a consequence *R*-pyridinium methoxide is present in the reaction medium, sufficient enough to slowly and smoothly produce mild conditions that lead to partial cluster deboronation. The BH²⁺ removed from the 1-CH₃-2-CO₂H-1,2-*closo*-C₂B₁₀H₁₀ ligand oxidizes to B(OCH₃)₃ reducing the Cu^{II} to Cu⁰ while the *closo* cluster is transformed to *nido*.

Figure 6 shows the ¹¹B{¹H}-NMR spectra that proves that the dimeric complex **A3** is unstable in CH₃OH, thus leading to the free ligand, a *nido*-shaped [7,8-C₂B₉H₁₀]⁻ species and B(OCH₃)₃.

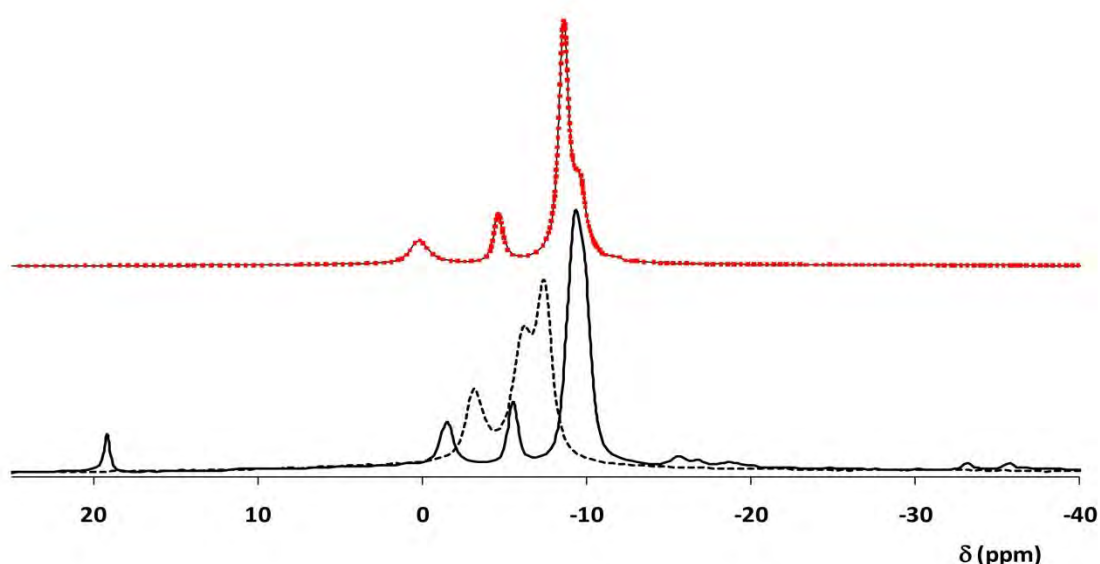


Figure 6. Top: ¹¹B{¹H}-NMR spectrum of a solution of free carborane ligand in CH₃OH. Bottom: ¹¹B{¹H}-NMR spectra of complex **A3** freshly prepared (---) and after 12 h in solution (—).

To complement the NMR spectroscopy data, the ESI-MS spectrum (Figure S4 Supporting Information) of a solution of complex **A3** in methanol after 18 hours of preparation was recorded. The molecular-ion peak of **A3** was not detected and the ionic peak that had the highest m/z value with the right isotopic distribution for a Cu complex was observed at m/z 467.3 (although in very weak intensity), which corresponds to the monomeric L_2Cu complex. The peak at m/z 403.4 (maximum intensity) corresponds to the dimeric form of the ligand $[1-CH_3-2-CO_2H-1,2-closo-C_2B_{10}H_{10}]_2$ in which two ligand units form two hydrogen bonds between themselves (calculated energy 7 kJmol^{-1} bond) as it has been reported.^[29] The peak found at m/z 157 (70.3%) corresponds to $1-CH_3-1,2-C_2B_{10}H_{11}$. The weak intensity ionic peaks at 201.1 and 191.1 correspond, respectively, to the free ligand, $[1-CH_3-2-CO_2-1,2-closo-C_2B_{10}H_{10}]^-$ and to the *nido*- $[7-CH_3-8-CO_2H-7,8-C_2B_9H_{10}]^-$ species.

The electronic UV-vis spectra of the complexes **A1-A6** are shown in Figure 7. The spectra show two characteristic bands, one in the range 380-420 nm and the other in the range 700-800 nm. The transitions have been analysed with the help of time-dependent DFT calculations and they correspond to the transfer of one electron to the empty $d_{x^2-y^2}$ orbitals of the Cu^{II} cations. Hence, there are eight d-d bands above 600 nm. The transition from the d_z^2 orbital to the $d_{x^2-y^2}$ usually appears above 1000 nm (out of the selected window). Thus, the lower energy bands of the spectra correspond to d-d transitions from the d_{xz} , d_{yz} and d_{xy} orbitals. The higher-energy transition can be assigned to LMCT bands from π orbitals of the carboxylate ligands to the empty $d_{x^2-y^2}$ orbitals of the Cu^{II} cations.

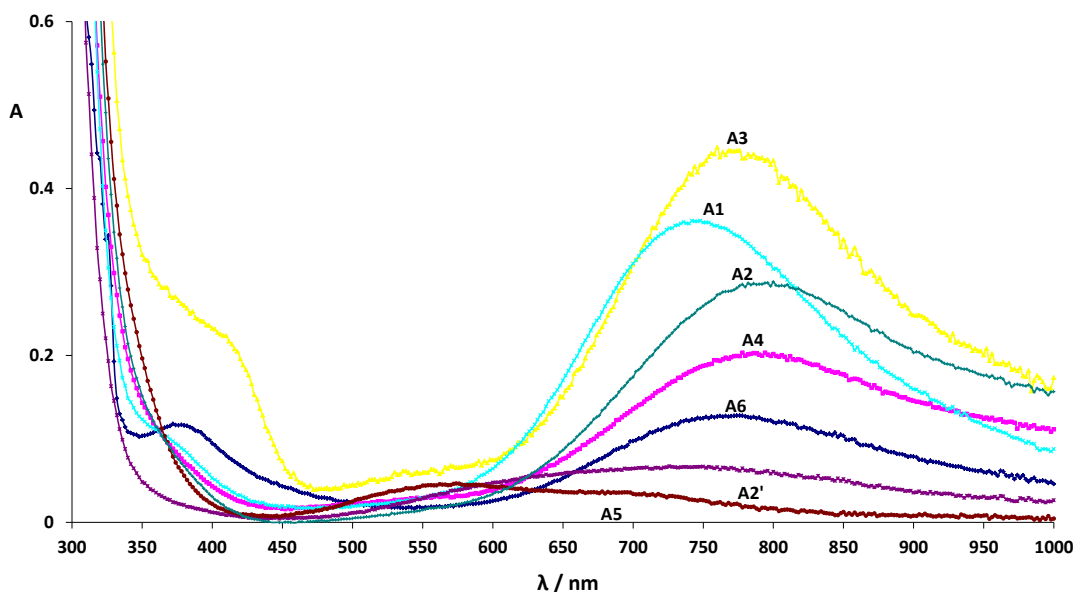
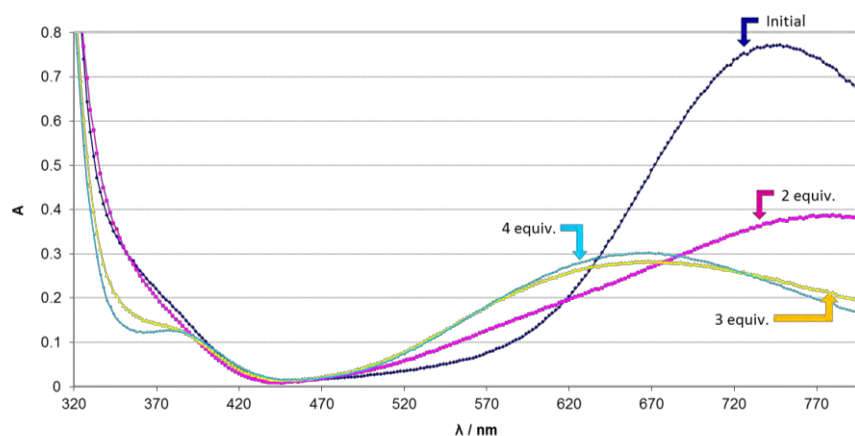


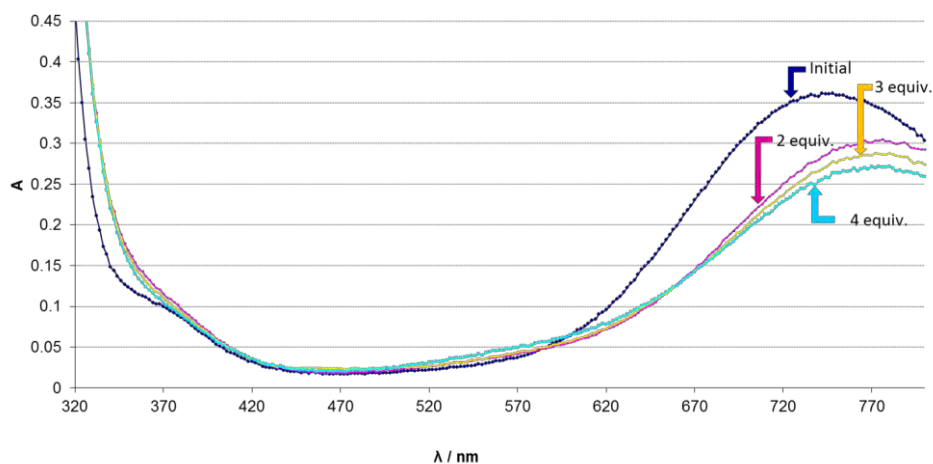
Figure 7. UV-vis spectral for complexes **A1-A6**.

As mentioned earlier in the description of the synthesis, addition of the terminal L_t pyridine-based ligands to the starting binuclear complex **A1** leads in some cases (when $L_t = \text{py}$, $p\text{-CH}_3\text{-py}$ or $o\text{-(CH}_3)_2\text{-py}$) to a mixture of compounds with different nuclearity. In order to have a better understanding of this synthetic behaviour, we have investigated the UV-visible spectral changes of the starting material upon the progressive addition of four equivalents of pyridine, p -trifluoromethylpyridine or $o\text{-(CH}_3)_2\text{-py}$ (2,6-lutidine) ligands to a solution of complex **A1** in dichloromethane. The initial UV-visible spectrum of **A1** is modified by the addition of two equivalents of pyridine (Figure 8a). The resulting spectrum exhibits a band at higher wavelengths (771 nm) with an increase in absorbance in the range 540-610 nm, probably indicating the presence of a binuclear compound together with a mononuclear one. This is confirmed by comparison with the UV-visible spectra of both pure compounds **A2** and **A2'**. The further addition of two equivalents of pyridine induces a drastic change in the UV-visible region with the disappearance of the band at 771 nm and the formation of a new absorption band at 667 nm. Slow evaporation at room temperature of the final solution leads to the “in situ” formation of the mononuclear compound **A2'**. On the other hand, the spectrum of **A1** is initially modified in an analogous way by the addition of two equivalents of $p\text{-CF}_3\text{-py}$ (with the band also shifted to higher wavelength, 768 nm, Figure 8b), but the spectrum is maintained after the successive addition of two more equivalents of ligand, which indicates the stability of the $\text{Cu}_2(\mu\text{-O}_2\text{CR})_4$ core in the presence of this terminal ligand. The spectrum of the compound obtained “in situ” is coincident with that of complex **A3** isolated from the synthetic process. Finally, for the 2,6-lutidine ligand, the addition of either two, three or four equivalents to complex **A1** leads to a shift of the maximum wavelength towards lower values thus revealing the direct formation of a monomer complex, with a spectrum fully coincident with that of the synthesized compound **A5** (Figure 8c).

a)



b)



c)

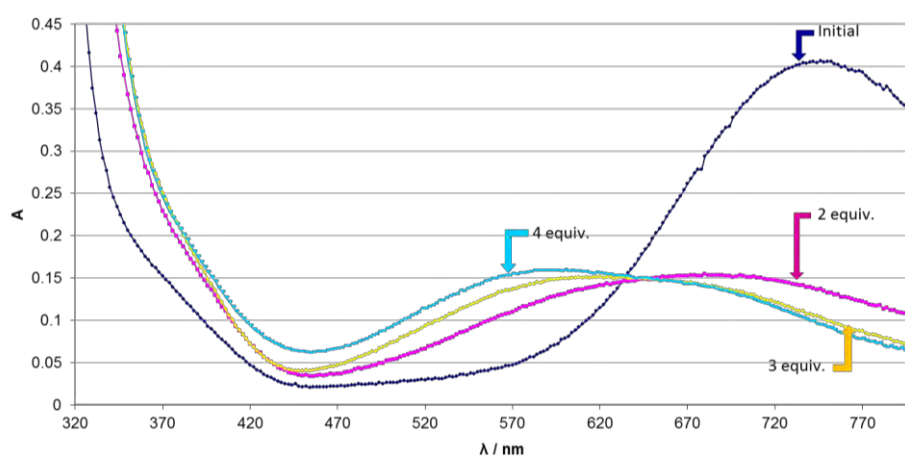


Figure 8. UV-vis spectral changes for complex **A1** obtained by the addition from one to four equivalents of a) pyridine, b) *p*-trifluoromethylpyridine and c) 2,6-lutidine

Addition of *p*-methylpyridine also breaks the paddle-wheel cage structure of the binuclear complex **A1** as confirmed by the X-ray structures obtained for the mononuclear and tetranuclear complexes **A4'** and **A4''** (see Figure S5 at the Supporting Information).

Then we investigated whether the behaviour of 2,6-lutidine (which leads directly to the rupture of the binuclear moiety and the formation of the mononuclear complex) was governed by steric or electronic (basicity) factors. An equimolar mixture of 2,6-lutidine and *p*-CF₃-py was slowly added to a solution of complex **A1** in dichloromethane and the subsequent spectral changes were followed by UV-visible spectroscopy. The shift of the maximum wavelength to lower values (as previously seen by addition of 2,6-lutidine itself) clearly demonstrated the

immediate formation of the mononuclear complex **A5**. Thus, the competition between the two pyridyl L_t ligands shows that the highly basic character of 2,6-lutidine is the key factor governing its reactivity since otherwise the coordination of the less encumbered *p*-CF₃-py would have occurred preferentially.

III.3.4. Magnetic properties

Compounds **A1**, **A3**, **A4**, and **A6** are the latest additions to the well-established family of binuclear paddle-wheel copper(II) complexes, with general formula [Cu₂(μ-O₂CR)₄L₂] in which the apical position is normally occupied by a solvent molecule or a monocoordinated ligand.^[31] Among this group of complexes, one of the best characterized compounds is [Cu₂(μ-O₂CMe)₄(H₂O)₂] that presents antiferromagnetic behaviour with a *J* value of -296 cm⁻¹.^[31b] Several magnetic studies have been performed varying the nature of such bridging molecules as well as the axial ligands (L_t).^[31a, 32] In addition, computational calculations of the exchange coupling have provided insight on the parameters that affect the interactions between the two copper centres involved, such as the electron-withdrawing power of the carboxylates or structural distortions, among others.^[33] All together, it has been established that the unpaired electron on each copper atom occupies the $d_{x^2-y^2}$ orbital and that it is oriented toward the oxygen atoms of the four carboxylate groups. Also, it is well known that the short Cu...Cu distance in the core (between 2.60 and 2.75 Å) does not significantly affect the *J* value it is, however, extremely sensitive to the electron density on the carboxylate of the bridging ligands (superexchange mechanism), where the greater the electron-donor ability of the carboxylate is, the stronger the exchange interaction appears.^[31-33]

One of the novelties of this study resides in the nature of the R group of the carboxylic ligand; in this case, carborane (R = 1-CH₃-*closo*-C₂B₁₀H₁₀). Following previous premises, a decrease of the coupling constant values with respect to the acetate analogue was already expected due to the electron-withdrawing character of the ligand 1-CH₃-2-CO₂H-1,2-*closo*-C₂B₁₀H₁₀. In addition, a variety of axial ligands “L” were used. This way, complex **A1** has two THF molecules as terminal species and compounds **A3**, **A4** and **A6** contain *p*-trifluoromethylpyridine, *p*-methylpyridine and pyrazine molecules, respectively.

In the present work, solid-state, variable-temperature (2.0-300.0 K) direct-current (dc) magnetic susceptibility data using a 1.0 T field were collected on polycrystalline samples of complexes. Their magnetic behaviours are depicted in Figure 9 and Figure S6 (see Supporting Information section) as plots of $\chi_M T$ vs T. Table 3 shows a comparison of the average dimensions in all four compounds.

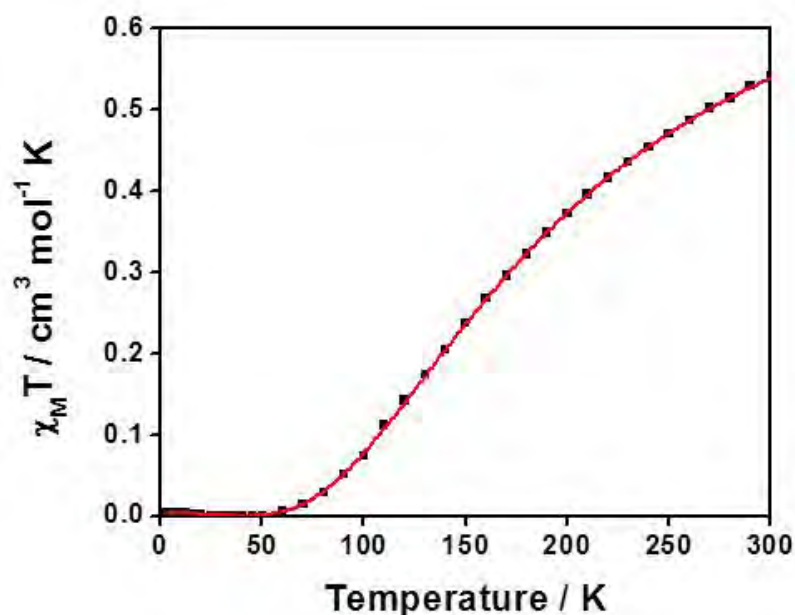


Figure 9. Fitting of the $\chi_{\text{M}}T$ vs T of **A1**, between 2.0 and 300.0 K. The experimental data is shown as black spheres and the red line corresponds to the theoretical values

Table 3. Comparison of the average structural parameters for the complexes studied ^[a].

	A1	A3	A4	A6
Cu...Cu [Å]	2.672	2.721	2.717	2.722
Cu—L [Å]^[b]	2.114	2.137	2.104	2.144
Cu—O [Å]	1.956	1.945	1.964	1.963
O—C—O [°]	127.6	127.3	126.9	127.4

[a] L = THF (**A1**), *p*-CF₃-py (**A3**), *p*-CH₃-py (**A4**) and pz (**A6**).

[b] The smallest values were taken for distances and angles.

For all species under study, the experimental curve show the typical features for strong, antiferromagnetic coupling between two Cu^{II} ions, where $\chi_{\text{M}}T$ values drop faster upon cooling. For complex **A1**, the $\chi_{\text{M}}T$ value decreases abruptly from 0.52 cm³mol⁻¹K at 300.0 K to 0.06 cm³mol⁻¹K at 50.0 K reaching a plateau that continues almost without variation until 2.0 K. In the case of complex **A6**, the $\chi_{\text{M}}T$ value at 300.0 K was 0.59 cm³mol⁻¹K decreasing towards values close to zero at the lowest temperatures. Upper values for complexes **A3** and **A4**, respectively, were 0.76 and 0.56 cm³mol⁻¹K, with the lower for both being 0.02 cm³mol⁻¹K at 2.0 K.

The experimental magnetic data were fitted using the equation for binuclear copper(II) complexes with the Hamiltonian in the form $H = -JS_1S_2$ in which the exchange parameter J is

negative for antiferromagnetic and positive for ferromagnetic interaction.^[31a] The magnetic data were fitted to the Bleaney-Bowers equation^[31b] and the best-fit parameters for all the studied molecules are shown in Table 4, where ρ is related to magnetic impurities and N_A , g , β , k and T have their usual meanings.

Table 4. Magnetic parameters for the studied molecules^[a]

	A1	A3	A4	A6
$J (\text{cm}^{-1})$	-261 ± 2	-255 ± 3	-241 ± 2	-249 ± 1
g	2.10 ± 0.01	2.19 ± 0.01	2.13 ± 0.007	2.17 ± 0.004
$\rho (\%)^{[b]}$	< 0.01	0.5	0.3	1.7
R	$2 \cdot 10^{-4}$	$8 \cdot 10^{-4}$	$4 \cdot 10^{-4}$	$2 \cdot 10^{-4}$

[a] Temperature independent parameter (TIP) = $12 \cdot 10^{-5}$, fixed for 2 Cu^{2+} . [b] ρ =paramagnetic impurity.

The parameter J is in the range of the values observed for binuclear paddle-wheel copper(II) cage structures containing acetates (above 280-300 cm^{-1}). In fact, as we expected, the lower numbers are due to the electron-withdrawing nature of the ligand 1- CH_3 -2- CO_2H -1,2-*closo*- $\text{C}_2\text{B}_{10}\text{H}_{10}$. By comparing this new addition of carborane paddle-wheel copper(II) compounds ($J \approx -250 \text{ cm}^{-1}$) with analogues^[34] (in which $R = \text{SiH}_3$, CH_3 , CF_3 and CCl_3) we may conclude that the electron-withdrawing behaviour of our compounds ($R = [1\text{-CH}_3\text{-2-CO}_2\text{-1,2-closo-C}_2\text{B}_{10}\text{H}_{10}]$) is in between of those with $R = \text{CF}_3$ and $R = \text{CCl}_3$ ^[34] (Table 5).

Table 5. Parameter J for binuclear Cu^{II} acetates R-COO^- ^[a].

R =	SiH_3	H	CH_3	CF_3	$\text{C}_2\text{B}_{10}\text{H}_{10}\text{-CH}_3$ -	CCl_3
$J (\text{cm}^{-1})$	-1000	-550	-300	-300	-250	-200

[a] The J parameters indicated in this table are average, experimental values from compounds with slightly different geometries and/or axial ligands. Data obtained from reference^[35].

Most of the published works agree with the difficulties quantifying the effect of the axial ligand L_t , being normally small and not necessarily connected to the superexchange pathway. Basicity may be also implicated in the process but in all cases, detailed analyses are needed to establish the real mechanism.^[34, 36] Here, in a qualitative way and following just the results on Table 4 we observe that the trend of J values follows, to a certain extent, the basic strength of the terminal ligands (L_t) although the differences are too small to consider this as the only factor involved. In addition, the bulky properties of the ligand seems to prevent the formation

of polymeric structures that normally appear from the intermolecular interactions between the second lone pair of each oxygen atom of the carboxylate in a paddle-wheel unit with a metal ion of another unit or through the ligand of the axial position.^[37]

EPR spectra for compound **A4** were recorded in the solid state at 300, 200 and 130 K, respectively, from 0 to 6000 Gauss (Figure 10). All three spectra show two bands at 450 and 4700 Gauss typical for a triplet state (H_{z1} and H_{\perp} , $S = 1$). The central band (around 3300 Gauss) corresponds to mononuclear Cu^{II} species. These impurities are frequent in bulky samples and easy to observe when temperature decreases. Also, at the lowest temperatures it is possible to observe the splits of the H_{z1} , due to hyperfine interactions of the unpaired electron with the two Cu^{II} nuclei. Similar spectra have been observed for other paddle-wheel binuclear Cu^{II} complexes in the past.^[38] Simulation on the EPR data at the highest temperature (Figure 11.) provided an estimated zero-field splitting parameter (D) of 0.36 cm^{-1} , which is in the range of literature values for these type of species (between 0.26 to 0.40 cm^{-1}).^[36, 38c]

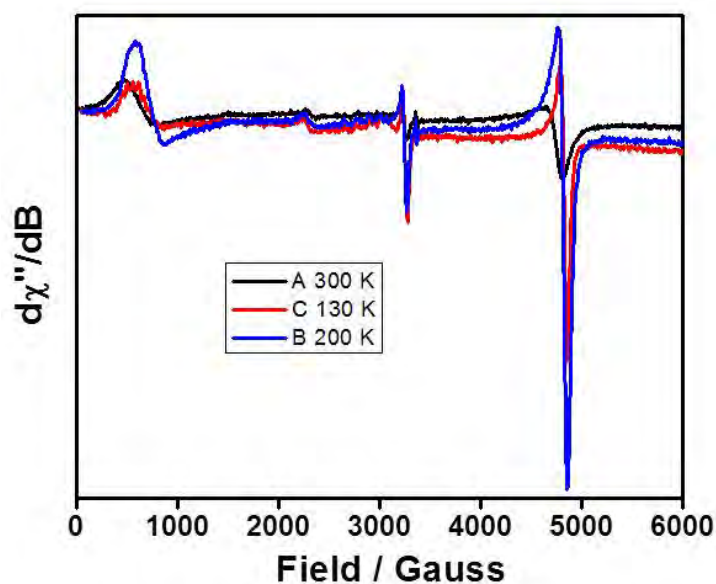


Figure 10. EPR spectra of **A4** in the solid state at A) 300 K, B) 200 K and C) 130 K, respectively.

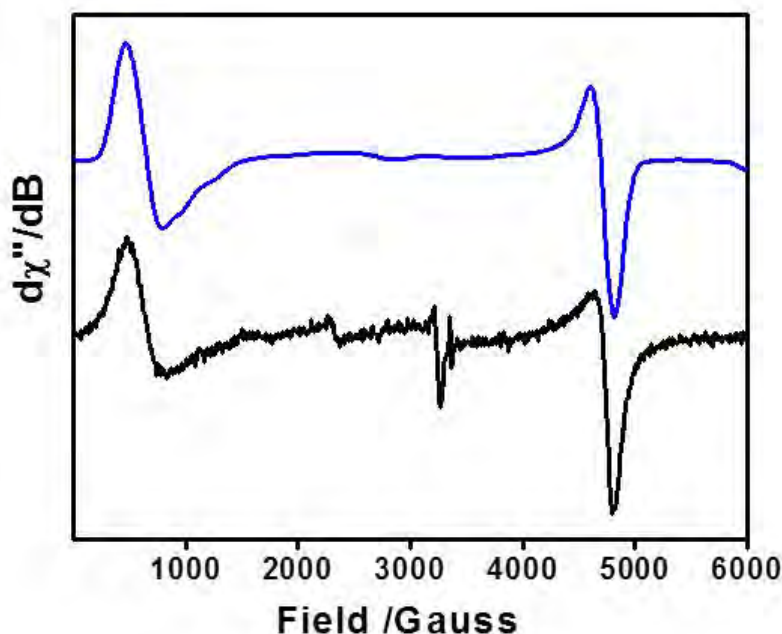


Figure 11. EPR spectra of **A4** (black) and simulation (blue) in the solid state at 300 K.

III.3.5. Electronic Structure Calculations

The electronic structure calculations have been carried out with two different goals. The first goal was to analyse the strength of the bond between the Cu^{II} cations and the axial ligands (THF, py and so on) while the second one was to calculate the exchange coupling constants for this family of copper complexes. The results are collected in Table 6. The calculated Cu-X axial bond energies confirm the stronger stability of the pyridine complexes over the THF complex, as we have seen experimentally through the UV-visible spectra. The relatively low calculated bond energies are consistent with the interaction of two fully occupied orbitals, that is, the d_z^2 orbital of the Cu^{II} cation interacting with the lone pair of the pyridine. The weakness of such axial bonds will be confirmed for the easy loss of the axial ligands in the thermal gravimetric analysis (TGA) experiments (next section). Despite the fact that the Cu-X axial interaction must be predominantly σ between the lone pair of the nitrogen of the pyridine ligand and the Cu^{II} cation, we found a correlation between the calculated energy bond value and the Hammett parameter of the substituents of the pyridine ligands. Thus, the energy bond is higher for electron-donating groups, like methyl, whereas for electron-withdrawing substituents the bond is weaker. Considering that the Hammett parameter is related with the electron density of the π system of the aromatic ring, this correlation should indicate some participation of such π system in the Cu-N bond. This participation has been confirmed by the orbital mixing between the d_{xz} copper orbital and one bonding π orbital of the axial pyridine ligand.

CHAPTER III

Concerning the calculated exchange coupling constants, the values confirm the fitted values obtained from the experimental magnetic susceptibility, indicating a relatively strong antiferromagnetic coupling. The theoretical results also confirm that the presence of methyl groups in the axial pyridine groups reduces the strength of the exchange interaction. There is not a clear correlation between the calculated J values and the Hammett parameters because the J value remains almost unchanged for the substitution of one hydrogen atom by a withdrawing CF_3 group (see Table 6).

Table 6. Calculated Cu-X axial bond energies [$\text{Kcal}\cdot\text{mol}^{-1}$] and exchange coupling constants. Experimental J values are provided for comparison.

	A1	A2	A3	A4
$E(\text{Cu-X})^{[a]}$	-9.8	-13.5	-11.7	-15.4
$J_{\text{calc}} (\text{cm}^{-1})$	-202	-204	-203	-180
$J_{\text{exp}} (\text{cm}^{-1})$	-261 ± 2	-	-255 ± 3	-241 ± 2

[a] L = THF (**A1**), py (**A2**), $p\text{-CF}_3\text{-py}$ (**A3**) and $p\text{-CH}_3\text{-py}$ (**A4**)

III.3.6. Thermal decomposition

Data obtained by TGA are compiled in Table 7. Heating **A1** to 166°C leads to a weight loss of 13% that almost certainly corresponds to two axial THF molecules. At 222° a weight loss of 41% suggests two carboranyl ligands LH and one CO_2 molecule, and a later loss of 15% corresponds to $1\text{-CH}_3\text{-1,2-closo-C}_2\text{B}_{10}\text{H}_{11}$. 32% of weight remains as residuum that corresponds to one LH and two Cu. This last residuum is found at the end of the experiments in all the samples. A similar behaviour has been observed in other binuclear paddle-wheel copper (II) complexes.^[13, 39]

Table 7. Thermal gravimetric analysis (TGA) data.

Compound	% weight loss (T [$^\circ\text{C}$])
A1	13(166); 41(222); 15(255)
A3	23(211); 34(235); 12(305)
A6	8.4(177); 50(207)
A7	19.5(168); 42(260)

For the pyridyl binuclear complexes, higher temperatures are needed to reach the loss of the axial ligands compared to **A1** (see Figure S7 at the supporting information section). In some cases, such as for complex **A7**, the first weight loss corresponds to a molecule of axial ligand together with CO₂ molecules originating from the breaking of carboranyl ligands. Later mass loss at high temperatures corresponds to carboranyl molecules, methyl groups, or CO₂ molecules arising from the rupture of these molecules.

III.4. Conclusions

A family of new mononuclear and binuclear copper(II) complexes containing the carboranylcarboxylate ligand 1-CH₃-2-CO₂H-1,2-*closo*-C₂B₁₀H₁₀, LH, have been synthesized and fully characterized by X-Ray diffraction, spectroscopic methods (IR, UV-vis, NMR, ESI-MS) as well as through thermal gravimetric analysis (TGA). Magnetics measurements of the binuclear complexes were performed showing in all cases strong antiferromagnetic interactions between the copper atoms.

Compounds **A1-A4** and **A6** display an overall geometry corresponding to a binuclear *paddle-wheel* structure where each copper ion is coordinated by four oxygen atoms one of each of the four syn,syn η¹: η¹: μ₂-carboxylate bridge and one donor atom (oxygen or nitrogen) of the different terminal ligands displaying a square pyramidal geometry. Mononuclear complex **A5** shows a square planar structure, where the copper atom is coordinated by two nitrogen atoms from two lutidine ligands and by two oxygen atoms from the two carboranylcarboxylate ligands that adopt a monodentate coordination. Finally, the X-ray structure of complex **A8** disclosed a 1D polymer chain in which, each copper ion adopt a distorted octahedral geometry coordinated by four oxygen atoms (two from two carboranylcarboxylate ligands and two from two ethanol molecules) and two pyridyl nitrogen atoms.

It was experimentally demonstrated that the electronic effects govern the reactivity toward the rupture of the binuclear structure, a conclusion that has been corroborated by electronic-structure calculations. The calculated Cu-X axial bond energies confirm a stronger interaction of the pyridyl axial ligands with the copper metal centre in comparison with the THF ligand, thus leading in some cases to the de-coordination of the carboranylcarboxylate bridging ligand and the subsequent formation of secondary products with different nuclearities.

We have also found a correlation between the calculated bond-energy value and the Hammett parameter of the substituents of the pyridine terminal ligands. Thus, the bond energy is higher for electron-donating groups, like methyl, whereas for electron-withdrawing substituents the bond is weaker. The calculated exchange coupling constants confirm the fitted values obtained from the experimental magnetic susceptibility.

Besides, the stability of the binuclear compounds was studied in different solvents observing that these compounds are stable in THF and CH₂Cl₂ whereas a partial degradation of the 1-CH₃-2-CO₂H-1,2-*closo*-C₂B₁₀H₁₀ ligand, LH, takes place in CH₃OH. The partial degradation reaction of the LH ligand is due to a nucleophilic attack, which leads to the removal of a BH²⁺ from the 1-CH₃-2-CO₂H-1,2-*closo*-C₂B₁₀H₁₀ ligand that oxidizes to B(OCH₃)₃ reducing the Cu^{II} to Cu⁰ while the *closo* cluster is transformed to *nido*.

Finally, similarities and differences between the collection of binuclear complexes presented here and the well-known, paddle-wheel copper acetate, $[\text{Cu}_2(\mu\text{-CH}_3\text{COO})_4(\text{H}_2\text{O})_2]$, have been found concluding that, although the reactivity of copper acetate with regard to the replacement of the apical H_2O or THF ligands by pyridyl ligands follows similar trends, the presence of the carboranylcarboxylate groups induces particular electronic and structural properties that establish remarkable differences with the analogous μ -acetate compounds such as their behaviour in nucleophilic solvents or their solubility.

III.5. Experimental section

III.5.1. Instrumentation and measurements

FT-IR spectra were taken in a Mattson-Galaxy Satellite FT-IR spectrophotometer containing a MKII Golden Gate Single Reflection ATR System. Elemental analyses were performed using a CHNS-O Elemental Analyser EA-1108 from Fisons. UV-Vis spectroscopy was performed on a Cary 50 Scan (Varian) UV-Vis spectrophotometer with 1 cm quartz cells or with an immersion probe of 5 mm path length. ISE-MS spectra have been performed on a Navigator LC/MS chromatograph from Thermo Quest Finnigan. NMR spectra have been recorded with a Bruker ARX 300 or a DPX 400 instrument equipped with the appropriate decoupling accessories (^1H and $^1\text{H}\{^{11}\text{B}\}$ NMR (300.13/400.13 MHz), $^{13}\text{C}\{^1\text{H}\}$ NMR (75.47/100.62 MHz) and ^{11}B and $^{11}\text{B}\{^1\text{H}\}$ NMR (96.29/128.37 MHz) spectra were recorded in d_6 -acetone, CDCl_3 and CH_3OH . Chemical shift values for ^{11}B NMR spectra were referenced to external $\text{BF}_3\leftarrow\text{OEt}_2$ and those for ^1H , $^1\text{H}\{^{11}\text{B}\}$ and $^{13}\text{C}\{^1\text{H}\}$ NMR spectra were referenced to SiMe_4 . Chemical shifts are reported in units of parts per million downfield from reference, and all coupling constants in Hz. Deconvolution of $^{11}\text{B}\{^1\text{H}\}$ spectra has been performed with the software OriginPro 8 SR0, v. 8.0724. Cyclic Voltammetric (CV) experiments were performed in a IJ-Cambria IH-660 potentiostat using a three electrode cell. A Pt (2 mm diameter) or graphite (3 mm diameter) electrodes were used as working electrode, platinum wire as auxiliary and SCE as the reference electrode. Measurements were recorded in acetonitrile solutions at scan rate of $100\text{ mV}\cdot\text{s}^{-1}$, using 0.1 M TBAH as supporting electrolyte. All cyclic voltammograms presented in this work were recorded under nitrogen atmosphere. All $E_{1/2}$ values estimated from cyclic voltammetry were calculated as the average of the oxidative and reductive peak potentials $(E_{\text{pa}}+E_{\text{pc}})/2$ at a scan rate of 100 mV/s . Thermal decomposition was performed using a Mettler Toledo TG/SDTA 851e system (25-600°) heating rate 10° min^{-1} .

X-ray structure determination: measurement of the crystals were performed on a Bruker Smart Apex CCD diffractometer using graphite-monochromated Mo $K\alpha$ radiation ($\lambda = 0.71073\text{Å}$) from an X-Ray tube. Data collection, Smart V. 5.631 (BrukerAXS 1997-02); data reduction, Saint+ Version 6.36A (Bruker AXS 2001); absorption correction, SADABS version 2.10 (Bruker AXS 2001) and structure solution and refinement, SHELXTL Version 6.14 (Bruker AXS 2000-2003).

Magnetic Susceptibility Studies: magnetic susceptibility measurements between 300 – 2 K were carried out in a SQUID magnetometer Quantum Design Magnetometer, model MPMP at the “Unitat de Mesures Magnètiques” (Universitat de Barcelona). Susceptibility measurements

were performed using a field of 1.0 T. Pascal's constants were used to estimate the diamagnetic corrections for the compound. The fit was performed by minimizing the function $R = \Sigma(\chi_{MT})_{\text{exp}} - (\chi_{MT})_{\text{calc}}]^2 / \Sigma(\chi_{MT})_{\text{exp}}]^2$.

Electronic Structure Calculations: Since a detailed description of the computational strategy adopted in this work to calculate the exchange coupling constants can be found elsewhere^[35, 40] we will only briefly sketch its most relevant aspects here. Using a phenomenological Heisenberg Hamiltonian $\hat{H} = -J\hat{S}_1 \cdot \hat{S}_2$ to describe the exchange coupling in a binuclear complex, where J is the exchange coupling constant, and S_1 and S_2 the local spins on centres 1 and 2, respectively. It has been found that, when using DFT-based wavefunctions, a reasonable estimate of the exchange coupling constants can be obtained from the energy difference between the state with highest spin, E_{HS} and the low spin wavefunction, E_{LS} (traditionally called broken-symmetry solution) obtained just flipping one of the spins through the following equation:

$$J = \frac{E_{LS} - E_{HS}}{2S_1S_2 + S_2} \quad (1)$$

This equation does not include the spin projection as the originally proposed by Noodleman et al.^[41] The presence of the self-interaction error in the exchange-correlation functional includes an unspecified amount of non-dynamic correlation energy resulting in the fact that the monodeterminantal solution corresponding to the low spin wavefunction provides an energy value close to that corresponding to the low spin state.^[35] The hybrid, DFT-based B3LYP functional^[42] has been used in all calculations as implemented in Gaussian-03,^[43] mixing the exact exchange with Becke's expression for the exchange functional^[44] and using the Lee-Yang-Parr correlation functional.^[45] The all electron triple- ζ basis set 6-311G(d,p) was employed. The calculated axial Cu-X bond energies were obtained as the difference with system with the Cu-X distance for one of the axial substituents of the molecules increased until a value of 5 Å.

III.5.2. Materials

All reagents used in the present work were obtained from Aldrich Chemical Co and were used without further purification. Reagent grade organic solvents were obtained from SDS and high purity de-ionized water was obtained by passing distilled water through a nano-pure Mili-Q water purification system. 1-CH₃-1,2-closo-C₂B₁₀H₁₁ was purchased from Katchem.

III.5.3. Preparations

All synthetic manipulations were routinely performed under ambient conditions.

Synthesis of 1-CH₃-2-CO₂H-1,2-closo-C₂B₁₀H₁₀, LH.

The 1-CH₃-2-CO₂H-1,2-closo-C₂B₁₀H₁₀ ligand was prepared according to literature procedures^[46] with small modifications.

To a stirred solution of 1-CH₃-1,2-closo-C₂B₁₀H₁₁ (1.08 g, 6.84 mmol) in diethyl ether (12 ml) at 0 °C was added dropwise 1.1 equivalents of n-BuLi (4.7 mL, 7.52 mmol). The solution was allowed to warm to room temperature, at which point dry ice was bubbled through the solution for about 20–30 min. The milky solution thus formed was hydrolysed with 2M HCl and transferred to a separating funnel. The ethereal layer plus ethereal washings of the aqueous layer were dried over MgSO₄ and then filtered. Removal of solvent afforded a white solid which was recrystallized in dichloromethane to obtain a white microcrystalline solid of LH. Yield: 1.30 g, 94%. ¹H{¹¹B} NMR (400.13 MHz, CDCl₃, 25 °C): δ= 7.18 (s; COOH), 2.39 (br s; B-H), 2.19 ppm (br s; B-H), 2.17 (s; CH₃) ppm. ¹³C{¹H} NMR (100.62 MHz, CDCl₃, 25 °C): δ= 165.10 (COOH), 75.91 (C_c), 71.62 (C_c), 24.78 (CH₃) ppm. ¹¹B{¹H} NMR (128.37 MHz, CDCl₃, 25 °C): δ= 0.6 (¹J(B,H)= 142 Hz, 1B), 5.5 (¹J(B,H)= 153 Hz, 1B), (-9.5 (¹J(B,H)= 151 Hz), -10.4 ppm), 8B. IR: $\bar{\nu}$ = 721ν(B-C), 903, 1011, 1270, 1409 ν(COO⁻)_{sim}, 1721ν(COO⁻)_{as}, 2531-2649 ν (B-H), 2845, 2971 cm⁻¹. Elemental analysis calcd (%) for C₄H₁₄O₂B₁₀: C 23.75, H 6.98; found: C 23.70, H 6.80.

Synthesis of [Cu₂(1-CH₃-2-CO₂-1,2-closo-C₂B₁₀H₁₀)₄(THF)₂], A1. 1-CH₃-2-CO₂H-1,2-closo-C₂B₁₀H₁₀, LH, (0.2 g, 0.99 mmols) in ethanol (1.5 mL) was neutralized with a 0.1 M aqueous NaOH solution with phenolphthalein as indicator at room temperature and immediately mixed with a solution of CuSO₄·5H₂O (0.12 g, 0.489 mmols) in water (1.5 mL). The temperature of the blue solution gradually rose to 30 °C. After 2h the solvent was removed under vacuum, the solid residue was redissolved in THF (30 mL) and again dried under vacuum. The last process was repeated three times. The obtained residue was once more dissolved in THF, the solution was filtrated to remove solid Na₂SO₄ and the solvent was again removed under vacuum. The resulting solid was recrystallized in CH₂Cl₂. Yield: 0.24 g (88%). ¹H{¹¹B} NMR (300.13 MHz, acetone-d₆, 25 °C): δ= 3.85 (s; O-CH₂), 2.93 (br s; B-H), 1.90 ppm (s; CH₂). ¹³C{¹H} NMR (75.47 MHz, acetone-d₆, 25 °C): δ= 113.14 (COO⁻), 92.48 (C_c), 78.61 (C_c), 69.44 (O-CH₂), 25.72 (CH₂), 24.33 ppm (CH₃). ¹¹B{¹H} NMR (96.29 MHz, acetone-d₆, 25 °C): δ= -1.6 (¹J(B,H)= 150 Hz, 1B), -4.3 (1B), -5.7 (1B), -6.9 ppm (¹J(B,H)= 130 Hz, 7B). IR: $\bar{\nu}$ = 727, 783, 914, 1038, 1386, 1443, 1621, 1665, 2588 cm⁻¹. UV-Vis (CH₂Cl₂, 1.10⁻³M) λ_{max} (ε)= 742 nm (361 M⁻¹cm⁻¹). Elemental analysis calcd (%) for C₂₄H₆₈O₈B₄₀Cu₂·0.3THF: C 27.57, H 6.46; found: C 27.77, H 6.39.

Synthesis of $[\text{Cu}_2(1\text{-CH}_3\text{-2-CO}_2\text{-1,2-closo-C}_2\text{B}_{10}\text{H}_{10})_4(\text{H}_2\text{O})_2]$, **A1'.** LH (0.069 g, 0.343 mmols) dissolved in water (3 mL) was mixed with a suspension of $\text{CuCO}_3\cdot\text{Cu}(\text{OH})_2$ (0.019 g, 0.0859 mmols) in water (2.5 mL). The resulting mixture was stirred for 3 h and the temperature was kept at 40°C. Afterwards the blue solution was filtered and the solvent was removed under vacuum. The resulting solid was recrystallized in diethyl ether. Yield: 0.032 (39%). Elemental analysis calcd (%) for $\text{C}_{16}\text{H}_{56}\text{O}_{10}\text{B}_{40}\text{Cu}_2$: C 19.85, H 5.83; found: C 19.81, H 5.80

Synthesis of $[\text{Cu}_2(1\text{-CH}_3\text{-2-CO}_2\text{-1,2-closo-C}_2\text{B}_{10}\text{H}_{10})_4(\text{py})_2]$, **A2.** A solution of pyridine (9.16 μL , 0.114 mmols) in CH_2Cl_2 (2.5 ml) was added to a solution of **A1** (0.060 g, 0.056 mmols) in CH_2Cl_2 (12 mL). The resulting blue solution was stirred for 20 min at room temperature. Afterwards the solution was concentrated to 6 mL and a blue solid was precipitated upon the addition of pentane. The resulting solid was recrystallized by slow diffusion of pentane into a diethyl ether solution. After several days, air-stable, green crystals of **A2** suitable for X-ray diffraction analysis were obtained, together with other blue crystals, that correspond to the monomer compound $[\text{Cu}(1\text{-CH}_3\text{-2-CO}_2\text{-1,2-closo-C}_2\text{B}_{10}\text{H}_{10})_2(\text{py})_2(\text{H}_2\text{O})]$, **A2'**. Yield of **A2**: 0.050 g (80%). $^1\text{H}\{^{11}\text{B}\}$ NMR (300.13 MHz, CDCl_3 , 25°C): δ = 24.92 (br s, 3H; $\text{C}_{\text{aryl}}\text{-H}$), 14.72 (br s, 2H; $\text{C}_{\text{aryl}}\text{-H}$), 3.87 (b s, 1H; B-H), 3.30, 3.05 (br s, 6H; B-H), 2.52, 2.44, 2.34, 2.29 (br s, 3H; B-H), 2.19 ppm (s, 3H; CH_3). $^{13}\text{C}\{^1\text{H}\}$ NMR (75.47 MHz, CDCl_3 , 25°C): δ = 137.38 (s; N- C_{aryl}), 126.50 (s; C_{aryl}), 126.22 (s; C_{aryl}), 119.92 (COO^-), 22.85 ppm (CH_3). $^{11}\text{B}\{^1\text{H}\}$ NMR (96.29 MHz, CDCl_3 , 25°C): δ = 1.9 ($^1J(\text{B,H})=108$ Hz), -6.6 ($^1J(\text{B,H})=105$ Hz), -8.4 ($^1J(\text{B,H})=239$ Hz), -9.2 ppm ($^1J(\text{B,H})=117$ Hz). IR: $\bar{\nu}$ = 694, 781, 1366, 1448, 1449, 1607, 1661, 2578 cm^{-1} . UV-Vis (CH_2Cl_2 , 1.10^{-3}M) λ_{max} (ϵ): 796 nm (287 $\text{M}^{-1}\text{cm}^{-1}$). Elemental analysis calcd (%) for $\text{C}_{26}\text{H}_{62}\text{O}_8\text{B}_{40}\text{Cu}_2\text{N}_2$: C 28.60, H 5.73, N 2.57; found: C 28.40, H 5.20, N 2.50.

Compound A2': $^1\text{H}\{^{11}\text{B}\}$ NMR (400.13 MHz, CDCl_3 , 25°C): δ = 3.39 (br s; B-H), 2.93 (br s; B-H), 2.17 ppm (s; CH_3). $^{13}\text{C}\{^1\text{H}\}$ NMR (75.47 MHz, CDCl_3 , 25°C): δ = 24.29 ppm (CH_3). $^{11}\text{B}\{^1\text{H}\}$ NMR (128.37 MHz, CDCl_3 , 25°C): δ = -1.7 ($^1J(\text{B,H})=145$ Hz; 1B), -6.4 ppm ($^1J(\text{B,H})=137$ Hz; 9B).

Synthesis of $[\text{Cu}_2(1\text{-CH}_3\text{-2-CO}_2\text{-1,2-closo-C}_2\text{B}_{10}\text{H}_{10})_4(\text{p-CF}_3\text{-Py})_2]$, **A3.** This compound was prepared following a method analogous to that described for **A2** starting from compound **A1** (0.060 g, 0.056 mmols) and 4-trifluoromethylpyridine (13.4 μL , 0.112 mmols) to afford air-stable green crystals of **A3**, suitable for X-ray diffraction analysis. Yield: 0.034 g (50%). $^1\text{H}\{^{11}\text{B}\}$ NMR (300.13 MHz, CDCl_3 , 25°C): δ = 3.98 (br s; 1H, B-H), 3.31 (br s; 1H, B-H), 3.15 (br s; 4H, B-H), 2.99 (br s; 4H, B-H), 2.23 ppm (s; CH_3). $^{13}\text{C}\{^1\text{H}\}$ NMR (75.47 MHz, MeOH, 25°C): δ = 161.27 (s; N- C_{aryl}), 151.01 (s; C_{aryl}), 146.48 (s; C_{aryl}), 119.91 (COO^-), 82.36 (C_c), 76.28 (C_c), 24.17 ppm (CH_3). $^{11}\text{B}\{^1\text{H}\}$ NMR (96.29 MHz, MeOH, 25°C): δ = -3.1 ($^1J(\text{B,H})=146$ Hz, 2B), -6.2 ($^1J(\text{B,H})=128$ Hz, 4B),

CHAPTER III

-7.3 ppm ($^1J(\text{B,H})=123$ Hz, 4B). IR: $\bar{\nu}=671, 832, 1065, 1115, 1323, 1384, 1418, 1666, 2583$ cm $^{-1}$. UV-Vis (CH $_2$ Cl $_2$, 1.10 $^{-3}$ M) $\lambda_{\text{max}}(\epsilon): 768$ nm (446 M $^{-1}$ cm $^{-1}$). Elemental analysis calcd (%) for C $_{28}$ H $_{60}$ O $_8$ B $_{40}$ N $_2$ F $_6$ Cu $_2$: C 27.43, H 4.93, N 2.28; found: C 27.41, H 4.75, N 2.52.

Synthesis of [Cu $_2$ (1-CH $_3$ -2-CO $_2$ -1,2-closo-C $_2$ B $_{10}$ H $_{10}$) $_4$ (*p*-CH $_3$ -Py) $_2$], A4. This compound was prepared in a similar manner to the method described for **A2** starting from compound **A1** (0.060 g, 0.056 mmols) and 4-methylpyridine (10.8 μ L, 0.112 mmols) to afford blue, air-stable crystals of **A4** after several days, together with other crystals corresponding to a monomer (**A4'**) and a tetramer (**A4''**) compounds. Yield of **A4**: 0.034 g (50%). $^1\text{H}\{^{11}\text{B}\}$ NMR (300.13 MHz, CDCl $_3$, 25 $^\circ$ C): $\delta=4.07$ (br s; B-H), 3.25 (br s; B-H), 3.11 (br s; B-H), 2.19 (s; CH $_3$), 1.26 ppm (s; CH $_3$). $^{13}\text{C}\{^1\text{H}\}$ NMR (75.47 MHz, CDCl $_3$, 25 $^\circ$ C): $\delta=29.98$ (CH $_3$), 24.55 ppm (CH $_3$). $^{11}\text{B}\{^1\text{H}\}$ NMR (128.37, CDCl $_3$, 25 $^\circ$ C): $\delta=-3.7$ ($^1J(\text{B,H})=133$ Hz, 3B), -5.3 (br s, 1B), -7.2 ppm ($^1J(\text{B,H})=139$ Hz, 6B). IR: $\bar{\nu}=725, 782, 1384, 1444, 1624, 1666, 2584, 2821, 2920$ cm $^{-1}$. UV-Vis (CH $_2$ Cl $_2$, 1.10 $^{-3}$ M) $\lambda_{\text{max}}(\epsilon): 778$ nm (203 M $^{-1}$ cm $^{-1}$).

Synthesis of [Cu(1-CH $_3$ -2-CO $_2$ -1,2-closo-C $_2$ B $_{10}$ H $_{10}$) $_2$ (*o*-(CH $_3$) $_2$ -py) $_2$], A5. This compound was prepared analogously to the method described for **A3** starting from compound **A1** (0.060 g, 0.056 mmols) and 2,6-lutidine (21.86 μ L, 0.186 mmols) to afford blue-violet air stable crystals of **A5**. Yield: 0.54 g (85%). $^1\text{H}\{^{11}\text{B}\}$ NMR (400.13 MHz, CDCl $_3$, 25 $^\circ$ C): $\delta=3.82$ (br s; B-H), 3.50 (br s; B-H), 3.09 (br s; B-H), 2.75 (br s; B-H), 1.26 (s; CH $_3$), 0.88-0.84 ppm (m; CH $_3$). $^{13}\text{C}\{^1\text{H}\}$ NMR (75.47 MHz, MeOH, 25 $^\circ$ C): $\delta=23.70$ ppm (CH $_3$). $^{11}\text{B}\{^1\text{H}\}$ NMR (128.37 MHz, MeOH, 25 $^\circ$ C): $\delta=-4.3$ (9B), -7.4 ppm (11B). IR: $\bar{\nu}=724, 780, 1331, 1472, 1611, 1659, 2580$ cm $^{-1}$. UV-Vis (CH $_2$ Cl $_2$, 1.10 $^{-3}$ M) $\lambda_{\text{max}}(\epsilon): 574$ nm (50 M $^{-1}$ cm $^{-1}$). Elemental analysis calcd (%) for C $_{22}$ H $_{44}$ O $_4$ B $_{20}$ N $_2$ Cu: C 38.80, H 6.52, N 4.12; found: C 38.60, H 6.34, N 3.85.

Synthesis of [Cu $_2$ (1-CH $_3$ -2-CO $_2$ -1,2-closo-C $_2$ B $_{10}$ H $_{10}$) $_4$ (pz) $_2$], A6 . A solution of pyrazine (0.009 g, 0.111 mmols) in CH $_2$ Cl $_2$ (3 ml) was added to a solution of **A1** (0.060 g, 0.056 mmols) in CH $_2$ Cl $_2$ (30 mL). The resulting solution was stirred for 20 minutes at room temperature. An unidentified blue solid was formed which was removed by filtration. The solution was then left to slowly evaporate at room temperature. After several days, air-stable, green-blue crystals of **A6**, suitable for X-ray diffraction analysis, were obtained. Yield: 0.49g (40%). $^{11}\text{B}\{^1\text{H}\}$ NMR (96.29 MHz, MeOH, 25 $^\circ$ C): $\delta=-2.7$ ($^1J(\text{B,H})=144$ Hz, 2B), -6.0 ($^1J(\text{B,H})=79$ Hz, 2B) and -7.2 ppm ($^1J(\text{B,H})=129$ Hz, 6B). IR: $\bar{\nu}=727, 780, 1150, 1355, 1444, 1672, 2583$ cm $^{-1}$. UV-Vis (diethyl ether, 1.10 $^{-3}$ M) $\lambda_{\text{max}}(\epsilon): 372$ nm (117 M $^{-1}$ cm $^{-1}$), 774 nm (127 M $^{-1}$ cm $^{-1}$). Elemental analysis calcd (%) for C $_{20}$ H $_{60}$ O $_8$ B $_{40}$ N $_4$ Cu \cdot 1.4 THF: C 29.80, H 6.01, N 4.70; found: C 29.69, H 6.27, N 4.45.

Synthesis of $[\text{Cu}_2(1\text{-CH}_3\text{-2-CO}_2\text{-1,2-closo-C}_2\text{B}_{10}\text{H}_{10})_4(4,4'\text{-bpy})_2]$, **A7.** This compound was prepared in an analogous manner to that described for **A3** starting from compound **A1** (0.060 g, 0.056 mmols) and 4,4'-bipyridine (0.018 g, 0.113 mmols) to afford a blue solid. Yield: 0.031 g (45%). IR: $\bar{\nu}$ = 726, 814, 1222, 1340, 1386, 1650, 1669, 2579 cm^{-1} . Elemental analysis calcd (%) for $\text{C}_{36}\text{H}_{68}\text{O}_8\text{B}_{40}\text{N}_4\text{Cu}_2 \cdot 0.5\text{CH}_2\text{Cl}_2$: C 34.06, H 5.40, N 4.35; found: C 33.86, H 5.49, N 4.22.

Synthesis of $[\text{Cu}(1\text{-CH}_3\text{-2-CO}_2\text{-1,2-closo-C}_2\text{B}_{10}\text{H}_{10})_2(4,4'\text{-bpy})(\text{EtOH})_2]$, **A8.** Addition of 0.093g (0.058 mmols) of 4,4'-bipyridine to a solution of 0.063 g (0.058 mmols) of **A1** in CH_2Cl_2 quickly generates a blue precipitate. After filtering and drying the sample, the reaction yield is 0.044 g (69%) but no crystals suitable for X-ray analysis are obtained by this method due to the insolubility of the product. Using an H-tube with 0.048 g (0.044 mmol) of **A1** dissolved in a few millilitres of ethanol in one side, 0.007g (0.044 mmol) of 4,4'-bipyridine dissolved in few millilitres of ethanol on the other side, and filling the H-tube with ethanol blue crystals of **A8** were grown after a few weeks. IR: $\bar{\nu}$ = 725, 783, 812, 1222, 1386, 1611, 1665, 2581 cm^{-1} .

III.6. References

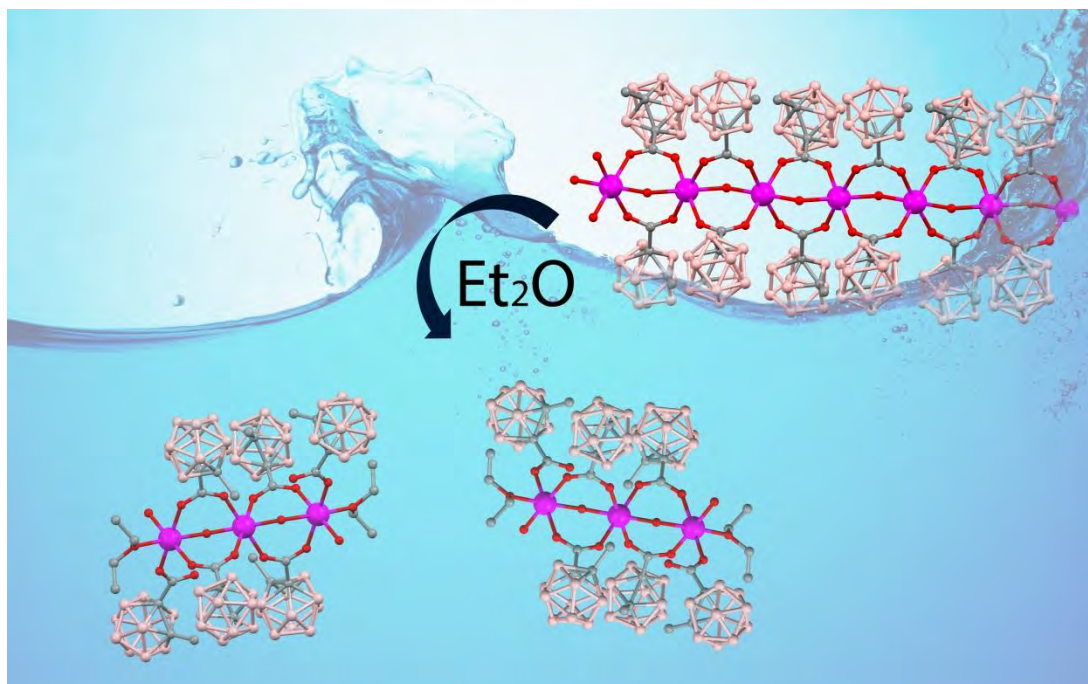
- [1] a) A. L. Briseno, J. Aizenberg, Y-J. Han, R. A. Penkala, H. Moon, A. J. Lovinger, C. Kloc, Z. Bao, *J. Am. Chem. Soc.*, 2005, 127, 12164 ; b) V. C. Sundar, J. Zaumseil, V. Podzorov, E. Menard, R. L. Willett, T. Someya, M. E. Gershenson, J. A. Rogers, *Science*, 2004, 303, 1644 ; c) H. E. Katz, C. Kloc, V. Sundar, J. Zaumseil, A. L. Briseno, Z. Bao, *J. Mater. Res*, 2004, 19, 1995 ; d) H. Z. Chen, M. M. Ling, X. Mo, M. M. Shi, M. Wang, Z. Bao, *Chem. Mater.*, 2007, 19, 816
- [2] G. A. Timco, S. Carretta, F. Troiani, F. Tuna, R. J. Pritchard, C. A. Muryn, E. J. L. McInnes, A. Ghirri, A. Candini, P. Santini, G. Amoretti, M. Affronte, E. P. Winpenny, *Nat. Nanotechnol.*, 2009, 4, 173
- [3] a) S. S.-Y. Chui, S. M.-F. Lo, J. P. H. Charmant, A. G. Orpen, I. D. Williams, *Science* 1999, 283, 1148 ; b) M. Eddaoudi, J. Kim, N. Rosi, D. Vodak, J. Wachter, M. O Keeffe, O. M. Yaghi, *Science*, 2002, 295, 469
- [4] O. K. Farha, A. M. Spokoyny, K. L. Mulfort, M. F. Hawthorne, C. A. Mirkin, J. T. Hupp, *J. Am. Chem. Soc.*, 2007, 129, 12680
- [5] a) M. F. Hawthorne, *Advances in Boron Chemistry*, The Royal Society of Chemistry, Cornwall, U.K, 1997; b) R. N. Grimes, *Carboranes*, Academic Press, New York, 1970, 54.
- [6] a) H. Kimura, K. Okita, M. Ichitani, T. Sugimoto, S. Kuroki, I. Ando, *Chem. Mater.*, 2003, 15, 355 ; b) M. K. Kolel-Vetil, T. M. Keller, *J. Polym. Sci. A*, 2006, 44, 147 ; c) A. González-Campo, B. Boury, F. Teixidor, R. Nuñez, *Chem. Mater.*, 2006, 18, 4344 ; d) E. Hao, B. Fabre, F. R. Fronczek, M. G. H. Vicente, *Chem. Mater.*, 2007, 19, 6195 ; e) A. M. Spokoyny, O. K. Farha, K. L. Mulfort, J. T. Hupp, C. A. Mirkin, *Inorg. Chim. Acta*, 2010, 364, 266.
- [7] a) F. Teixidor, R. Nuñez, C. Viñas, R. Sillanpää, R. Kivekäs, *Angew. Chem. Int. Ed.*, 2000, 112, 4460 ; b) F. Teixidor, R. Nuñez, C. Viñas, R. Sillanpää, R. Kivekäs, *Angew. Chem. Int. Ed.*, 2000, 39, 4290 ; c) R. Nuñez, P. Farrás, F. Teixidor, C. Viñas, R. Sillanpää, R. Kivekäs, *Angew. Chem.*, 2006, 118, 1292 ; d) R. Nuñez, P. Farrás, F. Teixidor, C. Viñas, R. Sillanpää, R. Kivekäs, *Angew. Chem. Int. Ed.*, 2006, 45, 1270 ; e) F. Teixidor, G. Barbera, A. Vaca, R. Kivekäs, R. Sillanpää, *J. Am. Chem. Soc.*, 2005, 127, 10158
- [8] a) M. F. Hawthorne, *Angew. Chem.*, 1993, 105, 997 ; b) M. F. Hawthorne, *Angew. Chem. Int. Ed. Engl.* , 1993, 32, 950 ; c) A. H. Soloway, W. Tjarks, B. A. Barnum, F-G. Rong, R. F. Barth, I. M. Codogni, J. G. Wilson, *Chem. Rev.* , 1998, 98, 1515 ; d) J. F. Valliant, K. J. Guenther, A. S. King, P. Morel, P. Schaffer, O. O. Sogbein, K. A. Stephenson, *Coord. Chem. Rev.* , 2002, 232, 173 ; e) I. B. Sivaev, V. Bregadze, S. Sjöberg, *Research and Development in Neutron Capture Therapy*, (Eds.: W. Sauerwein, R. Moss, A. Wittig) Monduzzi Editore, Bologna, 2002, 19 -23; f) P. Cigler, M. Kozisek, P. Rezáčová, J. Brynda, Z. Otwinowski, J. Pokorná, J. Plešek, B. Grüner, L. Dolecková-Maresová, M. Mása, *Proc. Natl. Acad. Sci. USA*, 2005, 102, 15394 ; g) R. Julius, O. Farha, J. Chiang, L. Perry, M. F. Hawthorne, *Proc. Natl. Acad. Sci. USA* 2007, 104, 4808
- [9] K. Kokado, Y. Chujo, *Macromolecules*, 2009, 42, 1418
- [10] a) F. Teixidor, C. Viñas, *Sci. Synth.*, 2005, 6, 1235; b) V. I. Bregadze, *Chem. Rev.*, 1992, 92, 209
- [11] a) R. B. King, *Chem. Rev.*, 2001, 101, 1119 ; b) J. Llop, C. Masalles, C. Viñas, F. Teixidor, R. Sillanpää, R. Kivekäs, *Dalton Trans.*, 2003, 556 ; c) H. Yao, M. Sabat, R. N. Grimes, F. F. de Biani, P. Zanello, *Angew. Chem.* , 2003, 115, 1032 ; d) H. Yao, M. Sabat, R. N. Grimes, F. F. de Biani, P. Zanello, *Angew. Chem. Int. Ed.* , 2003, 42, 1002 ; e) F. Teixidor, C. Viñas, A. Demonceau, R. Nuñez, *Pure Appl. Chem.* , 2003, 75, 1305 ; f) A. I. Stoica, C. Viñas, F. Teixidor,

- Chem. Commun.*, 2009, 4988 ; g) L. Schwartz, L. Eriksson, R. Lomoth, F. Teixidor, C. Viñas, S. Ott, *Dalton Trans.*, 2008, 2379 ; h) A.-I. Stoica, C. Viñas, F. Teixidor, *Chem. Commun.*, 2008, 6492
- [12] a) R. N. Grimes, *Angew. Chem.*, 1993, 105, 1350 ; b) R. N. Grimes, *Angew. Chem. Int. Ed. Engl.*, 1993, 32, 1289 ; c) M. A. Fox, A. K. Hughes, *Coord. Chem. Rev.*, 2004, 248, 457 ; d) H. Jude, H. Disteldorf, S. Fischer, T. Wedge, A. M. Hawkrige, A. M. Arif, M. F. Hawthorne, D. C. Muddiman, P. J. Stang, *J. Am. Chem. Soc.*, 2005, 127, 12131 ; e) A. V. Puga, F. Teixidor, R. Kivekäs, R. Sillanpää, C. Viñas, *Chem. Eur. J.*, 2009, 15, 9764
- [13] O. Kriz, A. L. Rheingold, M. Y. Shang, T. P. Fehlner, *Inorganic Chemistry*, 1994, 33, 3777.
- [14] a) Y. B. Koh, G. G. Cristoph, *Inorg. Chem.*, 1979, 18, 1122; b) M. Bukowska-Stryewska, J. Skoweranda, A. Tosik, *Acta Cryst.*, 1982, B38, 2904 ; c) M. Melník, *Coord. Chem. Rev.*, 1982, 42, 259; d) V. M. Rao, D. N. Satharayana, H. Manohar, *Dalton Transactions*, 1983, 2167.
- [15] a) M. Cavicchioli, A. C. Massabni, L. R. Guilherme, *Transition Metal Chemistry*, 2007, 355; b) R. C. Mehrotra, R. Bohra, *Metal Carboxylates*, Academic Press, New York, 1983, ; c) L. P. Battaglia, A. B. Corradi, L. Menabue, *J. Chem. Soc., Dalton Trans.*, 1986, 1653.
- [16] W. D. Phillips, H. C. Miller, E. L. J. Muetterties, *J. Am. Chem. Soc.*, 1959, 81, 4496.
- [17] a) Shu-Ting Wu, La-Sheng Long, Rong-Bin Huang, L.-S. Zheng, *Crystal Growth & Design*, 2007, 7, 1746; b) T. Liu, *Jiegou Huaxue (Chin. J. Struct. Chem.)* 2010, 29, 195.
- [18] a) L. A. Leites, *Chem. Rev.*, 1992, 92, 279 ; b) A. Laromaine, F. Teixidor, R. Kivekäs, R. Sillanpää, M. Arca, V. Lippolis, E. Crespo, C. Viñas, *Dalton Trans.*, 2006, 5240
- [19] R. C. Mehrotra, R. Bohra, *Metal Carboxylates*, Academic, New York, 1983, 396.
- [20] L. J. Todd, A. R. Siedle, *Prog. Nucl. Magn. Reson. Spectrosc.*, 1979, 13, 87
- [21] a) F. Teixidor, C. Viñas, *Sci. Synth.*, 2005, 6, 1235; b) V. I. Bregadze, *Chem. Rev.*, 1992, 92, 209
- [22] a) P. M. Garrett, F. N. Tebbe, M. F. Hawthorne, *J. Am. Chem. Soc.*, 1964, 86, 5016 ; b) R. A. Wiesboeck, M. F. Hawthorne, *J. Am. Chem. Soc.*, 1964, 86, 1642 ; c) M. F. Hawthorne, D. C. Young, P. M. Garrett, D. A. Owen, S. G. Schwerin, F. N. Tebbe, P. M. Wegner, *J. Am. Chem. Soc.*, 1968, 90, 862
- [23] a) L. I. Zakharkin, U. N. Kalinin, *Tetrahedron Lett.*, 1965, 6, 407; b) L. I. Zakharkin, V. S. Kirillova, *Izv. Akad. Nauk SSSR Ser. Khim.*, 1975, 11, 2596; c) Y. Taoda, T. Sawabe, Y. Endo, K. Yamaguchi, S. Fujii, H. Kagechika, *Chem. Commun.*, 2008, 2049
- [24] a) M. A. Fox, J. A. H. MacBride, K. Wade, *Polyhedron*, 1997, 16, 2499 ; b) M. A. Fox, K. Wade, *Polyhedron* 1997, 16, 2517 ; c) J. Yoo, J. W. Hwang, Y. Do, *Inorg. Chem.*, 2001, 40, 568 ; d) M. A. Fox, W. G. Gill, P. L. Herbertson, J. A. H. MacBride, K. Wade, *Polyhedron*, 1996, 15, 565
- [25] M. G. Davidson, M. A. Fox, T. G. Hibbert, J. A. K. Howard, A. Mackinnon, I. S. Neretin, K. Wade, *Chem. Commun.*, 1999, 1649.
- [26] H. Nöth, B. Wrackmeyer, *NMR Basic Principles and Progress*, Vol. 14, (Eds.: P. Diehl, E. Fluck, R. Kosfeld), Springer, Berlin, 1978,
- [27] G. P. Van der Keler, J. E. DeMoor, *J. Organomet. Chem.*, 1966, 6, 235.
- [28] W. D. Phillips, H. C. Miller, E. L. J. Muetterties, *J. Am. Chem. Soc.*, 1959, 81, 4496
- [29] a) T. P. Onak, H. Landesman, R. E. Williams, I. Shapiro, *J. Phys. Chem.*, 1959, 63, 1533 ; b) K. M. Harmon, F. E. Cummings, *J. Am. Chem. Soc.*, 1962, 84, 1751.
- [30] J. A. Hirsch, *Top Stereochem*, 1967, 1, 199.

CHAPTER III

- [31] a) M. Yamanaka, H. Uekusa, S. Ohba, Y. Saito, S. Iwata, *Acta Crystallogr. B*, 1991, 47, 344 ;
b) F. Sapiña, M. Burgos, E. Escrivá, J-V. Folgado, D. Beltrán, *Inorg. Chim. Acta* 1994, 216, 185
- [32] a) H.G. Guedel, A. Stebler, A. Furrer, *Inorg. Chem.*, 1979, 18, 1021 ; b) O. Kahn, *Molecular Magnetism*, VCH, Weinheim, 1993,
- [33] M. Melník, *Coord. Chem. Rev.*, 1981, 36, 1.
- [34] A. Rodríguez-Forteza, P. Alemany, S. Alvarez, E. Ruiz, *Chem. Eur. J.*, 2001, 7, 627
- [35] E. Ruiz, S. Alvarez, J. Cano, V. J. Polo, *J. Chem. Phys.*, 2005, 123, 164110.
- [36] R. Cejudo, G. Alzuet, J. Borrás, M. Liu-González, F. Sanz-Ruiz, *Polyhedron*, 2002, 21, 1057
- [37] F. P. W. Agterberg, H. A. J. Provó Kluit, W. L. Driessen, H. Oevering, W. Buijs, M. T. Lakin, A. L. Spek, J. Reedijk, *Inorg. Chem.*, 1997, 36, 4321
- [38] a) J. Jezierska, T. Glowiak, A. Ozarowski, Y. V. Yablokov, Z. Rzaczyńska, *Inorg. Chim. Acta*, 1998, 275 ; b) S. Youngme, A. Cheansirisomboon, C. Danvirutai, C. Pakawatchai, N. Chaichit, C. Engkagul, G. A. VanAlbada, J. Sánchez-Costa, J. Reedijk, *Polyhedron*, 2008, 27, 1875 ; c) B. Kozlevcar, I. Leban, M. Petric, S. Petricek, O. Roubeau, J. Reedijk, P. Segedin, *Inorg. Chim. Acta*, 2004, 357, 4220
- [39] R. E. Del Sesto, A. M. Arif, J. S. Miller, *Inorg. Chem.*, 2000, 39, 4894
- [40] a) E. Ruiz, S. Alvarez, A. Rodríguez-Forteza, P. Alemany, Y. Pouillon, C. Massobrio, *Magnetism: Molecules to Materials, Vol. II, Models and Experiments*, Eds.: J. S. Miller, M. D., Wiley-VCH, Weinheim, 2001, p. ; b) E. Ruiz, J. Cano, S. Alvarez, P. Alemany, *J. Comput. Chem.*, 1999, 20, 1391 ; c) E. Ruiz, A. Rodríguez-Forteza, J. Tercero, T. Cauchy, C. Massobrio, *J. Chem. Phys.*, 2005, 123, 074102.
- [41] L. J. Noodleman, *J. Chem. Phys.*, 1981, 74, 5737
- [42] A. D. J. Becke, *J. Chem. Phys.*, 1993, 98, 5648
- [43] G. 03, R. D.2, M. J. Frisch, G. W. Trucks, H. B. Schlegel, G. E. Scuseria, M. A. Robb, J. R. Cheeseman, J. A. M. Jr., T. Vreven, K. N. Kudin, J. C. Burant, J. M. Millam, S. S. Iyengar, J. Tomasi, V. Barone, B. Mennucci, M. Cossi, G. Scalmani, N. Rega, G. A. Petersson, H. Nakatsuji, M. Hada, M. Ehara, K. Toyota, R. Fukuda, J. Hasegawa, M. Ishida, T. Nakajima, Y. Honda, O. Kitao, H. Nakai, M. Klene, X. Li, J. E. Knox, H. P. Hratchian, J. B. Cross, V. Bakken, C. Adamo, J. Jaramillo, R. Gomperts, R. E. Stratmann, O. Yazyev, A. J. Austin, R. Cammi, C. Pomelli, J. W. Ochterski, P. Y. Ayala, K. Morokuma, G. A. Voth, P. Salvador, J. J. Dannenberg, V. G. Zakrzewski, S. Dapprich, A. D. Daniels, M. C. Strain, O. Farkas, D. K. Malick, A. D. Rabuck, K. Raghavachari, J. B. Foresman, J. V. Ortiz, Q. Cui, A. G. Baboul, S. Clifford, J. Cioslowski, B. B. Stefanov, G. Liu, A. Liashenko, P. Piskorz, I. Komaromi, R. L. Martin, D. J. Fox, T. Keith, M. A. Al-Laham, C. Y. Peng, A. Nanayakkara, M. Challacombe, P. M. W. Gill, B. Johnson, W. Chen, M. W. Wong, C. Gonzalez, J. A. Pople, *Gaussian, Inc., Wallingford CT*, 2004.
- [44] A. D. Becke, *Phys. Rev. A*, 1988, 38, 3098
- [45] C. Lee, W. Yang, R. G. Parr, *Phys. Rev. B*, 1988, 37, 785
- [46] U. Venkatasubramanian, D. J. Donohoe, D. Ellis, B. T. Giles, S. A. Macgregor, S. Robertson, G. M. Rosair, A. J. Welch, A. S. Batsanov, L. A. Boyd, R. C. B. Copley, M. A. Fox, J. A. K. Howard, K. Wade, *Polyhedron*, 2004, 23, 629

CHAPTER IV. Mn(II) complexes containing the carboranylcarboxylate ligand 1-CH₃-2-CO₂H-1,2-closo-C₂B₁₀H₁₀: a water soluble Mn(II) polymer with aqua metal bridges and its derivatives.



The first water soluble and crystallographically determined polynuclear Mn(II) complex has been synthesized utilizing the carboranylcarboxylate ligand, 1-CH₃-2-CO₂H-1,2-closo-C₂B₁₀H₁₀. It has been obtained in water with total atom economy and has been fully characterized by analytical, spectroscopic (NMR, IR, UV-visible, ESI-MS), electrochemical, magnetic, microscopic (Cryo-TEM) and scattering (DLS, SAXS) techniques. Besides, its reactivity in coordinating solvents and with chelating ligand such as, 2,2'-bpy or 2,2'-bpm, has been studied leading to the formation of compounds with different nuclearities (mononuclear, binuclear, trinuclear and polymeric). The crystallographic structure of all of them has been obtained by X-Ray diffraction. DLS studies have demonstrated that the polymeric structure is preserved to a certain extent in water and the structure is broken in diethyl ether solution. The magnetic properties of the compounds studied show, in all cases, a weak antiferromagnetic coupling.

TABLE OF CONTENTS

CHAPTER IV. Mn(II) complexes containing the carboranylcarboxylate ligand 1-CH₃-2-CO₂H-1,2-closo-C₂B₁₀H₁₀: a water soluble Mn(II) polymer with aqua metal bridges and its derivatives.

IV.1.	Introduction	77
IV.2.	Objectives	79
IV.3.	Results and discussion	80
IV.3.1.	Synthesis and structure	80
IV.3.2.	Electrochemical properties	90
IV.3.3.	Spectroscopic and microscopic properties	92
IV.3.4.	Magnetic properties.....	96
IV.4.	Conclusions	100
IV.5.	Experimental section	102
V.5.1.	Instrumentation and measurements	102
V.5.2.	Materials	103
V.5.3.	Preparations	104
IV.6.	References	106

IV.1. Introduction

Chemical transformations, as well as other industrial productive processes, are experiencing a profound transformation to meet sustainability criteria, moving from old methods to new ones developed in agreement with green chemistry principles.^[1] Water has been much under-investigated as a solvent for chemical transformations basically because of poor solubility of organic molecules; however, water is the “ideal solvent”^[2] being economic, non-toxic, non-inflammable and compatible with the environment. Substitution of organic solvents by water is desirable, but it becomes especially suited for those chemical transformations in which water is one of the reagents.

Coordination polymers are currently of great interest and represent an active area of coordination chemistry because of their special role in multiple fields such as ion exchange, gas storage, chemical separation, sensor technology, magnets, energy conversion and storage, optoelectronics, and catalysis.^[3] Also, polynuclear manganese complexes attract great interest owing to their relevance in many important naturally occurring processes.^[4]

Concerning organic spacers, carboxylic ligands are frequent choices for metal-organic networks, among other reasons due to their rich modes of coordination.^[5] With monocarboxylate ligands, binuclear complexes with the $[\text{Mn}_2(\mu\text{-OH}_2)(\mu_{1,3}\text{-O}_2\text{CR})_2]^{2+}$ core have been reported^[6] and trinuclear compounds have also been described;^[7] being the latter either linear or triangular.^[7] On the other hand, the search in the Cambridge Structural Database (CSD) of the motif “[$\text{Mn}_3(\mu_{1,3}\text{-O}_2\text{CR})_6$]” provides a large number of trinuclear clusters “ Mn_3 ”, few dodecanuclear “ Mn_{12} ” and tetranuclear “ Mn_4 ” complexes and, in much less ratio hexanuclear “ Mn_6 ” and henicosanuclear “ Mn_{21} ” species. Regarding the trinuclear systems, the most part are linear. Complexes with μ_2 -oxo, -hydroxo or aqua bridges have not been found in any of the structures studied. Therefore, no nuclearities higher than 21 incorporating the scrutinized motif “[$\text{Mn}_3(\mu_{1,3}\text{-O}_2\text{CR})_6$]” have been found; hence no coordination polymers with this motif have been described until now.

The use of carboranes in supramolecular chemistry is a topic that raises great interest for their particular properties^[8] that may induce unconventional characteristics in the supramolecular structures in which they are inserted. In earlier works with [1-CO₂-1,2-*closo*-C₂B₁₀H₁₁]⁻ ligand and Zn^{II}, Cu^{II}, Ni^{II} and Mo^{II} ions, the geometrical features found in the resulting complexes were not distinctive to conventional monocarboxylate ligands.^[9] Our vision of the carboranyl substituent, however, is that it provides good space filling, hydrophobicity and electron withdrawing properties, suggesting the possibility of inducing distinct geometrical behaviour in polynuclear complexes. If the expected structural change had not been observed,

CHAPTER IV

it could be due to the metal ions studied, and their dominant prevalence for a specific nuclearity and arrangement. Mn^{II} is a metal ion that offers different structural possibilities and has never been studied with this kind of ligands.

IV.2. Objectives

In the previous Chapter, the coordination complexes of the carboranylcarboxylate, $[1\text{-CH}_3\text{-2-CO}_2\text{-1,2-closo-C}_2\text{B}_{10}\text{H}_{10}]^-$, **L**, with Cu^{2+} have been reported. In most of them, the monocarboxylate ligand was bridging two Cu^{2+} ions leading to a paddle-wheel structure. If structural changes had not been observed in these complexes could be due to the prevalence of the Cu^{II} ions for a specific nuclearity and arrangement with monocarboxylate ligands. However, as it has been shown in the introduction, the motif $[\text{Mn}_3(\mu\text{-O}_2\text{CR})_6]$ offers different structural possibilities with the carboxylate ligands, moreover, the reactivity of this metal with this kind of ligand has been unexplored.

With this in mind, the main goal of this chapter was the synthesis and characterization of a series of new polynuclear and mononuclear manganese(II) complexes containing the carboranylcarboxylate $[1\text{-CH}_3\text{-2-CO}_2\text{-1,2-closo-C}_2\text{B}_{10}\text{H}_{10}]^-$.

First of all, a water soluble polymeric manganese(II) complex was synthesized and fully characterized through structural, analytical, spectroscopic, microscopic and magnetic techniques.

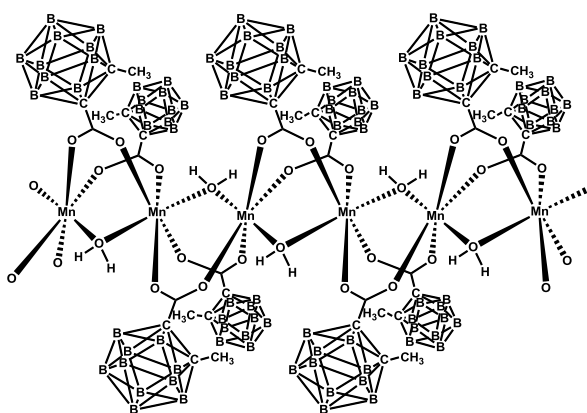


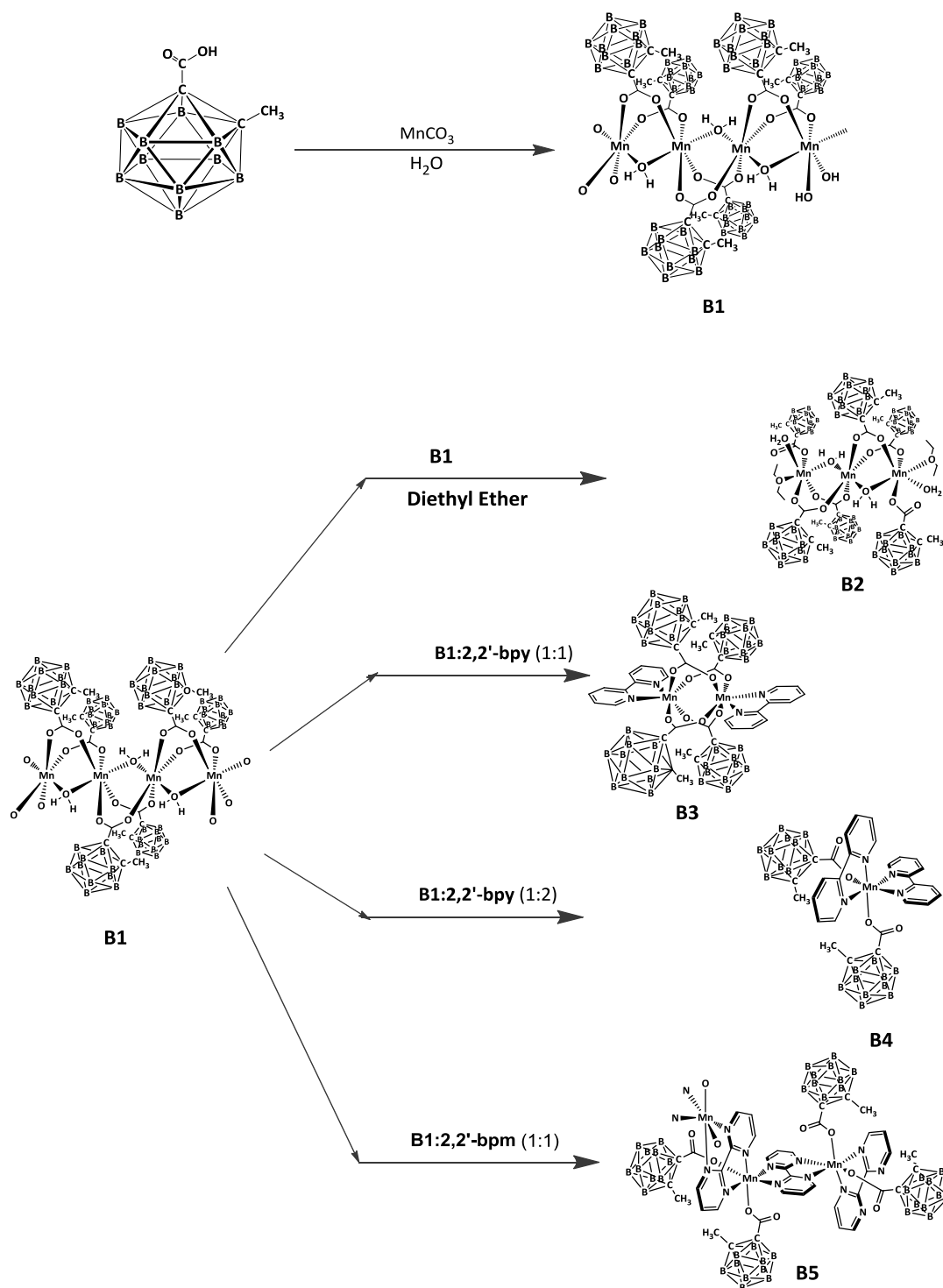
Chart 1. Polymeric structure of $[\text{Mn}(\mu\text{-H}_2\text{O})(\mu\text{-1-CH}_3\text{-2-CO}_2\text{-1,2-closo-C}_2\text{B}_{10}\text{H}_{10}\cdot)_2]_n \cdot (\text{H}_2\text{O})_n$, **B1**.

We were also concerned in evaluate the influence and reactivity of chelating polipyridylic ligands over the polymeric structure of this starting material. With this aim bidentate 2,2'-bipyridine and tetradentate 2,2'-bipyrimidine were chosen. The resulting products were fully characterized through structural, analytical, spectroscopic, electrochemical and magnetic techniques.

IV.3. Results and discussion

IV.3.1. Synthesis and structure

The synthetic strategy for the preparation of the Mn(II) water soluble polymer, **B1**, as well as the Mn(II) complexes **B2-B5**, containing the carboranylcarboxylate ligand 1-CH₃-2-CO₂H-1,2-*closo*-C₂B₁₀H₁₀ (**LH**) and 2,2'-bipyridine or 2,2'-bipyrimidine is outlined in Scheme 1



Scheme 1. Synthetic strategy for the preparation of Mn(II) complexes B1-B5

The strategy used to obtain the water soluble polymer, **B1**, consists in mixing a suspension of the carboranylcarboxylic acid 1-CH₃-2-CO₂H-1,2-closo-C₂B₁₀H₁₀, **LH**, and MnCO₃ in a 1:1 ratio, in water at 40 °C and stirring for 2h. Afterwards, the solvent was removed and the white polymer [Mn(μ-H₂O)(μ-1-CH₃-2-CO₂-1,2-closo-C₂B₁₀H₁₀)₂]_n·(H₂O)_n, **B1**, was obtained.

The polymeric structure of **B1** is broken in coordinating solvents such as diethyl ether leading to the first linear trinuclear Mn(II) compound [Mn₃(H₂O)₄(1-CH₃-2-CO₂-1,2-closo-C₂B₁₀H₁₀)₆(C₄H₁₀O)₂], **B2**.

Compound **B1** was used as starting material and was reacted with two different nitrogen containing heterocyclic aromatic ligands, 2,2'-bipyridine and 2,2'-bipyrimidine, with the aim to examine the stability of the polymeric structure in front of this coordinating ligands, as well as to study and characterize the new compounds obtained.

When the bidentate ligand 2,2'-bpy dissolved in ethanol is added to an ethanolic solution of complex **B1**, with a ligand/complex ratio of 1:1 (see Scheme 1) a slightly yellow solution was formed that after slow evaporation leads to colourless crystals of the binuclear complex [Mn₂(1-CH₃-2-CO₂-1,2-closo-C₂B₁₀H₁₀)₄(bpy)₂], **B3**. On the other hand, when the ratio ligand/complex was 2:1 the solution was become bright yellow and after slow evaporation yellow crystals suitable for X-Ray diffraction of the mononuclear complex [Mn(1-CH₃-2-CO₂-1,2-closo-C₂B₁₀H₁₀)₂(bpy)₂], **B4**, were obtained.

Finally, the addition of the tetradentate ligand 2,2'-bipyrimidine (bpm) as a coordinating ligand in CH₂Cl₂ leads to the formation of the yellow polymer [Mn(1-CH₃-2-CO₂-1,2-closo-C₂B₁₀H₁₀)₂(bpm)]_n, **B5**, (Scheme 1).

Crystallographic data and selected bond distances and angles for compounds **B1-B5** are presented in Table S1 (see supporting information section) and Table 1. and Table 2, respectively. ORTEP plots with the corresponding atom labels for the X-ray structures of all compounds are presented in Figure 1. and Figure 5.

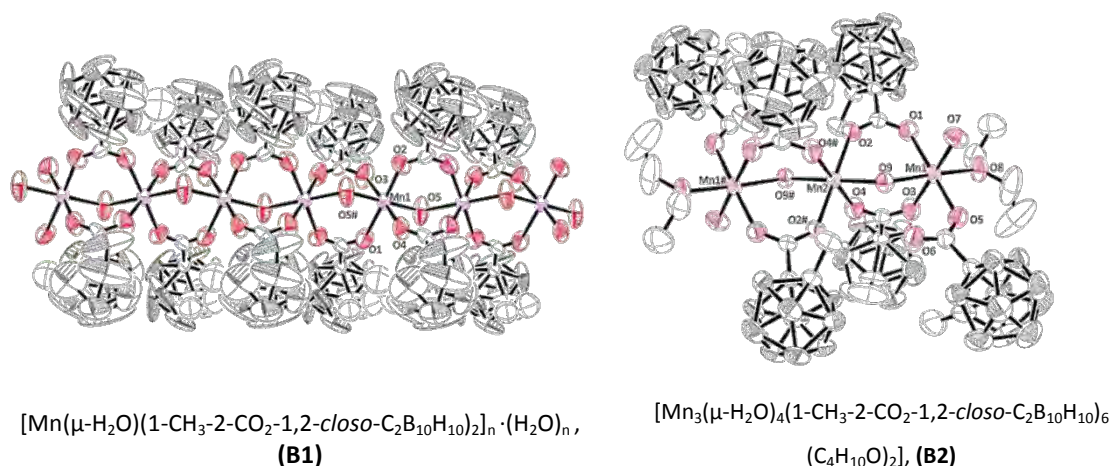


Figure 1. X-ray structures (ORTEP plots with ellipsoids at 40% probability level) and labelling scheme for complexes **B1** and **B2**.

Polymer **B1** displays an unusual feature in 1D oligomer Mn(II) complexes with a nuclearity higher than 2 that is the existence of water molecules bridging each two Mn centres. Each of the Mn(II) centres possesses a distorted octahedral geometry and the ligands are disposed in a zigzag fashion through the chain. The bulky nature of the ligand prevents intermolecular interactions among these lineal arrays. Each Mn(II) atom is coordinated by four carboxylate oxygen atoms and two aqua oxygen atoms and is bridged to other Mn atoms by two carboranylcarboxylate ligands and by an aqua ligand. The two $\mu_{1,3}$ -carboxylate groups are similar, with comparable Mn-O_{carb} distances. The bridging aqua was identified on the basis of the Mn-O distances, Mn(1)-O(5), 2.338(13) Å and Mn(1)-O(5)#1, 2.302(11) Å, which are significantly longer than those in $\mu\text{-O-Mn}_2^{\text{III}}$ compounds (1.78-1.81Å),^[10] in the $(\mu\text{-OH-Mn}^{\text{III}})_n$ polymer (1.89Å)^[11] and those in previous $\mu\text{-OH-Mn}_2^{\text{II}}$ molecular systems (2.05-2.09Å).^[10] The non-bridging water molecules are situated in the cavity formed by the carboranylcarboxylate ligands, and are linked through hydrogen bonds to the coordinated aqua ligand (O-H, 1.938Å and 2.485Å) (Figure 2). It is remarkable the packing structure of this polymer that displays polymeric chiral chains because the methyl group of the carboranylcarboxylate ligand is shifted respect to the centre of the coordinated carboxylate group. Then, two different conformations for these chains (λ and δ) can be found (Figure 3a). In this figure each methyl group is oriented toward the methyl group of a neighbouring ligand, with a C...C distance of 2.66 Å. Moreover, the orientation of all methyl groups is the same within a chain, and opposite to the methyl groups from a different chain. The imaginary helical path defined by the positions of the methyl groups along each polymeric chain allows to assign them either Δ or Λ conformation. The chains are spatially arranged in the network so that they define a sort of

"chiral layers" conformed by adjacent chains having the same conformation. Figure 3b shows the packing structure of these "chiral layers" that lead to a 2D structure. It can be concluded that this polymer is formed by a sequence of chiral chains due to the orientation of the methyl groups from the carboranylcarboxylate ligands.

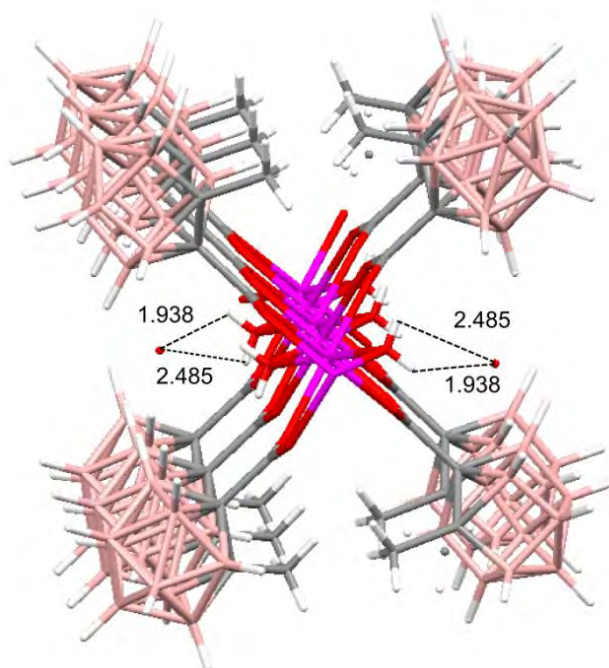


Figure 2. X-ray structure of **B1** showing the polymeric chains and hydrogen bonds connecting the hydration water with the polymeric chain.

Table 1. Selected bond lengths (Å) and angles (°) for complexes **B1** and **B2**.

	B1		B2		B2
Mn(1)-O(2)	2.108(9)	Mn(1)-O(1)	2.129(2)	Mn(2)-O(2)	2.1528(18)
Mn(1)-O(4)	2.119(9)	Mn(1)-O(3)	2.136(2)	Mn(2)-O(4)	2.1179(19)
Mn(1)-O(3)	2.176(9)	Mn(1)-O(5)	2.151(2)	Mn(2)-O(9)	2.228(2)
Mn(1)-O(1)	2.201(9)	Mn(1)-O(7)	2.157(2)	Mn(2)-O(2)#1	2.1528(18)
Mn(1)-O(5)#1	2.312(13)	Mn(1)-O(8)	2.194(2)	Mn(2)-O(4)#1	2.1179(19)
Mn(1)-O(5)	2.344(13)	Mn(1)-O(9)	2.346(2)	Mn(2)-O(9)#1	2.228(2)
O(2)-Mn(1)-O(4)	92.9(4)	O(7)-Mn(1)-O(8)	92.72(9)	O(4)-Mn(2)-O(4)#1	180.00(13)
O(2)-Mn(1)-O(3)	89.5(4)	O(1)-Mn(1)-O(9)	90.16(8)	O(4)-Mn(2)-O(2)	90.79(9)
O(4)-Mn(1)-O(3)	177.0(5)	O(3)-Mn(1)-O(9)	90.95(9)	O(4)#1-Mn(2)-O(2)	89.21(9)
O(2)-Mn(1)-O(1)	177.2(6)	O(5)-Mn(1)-O(9)	84.69(8)	O(4)-Mn(2)-O(2)#1	89.21(9)
O(4)-Mn(1)-O(1)	87.3(4)	O(7)-Mn(1)-O(9)	87.03(9)	O(4)#1-Mn(2)-O(2)#1	90.79(9)
O(3)-Mn(1)-O(1)	90.2(4)	O(8)-Mn(1)-O(9)	176.93(8)	O(2)-Mn(2)-O(2)#1	180.00(12)
O(2)-Mn(1)-O(5)#1	82.6(4)	O(1)-Mn(1)-O(3)	92.64(9)	O(4)-Mn(2)-O(9)#1	85.76(9)
O(4)-Mn(1)-O(5)#1	88.7(4)	O(1)-Mn(1)-O(5)	173.32(8)	O(4)#1-Mn(2)-O(9)#1	94.24(9)
O(3)-Mn(1)-O(5)#1	89.7(4)	O(3)-Mn(1)-O(5)	91.70(9)	O(2)-Mn(2)-O(9)#1	91.10(8)
O(1)-Mn(1)-O(5)#1	94.5(4)	O(1)-Mn(1)-O(7)	87.95(9)	O(2)#1-Mn(2)-O(9)#1	88.90(9)
O(2)-Mn(1)-O(5)	97.0(4)	O(3)-Mn(1)-O(7)	177.89(9)	O(4)-Mn(2)-O(9)	94.24(9)
O(4)-Mn(1)-O(5)	91.2(4)	O(5)-Mn(1)-O(7)	87.54(9)	O(4)#1-Mn(2)-O(9)	85.76(9)
O(3)-Mn(1)-O(5)	90.5(3)	O(1)-Mn(1)-O(8)	92.89(9)	O(2)-Mn(2)-O(9)	88.90(8)
O(1)-Mn(1)-O(5)	85.8(4)	O(3)-Mn(1)-O(8)	89.28(9)	O(2)#1-Mn(2)-O(9)	91.10(8)
O(5)#1-Mn(1)-O(5)	179.6(5)	O(5)-Mn(1)-O(8)	92.24(8)	O(9)#1-Mn(2)-O(9)	180.0

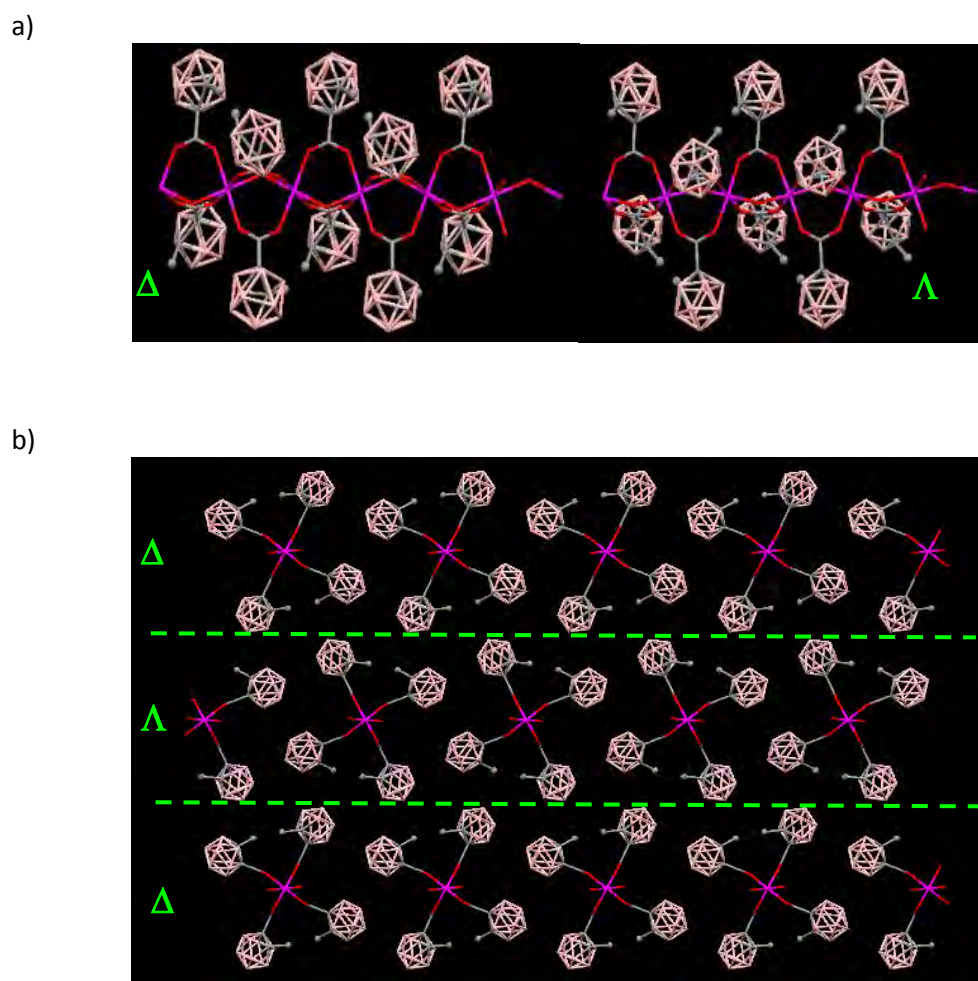


Figure 3. a) X-ray structure of **B1** showing different conformations for the polymeric chains; b) packing diagram for the “chiral layers” of polymer **B1**.

It was observed, that the polymeric structure of **B1** is broken in coordinating solvents such as diethyl ether, leading to the first linear trinuclear Mn(II) complex, **B2**, with water bridging entities. The structure of this compound (Figure 1.) consists in a linear array of three Mn(II) ions. The central Mn(2), which is located on a crystallographic inversion centre, is coordinated octahedrally by four carboxylate oxygen atoms and two aqua oxygen atoms, similar to the Mn(II) atoms in **B1**. The Mn(2) is bonded to both terminals Mn(1) by two carboranylcarboxylate ligands and by an aqua ligand. The two terminal Mn(II) ions are hexacoordinated and their coordination is completed by one monodentate carboxylate, one terminal aqua ligand and one oxygen atom from one diethyl ether molecule. It is worth noticing the existence of two intramolecular hydrogen bonds between the non-coordinating oxygen atom of the carboxylate (O6) and the H9A and H9B of the bridging aqua (H9A-O6, 1.445Å; H9B-O6, 2.714Å). Another intramolecular weak hydrogen bond is observed between H9B and O7 of the terminal aqua ligand, H9B-O7, 2.799Å. Two additional intermolecular H-

bonds are formed between the two hydrogen atoms of the terminal aqua ligand and two oxygen atoms from two molecules of diethyl ether solvent (H7D-O1Y , 1.895Å; H7C-O1V , 2.075Å) (see Figure S1 at the supporting information section).

The clean cleavage of **B1** by Et₂O to yield **B2** is shown in Figure 4. In this process only Et₂O and H₂O participate, whereas follow up cleavage of bridging carboxylates leads to monodentate ligands. Interestingly, terminal Mn atoms in each oligomer keep coordinated to one of the two originally shared (in the polymer structure) carboranylcarboxylate ligands. This clean process of generating oligomers can easily be reversed since removal of the diethyl ether solvent quantitatively restores the original polymer in the solid state; this could explain the solubility properties of this Mn polymer in diethyl ether by an easy assembling/disassembling process. This reversible process has also been evidenced in solution when using water as solvent, as will be described below.

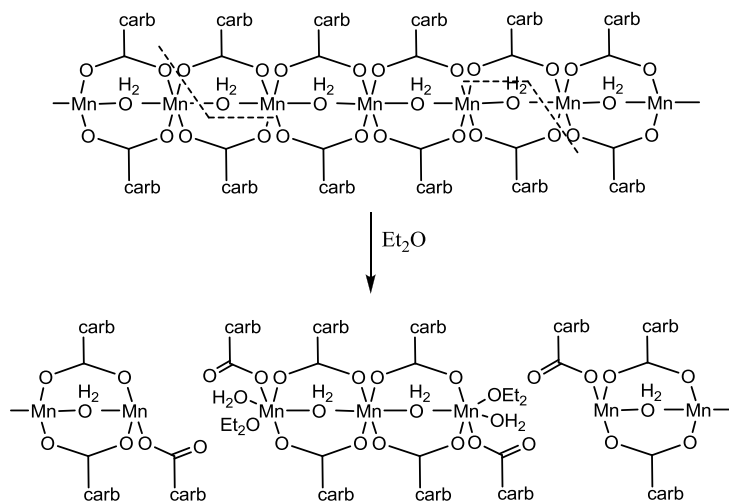


Figure 4. Cleavage of **B1** by Et₂O to yield **B2**.

Recently, Unema et al.^[12] have reported the crystal structure of the oxygen-evolving centre in photosystem II in which water molecules are bound to the Mn₄CaO₅ cluster. The process described here may provide the opportunity for further design and construction of new supramolecular assemblies as models of the oxygen-evolving centre (OEC) and also understand the role of the water molecules in the catalytic process of water splitting.

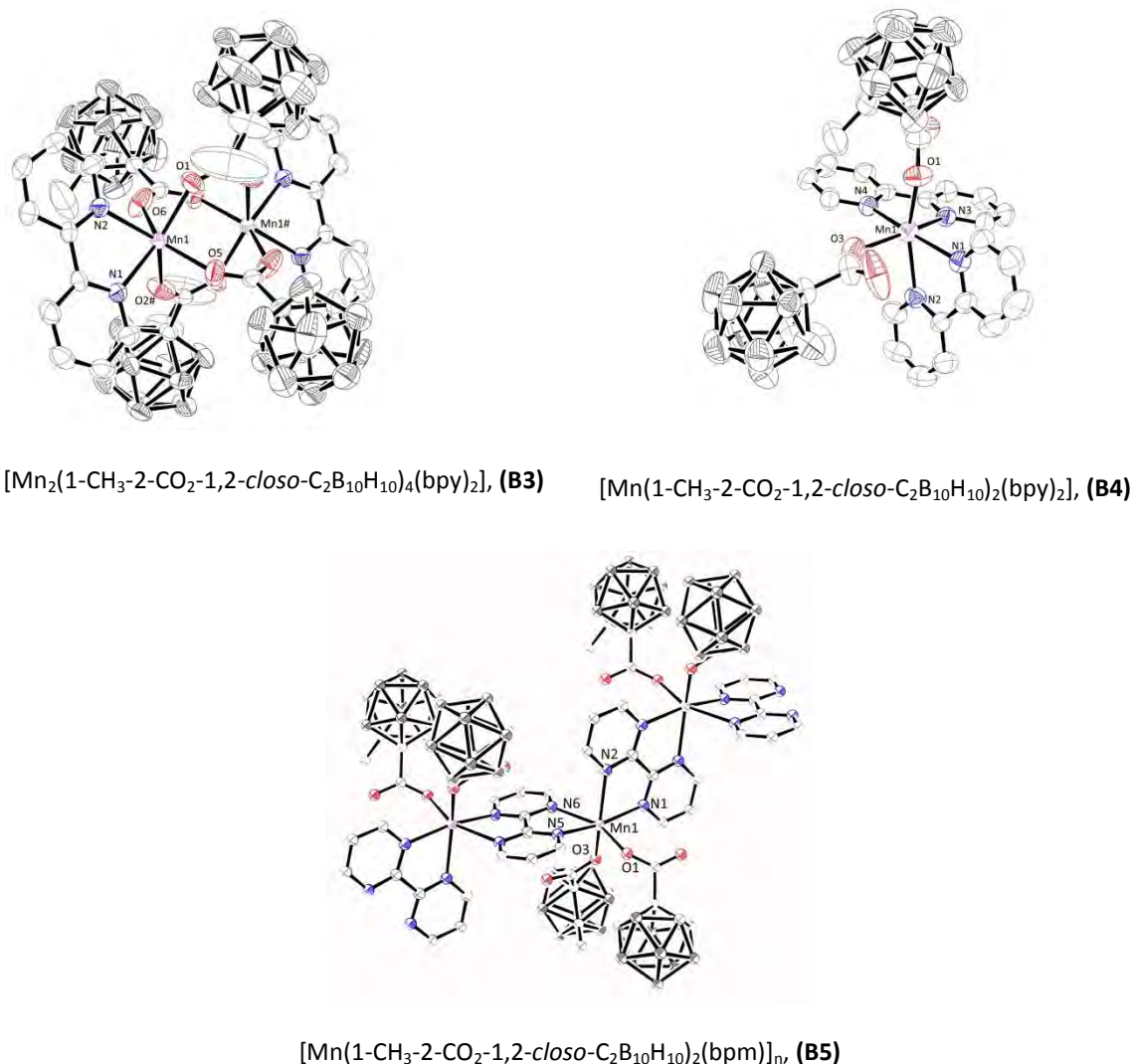


Figure 5. X-ray structures (ORTEP plots with ellipsoids at 30% probability level) and labelling scheme for complexes **B3-B5**.

Binuclear compound **B3** is a novel binuclear Mn(II) cluster which displays a centrosymmetric structure with the symmetry centre located between the two manganese atoms. These Mn(II) ions are holding together through four syn,syn $\eta^1: \eta^1: \mu^2$ -carboxylate bridges in which each Mn(II) ion displays an almost perfect N_2O_4 trigonal prismatic geometry that is completed by the two nitrogen donor atoms of the 2,2'-bipyridine ligand (see Figure 6. . Compound **B3** is the first example of a binuclear Mn(II) compound with carboxylate bridges found in the literature, where the manganese atoms are displaying a trigonal prismatic geometry. Only one example has been described in the literature of a binuclear compound displaying similar coordination environment with two manganese atoms bridged by four carboxylate anions and two 1,10-phenanthroline ligands but a distorted octahedral geometry around the metal centres was described.^[13] O-Mn-N/O angles are in the range 82.04(11)-85.88(1)° for adjacent atoms and in

the range 130.00(9)-141.74(9)° for the angles formed between the manganese atom and the atoms that described the diagonal of the rectangular faces of the prism. These angles totally agree with a prismatic trigonal geometry.^[14] Mn-O bond lengths are in the range 2.148(2)-2.168(2)Å and are shorter than distances Mn-N (average of 2.286(2)Å). The packing structure displays $\pi\cdots\pi$ stacking interactions among the aromatic rings of 2,2'-bpy ligands of two neighbouring molecules.(Figure S2 supporting information section).

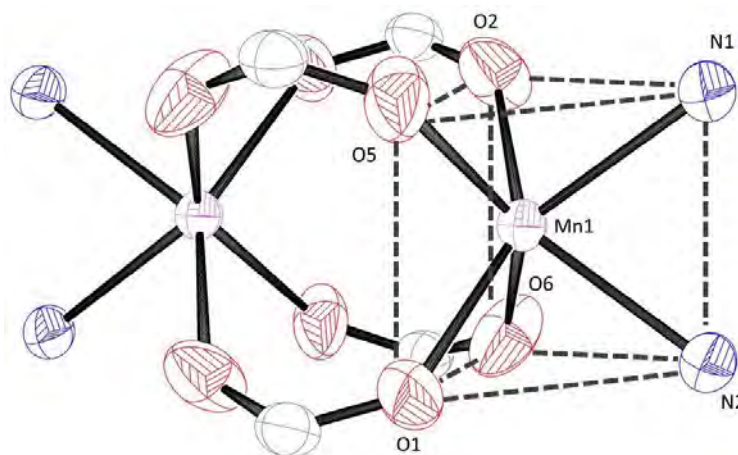


Figure 6. Trigonal prismatic geometry in detail of **B3**

The X-ray crystallography performed on the mononuclear complex **B4**, $\text{Mn}(1\text{-CH}_3\text{-2-CO}_2\text{-1,2-closo-C}_2\text{B}_{10}\text{H}_{10})_2(\text{bpy})_2$, reveals a six-coordinate Mn atom with a distorted octahedral geometry. The Mn(II) ion is coordinated by two chelating 2,2'-bipyridine ligands and two monodentate carboranylcarboxylate oxygen atoms, both adopting a *cis* configuration around the metal. The distances Mn-O (2.099(3) and 2.135(3) Å) and Mn-N (in the range 2.247(4)-2.298(4) Å) are similar and comparable to other Mn compounds with 2,2'-bpy and carboxylate ligands^[15] as well as to the binuclear complex **B3**. Compared to the ideal octahedral geometry, the angles show significant distortions with deviations from the theoretical value of 90°.

Finally, the structure of the complex **B5**, $[\text{Mn}(1\text{-CH}_3\text{-2-CO}_2\text{-1,2-closo-C}_2\text{B}_{10}\text{H}_{10})_2(\text{bpm})]_n$, is a novel 1D Mn (II) assembly where the metallic ions are linked by 2,2'-bipyrimidine groups in a zigzag manner (Figure 5.). Each Mn(II) ion coordinates to two $[1\text{-CH}_3\text{-2-CO}_2\text{-1,2-closo-C}_2\text{B}_{10}\text{H}_{10}]^-$ ligands in a monodentate mode completing this way the distorted octahedral geometry of the metal centres. The two carboranylcarboxylate ligands adopt a *cis*-configuration around the metal. No other example of a manganese compound containing 2,2'-bpm and carboxylate ligands displaying similar features has been found in the literature. However, similar structures containing water, chlorine or cyanate as monodentate ligands have been previously reported.^[16] It is observable that the Mn-O distance (2.075(3) and 2.095(3)Å) are shorter than the Mn-O distances found for similar complexes with 2,2'-bpm and water ligands ($d_{(\text{Mn-OH}_2)} =$

2.161(3) Å).^[16a] Nevertheless, Mn-N distances (average of 2.313 Å) are in the range found in other 2,2'-bpm-bridged manganese (II) complexes.^[16] The longest Mn-N in relation to the Mn-O bond distances and the small bite angle at the 2,2'-bpm ligands (71.24(12)° for N(1)-Mn(1)-N(2)) and 71.77(12)° for N(5)-Mn(1)-N(6)) leads to the main distortions of the ideal octahedral geometry around each metal atom. The two bpm ligands are planar but the manganese atom is 0.137 and 0.459 Å out of these planes. The dihedral angle between two adjacent 2,2'-bpm ligands is of 90.43°. The molecule crystallizes with an ethanol molecule of crystallization which is hydrogen-bonded to the non-bond oxygen atom of one of the two carboranylcarboxylate ligands likely stabilizing the zigzag chain structure (see further details in Figure S3 at the Supporting Information Section). Finally, the packing structure of the **B5** (Figure S2) shows an alternated distribution of the carboranylcarboxylate ligands of different chains in the space along the *a* axis.

Table 2. Selected bond lengths (Å) and angles (°) for complexes **B3-B5**.

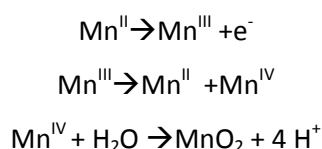
	B3		B4		B5	
Mn(1)-O(5)	2.148(2)	Mn(1)-O(1)	2.099(3)	Mn(1)-O(1)	2.075(3)	
Mn(1)-O(2)#1	2.154(2)	Mn(1)-O(3)	2.135(3)	Mn(1)-O(3)	2.095(3)	
Mn(1)-O(6)	2.155(2)	Mn(1)-N(3)	2.247(4)	Mn(1)-N(5)	2.279(4)	
Mn(1)-O(1)	2.168(2)	Mn(1)-N(2)	2.256(4)	Mn(1)-N(1)	2.294(3)	
Mn(1)-N(1)	2.295(2)	Mn(1)-N(1)	2.293(4)	Mn(1)-N(6)	2.335(4)	
Mn(1)-N(2)	2.277(2)	Mn(1)-N(4)	2.298(4)	Mn(1)-N(2)	2.344(3)	
O(5)-Mn(1)-O(2)#1	85.88(11)	O(1)-Mn(1)-O(3)	97.04(14)	O(1)-Mn(1)-O(3)	96.21(15)	
O(5)-Mn(1)-O(6)	141.74(9)	O(1)-Mn(1)-N(3)	90.07(15)	O(1)-Mn(1)-N(5)	84.38(12)	
O(2)#1-Mn(1)-O(1)	141.73(9)	O(3)-Mn(1)-N(3)	104.82(14)	O(3)-Mn(1)-N(5)	107.03(13)	
O(6)-Mn(1)-O(1)	85.24(12)	O(1)-Mn(1)-N(2)	96.01(13)	O(1)-Mn(1)-N(1)	93.77(13)	
O(5)-Mn(1)-N(2)	131.24(9)	O(3)-Mn(1)-N(2)	87.50(15)	O(3)-Mn(1)-N(1)	87.69(13)	
O(2)#1-Mn(1)-N(2)	130.00(9)	N(3)-Mn(1)-N(2)	165.53(14)	N(5)-Mn(1)-N(1)	165.27(12)	
O(6)-Mn(1)-N(2)	82.40(8)	O(1)-Mn(1)-N(1)	94.39(13)	O(1)-Mn(1)-N(6)	154.20(13)	
O(1)-Mn(1)-N(2)	83.30(8)	O(3)-Mn(1)-N(1)	156.95(15)	O(3)-Mn(1)-N(6)	81.96(13)	
O(5)-Mn(1)-N(1)	85.52(8)	N(3)-Mn(1)-N(1)	95.09(14)	N(5)-Mn(1)-N(6)	71.77(12)	
O(2)#1-Mn(1)-N(1)	83.14(8)	N(2)-Mn(1)-N(1)	71.41(15)	N(1)-Mn(1)-N(6)	111.81(12)	
O(6)-Mn(1)-N(1)	131.54(9)	O(1)-Mn(1)-N(4)	161.54(17)	O(1)-Mn(1)-N(2)	109.35(14)	
N(2)-Mn(1)-N(1)	70.53(7)	O(3)-Mn(1)-N(4)	86.07(17)	O(3)-Mn(1)-N(2)	147.43(15)	
O(5)-Mn(1)-O(1)	82.16(10)	N(3)-Mn(1)-N(4)	71.58(18)	N(5)-Mn(1)-N(2)	95.54(12)	
O(1)-Mn(1)-N(1)	131.54(9)	N(2)-Mn(1)-N(4)	102.31(17)	N(1)-Mn(1)-N(2)	71.24(12)	
N(2)-Mn(1)-N(1)	70.53(7)	N(1)-Mn(1)-N(4)	89.39(13)	N(6)-Mn(1)-N(2)	83.25(12)	

IV.3.2. Electrochemical properties

The redox potentials of complexes **B1**, **B3** and **B4** were determined by cyclic voltammetry (CV) in water + 0.1 M KPF₆ at pH 4.9, MeOH + 0.1M NH₄ClO₄ and CH₂Cl₂ + 0.1 M TBAH, respectively. Cyclic voltammograms obtained for **B3** and **B4** are shown in Figure S4 at the supporting information section.

The cyclic voltammetry of a solution of complex **B1** at pH= 5 is shown in Figure 7; around E_{ap} = 1 V vs SCE, there is an oxidation peak corresponding to the oxidation of Mn(II) to Mn(III)

and an increased background water oxidation is observed above 1.4 V. The redox process at 1 V is quasi-reversible, $\Delta E = 200$ mV, which implies that there is slow interfacial electron transfer, a subsequent chemical process which occurs following oxidation, or that there are contributions of multiple species to the voltammetry. The reductive peaks at $E_{cp} = 0.8$ V and -0.09 V are attributed to two reduction processes. After bulk electrolysis carried out at $E_{ap} = 1.1$ V where 0.8 electrons per manganese were consumed, a slight black solid was observed. All these facts together with other studies described in the literature,^[17] lead us to postulate the following mechanism,



The $\text{Mn}^{\text{3+}}$ species generated after oxidation can undergo disproportion leading to Mn^{II} and Mn^{IV} species and subsequent formation of MnO_2 after the reaction of Mn^{IV} with H_2O .

The cathodic peak at $E_{cp} = 0.8$ V is attributed to the reduction of Mn^{IV} to Mn^{III} which is reduced to Mn^{II} at $E_{cp} = -0.09$ V.

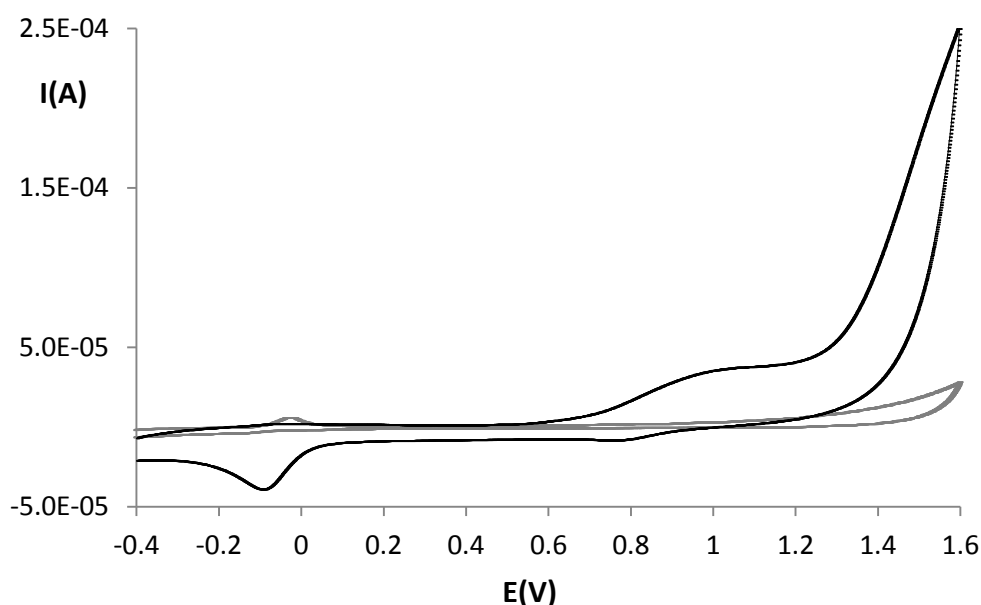
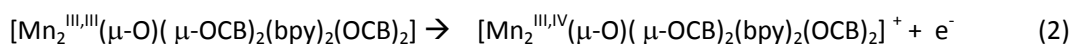
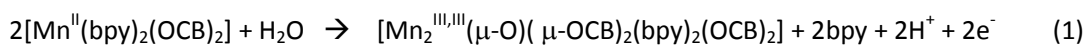


Figure 7. Cyclic voltammetry recorded for complexes **B1** in water, (**black**), and background, (**grey**).

Electrochemistry of compound **B3** was carried out in MeOH using NH_4ClO_4 as supporting electrolyte due to the low solubility of this compound. The cyclic voltammogram for **B3** (Figure S4a) shows a series of irreversible broad ill-defined oxidative peaks between 0.67 V and 1.30 V and also a reductive peak at 0.10 V, these peaks are associated with the formation of unidentified products. However, an exhaustive electrolysis of a solution of **B3** at 0.9 V

consumes 1.3 electrons per molecule and leads to a brown solution that could be correspond to the formation of a dimanganese (II,III) complex unstable on the time scale of the electrolysis.

The cyclic voltammogram of complex **B4** (Figure S4b at the supporting information section), exhibits two oxidation peaks at 1.08 and 1.47 V respectively; the shape of the VC is similar to others Mn acetate complexes described in the literature.^[18] The one oxidation peak at 1.08 V could be assigned to the metal oxidation process together with a subsequent dimerization of the product species to generate a Mn^{III,III} compound (eq. 1 below) that is formed as a result of the metal oxidation. This compound is proven by the presence of a new peak around 1.47 V involving the generation of a new dimeric compound where this last peak could be associated probably to a one electron oxidised unstable form (eq.2) follow to a chemical reaction with residual water of the solvent (eq.3). No distinguishable reduction peaks are detected on the cathodic sweep which can be assigned also to the formation of binuclear species.^[18] The monoelectronic nature of the first wave was confirmed by controlled-potential electrolysis at 1.06 V where one electron per initial amount of **B4** has been consumed.^[19] We have tentatively proposed the following electrochemical behaviour but more studies related to the electrochemistry are being developed in our laboratory to confirm this behaviour.



IV.3.3. Spectroscopic and microscopic properties

The IR spectra of all complexes described display typical $\nu(\text{B-H})$ absorption at frequencies above 2590 cm^{-1} , characteristic of *closo* carborane derivatives.^[20] Differences between the frequencies of the symmetric and antisymmetric stretches for the carboxylate ligands lies within the ranges quoted for bidentate bridging ligands.^[20b]

The study of the polymeric structure, **B1**, in water solution has been performed by $^1\text{H}\{^{11}\text{B}\}$ -, $^{11}\text{B}\{^1\text{H}\}$ - NMR, ESI-MS spectroscopy, Cryo-TEM microscopy and Dynamic Light Scattering (DLS). For the remainder complexes $^{11}\text{B}\{^1\text{H}\}$ -NMR and ESI-MS were carried out. The $^1\text{H}\{^{11}\text{B}\}$ - and $^{11}\text{B}\{^1\text{H}\}$ -NMR spectra of **B1** fully agree with the solid structure confirmed by X-ray crystallography (Figure S6 at the supporting information section). It can be observed that the $^1\text{H}\{^{11}\text{B}\}$ -spectrum exhibits a resonance at $\delta = 1.93 \text{ ppm}$ attributed to the $\text{C}_c\text{-CH}_3$ protons. The resonances of the protons bonded to the B atoms appear as broad singlets over a wide chemical shift range in the region from $\delta = 0$ to $+3 \text{ ppm}$. The $^{11}\text{B}\{^1\text{H}\}$ -NMR resonances for

complexes studied featured similar patterns in the range from -4.1 to -11 ppm that agree with a *closo* cluster.^[20a] ESI-MS spectrum of the polymer **B1** in water in the scan region 100 m/z to 2000 m/z shows different peaks that could be assigned to the $\{[\text{Mn}(\text{L})_2(\text{H}_2\text{O})]_4 + \text{H}^+\}$ fragment (m/z 1902.4) and $\{[\text{Mn}(\text{L})_2(\text{H}_2\text{O})]_3 + \text{LH} + \text{H}^+\}$ fragment (m/z 1628.7) together with other peaks of less intensity corresponding to the $\{[\text{Mn}(\text{L})_2(\text{H}_2\text{O})]_2 - (\text{L}) + 2\text{H}^+\}$ fragment (m/z 795.4) and $\{[\text{Mn}(\text{L})_2(\text{H}_2\text{O})]_2 - (\text{LH}) + \text{Na}^+\}$ fragment (m/z 772.4). For complex **B3**, the ESI-MS spectrum in methanol in the scan region 400 m/z to 1500 m/z shows two main peaks assigned to the $\{[\text{Mn}_2(\text{L})_4(\text{bpy})_2] + \text{Na}^+\}$ fragment (m/z 1250.2) and $\{[\text{Mn}_2(\text{L})_4(\text{bpy})_2] - (\text{L})\}^+$ fragment (m/z 1026.5) and a lower intensity peak corresponding to $\{[\text{Mn}_2(\text{L})_4(\text{bpy})_2] + \text{H}^+\}$ fragment (m/z 568.6). In case of complex **B4**, the ESI-MS in the scan region 100 m/z to 1000 m/z reveals two low intensity peaks assigned to $\{[\text{Mn}(\text{L})_2(\text{bpy})_2] - (\text{L}) + \text{H}_2\text{O}\}^+$ fragment (m/z 577.1) and $\{[\text{Mn}(\text{L})_2(\text{bpy})_2] - (\text{L})\}^+$ fragment (m/z 569.2). (Figure S7 in supporting information).

Cryo-TEM microscopy

Cryo-TEM microscopy analysis of a water solution of **B1** corroborated that either a polymeric or aggregate structure exists in solution. The micrographies show a wide range of aggregates with some morphological differences as is shown in Figure 8. Motifs with different lengths (300-700 nm) are indicative that a polymer structure or aggregates exist in solution.

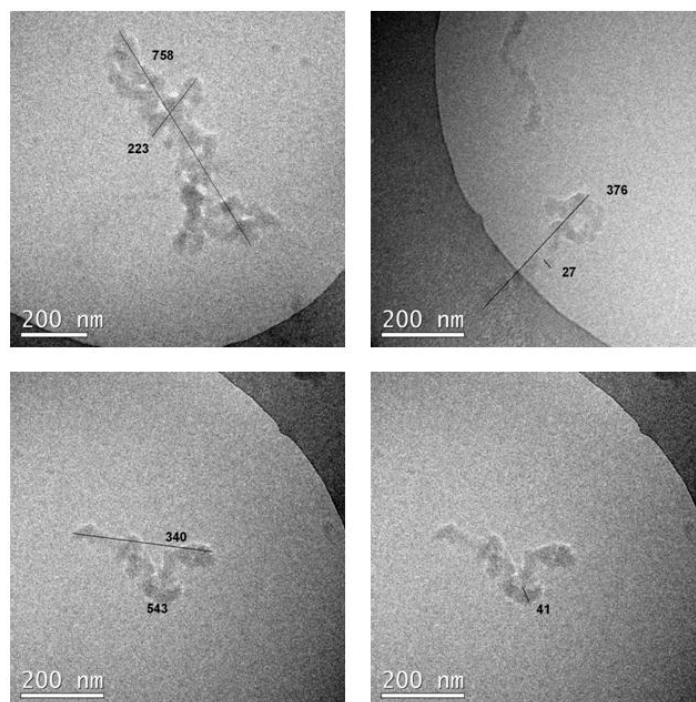


Figure 8. Cryo-TEM micrograph of a solution of **B1** in water

Dynamic Light Scattering (DLS)

The sample studied was a white powder forming colourless solutions in water, diethyl ether and wet dichloromethane. However, aqueous solutions at the highest concentrations (around 100 g/L) were very slightly yellowish with intensive opalescence due to the presence of nanoparticles capable to scatter the light.

No nanoparticles were detected by DLS in diethyl ether solutions meaning that the polymer has been cleaved into small particles with dimensions less than few nanometres. This is in agreement with the trinuclear species described in previous section. A relatively low fraction of nanoparticles with hydrodynamic radius, R_H , around 130 nm in wet dichloromethane were observed. Nevertheless, the structures of these aggregates are difficult to estimate because the preferential sorption of water or stabilization of small droplets of water by surface-active carborane molecules may take also place; the systems have not been therefore further studied.

Aqueous solutions were analysed in detail by means of light scattering. First, samples of different concentration were measured (Figure 9). It is clear that the self-assembly of polymer in water strongly depends on concentration. In very diluted samples ($c < 0.1$ g/L), the infinite polymer structure is completely broken with fragments smaller than 1 nm. At concentrations higher than 0.1 g/L, which can be regarded as so called critical aggregation concentration (CAC), nanoparticles with R_H in range 200-800 nm were observed. The detection of CAC is quite surprising, because it is not usually the case for other carboranes in water.^[21] The distribution of R_H is always monomodal but fairly broad at the highest concentrations (Figure 10.). The worth noticing is the fact that dimensions of nanoparticles increase with concentration especially at $c > 10$ g/L. It means that the process does not obey the so called closed association typical for polymeric micelles and surfactants.^[22] The probable explanation is as follows: the further addition of polymer leads to the elongation of worm-like structures observed by Cryo-TEM (see Figure 8) by merging of small domains with the larger supramolecular structure. The existence of such small domains in water was unambiguously proven by ESI-MS spectrum (mentioned above). This effect is pronounced at the highest concentrations resembling a transition of surfactant micelles to more complex morphologies like cylinders or lamellae.^[23]

In order to reveal the inner structure of the nanoparticles, we studied aqueous solutions with weight fractions of 1.0%, 2.8% and 9.0% by means of X-ray scattering (SAXS and WAXS), which is sensitive to the presence of a periodic structure. Unfortunately, we did not prove the infinite structure in solution, which was otherwise determined by X-ray diffraction in solid

state. Thus, the layers are probably somehow distorted by swelling with water. Nevertheless, the self-assembly in solution should be at least comparable to the situation in crystal. The nanoparticles have worm-like structure that is probably pre-determined by the 1D manganese polymeric structure. The dimensions of nanoparticles (Figure 9 and Figure 10.) are much larger than the thickness of periodic layers in the crystal, and $[\text{Mn}(\text{L})_2(\text{H}_2\text{O})]_n$ units have to be therefore present inside the aggregates as indirectly shown by ESI-MS.

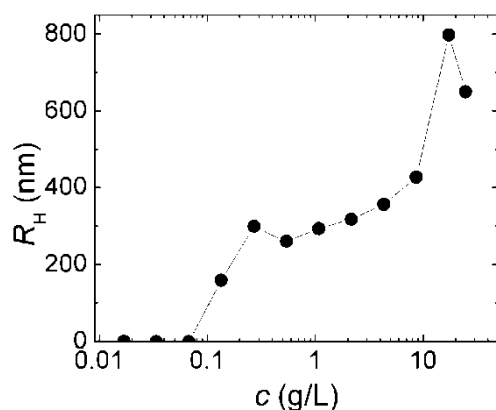


Figure 9. Concentration dependence of hydrodynamic radius of nanoparticles in aqueous solutions of “polymer” measured at scattering angle 90deg

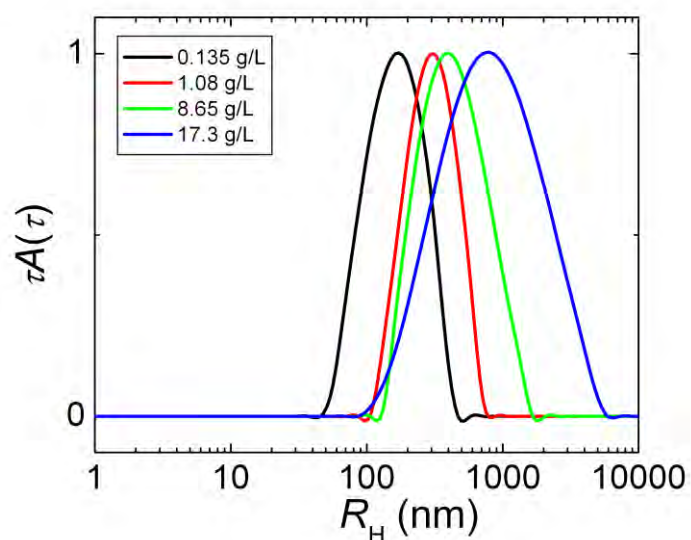


Figure 10. Distribution of hydrodynamic radii of nanoparticles in aqueous solutions of “polymer” at scattering angle 90deg for different concentrations as indicated in graph.

It can be concluded then that the infinite polymeric structure of the sample does not exist in diethyl ether solution. However, it is preserved to a certain extent in water. We can assert that increasing the concentration of polymer in water leads to reassembling of smaller oligomer

units initially generated upon dissolution. By light scattering, the nanoparticles with radii of several hundreds of nanometres at concentrations above CAC (0.1 g/L) were observed. Their shape is quite loose and worm-like. Since the light scattering is an indirect method and SAXS/WAXS experiments were not successful, the exact inner structure of the nanoparticles could not be determined. The formation of the fairly large associates is most probably driven by hydrophobicity of carborane clusters and complexation of $[1\text{-CH}_3\text{-2-CO}_2\text{-1,2-closo-C}_2\text{B}_{10}\text{H}_{10}]^-$ to Mn^{II} . The structure is probably swelled by water. However, it still retains its organized structure comparable to that in solid state and can be imagined as the merging of small $[\text{Mn}(\text{L})_2(\text{H}_2\text{O})]_n$ units into worm-like nanoparticles.

IV.3.4. Magnetic properties

Magnetic structural correlations were performed for compounds **B1**, **B3** and **B5**. As described above, **B1** is a novel 1D Mn^{II} assembly, in which the metallic ions are linked by two $[1\text{-CH}_3\text{-2-CO}_2\text{-1,2-closo-C}_2\text{B}_{10}\text{H}_{10}]^-$ ligands and one H_2O molecule. In the crystal, all $\text{Mn}\cdots\text{Mn}$ distances are equivalent, therefore the system could be magnetically described just using one exchange coupling, J . Plots showing the thermal evolution of the magnetic molar susceptibility, χ_{M} and $\chi_{\text{M}}T$ are shown in Figure 11a. These solid-state, variable-temperature (2.0- 300 K) data were collected on polycrystalline samples using 0.02 T (from 2 to 30 K) and 0.3 T (from 2 to 300 K) fields.

The $\chi_{\text{M}}T$ data at room temperature ($4.47 \text{ cm}^3 \text{ mol}^{-1} \text{ K}$) agrees well with the spin-only value expected for a high-spin Mn^{II} ion ($4.375 \text{ cm}^3 \text{ mol}^{-1} \text{ K}$ when $g = 2$). The magnetic answer decreases continuously from 300 K down to 50 K, and then rapidly upon further cooling. This behaviour is indicative of a weak antiferromagnetically coupled system and it is also portrayed in the χ_{M} vs T graph. The magnetic molar susceptibility displays a maximum at 5 K and decreases very quickly afterwards (Figure 11a). The interaction through the triple bridge was evaluated by the modified expression for a classical Heisenberg chain, derived by Fisher, based on the exchange Hamiltonian $H = -J\sum_i S_i S_{i+1}$.^[24] The best fit parameters were found for $J = -0.91 \text{ cm}^{-1}$, $g = 2.01$, TIP of $80 \times 10^{-6} \text{ cm}^3 \text{ mol}^{-1}$ and $R = 8 \times 10^{-5}$.

The water bridge and syn-syn arrangement of the two carboxylate ligands lead the magnetic answer of this new array providing a good overlap of magnetic orbitals and therefore displaying antiferromagnetic behaviour. The weakness of the coupling has been already observed in similar aqua-bridged MOFs^[25] and binuclear complexes, where $\text{Mn-O}_{\text{H}_2\text{O}}$ and $\text{Mn}^{\text{II}}\cdots\text{Mn}^{\text{II}}$ distances are relatively long and the $\text{Mn}-(\text{OH}_2)\text{-Mn}$ angle is always higher than 108° (Table 3). The coupling through the water bridge has been proven even weaker than the

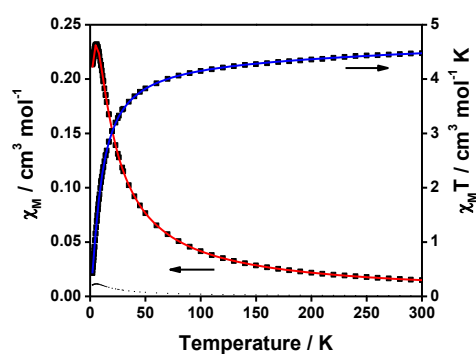
coupling observed for OH- and OR-bridged species (strength order: $O_2^- > OH^- > H_2O$).^[6c, 26] **Table**

3. Crystallographic and magnetic comparison between complex B1 and previous literature works.

	B1*	2	3*	4	5*	6*	7*	8
Mn...Mn (Å)	3.78	3.51	3.77	3.75	3.59	3.62	3.61	3.77
Mn(OH ₂)-Mn(°)	109.	-	114.	114.	110.	110.	108.	114.
Mn-OH ₂ (Å)	2.32	2.26	2.24	2.22	2.18	2.21	2.25	2.24
<i>G</i>	2.01	-	1.97	-	1.93	2.01	2.0	-
<i>J</i> (cm ⁻¹)	-	-	-1.26	-	-2.73	2.95	-1.0	-

* $H = -2JS_{i+1}$. ** Number **B1** corresponds to this work where $H = -JS_{i+1}$.

a)



b)

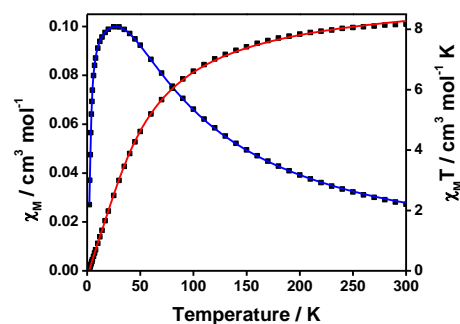


Figure 11. Experimental data including χ_M vs T (y axis on the left side) and $\chi_M T$ vs T (y axis on the right side) between 2.0 and 300.0 K. The experimental points are shown as black squares and the red and blue lines correspond to the theoretical values, also in that order of a) **B1**, b) **B3**.

Compound **B3** is a novel binuclear Mn^{II} cluster, where the metallic ions are linked by four [1-CH₃-2-CO₂-1,2-*closo*-C₂B₁₀H₁₀]⁻ ligands, in a so-called paddle-wheel arrangement. The bulky nature of the ligand prevents intermolecular interactions among neighbouring molecules. Plots showing the thermal evolution of the magnetic molar susceptibility, χ_M , and $\chi_M T$ are shown in Figure 11b. These solid-state, variable-temperature (2.0K - 300.0K) data were collected on polycrystalline samples using 1.0 T field. The $\chi_M T$ data of 8.17 cm³ mol⁻¹ K at room temperature is closer to the expected value for two isolated Mn^{II} atoms. Magnetic susceptibility data decreases continuously from 300K up to 100K, and then rapidly to 0.05 cm³ mol⁻¹ K upon

further cooling. This behaviour is indicative of a weak antiferromagnetically coupled system and it is also portrayed in the χ_M vs T graph. The magnetic molar susceptibility displays a maximum at 25 K and decreases very quickly afterwards (Figure 11b). The interaction through the triple bridge was evaluated by the modified expression for a classical Heisenberg based on the exchange Hamiltonian $H = -J\sum S_i S_{i+1}$ modified to take into account the presence of impurities (ρ).^[24b] The equation used was described for a binuclear system with $S_1 = S_2 = 5/2$ and applied to fit the experimental $\chi_M T$ vs T plot by means of a least-square method. The best fit parameters were found for $J = -6.58 \pm 0.04 \text{ cm}^{-1}$, $g = 2.02 \pm 0.003$, $\rho = 0.2 \%$, a constant TIP value of $60 \times 10^{-6} \text{ cm}^3 \text{ mol}^{-1}$ and $R = 1.2 \times 10^{-5}$.

Finally, compound **B5** is also a novel 1D Mn^{II} assembly, where the metallic ions are linked by 2,2'-bipyrimidine groups and each Mn^{II} ion coordinates to two [1- CH_3 -2- CO_2 -1,2-*closo*- $\text{C}_2\text{B}_{10}\text{H}_{10}$] $^-$ ligands in a monodentate mode completing this way the octahedral geometry of the metal centres. Here, the carboxylate group does not get involved in the magnetic exchange but assist separating the chains among each other. In the crystal, all the manganese distances are equivalent and magnetically the system could be described just using one exchange coupling, J .

Plots showing the magnetic molar susceptibility, χ_M (inset), and $\chi_M T$ are shown in Figure 12. These solid-state, variable-temperature (2K - 300K) data were collected on polycrystalline samples using 0.02 T (from 2 to 30K) and 0.3 T (from 2 to 300K) fields. The $\chi_M T$ data of **B5** at room temperature ($4.43 \text{ cm}^3 \text{ mol}^{-1} \text{ K}$) agrees well with the spin-only value expected for a high-spin Mn^{II} ion ($4.38 \text{ cm}^3 \text{ mol}^{-1} \text{ K}$ when $g = 2.0$). The magnetic answer remains practically unchanged from the highest temperatures until 100 K providing a plateau that decreases then rapidly upon further cooling (2K). This behaviour is indicative of a weak antiferromagnetically coupled system indicative of not strong magnetic exchanges through the 2,2'-bipyrimidine groups. This fact is also indicated in the magnetic molar susceptibility that displays a maximum at 5K and decreases very quickly afterwards (Figure 12, inset). In addition, the plot of the reduced magnetization vs. field does not follow the Brillouin function due to the small AF exchange among the Mn^{II} within the chain (Figure 13).

The interaction through the 2,2'-bipyrimidine bridge was evaluated by the modified expression for a classical Heisenberg chain derived by Fisher based on the exchange Hamiltonian $H = -J\sum S_i S_{i+1}$.^[24] The best fit parameters were found for $J = -0.70 \text{ cm}^{-1}$, $g = 2.01$, TIP of $780 \times 10^{-6} \text{ cm}^3 \text{ mol}^{-1}$ and $R = 1 \times 10^{-4}$.

Overall, it can be concluded that the bridging ligands do provide weak antiferromagnetic interactions among the Mn^{II} centres and that each chain is well-isolated to the neighbours thanks to the $[1-CH_3-2-CO_2-1,2-closo-C_2B_{10}H_{10}]^-$ ligands.

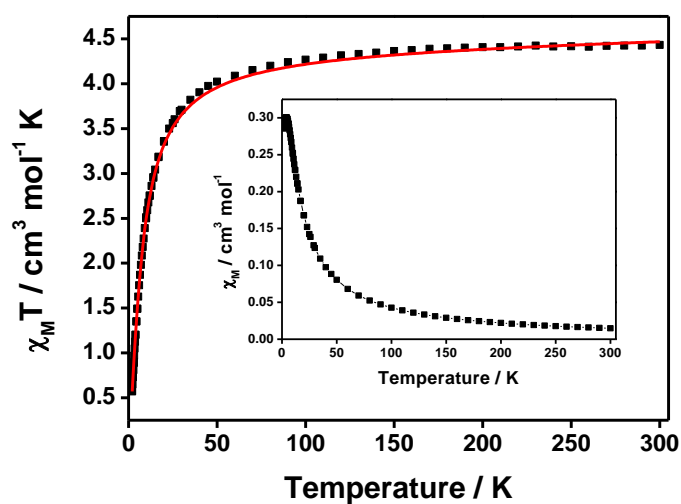


Figure 12. Experimental data including $\chi_M T$ vs T and χ_M vs T (inset) of **B5** between 2.0 and 300.0 K. The experimental points are shown as black squares and the red line corresponds to the theoretical fitting.

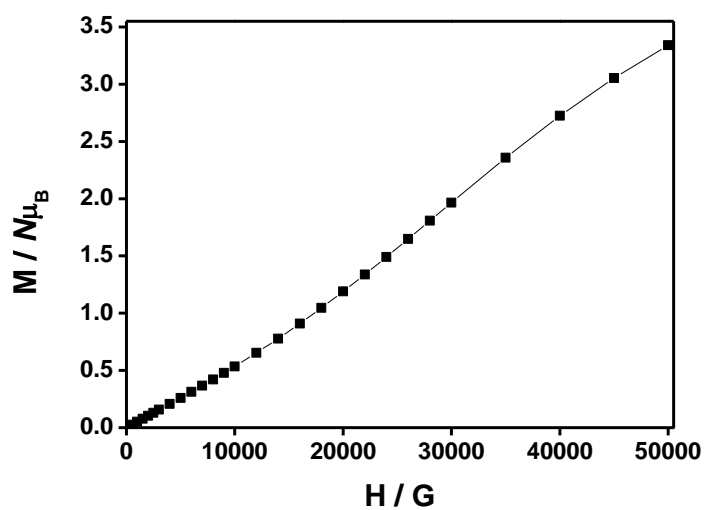


Figure 13. Experimental data including $\chi_M T$ vs T and χ_M vs T (inset) of **B5** between 2 and 300 K. The experimental points are shown as black squares and the red line corresponds to the theoretical fitting.

IV.4. Conclusions

A family of new manganese (II) complexes containing the ligand [1-CH₃-2-CO₂-1,2-closo-C₂B₁₀H₁₁], LH, has been synthesized and thoroughly characterized by analytical, spectroscopic (IR, NMR, UV-vis, ESI-MS), electrochemical, microscopic (Cryo-TEM) and scattering (DLS, SAXS) techniques. Magnetics measurements were carried out of polynuclear compounds showing in all cases weak antiferromagnetic interactions between the manganese atoms. The X-Ray structure of all complexes has been obtained showing uncommon nuclearities. Besides, Mn···Mn bridging water units have been observed for the first time.

The X-Ray structure of compound **B1** disclosed an unusual 1D manganese(II) polymer chain in which each of the Mn(II) ions is coordinated by four carboxylate oxygen atoms and two aqua oxygen atoms displaying a distorted octahedral geometry. The manganese centres are bridged by two carboranylcarboxylate and one aqua ligands.

The polymeric nature of **B1** can be easily fragmented with coordinating solvents, e.g. diethyl ether or by reaction with chelating ligands such as 2,2'-bpy or 2,2'-bpm.

Trinuclear compound **B2** displays a structure in which the inner Mn···Mn pairs maintain the precise picture found in **B1** with the bridging water unit and the two bridging carboxylate ligands while the terminal Mn ions evidence their origin as a result of fragmenting the polymer. Terminal Mn centres in the oligomers contain one monodentate carboranylcarboxylate ligand, one terminal water molecule and one terminal fragmenting solvent, Et₂O in this case. The clean way of fragmentation of the polymer enables a reverse process, allowing the regeneration of the polymer structure. This easy assembling disassembling process is, most probably, what endows **B1** its notorious solubility properties, and its aggregation concentration dependent ability as shown by the DLS studies.

It was observed that, when **B1** reacts with the ligand 2,2'-bpy the result product is depending of the ligand/complex ratio. When the ligand/complex ratio is 1:2, the binuclear complex **B3** is obtained in which each manganese(II) atom is coordinated by four oxygen atoms one of each of the four syn,syn η¹: η¹: μ²-carboxylate bridge and two nitrogen atoms of one 2,2'-bpy ligand displaying trigonal prismatic geometry. Nevertheless, if the ligand/complex ratio is 1:1 the mononuclear compound **B4** is synthesized which shows a distorted octahedral structure where the Mn(II) atom is coordinated by two oxygen atoms from two monodentate carboranylcarboxylate ligands and four nitrogen atoms from two 2,2'-bpy ligands. Finally, when complex **B1** reacts with the tetradentate ligand 2,2'-bpm, a novel 1D Mn(II) polymeric structure, **B5**, is obtained consisting of neutral zigzag chains of manganese (II) ions linked by

2,2'-bpm. Each Mn(II) ion coordinates to two **L** ligands in a monodentate mode completing this way the distorted octahedral geometry of the metal centres.

Cyclic voltammogram of complexes in general exhibits oxidation waves corresponding to the oxidation of Mn(II) to Mn(III). In the case of polymer **B1** an increased background water oxidation is also observed above 1.4 V. For the mononuclear compound **B4**, the CV exhibits two anodic peaks that could be assigned to a metal oxidation process together with chemical reactions leading to the formation of binuclear species.

IV.5. Experimental section

V.5.1. Instrumentation and measurements

Instrumentation and Measurements. FT-IR spectra were taken in a Mattson-Galaxy Satellite FT-IR spectrophotometer containing a MKII Golden Gate Single Reflection ATR System. Elemental analyses were performed using a CHNS-O Elemental Analyser EA-1108 from Fisons. ESI-MS spectra have been performed in a Thermo Quest Finnigan Navigator LC/MS chromatograph. UV-Vis spectroscopy was performed on a Cary 50 Scan (Varian) UV-Vis spectrophotometer with 1 cm quartz cells or with an immersion probe of 5 mm path length. NMR spectra have been recorded with a Bruker ARX 300 or a DPX 400 instrument equipped with the appropriate decoupling accessories $^1\text{H}\{^{11}\text{B}\}$ NMR (300.13/400.13 MHz), and $^{11}\text{B}\{^1\text{H}\}$ NMR (96.29/128.37 MHz) spectra were recorded in D_2O and CH_3OD . Chemical shift values for ^{11}B NMR spectra were referenced to external $\text{BF}_3\leftarrow\text{OEt}_2$ and those for $^1\text{H}\{^{11}\text{B}\}$ spectra were referenced to SiMe_4 . Chemical shifts are reported in units of parts per million downfield from reference, and all coupling constants in Hz. Cyclic Voltammetric (CV) experiments were performed in a IJ-Cambria IH-660 potentiostat using a three electrode cell. A Pt (2 mm diameter) or graphite (3 mm diameter) electrodes were used as working electrode, platinum wire as auxiliary and SCE as the reference electrode. Measurements were recorded in water solutions using 0.1 M KPF_6 as supporting electrolyte, dichloromethane solutions, using 0.1 M TBAH as supporting electrolyte or methanol solutions using NH_4ClO_4 as supporting electrolyte at scan rate of $100 \text{ mV}\cdot\text{s}^{-1}$. All cyclic voltammograms presented in this work were recorded under nitrogen atmosphere. All $E_{1/2}$ values estimated from cyclic voltammetry were calculated as the average of the oxidative and reductive peak potentials $(E_{\text{pa}}+E_{\text{pc}})/2$ at a scan rate of 100 mV/s.

Magnetic Susceptibility Studies. Magnetic susceptibility measurements between 2.0 and 300.0 K were carried out in a SQUID magnetometer Quantum Design Magnetometer, model MPMP. Susceptibility measurements were performed using a field of 1.0 T. Pascal's constants were used to estimate the diamagnetic corrections for the compound. The fit was performed by minimizing the function $R = \sum(\chi\text{MT})_{\text{exp}} - (\chi\text{MT})_{\text{calc}}/2/\sum(\chi\text{MT})_{\text{exp}}^2$.

Microscopy Studies (Cryo-TEM). The studies were performed by using a Jeol JEM-1400 electron microscope operating at 120 kV and equipped with a CCD multiscan camera (Gatan). The microscope was equipped with a Gatan cryoholder and the samples were maintained at -177°C during imaging. Micro drops (2 μL) of the water solutions of amphiphiles were blotted onto holey carbon grids (Quantifoil) previously glow discharged in a BAL-TEC MSC 010 glow

discharger unit, which were immediately plugged into liquid ethane at -180 °C using a Leica EM CPC cryoworkstation.

Scattering Studies: Dynamic Light Scattering (DLS) and Static Light Scattering (SLS). In the Dynamic Light Scattering (DLS) and Static Light Scattering (SLS) studies the light scattering setup (ALV, Langen, Germany) consisted of a 633 nm He-Ne laser, an ALV CGS/8F goniometer, an ALV High QE APD detector, and an ALV 5000/EPP multibit, multitaup autocorrelator. DLS data analysis was performed by fitting the measured normalized intensity autocorrelation function $g_2(t) = 1 + \beta |g_1(t)|^2$, where $g_1(t)$ is the electric field correlation function, t is the lag-time and β is a factor accounting for deviation from the ideal correlation. An inverse Laplace transform of $g_1(t)$ with the aid of a constrained regularization algorithm (CONTIN) provides the distribution of relaxation times, $\tau A(\tau)$. Effective angle- and concentration-dependent hydrodynamic radii, $R_H(q,c)$, were obtained from the mean values of relaxation times, $\tau_m(q,c)$, of individual diffusive modes using the Stokes-Einstein equation. The SLS data were treated by the standard Zimm or Berry method. As the refractive index increment is unknown, SLS scattering curves were used only for calculation of radius of gyration R_g . Samples for DLS measurements were dissolved in deionized water in concentration range 0.0169 – 24.8 g/L, where solutions of lower concentrations were typically prepared by dilution of the stock solution by filtered water. Solutions in diethyl ether and dichloromethane with concentrations about 1 g/L were also prepared. In case of dichloromethane, few droplets of water had to be added in order to obtain a clear solution. For combined SAXS/WAXS experiments, aqueous solutions with weight fractions of the sample 1.0%, 2.8% and 9.0% were prepared.

X-ray structure determination. Measurement of the crystals were performed on a Bruker Smart Apex CCD diffractometer using graphite-monochromated Mo $K\alpha$ radiation ($\lambda = 0.71073\text{\AA}$) from an X-Ray tube. Data collection, Smart V. 5.631 (BrukerAXS 1997-02); data reduction, Saint+ Version 6.36A (Bruker AXS 2001); absorption correction, SADABS version 2.10 (Bruker AXS 2001) and structure solution and refinement, SHELXTL Version 6.14 (Bruker AXS 2000-2003).

V.5.2. Materials

All reagents used in the present work were obtained from Aldrich Chemical Co and were used without further purification. Reagent grade organic solvents were obtained from SDS and high purity de-ionized water was obtained by passing distilled water through a nano-pure Mili-Q water purification system. 1-CH₃-1,2-closo-C₂B₁₀H₁₁ was purchased from Katchem.

V.5.3. Preparations

The 1-CH₃-2-CO₂H-1,2-closo-C₂B₁₀H₁₀ ligand was prepared according to literature procedures^[27] with some modifications as described in Chapter III. All synthetic manipulations were routinely performed under ambient conditions.

Synthesis of [Mn(μ-H₂O)(1-CH₃-2-CO₂-1,2-closo-C₂B₁₀H₁₀)₂]_n · (H₂O)_n, B1. To a suspension of 0.249 g (1.233 mmols) of 1-CH₃-2-CO₂H-1,2-closo-C₂B₁₀H₁₀, LH, in 20 mL of water was added 0.142 g (1.233 mmols) of MnCO₃ in 5 mL of water. The solution was stirred and heated to 40°C for 2h. Afterward, the solution was filtered and the solvent was removed under vacuum to obtain a white solid. The latter was crystallized by slow evaporation of a dichloromethane solution. Yield: 0.274g (94%). ¹H{¹¹B} NMR (400.13 MHz, D₂O, 25°C): δ= 2.33 (br s, B-H), 2.20 (br s, B-H), 2.10 (br s, B-H), 2.03 (br s, B-H), 1.96 (br s, B-H), 1.93 (s, CH₃). ¹¹B{¹H} NMR (128.37, D₂O, 25°C): δ= -4.1 (¹J(B,H)= 148.9, 2B), -7.0 (¹J(B,H)= 150.3, 2B), -10.10 (¹J(B,H)= 118.1, 3B), -10.93 (¹J(B,H)= 142.5, 3B). IR: $\bar{\nu}$ = 3632, 3379 ν (OH), 3201 ν (CH₃), 2627, 2583 ν (B-H), 1619, 1568 ν (COO⁻)_{as}, 1381 ν (COO⁻)_{sim}, 1196, 1149, 844 δ (O-H), 725 ν (B-C) cm⁻¹. Anal. Found (calcd.) (%) for C₈H₂₈O₅B₂₀Mn: C 20.24(20.21); H 5.81(5.94).

Synthesis of [Mn₃(H₂O)₄(1-CH₃-2-CO₂-1,2-closo-C₂B₁₀H₁₀)₆(C₄H₁₀O)₂], B2. By recrystallization of **B1** in a diethyl ether solution and then slow diffusion of pentane into this solution, colourless needles suitable for X-ray diffraction were obtained corresponding to complex **B2**.

Synthesis of [Mn₂(1-CH₃-2-CO₂-1,2-closo-C₂B₁₀H₁₀)₄(bpy)₂], B3. To a solution of 0.063 g (0.132 mmols) of [Mn(μ-H₂O)(μ-Me-COO-C₂B₁₀H₁₀)₂]_n, **B1**, in 2 mL of ethanol was added 0.021 g (0.132 mmols) of 2, 2'-bipyridine in 1 mL of ethanol. The solution pale yellow was stirred for 30 min and filtered. Afterward the volume of the resulting solution was reduced to 1 ml, obtaining a precipitate that was washed with diethyl ether. The resulting solid was recrystallized in EtOH. Yield: 0.060g (74%). ¹¹B{¹H} NMR (128.37, CH₃OD, 25°C): δ= -3.3 (6B), -6.4 (2B), -7.8 (2B). IR: $\bar{\nu}$ = 2577 ν (B-H), 1692 ν (COO⁻)_{as}, 1597, 1577, 1474, 1440, 1362 ν (COO⁻)_{sim}, 1017, 845, 758 ν (B-C), 735 cm⁻¹. UV-Vis (CH₂Cl₂, 1.10⁻⁴ M) λ_{max} (ϵ): 470 nm (307 M⁻¹cm⁻¹), 650 nm (134 M⁻¹cm⁻¹). Anal. Found (calcd.) (%) for C₃₆H₆₈O₈B₄₀N₄Mn₂: C 35.06(35.23); N 4.40(4.57); H 5.56(5.58).

Synthesis of [Mn(1-CH₃-2-CO₂-1,2-closo-C₂B₁₀H₁₀)₂(bpy)₂], B4. This compound was prepared following a method analogous to that described for **B3** using 0.06 g (0.127 mmols) of **B1** and 0.04 g (0.254 mmols) of 2,2'-bipyridine as starting materials to afford air-stable yellow crystals of **B4**, suitable for X-ray diffraction analysis. Yield: 0.060 g (62 %). IR: $\bar{\nu}$ = 3329, 2576 ν (B-H), 1693, 1664 ν (COO⁻)_{as}, 1598, 1576, 1474, 1439, 1363 ν (COO⁻)_{sim}, 1016, 831, 760 ν (B-C), 736

cm^{-1} . UV-Vis (CH_2Cl_2 , 1.10^{-4} M) λ_{max} (ϵ): 772 nm ($7 \text{ M}^{-1}\text{cm}^{-1}$). Anal. Found (calcd.) (%) for $\text{C}_{28}\text{H}_{42}\text{O}_4\text{B}_{20}\text{N}_4\text{Mn}$: C 43.65(43.69); H 5.37(5.50); N 7.40(7.28).

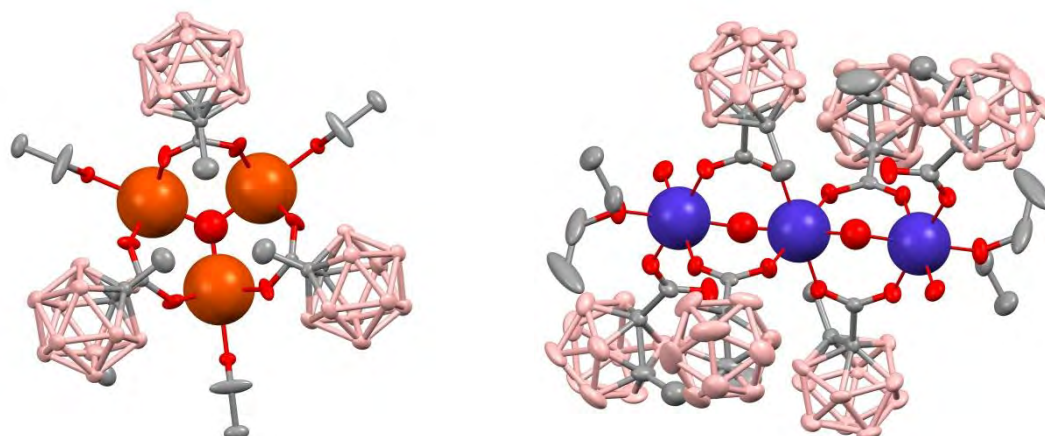
Synthesis of $[\text{Mn}(\mathbf{1}\text{-CH}_3\text{-2-CO}_2\text{-1,2-closo-C}_2\text{B}_{10}\text{H}_{10})_2(\text{bpm})]_n$, **B5.** Addition of a solution of 2,2'-bipyrimidine (0.017 g, 0.105 mmols) in CH_2Cl_2 (2 ml) to a solution of **B1** (0.049 g, 0.103 mmols) in CH_2Cl_2 (3 mL) quickly generates a yellow precipitate. The resulting solid was recrystallized in EtOH. After several days, air-stable, yellow crystals of **B5**, suitable for X-ray diffraction analysis, were obtained. Yield: 0.055 g (88 %). Anal. Found (calcd.) (%) for $\text{C}_{16}\text{H}_{32}\text{O}_4\text{B}_{20}\text{N}_4\text{Mn} \cdot 0.35 \text{CH}_2\text{Cl}_2$: C 30.40(30.43); H 5.20(5.11); N 8.38(8.68). IR(cm^{-1}): $\nu = 3403, 2975, 2592, 2579 \nu$ (B-H), $1651 \nu(\text{COO}^-)_{\text{as}}$, $1629, 1572, 1409, 1353 \nu(\text{COO}^-)_{\text{sim}}$, $1342, 1276, 1047, 1019, 725 \nu$ (B-C), 690, 666.

IV.6. References

- [1] a) P.T. Anastas, J. C. Warner, *Green Chemistry: Theory and Practice*, Oxford University Press, Oxford, U.K., 1998.; b) M. Lancaster, *Green Chemistry: An Introductory Text*, RSC, London, 2002.; c) M. Poliakov, J.M. Fitzpatrick, T.R. Farren, P. T. Anastas, *Science*, 2002, 297, 807; d) P.T. Anastas, M. M. Kirchhoff, *Acc. Chem. Res.*, 2002, 35, 686; e) R. A. Sheldon, *Green Chem.*, 2005, 7, 267; f) M. Lancaster, J.H. Clark, D. J. Macquarrie, *In Handbook of Green Chemistry and Technology*, Eds. Blackwell Publishing: Abingdon, U.K., 2002.; g) R.A.Sheldon, I. Arends, U. Hanefeld, Wiley-VCH: Weinheim, Germany, 2007,
- [2] a) C.-J. Li, *J. Chem. Rev.*, 2005, 105, 3095; b) J.H. Clark, S. Taverner, *J. Org. Process Res. Dev.*, 2007, 11, 149; c) C.I. Herreras, X. Yao, L. Z.C.-J. Li, *Chem. Rev.*, 2007, 107, 2546; d) C.-J. Li, T. H. Chan, *Comprehensive Organic Reactions in Aqueous Media*, Wiley-VCH: Weinheim, Germany, 2007.; e) U. M. Lindström, *Organic Reactions in water*, Blackwell Publishing, Oxford, U. K., 2007.; f) A. Chanda, V. V. Fokin, *Chem. Rev.*, 2009, 109, 725; g) F. M. Kerton, *Alternatives Solvents for Green Chemistry*, RSC Publishing, Cambridge, U.K., 2009.; h) R. Skouta, *Green Chem. Lett. Rev.*, 2009, 2, 121; i) P. T. Anastas, C.-J. Li, Eds. *Handbook of Green Chemistry*, Vol.5, Wiley-VCH, Weinheim, Germany, 2010,
- [3] a) M. Eddaoudi, D.B. Moler, H. Li, B. Chen, T.M. Reineke, M. O'Keeffe, O. M. Yaghi, *Acc. Chem. Res.*, 2001, 34, 319; b) B. Moulton, M. J. Zaworotko, *Curr. Opin. Solid State Mater. Sci.*, 2002, 6, 117; c) C. Janiak, *J. Chem. Soc., Dalton Trans.*, 2003, 2781; d) O.M. Yaghi, M. O'Keeffe, N.W. Ockwig, H.K. Chae, M. Eddaoudi, J. Kim, *Nature Chemical Biology*, 2003, 423, 705; e) U. Mueller, M. Schubert, F. Teich, H. Puetter, K. Schierle-Arndt, J. Pastre, *J. Mater. Chem.*, 2006, 16, 626; f) M. Andruh, *Chem. Commun.*, 2007, 2565; g) B. Wang, A.P. Cote, H. Furukawa, M. O'Keeffe, O. M. Yaghi, *Nature Chemical Biology*, 2008, 453, 207; h) B. Moulton, M. J. Zaworotko, *Chem. Rev.*, 2001, 101, 1629; i) A.K. Cheetham, C.N.R. Rao, R. K. Feller, *Chem. Commun.*, 2006, 4780.
- [4] a) D.C. Weatherburn, S. Mandal, S. Mukhopadhyay, S. Bahduri, L. F. Lindoy, *Manganese in Comprehensive Coordination Chemistry II*, 5, (Eds.: J. A. McCleverty, T. J. Meyer) Elsevier Pergamon, Oxford 2004, 1; b) S Mukhopadhyay, S. K. Mandal, S. Bhaduri, W. H. Armstrong, *Chem. Rev.*, 2004, 104,, 3981.
- [5] a) D. MasPOCH, D. Ruiz-Molina, J. Veciana, *Chem. Soc. Rev.*, 2007, 36, 770; b) X. Lin, J. Jia, P. Hubberstey, M. Schroeder, N. R. Champness, *CrystEngComm*, 2007, 9, 438; c) C.L. Cahill, D.T. de Lill, M. Frisch, *CrystEngComm*, 2007, 9, 15.
- [6] a) A. Caneschi, F. Ferraro, D. Gatteschi, M. Ch. Melandri, P. Rey, R. Sessoli,, *Angew. Chem. Int. Ed. Engl.*, 1989, 28, 1365; b) S.B. Yu, A. Bino, I. Shweky, S. J. Lippard, *Inorg. Chem.*, 1992, 31, 3502; c) B-H. Ye, T. Mak, I.D. Williams, X. Y. Li, *Chem. Commun.*, 1997, 1813.
- [7] a) R.L. Rardin, P. Poganiuch, A. Bino, D.P Goldberg, W.B. Tolman, S. Liu, S. J. Lippard, *J. Am. Chem. Soc.*, 1992, 114,, 5240; b) M-H. Zeng, M-C. Wu, H. Liang, Y-L. Zhou, X-M. Chen, S. W. Ng,, *Inorg. Chem.*, 2007, 46, 7241.
- [8] a) H. Jude, H. Disteldorf, S. Fischer, T. Wedge, A. M. Hawkrige, A. M. Arif, M. F. Hawthorne, D. C. Muddiman, P. Stang, *J. Am. Chem. Soc.*, 2005, 127, 12131; b) R. N. Grimes, *Angew. Chem. Int. Ed. Engl.*, 1993, 32, 1289; c) M. A. Fox, A. K. Hughes, *Coord. Chem. Rev.*, 2004, 248, 457
- [9] a) O. Kriz, A. L. Rheingold, M. Y. Shang, T. P. Fehlner, *Inorganic Chemistry*, 1994, 33, 3777; b) M. Fontanet, A. R. Popescu, X. Fontrodona, M. Rodriguez, I. Romero, F. Teixidor, C. Viñas, E. Ruiz, *Chem. Eur. J.*, 2011, 17, 13217.
- [10] a) V.L. Pecoraro, M.J. Baldwin, A. Gelasso, *Chem. Rev.*, 1994, 94, 807; b) L. Que, J. A. E. Trye, *Prog. Inorg. Chem.*, 1990, 38, 97.
- [11] D.J. Price, S.R. Batten, B. Moubaraki, K. S. Murray, *Polyhedron*, 2003, 22, 2161.
- [12] Y. Umena, K. Kawakami, J-R. Shen, N. Kamiya, *Nature*, 2011, 473, 55.
- [13] D. H. Wu, J. Shi, Y. J. Shi, G. Q. Jang, *Act. Crystallorg., Sect. E: Struc. Rep. Online.*, 2008, 64, m161.
- [14] Remy van Gorkum, Francesco Buda, Huub Kooijman, Anthony L. Spek, Elisabeth Bouwman, J. Reedijk, *Eur. J. Inorg. Chem.*, 2005, 2255.

- [15] a) E. Garribba, G. Micera, M. Zema, *Inorganica Chimica Acta*, 2004, 357, 2038; b) V. Gómez, M. Corbella, *J. Chem. Crystallogr.*, 2011, 41, 843; c) N. Palanisami, R. Murugavel, *Inorganica Chimica Acta*, 2011, 365, 430; d) B. Albela, M. Corbella, J. Ribas, I. Castro, J. Sletten, H. Stoeckli-Evans, *Inorg. Chem.*, 1998, 37, 788.
- [16] a) D.M. Hong, H.H. Wei, L.L. Gan, G.H. Lee, Y. Wang, *Polyhedron* 1996, 15, 2335; b) G. D. Munno, T. Poerio, M. Julve, F. Lloret, G. Viau, A. Caneschi, *J. Chem. Soc., Dalton Trans.*, 1997, 601; c) D. Armentano, G. d. Munno, F. Guerra, J. Faus, F. Lloret, M. Julve, *Dalton Trans.*, 2003, 4626.
- [17] a) A. Manivel, N. Ilayaraja, D. Velayutham, M. Noel, *Electrochimica Acta*, 2007, 52, 7841; b) Y. Gao, R. H. Crabtree, G. W. Brudvig, *Inorganic Chemistry*, 2012, 51, 4043.
- [18] a) M. M. Morrison, D. T. Sawyer, *Inorganic Chemistry*, 1978, 17, 333; b) M.-N. C. Dunand-Sauthier, A. Deronzier, I. Romero, *Journal of Electroanalytical Chemistry*, 1997, 436, 219; c) M.-N. Collomb Dunand-Sauthier, A. Deronzier, X. Pradon, S. Ménage, C. Philouze, *Journal of the American Chemical Society*, 1997, 119, 3173.
- [19] a) T. S. Davis, J. P. Fackler, M. J. Weeks, *Inorganic Chemistry*, 1968, 7, 1994; b) R. Dingle, *Acta Chem. Scand.*, 1966, 20, 33.
- [20] a) L. J. Todd, A. R. Siedle, *Prog. Nucl. Magn. Reson. Spectrosc.*, 1979, 13, 87; b) R. C. Mehrotra, R. Bohra, *Metal Carboxylates*, Academic, New York, 1983, 396; c) L. A. Leites, *Chem. Rev.*, 1992, 92, 279
- [21] a) P. Matejicek, P. Cigler, K. Prochazka, V. Kral, *Langmuir* 2006, 22, 575; b) P. Matejicek, P. Cigler, A. B. Olejniczak, A. Andrysiak, B. Wojtczak, K. Prochazka, Z. J. Lesnikowski, *Langmuir*, 2008, 24, 2625; c) M. Uchman, P. Jurkiewicz, P. Cigler, B. Gruner, M. Hof, K. Prochazka, P. Matejicek, *Langmuir* 2010, 26, 6268.
- [22] P. Alexandridis, J. F. Holzwarth, T. A. Hatton, *Macromolecules*, 1994, 27, 2414.
- [23] A. Bernheim-Groswasser, R. Zana, Y. Talmon, *J. Phys. Chem. B*, 2000, 104, 4005.
- [24] a) M. E. Fisher, *Am. J. Phys.*, 1964, 32, 343; b) O. Kahn, *Molecular Magnetism*, VCH, New York, 1993, 258.
- [25] a) Z. Su, S.-S. Chen, J. Fan, M.-S. Chen, Y. Zhao, W.-Y. Sun, *Cryst. Growth. Des.*, 2010, 10, 3675; b) C.-Y. Niu, X.-F. Zheng, X.-S. Wan, C.-H. Kou, *Cryst. Growth. Des.*, 2011, 11, 2874.
- [26] a) R. A. Reynolds III, W. R. Dunham, D. Coucouvanis, *Inorg. Chem.*, 1998, 37, 1232; b) B.-H. Ye, I. D. Williams, X.-Y. Li, *J. Inorg. Biochem.*, 2002, 92, 128; c) D. Coucouvanis, R. A. Reynolds III, W. R. Dunham, *J. Am. Chem. Soc.*, 1995, 117, 7570; d) Y.-L. Shen, S.-L. Sun, W.-D. Song, *Acta Cryst. Section E*, 2007, E63, m1309.
- [27] U. Venkatasubramanian, D. J. Donohoe, D. Ellis, B. T. Giles, S. A. Macgregor, S. Robertson, G. M. Rosair, A. J. Welch, A. S. Batsanov, L. A. Boyd, R. C. B. Copley, M. A. Fox, J. A. K. Howard, K. Wade, *Polyhedron*, 2004, 23, 629

CHAPTER V. Study of the reactivity of the carboranyl-carboxylate ligand 1-CH₃-2-CO₂H-1,2-closo-C₂B₁₀H₁₀ with Fe and Co.



Four new polynuclear complexes containing the carboranylcarboxylate ligand, 1-CH₃-2-CO₂H-1,2-closo-C₂B₁₀H₁₀ and iron or cobalt atoms have been synthesized and thoroughly characterized by analytical and spectroscopic (NMR, IR, UV-visible) techniques. X-ray crystallographic structure of all complexes has been resolved showing trinuclear oxo-centred mixed valence carboxylate bridged complexes for iron ion and bi- and trinuclear complexes for cobalt ion, in which the metal ions are held together through two carboranylcarboxylate ligands and one aqua molecule.

TABLE OF CONTENTS

CHAPTER V. Study of the reactivity of the carboranyl-carboxylate ligand 1-CH₃-2-CO₂H-1,2-closo-C₂B₁₀H₁₀ with Fe and Co.

V.1.	Introduction	113
V.2.	Objectives	115
V.3.	Results and discussion	116
V.3.1.	Synthesis and structure	116
V.3.1.1.	Iron complexes	116
V.3.1.2.	Cobalt complexes	121
V.3.2.	Spectroscopic properties	127
V.4.	Conclusions	130
V.5.	Experimental section	131
V.5.1.	Instrumentation and measurements	131
V.5.2.	Materials	131
V.5.3.	Preparations	131
V.6.	References	134

V.1. Introduction

Systems with polynuclear transition-metal complexes are widely seen in nature and their study spread fields from biology to photophysics.^[1] It is known that in the active centres of enzymes, the transition metal atoms are often joined by aquo, hydroxo or oxo bridges.^[2] In this systems, iron is one of the most essential elements, different biological activities of Fe(II) and Fe(III) are well known,^[3] for example, in the oxidation of methane to methanol, proteins with oxo-bridged iron aggregates in the active centre are involved.^[1] Tetracarboxylate-bridged diiron(II) complexes have been investigated to model enzyme active sites of carboxylate-bridged diiron metalloproteins.^[4] However, Fe(II) carboxylate ligands present strong tendency to form species of higher nuclearity.^[1, 5] In particular, trinuclear mixed-valence iron complexes oxo-centred and carboxylate-bridged type $[\text{Fe}^{\text{III}}_2\text{Fe}^{\text{II}}\text{O}(\text{O}_2\text{CR})_6\text{L}_3] \cdot n\text{S}$ in which L is a monodentate ligand and S is a solvent molecule of crystallization, have been broadly studied due to their simplicity, their potential use in oxidation catalysis and their interesting physical properties.^[6]

Moreover, this type of complexes can be used as frameworks to study metal-metal interactions in clusters, especially, they have been of considerable interest to study intramolecular electron transfer processes.^[6a, 7] The understanding of these processes is fundamental for the synthesis of new coordination clusters which can be precursors for clusters of higher nuclearity showing interesting magnetic properties than can act as new magnetic materials such as single molecule magnets (SMMs).^[8] SMMs are currently of great interest due to their potential applications in quantum computing, high-density information storage and biomedicine.^[9]

Carboxylate-bridged cobalt(II) compounds are also involved in many enzymatic but non-redox active processes.^[10] Binuclear high-spin cobalt(II) complexes are analogous to metalloenzymes such as xylose glucose isomerase, aminopeptidase, hydroxylase or urease.^[11] Besides, cobalt(II) is a good precursor to generate supramolecular structures (MOF's) which are of great interest for applications in fields related to porous materials such as storage, separation and catalysis as well as in biomedical applications or their use as sensor materials.^[12] Furthermore, use of cobalt as component in nanomaterials has a great interest due to their size as well as their electrical, magnetic, optical and catalytic properties.^[13]

Synthesis and characterization of complexes containing the $[1\text{-CO}_2\text{-}1,2\text{-}closo\text{-C}_2\text{B}_{10}\text{H}_{11}]^-$ ligand and the transition metals Zn^{II} , Cu^{II} , Ni^{II} and Mo^{II} ions were previously performed.^[14] However, the coordination of Fe^{II} and Co^{II} ions to carboranylcarboxylate ligands has never been studied instead of their relevance in significant biological processes and their multiple potential uses in biomedicine or in synthesis of new nanomaterials among others.

V.2. Objectives

As discussed above, carboranylcarboxylate ligands have not been studied ever with metals such as iron(II) or cobalt(II) and it is why we were interested in the behaviour of the carboranylcarboxylate ligand [1-CH₃-2-CO₂-1,2-*closo*-C₂B₁₀H₁₀]-, LH, against its coordination to transition metals such as iron or cobalt.

The main goal of this chapter was therefore, the synthesis and fully characterization of the resulting complexes through structural, analytical and spectroscopic (IR, UV-visible, RMN) techniques.

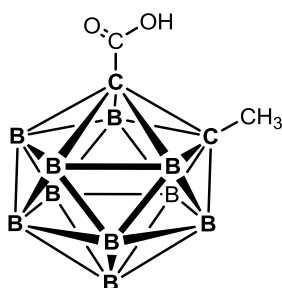


Chart 1. 1-CH₃-2-CO₂H-1,2-*closo*-C₂B₁₀H₁₀ ligand (LH)

The first goal was to coordinate the ligand LH to the iron salt Fe(CF₃SO₃)₂ and characterize the resulting complexes. The coordination of this ligand to iron atoms will provide complexes with potential applications in catalytic processes.

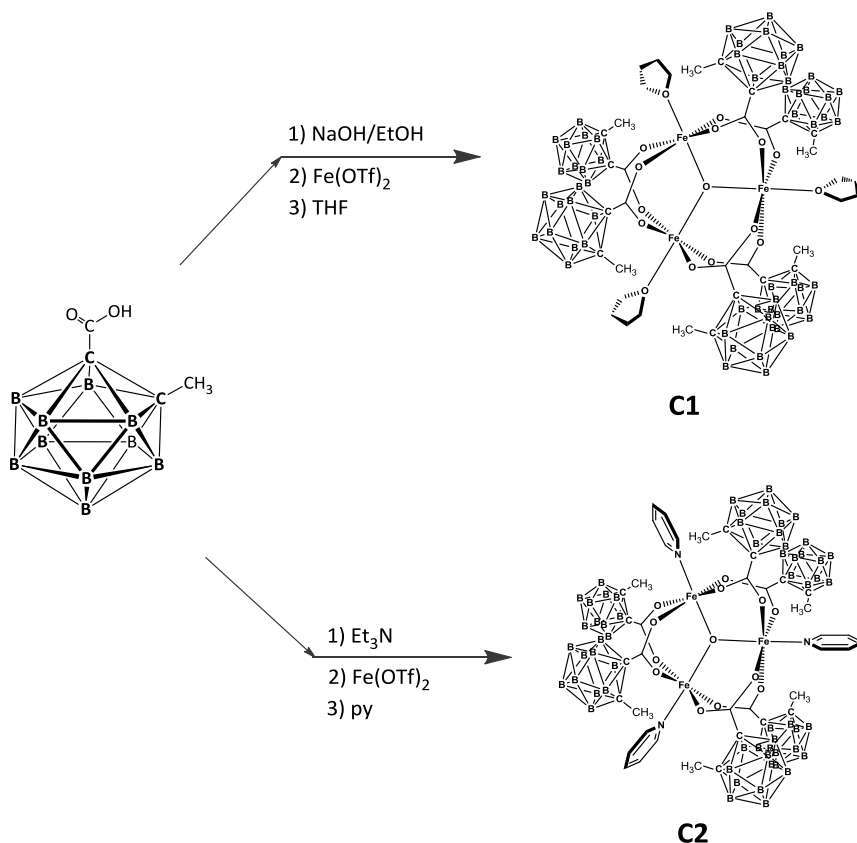
Another goal was the study of the reactivity of LH ligand with two different cobalt(II) salts with the idea of studying and characterize the compounds obtained and thus can also make comparisons with Cu and Mn compounds obtained in the previous chapters.

V.3. Results and discussion

V.3.1. Synthesis and structure

V.3.1.1. Iron complexes

The synthetic strategy for the preparation of the trinuclear iron complexes, **C1** and **C2** containing the carboranylcarboxylate ligand 1-CH₃-2-CO₂H-1,2-*closo*-C₂B₁₀H₁₀ (**LH**) and THF or py molecules is outlined in Scheme 1.

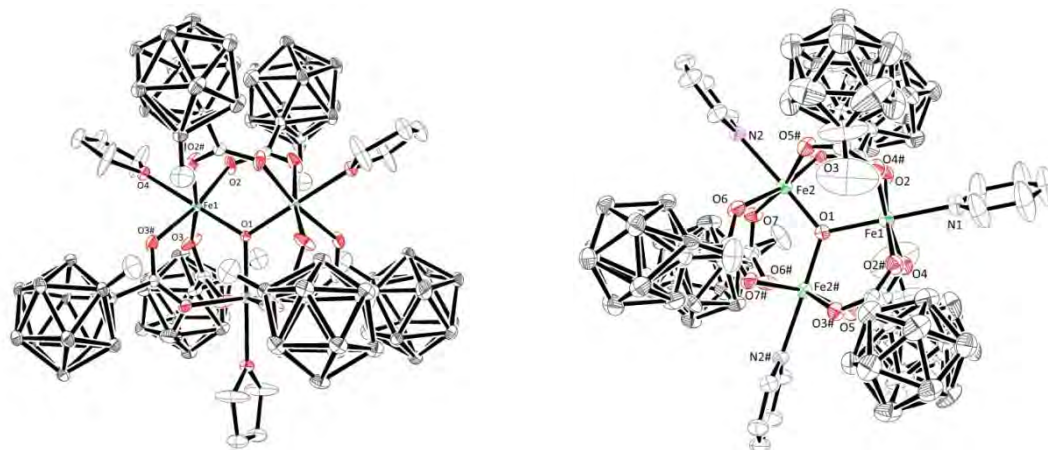


Scheme 1. Synthetic strategy for the preparation of mixed Fe(II), Fe(III) complexes **C1** and **C2**.

Two different strategies shown in Scheme 1. were used leading in all cases mixed valence carboxylate bridged iron complexes. The trinuclear complex [Fe₃(μ-O)(1-CH₃-2-CO₂-1,2-*closo*-C₂B₁₀H₁₀)₆(THF)₃], **C1**, was obtained by neutralization of carboranylcarboxylic acid, **LH**, with NaOH followed by reaction with Fe(CF₃SO₃)₂ in THF. This method is similar to the one used in Chapter III^[14a] to obtain the compound **A1**, [Cu₂(1-CH₃-2-CO₂-1,2-*closo*-C₂B₁₀H₁₀)₄(THF)₂]. Synthesis of trinuclear iron complex [Fe₃(μ-O)(1-CH₃-2-CO₂-1,2-*closo*-C₂B₁₀H₁₀)₆(py)₃], **C2**, lies in the neutralization of carboranylcarboxylic acid, **LH**, with Et₃N followed by reaction with Fe(CF₃SO₃)₂ in CH₂Cl₂.and subsequent reaction with pyridine ligand in a ratio metal:ligand of 1:1. ^[15] This method was used expecting a binuclear compound, however, a trinuclear iron

complex similar to **C1** was obtained but containing py instead of THF. In both cases, all the manipulations were performed under nitrogen atmosphere.

Crystallographic data and selected bond distances and angles for compounds **C1** and **C2** are presented in Table 1. and Table 2. , respectively. ORTEP plots with the corresponding atom labels for the X-ray structures of both compounds are presented in Figure 1.



$[\text{Fe}_3(\mu_3\text{-O})(1\text{-CH}_3\text{-2-CO}_2\text{-1,2-closo-C}_2\text{B}_{10}\text{H}_{10})_6(\text{THF})_3]$, (**C1**) $[\text{Fe}_3(\mu\text{-O})(1\text{-CH}_3\text{-2-CO}_2\text{-1,2-closo-C}_2\text{B}_{10}\text{H}_{10})_6(\text{py})_3]$, (**C2**)

Figure 1. X-ray structures (ORTEP plots with ellipsoids at 20% probability level) and labelling scheme for complexes **C1** and **C2**.

Compound **C1** crystallizes in the space group P63/m and the structure consists in a planar $\text{Fe}_3(\mu_3\text{-O})$ core, six carboxylate groups acting as bidentate syn,syn bridges linking pairs of iron atoms in the cluster and three THF molecules which complete the distorted octahedral sphere around each iron atom (Figure 1). The electroneutrality of these complexes indicates that the compound is formed by two Fe(III) and one Fe(II) leading to a mixed valence complex. However, it is remarkable observed that in this compound the three iron ions are crystallographically indistinguishable. This fact is due to the collocation of the central $\mu_3\text{-oxo}$ atom on a special position on the crystallographic 3-fold rotation axis and is attributed to a dynamic disorder induced by a rapid internal electron transfer.^[16] An evidence of this fact is that the central Fe_3O atoms form a perfect equilateral triangle with distances $\text{Fe}(1)\text{-Fe}(1)\#1$ of 3.303 Å and angles $\text{Fe}(1)\#1\text{-Fe}(1)\text{-Fe}(1)\#2$ of 60°. The Fe-O distances are 2.0298(16) Å and 2.0353(15) Å for $\text{Fe-O}_{\text{Carbox}}$, 2.118(2) Å for Fe-O_{THF} and 1.9073(4) Å for $\text{Fe}(\mu\text{-O})$. These distances are in total agreement with the only two structures reported in the literature for similar complexes.^[17] The Fe atoms present a deviation from the equatorial plane of their octahedra formed by the four oxygen atoms of the carboranylcarboxylate ligands of 0.186 Å toward the $\mu_3\text{-O}$ atom (see Figure S1 at the supporting information section). It is observable than the planes of the THF ligands are perpendicular to the $\text{Fe}_3(\mu_3\text{-O})$ core plane with a dihedral angle of

90°. The octahedral geometry around each iron atom is not ideal with angles in the range from 84.38° to 95.35°.

There are two noteworthy packing arrangements in this compound along the *b* and the *c* axis (see Figure 2b). It is observable along the *b* axis that the Fe₃O complexes are forming parallel layers in which the six carboranylcarboxylate ligands are placed three in the right side of the molecule and three in the left one leaving a cavity between them where are seated the THF molecules. Besides, the carboranylcarboxylate ligands belonging to different chains are stacked one upon another. A different vision of the packing arrangement for this molecule can be observed along the *c* axis (

Figure 2b). It is notice than the six bridged carboranylcarboxylate ligands of each molecule are overlapped in pairs and alternated in the space with the THF molecules. It is also observed than the methyl groups of all the carboranylcarboxylate ligands are orientated towards the central μ -oxygen atom of the Fe₃O core. All these arrangements allow the formation of a perfect hexagon with average distances between the central oxygen atom (O(1)) of the different molecules of 14.377 Å (see Figure 3). It is remarkable that the presence of the carboranylcarboxylate ligands in the cavity of the hexagon leads to the existence of a hydrophobic environment in this cavity.

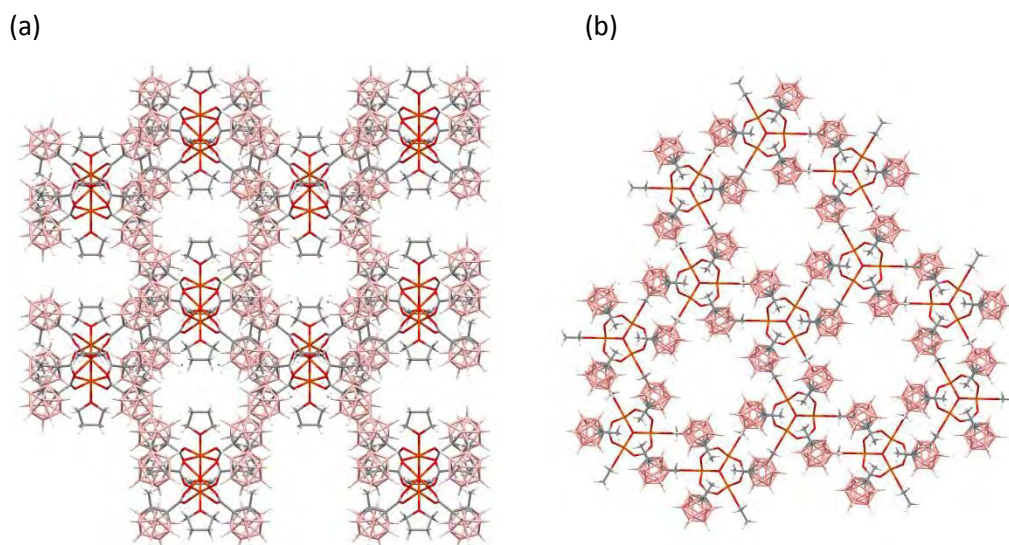


Figure 2. Packing diagram of complex **C1** along the *b* axis (a) and the *c* axis (b).

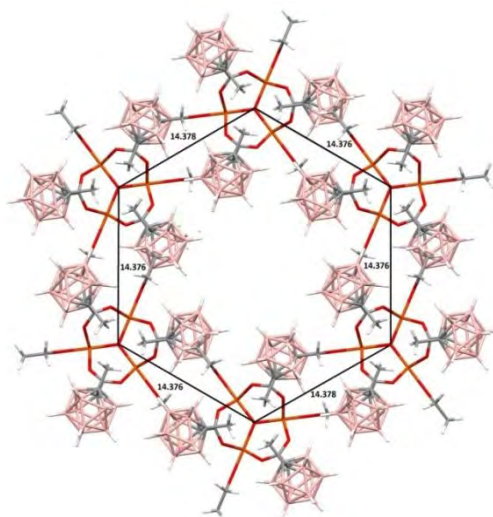


Figure 3. Details of the hexagon formed for six adjacent molecules of the complex **C1** in the packing arrangement along the *c* axis.

Table 1. Crystal Data for X-ray structures of **C1** and **C2**.

	C1	C2
Empirical formula	C ₃₆ H ₁₀₂ B ₆₀ O ₁₆ Fe ₃	C ₃₉ H ₉₃ B ₆₀ O ₁₃ N ₃ Fe ₃
Formula weight	1607.37	1628.31
Crystal system	Hexagonal	Monoclinic
Space group	P63/m	C2/c
a [Å]	17.938(2)	19.572(3)
b [Å]	17.938(2)	20.342(3)
c [Å]	19.943(5)	23.179(3)
α [°]	90	90
β [°]	90	94.871(2)
γ [°]	120	90
V [Å ³]	5557.4(16)	9195(2)
Formula Units/Cell	2	4
ρ _{calc.} [g cm ⁻³]	1.265	1.176
μ [mm ⁻¹]	0.723	0.516
R1 ^[a] , [I > 2σ(I)]	0.0570	0.0717
wR2 ^[b] [all data]	0.1679	0.2555

$$[a] R_1 = \frac{\sum ||F_o| - |F_c||}{\sum |F_o|}$$

$$[b] wR_2 = \left[\frac{\sum \{w(F_o^2 - F_c^2)^2\}}{\sum \{w(F_o^2)^2\}} \right]^{1/2}, \text{ where } w = 1/[\sigma^2(F_o^2) + (0.0042P)^2] \text{ and } P = (F_o^2 + 2F_c^2)/3$$

Table 2. Selected bond lengths (Å) and angles (°) for complexes **C1** and **C2**.

	C1		C2		C2
Fe(1)-O(1)	1.9073(4)	Fe(1)-O(1)	2.014(4)	O(2)#1-Fe(1)-O(2)	174.5(2)
Fe(1)-O(3)	2.0298(16)	Fe(1)-O(4)	2.100(4)	O(1)-Fe(1)-N(1)	180.000(1)
Fe(1)-O(3)#1	2.0298(16)	Fe(1)-O(4)#1	2.100(4)	O(4)-Fe(1)-N(1)	86.93(10)
Fe(1)-O(4)	2.118(2)	Fe(1)-O(2)	2.101(4)	O(4)#1-Fe(1)-N(1)	86.93(10)
Fe(1)-O(2)	2.0353(15)	Fe(1)-O(2)#1	2.101(4)	O(2)-Fe(1)-N(1)	87.26(10)
Fe(1)-O(2)#1	2.0353(15)	Fe(1)-N(1)	2.176(7)	O(2)#1-Fe(1)-N(1)	87.26(10)
O(1)-Fe(1)-O(3)	95.14(5)	Fe(2)-O(1)	1.866 (2)	O(1)-Fe(2)-O(3)	98.30(13)
O(1)-Fe(1)-O(3)#1	95.14(5)	Fe(2)-O(5)#1	2.009(3)	O(1)-Fe(2)-O(5)#1	95.91(13)
O(3)#1-Fe(1)-O(3)	90.75(13)	Fe(2)-O(6)	2.042(3)	O(5)#1-Fe(2)-O(3)	93.14(15)
O(1)-Fe(1)-O(2)	95.35(4)	Fe(2)-O(3)	2.015(3)	O(1)-Fe(2)-O(6)	94.09(13)
O(3)#1-Fe(1)-O(2)	169.52(7)	Fe(2)-O(7)	2.054(3)	O(5)#1-Fe(2)-O(6)	88.35(16)
O(3)-Fe(1)-O(2)	88.17(9)	Fe(2)-N(2)	2.202(4)	O(3)-Fe(2)-O(6)	167.29(14)
O(1)-Fe(1)-O(2)#1	95.35(4)	O(1)-Fe(1)-O(4)	93.07(10)	O(1)-Fe(2)-O(7)	96.08(13)
O(3)#1-Fe(1)-O(2)#1	88.17(9)	O(1)-Fe(1)-O(4)#1	93.07(11)	O(5)#1-Fe(2)-O(7)	167.93(15)
O(3)-Fe(1)-O(2)#1	169.52(7)	O(4)-Fe(1)-O(4)#1	173.9(2)	O(3)-Fe(2)-O(7)	86.49(14)
O(2)-Fe(1)-O(2)#1	90.99(12)	O(1)-Fe(1)-O(2)	92.74(10)	O(6)-Fe(2)-O(7)	89.43(16)
O(1)-Fe(1)-O(4)	179.61(6)	O(1)-Fe(1)-O(2)#1	92.74(10)	O(1)-Fe(2)-N(2)	175.99(11)
O(3)#1-Fe(1)-O(4)	85.13(6)	O(4)-Fe(1)-O(2)	87.18(15)	O(5)#1-Fe(2)-N(2)	82.85(14)
O(3)-Fe(1)-O(4)	85.13(6)	O(4)#1-Fe(1)- O(2)#1	87.18(15)	O(3)-Fe(2)-N(2)	85.59(14)
O(2)-Fe(1)-O(4)	84.38(6)	O(4)-Fe(1)-O(2)#1	92.53(15)	O(6)-Fe(2)-N(2)	82.07(14)
O(2)#1-Fe(1)-O(4)	84.38(6)	O(4)#1-Fe(1)-O(2)	92.53(15)	O(7)-Fe(2)-N(2)	85.10(14)

Complex **C2** crystallizes in space group C2/c and displays a similar structure to **C1** with a central planar Fe₃(μ₃-O) core, six carboxylate groups and three pyridine molecules completing the distorted octahedral sphere for each iron atom. In contrast, to compound **C1**, **C2** presents only two of the three iron atoms equivalents leading to an isosceles triangle for the central Fe₃O unit, with one short distance Fe(2)-Fe(2)#1 of 3.273 Å and two longer distances Fe(1)-Fe(2)/Fe(2)#1 of 3.340 Å. Two different angles have also been observed two larger Fe(1)-Fe(2)-Fe(2)#1 and Fe(2)-Fe(2)#1-Fe(1), 60.66° and one smaller Fe(2)-Fe(1)-Fe(2)#1, 58.68°. In the same way than for **C1**, the electroneutrality of the complex indicates that the compound is formed by two Fe(III) and one Fe(II) leading to a mixed valence complex. It is well known^{[7b, 7c,}

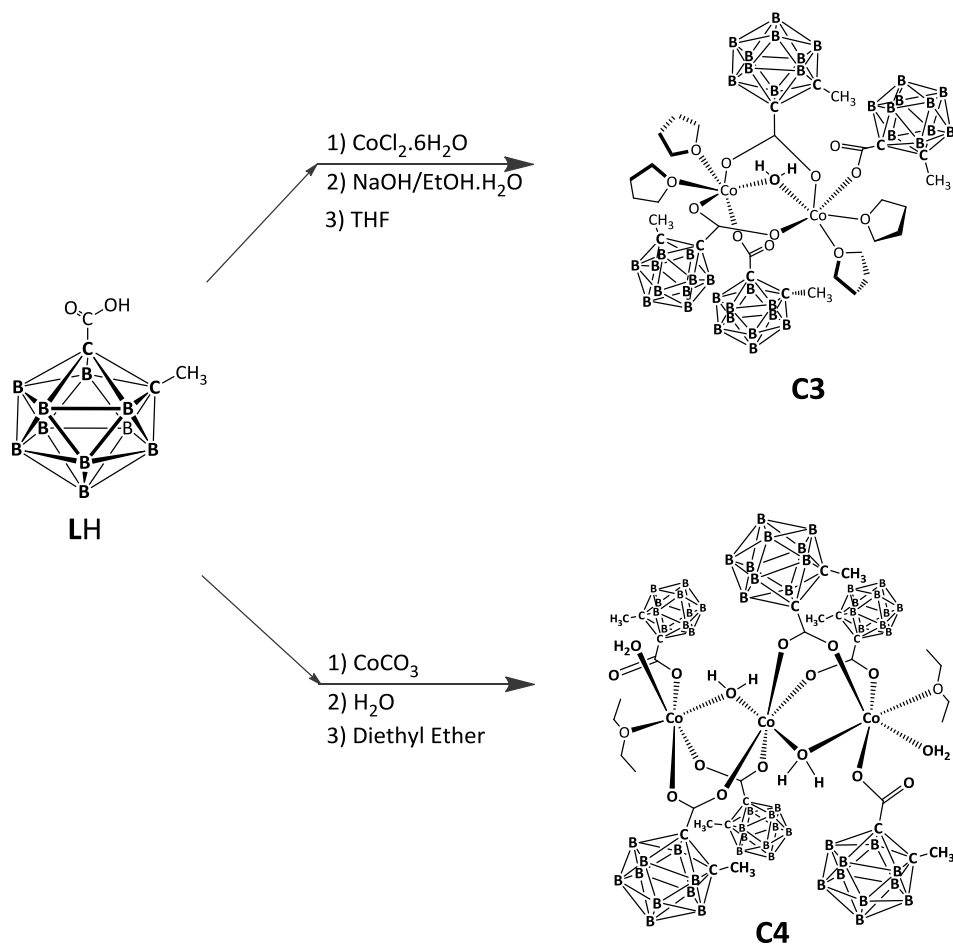
^{18]} that the bond distances Fe-(μ -O) and the angles (μ -O)-Fe-O_{carbox} are depending on the valence states of the iron ions, being $d_{(\text{Fe}^{\text{II}}-\text{O})} > d_{(\text{Fe}^{\text{III}}-\text{O})}$ and $\alpha_{(\text{O}-\text{Fe}^{\text{II}}-\text{O}_{\text{carbox}})} < \alpha_{(\text{O}-\text{Fe}^{\text{III}}-\text{O}_{\text{carbox}})}$. It is also known that the distances Fe-O_{carbox} present the same dependency^[18c] being $d_{(\text{Fe}^{\text{II}}-\text{O}_{\text{carbox}})} > d_{(\text{Fe}^{\text{III}}-\text{O}_{\text{carbox}})}$. Although this fact was not observed for **C1**, it is clearly evidenced in **C2** in which Fe(1)-O(1) bond distance (2.014(4) Å) is longer than Fe(2)/Fe(2)#-O(1) distances (1.866(2) Å); also the angle O(1)-Fe(1)-O_{carbox} (average 92.91°), is shorter than O(1)-Fe(2)/Fe(2)#-O_{carbox} angles (average 96.10°) and averaged distance Fe(1)-O_{carbox} (2.1005 Å) is longer than Fe(2)/Fe(2)#-O_{carbox} (2.030 Å) ones. With this evidences, it can be concluded that in compound **C2**, Fe(1) ion presents a Fe(II) oxidation state whereas Fe(2) and Fe(2)# are in an Fe(III) state.

It is observable in compound **C2** than the shortest metal-pyridine bond distances are opposite to the longest metal-central oxygen bonds ($d_{(\text{Fe}(1)-\text{O}(1))} = 2.014(4)$ Å) and $d_{(\text{Fe}(1)-\text{N}(1))} = 2.176(7)$ Å) and vice versa, $d_{(\text{Fe}(2)/\text{Fe}(2)\#-\text{O}(1))} = 1.866(2)$ and $d_{(\text{Fe}(2)-\text{N}(2))} = 2.202(4)$ Å. This behaviour has been observed in similar mixed-valence complexes containing carboxylate and pyridine ligands.^[7c] Besides, the coordinated pyridines bonded to Fe(1) and Fe(2)/Fe(2)# present different orientation with respect to the plane formed for the three iron atoms. The planes of the two py ligand bonded to Fe(2) and Fe(2)# are nearly perpendicular (dihedral angle, 88.17°), while the plane of the third py ligand presents an angle of 66.07° respect the plane defined for the three iron atoms.

Packing diagram of **C2** along *b* axis displays diagonal chains in which pyridine and carboranylcarboxylate ligands located in the diagonal are overlapped and the remaining carboranylcarboxylate ligands are stacked one upon another. Along *c* axis, **C2** presents a pattern packing in which the carboranylcarboxylate ligands of the same molecule are in pairs and alternated with the pyridine ligands. Besides, two of the three methyl groups of these carboranylcarboxylate ligands are oriented towards the central μ -oxo atom. One of the pyridine ligands from each molecule is overlapped by a pair of carboranylcarboxylate ligands of the adjacent molecule. (see Figure S2 at the supporting information section)

V.3.1.2. Cobalt complexes

The synthetic strategy for the preparation of the Co(II) complexes, **C3** and **C4**, containing the carboranylcarboxylate ligand 1-CH₃-2-CO₂H-1,2-*closo*-C₂B₁₀H₁₀ (LH) and THF, aqua or diethyl ether ligands is outlined in Scheme 1.



Scheme 2. Synthetic strategy for the preparation of Co(II) complexes **C3** and **C4**.

The binuclear cobalt compound $[\text{Co}_2(\mu\text{-H}_2\text{O})(1\text{-CH}_3\text{-2-CO}_2\text{-1,2-closo-C}_2\text{B}_{10}\text{H}_{10})_4(\text{THF})_4]$, **C3**, was obtained by neutralization of carboranylcarboxylic acid, **LH**, with NaOH followed by reaction with $\text{CoCl}_2 \cdot 6\text{H}_2\text{O}$ in ethanol/ H_2O and subsequent extraction in THF.^[14a] This method was used in Chapter III to obtain the binuclear compound **A1**, $[\text{Cu}_2(1\text{-CH}_3\text{-2-CO}_2\text{-1,2-closo-C}_2\text{B}_{10}\text{H}_{10})_4(\text{THF})_2]$. Compound $[\text{Co}_3(\mu\text{-H}_2\text{O})_2(1\text{-CH}_3\text{-2-CO}_2\text{-1,2-closo-C}_2\text{B}_{10}\text{H}_{10})_6(\text{H}_2\text{O})_2(\text{C}_4\text{H}_{10}\text{O})_2]$, **C4**, was obtained by recrystallization of the compound **C5** in diethyl ether. Compound **C5**, was synthesized by reaction of a suspension of the carboranylcarboxylic acid $1\text{-CH}_3\text{-2-CO}_2\text{H-1,2-closo-C}_2\text{B}_{10}\text{H}_{10}$, **LH**, with CoCO_3 in water.

Complex **C5** was not possible to crystallize but its X-ray powder diffraction (XRD) was performed and compared with the calculate XRD for **C4** complex (Figure S2 at the supporting information section). It was observed that both diagrams are not similar. We propose that complex **C5** presents a polymeric structure similar to complex **B1**, $[\text{Mn}(\mu\text{-H}_2\text{O})(\mu\text{-1-CH}_3\text{-2-CO}_2\text{-1,2-closo-C}_2\text{B}_{10}\text{H}_{10})_2]_n \cdot (\text{H}_2\text{O})_n$, where the Co(II) ions are bonded by two carboranylcarboxylate ligands and by one aqua ligand. More evidences to this fact were found in the elemental

analysis of compound **C5**, which totally agree with the proposed compound (see experimental section).

Crystallographic data and selected bond distances and angles for compounds **C3** and **C4** are presented in Table 3 and Table 4, respectively. ORTEP plots with the corresponding atom labels for the X-ray structures of both compounds are presented in Figure 4.

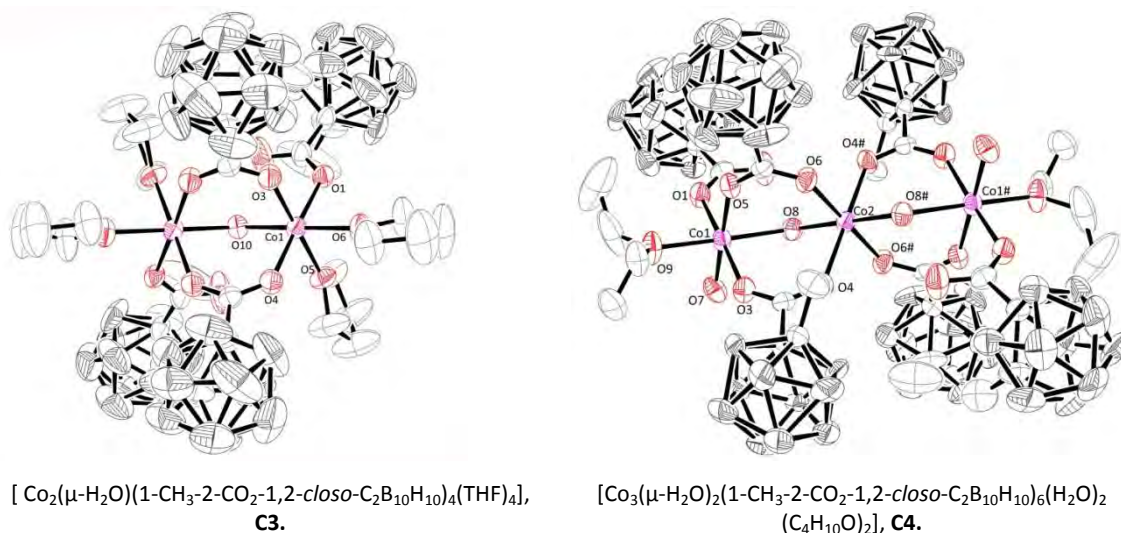


Figure 4. X-ray structures (ORTEP plots with ellipsoids at 40% probability level) and labelling scheme for complexes **C3** and **C4**.

Binuclear compound **C3** displays a structure with the two cobalt(II) atoms held together through two syn,syn $\eta^1:\eta^1$: μ_2 -carboxylate bridges and one bridged aqua molecule as shown in Figure 4. The distorted octahedral geometry around each metal ion is completed by one additional monodentate carboranylcarboxylate ligand and two oxygen donor atoms from two THF ligands leading to a local *cis*- $\text{Co}(\text{O}_{\text{THF}})_2(\text{O}_{\text{carboxy}})_4$ coordination. Although there are several reported cobalt(II) complexes with a similar environment,^[19] compound **C3** is the first one containing carboxylate groups, one μ_2 -bridged aqua molecule and THF molecules. The molecule is located in a crystallographically imposed two-fold axis which passes through the oxygen O(10) belonging to the μ_2 -bridged aqua molecule. The hydrogen atoms of the bridged aqua molecule are involved in intramolecular O(10)-H...O hydrogen bonds with the uncoordinated O atoms of the monodentate carboranylcarboxylate ligands (O(10)-H(10C)...O(2), 1.607Å) (see Figure 5). The bond length Co(1)-O(10)_w distance is 2.083(17) Å while the corresponding Co(1)-O(10)-Co(1)#1 angle is 117.82(14)°. This bond distance is shorter and the angle is larger than those for similar carboxylate compounds containing py in spite of THF.^[19c-e] This fact could be due to the strong electron-withdrawing character of the py versus THF. The Co-O_{THF} bond length corresponding to the THF molecule in *trans* position to the bridged aqua oxygen atom is significantly shorter (2.083Å) than the Co-O_{THF} distance for

the THF molecule *trans* to the bridged carboranylcarboxylate oxygen atom (2.092 Å) due to the well-known *trans* influence.^[20]

The structural packing of this complex (Figure S3 at the supporting information section) along the *a* axis shows parallel chains of molecules in which the carboranylcarboxylate ligands of one molecule are placed close to the THF ligands of the parallel molecule.

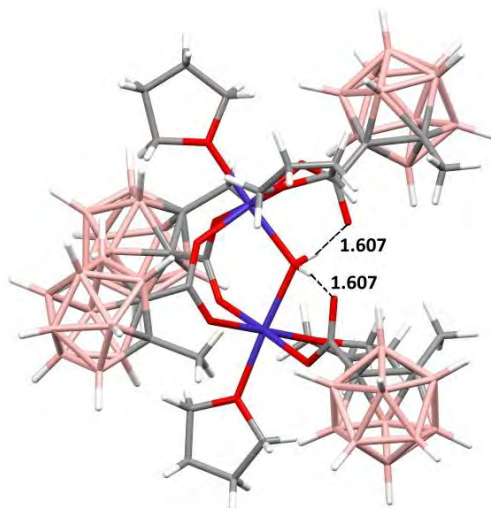


Figure 5. X-ray structure of **C3** showing the intramolecular hydrogen bonds.

The X-ray diffraction of compound **C4** discloses a trinuclear cobalt complex with aqua bridged entities which consists in a linear array of three Co(II) ions with a crystallographic inversion centre located on the central Co(2). Each Co(II) ion is hexacoordinated; the central Co(2) is coordinated by four carboxylate and two aqua oxygen atoms. This Co(2) is bonded to both terminal Co(1) by two carboranylcarboxylate ligands and by an aqua ligand. The coordination of the two terminal Co(II) ions is completed by one monodentate carboxylate, one terminal aqua ligand and one oxygen atom from one diethyl ether molecule. The cobalt centres display a tetragonal distortion; for the terminal Co(1) the equatorial Co(1)-O(1), Co(1)-O(3) and Co(1)-O(5) distances to the carboranylcarboxylate ligand present an average of 2.06 Å; the equatorial Co(1)-O(7) distance to the non-bridged water is 2.021 Å, while the axial distance to the diethyl ether molecule, Co(1)-O(9), is 2.111 Å, and the axial distance to the bridging water, Co(1)-O(8), is 2.217 Å; for Co(2), the average of the four equatorial Co-O distances is 2.06 Å, whereas the two axial are 2.13 Å defining a tetragonally distorted octahedron. Distances Co-O_{Carbox} are in the range 2.021-2.099 Å for Co(1) and 2.052-2.072 Å for Co(2). Distance Co-O_w are 2.217(4) Å for Co(1) and 2.134(4) Å for Co(2). The Co(1)-O(8)-Co(2) angle found is 114.21(17)°. These Co-O bond distances and the angle Co-O_w-Co agree with thus reported for similar trinuclear cobalt(II) complexes containing bridged carboxylate groups.^[21] It is worth noticing the existence of two intramolecular hydrogen bonds between the

uncoordinated oxygen atom of the monodentate carboxylate (O(2)) and the H8A and H8B of the bridged aqua (H(8A)-O(2), 1.666Å; H(8B)-O(2) 2.955Å). Another intramolecular weak hydrogen bond is observed between H7B of the terminal aqua ligand and O(9) of the terminal diethyl ether molecule, H(9B)-O(7), 2.891Å (Figure 6).

The packing arrangement of compound **C4** along *c* axis present parallel lineal chains where the terminal diethyl ether ligands of adjacent molecules from the same chain are facing each other (see Figure S3 at the supporting information section).

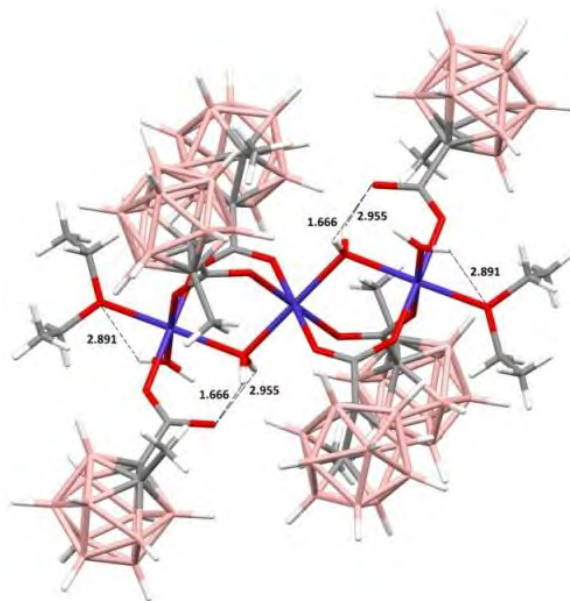


Figure 6. X-ray structure of **C4** showing the intramolecular and intermolecular hydrogen bonds.

The synthetic strategy followed to obtain complexes **C3** and **C4** was the same to the strategy followed to obtain **A1**, $[\text{Cu}_2(1\text{-CH}_3\text{-2-CO}_2\text{-1,2-closo-C}_2\text{B}_{10}\text{H}_{10})_4(\text{THF})_2]$, and **B2**, $[\text{Mn}_3(\mu\text{-H}_2\text{O})_4(1\text{-CH}_3\text{-2-CO}_2\text{-1,2-closo-C}_2\text{B}_{10}\text{H}_{10})_6(\text{C}_4\text{H}_{10}\text{O})_2]$, presented in previous chapters. In both cases binuclear compounds were obtained in which the metal atoms are held through syn,syn η^1 : η^1 : μ_2 -carboxylate bridges. However, whereas compound **A1** presents a paddle-wheel type structure in which each copper atom displays a square pyramidal geometry completed by one oxygen atom from a THF molecule; in compound **C3** the cobalt(II) ions are held through two bridged carboranylcarboxylate and one aqua ligands and each cobalt atom shows an additional carboranylcarboxylate ligand in a monodentate mode and two THF molecules completing a distorted octahedral geometry around each metal ion..

The strategy used to obtain compounds **C4** and **B2** was also the same and in both cases trinuclear compounds were obtained, in which the metal ions are linked each other through two bridged carboranylcarboxylate ligands and one bridged aqua ligand. In both compounds the terminal metal atoms present one monodentate carboranylcarboxylate ligand, one aqua

ligand and one diethyl ether molecule. The structures of both complexes present octahedral geometry around each metal ion and an inversion centre located in the central metal atom.

Table 3. Crystal Data for X-ray structures of **C3** and **C4**.

	C3	C4
Empirical formula	C ₃₂ H ₈₆ B ₄₀ O ₁₃ CO ₂	C ₄₈ H ₁₄₆ B ₆₀ O ₂₂ CO ₃
Formula weight	1229.27	1901.04
Crystal system	Orthorhombic	Triclinic
Space group	Pccn	P-1
a [Å]	12.392(5)	14.420(9)
b [Å]	22.830(10)	14.806(10)
c [Å]	23.802(10)	15.656(10)
α [°]	90	63.006(12)
β [°]	90	73.533(13)
γ [°]	90	67.443(11)
V [Å ³]	6734(5)	2726(3)
Formula Units/Cell	4	1
ρ _{calc.} [g cm ⁻³]	1.212	1.158
μ [mm ⁻¹]	0.542	0.506
R1 ^[a] , [I > 2σ(I)]	0.0636	0.0979
wR2 ^[b] [all data]	0.2183	0.2603

$$[a] R_1 = \frac{\sum ||F_o| - |F_c||}{\sum |F_o|}$$

$$[b] wR_2 = \left[\frac{\sum \{w(F_o^2 - F_c^2)^2\}}{\sum \{w(F_o^2)^2\}} \right]^{1/2}, \text{ where } w = 1/[\sigma^2(F_o^2) + (0.0042P)^2] \text{ and } P = (F_o^2 + 2F_c^2)/3$$

Table 4. Selected bond lengths (Å) and angles (°) for complexes **C3** and **C4**.

	C3		C4		C4
Co(1)-O(3)	2.039(2)	Co(1)-O(1)	2.099(5)	Co(2)-O(6)	2.052(4)
Co(1)-O(6)	2.083(2)	Co(1)-O(3)	2.059(5)	Co(2)-O(4)	2.072(4)
Co(1)-O(10)	2.0832(17)	Co(1)-O(5)	2.027(5)	Co(2)-O(8)	2.134(4)
Co(1)-O(5)	2.092(2)	Co(1)-O(7)	2.021(5)	Co(2)-O(6)#1	2.052(4)
Co(1)-O(4)	2.092(2)	Co(1)-O(8)	2.217(4)	Co(2)-O(4)#1	2.072(4)
Co(1)-O(1)	2.121(2)	Co(1)-O(9)	2.111(5)	Co(2)-O(8)#1	2.134(4)
O(3)-Co(1)-O(6)	90.64(10)	O(7)-Co(1)-O(8)	88.09(16)	O(4)-Co(2)-O(4)#1	180.0(2)
O(3)-Co(1)-O(10)	91.76(8)	O(1)-Co(1)-O(9)	90.96(19)	O(4)-Co(2)-O(6)	91.91(19)
O(6)-Co(1)-O(10)	176.61(9)	O(3)-Co(1)-O(9)	89.45(19)	O(4)#1-Co(2)-O(6)	88.09(19)
O(3)-Co(1)-O(5)	178.25(10)	O(5)-Co(1)-O(9)	88.78(18)	O(4)-Co(2)-O(6)#1	88.09(19)
O(6)-Co(1)-O(5)	88.23(10)	O(7)-Co(1)-O(9)	92.40(19)	O(4)#1-Co(2)-O(6)#1	91.91(19)
O(10)-Co(1)-O(5)	89.42(8)	O(8)-Co(1)-O(9)	178.67(19)	O(6)-Co(2)-O(6)#1	180.0(1)
O(3)-Co(1)-O(4)	90.10(10)	O(1)-Co(1)-O(3)	175.49(19)	O(4)-Co(2)-O(8)#1	90.43(17)
O(6)-Co(1)-O(4)	89.01(9)	O(1)-Co(1)-O(5)	92.1(2)	O(4)#1-Co(2)-O(8)#1	89.57(17)
O(10)-Co(1)-O(4)	93.39(8)	O(3)-Co(1)-O(5)	92.42(19)	O(6)-Co(2)-O(8)#1	84.84(16)
O(5)-Co(1)-O(4)	88.54(9)	O(1)-Co(1)-O(7)	87.08(19)	O(6)#1-Co(2)-O(8)#1	95.16(16)
O(3)-Co(1)-O(1)	90.37(10)	O(3)-Co(1)-O(7)	88.4(2)	O(4)-Co(2)-O(8)	89.57(17)
O(6)-Co(1)-O(1)	88.95(9)	O(5)-Co(1)-O(7)	178.56(18)	O(4)#1-Co(2)-O(8)	90.43(17)
O(10)-Co(1)-O(1)	88.63(8)	O(1)-Co(1)-O(8)	87.83(16)	O(6)-Co(2)-O(8)	95.16(16)
O(5)-Co(1)-O(1)	90.95(9)	O(3)-Co(1)-O(8)	91.79(16)	O(6)#1-Co(2)-O(8)	84.84(16)
O(4)-Co(1)-O(1)	177.91(8)	O(5)-Co(1)-O(8)	90.71(16)	O(8)#1-Co(2)-O(8)	180.0(1)

V.3.2. Spectroscopic properties

The IR spectra of all complexes described typical $\nu(\text{B-H})$ absorption at frequencies above 2590 cm^{-1} , characteristic of *closo* carborane derivatives.^[22] Differences between the frequencies of the symmetric and antisymmetric stretches for the carboxylate ligands lies within the ranges quoted for bidentate bridged ligands.^[22b]

The electronic UV-vis spectra of complexes **C1**, **C2**, **C3** and **C5** are shown in Figure 7 and

Figure 8, respectively. Spectra of the trinuclear iron complexes, **C1** and **C2**, show three characteristic bands at 351 nm, 479 nm and 554 nm for **C1** and 352 nm, 490 nm and 558 nm for complex **C2**. Both complexes are orange-brown so it is expect than the bands observed in

the near IR are due to transitions in the iron (III) atoms. The absorptions at 479 nm and 490 nm have been tentatively assigned to MLCT transitions,^[23] the lower energy absorptions (554 nm and 558 nm) to d-d transitions^[24] while the higher energy ones (351 nm and 352 nm) have been attributed to an O → Fe(III) charge-transfer transition.^[25]

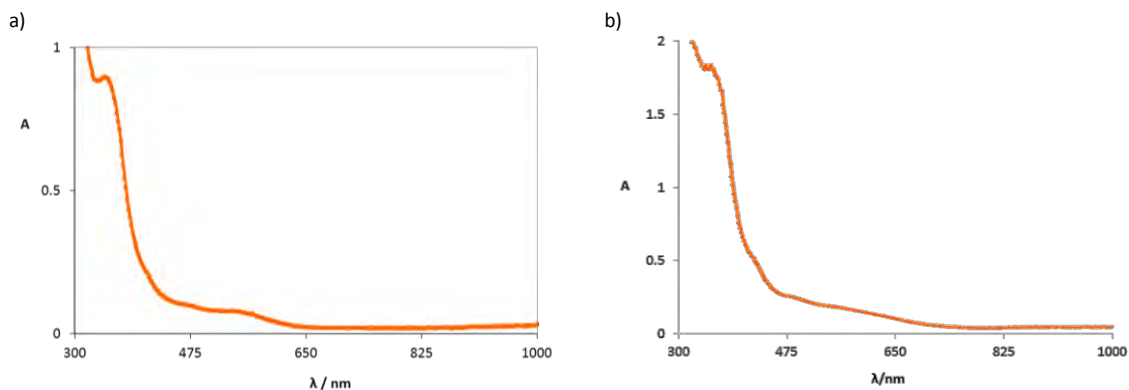


Figure 7. UV-vis spectra for complexes a) C1, b) C2

For cobalt(II) complexes, UV-vis spectra of octahedral Co(II) complexes show two characteristic bands, one in the range 300-400 nm and the other in the range 420-570 nm. The pink binuclear compound **C3** revealed two bands at 353 nm and 534 nm respectively, whereas that the spectrum for the pink solid **C5** presents one band at 510 nm, and two shoulders at 356 and 472 nm, respectively (

Figure 8). The higher energy bands observed in **C3** and **C5** can be assigned to LMCT transitions.^[26] Absorptions in the visible region at 534 nm for **C3** and at 472 and 510 nm for **C5** are assigned to the two spin-allowed d-d transitions, ${}^4T_{1g}(F) \rightarrow {}^4A_{2g}(F)$ and ${}^4T_{1g}(F) \rightarrow {}^4T_{1g}(P)$.^[19b, 19e, 27]

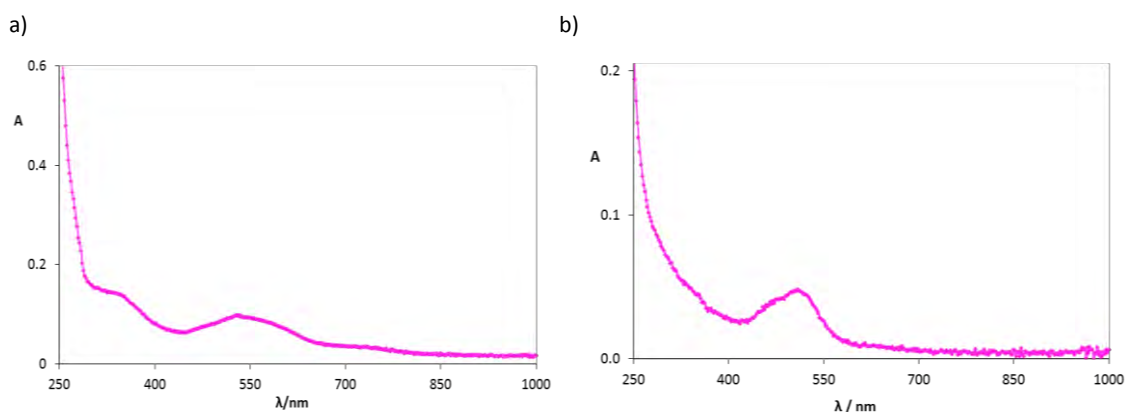


Figure 8. UV-vis spectra for complexes a) C3, b) C5

The ${}^1\text{H}\{{}^{11}\text{B}\}$ -, ${}^{11}\text{B}$ -, ${}^{11}\text{B}\{{}^1\text{H}\}$ - and ${}^{13}\text{C}\{{}^1\text{H}\}$ -NMR spectra of these complexes were performed. It can be observed that the ${}^1\text{H}\{{}^{11}\text{B}\}$ - spectra exhibit resonances around $\delta = 2$ ppm attributed to

the C_c-CH₃ protons and the resonances of the protons bonded to the B atoms appear as broad singlets over a wide chemical-shift range in the region from $\delta = 0$ to +5 ppm. The $^{11}\text{B}\{^1\text{H}\}$ -NMR resonances for all the complexes featured similar patterns in the range from $\delta = 2$ to -15 ppm that agree with a *closo* cluster.^[22a]

V.4. Conclusions

Four new complexes containing the ligand [1-CH₃-2-CO₂-1,2-closo-C₂B₁₀H₁₁], LH, and iron(II) or cobalt(II) ions has been synthesized and thoroughly characterized by analytical, and spectroscopic techniques as well as through X-Ray structure.

For iron complexes, two different synthetic strategies were carried out, obtaining in both cases trinuclear mixed valence iron(III,II) complexes with a Fe₃(μ₃-O) core. The structure of these complexes consist in a planar trigonal Fe₃O core, six syn,syn bridged carboxylate ligands and three THF (**C1**) or py (**C2**) molecules completing the distorted octahedral sphere for each iron atom. It was observed that in compound **C1** the three iron atoms are crystallographically indistinguishable probably due to the dynamic disorder induced by a rapid internal electron transfer whereas than in **C2** the oxidation state of each iron atom could be assigned according to the bond distances Fe-(μ-O) and Fe-O_{carbox} and to the angles(μ-O)-Fe-O_{carbox}.

UV-visible spectra of both compounds were performed and three characteristic bands were observed around 350 nm, in the range 479-490 nm and the third one around 555 nm. These bands were tentatively assigned to LMCT , MLCT and d-d transitions, respectively.

For cobalt complexes, two different nuclearity compounds, **C3** and **C4**, were obtained dependent on the cobalt(II) salt used as starting material, the solvent medium and the synthetic strategy followed. Although both compounds display different nuclearity, binuclear for **C3** and trinuclear for **C4**, in both structures the cobalt atoms are held together through two carboranylcarboxylate and one aqua ligands. Besides, terminal cobalt atoms from both complexes present a monodentate carboranylcarboxylate ligand and two additional oxygen atoms from the solvent medium leading to an octahedral geometry around each cobalt atom.

Compound **C4**, was obtained by recrystallization of complex **C5** in diethyl ether, whose structure has been propose as a polymer of stoichiometry [Co(μ-H₂O)(μ-1-CH₃-2-CO₂-1,2-closo-C₂B₁₀H₁₀·)₂]_n·(H₂O)_n.

UV-visible spectra of compounds **C3** and **C5** were performed and characteristic bands for both complexes were observed. The higher energy bands were assigned to LMCT transitions, and the other bands to the two spin-allowed d-d transitions, ⁴T₁(F)→⁴A₂(F) and ⁴T₁g(F)→⁴T₁g(P).

V.5. Experimental section

V.5.1. Instrumentation and measurements

Instrumentation and Measurements. FT-IR spectra were taken in a Mattson-Galaxy Satellite FT-IR spectrophotometer containing a MKII Golden Gate Single Reflection ATR System. Elemental analyses were performed using a CHNS-O Elemental Analyser EA-1108 from Fisons. UV-Vis spectroscopy was performed on a Cary 50 Scan (Varian) UV-Vis spectrophotometer with 1 cm quartz cells or with an immersion probe of 5 mm path length. NMR spectra have been recorded with a Bruker ARX 300 or a DPX 400 instrument equipped with the appropriate decoupling accessories (^1H and $^1\text{H}\{^{11}\text{B}\}$ NMR (300.13/400.13 MHz), $^{13}\text{C}\{^1\text{H}\}$ NMR (75.47/100.62 MHz) and ^{11}B and $^{11}\text{B}\{^1\text{H}\}$ NMR (96.29/128.37 MHz) spectra were recorded in d_6 -acetone, CD_2Cl_2 and D_2O . Chemical shift values for ^{11}B NMR spectra were referenced to external $\text{BF}_3\leftarrow\text{OEt}_2$ and those for ^1H , $^1\text{H}\{^{11}\text{B}\}$ and $^{13}\text{C}\{^1\text{H}\}$ NMR spectra were referenced to SiMe_4 . Chemical shifts are reported in units of parts per million downfield from reference, and all coupling constants in Hz. Deconvolution of $^{11}\text{B}\{^1\text{H}\}$ spectra has been performed with the software OriginPro 8 SR0, v. 8.0724.

X-ray structure determination. Measurement of the crystals were performed on a Bruker Smart Apex CCD diffractometer using graphite-monochromated Mo $K\alpha$ radiation ($\lambda = 0.71073\text{\AA}$) from an X-Ray tube. Data collection, Smart V. 5.631 (BrukerAXS 1997-02); data reduction, Saint+ Version 6.36A (Bruker AXS 2001); absorption correction, SADABS version 2.10 (Bruker AXS 2001) and structure solution and refinement, SHELXTL Version 6.14 (Bruker AXS 2000-2003).

V.5.2. Materials

All reagents used in the present work were obtained from Aldrich Chemical Co and were used without further purification. Reagent grade organic solvents were obtained from SDS and high purity de-ionized water was obtained by passing distilled water through a nano-pure Mili-Q water purification system. 1- CH_3 -1,2-closo- $\text{C}_2\text{B}_{10}\text{H}_{11}$ was purchased from Katchem.

V.5.3. Preparations

The 1- CH_3 -2- CO_2H -1,2-closo- $\text{C}_2\text{B}_{10}\text{H}_{10}$ ligand was prepared according to literature procedures^[28] with some modifications as was described in Chapter III of the present thesis. The synthetic manipulations for iron complexes were routinely performed under inert atmosphere and for cobalt complexes under ambient conditions. Synthesis of $\text{Fe}(\text{CF}_3\text{SO}_3)_2$ was performed following the literature preparation^[29] with some modifications.

Synthesis of $[\text{Fe}(\text{CF}_3\text{SO}_3)_2]$. A small excess of $\text{CF}_3\text{SO}_3\text{H}$ (3.63 mL, 40.767 mmol) was dropwise and carefully added, as the reaction is highly exothermic, into an aqueous suspension of Fe powder (1.034 g, 18.51 mmol). The resulting suspension was stirred at ambient temperature for 2 days. Then, the unreacted iron powder was filtrated and the solvent was removed under vacuum obtaining a paleblue powder. Finally, the contained water was completely removed by heating the paleblue powder at 250 °C, obtaining a white powder of $\text{Fe}(\text{CF}_3\text{SO}_3)_2$. Yield: 5.758 g (88%) Anal. Found (calcd.) (%) for $\text{C}_2\text{F}_6\text{O}_6\text{S}_2\text{Fe}$: C 6.63 (6.79), H 0.00 (0.00). IR: $\bar{\nu}$ = 630-889 $\nu(\text{CF}_3)_{\text{str}}$, 1024, 1170-1223 $\nu(\text{S}=\text{O})_{\text{str}}$, 1391 $\nu(\text{R}-\text{SO}_2\text{OR})_{\text{str}}$, 1430, 1535, 1614, 1632, 1655, 1740, 3459 cm^{-1} .

Synthesis of $[\text{Fe}_3(\mu\text{-O})(1\text{-CH}_3\text{-2-CO}_2\text{-1,2-closo-C}_2\text{B}_{10}\text{H}_{10})_6(\text{THF})_3]$, **C1.** 1- $\text{CH}_3\text{-2-CO}_2\text{H-1,2-closo-C}_2\text{B}_{10}\text{H}_{10}$, LH, (0.103 g, 0.51 mmols) in ethanol (1 mL) was neutralized with a 0.1 M aqueous NaOH solution with phenolphthalein as indicator at room temperature and then the solvent was removed under vacuum. Then, under inert atmosphere, 5 mL of THF were added and the resulting solution was immediately mixed with a solution of $\text{Fe}(\text{CF}_3\text{SO}_3)_2$ (0.09 g, 0.255 mmols) in THF (5 mL). After stirring overnight, the solvent was removed under vacuum obtaining a brown solid that was recrystallized by slow diffusion of pentane into a dichloromethane solution to afford, air-stable, brown crystals of **C1** suitable for X-ray diffraction analysis. Yield: 0.61 g (45%). $^1\text{H}\{^{11}\text{B}\}$ NMR (400.13 MHz, CD_2Cl_2 , 25 °C): δ = 3.98 (s; O- CH_2), 3.22 (br s; B-H), 2.04 (s, CH_3), 1.99 ppm (s; CH_2). $^{13}\text{C}\{^1\text{H}\}$ NMR (MHz, CD_2Cl_2 , 25 °C): δ = 30.25 (CH_2), 29.92 (CH_2), 23.26 ppm (CH_3). $^{11}\text{B}\{^1\text{H}\}$ NMR (128.37 MHz, CD_2Cl_2 , 25 °C): δ =-1.4, -4.5, -8.6, -10.0, -13.5. IR: $\bar{\nu}$ = 2963, 2584 ν (B-H), 1749, 1647 $\nu(\text{COO}^-)_{\text{as}}$, 1445, 1371 $\nu(\text{COO}^-)_{\text{sim}}$, 1261, 1192, 1148, 1092, 1015, 943, 913, 870, 845, 802, 772, 724, 680 cm^{-1} . UV-Vis (CH_2Cl_2 , 1.10^{-3}M) $\lambda_{\text{max}}(\epsilon)$ = 554 nm ($311 \text{ M}^{-1}\text{cm}^{-1}$), 479 nm ($398 \text{ M}^{-1}\text{cm}^{-1}$), 352 nm ($3750 \text{ M}^{-1}\text{cm}^{-1}$). Elemental analysis calcd (%) for $\text{C}_{36}\text{H}_{102}\text{B}_{60}\text{O}_{16}\text{Fe}_3 \cdot 0.6\text{THF}$: C 27.94, H 6.52; found: C 28.16, H 6.16.

Synthesis of $[\text{Fe}_3(\mu\text{-O})(1\text{-CH}_3\text{-2-CO}_2\text{-1,2-closo-C}_2\text{B}_{10}\text{H}_{10})_6(\text{py})_3]$, **C2.** A solution of LH (0.075 g, 0.38 mmols) and Et_3N (52.5 μL , 0.37 mmols) in CH_2Cl_2 (1 mL) was added dropwise to a solution of $\text{Fe}(\text{OTf})_2$ (0.082 g, 0.231 mmols) in CH_2Cl_2 (1 mL), all under N_2 atmosphere. Pyridine (18.2 μL , 0.23 mmols) was added to this mixture and the solution was allowed to stir for 16 h. Then, the solution was concentrate to dryness. The resulting brown product was extracted into diethyl ether, filtered and exposed to pentane vapour diffusion. After several days, brown crystals of **C2**, suitable for X-ray diffraction analysis, were obtained. Yield: 0.071g (70%). IR: $\bar{\nu}$ = 2583 ν (B-H), 1649 $\nu(\text{COO}^-)_{\text{as}}$, 1371 $\nu(\text{COO}^-)_{\text{sim}}$, 1015, 695, 675, 619, 515 cm^{-1} . UV-Vis (CH_2Cl_2 , 1.10^{-3}M) $\lambda_{\text{max}}(\epsilon)$ = 558 nm ($182 \text{ M}^{-1}\text{cm}^{-1}$), 490 nm ($244 \text{ M}^{-1}\text{cm}^{-1}$), 352 nm ($1840 \text{ M}^{-1}\text{cm}^{-1}$). Anal. Found (calcd.) (%) for $\text{C}_{39}\text{H}_{93}\text{B}_{60}\text{O}_{13}\text{N}_3\text{Fe}_3$: C 26.03(26.05); N 1.61(1.79); H 5.76(5.78).

Synthesis of $[\text{Co}_2(\mu\text{-H}_2\text{O})(1\text{-CH}_3\text{-2-CO}_2\text{-1,2-closo-C}_2\text{B}_{10}\text{H}_{10})_4(\text{THF})_4]$, **C3.** 1-CH₃-2-CO₂H-1,2-closo-C₂B₁₀H₁₀, LH, (0.2 g, 0.99 mmols) in ethanol (1.5 mL) was neutralized with a 0.1 M aqueous NaOH solution with phenolphthalein as indicator at room temperature and immediately mixed with a solution of CoCl₂·6H₂O (0.12 g, 0.490 mmols) in water (1 mL). The temperature of the pink solution gradually rose to 40°C. After 2 h the solvent was removed under vacuum, the solid residue was redissolved in THF (30 mL) and again dried under vacuum. The last process was repeated three times. The obtained residue was once more dissolved in THF, the solution was filtrated to remove solid Na₂SO₄ and the solvent was again removed under vacuum. The resulting pink solid was recrystallized by slow diffusion of pentane into a diethyl ether solution to afford, air-stable pink crystals of **C3** suitable for X-ray diffraction analysis. Yield: 0.28 g (93%). ¹H{¹¹B} NMR (400.13 MHz, acetone-d₆, 25°C): δ= 4.70 (s, μ-H₂O), 2.30 (br s, B-H), 2.23 (br s, B-H), 2.13 (s, CH₃). ¹¹B{¹H} NMR (128.37 MHz, acetone-d₆, 25°C): δ= -1.4 (1B), -2.5(1B), -3.7(1B), -6.9 (2B), -9.6(1B), -10.5(1B), -11.1(1B), -12.8 (2B) ppm. IR: $\bar{\nu}$ = 2985ν(OH), 2894, 2581ν (B-H), 1677ν(COO⁻)_{as}, 1443, 1361ν(COO⁻)_{sim}, 916, 871δ(O-H), 761, 725ν(B-C) cm⁻¹. UV-Vis (CH₂Cl₂, 1.10⁻³M) λ_{max} (ε)= 353 nm (134 M⁻¹cm⁻¹), 534 nm (97 M⁻¹cm⁻¹). Elemental analysis calcd (%) for C₃₂H₈₆B₄₀O₁₃Co₂·0.3 THF: C 31.88, H 7.12; found: C 31.77, H 7.34.

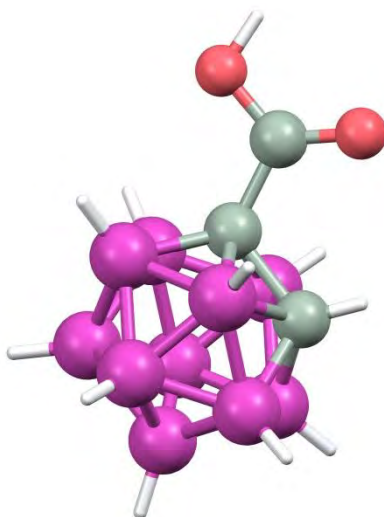
Synthesis of $[\text{Co}(\mu\text{-H}_2\text{O})(1\text{-CH}_3\text{-2-CO}_2\text{-1,2-closo-C}_2\text{B}_{10}\text{H}_{10})_2]_n \cdot (\text{H}_2\text{O})_n$, **C5.** To a suspension of 0.093 g (0.458 mmols) of 1-CH₃-2-CO₂H-1,2-closo-C₂B₁₀H₁₀, LH, in water (20 mL) was added 0.055 g (0.458 mmols) of CoCO₃ in water (5mL). The solution was stirred and heated to 40 °C for 2h. Afterward, the solution was filtered and the solvent was removed under vacuum to obtain a palepink solid. The resulting product was recrystallized by slow diffusion of pentane into a diethyl ether solution. After several days, pink crystals suitable for X-ray diffraction were obtained corresponding to [Co₃(μ-H₂O)₄(1-CH₃-2-CO₂-1,2-closo-C₂B₁₀H₁₀)₆(C₄H₁₀O)₂], **C4**. Yield: 0.103g (94%). ¹H{¹¹B} NMR (400.13 MHz, D₂O, 25°C): δ= 2.19 (br s, B-H), 2.10 (br s, B-H), 1.96 (br s, B-H), 1.90 (br s, B-H), 1.79 (s, CH₃). ¹¹B{¹H} NMR (128.37, D₂O, 25°C): δ= -4.0 (¹J(B,H)= 148.9, 1B), -6.9 (¹J(B,H)= 151.5, (1B), -10.09 3B), -10.91 (¹J(B,H)= 147.6, 5B). IR: $\bar{\nu}$ = 3585, 3556 ν(OH), 2583 ν (B-H), 1618ν(COO⁻)_{as}, 1376 ν(COO⁻)_{sim}, 1149, 1015, 846 δ(O-H), 772, 725 ν(B-C) cm⁻¹. UV-Vis (H₂O, 1.10⁻³M) λ_{max} (ε)= 356 nm (5 M⁻¹cm⁻¹), 472 nm (4 M⁻¹cm⁻¹), 510 nm (5 M⁻¹cm⁻¹). Anal. Found (calcd.) (%) for C₈H₂₈O₅B₂₀Co·1H₂O: C 19.52(19.32); H 6.17(6.08).

V.6. References

- [1] S. J. Lippard, *Angew Chem. Int. Ed. Engl.*, **1988**, 27, 344.
- [2] J. Limburg, J. S. Vrettos, L. M. Liable-Sands, A. L. Rheingold, R. H. Crabtree, G. W. Brudvig, *Science*, **1999**, 283, 1524.
- [3] a) H. G. Seiler, A. Sigel, H. Sigel, *Handbook on Metals in Clinical and Analytical Chemistry*, Marcel Dekker, New York **1994**; b) J. B. Vincent, G. L. Olivier-Lilley, B. A. Averill, *Chemical Reviews*, **1990**, 90, 1447; c) R. R. Crichton, *Inorganic Biochemistry of Iron Metabolism*, Hardvar, New York, **1991**,
- [4] a) R. H. Holm, P. Kennepohl, E. I. Solomon, *Chem. Rev.*, **1996**, 96, 2239; b) E. I. Solomon, T. C. Brunold, M. I. Davis, J. N. Kemsley, S.-K. Lee, N. Lehnert, F. Neese, A. J. Skulan, Y.-S. Yang, J. Zhou, *Chem. Rev.*, **2000**, 100, 235; c) J. Du Bois, T. J. Mizoguchi, S. J. Lippard, *Coord. Chem. Rev.*, **2000**, 200; d) E. Y. Tshuva, S. J. Lippard, *Chem. Rev.*, **2004**, 987.
- [5] R. L. Rardin, W. B. Tolman, S. J. Lippard, *New J. Chem.*, **1991**, 15, 417.
- [6] a) R. D. Cannon, A. J. P. White, *Prog. Inorg. Chem.*, **1988**, 36, 195; b) V. Rabe, W. Frey, A. Baro, S. Laschat, M. Bauer, H. Bertagnolli, S. Rajagopalan, T. Asthalter, E. Roduner, H. Dilger, T. Glaser, D. Schnieders, *Eur. J. Inorg. Chem.*, **2009**, 2009, 4660.
- [7] a) H. G. Jang, S. J. Geib, Y. Kaneko, M. Nakano, M. Sorai, A. L. Rheingold, B. Montez, D. N. Hendrickson, *Journal of the American Chemical Society*, **1989**, 111, 173; b) J. Overgaard, E. Rentschler, G. A. Timco, N. V. Gerbeleu, V. Arion, A. Bousseksou, J. P. Tuchagues, F. K. Larsen, *Journal of the Chemical Society, Dalton Transactions*, **2002**, 0, 2981; c) R. Wu, M. Poyraz, F. E. Sowrey, C. E. Anson, S. Wocadlo, A. K. Powell, U. A. Jayasooriya, R. D. Cannon, T. Nakamoto, M. Katada, H. Sano, *Inorg. Chem.*, **1998**, 37, 1913; d) C.-C. Wu, S. A. Hunt, P. K. Gantzel, P. Gülich, D. N. Hendrickson, *Inorganic Chemistry*, **1997**, 36, 4717.
- [8] a) R. Sessoli, A. K. Powell, *Coord. Chem. Rev.*, **2009**, 253, 2328; b) G. Aromi, E. K. Brechin, *Struct. Bond.*, **2006**, 122, 1; c) Y.-Z. Zheng, M.-L. Tong, W. Xue, W.-X. Zhang, X.-M. Chen, F. Grandjean, G. J. Long, *Angew. Chem. Int. Ed.*, **2007**, 46, 6076; d) E. K. Brechin, J. C. Huffman, G. Christou, J. Yoo, M. Nakano, D. N. Hendrickson, *Chem. Comm.*, **1999**, 0, 783.
- [9] a) R. Bircher, G. Chaboussant, C. Dobe, H. U. Gudel, S. T. Ochsenbein, A. Sieber, O. Waldmann, *Adv. Funct. Mater.*, **2006**, 16, 209; b) E. Coronado, D. Gatteschi, *J. Mater. Chem.*, **2006**, 16(26), 2513; c) C. J. Milios, S. Piligkos, E. K. Brechin, *Dalton Trans.*, **2008**, 14, 1809; d) D. Gatteschi, R. Sessoli, A. Cornia, *Chem. Commun.*, **2000**, 9, 725; e) G. Christou, *Polyhedron*, **2005**, 24, 2065; f) B. Cage, S. E. Russek, R. Shoemaker, A. J. Barker, C. Stoldt, V. Ramachandaran, N. S. Dalal, *Polyhedron*, **2007**, 26, 2413.
- [10] J. A. Larrabee, S.-A. Chyun, A. S. Volwiler, *Inorg. Chem.*, **2008**, 47, 10499.
- [11] a) H. L. Carrell, J. P. Glusker, V. Burger, F. Manfre, D. Tritsch, J.-F. Biellmann, *Proc. Natl. Acad. Sci. USA*, **1989**, 86, 4440; b) A. Lavie, K. N. Allen, G. A. Petsko, D. Ringe, *Biochemistry*, **1994**, 33, 5469; c) K. N. Allen, A. Lavie, G. A. Petsko, D. Ringe, *Biochemistry*, **1995**, 34, 3742; d) T. D. Fenn, D. Ringe, G. A. Petsko, *Biochemistry*, **2004**, 43, 6464; e) D. A. Brown, W. Errington, W. K. Glass, W. Haase, T. J. Kemp, H. Nimir, S. M. Ostrovsky, R. Werner, *Inorg. Chem.*, **2001**, 40, 5962; f) M. H. Sazinsky, M. Merckx, E. Cadieux, S. Tang, S. J. Lippard, *Biochemistry*, **2004**, 43, 16263; g) R. C. Holz, *Coord. Chem. Rev.*, **2002**, 232.
- [12] a) J. Luo, M. Hong, R. Wang, R. Cao, L. Han, D. Yuan, Z. Lin, Y. Zhou, *Inorganic Chemistry*, **2003**, 42, 4486; b) Q. Yang, L. Huang, M. Zhang, Y. Li, H. Zheng, Q. Lu, *Crystal Growth & Design*, **2013**, 13, 440; c) Y.-H. Liu, H.-L. Tsai, Y.-L. Lu, Y.-S. Wen, J.-C. Wang, K.-L. Lu, *Inorg. Chem.*, **2001**, 40, 6426; d) N. Stock, S. Biswas, *Chem. Rev.*, **2012**, 112, 933; e) C. Janiak, J. K. Vieth, *New Journal of Chemistry*, **2010**, 34, 2366.
- [13] a) V. F. Puentes, D. Zanchet, C. K. Erdonmez, A. P. Alivisatos, *J. Am. Chem. Soc.*, **2002**, 124, 12874; b) V. F. Puentes, K. M. Krishnan, A. P. Alivisatos, *Science*, **2001**, 291, 2115; c) S. M. Ostrovsky, R. Werner, D. A. Brown, W. Haase, *Chemical Physics Letters*, **2002**, 353, 290.
- [14] a) O. Kriz, A. L. Rheingold, M. Y. Shang, T. P. Fehlner, *Inorganic Chemistry*, **1994**, 33, 3777; b) M. Fontanet, A. R. Popescu, X. Fontrodona, M. Rodriguez, I. Romero, F. Teixidor, C. Viñas, E. Ruiz, *Chem. Eur. J.*, **2011**, 17, 13217.
- [15] F. A. Chavez, R. Y. N. Ho, M. Pink, J. V. G. Young, S. V. Kryatov, E. V. Rybak-Akimova, H. Andres, E. Münck, J. L. Que, W. B. Tolman, *Angew. Chem. Int. Ed.*, **2002**, 41, 149.
- [16] A. I. Vogel, *A Textbook of Quantitative Inorganic Analysis 3rd ed.*, Longman, London, **1961**,
- [17] a) E. Yu. Fursova, G. V. Romanenko, V. I. Ovcharenko, *Izv. Akad. Nauk SSSR, Ser. Khim. (Russ.) (Russ. Chem. Bull.)*, **2005**, 795; b) F. Marchetti, B. Melai, G. Pampaloni, S. Zacchini, *Inorg. Chem.*, **2007**, 46, 3378.

- [18] a) T. Sato, F. Ambe, K. Endo, M. Katada, H. Maeda, T. Nakamoto, H. Sano, *J. Am. Chem. Soc.*, **1996**, 118, 3450; b) J. Overgaard, F. K. Larsen, B. Schiøtt, B. B. Iversen, *J. Am. Chem. Soc.*, **2003**, 125, 11088; c) P. Poganiuch, S. Liu, G. C. Papaefthymiou, S. J. Lippard, *J. Am. Chem. Soc.*, **1991**, 113, 4645.
- [19] a) D. Lee, P.-L. Hung, B. Spingler, S. J. Lippard, *Inorg. Chem.*, **2002**, 41, 521; b) D. A. Brown, W. K. Glass, N. J. Fitzpatrick, T. J. Kemp, W. Errington, G. J. Clarkson, W. Haase, F. Karsten, A. H. Mahdy, *Inorg. Chim. Acta*, **2004**, 357, 1411; c) T. J. Prior, J. C. Burley, *Acta Crystallographica Section E*, **2005**, 61, m1422; d) A. Karmakar, R. J. Sarma, J. B. Baruah, *Eur. J. Inorg. Chem.*, **2007**, 5, 643; e) A. Karmakar, R. J. Sarma, J. B. Baruah, *Polyhedron*, **2007**, 26, 1347.
- [20] J. K. Burdett, T. A. Albright, *Inorganic Chemistry*, **1979**, 18, 2112.
- [21] a) V. Calvo-Pérez, S. Ostrovsky, A. Vega, J. Pelikan, E. Spodine, W. Haase, *Inorg. Chem.*, **2006**, 45, 644; b) A. O. Tokareva, D. S. Tereshchenko, A. I. Boltalin, S. I. Troyanov, *Koord. Khim. (Russ.) (Coord. Chem.)* **2006**, 32, 691; c) P. Nockemann, B. Thijs, K. V. Hecke, L. V. Meervelt, K. Binnemans, *Crystal Growth & Design*, **2008**, 8, 1353; d) Z. Hulvey, D. S. Wragg, Z. Lin, R. E. Morris, A. K. Cheetham, *Dalton Trans.*, **2009**, 0, 1131.
- [22] a) L. J. Todd, A. R. Siedle, *Prog. Nucl. Magn. Reson. Spectrosc.*, **1979**, 13, 87; b) R. C. Mehrotra, R. Bohra, *Metal Carboxylates*, Academic, New York, **1983**, 396; c) L. A. Leites, *Chem. Rev.*, **1992**, 92, 279
- [23] V. Paredes-García, D. Venegas-Yazigi, R. O. Latorre, E. Spodine, *Polyhedron*, **2006**, 25, 2026.
- [24] J. S. Pap, J. Kaizer, M. Giorgi, G. Speier, *Inorganic Chemistry Communications*, **2010**, 13, 1069.
- [25] A. K. Dutta, S. K. Maji, S. Dutta, *Journal of Molecular Structure*, **2012**, 1027, 87.
- [26] Z. Salman, R. Khalaf, H. D. Ashour, *Iraqi National Journal Of Chemistry*, **2009**, 489.
- [27] a) K. B. Gudasi, S. A. Patil, R. S. Vadavi, R. V. Shenoy, *Transition Metal Chemistry*, **2006**, 31, 586; b) R. V. S. N. Ravikumara, K. Ikedaa, A. V. Chandrasekhar, Y. P. Reddy, P. S. Raod, J. Yamauchie, *Journal of Physics and Chemistry of Solids*, **2003**, 64, 2433.
- [28] U. Venkatasubramanian, D. J. Donohoe, D. Ellis, B. T. Giles, S. A. Macgregor, S. Robertson, G. M. Rosair, A. J. Welch, A. S. Batsanov, L. A. Boyd, R. C. B. Copley, M. A. Fox, J. A. K. Howard, K. Wade, *Polyhedron*, **2004**, 23, 629
- [29] Y. Inada, Y. Nakano, M. Inamo, M. Nomura, S. Funahashi, *Inorg. Chem.*, **2000**, 39, 4793.

CHAPTER VI. Cu(II) and Mn(II) complexes containing the carboranylcarboxylate ligand 1-CO₂H-1,2-closo-C₂B₁₀H₁₁.



A series of new mono- and polynuclear copper(II) and manganese(II) compounds containing the 1-CO₂H-1,2-closo-C₂B₁₀H₁₁ carborane ligand (*L'H*) has been synthesized and fully characterized through analytical, spectroscopic (NMR, IR, UV-visible) and electrochemical techniques. X-ray structural analysis has been performed on all compounds. A comparison of these compounds with the analogous containing the carboranylcarboxylate ligand [1-CH₃-2-CO₂-1,2-closo-C₂B₁₀H₁₁], *LH*, revealed in most cases a similarity in the structure of the compounds. However, some differences were found in these compounds arising from the presence of different substituents on the carboranylcarboxylate ligands. An evaluation of this behaviour is presented in this chapter.

TABLE OF CONTENTS

CHAPTER VII. Cu(II) and Mn(II) complexes containing the carboranylcarboxylate ligand 1-CO₂H-1,2-closo-C₂B₁₀H₁₀.

VI.1. Introduction	141
VI.2. Objectives	142
VI.3. Results and discussion	143
VI.3.1. Synthesis and characterization of copper complexes.....	143
VI.3.2. Electrochemical properties	151
VI.3.3. Spectroscopic properties	152
VI.3.4. Synthesis and characterization of manganese complexes	153
VI.4. Conclusions	162
VI.5. Experimental section	164
VI.5.1. Instrumentation and measurements	164
VI.5.2. Materials	164
VI.5.3. Preparations	165
VI.6. References	169

VI.1. Introduction

As commented in Chapter III and IV, mono- and polynuclear copper(II) and manganese(II) compounds have great interest due to their multiple applications in different fields such as molecular semiconductors, nanomagnets, ions exchange, chemical separation, sensor technology, energy conversion, optoelectronics or catalysis^[1], as well as for their potential use as frameworks for the assembling of complexes in two or three dimensions to generate supramolecular structures (MOFs)^[2] which have attractive applications among which are their use as sensors, catalysts, or H₂-storage devices.^[3]

Synthesis and characterization of complexes containing the carboranylcarboxylate ligand, [1-CH₃-2-CO₂-1,2-*closo*-C₂B₁₀H₁₀]⁻, and copper^[4] or manganese^[5] atoms has been reported and presented in Chapter III and IV. Most of the copper(II) complexes reported display a binuclear *paddle-wheel* structure whereas than for Mn(II) complexes, mono-, bi- and polynuclear compounds have been described. Moreover, copper compounds containing the carboranylcarboxylate ligand present notable differences respect the analogous μ -acetate compounds such as their behaviour in nucleophilic solvents (carboranylcarboxylate complexes are unstable in MeOH whereas the analogous μ -acetate complex. are stable) or their solubility (complexes containing the carboranylcarboxylate ligand are readily soluble in dichloromethane, diethyl ether or toluene, where copper acetate is completely insoluble).^[4]

On the other hand, complexes containing the [1-CO₂-1,2-*closo*-C₂B₁₀H₁₁]⁻ ligand and the transition metals Zn^{II}, Cu^{II}, Ni^{II} and Mo^{II} ions have been found in the literature,^[6] however, the coordination of Mn^{II} ions to this carboranylcarboxylate ligand has never been studied.

In this chapter we focused our investigations on the differences that the substitution of a methyl group by a hydrogen atom on the cluster of the carboranylcarboxylate ligand can produce in the reactivity of this ligand in front of Cu(II) and Mn(II).

VI.2. Objectives

In previous chapters we have synthesized complexes with Cu(II) and Mn(II) both containing the carboranylcarboxylate ligand $[1\text{-CH}_3\text{-2-CO}_2\text{-1,2-closo-C}_2\text{B}_{10}\text{H}_{10}]^-$, in this chapter, we expect that the substitution of the methyl group by a hydrogen atom on this carboranylcarboxylate ligand could lead to a different reactivity of this new ligand with these metals.

With all this in mind, the main goal of this chapter was the synthesis, characterization and study of the main chemical properties of new mono- and polynuclear copper(II) or manganese(II) complexes containing the ligand carboranylcarboxylate $[1\text{-CO}_2\text{-1,2-closo-C}_2\text{B}_{10}\text{H}_{11}]^-$.

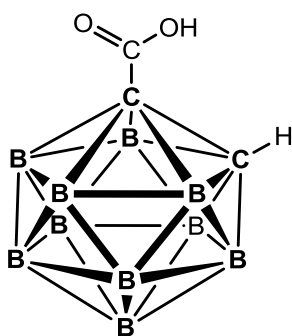


Chart 1. $1\text{-CO}_2\text{H-1,2-closo-C}_2\text{B}_{10}\text{H}_{10}$ ligand ($L'H$)

First of all, a binuclear Cu(II) starting material complex having THF molecules as terminal ligands was synthesized and fully characterized. The reactivity of this starting material with respect to different pyridyl ligands was also studied.

Secondly, a Mn(II) starting material complex was synthesized and fully characterized through structural, analytical and spectroscopic techniques. We were also concerned in evaluate the influence and reactivity of the bidentate chelating ligand 2,2'-bipyridine over the structure of this starting material.

Finally, we have proposed to establish structural and chemical differences among the synthesized compounds and the analogous ones containing the carboranylcarboxylate ligand LH, where a methyl group instead a hydrogen atom is presented.

VI.3. Results and discussion

VI.3.1. Synthesis and characterization of copper complexes

The synthetic strategy for the preparation of the ligand **L'H** and the Cu(II) complexes **D1-D5**, containing the carboranylcarboxylate ligand 1-CO₂H-1,2-*closo*-C₂B₁₀H₁₁ (**L'H**) and different terminal ligands, **L_t**, is outlined in

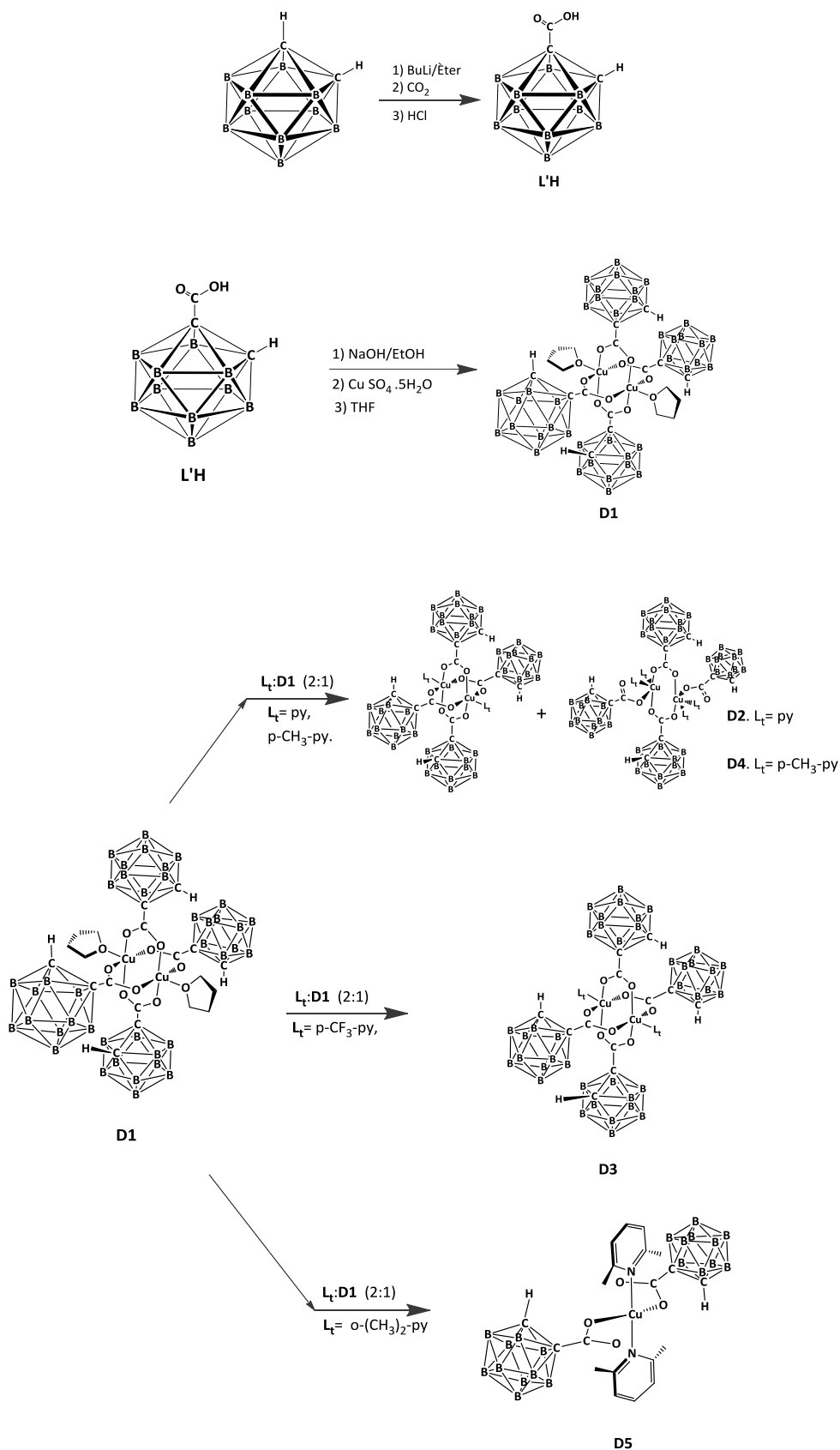
Scheme 1.

Binuclear copper(II) compound [Cu₂(1-CO₂-1,2-*closo*-C₂B₁₀H₁₁)₄(THF)₂], **D1**, was obtained by neutralization of carboranylcarboxylic acid, **L'H**, with NaOH followed by reaction with CuSO₄ in ethanol/H₂O and subsequent extraction in THF.^[6a]

Compound **D1** was used as starting material and it was reacted with monodentate and bidentate pyridylic ligands, **L_t**, (**L_t** = py, *p*-CF₃-py, *p*-CH₃-py and *o*-(CH₃)₂-py), which were also used in Chapter III.

When the corresponding ligands **L_t** dissolved in CH₂Cl₂ are added to a solution of complex **D1** in CH₂Cl₂ (with a ligand:complex ratio of 2:1), blue-green solutions are formed that after slow evaporation lead, in most cases, to the precipitation of binuclear complexes of general formula [Cu₂(L')₄(L_t)₂] as main products. In the case of the binuclear compounds **D2** and **D4**, obtained upon addition of pyridine and *p*-methylpyridine respectively, we have also observed the parallel formation of other binuclear compounds with general formula [Cu₂(L')₄(L_t)₄] in lower yield (complexes **D2'** and **D4'**, see experimental section and Figure S1 at the supporting information section) with a ratio **D2**:**D2'** of 0.55:0.45 and **D4**:**D4'** of 0.90:0.10. Finally, the addition of 2,6-lutidine as axial **L_t** ligand leads to the formation of the mononuclear complex **D5** as main product.

Crystallographic data and selected bond distances and angles for compounds **D1-D5** are presented in Table S1 (see supporting information section), Table 1. and Table 2, respectively (the corresponding data for compounds **D2'**, **D4'** and **D5'** are gathered in the supporting information section, Table S2 and Table S3). ORTEP plots with the corresponding atom labels for the X-ray structures of all compounds are presented in Figure 1 and Figure S1.



Scheme 1. Synthetic strategy for the preparation of **L'H** and Cu(II) complexes **D1-D5**

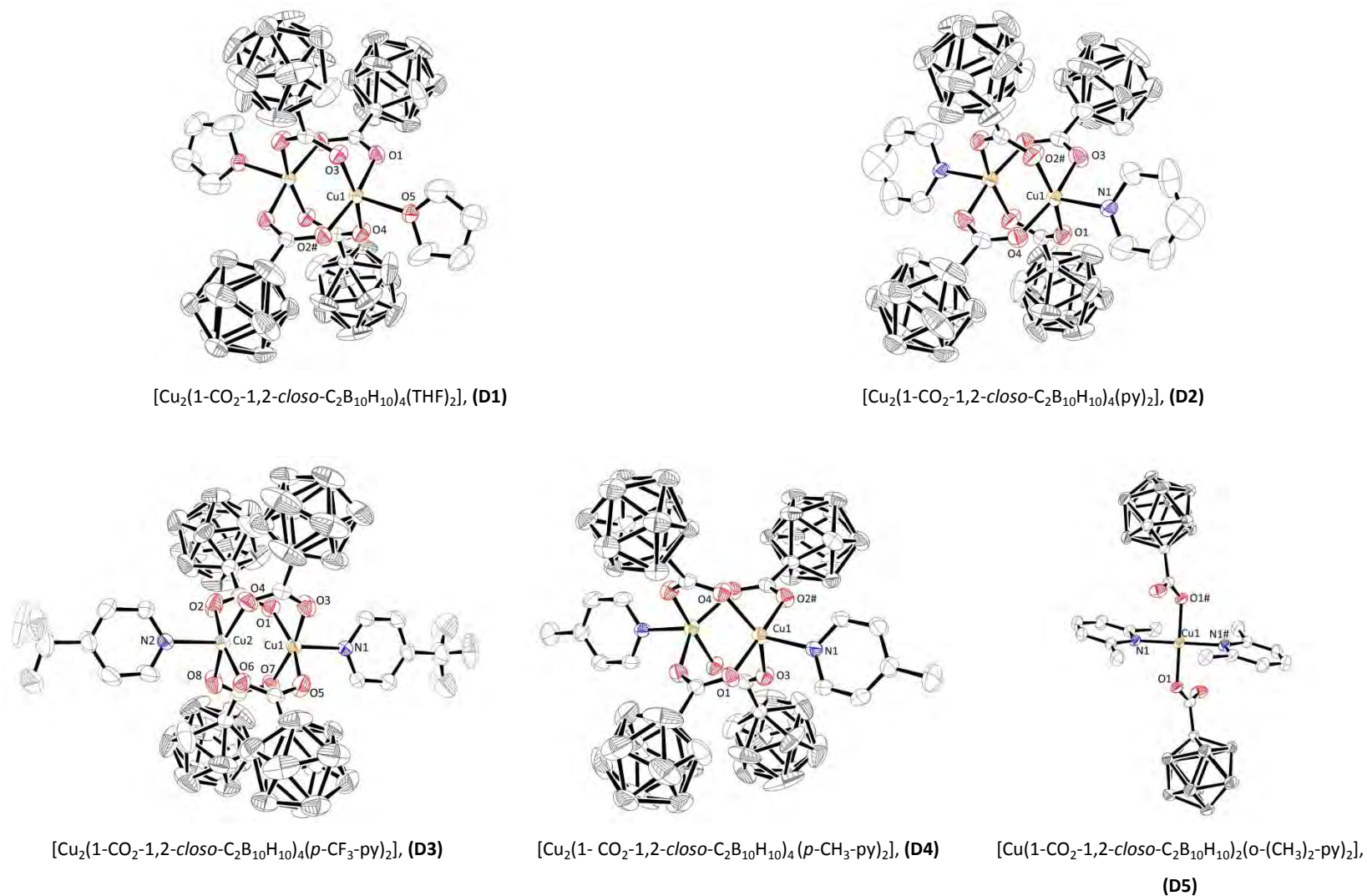


Figure 1. X-ray structures (ORTEP plots with ellipsoids at 40% probability level) and labelling scheme for complexes **D1-D5**.

Table 1. Selected bond lengths (Å) and angles (°) for complexes **D1-D4**.

	D1	D2	D4		D3	D3	D3
Cu(1)-O(1)	1.959(2)	1.962(4)	1.922(4)	Cu(1)-O(1)	1.986(2)	Cu(2)-O(2)	1.941(2)
Cu(1)-O(2)#1	1.960(2)	1.957(4)	1.913(3)	Cu(1)-O(3)	1.953(2)	Cu(2)-O(4)	1.965(2)
Cu(1)-O(3)	1.959(2)	1.972(4)	2.139(4)	Cu(1)-O(5)	1.973(2)	Cu(2)-O(6)	1.952(2)
Cu(1)-O(4)	1.960(2)	1.967(4)	2.040(4)	Cu(1)-O(7)	1.959(2)	Cu(2)-O(8)	1.977(2)
Cu(1)-X	2.100(2)	2.113(3)	2.060(5)	Cu(1)-N(1)	2.126(2)	Cu(2)-N(2)	2.127(2)
Cu(1)-Cu(1)#	2.6786(6)	2.7308(12)	3.009(2)	Cu(1)-Cu(2)	2.7439(5)	O(2)-Cu(2)-O(6)	167.88(10)
O(1)-Cu(1)-O2#	166.83(10)	165.07(17)	175.10(16)	O(1)-Cu(1)-O(5)	161.41(9)	O(2)-Cu(2)-O(4)	88.92(12)
O(1)-Cu(1)-O(4)	89.09(12)	89.30(18)	89.21(18)	O(1)-Cu(1)-O(7)	89.35(11)	O(6)-Cu(2)-O(4)	89.95(11)
O(2) #1-Cu(1)-O(4)	88.84(12)	89.0(2)	91.16(18)	O(5)-Cu(1)-O(7)	88.71(11)	O(2)-Cu(2)-O(8)	88.53(13)
O(3)-Cu(1)-O(1)	89.88(11)	88.60(2)	89.26(18)	O(3)-Cu(1)-O(1)	88.06(11)	O(6)-Cu(2)-O(8)	88.86(12)
O(3)-Cu(1)-O(2)#	89.17(11)	89.4(2)	87.42(18)	O(3)-Cu(1)-O(5)	89.79(12)	O(4)-Cu(2)-O(8)	162.16(10)
O(3)-Cu(1)-O(4)	166.79(9)	166.04(18)	141.66(15)	O(3)-Cu(1)-O(7)	167.32(10)	O(6)-Cu(2)-N(2)	94.16(9)
O(1)-Cu(1)-X	99.38(9)	99.82(16)	92.06(17)	O(1)-Cu(1)-N(1)	96.49(9)	O(4)-Cu(2)-N(2)	99.49(9)
O(2)#-Cu(1)-X	93.75(10)	95.07(16)	92.04(17)	O(5)-Cu(1)-N(1)	102.09(9)	O(8)-Cu(2)-N(2)	98.35(9)
O(3)-Cu(1)-X	98.24(9)	93.29(17)	99.48(16)	O(3)-Cu(1)-N(1)	98.58(9)	O(2)-Cu(2)-N(2)	97.93(10)
O(4)-Cu(1)-X	94.92(10)	100.66(16)	118.86(7)	O(7)-Cu(1)-N(1)	94.05(9)	O(6)-Cu(2)-Cu(1)	83-17(6)
O(1)-Cu(1)- Cu(1)#	83.83(7)	82.36(13)	89.20(12)	O(1)-Cu(1)- Cu(2)	79.83(6)	O(4)-Cu(2)-Cu(1)	80.73(7)
O(2)#-Cu(1)-Cu(1)#	83.02(7)	82.71(12)	86.27(13)	O(5)-Cu(1)-Cu(2)	81.59(7)	O(8)-Cu(2)-Cu(1)	81.45(7)
O(3)-Cu(1)-Cu(1)#	83.26(7)	82.40(13)	69.83(11)	O(3)-Cu(1)-Cu(2)	83.75(7)	O(2)-Cu(2)-Cu(1)	84.74(7)
O(4)-Cu(1)-Cu(1)#	83.54(7)	83.64(13)	71.85(12)	O(7)-Cu(1)-Cu(2)	83.57(6)	N(2)-Cu(2)-Cu(1)	177.32(7)
X-Cu(1)-Cu(1)#	176.44(7)	175.15(11)	169.22(13)	N(1)-Cu(1)-Cu(2)	175.60(6)		

X= O(5), complex **D1**; X = N(1), complexes **D2, D4**;**Table 2.** Selected bond lengths (Å) and angles (°) for complex **D5**.

	D5		D5
Cu(1)-O(1)	1.9409(14)	O(1)#-Cu(1)-N(1)#	92.23(7)
Cu(1)-O(1)#	1.9409(14)	O(1)-Cu(1)-N(1)#	87.77(7)
Cu(1)-N(1)	2.0288(16)	O(1#)-Cu(1)-N(1)	87.77(6)
Cu(1)-N(1)#	2.0288(16)	O(1)-Cu(1)-N(1)	92.23(6)
O(1)#-Cu(1)-O(1)	180.00(1)	N(1) #-Cu(1)-N(1)	180.00(13)

Binuclear compounds **D1-D4** display a similar structure with the two copper (II) atoms held together through four syn,syn $\eta^1: \eta^1: \mu^2$ -carboxylate bridges acting as equatorial ligands for each Cu(II) atom. The square pyramidal geometry around each metal ion is completed by the oxygen donor atom of a THF molecule in **D1** or by the donor nitrogen atom of the different

pyridylic terminal ligands in **D2-D4**. The overall geometry of the complexes corresponds to a binuclear paddle-wheel cage type.

The structures are centrosymmetric with the symmetry centre located between the two copper atoms. The Cu-O_{carboxy} bond distances are similar and comparable to other similar coordinated carboxylates,^[4, 7] and are in the range 1.91-2.14 Å.

For complex **D1**, the apical distance Cu-O_{THF} is 2.11 Å and is longer than the basal distances, but it is within the range observed for other similar carboxylate structures with water as axial ligand.^[8] The Cu-L_t bond distances in the pyridyl complexes follow the trend L_t= p-CF₃-py (2.13 Å) > py (2.11 Å) > p-CH₃-py (2.06 Å) an order that could be related to the basic strength of the ligands, the lower basicity of the pyridylic ligands increases the distance Cu-L_t observed in these complexes. The Cu...Cu distances, in the range 2.68-3.00 Å, are similar to the complexes synthesized in Chapter III as well as to other carboranylcarboxylate compounds reported in the literature.^[6a]

The distortion of the coordination polyhedron in compounds **D1-D4** is evidenced by the trans O-Cu-O angles, which range from 161.4 to 175.1°. Moreover, each copper atom is displaced out of the mean plane towards the corresponding apical ligand (the bond angles involving the apical ligand, O-Cu-O/N, range from 92.1 to 102.1°, and the distances from each Cu atom to its mean basal plane range between 0.225 and 0.380 Å for the set of binuclear complexes). For complexes **D2-D4**, with N-pyridines as apical ligands this displacement (average of 0.298 Å) is more pronounced than for complex **D1**, containing THF (0.225 Å). Also, in these compounds **D1-D4** the displacement of the copper atom towards the terminal ligand observed in compounds **D1-D4** is slightly higher than the observed for similar complexes [Cu₂(1-CH₃-2-CO₂-1,2-*closo*-C₂B₁₀H₁₀)₄(THF)₂], **A1**, [Cu₂(1-CO₂-1,2-*closo*-C₂B₁₀H₁₀)₄(py)₂], **A2**, [Cu₂(1-CH₃-2-CO₂-1,2-*closo*-C₂B₁₀H₁₀)₄(p-CF₃-Py)₂], **A3**, [Cu₂(1-CH₃-2-CO₂-1,2-*closo*-C₂B₁₀H₁₀)₄(p-CH₃-Py)₂], **A4**, synthesized in chapter III (range from 0.214 to 0.253 Å). The cis O-Cu-O angles around the copper atoms in **D1-D4** show slight differences with regard to the 90° ideal value and are in the range 87.4-91.2°. Intramolecular C-H...O hydrogen bonds between the hydrogen atoms bond to the carbon atom in the carborane and the oxygen atoms of the carboranylcarboxylate ligand are observed for all complexes.

It is noteworthy to comment the arrangement of the molecules of complex **D4** along *a* axis, which are displaying vertical layers in which two of the four carboranylcarboxylate ligands are opposite to two carboranylcarboxylate ligands from two adjacent molecules leading a helix form along each pair of chains. The other two carboranylcarboxylate ligands are alternated to another pair from an adjacent chain. The solvent water molecules are sandwiched between

two *p*-CH₃-py ligands fulfilling the cavities between molecules along the *c* axis. (Figure S2 at the supporting information section).

The X-ray crystallography diffraction performed on complex **D2'** ([Cu₂(1-CO₂-1,2-*closo*-C₂B₁₀H₁₀)₄(py)₄], Figure S1a, reveals a centrosymmetric binuclear copper (II) complex in which the two copper atoms are held through two *syn-anti* carboranylcarboxylate bridges acting as axial ligand (O2) and equatorial ligand (O1), respectively. The square pyramidal geometry around each copper atom is completed by one oxygen atom from a monodentate carboranylcarboxylate and two nitrogen atoms from two pyridine molecules in the equatorial plane. It is noteworthy the existence of C_c-H...H-B interactions between monodentate and bridged carboranylcarboxylate ligand, C-H(3)...H(11)-B, *d*=3.054 Å, and C-H(6)...H(9)-B, *d*=2.721 Å. These interactions probably are responsible of the asymmetry observed in the bridged ligands (Figure 2.). Due to this asymmetry, two intramolecular C-H...O hydrogen-bonds are observed, one between the substituent hydrogen from the bridged carborane and the oxygen atom coordinated to the metal, from the monodentate ligand (C(3)-H(3B)...O(5); *d*=2.279 Å) and another between the same hydrogen atom and its own oxygen *anti* (C(3)-H(3B)...O(2); *d*=2.534 Å), (see Figure S3 at the supporting information section). This last oxygen atom, O(2), present the longest distance Cu-O, (*d*_{Cu-O2}=2.288(5) Å), in comparison with the other two Cu-O bond distances (*d*_{Cu-O1}=1.954(4) Å and *d*_{Cu-O5}=1.977(5) Å). It is observed that the plane containing py_{N1} is 26.40° tilted with regard to the plane containing py_{N2}. The angles between the axial and the equatorial positions show significant distortions in comparison to the ideal square pyramid, with deviations from the theoretical value and are in the range 85.72°- 109.93°, it is remarkably that the carboranylcarboxylate oxygen displaying the longest Cu-O distance is involved in the angles with the highest deviations. Binuclear compound **D4'** (see Figure S1b at the supporting information section) displays a similar structure, where minor distortions are observed.

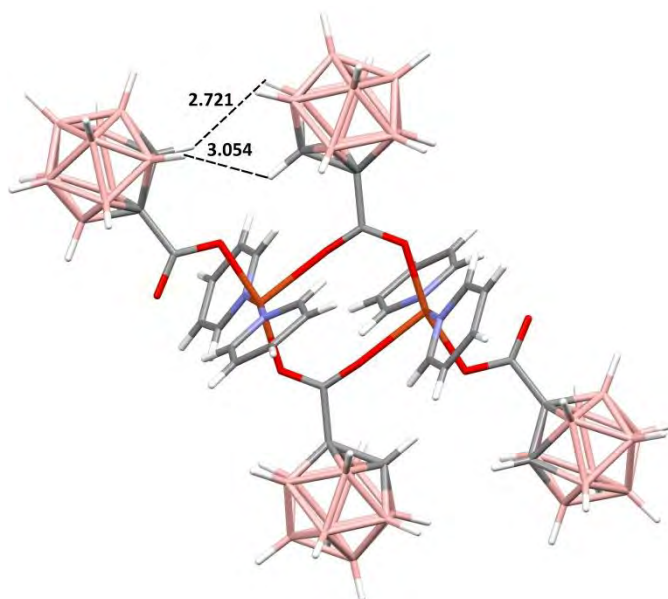


Figure 2. Interaction C-H...H-B on complex **D2'**

Mononuclear complex **D5** displays a centrosymmetric square planar structure, in which the copper atom is coordinated by two nitrogen atoms from the lutidine ligands and by two oxygen atoms from the two carboranylcarboxylate ligands that adopt a monodentate coordination mode. It is also noteworthy the existence of two hydrogen bonds one intramolecular involving the methyl group of one of the lutidine ligands and the non-coordinated oxygen atom of the carboranylcarboxylate ligand and other intermolecular with the methyl group of a neighbouring molecule which leads to the packing shown in Figure 3. Compound **D5** crystallizes together with compound **D5'** (Figure S1c in supporting information section). **D5'** consists in a copper(II) ion coordinated by four oxygen atoms of four carboranylcarboxylate ligands in a monodentate mode, leading to a square planar geometry. The molecule presents an inversion centre located in the copper atom. Cu-O distances are similar (1.919(2) Å and 1.926(2) Å) and the O-Cu-O angles are quite similar to the ideal value for a square planar geometry (89.52(11)° and 90.49(11)°). It is noteworthy the packing structure of compound **D5'** (Figure S3), molecules of **D5'** are arranged in chains in which two 2,6-lutidine molecules are located between adjacent molecules of compound **D5'**. Besides, carboranylcarboxylate ligands from molecules of different chains are alternated occupying the space fulfilled by the 2,6-lutidine ligands from the other chain. Each molecule of **D5'** present four O-H...N bonds between the four uncoordinated oxygen atoms of the monodentate carboranylcarboxylate ligands and two solvent 2,6-lutidine molecules.

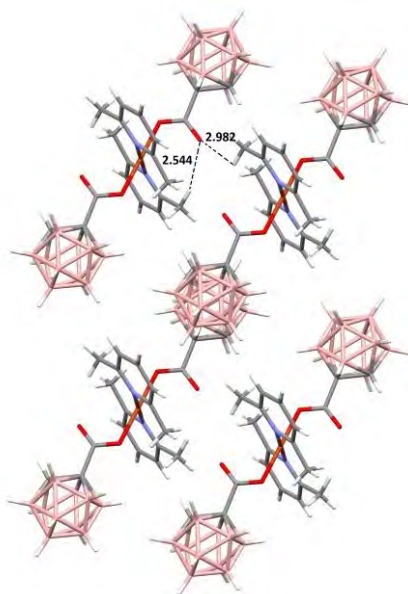


Figure 3. Packing diagram for the X-ray diffraction structure of complex **D5** showing the intramolecular and intermolecular hydrogen bonds.

X-ray crystallographic structure of compounds **D1-D5** provided a collection of binuclear and mononuclear compounds really similar to their analogous compounds **A1-A4** reported in Chapter III. No important differences are observed in the starting materials compounds obtained with both carboranylcarboxylate ligands, $[\text{Cu}_2(1\text{-CH}_3\text{-2-CO}_2\text{-1,2-}i\text{closo-C}_2\text{B}_{10}\text{H}_{10})_4(\text{THF})_2]$, **A1**, and $[\text{Cu}_2(1\text{-CO}_2\text{-1,2-}i\text{closo-C}_2\text{B}_{10}\text{H}_{11})_4(\text{THF})_2]$, **D1**. It is probably due to the prevalence of the Cu(II) ions for a specific nuclearity and arrangement with the monocarboxylate ligands.^[6a, 9] Moreover, the behaviour of this starting material with the pyridylic ligands is also similar for both ligands leading to binuclear compounds as a main product when py, *p*-CH₃-py or *p*-CF₃-py are used as terminal ligands and a mononuclear compound with *o*-(CH₃)₂-py. However, important differences are found in the side products obtained with the pyridylic ligands py and *p*-CH₃-py; compound **A1**, containing 1-CH₃-2-CO₂-1,2-*closo*-C₂B₁₀H₁₀ ligand, **LH**, leads to the formation of mononuclear side products whereas that compound **D1** with the 1-CO₂-1,2-*closo*-C₂B₁₀H₁₁ ligand, **L'H**, presents binuclear compounds as a side products. This difference has been attributed to the above commented short contacts C_c-H...H-B between neighbouring carborane ligands, which probably are the responsible for keeping the binuclear structures avoiding the evolution to the mononuclear compounds. This H...H short contacts are mainly hydrogen interactions between the acidic C_c-H protons and the B-H hydrides atoms and could be considered as dyhydrogen bonds^[10] and/or H-H bonding interactions.^[11] These interactions has been previously observed in carborane groups and their role in establishing rotamer configurations has been previously reported by Teixidor et al.^[12] It should be point out that these interactions has not been observed for compounds with the ligand **LH**, , where only

mononuclear compounds as side products were observed, as in the case of **A2** and **A4**, also probably due to the steric encumbrance of the methyl groups that could hinder the prevalence of the binuclear structures. Other consequence of these $C_c-H \cdots H-B$ interactions could be the proportion in the isolated products; thus, for compounds obtained with pyridine ligand, when the ligand used was **L'H**, a comparable ratio of the corresponding compounds were obtained (ratio **D2:D2'** of 0.55:0.45), however, when the ligand was **LH**, is mainly obtained the binuclear compound **A2** and only traces of mononuclear compound are detected.

VI.3.2. Electrochemical properties

Electrochemical properties of complexes **D1-D5** were studied by cyclic voltammetry (CV) and differential pulse voltammetry (DPV). The cyclic voltammograms of these complexes in acetonitrile (0.1 M TBAH) at room temperature, with a scan rate of $100 \text{ mV}\cdot\text{s}^{-1}$ are reported in Figure 3. and Figure S5). The CV display similar electrochemical behaviour as expected from their analogous structures, though no differences in the potential values are observed in accordance with the electron character of the pyridylic terminal ligands. All complexes present electrochemically irreversible redox waves that can be assigned to the $\text{Cu}^{\text{II}}/\text{Cu}^0$. One reduction wave in the cathodic sweep of the CV curve was observed ($E_{\text{pc}} = -0.49 \text{ V}$ for **D1-D3** and **D5** and $E_{\text{pc}} = -0.48 \text{ V}$ for **D4**) that probably correspond to reduction of Cu^{II} to Cu^0 , and in the anodic sweep two successive oxidation waves at $E_{\text{pa}} = -0.27$ and -0.21 V for **D1**; $E_{\text{pa}} = -0.26$ and -0.20 V for **D2**; $E_{\text{pa}} = -0.24$ and -0.15 V for **D3**; $E_{\text{pa}} = -0.23$ and -0.16 V for **D4** and $E_{\text{pa}} = -0.27$ and -0.20 V for **D5** were observed and were assigned to the $\text{Cu}^0/\text{Cu}^{\text{I}}$ and $\text{Cu}^{\text{I}}/\text{Cu}^{\text{II}}$ redox processes, respectively. The reduction to Cu^0 should almost certainly involve the rupture of the binuclear structure in the compound and indeed, coulometry performed at a fixed potential of $E_{\text{po}} = -0.8 \text{ V}$ for 3 minutes leads to the formation of a Cu^0 metallic deposit clearly visible on the working electrode surface.

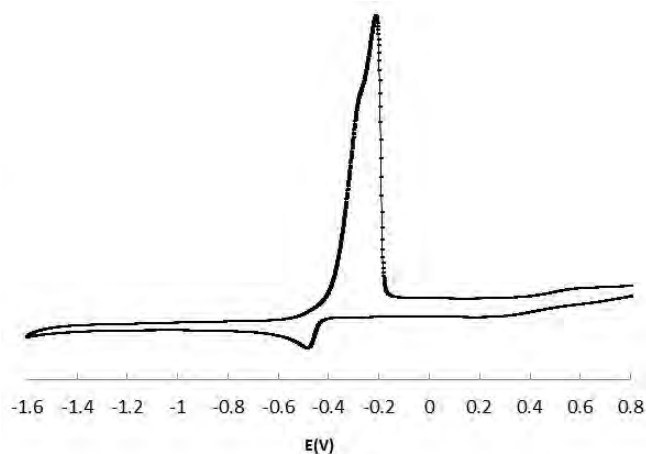


Figure 4. Cyclic voltammetry recorded for complex **D1** in acetonitrile.

Differential pulse Voltammetry (DPV) of these complexes were studied in acetonitrile (0.1 M TBAH) at room temperature in the range corresponding to the oxidation processes, with the initial idea of finding the relationship between the compound mixtures (**D2/D2'**, **D4/D4'** and **D5/D5'**). However, a great similarity in the DPV of all compounds was observed, probably due to the similar potential oxidation values of these mixtures of compounds (see Figure 5 and Figure S6).

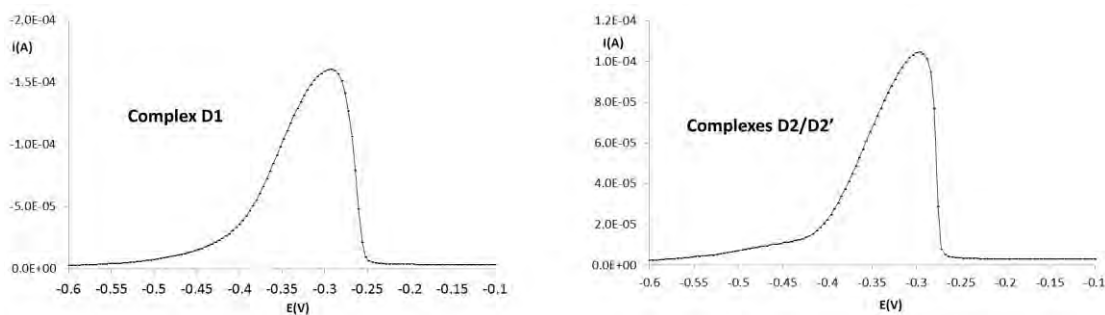


Figure 5. DPV voltammograms for complexes **D1** and the mixture **D2/D2'** in acetonitrile (0.1 M TBAH). Starting scan at -0.6V.

VI.3.3. Spectroscopic properties

The IR spectra of all complexes described display typical $\nu(\text{B-H})$ absorption at frequencies above 2580 cm^{-1} , characteristic of *closo* carborane derivatives^[13] difference between the frequencies of the symmetric and antisymmetric stretches lies between the ranges quoted for bidentate and monodentate bridged ligands.^[14] The $^1\text{H}\{^{11}\text{B}\}$ -, ^{11}B -, $^{11}\text{B}\{^1\text{H}\}$ - and $^{13}\text{C}\{^1\text{H}\}$ -NMR spectra of these compounds are in complete agreement with the solid structures confirmed by X-ray crystallography. It can be observed that the $^{11}\text{B}\{^1\text{H}\}$ -NMR resonances for all the complexes featured similar patterns in the range from $\delta = 2$ to -15 ppm that agree with a *closo* cluster.^[15] The $^1\text{H}\{^{11}\text{B}\}$ - spectra exhibit the resonances of the protons bonded to the B atoms as broad singlets over a wide chemical-shift range in the region from $\delta = 0$ to $+5$ ppm and resonances attributed to the $\text{C}_c\text{-H}$ protons appear in the range $\delta = 3.42$ to 4.40 ppm.

It was observed for all complexes that the aromatic protons were not observed in the $^1\text{H}\{^{11}\text{B}\}$ -NMR at 298K. With the aim to observe these aromatic protons, ^1H and $^1\text{H}\{^{11}\text{B}\}$ -NMR spectra of complex **D3** were carried on at 273 K. Aromatic protons were then observed. Moreover, it is worthy of mention that the ^1H -NMR chemical shifts of the protons bonded to the boron atoms change to higher frequencies when decreasing temperature (see Figure S9b at the supporting information section). The chemical shift range for these protons is from 2.12 to 3.11 ppm at 298 K whereas it moves from 2.54 to 3.65 ppm at 260K. This probably can be

related to intermolecular interactions B-H...H-B between several B-H vertexes that are observed in the crystal structure.^[12, 16] (Figure S10 at the supporting information section)

The electronic UV-vis spectra of complexes **D1-D5** are shown in Figure 6. The spectra show one characteristic band in the range 600-800 nm. These transitions can be assigned to d-d transitions from the d_{xz} , d_{yz} and d_{xy} orbitals. .^[4]

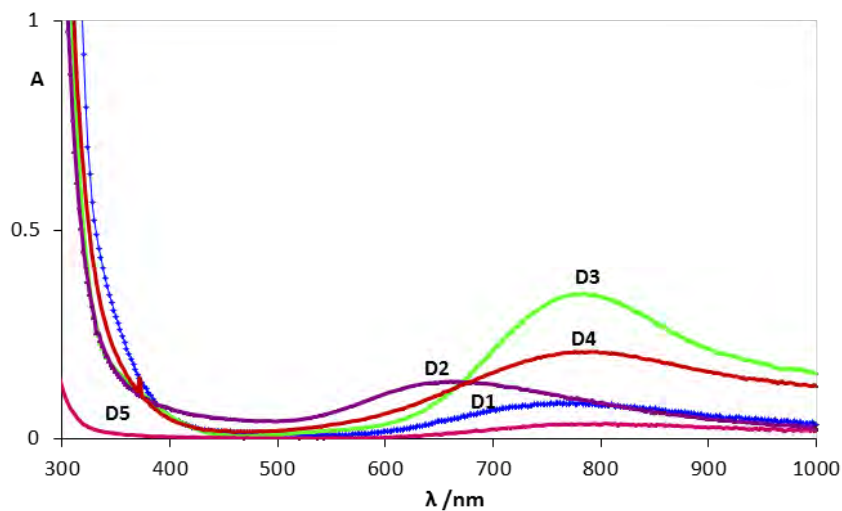
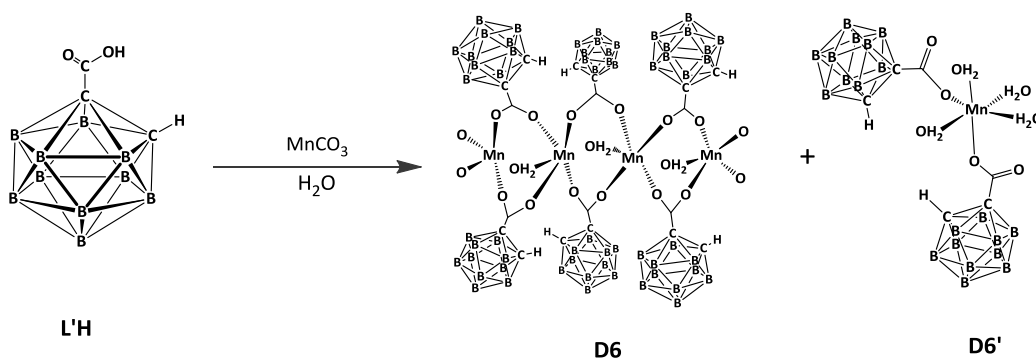
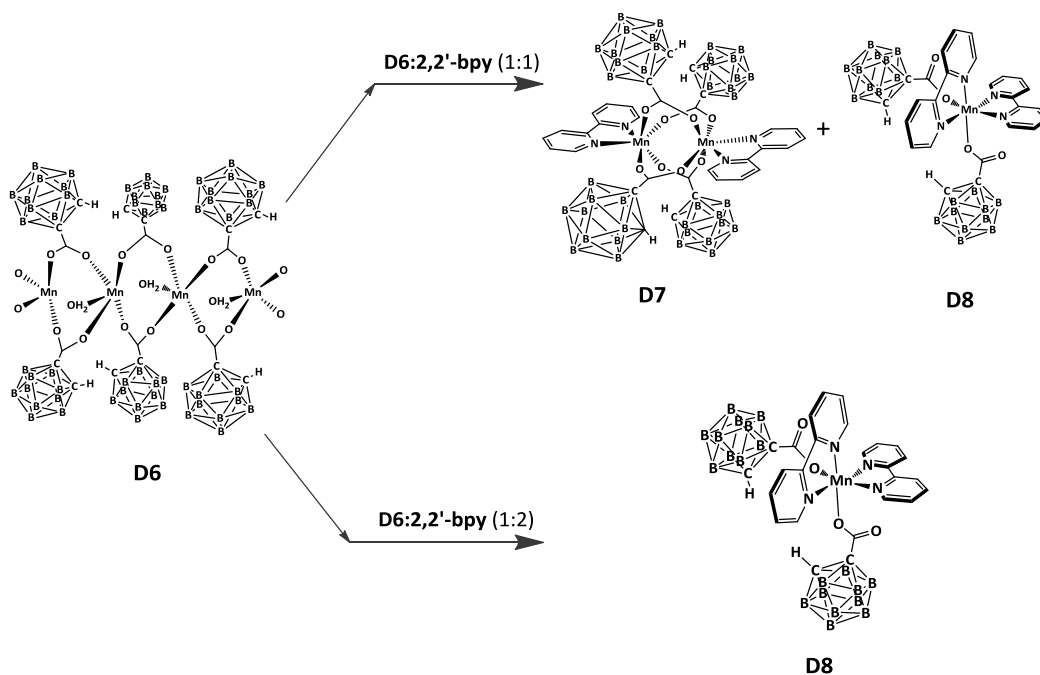


Figure 6. UV-vis spectral for complexes **D1-D5**.

VI.3.4. Synthesis and characterization of manganese complexes

The synthetic strategy for the preparation of the Mn(II) complexes **D6-D8** containing the carboranylcarboxylate ligand 1-CO₂H-1,2-*closo*-C₂B₁₀H₁₀ (**L'H**) and H₂O or 2,2'-bipyridine molecules is outlined in Scheme 2.





Scheme 2. Synthetic strategy for the preparation of Mn(II) complexes **D6-D8**

The strategy used to obtain the polymer **D6**, consists in mixing a suspension of the carboranylcarboxylic acid 1-CO₂H-1,2-closo-C₂B₁₀H₁₀, **L'H**, and MnCO₃ in a 1:1 ratio, in water at 40 °C and stirring for 2h. Afterwards, the solvent was removed and a white solid was obtained corresponding to the water soluble polymer [Mn(H₂O)(μ-1-CO₂-1,2-closo-C₂B₁₀H₁₀)₂]_n · 2H₂O, **D6**, together with a mononuclear compound, [Mn(1-CO₂-1,2-closo-C₂B₁₀H₁₀)₂(H₂O)₄], **D6'**.

Compound **D6** was used as starting material and was reacted with 2,2'-bipyridine with the aim to examine its reactivity in front of this chelating ligand, as well as to study and characterize the new compounds obtained.

When the bidentate ligand 2,2'-bpy dissolved in dichloromethane is added to a dichloromethane solution of complex **D6**, with a ligand/complex ratio of 1:1 (see Scheme 2.) a slightly yellow solution was formed that after slow evaporation leads to colourless crystals of the binuclear complex [Mn₂(1-CO₂-1,2-closo-C₂B₁₀H₁₀)₄(bpy)₂], **D7**. On the other hand, when the ratio ligand/complex was 2:1 the solution was become bright yellow and an insoluble yellow precipitate of [Mn(1-CO₂-1,2-closo-C₂B₁₀H₁₀)₂(bpy)₂], **D8**, was obtained.

Crystallographic data and selected bond distances and angles for compounds **D6-D8** are presented in Table S4 (see supporting information section),

Table 3. and Table 4, respectively. ORTEP plots with the corresponding atom labels for the X-ray structures of all compounds are presented in Figure 7 and Figure 9.

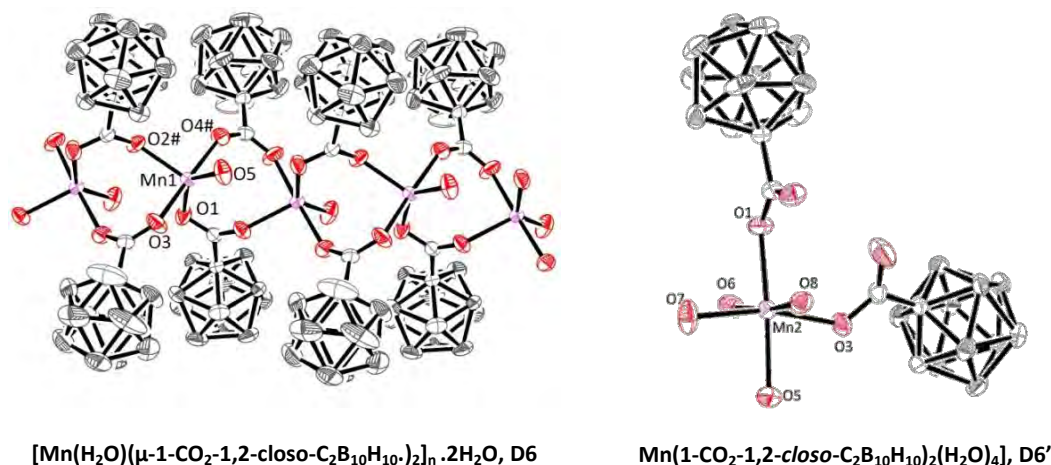


Figure 7. X-ray structures (ORTEP plots with ellipsoids at 40% probability level) and labelling scheme for complexes **D6** and **D6'**.

The X-ray structure of the complex **D6** discloses an unusual 1D polymeric structure in which water molecules are coordinated to each Mn(II) centre acting as a terminal ligand. A square pyramidal geometry is observed around each Mn(II) ion where three carboxylate oxygen atoms and one aqua oxygen atom occupy the equatorial position and a fourth carboxylate oxygen atom acts as axial ligand. Mn(II) atoms are bridged by two carboranylcarboxylate ligands, one of them in a *syn-syn* conformation and the other one in a *syn-anti* conformation. The carboranylcarboxylate ligands together with the metal are disposed in a zig-zag fashion through the chain. No similar compounds have been found in the literature.

The conformation of the carboxylate ligands is probably due to the existence of dihydrogen bonds $\text{C}_c\text{-H}\cdots\text{H-B}$ between the hydrogen atom from the carbon in the carboranylcarboxylate in *syn-anti* and the H-B from an adjacent carboranylcarboxylate in *syn-syn*, ($\text{C-H}(3)\cdots\text{H}(12)\text{-B}$, $d = 2.999 \text{ \AA}$ and $\text{C-H}(3)\cdots\text{H}(13)\text{-B}$, $d = 2.338 \text{ \AA}$), (Figure 8). These contacts are also responsible of the orientation of the hydrogen substituents on the cluster, which are describing a circle around the metal centre and the terminal water molecule, leading to a zig-zag distribution of the Mn atoms along the polymeric chain. These $\text{H}\cdots\text{H}$ short contacts are the same commented above for copper complexes and have been previously observed in the literature.^[12] It is remarkable that these interactions are not observed when the carboranylcarboxylate presents a *syn-syn* conformation, however, an intramolecular hydrogen bond is observed then between the H(5B) from the terminal aqua ligand and the O(3) atom from the carboxylate in *syn-syn* ($\text{H}(5\text{B})\text{-O}(3)$,

$d = 2.919 \text{ \AA}$) which probably is the responsible of the different distances Mn-O in this *syn-syn* ligand (Mn-O(3), $d = 2.112 \text{ \AA}$ and Mn-O(4) $d = 2.080 \text{ \AA}$). An additional H-bond is observed between the H5A from the terminal aqua ligand and the O(1) atom from the carboxylate in *syn-anti* (H5A-O(1), 1.872 \AA) (see Figure 7). The Mn-O distances for the carboranylcarboxylate bridge ligand in a *syn-syn* conformation are shorter than the ones for the ligand in *syn-anti* conformation (average 2.096 \AA and 2.143 \AA , respectively). The bond distance for Mn-O_w is $2.124(3) \text{ \AA}$. The trans O-Mn-O angle for the carboranylcarboxylate bridge ligand in *syn-syn* conformation is higher than that for the ligand in *syn-anti* conformation (175.4° and 105.0° , respectively). The displacement of one of the oxygen atoms from the bridged carboranylcarboxylate ligands in *syn-anti* conformation respect the plane form by the other oxygen atom and the two Mn atoms is 0.832 \AA and 0.691 \AA for O(2)#1 and O(3), respectively (Figure S11 at the supporting information section). The cis O-Mn-O angles around the manganese atoms show slight differences with regard to the 90° ideal value and they are in the range 89.6 - 94.0° . It is also noteworthy the existence of two more B-H...O bonds between the B-H closer to the carbon atoms in the cluster and the oxygen atoms of the bridge carboxylate ($d(\text{H}(1)\text{-O}(2)) = 2.749 \text{ \AA}$ and $d(\text{H}(4)\text{-O}(1)) = 3.048 \text{ \AA}$). The molecules of compound **D6** along *b* axis (Figure S3 at the supporting information section) are arranged in layers in which the carboranylcarboxylate ligands are alternated. It is also observable in this packing diagram the two different conformation of the carboranylcarboxylate ligand (*syn-syn* and *syn-anti*) previously commented.

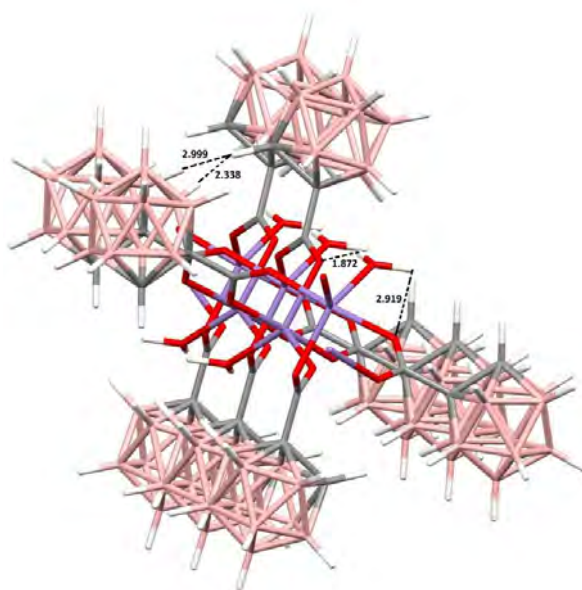


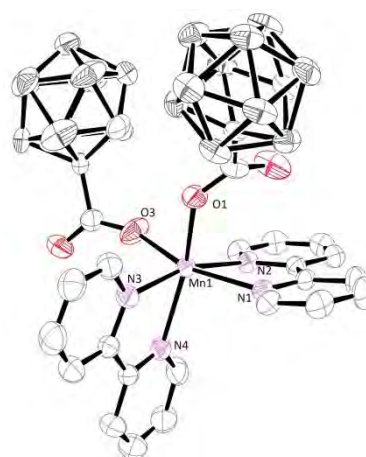
Figure 8. X-ray structure of **D6** showing the interactions C-H...H-B and the hydrogen bonds in the polymeric chain.

Mononuclear compound **D6'** reveals a six-coordinated Mn atom displaying a distorted octahedral geometry. The Mn(II) ion is coordinated by four oxygen atoms from four water molecules and by the donor oxygen atoms from two carboranylcarboxylate ligands that are coordinated to the metal in a monodentate mode, both adopting a *cis* configuration around the metal centre. This compound crystallise with one solvate molecule of water. The Mn-O_{carboxyl} bond distances are 2.165(13) and 2.121(13) Å whereas the average Mn-O_w bond distances is 2.203 Å. These Mn-O distances are in the range for other similar compounds containing Mn, aqua and carboxylate ligands.^[17] Compound **D6'** presents one intramolecular H...O hydrogen bond involving the uncoordinated O atom of one of the monodentate carboranylcarboxylate ligands and the H atom of the closest aqua ligand (O(8)-H(8A)...O(2), 2.680Å). Moreover, it is noteworthy to observed the existence of nine intermolecular hydrogen bond with the neighbour molecules of complex **D6'** and with the solvent water molecule located between adjacent layers (Figure S10 at the supporting information section).

A comparison of **D6** and the polymer [Mn(μ-H₂O)(1-CH₃-2-CO₂-1,2-*closo*-C₂B₁₀H₁₀)₂]_n·(H₂O)_n, **B1**, allow us to establish differences between the carboranylcarboxylate L'H and the ligand LH in the reactivity with manganese(II) ion, where the C_c-H...H-B interactions present only in **D6** are responsible of the observed differences. The first great difference is the geometry around the central metal (square pyramidal for **D6** and octahedral for **B1**) and the coordination of the aqua molecule in both complexes (bridge in **B1** and terminal in **D6**). Moreover, although in both complexes Mn(II) ions are bridged by two carboranylcarboxylate ligands, in compound **B1** both are in a *syn-syn* conformation whilst for **D6** one of them is in a *syn-syn* conformation and the other one is in a *syn-anti* conformation which is also a consequence of the mentioned interactions. Furthermore, complex **B1** presents solvent water molecules not seen for **D6** which are linked through hydrogen bonds to the coordinated bridge aqua ligand. Another important difference is the packing structure of both complexes, complex **B1** displays polymeric chiral chains due to the methyl group of the carboranylcarboxylate ligand is shifted respect to the centre of the coordinated carboxylate group, thus observing two different conformations for these chains (lambda and delta), however, in complex **D6** the hydrogen substituents in the clusters have the same disposition in the different chains, fact that makes that the packing arrangement displays polymeric chains with the same conformation preventing any chirality between them (Figure S13 at the supporting information section).

Table 3. Selected bond lengths (Å) and angles (°) for complexes **D6** and **D6'**.

	D6		D6'
Mn(1)-O(4)#1	2.080(3)	Mn(2)-O(1)	2.165(13)
Mn(1)-O(3)	2.112(3)	Mn(2)-O(3)	2.121(13)
Mn(1)-O(2)#1	2.115(3)	Mn(2)-O(5)	2.221(16)
Mn(1)-O(5)	2.124(3)	Mn(2)-O(6)	2.159(16)
Mn(1)-O(1)	2.170(3)	Mn(2)-O(7)	2.171(15)
O(4)#1-Mn(1)-O(3)	175.35(14)	Mn(2)-O(8)	2.261(13)
O(4)#1-Mn(1)-O(2)#2	90.90(12)	O(3)-Mn(2)-O(6)	94.10(7)
O(3)-Mn(1)-O(2)#2	91.07(12)	O(3)-Mn(2)-O(1)	104.09(6)
O(4)#1-Mn(1)-O(5)	90.47(13)	O(6)-Mn(2)-O(1)	85.34(6)
O(3)-Mn(1)-O(5)	84.88(13)	O(3)-Mn(2)-O(7)	165.25(7)
O(2)#2-Mn(1)-O(5)	113.25(13)	O(6)-Mn(2)-O(7)	87.28(7)
O(4)#1-Mn(1)-O(1)	94.02(13)	O(1)-Mn(2)-O(5)	174.80(6)
O(3)-Mn(1)-O(1)	89.54(13)	O(1)-Mn(2)-O(7)	90.66(7)
O(2)#2-Mn(1)-O(1)	105.03(11)	O(3)-Mn(2)-O(5)	80.48(6)
O(5)-Mn(1)-O(1)	141.37(13)	O(6)-Mn(2)-O(5)	96.89(8)
		O(7)-Mn(2)-O(5)	84.76(7)
		O(3)-Mn(2)-O(8)	90.92(6)
		O(6)-Mn(2)-O(8)	172.04(6)
		O(1)-Mn(2)-O(8)	87.46(5)
		O(7)-Mn(2)-O(8)	89.43(6)
		O(5)-Mn(2)-O(8)	90.02(7)

[Mn₂(1-CO₂-1,2-*closo*-C₂B₁₀H₁₀)₄(bpy)₂], (**D7**)[Mn(1-CO₂-1,2-*closo*-C₂B₁₀H₁₀)₂(bpy)₂], (**D8**)**Figure 9.** X-ray structures (ORTEP plots with ellipsoids at 40% probability level) and labelling scheme for complexes **D7** and **D8**.

Binuclear compound **D7** is a novel binuclear Mn(II) cluster which displays a centrosymmetric structure with the symmetry centre located between the two manganese atoms. These Mn(II) ions are holding together through four syn,syn $\eta^1: \eta^1: \mu_2$ -carboxylate bridges in which each Mn(II) ion displays a trigonal prismatic geometry that is completed by the two nitrogen donor atoms of the 2,2'-bipyridine ligand (see Figure 10.). O-Mn-N/O angles are in the range $81.30(13)$ - $85.85(16)^\circ$ for adjacent atoms and in the range $129.66(14)$ - $142.20(14)^\circ$ for the angles formed between the manganese atom and the atoms that describe the diagonal of the rectangular faces of the prism. These angles agree with the ideal 90° and 135.4° for prismatic trigonal geometry.^[18] Mn-O bond lengths are in the range 2.144-2.175 Å and are shorter than distances Mn-N (average of 2.271 Å). The packing structure displays $\pi \cdots \pi$ stacking interactions among the aromatic rings of 2,2'-bpy ligands of two neighbouring molecules (Figure S2 supporting information section).

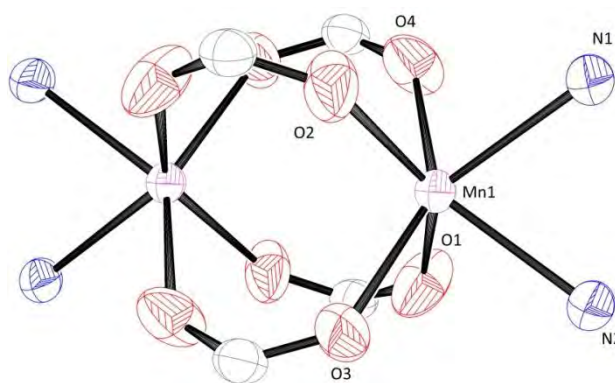


Figure 10. Trigonal prismatic geometry in detail of **D7**

The X-ray crystallography performed on the mononuclear complex **D8**, $[\text{Mn}(1\text{-CO}_2\text{-1,2-closo-C}_2\text{B}_{10}\text{H}_{10})_2(\text{bpy})_2]$, reveals a six-coordinate Mn atom with a distorted octahedral geometry. The Mn(II) ion is coordinated by four nitrogen atoms from two chelating 2,2'-bipyridine ligands and two oxygen atoms from two monodentate carboranylcarboxylate ligands, both adopting a *cis* configuration around the metal. The distances Mn-O (2.093(2) and 2.138(2) Å) and Mn-N (in the range 2.255(2)-2.295(3) Å) are similar and comparable to other Mn compounds with 2,2'-bpy and carboxylate ligands^[19] as well as to the mononuclear complex **B4**, $[\text{Mn}(1\text{-CH}_3\text{-2-CO}_2\text{-1,2-closo-C}_2\text{B}_{10}\text{H}_{10})_2(\text{bpy})_2]$, described in Chapter IV. Compared to the ideal octahedral geometry, the angles show significant distortions with deviations from the theoretical value of 90° and are in the range 88.2 - 103.1° .

It is noteworthy to observe that compound **D7** display the same geometry than compound **B3**, $[\text{Mn}_2(1\text{-CH}_3\text{-2-CO}_2\text{-1,2-closo-C}_2\text{B}_{10}\text{H}_{10})_4(\text{bpy})_2]$, from Chapter IV containing the methyl group in the carboranylcarboxylate ligand, however, the packing diagram for both complexes is

different due to the different arrangement of the substituents in the carboranylcarboxylate ligands; in the case of the hydrogen atoms, all of them are directed toward the 2,2'-bpy ligands, whereas that methyl groups display different arrangement probably due to increased steric encumbrance of these methyl groups (see Figure S13b at the supporting information section).

Table 4. Selected bond lengths (Å) and angles (°) for complexes **D7** and **D8**.

	D7		D8
Mn(1)-O(1)	2.147(3)	Mn(1)-O(1)	2.138(2)
Mn(1)-O(2)#1	2.144(3)	Mn(1)-O(3)	2.093(2)
Mn(1)-O(3)	2.175(3)	Mn(1)-N(1)	2.287(2)
Mn(1)-O(4)	2.147(3)	Mn(1)-N(2)	2.255(2)
Mn(1)-N(1)	2.280(3)	Mn(1)-N(3)	2.269(3)
Mn(1)-N(2)	2.262(3)	Mn(1)-N(4)	2.295(3)
O(4)-Mn(1)-O(2)#1	85.85(16)	O(1)-Mn(1)-O(3)	90.29(9)
O(1)-Mn(1)-O(4)	83.24(14)	O(1)-Mn(1)-N(3)	88.24(9)
O(2)#1-Mn(1)-O(1)	141.58(13)	O(3)-Mn(1)-N(3)	98.43(11)
O(2)#1-Mn(1)-O(3)	81.30(13)	O(1)-Mn(1)-N(2)	103.05(9)
O(1)-Mn(1)-O(3)	85.14(14)	O(3)-Mn(1)-N(2)	92.90(10)
O(4)-Mn(1)-O(3)	142.20(14)	N(3)-Mn(1)-N(2)	163.98(9)
O(4)-Mn(1)-N(2)	131.44(15)	O(1)-Mn(1)-N(1)	83.00(8)
O(2)#1-Mn(1)-N(2)	129.66(14)	O(3)-Mn(1)-N(1)	161.33(11)
O(1)-Mn(1)-N(2)	83.24(13)	N(3)-Mn(1)-N(1)	98.75(9)
O(3)-Mn(1)-N(2)	82.29(13)	N(2)-Mn(1)-N(1)	71.86(8)
O(4)-Mn(1)-N(1)	83.70(13)	O(1)-Mn(1)-N(4)	159.26(10)
O(2)#1-Mn(1)-N(1)	84.45(13)	O(3)-Mn(1)-N(4)	96.16(10)
O(1)-Mn(1)-N(1)	130.40(13)	N(3)-Mn(1)-N(4)	71.34(9)
O(3)-Mn(1)-N(1)	129.68(13)	N(2)-Mn(1)-N(4)	96.31(9)
N(2)-Mn(1)-N(1)	70.72(12)	N(1)-Mn(1)-N(4)	96.20(9)

VI.4. Conclusions

A family of new mononuclear and binuclear copper(II) complexes containing the carboranylcarboxylate ligand 1-CO₂H-1,2-*closo*-C₂B₁₀H₁₀, **L'H**, have been synthesized and fully characterized by X-Ray diffraction, spectroscopic methods (IR, UV-vis, NMR) and electrochemistry (CV and DPV).

Cu(II) complexes **D1-D4** present an overall geometry corresponding to a binuclear *paddle-wheel* structure where each copper ion is coordinated by four oxygen atoms one of each of the four syn,syn η¹: η¹: μ₂-carboxylate bridge and one donor atom (oxygen or nitrogen) from the different terminal ligands displaying a square pyramidal geometry. Mononuclear complex **D5** shows a square planar structure, where the copper atom is coordinated by two nitrogen atoms from two lutidine ligands and by two oxygen atoms from the two carboranylcarboxylate ligands that adopt a monodentate coordination.

Not important differences have been observed in the structure of the starting material, in the main products and in the reactivity with pyridylic ligands for compounds containing the carboranylcarboxylate ligand **L'H** or the ligand [1-CH₃-2-CO₂H-1,2-*closo*-C₂B₁₀H₁₀], **LH**; however, important differences have been found in the side products obtained with the pyridylic ligands py and *p*-CH₃-py. First of all, for compounds containing the ligand **LH**, mononuclear complexes were obtained as secondary products, whilst for compounds containing the ligand **L'H**, binuclear compounds have been got. This fact has been attributed to the existence of dihydrogen bonds C_c-H...H-B between neighbouring carborane ligands in complexes containing the ligand **L'H**. These interactions are probably responsible for keeping the binuclear structures avoiding the formation of the mononuclear compounds and also, of the ratio of isolate products obtained with pyridine ligand. Whereas with ligand **LH**, the binuclear compound **A2** is mainly obtained and only traces of mononuclear compound were detected, with ligand **L'H**, a comparable ratio of the corresponding compounds has been obtained.

It has been observed for complex **D3** that the ¹H-NMR chemical shifts of the proton bonded to the boron atoms in the carboranylcarboxylate ligand change to higher frequencies when decreasing the temperature, which might be due to the existence of intermolecular B-H...H-B interactions between several B-H vertexes.

The electronic UV-vis spectra of complexes **D1-D5** show one characteristic band in the range 600-800 nm, assigned to d-d transitions from the d_{xz}, d_{yz} and d_{xy} orbitals.

CV of compounds **D1-D5** show irreversible redox processes that can be assigned respectively to Cu^{II}/Cu^I and Cu^I/Cu⁰ redox pairs. We have not observed a noticeable shift in the potential values with the different electron-withdrawing character of the pyridylic ligands present in

these compounds. Moreover, it was observed a great similarity in the DPV of all compounds probably due to the similar potential oxidation values of these mixtures of compounds.

For Mn(II) compounds, it was observed that compound **D6** discloses an unusual 1D manganese(II) polymer in which each of the Mn(II) ions is coordinated by four carboxylate oxygen atoms from two bridge carboranylcarboxylate, one in a *syn-syn* and another in a *syn-anti* conformation, and one aqua oxygen atom displaying a square pyramidal geometry. This difference in the polymeric structure by respect to that obtained with the ligand [1-CH₃-2-CO₂H-1,2-*closo*-C₂B₁₀H₁₀], **LH**; has been attributed to the existence of dyhydrogen C_c-H...H-B bonds, interactions that are not present in the polymer **B1**. A possible consequence of these interactions is also the presence of chiral layers in compound **B1** containing the ligand **LH**, which are not observed in compound **D6** containing the ligand **L'H**.

It was observed that, when **D6** reacts with the ligand 2,2'-bpy in a 1:2 ligand/complex ratio, a binuclear complex, **D7**, was obtained where four *syn,syn* η¹: η¹: μ²-carboxylate bridges join the two manganese(II) centres, whereas than if the ligand/complex ratio is 1:1 a mononuclear compound, **D8**, is obtained, where two carboranylcarboxylate ligands are coordinated to the manganese ion in a monodentate mode.

In general, it could be conclude that important differences in the reactivity with Mn(II) and Cu(II) ions have been observed due to the presence of a hydrogen atom instead of a methyl group in the carboranylcarboxylate ligand.

VI.5. Experimental section

VI.5.1. Instrumentation and measurements

FT-IR spectra were taken in a Mattson-Galaxy Satellite FT-IR spectrophotometer containing a MKII Golden Gate Single Reflection ATR System. Elemental analyses were performed using a CHNS-O Elemental Analyser EA-1108 from Fisons. UV-Vis spectroscopy was performed on a Cary 50 Scan (Varian) UV-Vis spectrophotometer with 1 cm quartz cells or with an immersion probe of 5 mm path length. NMR spectra have been recorded with a Bruker ARX 300 or a DPX 400 instrument equipped with the appropriate decoupling accessories (^1H and $^1\text{H}\{^{11}\text{B}\}$ NMR (300.13/400.13 MHz), $^{13}\text{C}\{^1\text{H}\}$ NMR (75.47/100.62 MHz) and ^{11}B and $^{11}\text{B}\{^1\text{H}\}$ NMR (96.29/128.37 MHz) spectra were recorded in d_6 -acetone, CDCl_3 and CH_3OH . Chemical shift values for ^{11}B NMR spectra were referenced to external $\text{BF}_3\leftarrow\text{O}(\text{C}_2\text{H}_5)_2$ and those for ^1H , $^1\text{H}\{^{11}\text{B}\}$ and $^{13}\text{C}\{^1\text{H}\}$ NMR spectra were referenced to SiMe_4 . Chemical shifts are reported in units of parts per million downfield from reference, and all coupling constants in Hz. Deconvolution of $^{11}\text{B}\{^1\text{H}\}$ spectra and DPV voltammograms has been performed with the software OriginPro 8 SR0, v. 8.0724. Cyclic Voltammetric (CV) and Differential Pulse Voltammetry (DPV) experiments were performed in a IJ-Cambria IH-660 potentiostat using a three electrode cell. A Pt (2 mm diameter) electrode was used as working electrode, platinum wire as auxiliary and SCE as the reference electrode. Measurements were recorded in acetonitrile solutions at scan rate of $100 \text{ mV}\cdot\text{s}^{-1}$ for CV and pulse amplitude of 0.05 V, pulse width of 0.05 s, sampling width of 0.02 s, and pulse period of 0.5 s for DPV, using 0.1 M TBAH as supporting electrolyte. All cyclic voltammograms presented in this work were recorded under nitrogen atmosphere.

X-ray structure determination: measurement of the crystals were performed on a Bruker Smart Apex CCD diffractometer using graphite-monochromated Mo $K\alpha$ radiation ($\lambda = 0.71073\text{\AA}$) from an X-Ray tube. Data collection, Smart V. 5.631 (BrukerAXS 1997-02); data reduction, Saint+ Version 6.36A (Bruker AXS 2001); absorption correction, SADABS version 2.10 (Bruker AXS 2001) and structure solution and refinement, SHELXTL Version 6.14 (Bruker AXS 2000-2003).

VI.5.2. Materials

All reagents used in the present work were obtained from Aldrich Chemical Co and were used without further purification. Reagent grade organic solvents were obtained from SDS and high purity de-ionized water was obtained by passing distilled water through a nano-pure Mili-Q water purification system. $o\text{-C}_2\text{B}_{10}\text{H}_{11}$ was purchased from Katchem.

VI.5.3. Preparations

All synthetic manipulations were routinely performed under ambient conditions.

Synthesis of 1,2-Dicarba-closo-dodecaborane-1-carboxylic Acid, L'H.

The 1-CO₂H-1,2-*closo*-C₂B₁₀H₁₀ ligand was prepared according to literature procedures^[20] with small modifications.

To a stirred solution of *o*-C₂B₁₀H₁₁ (1.66 g, 11.61 mmol) in diethyl ether (170 ml) at -80 °C was added dropwise 1.20 equivalents of *n*-BuLi (11.2 mL, 13.89 mmol) and stirring was continued for 1 hour at the same temperature. Dry ice was bubbled through the solution for about 2.5 hours and then was warmed to room temperature. Diethyl ether was removed by rotatory evaporator and the resulting solid was sublimated to eliminate *o*-carborane residues. The desired product was then hydrolysed with 3 M HCl, transferred to a separating funnel and extracted with hexanes. Combined extracts were dried over MgSO₄ and then filtered. Removal of solvent afforded a white microcrystalline solid of L'H. Yield: 1.59 g, 73%. ¹H{¹¹B} NMR (400.13 MHz, CDCl₃, 25 °C): δ= 1.42-2.99 (br ; B-H), 4.06 (s; 1H) ppm. ¹³C{¹H} NMR (100.62 MHz, CDCl₃, 25 °C): δ= 165.34 (COOH), 68.04 (C_c), 57.01 (C_c) ppm. ¹¹B{¹H} NMR (128.37 MHz, CDCl₃, 25 °C): δ= -2.4 (¹J(B,H)= 149 Hz, 2B), -9.2 (¹J(B,H)= 149 Hz, 2B), (-11.9, -13.6 (¹J(B,H)= 157 Hz), -10.4 ppm), 6B. IR: $\bar{\nu}$ = 710 ν (B-C), 893, 1010, 1194, 1277, 1426 ν (COO⁻)_{sim}, 1719 ν (COO⁻)_{as}, 2398-2628 ν (B-H), 2862, 3079 ν (C_c-H) cm⁻¹. Elemental analysis calcd (%) for C₃H₁₂O₂B₁₀: C 19.14, H 6.43; found: C 19.64, H 6.49.

Synthesis of [Cu₂(1-CH₃-2-CO₂-1,2-*closo*-C₂B₁₀H₁₀)₄(THF)₂], D1. 1-CO₂H-1,2-*closo*-C₂B₁₀H₁₀, L'H, (0.2 g, 1.18 mmols) in ethanol (2 mL) was neutralized with a 0.1 M aqueous NaOH solution with phenolphthalein as indicator at room temperature and immediately mixed with a solution of CuSO₄·5H₂O (0.15 g, 0.59 mmols) in water (1 mL). The temperature of the blue solution gradually rose to 40 °C. After 2 h the solvent was removed under vacuum, the solid residue was redissolved in THF (40 mL) and again dried under vacuum. The last process was repeated three times. The obtained residue was once more dissolved in THF, the solution was filtrated to remove solid Na₂SO₄ and the solvent was again removed under vacuum. The resulting solid was recrystallized in CH₂Cl₂. Yield: 0.2 g (67%). ¹H{¹¹B} NMR (300.13 MHz, acetone-d₆, 25 °C): δ= 3.71 (s; C_c-H) , 2.58 (br s; B-H), 1.83 (s; CH₂) ppm. ¹¹B{¹H} NMR (96.29 MHz, acetone-d₆, 25 °C): δ= 2.3 (¹J(B,H)= 131 Hz, 2B), -7.4 (¹J(B,H)= 128 Hz, 2B), -11.5 (¹J(B,H)= 126 Hz, 5B), -17.3 (1B), ppm. IR: $\bar{\nu}$ = 631, 683, 719 ν (B-C), 782, 839, 881, 910, 1015, ,1036, 1062, 1095, 1401 ν (COO⁻)_{sim}, 1671 ν (COO⁻)_{as}, 2581 ν (B-H), 2601, 2891, 2984, 3079 ν (C_c-H) cm⁻¹.

UV-Vis (CH_2Cl_2 , 1.10^{-3}M) λ_{max} (ϵ) = 740 nm ($85 \text{ M}^{-1}\text{cm}^{-1}$). Elemental analysis calcd (%) for $\text{C}_{20}\text{H}_{60}\text{O}_{10}\text{B}_{40}\text{Cu}_2$: C 23.55, H 5.93; found: C 23.46, H 5.79.

Synthesis of $[\text{Cu}_2(1\text{-CO}_2\text{-1,2-closo-C}_2\text{B}_{10}\text{H}_{10})_4(\text{py})_2]$, **D2.** To a solution of **D1** (0.049 g, 0.048 mmols) in CH_2Cl_2 (8 mL) was added a solution of pyridine (7.81 μl , 0.096 mmols) in CH_2Cl_2 (2 mL). The resulting blue solution was stirred for 20 minutes at room temperature. Afterwards the solution was concentrated and a blue solid was appeared. The resulting solid was recrystallized by slow diffusion of pentane into a dichloromethane solution. After several days, air-stable, green crystals of **D2** suitable for X-ray diffraction analysis were obtained, together with other blue crystals, that correspond to the compound $[\text{Cu}_2(1\text{-CO}_2\text{-1,2-closo-C}_2\text{B}_{10}\text{H}_{10})_4(\text{py})_4]$, **D2'**. The separation of the two compounds was not possible. Yield: 0.041 g. $^1\text{H}\{^{11}\text{B}\}$ NMR (400.13 MHz, CDCl_3 , -13°C): δ = 7.82 (br s; $\text{C}_{\text{aryl-H}}$), 7.59 (br; $\text{C}_{\text{aryl-H}}$), 7.52 (br s; $\text{C}_{\text{aryl-H}}$), 6.99 (br s; $\text{C}_{\text{aryl-H}}$), 4.40 (br s; $\text{C}_c\text{-H}$), 4.10 (br s; $\text{C}_c\text{-H}$), 4.04 (br s; B-H), 3.49 (br s; B-H), 3.48 (br s; B-H), 3.05 (br s; B-H), 2.97 (br s; B-H), 2.93 (br s; B-H) ppm. $^{11}\text{B}\{^1\text{H}\}$ NMR (128.37 MHz, CDCl_3 , 25°C): δ = -2.7, -5.8, -9.0, -15.5 ppm. IR: $\bar{\nu}$ = 693, 717v(B-C), 755, 776, 840, 881, 908, 1015, 1046, 1072, 1089, 1156, 1220, 1260, 1361v(COO^-)_{sim}, 1451, 1489, 1609, 1640, 1661v(COO^-)_{as}, 2576v(B-H), 2851, 2924, 2963, 3037, 3079v($\text{C}_c\text{-H}$) cm^{-1} . UV-Vis (CH_3CN) λ_{max} (ϵ): 690 nm. Elemental analysis calcd (%) for $\text{C}_{26.5}\text{H}_{58.5}\text{O}_8\text{B}_{40}\text{Cu}_2\text{N}_{2.9}$ (0.55·**D2**+0.45·**D2'**): C 28.80, H 5.33, N 3.67; found: C 28.68, H 5.41, N 3.62.

Synthesis of $[\text{Cu}_2(1\text{-CO}_2\text{-1,2-closo-C}_2\text{B}_{10}\text{H}_{10})_4(\text{p-CF}_3\text{-Py})_2]$, **D3.** This compound was prepared following a method analogous to that described for $[\text{Cu}_2(1\text{-CO}_2\text{-1,2-closo-C}_2\text{B}_{10}\text{H}_{10})_4(\text{py})_2]$, starting from compound **D1** (0.083 g, 0.081 mmols) and 4-trifluoromethylpyridine (18.8 μl , 0.162 mmols) to afford air-stable green crystals of **D3**, suitable for X-ray diffraction analysis. Yield: 0.041 g (43%). $^1\text{H}\{^{11}\text{B}\}$ NMR (400.13 MHz, acetone- d_6 , -13°C): δ = 9.72 (br; $\text{C}_{\text{aryl-H}}$), 8.70 (br s; $\text{C}_{\text{aryl-H}}$), 7.60 (br; $\text{C}_{\text{aryl-H}}$), 6.75 (br s; $\text{C}_{\text{aryl-H}}$), 6.17 (br s; $\text{C}_{\text{aryl-H}}$), 5.67 (br; $\text{C}_{\text{aryl-H}}$), 4.77 (br; $\text{C}_c\text{-H}$), 3.65 (br s; $\text{C}_c\text{-H}$), 3.45 (br s; B-H), 3.20 (br s; B-H), 2.85 (br s; B-H) ppm. $^{11}\text{B}\{^1\text{H}\}$ NMR (128.37 MHz, CDCl_3 , 25°C): δ = 0.53 ($^1J(\text{B,H}) = 141 \text{ Hz}$) -2.2 ($^1J(\text{B,H}) = 107 \text{ Hz}$), -7.1 ($^1J(\text{B,H}) = 127 \text{ Hz}$), -9.2 ($^1J(\text{B,H}) = 177 \text{ Hz}$), -10.7 ppm. IR: $\bar{\nu}$ = 671, 724v(B-C), 783, 833, 1022, 1065, 1090, 1145, 1173, 1226, 1323, 1385v(COO^-)_{sim}, 1423, 1666v(COO^-)_{as}, 2579v(B-H) cm^{-1} . UV-Vis (CH_2Cl_2 , 1.10^{-3}M) λ_{max} (ϵ): 794 nm ($347 \text{ M}^{-1}\text{cm}^{-1}$). Elemental analysis calcd (%) for $\text{C}_{24}\text{H}_{52}\text{O}_8\text{B}_{40}\text{N}_2\text{F}_6\text{Cu}_2$ ·0.5 pentane: C 27.78, H 5.07, N 2.24; found: C 27.74, H 5.17, N 2.33.

Synthesis of $[\text{Cu}_2(1\text{-CO}_2\text{-1,2-closo-C}_2\text{B}_{10}\text{H}_{10})_4(\text{p-CH}_3\text{-py})_2]$, **D4.** This compound was prepared in a similar manner to the method described for **D2** starting from compound **D1** (0.076 g, 0.075 mmols) and 4-methylpyridine (14.8 μl , 0.149 mmols) to afford green, air-stable crystals of **D4**

after several days, together with other blue crystals corresponding to the complex $[\text{Cu}_2(1\text{-CO}_2\text{-}1,2\text{-}closo\text{-C}_2\text{B}_{10}\text{H}_{10})_4(\rho\text{-CH}_3\text{-py})_4]$, **D4'**. The separation of the two compounds was not possible. Yield: 0.048 g. $^1\text{H}\{^{11}\text{B}\}$ NMR (400.13 MHz, CDCl_3 , -13°C): δ = 4.31 (br s; $\text{C}_c\text{-H}$), 3.99 (br s; B-H), 3.37 (br s; B-H), 2.96 (br s; B-H). $^{11}\text{B}\{^1\text{H}\}$ NMR (128.37, CDCl_3 , 25°C): δ = -3.3, -1.7, -5.8, -8.2, -9.1, -11.4, -12.8, -16.6 ppm. IR: $\bar{\nu}$ = 717, 781v(B-C), 805, 839, 909, 1015, 1071, 1092, 1218, 1231, 1364v(COO^-)_{sim}, 1435, 1508, 1623, 1666v(COO^-)_{as}, 2578v(B-H), 3077v($\text{C}_c\text{-H}$) cm^{-1} . UV-Vis (CH_2Cl_2) λ_{max} (ϵ): 776 nm. Elemental analysis calcd (%) for $\text{C}_{26.4}\text{H}_{60.8}\text{O}_8\text{B}_{40}\text{Cu}_2\text{N}_{2.4}$ (0.90·**D4**+0.10·**D4'**): C 28.00, H 5.54, N 2.85; found: C 28.21, H 5.56, N 2.99.

Synthesis of $[\text{Cu}(1\text{-CO}_2\text{-}1,2\text{-}closo\text{-C}_2\text{B}_{10}\text{H}_{10})_2(\text{o}-(\text{CH}_3)_2\text{-py})_2]$, **D5.** This compound was prepared analogously to the method described for **D3** starting from compound **D1** (0.060 g, 0.059 mmols) and 2,6-lutidine (27.26 μL , 0.234 mmols) to afford blue-violet air stable crystals of **D5** together with some blue crystals corresponding to the complex **D5'**. The separation of the two compounds was not possible. Yield: 0.036 g. $^1\text{H}\{^{11}\text{B}\}$ NMR (400.13 MHz, CDCl_3 , -13°C): δ = 8.03 (br; $\text{C}_{\text{aryl}}\text{-H}$), 7.38 (br s; $\text{C}_{\text{aryl}}\text{-H}$), 4.39 (br s; B-H), 3.81 (br s; B-H), 3.42 (s; $\text{C}_c\text{-H}$), 2.86 (br s; B-H), 2.32 (br s; B-H) ppm. $^{11}\text{B}\{^1\text{H}\}$ NMR (128.37 MHz, CDCl_3 , 25°C): δ = -2.3, -5.7, -8.2, -10.1, -12.8, -18.5 ppm. IR: $\bar{\nu}$ = 715, 731, 779v(B-C), 840, 908, 1012, 1041, 1084, 1112, 1166, 1254, 1339v(COO^-)_{sim}, 1377, 1406, 1470, 1584, 1610, 1660v(COO^-)_{as}, 2564v(B-H), 2598v(B-H), 2630, 3081v($\text{C}_c\text{-H}$) cm^{-1} . UV-Vis (CH_2Cl_2) λ_{max} (ϵ): 804 nm. Elemental analysis calcd (%) for $\text{C}_{20}\text{H}_{40}\text{O}_4\text{B}_{20}\text{N}_2\text{Cu}$.0.1 CH_2Cl_2 : C 36.54, H 6.13, N 4.24; found: C 36.42, H 6.32, N 4.23.

Synthesis of $[\text{Mn}(\text{H}_2\text{O})(1\text{-CO}_2\text{-}1,2\text{-}closo\text{-C}_2\text{B}_{10}\text{H}_{10})_2]_n \cdot 2\text{H}_2\text{O}$, **D6.** To a suspension of 0.192 g (1.024 mmols) of $1\text{-CO}_2\text{-}1,2\text{-}closo\text{-C}_2\text{B}_{10}\text{H}_{10}$, **L'H**, in 30 mL of water was added 0.0589 g (0.512 mmols) of MnCO_3 in 10 mL of water. The solution was stirred and heated to 40°C for 2h. Afterward, the solution was filtered and the solvent was removed under vacuum to obtain a white solid. The latter was recrystallized by slow diffusion of pentane into a dichloromethane solution. After several days, air-stable, colourless crystals of **D6** suitable for X-ray diffraction analysis were obtained, together with other colourless crystals, that correspond to the compound, $[\text{Mn}(1\text{-CO}_2\text{-}1,2\text{-}closo\text{-C}_2\text{B}_{10}\text{H}_{10})_2(\text{H}_2\text{O})_4]$, **D6'**. The separation of the two compounds was not possible. Yield: 0.271 g. $^{11}\text{B}\{^1\text{H}\}$ NMR (128.37, D_2O , 25°C): δ = -6.1 ($^1\text{J}(\text{B},\text{H})$ = 138.6, 1B), -7.3 ($^1\text{J}(\text{B},\text{H})$ = 150.2, 1B), -12.1 ($^1\text{J}(\text{B},\text{H})$ = 142.5, 2B), -14.2 ($^1\text{J}(\text{B},\text{H})$ = 119.4, 4B), -16.2 ($^1\text{J}(\text{B},\text{H})$ = 161.7, 2B). IR: $\bar{\nu}$ = 587, 597, 631, 725v(B-C), 844, 863, 914, 941, 1015, 1148, 1190, 1380v(COO^-)_{sim}, 1443, 1567, 1598, 1619v(COO^-)_{as}, 1644, 2569v(B-H), 2579v(B-H), 3631 cm^{-1} . Anal. Found (calcd.) (%) for $\text{C}_6\text{H}_{30}\text{O}_8\text{B}_{20}\text{Mn} \cdot 2\text{H}_2\text{O}$: C 14.62(14.91); H 5.95(5.84).

Synthesis of $[\text{Mn}_2(1\text{-CO}_2\text{-1,2-closo-C}_2\text{B}_{10}\text{H}_{10})_4(\text{bpy})_2]$, **D7.** To a solution of 0.067 g (0.148 mmols) of $[\text{Mn}(\text{H}_2\text{O})(1\text{-CO}_2\text{-1,2-closo-C}_2\text{B}_{10}\text{H}_{10})_2]_n$, **D6**, in 3 mL of CH_2Cl_2 was added 0.024 g (0.151 mmols) of 2, 2'-bipyridine in 1 mL of CH_2Cl_2 . The solution pale yellow was stirred for 30 min and filtered. Afterward the volume of the resulting solution was reduced to 1 mL, obtaining a precipitate that was washed with pentane. The resulting solid was recrystallized in EtOH to afford colourless, air-stable crystals of **D7** after several days, together with other yellow crystals corresponding to the complex $[\text{Mn}(1\text{-CO}_2\text{-1,2-closo-C}_2\text{B}_{10}\text{H}_{10})_2(\text{bpy})_2]$, **D8**. Yield: 0.065 g. IR: $\bar{\nu}$ = 718, 736, 761 ν (B-C), 841, 884, 908, 1013, 1059, 1083, 1157, 1178, 1187, 1242, 1326 ν (COO^-)_{sim}, 1437, 1472, 1493, 1577, 1596, 1663 ν (COO^-)_{as}, 1681, 2264, 2568 ν (B-H), 2599 ν (B-H), 2617, 3078, 3197 cm^{-1} . Anal. Found (calcd.) (%) for $\text{C}_{32}\text{H}_{60}\text{O}_8\text{B}_{40}\text{N}_4\text{Mn}_2 \cdot 1.1\text{CH}_2\text{Cl}_2$: C 31.44(31.44); N 4.62(4.43); H 4.89(4.96).

Synthesis of $[\text{Mn}(1\text{-CO}_2\text{-1,2-closo-C}_2\text{B}_{10}\text{H}_{10})_2(\text{bpy})_2]$, **D8.** This compound was prepared following a method analogous to that described for **D7** using 0.083 g (0.186 mmols) of **D6** and 0.059 g (0.373 mmols) of 2,2'-bipyridine as starting materials obtaining an insoluble yellow precipitate. Yield: 0.093 g (67 %). IR: $\bar{\nu}$ = 718, 736, 760 ν (B-C), 771, 844, 908, 1013, 1059, 1082, 1157, 1177, 1246, 1326 ν (COO^-)_{sim}, 1438, 1472, 1577, 1596, 1664 ν (COO^-)_{as}, 1683, 2550 ν (B-H), 2567 ν (B-H), 2591 ν (B-H), 2628, 3022, 3074 cm^{-1} . Anal. Found (calcd.) (%) for $\text{C}_{26}\text{H}_{38}\text{O}_4\text{B}_{20}\text{N}_4\text{Mn} \cdot 0.5\text{CH}_2\text{Cl}_2$: C 40.50(40.59); H 7.16(7.14); N 4.97(5.01).

VI.6. References

- [1] a) M. Eddaoudi, D.B. Moler, H. Li, B. Chen, T.M. Reineke, M. O'Keeffe, O. M. Yaghi, *Acc. Chem. Res.*, **2001**, 34, 319; b) B. Moulton, M. J. Zaworotko, *Curr. Opin. Solid State Mater. Sci.*, **2002**, 6, 117; c) C. Janiak, *J. Chem. Soc., Dalton Trans.*, **2003**, 2781; d) O.M. Yaghi, M. O'Keeffe, N.W. Ockwig, H.K. Chae, M. Eddaoudi, J. Kim, *Nature Chemical Biology*, **2003**, 423, 705; e) U. Mueller, M. Schubert, F. Teich, H. Puetter, K. Schierle-Arndt, J. Pastre, *J. Mater. Chem.*, **2006**, 16, 626; f) M. Andruh, *Chem. Commun.*, **2007**, 2565; g) B. Wang, A.P. Cote, H. Furukawa, M. O'Keeffe, O. M. Yaghi, *Nature Chemical Biology*, **2008**, 453, 207; h) B. Moulton, M. J. Zaworotko, *Chem. Rev.*, **2001**, 101, 1629; i) A.K. Cheetham, C.N.R. Rao, R. K. Feller, *Chem. Commun.*, **2006**, 4780; j) G. A. Timco, S. Carretta, F. Troiani, F. Tuna, R. J. Pritchard, C. A. Muryn, E. J. L. McInnes, A. Ghirri, A. Candini, P. Santini, G. Amoretti, M. Affronte, E. P. Winpenny, *Nat. Nanotechnol.*, **2009**, 4, 173
- [2] a) S. S.-Y. Chui, S. M.-F. Lo, J. P. H. Charmant, A. G. Orpen, I. D. Williams, *Science* **1999**, 283, 1148; b) M. Eddaoudi, J. Kim, N. Rosi, D. Vodak, J. Wachter, M. O'Keeffe, O. M. Yaghi, *Science*, **2002**, 295, 469; c) H. Jude, H. Disteldorf, S. Fischer, T. Wedge, A. M. Hawkrigde, A. M. Arif, M. F. Hawthorne, D. C. Muddiman, P. Stang, *J. Am. Chem. Soc.*, **2005**, 127, 12131; d) R. N. Grimes, *Angew. Chem.*, **1993**, 105, 1350; e) M. A. Fox, A. K. Hughes, *Coord. Chem. Rev.*, **2004**, 248, 457
- [3] O. K. Farha, A. M. Spokoiny, K. L. Mulfort, M. F. Hawthorne, C. A. Mirkin, J. T. Hupp, *J. Am. Chem. Soc.*, **2007**, 129, 12680
- [4] M. Fontanet, A.-R. Popescu, X. Fontrodona, M. Rodríguez, I. Romero, F. Teixidor, C. Viñas, N. Aliaga-Alcalde, E. Ruiz, *Chemistry – A European Journal*, **2011**, 17, 13217.
- [5] M. Fontanet, M. Rodriguez, I. Romero, X. Fontrodona, F. Teixidor, C. Vinas, N. Aliaga-Alcalde, P. Matejcek, *Dalton Transactions*, **2013**.
- [6] a) O. Kriz, A. L. Rheingold, M. Y. Shang, T. P. Fehlner, *Inorganic Chemistry*, **1994**, 33, 3777; b) M. Fontanet, A. R. Popescu, X. Fontrodona, M. Rodriguez, I. Romero, F. Teixidor, C. Viñas, E. Ruiz, *Chem. Eur. J.*, **2011**, 17, 13217.
- [7] a) Y. B. Koh, G. G. Cristoph, *Inorg. Chem.*, **1979**, 18, 1122; b) M. Melník, *Coord. Chem. Rev.*, **1982**, 42, 259.
- [8] a) M. Cavicchioli, A. C. Massabni, L. R. Guilherme, *Transition Metal Chemistry*, **2007**, 355; b) R. C. Mehrotra, R. Bohra, *Metal Carboxylates*, Academic Press, New York, **1983**; c) L. P. Battaglia, A. B. Corradi, L. Menabue, *J. Chem. Soc., Dalton Trans.*, **1986**, 1653.
- [9] a) S. Chavan, D. Srinivas, P. Ratnasamy, *Journal of Catalysis*, **2000**, 192, 286; b) S. Youngme, A. Cheansirisomboon, C. Danvirutai, C. Pakawatchai, N. Chaichit, *Inorganic Chemistry Communications*, **2008**, 11, 57; c) J.-J. Wang, Z. Chang, A.-S. Zhang, T.-L. Hu, X.-H. Bu, *Inorganica Chimica Acta*, **2010**, 363, 1377.
- [10] a) I. Alkorta, J. Elguero, S. Grabowski, *J. Phys. Chem. A* **2008**, 112, 2721; b) S. J. Grabowski, W. A. Sokalski, J. Leszczynski, *J. Chem. Phys.*, **2007**, 337, 68; c) S. J. Grabowski, W. A. Sokalski, J. Leszczynski, *J. Phys. Chem. A*, **2005**, 109, 4331.
- [11] C. F. Matta, J. Hernandez-Trujillo, T. H. Tang, R. F. W. Bader, *Chem. Eur. J.*, **2003**, 9, 1940.
- [12] E. J. Juárez-Pérez, R. Núñez, C. Viñas, R. Sillanpää, F. Teixidor, *European Journal of Inorganic Chemistry*, **2010**, 2010, 2385.
- [13] a) L. A. Leites, *Chem. Rev.*, **1992**, 92, 279; b) A. Laromaine, F. Teixidor, R. Kivekäs, R. Sillanpää, M. Arca, V. Lippolis, E. Crespo, C. Viñas, *Dalton Trans.*, **2006**, 5240
- [14] R. C. Mehrotra, R. Bohra, *Metal Carboxylates*, Academic, New York, **1983**, 396.
- [15] L. J. Todd, A. R. Siedle, *Prog. Nucl. Magn. Reson. Spectrosc.*, **1979**, 13, 87
- [16] M. A. Fox, A. K. Hughes, *Coordination Chemistry Reviews*, **2004**, 248, 457.
- [17] a) S. S.-Y. Chui, S. M.-F. Lo, J. P. H. Charmant, A. G. Orpen, I. D. Williams, *Science*, **1999**, 283, 1148; b) O. Kristiansson, *Z. Kristallogr.-New Cryst. Struct. (J)*, **2001**, 216, 86; c) N. Barooah, A. Karmakar, R. J. Sarma, J. B. Baruah, *Inorganic Chemistry Communications*, **2006**, 9, 1251; d) G.-W. Yang, Q.-Y. Li, Y. Zhou, G.-Q. Gu, Y.-S. Ma, R.-X. Yuan, *Inorganica Chimica Acta*, **2009**, 362, 1234; e) M.-L. Hu, *Acta Crystallogr., Sect. E: Struct. Rep. Online*, **2006**, 62, m32; f) F.-A. Li, *Acta Crystallogr., Sect. E: Struct. Rep. Online*, **2010**, 66, m1526; g) L. Huang, D.-B. Chen, *Acta Crystallogr., Sect. E: Struct. Rep. Online*, **2006**, 62, m2872.
- [18] a) Remy van Gorkum, Francesco Buda, Huub Kooijman, Anthony L. Spek, Elisabeth Bouwman, J. Reedijk, *Eur. J. Inorg. Chem.*, **2005**, 2255; b) S. Banerjee, A. Ghosh, B. Wu, P.-G. Lassahn, C. Janiak, *Polyhedron*, **2005**, 24, 593.

- [19] a) E. Garribba, G. Micera, M. Zema, *Inorganica Chimica Acta*, **2004**, 357, 2038; b) V. Gómez, M. Corbella, *J. Chem. Crystallogr.*, **2011**, 41, 843; c) N. Palanisami, R. Murugavel, *Inorganica Chimica Acta*, **2011**, 365, 430; d) B. Albela, M. Corbella, J. Ribas, I. Castro, J. Sletten, H. Stoeckli-Evans, *Inorg. Chem.*, **1998**, 37, 788.
- [20] R. A. Kasar, G. M. Knudsen, S. B. Kahl, *Inorganic Chemistry*, **1999**, 38, 2936.

CHAPTER VII. Catalytic activity of Mn(II) and Co(II) compound containing the carboranylcarboxylate ligand 1-CH₃-2-CO₂H-1,2-closo-C₂B₁₀H₁₀



The reactivity of some of the new manganese (II) and cobalt(II) complexes synthesized in previous chapters has been tested with regard to the epoxidation of aromatic and aliphatic alkenes with peracetic acid as oxygen donor in dichloromethane. In general, manganese complexes show good catalytic activity, however, this activity is moderate for the binuclear cobalt complex $[\text{Co}_2(\mu\text{-H}_2\text{O})(1\text{-CH}_3\text{-2-CO}_2\text{-1,2-closo-C}_2\text{B}_{10}\text{H}_{10})_4(\text{THF})_4]$ studied. Catalytic activity of polymeric manganese(II) complex $[\text{Mn}(\mu\text{-H}_2\text{O})(1\text{-CH}_3\text{-2-CO}_2\text{-1,2-closo-C}_2\text{B}_{10}\text{H}_{10})_2]_n \cdot (\text{H}_2\text{O})_n$ has been tested regarding the oxidation of water to molecular oxygen.

TABLE OF CONTENTS

CHAPTER VII. Catalytic activity of Mn(II) and Co(II) compound containing the carboranylcarboxylate ligand 1-CH₃-2-CO₂H-1,2-closo-C₂B₁₀H₁₀

VII.1. Introduction	175
VII.2. Objectives	177
VII.3. Results and discussion	179
VII.3.1. Catalytic epoxidation of alkenes.....	179
VII.3.2. Water oxidation.....	186
VII.4. Conclusions	189
VII.5. Experimental section	191
VII.5.1. Instrumentation and measurements	191
VII.5.2. Materials.....	191
VII.5.3. Preparations	191
VII.5.4. Catalytic epoxidation	191
VII.5.5. Water oxidation.....	192
VII.6. References	193

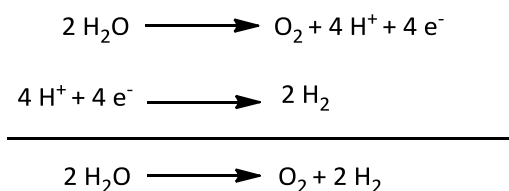
VII.1. Introduction

Metal-catalysed oxidation reactions are one of the most significant electron transfer reactions in chemistry and biology.^[1] Epoxides are an important class of functional groups that are widely employed in organic synthesis as many natural products possess epoxide units as essential structural moieties for their biological activities.^[2] Thus, the study of efficient metal-catalysed olefin epoxidation procedures is still receiving considerable attention due to the use of epoxides as building blocks in organic synthesis as well as in material science.^[3]

Epoxidation of olefins is usually carried on with organic peracids or with a combination of a transition metal catalyst and a co-oxidant such as H₂O₂, *t*-BuOOH, NaOCl or even oxygen. For this reason, although several methods have been developed,^[4] there is still an increasing need for more efficient and selective routes using stable and easily accessible catalyst under mild and neutral conditions.^[5]

Manganese complexes of tetradentate N₂O₂ Schiff-base ligands, Salen and derivatives, have been extensively studied as catalysts in epoxidation reactions.^[6] However, in the last decade, Stack and co-workers reported a method based on an *in-situ* synthesized mononuclear manganese(II) complexes by mixing Mn(CF₃SO₃)₂ and bi-, tri- or tetradentate nitrogen ligands and peracetic acid as oxidant, which generates acetic acid as side product being a good and clean oxidising agent.^[7] These systems presented higher activity, rapidity and efficiency in alkene epoxidation reactions than manganese complexes with Schiff base ligands, however, their stereoselectivity was poor. Few studies of manganese complexes containing carboxylate groups as catalyst have been reported, among them there are trinuclear manganese complexes with the structure [Mn₃(L)₂(OAc)₆], where L is a neutral bidentate nitrogen ligand, which are highly efficient catalysts in the epoxidation of alkenes using peracetic acid.^[8]

Another important oxidation reaction is the water oxidation reaction to molecular oxygen. This is an important process for the life on the earth and, in nature, it takes place in the photosystem II (PSII) using solar energy according to the redox reactions:



The complex responsible of this reaction in the PSII consists in a tetranuclear Mn cluster associated with Ca⁺² by oxo bonds, Cl⁻ and a redox-active tyrosine which is responsible of the coordination of seven amino acid side chains, mostly carboxylate, to the metal atoms.^[9]

CHAPTER VII

The use of water splitting as a way of converting solar energy to chemical energy holds promise for supplying future energy needs.^[10] This fact has contributed to an intensive research in the last decade of inexpensive and efficient catalysts for the solar-driven oxidation of water.^[11] Indeed, the most studied catalysts for this reaction are ruthenium^[12] and iridium^[13] complexes, being the manganese^[12b, 14] and cobalt^[15] complexes less studied in this area.

VII.2. Objectives

Complexes containing carboranylcarboxylate ligands have not ever been studied in metal-catalysed oxidation reactions. For this reason, the main goal of this chapter was to study the reactivity of some of the manganese and cobalt complexes described in previous chapters towards the epoxidation of some aromatic and aliphatic alkenes using peracetic acid as the oxidant.

We were also interested in the study of the reactivity of the trinuclear acetate manganese(II) complex $\text{Mn}_3(\text{OAc})_6(\text{bpy})_2$ containing 2,2'-bpy with the aim to make comparisons.

With this aim, catalytic activity of manganese and cobalt complexes presented in the Chart 1, together with the corresponding $\text{Mn}_3(\text{OAc})_6(\text{bpy})_2$, were tested in the epoxidation reaction of different alkenes.

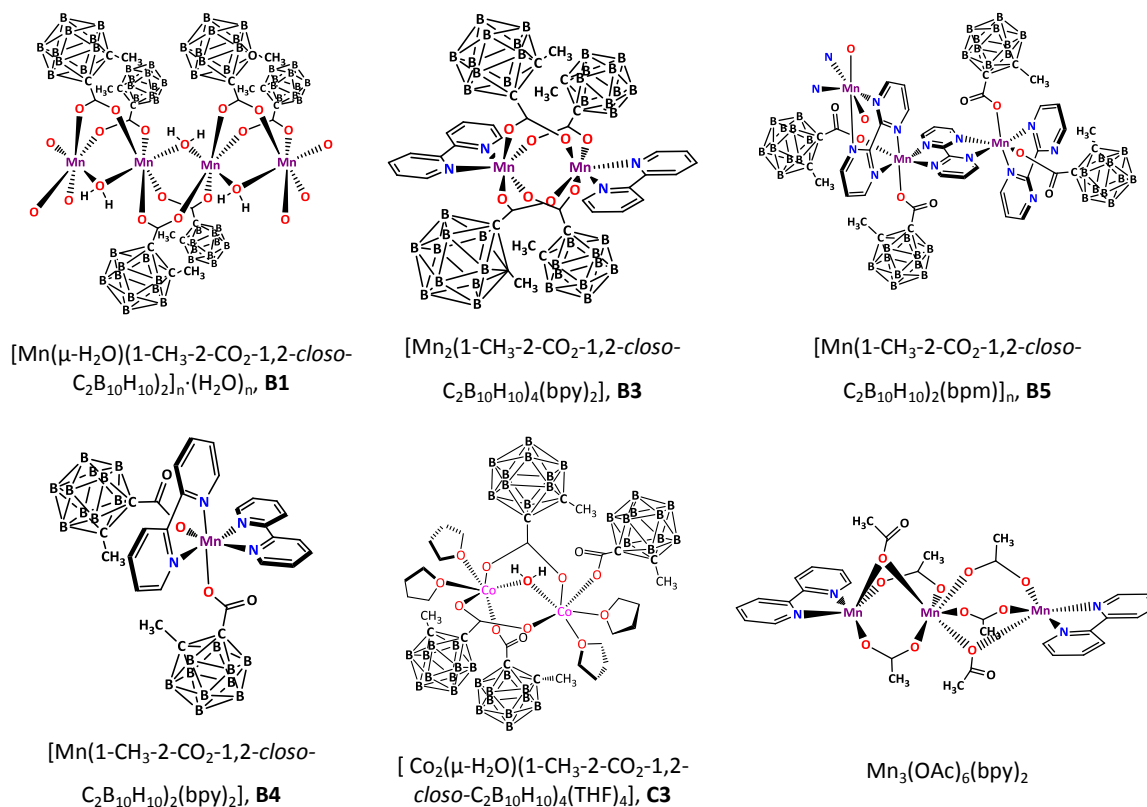


Chart 1. Complexes tested in the epoxidation reaction

We were also interested in the study of the role of the carboranylcarboxylate ligand $[1\text{-CH}_3\text{-2-CO}_2\text{-1,2-closo-C}_2\text{B}_{10}\text{H}_{10}]$, LH, in these reactions. With this aim, catalytic activity of ligand LH was tested using styrene as a substrate.

CHAPTER VII

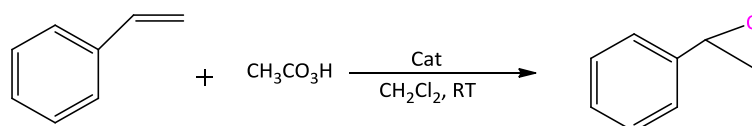
Another goal was to test the behaviour of the polymeric manganese(II) complex $[\text{Mn}(\mu\text{-H}_2\text{O})(1\text{-CH}_3\text{-2-CO}_2\text{-1,2-*cis*\text{-C}_2\text{B}_{10}\text{H}_{10})_2]_n \cdot (\text{H}_2\text{O})_n$, **B1**, with regard to the water oxidation reaction as a preliminary study.

VII.3. Results and discussion

VII.3.1. Catalytic epoxidation of alkenes

The catalytic activity of the manganese compounds **B1**, **B3-B5** and the cobalt (II) complex **C3** presented in Chart 1 was investigated in the epoxidation of representative terminal and internal double bonds of aliphatic and aromatic alkenes using commercial peracetic acid (32%) as oxidant. We were also interested in the catalytic behaviour of the acetate compound $\text{Mn}_3(\text{OAc})_6(\text{bpy})_2$, in the catalytic conditions used for our compounds, for comparison purpose. With this aim, $\text{Mn}_3(\text{OAc})_6(\text{bpy})_2$ was synthesized and characterized by X-ray diffraction (See Figure S1 and Table S1 at the supporting information section), although this compound has been previously synthesized and reported in the literature.^[8, 16] We have also studied the catalytic activity of the carboranylcarboxylate ligand **LH** in the same conditions of the catalysis. No epoxidation occurred on the substrates in presence of Mn(II) or Co(II) salts or in the absence of catalyst. Table 1 reports the conversion, the epoxide yield and selectivity values for the epoxide product using styrene as substrate, for manganese, cobalt complexes and ligand **LH**. All complexes were tested under analogous conditions (catalyst:substrate: peracetic acid, 1:100:200). In all cases, benzaldehyde was detected as a side product of the oxidation reaction.

Table 1. Catalytic oxidation of styrene by Mn and Co complexes and **LH** using $\text{CH}_3\text{CO}_3\text{H}$ as oxidant.^a



Entry	Compound	Conversion (%)	Epoxide yield (%)	Selectivity (%) ^a	Time (min)
1	B1	96	58	61	4
2	B1	100	77	77	30
3	B3	100	44	44	4
4	B4	100	44	44	4
5	B5	100	76	76	4
6	$\text{Mn}_3(\text{OAc})_6(\text{bpy})_2$	99	58	58	4
7	C3	21	12	56	4
8	C3	39	9	23	30
9	LH	10	0	2	4
10	LH	25	6	23	30
11	LH	29	16	55	120

Conditions (see experimental section for further details): catalyst (2.6 μmol), substrate (260 μmol), CH_2Cl_2 (2.5 mL). Peracetic acid 32% (520 μmol) added at 0°C, then reaction at RT.

^aCalculated as [epoxide yield/substrate conversion] x 100.

A quick glance to Table 1 suggests that for Mn compounds, conversions over 95% are found after 4 minutes of reaction together with moderate and high selectivity values. However, in the case of Co compounds moderate conversions and selectivities are observed with low epoxide yields that steadily decrease after 30 minutes of reaction. Catalytic activity of ligand LH was also tested with regard to the styrene substrate. Entries 10-12 show that after 4 minutes of reaction the epoxide was not detected whilst after 2 hours an increase was observed. Based in these results we can assert that the catalytic activity of the metallic compounds under study after 4 minutes is due to the coordination of the carboranylcarboxylate ligand to the metal.

It can be observed that the two polymeric complexes **B1** and **B5** show the highest selectivity values; in the case of **B1**, this value increase after 30 minutes of reaction. Entries 2 and 3 show that binuclear **B3** and mononuclear **B4** compounds, exhibit the same performance regarding the conversion of styrene with moderate values of selectivity (44%). Thus, we can conclude that the polymeric manganese structures present better conversion and selectivity than mononuclear and binuclear complexes containing 2,2'-bpy as ligands. Epoxidation reactions of aromatic olefins are known to be sluggish, leading to significant amounts of secondary products especially when the metal systems of Jacobsen^[17] or Stack,^[7a, 7b] are employed.

A comparison of the catalytic activity of complex $\text{Mn}_3(\text{OAc})_6(\text{bpy})_2$ with our complexes indicates that they display similar conversion values with a slight increase of selectivity values for the trinuclear complex $\text{Mn}_3(\text{OAc})_6(\text{bpy})_2$ over the binuclear **B3** and mononuclear **B4**, but with lower values with respect to polymeric compounds **B1** and **B5**.

Based on the good results obtained with styrene as substrate, we decided to test our complexes in the epoxidation of other olefins maintaining the reaction times at 4 minutes. The results are gathered in Table 2. As there is observed, high conversions and selectivities for the epoxide product are obtained in most of the cases.

When catalytic activity is studied with 4-vinyl-1-cyclohexene, it is noticed that the reaction is regioselective for epoxidation of the ring double bond. Moreover, it is observed that complexes containing pyridylic ligands, **B3-B5**, and acetate, $\text{Mn}_3(\text{OAc})_6(\text{bpy})_2$, show high conversion values but moderate selectivity. However, excellent selectivity is achieved by the polymeric complex **B1**, where only Mn(II), water and carboranylcarboxylate ligands are present.

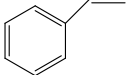
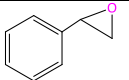
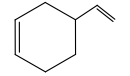
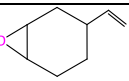
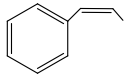
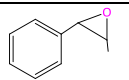
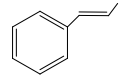
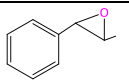
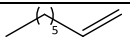
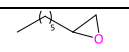
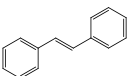
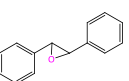
For *cis*- β -methylstyrene, all complexes containing the carboranylcarboxylate ligand show high conversion and selectivity values. It is remarkable that the epoxidation of *cis*- β -methylstyrene, is highly stereospecific for the formation of the *cis*-epoxide with all these compounds. However, when the trinuclear complex $\text{Mn}_3(\text{OAc})_6(\text{bpy})_2$ is used as the catalyst the process is less stereospecific and also lower values of conversion and selectivity are observed.

According with these results it could be said that if a radical mechanism was involved in the epoxidation pathway, the radical intermediate species containing the carboranylcarboxylate ligand must be shorter-lived than those containing the acetate ligand in order to exert a significant influence on the stereoselectivity of the reaction.^[7a, 18] Thus, it could also be said that the carboranylcarboxylate ligand plays an important role in the stereospecificity of this reaction greater than polipyridylic ligands since less percentage of *cis* epoxide is obtained when $\text{Mn}_3(\text{OAc})_6(\text{bpy})_2$, is used as catalyst, which only contains acetate and bipyridine groups.

In the case of *trans*- β -methylstyrene, all complexes display good performance and selectivity, presenting high values that in some cases are close to 100%. The catalytic activity was also tested with the aliphatic substrate 1-octene which usually tends to be the least reactive olefin in metal-catalysed epoxidation.^[19] In this case 1-octene was readily epoxidized with our compounds providing good conversion values and moderate selectivities. It is again remarkable the selectivity of **B1**.

Finally, excellent conversion and good selectivity values were obtained for complexes **B1-B3** and **B5** using *trans*-stilbene as a substrate, conversely, **B4** displayed moderate selectivity and epoxide conversion values.

Table 2. Epoxidation tests performed with manganese complexes **B1-B5** and $\text{Mn}_3(\text{OAc})_6(\text{bpy})_2$

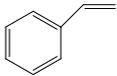
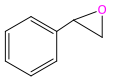
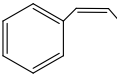
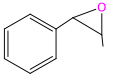
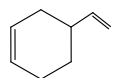
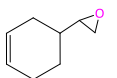
Substrate	Product	B1		B3		B4		B5		$\text{Mn}_3(\text{OAc})_6(\text{bpy})_2$	
		Conv. (%)	Select. (%) ^a	Conv. (%)	Select. (%) ^a						
		96	61	100	44	100	44	100	76	99	58
		70	91 ^c	89	40 ^c	100	45 ^c	100	55 ^c	97	68 ^c
		90	75 <i>c/t</i> =79% ^b	99	80 <i>c/t</i> =88% ^b	98	82 <i>c/t</i> =87% ^b	100	66 <i>c/t</i> =94% ^b	75	75 <i>c/t</i> =67% ^b
		95	80	100	97	100	88	100	95	100	100
		61	72	95	41	98	54	83	46	83	56
		86	70	100	63	100	48	100	74	100	83

Conditions (see experimental section for further details): catalyst (2.6 μmol), substrate (260 μmol), CH_2Cl_2 (2.5 mL). Peracetic acid 32% (520 μmol) added at 0 $^\circ\text{C}$, then reaction at RT.

^aCalculated as [epoxide yield/substrate conversion] x 100. ^b*c/t* represents the percentage of *cis* isomer obtained. ^c Epoxidation exclusively at the cyclohexene ring.

Finally, we focus our attention on the cobalt complex $[\text{Co}_2(\mu\text{-H}_2\text{O})(1\text{-CH}_3\text{-2-CO}_2\text{-1,2-closo-C}_2\text{B}_{10}\text{H}_{10})_4(\text{THF})_4]$, **C3**. Its catalytic activity was studied with styrene, *cis*- β -methylstyrene and 4-vinyl-1-cyclohexene as substrates. Results are gathered in Table 3. It is observed that this compound presents, in general, moderate performance and selectivity for all substrates tested. Moreover, it is noteworthy that these results improve after 30 minutes of reaction in the case of *cis*- β -methylstyrene and 4-vinyl-1-cyclohexene, however, in the case of styrene these values decrease.

Table 3. Epoxidation tests performed with cobalt complex **C3**

Substrate	Product	C3	
		Conv. (%)	Select. (%) ^a
		21 ^c	56 ^c
		39 ^d	23 ^d
		16 ^c	46 ^c <i>c/t</i> =49% ^b
		42 ^d	45 ^d <i>c/t</i> =62% ^b
		41 ^c	55 ^c
		67 ^d	70 ^d

Conditions (see experimental section for further details): catalyst (2.6 μmol), substrate (260 μmol), CH_2Cl_2 (2.5 mL). Peracetic acid 32% (520 μmol) added at 0 $^\circ\text{C}$, then reaction at RT.

^aCalculated as [epoxide yield/substrate conversion] x 100. ^b *c/t* represents the percentage of *cis* isomer obtained.

^c Aliquot taken after 4 minutes of reaction. ^d Aliquot taken after 30 minutes of reaction

The complexes under study are the first examples, to the best of our knowledge, of complexes containing carboranylcarboxylate ligands tested in alkene epoxidation catalysis.

A study of the stability of the ligand **LH** in the acid medium has been carried out by NMR and IR techniques. The ^{11}B - and $^{11}\text{B}\{^1\text{H}\}$ -NMR spectra of ligand **LH** in peracetic acid in the ratio 1:200 (same condition than in the catalysis) are shown in

Figure 1. . Spectra show that the ligand **LH** remains unaffected after reaction with peracetic acid. No signals of *nido*-shaped $[\text{7,8-C}_2\text{B}_9\text{H}_{10}]^-$ or $[\text{7,8-C}_2\text{B}_9\text{H}_9]^{2-}$ anions or $\text{B}(\text{OCH}_3)_3$ has been observed after reaction with peracetic acid.

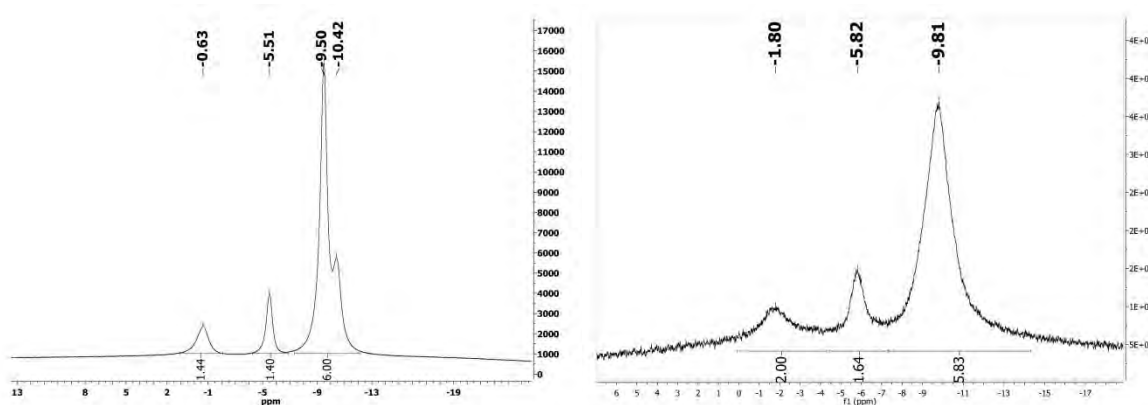
We have also studied the behaviour of ligand **LH** after addition of commercial peracetic acid by IR spectrometry, two ratios **LH**:oxidant were tested 1:1 and 1:200 (Figure 2); we did not observe changes in the typical $\nu(\text{B-H})$ absorption at frequencies above 2590 cm^{-1} , characteristic of *closo* carborane derivatives^[20] or in the frequencies of the symmetric and antisymmetric stretches, above 1270 and 1720 cm^{-1} , respectively, of the carboxylate groups of

CHAPTER VII

the LH ligand. We can conclude from these experiments that the carboranylcarboxylate ligand LH, remains unaltered after reaction with commercial peracetic acid 32%.

As a general conclusion, it may be said that the coordination of the carboranylcarboxylate ligand to the metal ion is crucial in the performance of the compounds as catalysts. Moreover, it has been observed that the catalytic activity also depends of the metal considered. Thus, when manganese is present in the complex, high catalytic activity is observed, however, when cobalt(II) ion is the metal centre, the compound shows very low catalytic activity in any case.

a)



b)

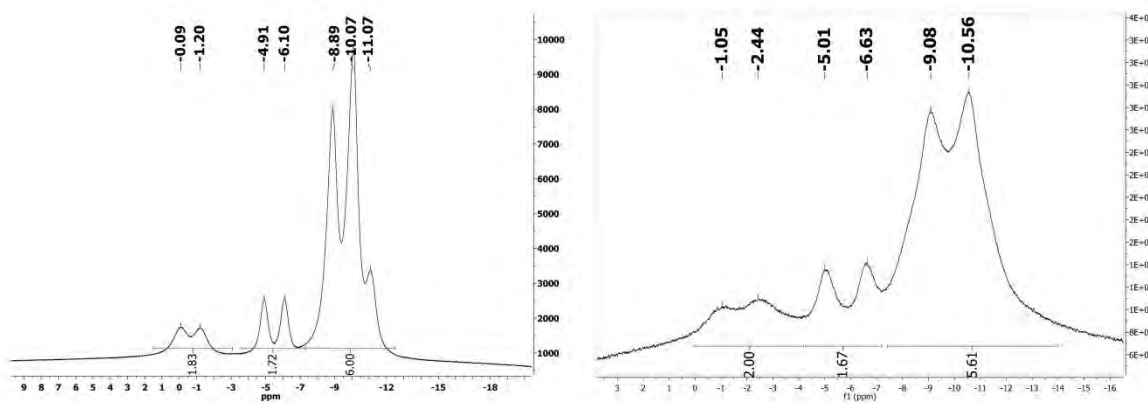
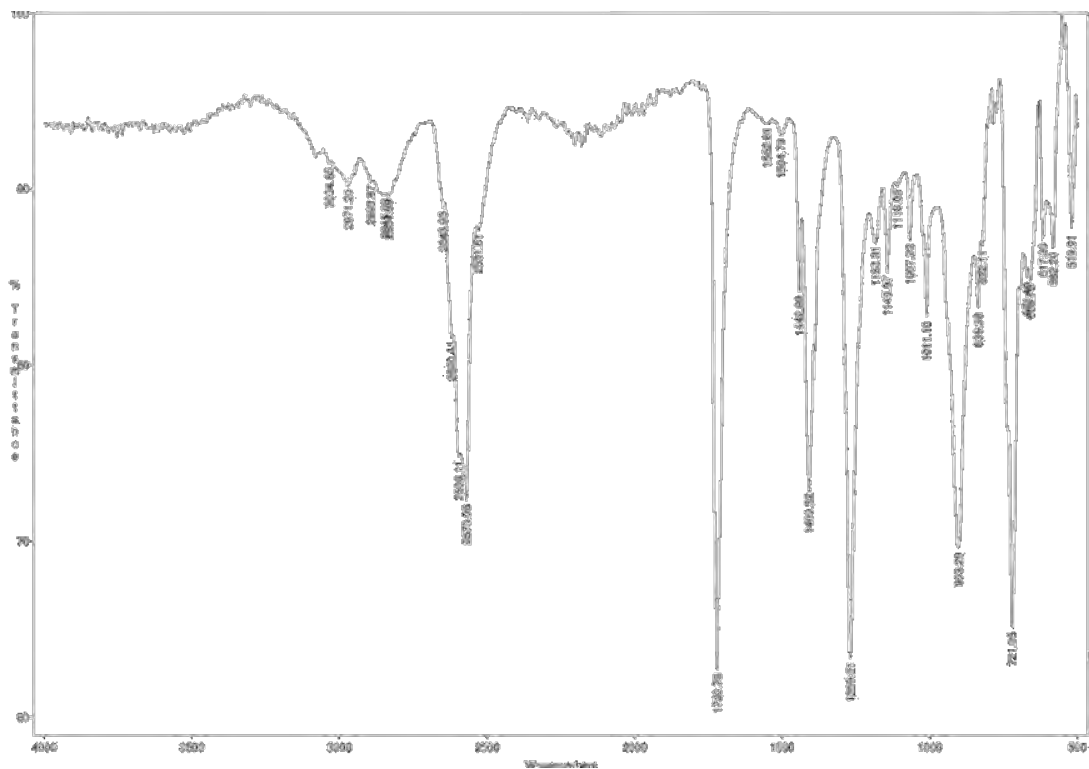
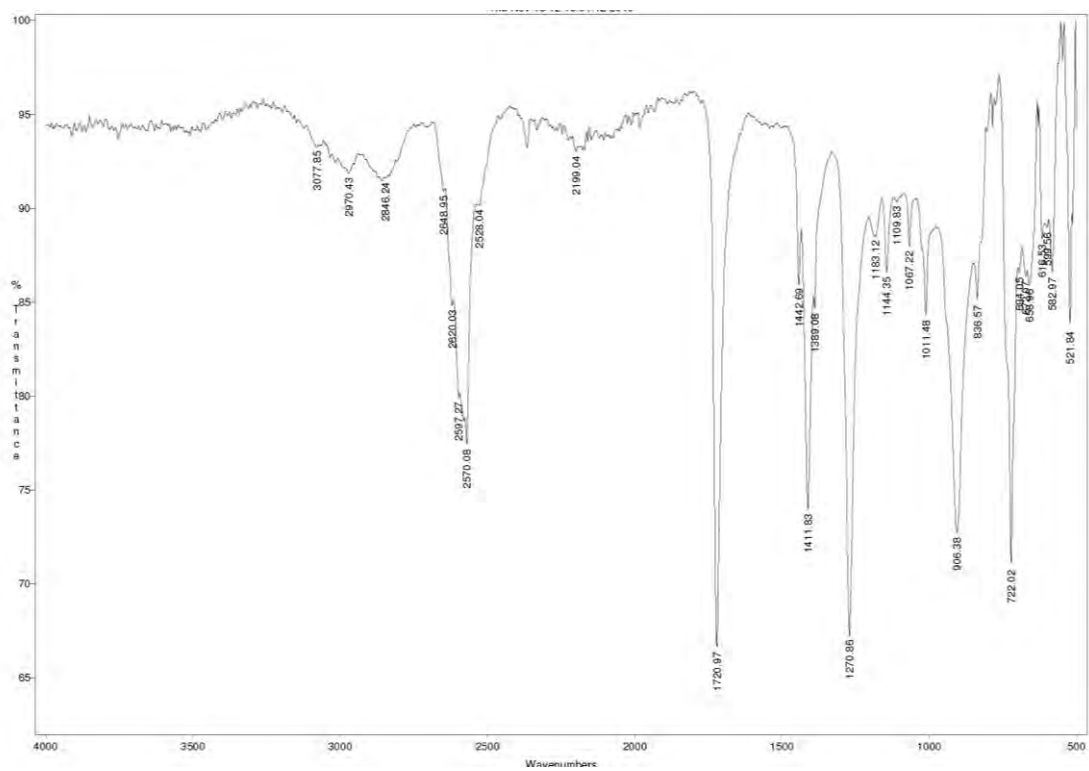


Figure 1. a) $^{11}\text{B}\{^1\text{H}\}$ -RMN and b) ^{11}B -RMN spectra of ligand LH after reaction with peracetic acid in $\text{H}_2\text{O}/\text{D}_2\text{O}$ (right side) and pure ligand LH in CDCl_3 (left side).

a)



b)



c)

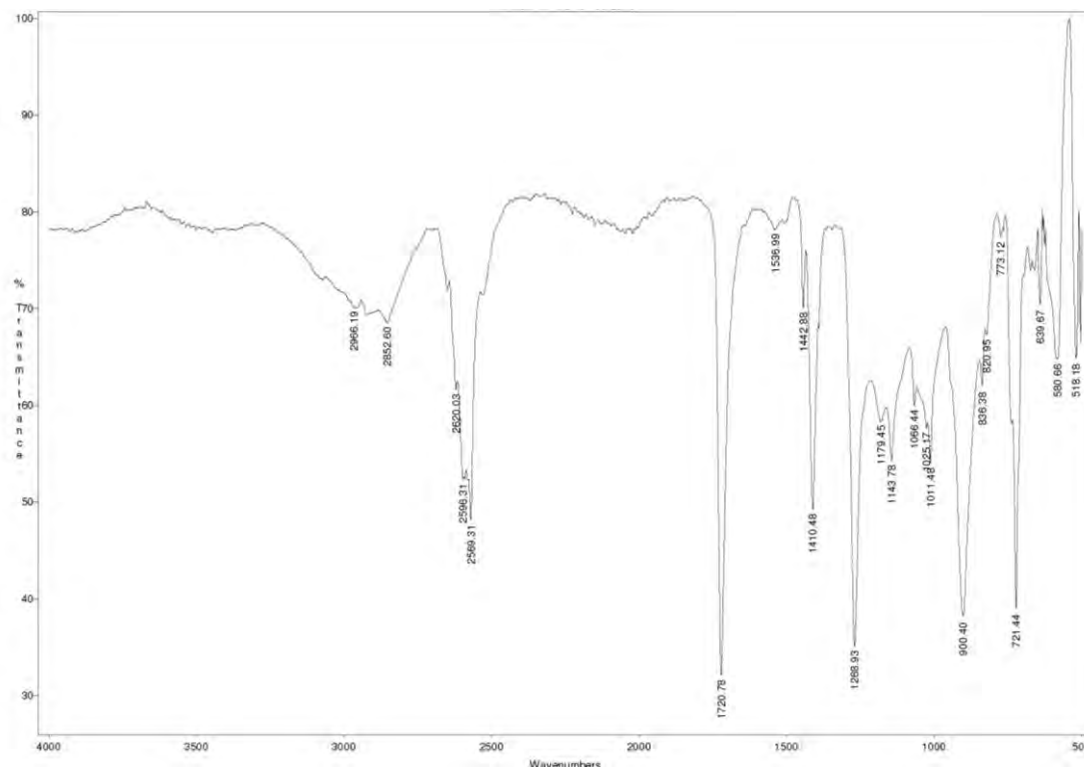


Figure 2. IR spectra of ligand LH a) pure, b) 1:1 ratio LH: peracetic acid 32% c) 1:200 ratio LH: peracetic acid 32%

VII.3.2. Water oxidation

Recently, the crystal structure of the oxygen-evolving centre in photosystem II has been reported by Umena et al.^[9b] and it has been seen that water molecules are bound to the Mn_4CaO_5 cluster. We are of the opinion that our polymer **B1** may provide a good example for further design and construction of new supramolecular assemblies as models of the oxygen-evolving center (OEC) and also to understand the role of the water molecules in the catalytic process of water splitting. All this, prompted us to study the catalytic activity of the manganese(II) complex $[Mn(\mu-H_2O)(1-CH_3-2-CO_2-1,2-closo-C_2B_{10}H_{10})_2]_n \cdot (H_2O)_n$, **B1** towards the oxidation of water to molecular oxygen.

Our investigation of the catalysis of water oxidation by complex **B1**, was carried out using spectroscopic methods, and GC-MS. A solution of complex **B1** was added to an aqueous CF_3SO_3H solution (initial pH 1.0), containing excess of Ce^{IV} ; generation of oxygen was immediately detected and was monitored by GC-MS. We could observe that the catalytic water oxidation reaction is completed in less than 2 minutes (Figure 3). No generation of CO_2 was detected.

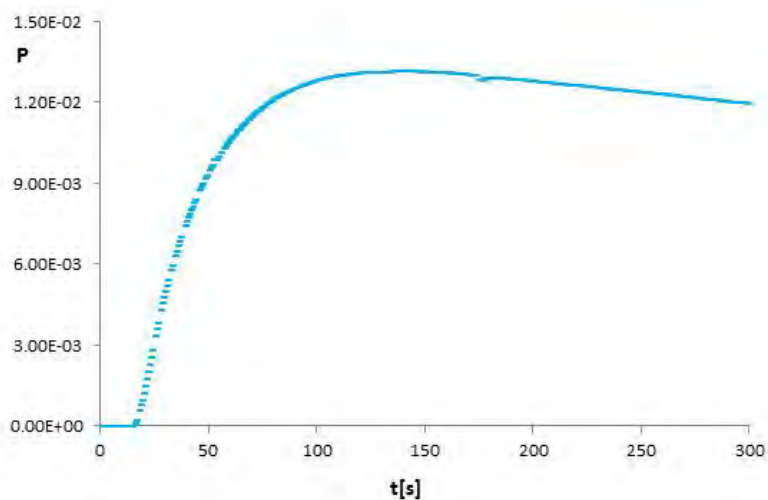
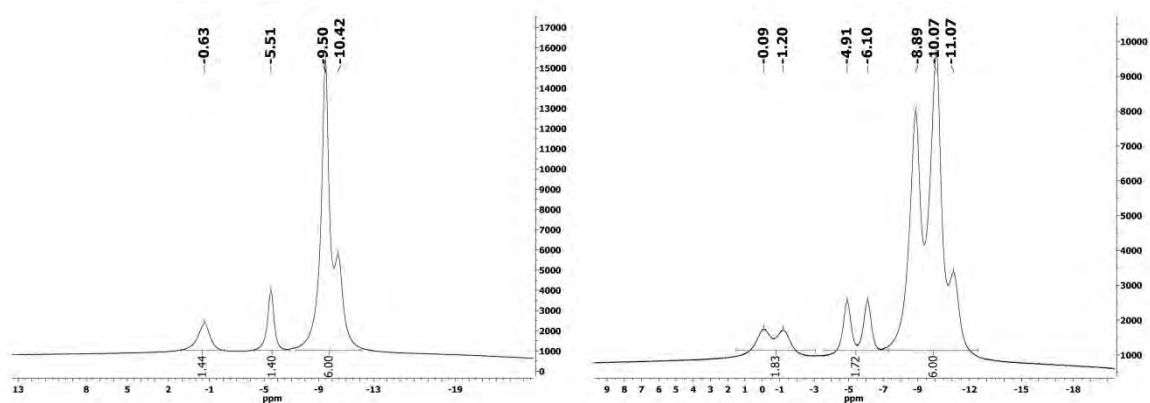


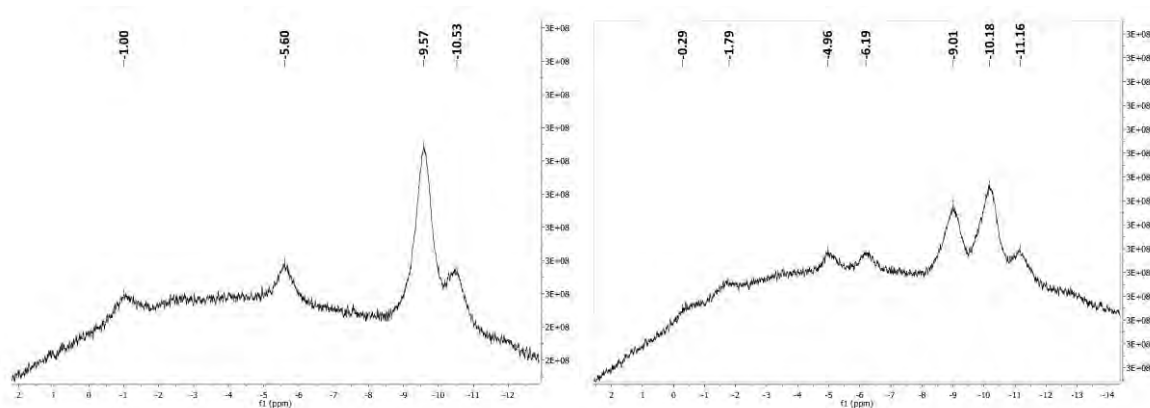
Figure 3. Kinetic plots of oxygen formation by **B1** versus time (conditions: $\text{CF}_3\text{SO}_3\text{H}$ aqueous solutions (2.0 ml) containing Ce^{IV} (0.204 mmol) and catalyst (1.02×10^{-3} mol)).

With the aim to learn if the generation of O_2 is due to the breaking of ligand **LH**, the stability of the latter was tested by ^{11}B and $^{11}\text{B}\{^1\text{H}\}$ -NMR spectra. Similarly as for complex **B1**, to an aqueous $\text{CF}_3\text{SO}_3\text{H}$ solution (initial pH 1.0), containing excess of Ce^{IV} , a solution of ligand **LH** was added. The resulting solution was dried under vacuum and extractions with D_2O and CDCl_3 were carried on. Then, ^{11}B and $^{11}\text{B}\{^1\text{H}\}$ -NMR of the two extractions were performed (see Figure 4.). No signals of *nido*-shaped $[\text{7,8-C}_2\text{B}_9\text{H}_{10}]^-$ or $[\text{7,8-C}_2\text{B}_9\text{H}_9]^{2-}$ anions or $\text{B}(\text{OCH}_3)_3$ were observed after water oxidation reaction, being the initial and final NMR spectra indistinguishable. Thus, it can be concluded that the generated O_2 is not due to the degradation of the *closo* to *nido* cluster of the ligand.

a)



b)



c)

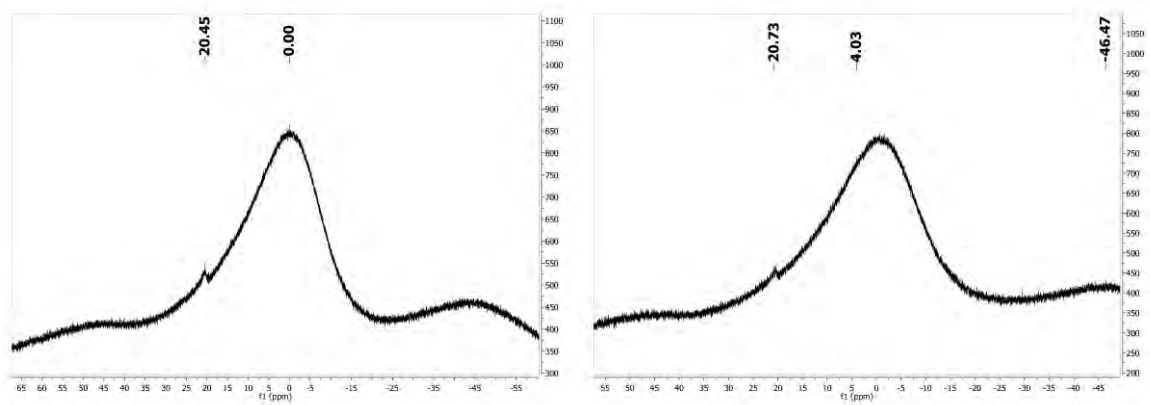


Figure 4. ^{11}B -RMN (right) and $^{11}\text{B}\{^1\text{H}\}$ -RMN (left) of ligand **LH** a) pure in CDCl_3 , b) extraction with CDCl_3 and c) extraction with D_2O after same conditions than water oxidation reaction.

As seen, these preliminary studies suggest that the polymer **B1** is readily capable to oxidize water to oxygen, however, these are preliminary results and more studies are required to quantify the generated O_2 .

VII.4. Conclusions

The catalytic activity of the manganese compounds $[\text{Mn}(\mu\text{-H}_2\text{O})(1\text{-CH}_3\text{-2-CO}_2\text{-1,2-closo-C}_2\text{B}_{10}\text{H}_{10})_2]_n \cdot (\text{H}_2\text{O})_n$, **B1**, $[\text{Mn}_2(1\text{-CH}_3\text{-2-CO}_2\text{-1,2-closo-C}_2\text{B}_{10}\text{H}_{10})_4(\text{bpy})_2]$, **B3**, $[\text{Mn}(1\text{-CH}_3\text{-2-CO}_2\text{-1,2-closo-C}_2\text{B}_{10}\text{H}_{10})_2(\text{bpy})_2]$, **B4**, $[\text{Mn}(1\text{-CH}_3\text{-2-CO}_2\text{-1,2-closo-C}_2\text{B}_{10}\text{H}_{10})_2(\text{bpm})]_n$, **B5**, the cobalt complex, $[\text{Co}_2(\mu\text{-H}_2\text{O})(1\text{-CH}_3\text{-2-CO}_2\text{-1,2-closo-C}_2\text{B}_{10}\text{H}_{10})_4(\text{THF})_4]$, **C3**, has been tested regarding the epoxidation of representative terminal and internal double bonds of aliphatic and aromatic alkenes epoxidation.

Catalytic activity of ligand **LH** was also tested with regard to the epoxidation of styrene as substrate. No epoxide was detected after 4 minutes of reaction, leading us to conclude that the coordination of the carboranylcarboxylate ligand to the metal is necessary to observe catalytic activity under the conditions studied.

Manganese complexes have shown good efficiency even after 4 minutes of reaction and revealed to be specific for the *cis* epoxide, when *cis*- β -methylstyrene is used as substrate and regioselective in the epoxidation of the ring double bond with 4-vinyl-1-cyclohexene. Moreover, with the aliphatic substrate 1-octene, good conversion values and moderate selectivities were achieved despite its tendency to be the least reactive olefin in metal-catalysed epoxidation, even with the polymeric compound **B1** which only contains carboranylcarboxylate and aquo ligands.

In order to make comparisons with our manganese complexes, $\text{Mn}_3(\text{OAc})_6(\text{bpy})_2$ was synthesized and characterized by X-ray diffraction and its catalytic activity was also assessed in the commented epoxidation reactions. It was observed that although conversions values of all manganese complexes tested are similar, the selectivity values for most substrates under study are higher for the complexes containing the carboranylcarboxylate ligand than for the trinuclear complex containing the acetate.

Catalytic activity of cobalt complex showed moderate performance and selectivity for all substrates tested, with values that improve in some cases after 30 minutes of reaction. It thus can be concluded that manganese complexes are the ones exhibiting the highest catalytic activity.

It was confirmed by spectroscopic techniques (IR and NMR) that the carboranylcarboxylate ligand **LH** is stable after reaction with commercial peracetic acid 32%. Thus, it was resolved that the coordination of the carboranylcarboxylate ligand to the metal ion is critical in the catalytic activity of these compounds as well as the metal considered, being compounds containing manganese(II) more efficient than those containing cobalt(II).

CHAPTER VII

Finally, manganese(II) complex $[\text{Mn}(\mu\text{-H}_2\text{O})(1\text{-CH}_3\text{-2-CO}_2\text{-1,2-}i\text{closo-C}_2\text{B}_{10}\text{H}_{10})_2]_n(\text{H}_2\text{O})_n$, **B1**, was preliminarily tested in the oxidation of water to molecular oxygen, showing catalytic activity. Moreover, the carboranylcarboxylate ligand **LH** was stable under the water oxidation reaction thus concluding that the generated O_2 is not produced by the degradation of the *closo* to *nido* cluster in the ligand.

VII.5. Experimental section

VII.5.1. Instrumentation and measurements

Instrumentation and Measurements. GC measurements were taken in a Shimadzu GC-2010 gas chromatography apparatus equipped with an Astec CHIRALDEX G-TA column and a FID detector. Water oxidation measurements were taken in an OmnistarTM GSD 301 C (Pfeiffer) quadrupole mass spectrometer. FT-IR spectra were taken in a Mattson-Galaxy Satellite FT-IR spectrophotometer containing a MKII Golden Gate Single Reflection ATR System. NMR spectra have been recorded with a Bruker ARX 300 or a DPX 400 instrument equipped with the appropriate decoupling accessories (^1H and $^1\text{H}\{^{11}\text{B}\}$ NMR (300.13/400.13 MHz), $^{13}\text{C}\{^1\text{H}\}$ NMR (75.47/100.62 MHz) and ^{11}B and $^{11}\text{B}\{^1\text{H}\}$ NMR (96.29/128.37 MHz) spectra were recorded in d_6 -acetone, CD_2Cl_2 and D_2O . Chemical shift values for ^{11}B NMR spectra were referenced to external $\text{BF}_3\leftarrow\text{OEt}_2$ and those for ^1H , $^1\text{H}\{^{11}\text{B}\}$ and $^{13}\text{C}\{^1\text{H}\}$ NMR spectra were referenced to SiMe_4 . Chemical shifts are reported in units of parts per million downfield from reference, and all coupling constants in Hz.

X-ray structure determination. Measurement of the crystals were performed on a Bruker Smart Apex CCD diffractometer using graphite-monochromated Mo $\text{K}\alpha$ radiation ($\lambda = 0.71073\text{\AA}$) from an X-Ray tube. Data collection, Smart V. 5.631 (BrukerAXS 1997-02); data reduction, Saint+ Version 6.36A (Bruker AXS 2001); absorption correction, SADABS version 2.10 (Bruker AXS 2001) and structure solution and refinement, SHELXTL Version 6.14 (Bruker AXS 2000-2003).

VII.5.2. Materials

All reagents used in the present work were obtained from Aldrich Chemical Co and were used without further purification. Reagent grade organic solvents were obtained from SDS and high purity de-ionized water was obtained by passing distilled water through a nano-pure Mili-Q water purification system.

VII.5.3. Preparations

The $\text{Mn}_3(\text{OAc})_6(\text{bpy})_2$ complex was prepared according to literature procedures^[16, 21]. All the water oxidation manipulations were performed under inert atmosphere.

VII.5.4. Catalytic epoxidation

A CH_2Cl_2 (2.5 mL) solution of alkene (260 μmol), catalyst (2.6 μmol) and biphenyl (250 μmol , internal standard) was prepared in a 5 mL flask and cooled in an ice bath. Afterwards, 32 %

peracetic acid (110 μmol) was slowly added via syringe under stirring at 0°C. The reaction vessel was then taken out of the ice bath (this is taken as the starting point of the catalysis) and allowed to progressively warm to RT. Each aliquot of the reaction taken for analysis was filtered through a basic alumina plug and was analysed in a Shimadzu GC-2010 gas chromatography apparatus equipped with an Astec CHIRALDEX G-TA column and a FID detector. Quantification was achieved from calibration curves.

NMR study

To an ethanolic solution of 0.006 g (0.030 mmols) of ligand LH, 1.25 mL (6.0 mmols) of peracetic acid 32% were added. Solution was stirring for 1 hour and then solvent was removed under vacuum. Solid was dissolved in CDCl_3 and the ^{11}B - and $^{11}\text{B}\{^1\text{H}\}$ -NMR spectra of the solution was carried on (see Figure 1 above).

IR study

Two portions of LH ligand were dissolved in dichloromethane and were reacted with peracetic acid in different ratio LH:oxidant (1:1 and 1:200). After 1 hour of reaction the solution was dried under vacuum and IR spectra of both experiments were registered. (Figure 2 above)

VII.5.5. Water oxidation

The water oxidation measurements were carried out by GC-MS. To a flask containing 112 mg (0.204 mmols) of $\text{Ce}(\text{NH}_4)_2(\text{NO}_3)_6$ under stirring and inert atmosphere, were added 2 mL of an aqueous solution of $\text{CF}_3\text{SO}_3\text{H}$ (pH 1.0). Once the Ce^{IV} was dissolved, 0.51 mL of a solution 2mM of catalyst **B1** in water or ligand LH in dichloromethane was injected to the above solution under stirring and under nitrogen atmosphere. Immediately, measurements of the evolution of O_2 vs time were recorded.

VII.6. References

- [1] a) R. A. Sheldon, J. K. Kochi, *Metal Catalyzed Oxidation of Organic Compounds*, Academic Press, New York, **1981**; b) P. Gamez, P. G. Aubel, W. L. Driessen, J. Reedijk, *Chem. Soc. Rev.*, **2001**, 30, 376; c) A. Robert, B. Meunier, *Biomimetic Oxidations Catalyzed by Transition Metal Complexes*, Ed. Meunier, B., Imperial College Press, **2000**, Ch. 12; d) P. C. A. Bruijninx, G. Van Koten, R. J. M. K. Gebbink, *Chem. Soc. Rev.*, **2008**, 37, 2716.
- [2] a) K. B. Sharpless, *Angewandte Chemie International Edition*, **2002**, 41, 2024; b) A. H. Hoveyda, D. A. Evans, G. C. Fu, *Chemical Reviews*, **1993**, 93, 1307.
- [3] a) S. Y. Ko, A. W. M. Lee, S. Masamune, L. A. Reed, K. B. Sharpless, F. J. Walker, **1983**, 220, 949; b) S. D. Gagnon, *Encyclopedia of Polymer Science and Engineering*, 2nd ed., H.F. Mark, N.M. Bikales, C.G. Overberger, G. Menges, J.I. Kroschwitz; Vol. 6, John Wiley & Sons, New York, **1985**, pp 273-307; c) K. C. Nicolaou, N. Winssinger, J. Pastor, S. Ninkovic, F. Sarabia, Y. He, D. Vourloumis, Z. Yang, T. Li, P. Giannakakou, E. Hamel, *Nature*, **1997**, 387, 268; d) D. J. Darensbourg, R. M. Mackiewicz, A. L. Phelps, D. R. Billodeaux, *Acc. Chem. Res.*, **2004**, 37, 836; e) I. E. Ojima, *Catalytic Asymmetric Synthesis*, 2nd ed., Wiley & Sons, New York, **2000**; f) G. de Faveri, G. Ilyashenko, M. Watkinson, *Chem. Soc. Rev.*, **2011**, 40, 1722.
- [4] a) K. A. Joergensen, *Chemical Reviews*, **1989**, 89, 431; b) T. Katsuki, *Adv. Synth. Catal.*, **2002**, 344, 131; c) D. E. De Vos, B. F. Sels, P. A. Jacobs, *Adv. Synth. Catal.*, **2003**, 345, 457.
- [5] a) R. Noyori, M. Aoki, K. Sato, *Chem. Commun.*, **2003**, 1977; b) B. S. Lane, K. Burgess, *Chem. Rev.*, **2003**, 103, 2457.
- [6] a) C. P. Horwitz, S. E. Creager, R. W. Murray, *Inorganic Chemistry*, **1990**, 29, 1006; b) Q. H. Xia, H. Q. Ge, C. P. Ye, Z. M. Liu, K. X. Su, *Chemical Reviews*, **2005**, 105, 1603; c) A. Martinez, C. Hemmert, C. Loup, G. Barré, B. Meunier, *The Journal of Organic Chemistry*, **2006**, 71, 1449.
- [7] a) A. Murphy, G. Dubois, T. D. P. Stack, *J. Am. Chem. Soc.*, **2003**, 125, 5250; b) A. Murphy, A. Pace, T. D. P. Stack, *Org. Lett.*, **2004**, 6, 3119; c) A. Murphy, T. D. P. Stack, *J. Mol. Catal. A: Chem.*, **2006**, 251, 78.
- [8] B. Kang, M. Kim, J. Lee, Y. Do, S. Chang, *The Journal of Organic Chemistry*, **2006**, 71, 6721.
- [9] a) P. E. M. Siegbahn, *Accounts of Chemical Research*, **2009**, 42, 1871; b) Y. Umena, K. Kawakami, J.-R. Shen, N. Kamiya, *Nature*, **2011**, 473, 55.
- [10] a) J. L. Dempsey, A. J. Esswein, D. R. Manke, J. Rosenthal, J. D. Soper, D. G. Nocera, *Inorganic Chemistry*, **2005**, 44, 6879; b) W. J. Youngblood, S.-H. A. Lee, K. Maeda, T. E. Mallouk, *Accounts of Chemical Research*, **2009**, 42, 1966; c) H. Dau, I. Zaharieva, *Accounts of Chemical Research*, **2009**, 42, 1861.
- [11] a) X. Sala, I. Romero, M. Rodríguez, L. Escriche, A. Llobet, *Angewandte Chemie International Edition*, **2009**, 48, 2842; b) G. C. Dismukes, R. Brimblecombe, G. A. N. Felton, R. S. Pryadun, J. E. Sheats, L. Spiccia, G. F. Swiegers, *Accounts of Chemical Research*, **2009**, 42, 1935.
- [12] a) S. Romain, L. Vigarà, A. Llobet, *Acc. Chem. Res.*, **2009**, 42, 1944; b) H. e. a. Dau, *ChemCatChem* **2010**, 2, 724; c) T. J. Meyer, *Acc. Chem. Res.*, **1989**, 22, 163; d) L. Duan, F. Bozoglian, S. Mandal, B. Stewart, T. Privalov, A. Llobet, L. Sun, *Nat Chem*, **2012**, 4, 418.
- [13] a) N. D. McDaniel, F. J. Coughlin, L. L. Tinker, S. Bernhard, *J. Am. Chem. Soc.*, **2008**, 130, 210; b) J. F. Hull et al., *J. Am. Chem. Soc.*, **2009**, 131, 8730; c) R. Lalrempuia, N. D. McDaniel, H. Müller-Bunz, S. Bernhard, M. Albrecht, *Angew. Chem. Int. Ed.*, **2010**, 49, 9765.
- [14] C. S. Mullins, V. L. Pecoraro, *Coord. Chem. Rev.*, **2008**, 252, 416.
- [15] a) D. J. Wasylenko, C. Ganesamoorthy, J. Borau-Garcia, C. P. Berlinguette, *Chem. Commun.*, **2011**, 47, 4249; b) D. K. Dogutan, R. McGuire, D. G. Nocera, *J. Am. Chem. Soc.*, **2011**, 133, 9178; c) Q. Yin et al., *Science*, **2010**, 328, 342.
- [16] S. Menage, S. E. Vitols, P. Bergerat, E. Codjovi, O. Kahn, J. J. Girerd, M. Guillot, X. Solans, T. Calvet, *Inorganic Chemistry*, **1991**, 30, 2666.
- [17] a) H. Jacobsen, L. Cavallo, *Organometallics*, **2005**, 25, 177; b) L. Cavallo, H. Jacobsen, *Inorganic Chemistry*, **2004**, 43, 2175.
- [18] M. Palucki, N. S. Finney, P. J. Pospisil, M. L. Güler, T. Ishida, E. N. Jacobsen, *Journal of the American Chemical Society*, **1998**, 120, 948.
- [19] K.-P. Ho, W.-L. Wong, K.-M. Lam, C.-P. Lai, T. H. Chan, K.-Y. Wong, *Chemistry – A European Journal*, **2008**, 14, 7988.

CHAPTER VII

[20] a) L. A. Leites, *Chem. Rev.*, **1992**, 92, 279 ; b) A. Laromaine, F. Teixidor, R. Kivekäs, R. Sillanpää, M. Arca, V. Lippolis, E. Crespo, C. Viñas, *Dalton Trans.*, **2006**, 5240

[21] B.-H. Ye, X.-M. Chen, F. Xue, L.-N. Ji, T. C. W. Mak, *Inorganica Chimica Acta*, **2000**, 299, 1.

CHAPTER VIII. General results and discussion

TABLE OF CONTENTS

CHAPTER VIII. General results and discussions

VIII.1.	Cu(II) complexes	199
VIII.2.	Mn(II) complexes.....	206
VIII.3.	Fe (II) complexes.....	212
VIII.4.	Co(II) complexes	214

This chapter attempts to provide a link between the proposed general objectives (Chapter II) and the reported experimental results (Chapters III-VII), being an adequate way to enter in the final chapter of this thesis, the general conclusions.

Three main closely projects were defined as objectives of this thesis considering the nature of the transition metal to be reacted with the two carboranylcarboxylate ligands. Here on, the results obtained and previously presented as separate chapters will be discussed, in a more compact way, for each metal ion described.

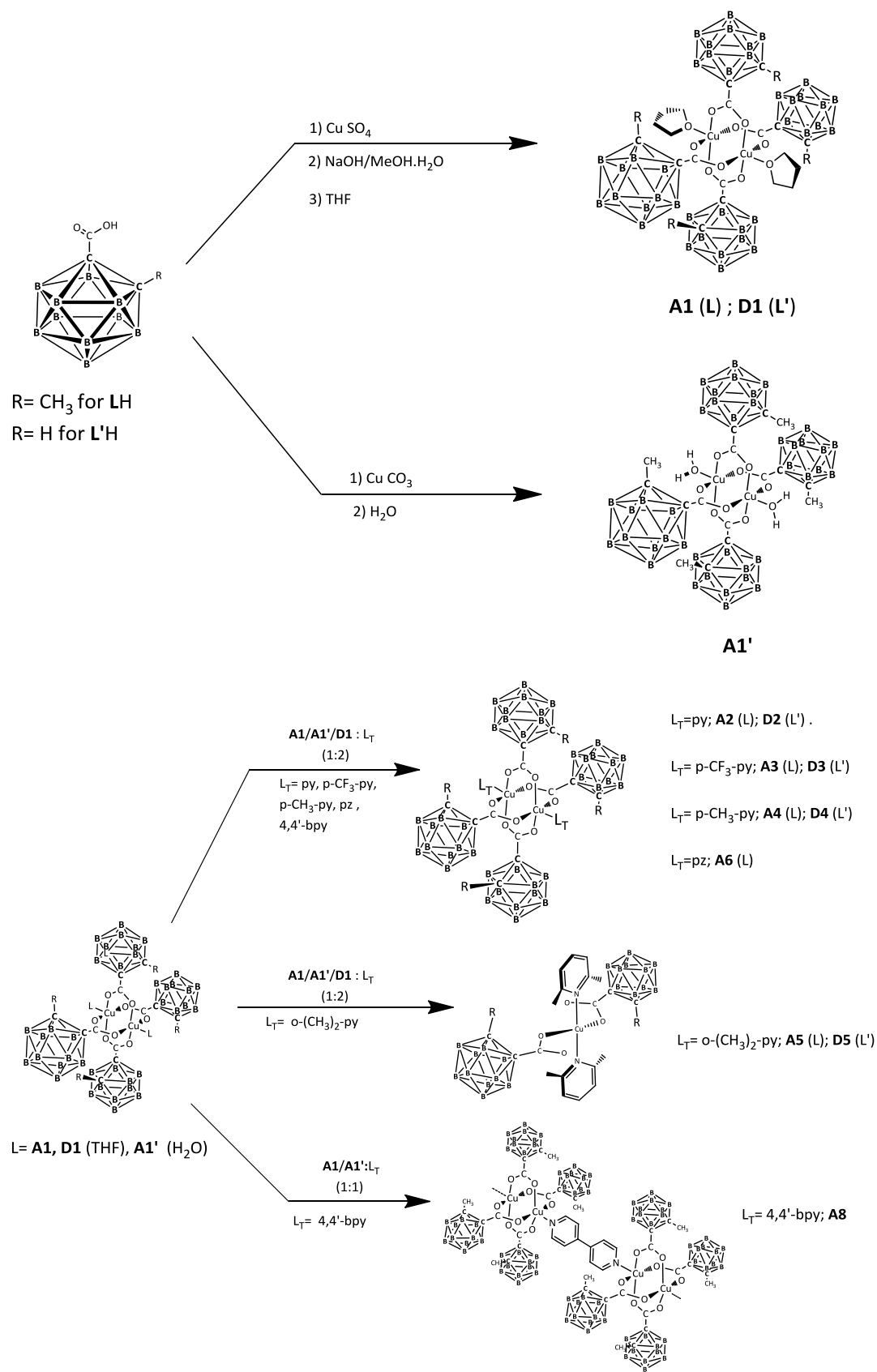
First of all, the carboranylcarboxylate ligands $[1\text{-CH}_3\text{-2-CO}_2\text{-1,2-closo-C}_2\text{B}_{10}\text{H}_{10}]^-$, **L**, or $[1\text{-CO}_2\text{-1,2-closo-C}_2\text{B}_{10}\text{H}_{11}]^-$, **L'**, were chosen due to the interesting properties presented by the 1,2-dicarba-closo-dodecaborane and its derivatives, which make them potentially applicable in the preparation of materials.^[1] Then, transition metals Cu^{II} , Mn^{II} , Co^{II} and Fe^{II} were selected based on their multiple applications in different fields such as molecular semiconductors, nanomagnets, ions exchange, chemical separation, sensor technology, energy conversion, optoelectronics or catalysis^[2], as well as for their potential use as frameworks for the assembling of complexes in two or three dimensions to generate supramolecular structures (MOFs).^[3] Moreover, it was known that only the coordination of the carboranylcarboxylate ligand $[1\text{-CO}_2\text{-1,2-closo-C}_2\text{B}_{10}\text{H}_{11}]^-$ to the transition metals Zn^{II} , Cu^{II} , Ni^{II} and Mo^{II} had been previously reported,^[4] making the study of carboranylcarboxylate ligands to generate polynuclear compounds and their potential applications a new and interesting topic of research.

VIII.1. Cu(II) complexes

As commented, few carboranylcarboxylate complexes containing copper (II) as metal have been previously synthesized; moreover, their coordination chemistry, together with their physical and chemical properties, have remained mostly unexplored. For this reason, a new family of mono- and polynuclear copper(II) complexes containing the carboranylcarboxylate ligands **L** and **L'** have been synthesised and fully characterized. Besides, the difference in reactivity due to the substitution of the methyl group in **LH** by a hydrogen atom on this carboranylcarboxylate ligand has been studied.

The first step was the synthesis of the starting compounds $[\text{Cu}_2(1\text{-CH}_3\text{-2-CO}_2\text{-1,2-closo-C}_2\text{B}_{10}\text{H}_{10})_4(\text{THF})_2]$, **A1**, $[\text{Cu}_2(1\text{-CH}_3\text{-2-CO}_2\text{-1,2-closo-C}_2\text{B}_{10}\text{H}_{10})_4(\text{H}_2\text{O})_2]$, **A1'**, and $[\text{Cu}_2(1\text{-CO}_2\text{-1,2-closo-C}_2\text{B}_{10}\text{H}_{11})_4(\text{THF})_2]$, **D1**, which were subsequently reacted with different pyridyl ligands, **L_t** (**L_t** = py, *p*-CF₃-py, *p*-CH₃-py, *o*-(CH₃)₂-py, pz, or 4,4'-bpy) obtaining, in most cases binuclear paddle-wheel cage type complexes of general formula $[\text{Cu}_2(\text{CB})_4(\text{L}_t)_2]$ as main products, where

CB= L, when **A1** or **A1'** is used as starting material or **L'** when **D1** is the starting compound (Scheme 1).



Scheme 1. Synthetic strategy for the preparation of Cu(II) complexes.

X-Ray diffraction of all complexes was performed, showing for the binuclear compounds a similar structure with the two copper (II) atoms held together through four syn,syn $\eta_1:\eta_1:\mu_2$ -carboxylate bridges acting as equatorial ligands for each Cu^{II} . The square pyramidal geometry around each metal ion is completed by the oxygen donor atom of a THF or a H_2O molecule in the starting compounds or by the nitrogen donor atom of the different pyridyl terminal ligands.

In the case of the binuclear compounds obtained upon addition of pyridine, **A2** and **D2**, and *p*-methylpyridine, **A4** and **D4**, we have observed the parallel formation of other compounds in lower yield, however, whilst mononuclear or tetranuclear compounds were obtained with ligand LH, binuclear compounds were obtained with ligand L'H. A representative example is shown in Figure 1. These differences in the reactivity have been attributed to the existence of dihydrogen bonds $\text{C}_c\text{-H}\cdots\text{H-B}$ between neighbouring carborane ligands in complexes containing the ligand L'H, which have not been observed in compounds with the ligand LH. These interactions might be responsible of the binuclear structures avoiding the formation of the mononuclear compounds as well as responsible of the ratio between the main and secondary products obtained.

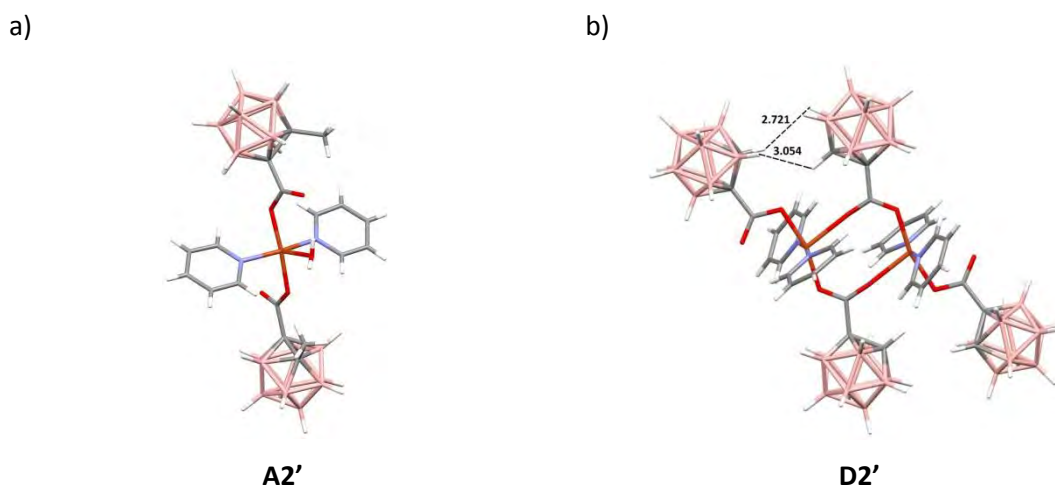


Figure 1. X-ray structures for a) **A2'**, b) **D2'** showing the $\text{C}_c\text{-H}\cdots\text{H-B}$ interactions.

It was seen that the IR spectra and the $^1\text{H}\{^{11}\text{B}\}$ -, ^{11}B -, $^{11}\text{B}\{^1\text{H}\}$ - and $^{13}\text{C}\{^1\text{H}\}$ -NMR spectra of all complexes agree with the solid structures confirmed by X-ray crystallography. Besides, it was observed for complex **D3** that the ^1H -NMR chemical shifts of the proton bonded to the boron atoms in the carboranylcarboxylate ligand changed to higher frequencies when decreases the temperature, which was attributed to the existence of intermolecular $\text{B-H}\cdots\text{H-B}$ interactions between several B-H vertexes. (Figure 2)

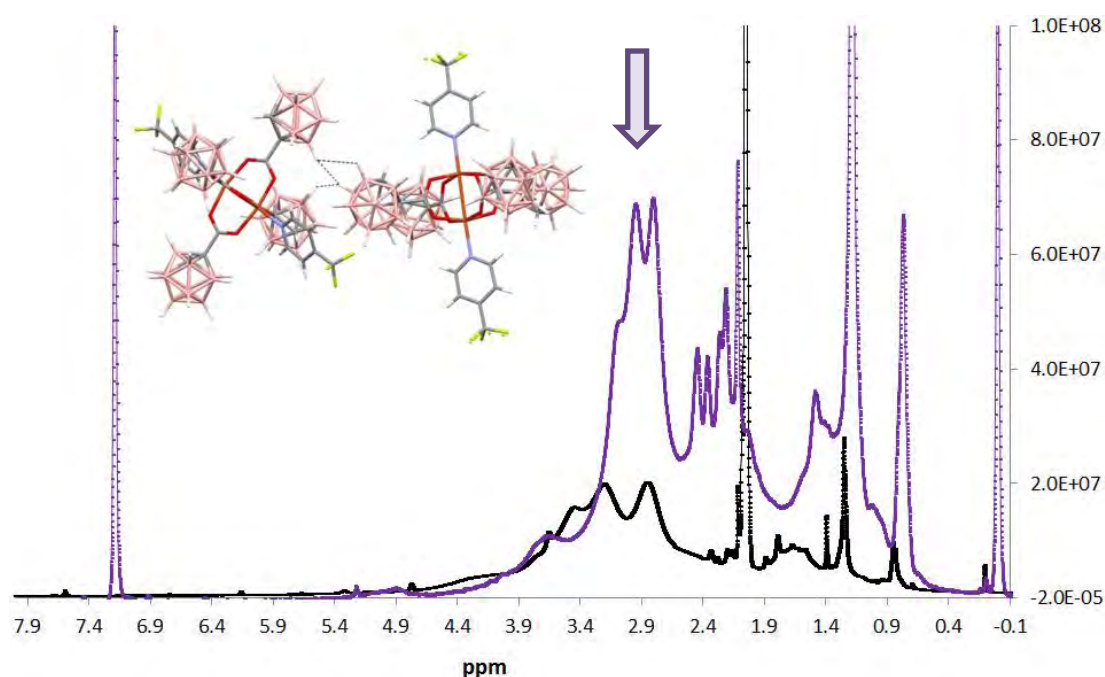


Figure 2. Structure of **D3** showing the B-H...H-B interactions and comparison of its $^1\text{H}\{^{11}\text{B}\}$ -RMN spectra in chloroform at 298K (purple) and in acetone at 260K (black).

Additionally, electrochemical properties of complex **A1**, the analogous μ -acetate complex $[\text{Cu}_2(\mu\text{-CH}_3\text{COO})_4(\text{THF})_2]$ and complexes **D1-D5**, were studied by cyclic voltammetry (CV) and, in the case of complexes **D1-D5**, containing the **L'H** ligand, differential pulse voltammetry (DPV) were also performed. CV of all complexes showed irreversible redox processes that can be assigned to $\text{Cu}^{\text{II}}/\text{Cu}^{\text{I}}$ and $\text{Cu}^{\text{I}}/\text{Cu}^0$ redox pairs, respectively. On the one hand, a comparison of complex **A1** with the analogous containing acetate ligands leads to observe that the latter is cathodically shifted with regard to complex **A1** in accordance with the higher electron-withdrawing character of the carboranylcarboxylate with respect to acetate ligand (Figure 3). On the other hand, for the complexes containing the ligand **L'H**, no noticeable shift in the potential values has been observed with the different electron-withdrawing character of the pyridyl ligands present in these compounds.

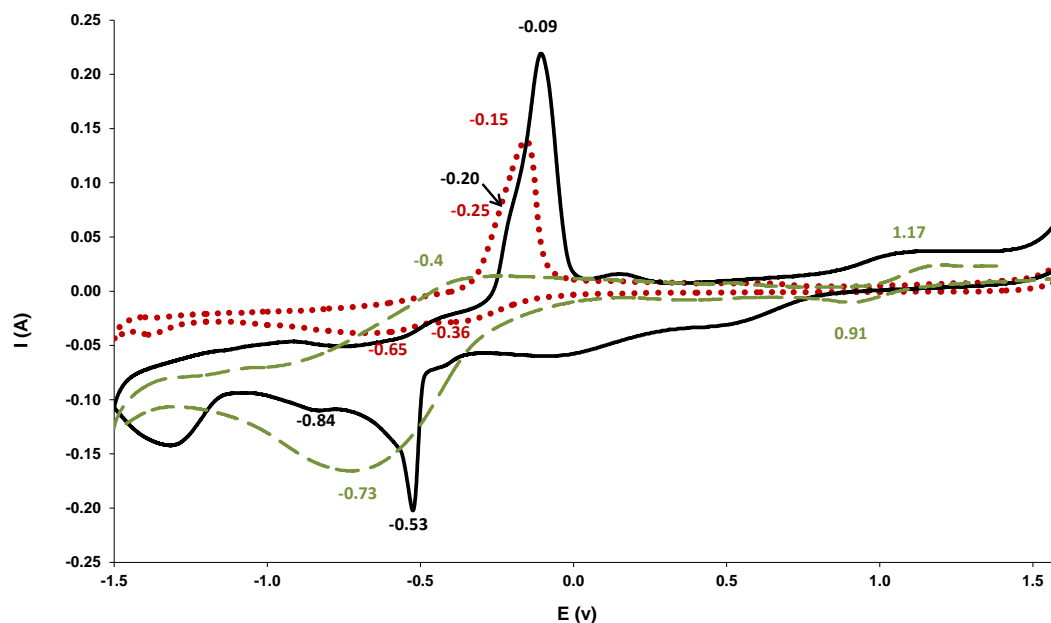


Figure 3. Cyclic voltammogram recorded for complexes $[\text{Cu}_2(\mu\text{-CH}_2\text{-COO})_2(\text{Tf})_2]$ (red), **A1** (black) and **LH** (green) in acetonitrile.

The electronic UV-vis spectra of complexes **A1-A6** and **D1-D5** were also performed, showing one characteristic band in the range 600-800 nm, assigned to d-d transitions from the d_{xz} , d_{yz} and d_{xy} orbitals in all complexes; a second band is also observed for the complexes containing the ligand **LH** around 380-420 nm assigned to LMCT bands from π orbitals of the carboxylate ligands to the empty $d_{x^2-y^2}$ orbitals of the Cu^{II} cations. (Figure 4)

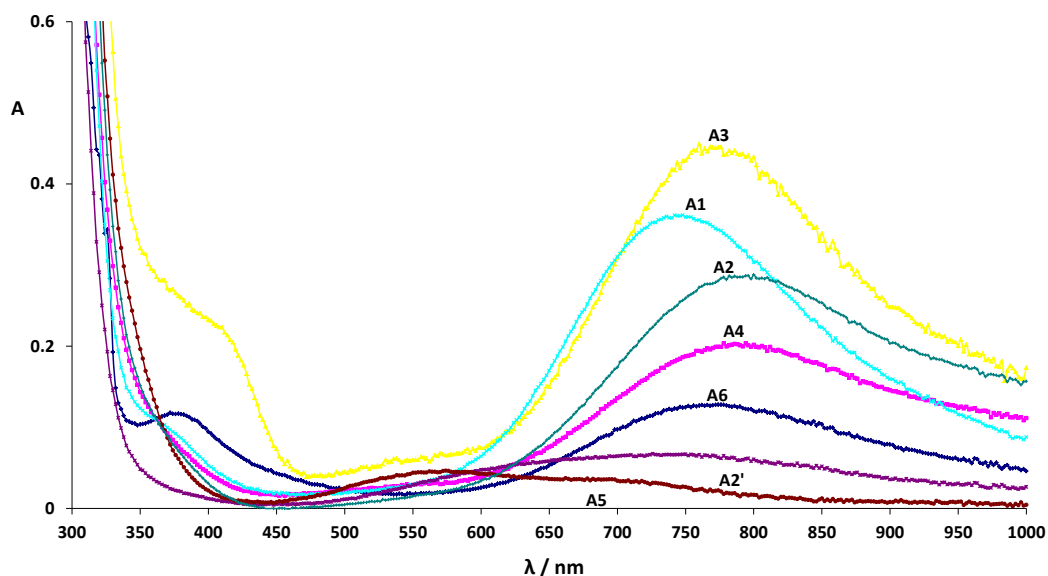


Figure 4. UV-vis spectral for complexes **A1-A6**.

In order to have a better understanding of these compounds, we have investigated the UV-visible spectra of **A1** upon the progressive addition of four equivalents of the terminal ligands

py, *p*-CH₃-py or *o*-(CH₃)₂-py. It has been seen that the initial UV-visible spectrum of **A1** is modified by the addition of two equivalents of pyridine exhibiting a band at higher wavelengths, probably indicating the presence of a binuclear compound together with a mononuclear one which was confirmed by comparison with the UV-visible spectra of both pure compounds **A2** and **A2'**. Also, the spectrum of **A1** was initially modified in an analogous way by the addition of two equivalents of *p*-CF₃-py (with the band also shifted to higher wavelength), but the spectrum is maintained after the successive addition of two more equivalents of ligand, indicating the stability of the Cu₂(μ-O₂CR)₄ core in the presence of this terminal ligand. The spectrum of the compound obtained "in situ" is coincident with that of complex **A3** isolated from the synthetic process. Finally, for 2,6-lutidine ligand, the addition of either two, three or four equivalents to complex **A1** leads to a shift of the maximum wavelength towards lower values thus revealing the direct formation of a monomer complex, with a spectrum fully coincident with that of the synthesized compound **A5**.

We then investigated whether the behaviour of 2,6-lutidine (which leads directly to the rupture of the binuclear moiety and the formation of the mononuclear complex) was governed by steric or electronic (basicity) factors. An equimolar mixture of 2,6-lutidine and *p*-CF₃-py was slowly added to a solution of **A1** and the subsequent spectral changes were followed by UV-vis. The shift of the maximum wavelength to lower values (as previously seen by addition of 2,6-lutidine itself) clearly demonstrated the immediate formation of the mononuclear complex **A5**. Thus, the competition between the two pyridyl L_t ligands evidences that the highly basic character of 2,6-lutidine is the key factor governing its reactivity since, otherwise, the coordination of the less encumbered *p*-CF₃-py would have occurred preferentially (Figure 5).

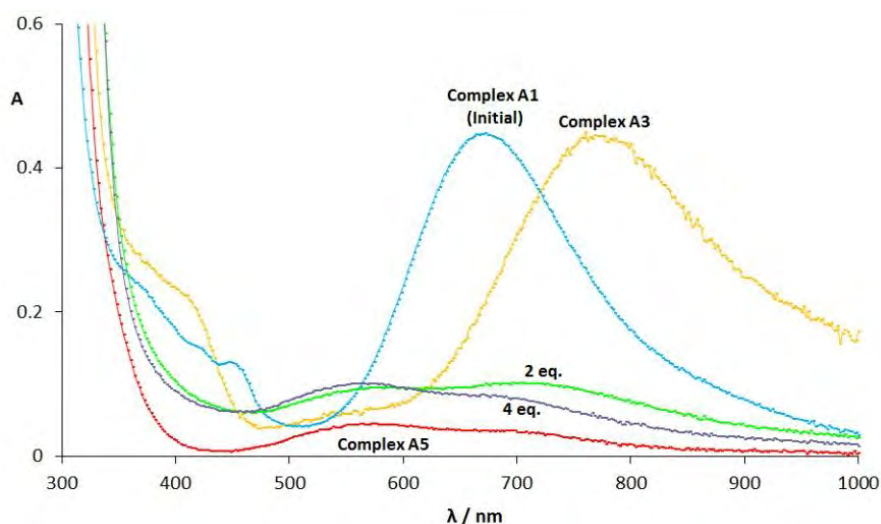
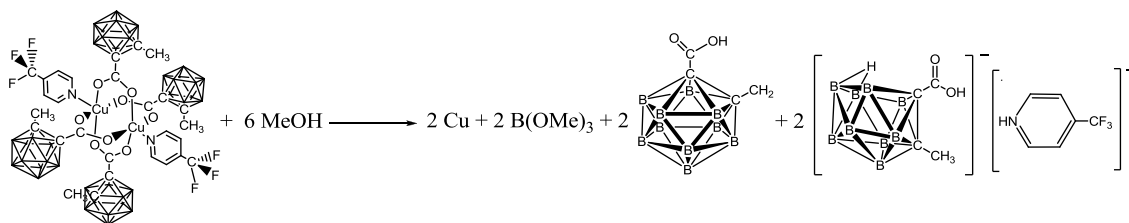


Figure 6. UV-vis monitoring of the addition of an equimolar mixture of 2,6-lutidine and *p*-CF₃-py to a solution of compound **A1** in dichloromethane.

This conclusion was also corroborated by electronic-structure calculations in which, the calculated Cu-N/O axial bond energies confirmed the stronger interaction of the pyridyl axial ligands with the copper metal centre in comparison with the THF ligand, thus leading in some cases to the decoordination of the carboranylcarboxylate ligand and the subsequent formation of secondary products with different nuclearities. A correlation between the calculated bond-energy value and the Hammett parameter of the substituents of the pyridine terminal ligands was also found being the bond energy higher for electron-donating groups, like methyl, than for electron-withdrawing substituents.

Besides, the stability of the binuclear compounds containing the ligand **LH** was studied in different solvents observing that these compounds were stable in THF and CH₂Cl₂ whereas a partial degradation of the 1-CH₃-2-CO₂H-1,2-*closo*-C₂B₁₀H₁₀ ligand, **LH**, took place in CH₃OH due to a nucleophilic attack, which lead to the removal of a BH²⁺ from the [1-CH₃-2-CO₂H-1,2-*closo*-C₂B₁₀H₁₀] ligand; this became oxidized to B(OCH₃)₃ reducing the Cu^{II} to Cu⁰ while the *closo* cluster was transformed to *nido* (Scheme 2). These results were confirmed by NMR and ESI-MS techniques observing clearly the signals corresponding to the *nido* species.



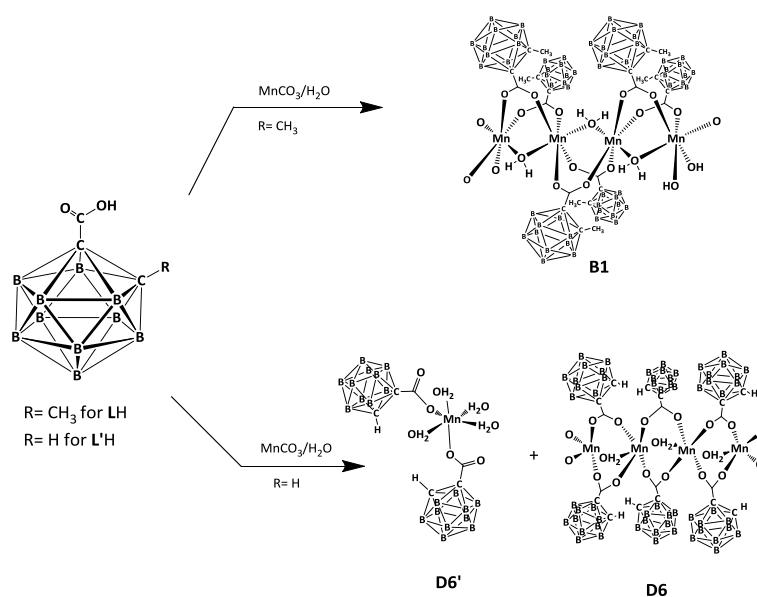
Scheme 2. Global reaction of the degradation of the ligand **L** from *closo* to *nido*

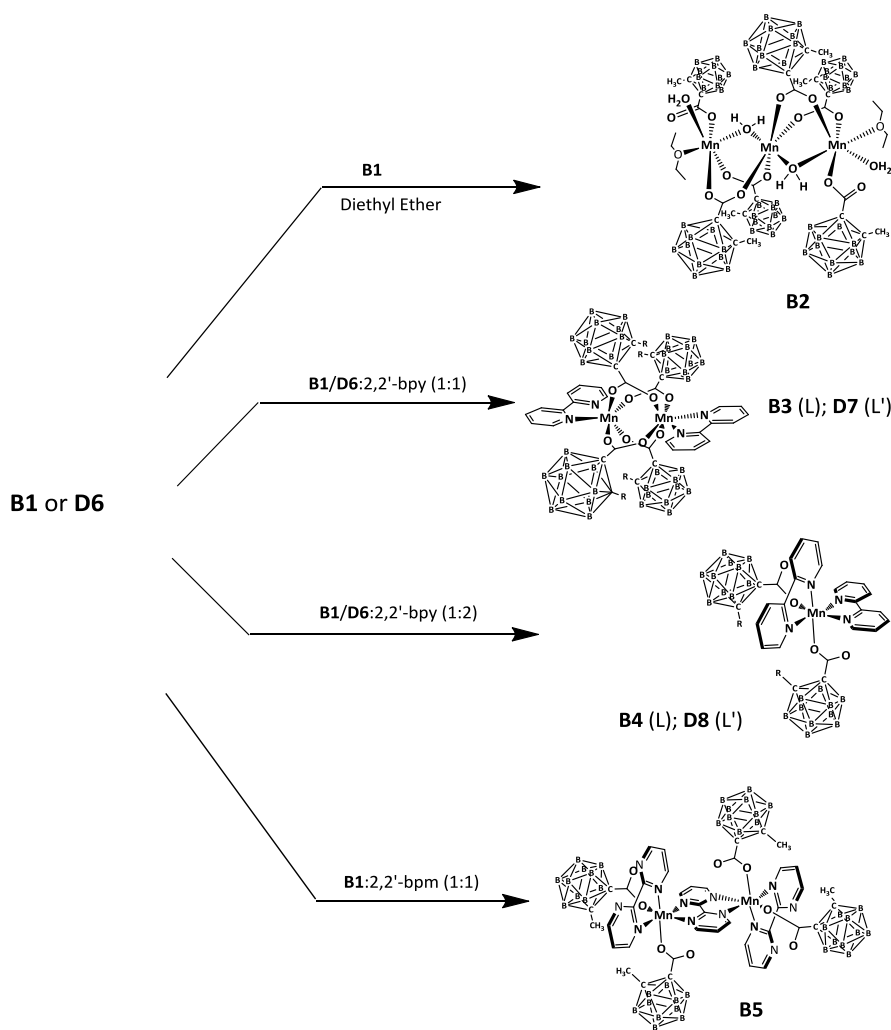
Finally, magnetic measurements of the binuclear complexes containing **LH** were performed showing, in all cases, strong antiferromagnetic interactions between the copper atoms whose coupling constant values, J , were in the range of those observed for binuclear paddle-wheel copper(II) cage structures containing acetates (above $280\text{-}300\text{ cm}^{-1}$). Exchange coupling constants were also calculated in the electronic structure calculations commented above, confirming the fitted values obtained from the experimental magnetic susceptibility.

VIII.2. Mn(II) complexes

Two new water soluble polymeric Mn(II) complexes were synthesized with the carboranylcarboxylate ligands **LH** and **L'H**. The polymeric compounds $[\text{Mn}(\mu\text{-H}_2\text{O})(\mu\text{-L})_2]_n \cdot (\text{H}_2\text{O})_n$, **B1** and $[\text{Mn}(\text{H}_2\text{O})(\mu\text{-L}')_2]_n \cdot 2\text{H}_2\text{O}$, **D6** were used as starting compounds to study their reactivity towards coordinating solvents and ligands such as 2,2'-bpy or 2,2'-bpm.

The polymeric structure of **B1** was broken in coordinating solvents such as diethyl ether leading to the first linear trinuclear Mn(II) compound $[\text{Mn}_3(\text{H}_2\text{O})_4(\text{L})_6(\text{C}_4\text{H}_{10}\text{O})_2]$, **B2**, with water bridging units and where the central manganese atom maintains the same coordination as in the polymer structure. The reactivity of polymers **B1** or **D6** with chelating ligands such as 2,2'-bpy was tested observing the formation of binuclear compounds with general formula $[\text{Mn}_2(\text{CB})_4(\text{bpy})_2]$ or mononuclear compounds $[\text{Mn}(\text{CB})_2(\text{bpy})_2]$, depending of the ligand:complex ratio used (CB= **L**, when **B1** is used as starting material or **L'** when **D6** is the starting compound). Finally, when complex **B1** reacted with the tetradentate ligand 2,2'-bpm, a novel 1D Mn(II) polymeric structure, $[\text{Mn}(\text{L})_2(\text{bpm})]_n$, **B5**, is obtained (Scheme 3).





Scheme 3. Synthetic strategy for the preparation of Mn(II) complexes.

Important differences were observed in the X-Ray structure of the polymeric compounds, **B1** and **D6** such as, the geometry around the Mn(II) ions (square pyramidal for **D6** and octahedral for **B1**) or the conformation of the bridged carboranylcarboxylate ligands **L** and **L'**, *syn-syn* in **B1** for the two carboxylate ligands and *syn-syn* and *syn-anti* in **D6** for every carboxylate ligands. Furthermore, in **B1** a coordinated bridged aqua ligand is observed whilst in **D6** the aqua ligand is acting as a terminal ligand. An important difference was observed in the packing diagram of both complexes; complex **B1** displayed polymeric chiral chains due to the methyl group of the carboranylcarboxylate ligand was shifted respect to the centre of the coordinated carboxylate group. This fact lead to two different conformations for these chains (λ and δ); however, in complex **D6**, the hydrogen substituents in the clusters have the same disposition in the different chains, fact that makes that the packing arrangement displayed polymeric chains with the same conformation preventing any chirality between them (see Figure 6). All these differences have been attributed to the existence of $C_c-H \cdots H-B$ dihydrogen bonds in **D6**

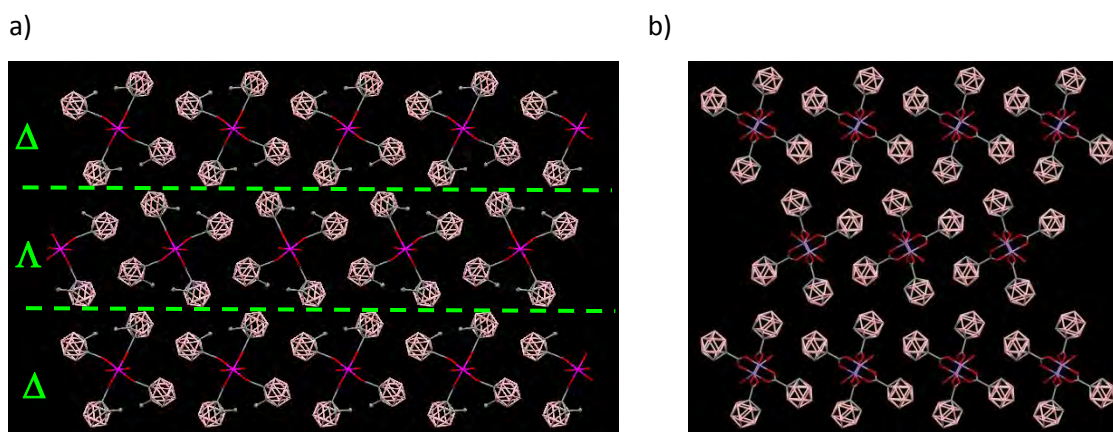


Figure 6. Packing arrangement of complexes a) **B1** and b) **D6** showing the structural differences between them.

The binuclear complexes **B3** and **D7** containing the ligand 2,2'-bpy display a similar structure with a trigonal prismatic geometry around each manganese(II) centre; however the mononuclear compounds **B3** and **D8** containing the same ligand, display a distorted octahedral structure, where two monodentate carboranylcarboxylate ligands are coordinated to the metal, both adopting a *cis* configuration around the metal (Figure 7).

IR spectra and $^1\text{H}\{^{11}\text{B}\}$ -, ^{11}B - and $^{11}\text{B}\{^1\text{H}\}$ -NMR spectra of these compounds were in complete agreement with the solid structures confirmed by X-ray crystallography, as well as ESI-MS spectra of the complexes.

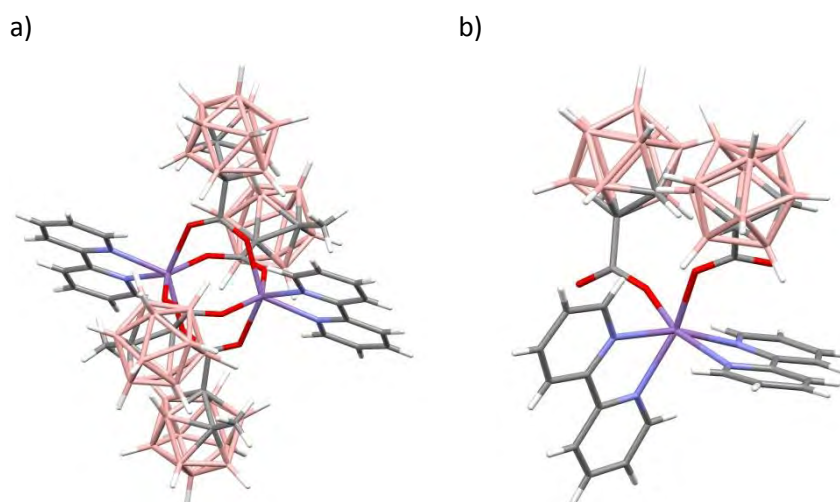


Figure 7. X-ray structure of complexes a) **B3** and b) **D8**.

Electrochemical properties of complexes containing the ligand LH were studied by cyclic voltammetry (CV) observing that all complexes exhibited waves corresponding to the oxidation of Mn(II) to Mn(III). For the polymer **B1**, it was also observed an increased background water oxidation above 1.4 V. In the case of the mononuclear compound **B4**, the CV exhibited two

anodic peaks that could be assigned to a metal oxidation process together with chemical reactions leading to the formation of binuclear species.

Additionally, the stability of the polymeric structure of **B1** in solution was studied by Cryo-TEM microscopy, Dynamic Light Scattering (DLS) and X-ray scattering (SAXS and WAXS) techniques. On the one hand, Cryo-TEM microscopy analysis of a water solution of complex **B1** showed a wide range of aggregates with motifs with different lengths (300-700 nm) which were an indicative that a polymer structure or aggregates existed in solution (Figure 8a). On the other hand, DLS studies of compound **B1** were carried out concluding that the infinite polymeric structure was preserved to a certain extent in water but this structure did not exist in diethyl ether solution because the polymer was cleaved into small particles each one less than few nanometres, which was in agreement with the trinuclear compound **B2** obtained experimentally. Moreover, it was observed that the self-assembly of the polymer in water strongly depends on concentration, noting that the dimensions of the nanoparticles increase with the concentration (Figure 8b). The probable explanation is as follows: the further addition of polymer leads to the elongation of wormlike structures observed by cryo-TEM by the merging of small domains with the larger supramolecular structure. This effect is pronounced at the highest concentrations resembling a transition of surfactant micelles to more complex morphologies like cylinders or lamellae.^[5] Finally, SAXS/WAXS experiments were not successful so that we did not prove the infinite structure in solution, nevertheless, it was concluded that the self-assembly in solution should be at least comparable to the situation in crystal.

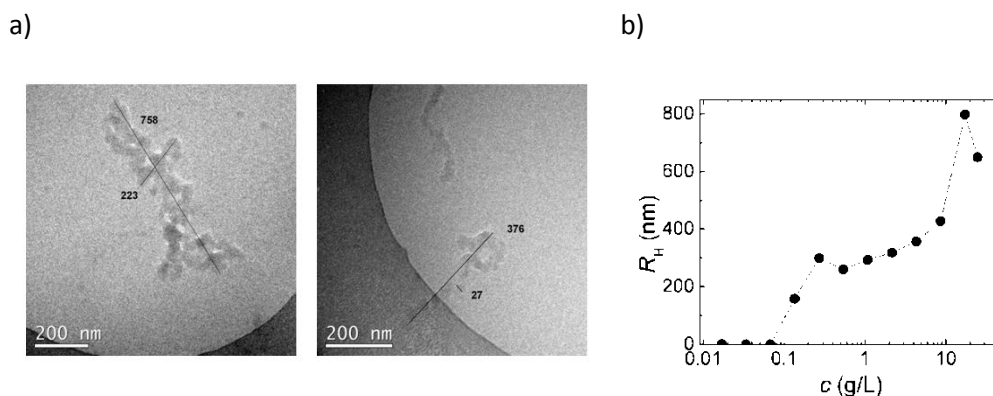


Figure 8. a) Cryo-TEM micrograph of a solution of **B1** in water; b) concentration dependence of hydrodynamic radius of nanoparticles in aqueous solutions of “polymer” measured at scattering angle 90deg

Magnetic measurements of compounds **B1**, **B3** and **B5** were performed, showing in all cases weak antiferromagnetic interactions between the manganese atoms; in **B1** the responsible of the weak antiferromagnetic interactions between the Mn(II) centres is the bridging water

molecule and the syn-syn arrangement of the two carboxylate ligands whereas for **B5** is the 2,2'-bpm bridging ligands .

The catalytic activity in oxidation reactions of compounds **B1**, **B3-B5** was tested regarding the epoxidation of alkenes using commercial peracetic acid (32%) as oxidant. In order to make comparisons with these complexes, $\text{Mn}_3(\text{OAc})_6(\text{bpy})_2$ was synthesized and characterized by X-ray diffraction and its catalytic behaviour was also assessed in the commented epoxidation reactions. Moreover, the catalytic activity of the ligand **LH** was tested with regard to the epoxidation of styrene concluding that the coordination of the carboranylcarboxylate ligand to the metal is necessary to observe catalytic activity under the conditions tested.

A quick glance to Table 1 suggests that when styrene was the substrate, for Mn compounds, conversions over 95% were found after 4 minutes of reaction together with moderate and high selectivity values. It could be observed that the polymeric manganese structures **B1** and **B5** presented better conversion and selectivity than mononuclear and binuclear complexes containing 2,2'-bpy as ligands, **B4** and **B3**, respectively.

When catalytic activity is studied with 4-vinyl-1-cyclohexene, it was noticed that the reaction was regiospecific for epoxidation of the ring double bond. Moreover, it was observed that complexes containing pyridyl ligands, **B3-B5**, and acetate, $\text{Mn}_3(\text{OAc})_6(\text{bpy})_2$, showed high conversion values but moderate selectivity. However, excellent selectivity was achieved by the polymeric complex **B1**, where only Mn(II), water and carboranylcarboxylate ligands were present.

For *cis*- β -methylstyrene, all complexes containing the carboranylcarboxylate ligand showed high conversion and selectivity values with high stereospecificity for the formation of the *cis*-epoxide. These values were larger than those obtained with the trinuclear complex $\text{Mn}_3(\text{OAc})_6(\text{bpy})_2$ for which the process was also less stereospecific. Based on these results it may be said that if a radical mechanism was involved in the epoxidation pathway, the radical intermediate species containing the carboranylcarboxylate ligand must be shorter-lived than those containing the acetate ligand in order to exert a significant influence on the stereoselectivity of the reaction.^[6] Thus, it could also be said that the carboranylcarboxylate ligand plays an important role in the stereospecificity of this reaction in larger extent than polypyridyl ligands since a lower percentage of *cis* epoxide was obtained when $\text{Mn}_3(\text{OAc})_6(\text{bpy})_2$ was used as catalyst, which only contains acetate and bipyridine groups.

In the case of *trans*- β -methylstyrene, all complexes displayed good performance and selectivity, presenting high values that in some cases are close to 100%. The catalytic activity was also tested with the aliphatic substrate 1-octene which usually tends to be the least reactive olefin in metal-catalysed epoxidation.^[7] In this case 1-octene was readily epoxidized

with our compounds providing good conversion values and moderate selectivities. The selectivity of **B1** is remarkable.

Finally, excellent conversion and good selectivity values were obtained for complexes **B1-B3** and **B5** using *trans*-stilbene as a substrate, however, **B4** displayed moderate selectivity and conversion.

Table 1. Epoxidation tests performed with manganese complexes **B1-B5** and $\text{Mn}_3(\text{OAc})_6(\text{bpy})_2$

Substrate	Product	B1		B3		B4		B5		$\text{Mn}_3(\text{OAc})_6(\text{bpy})_2$	
		Conv. (%)	Select. (%) ^a	Conv. (%)	Select. (%) ^a						
		96	61	100	44	100	44	100	76	99	58
		70	91 ^c	89	40 ^c	100	45 ^c	100	55 ^c	97	68 ^c
		90	75 <i>c/t</i> =79% ^b	99	80 <i>c/t</i> =88% ^b	98	82 <i>c/t</i> =87% ^b	100	66 <i>c/t</i> =94% ^b	75	75 <i>c/t</i> =67% ^b
		95	80	100	97	100	88	100	95	100	100
		61	72	95	41	98	54	83	46	83	56
		86	70	100	63	100	48	100	74	100	83

Conditions: catalyst (2.6 μmol), substrate (260 μmol), CH_2Cl_2 (2.5 mL). Peracetic acid 32% (520 μmol) added at 0 $^\circ\text{C}$, then reaction at RT.

^a Calculated as [epoxide yield/substrate conversion] x 100. ^b *c/t* represents the percentage of *cis* isomer obtained.

^c Epoxidation exclusively at the cyclohexene ring.

Additionally, a study of the stability of ligand **LH** in the peracetic acid medium was carried out through NMR and IR techniques, showing that the ligand **LH** remained unaffected after reaction with commercial 32%. Thus, it confirmed that the coordination of the carboranylcarboxylate ligand to the metal ion is relevant in the catalytic activity of these compounds.

Finally, catalytic activity of polymeric manganese(II) complex **B1** was tested regarding the oxidation of water to molecular oxygen, showing generation of oxygen (Figure 10). The stability of ligand **LH** was also tested by NMR under the same conditions as the water oxidation reaction concluding that the *closo* cluster is not degraded to *nido* and the generated O_2 is due to the compound **B1** containing the carboranylcarboxylate.

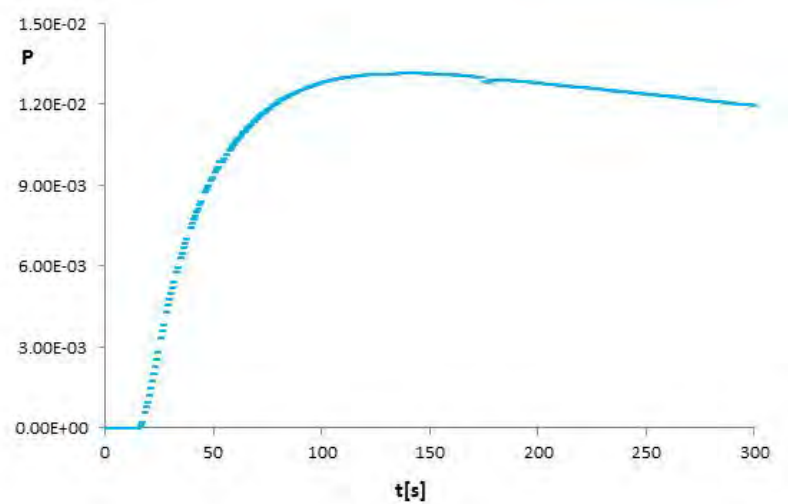
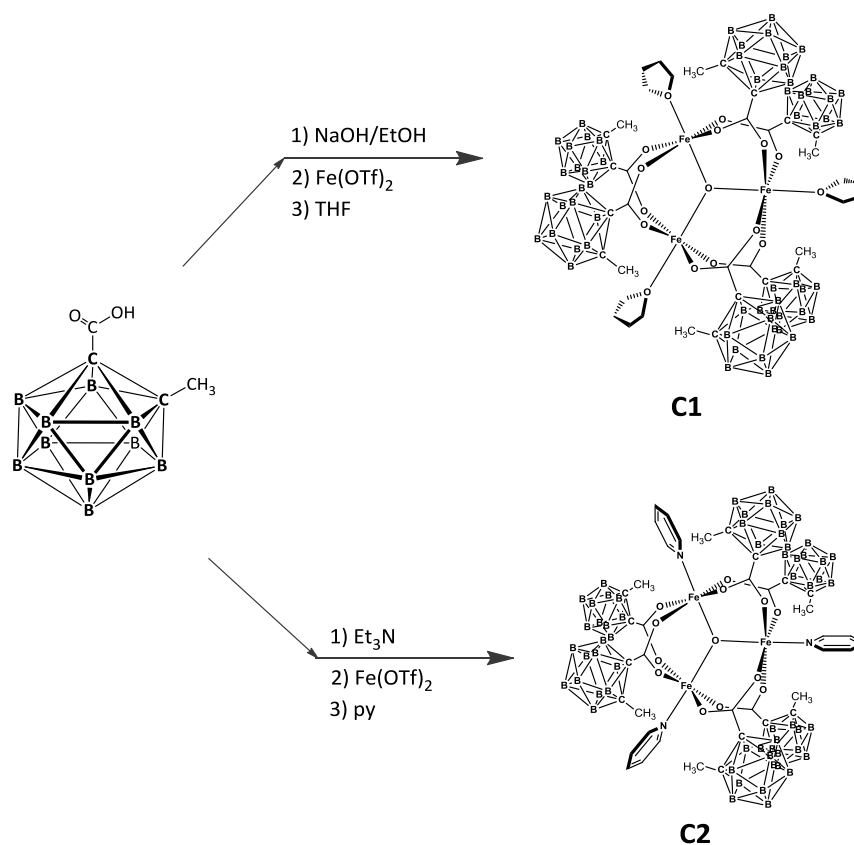


Figure 10. Kinetic plots of oxygen formation by **B1** versus time.

VIII.3. Fe (II) complexes

Two trinuclear mixed-valence iron(III,II) complexes containing the carboranylcarboxylate ligand [1-CH₃-2-CO₂-1,2-closo-C₂B₁₀H₁₁], LH, were synthesized and characterized by elemental analysis, spectroscopic and X-Ray diffraction techniques.

Two different synthetic strategies were carried out to synthesize the complexes, obtaining in both cases trinuclear mixed valence iron(III,II) complexes. The X-ray structure of these compounds revealed a planar trigonal Fe₃O core, with six syn,syn bridged carboxylate ligands and three THF ([Fe₃(μ-O)(L)₆(THF)₃], **C1**) or py ([Fe₃(μ-O)(L)₆(py)₃], **C2**) molecules completing the distorted octahedral sphere around each iron atom. Furthermore, it was seen that the three iron ions in complex **C1** were crystallographically indistinguishable, probably due to the dynamic disorder induced by a rapid internal electron transfer whereas in **C2** there are two iron (III) and one iron (II) which could be assigned according to the bond distances Fe-(μ-O) and Fe-O_{carbox} and to the angles(μ-O)-Fe-O_{carbox}. (Scheme 4)



Scheme 4. Synthetic strategy for the preparation of Fe(II) complexes.

It is notable the packing arrangement along *c* axis in **C1** which allowed the formation of a perfect hexagon with similar distances between the central oxygen atom of the different molecules. Moreover, carboranylcarboxylate ligands are located in the cavity of the hexagon leading to the existence of a hydrophobic environment in this one (Figure 10).

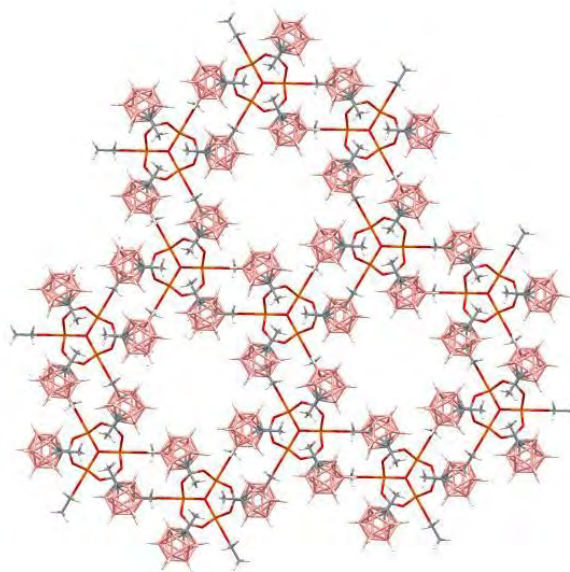


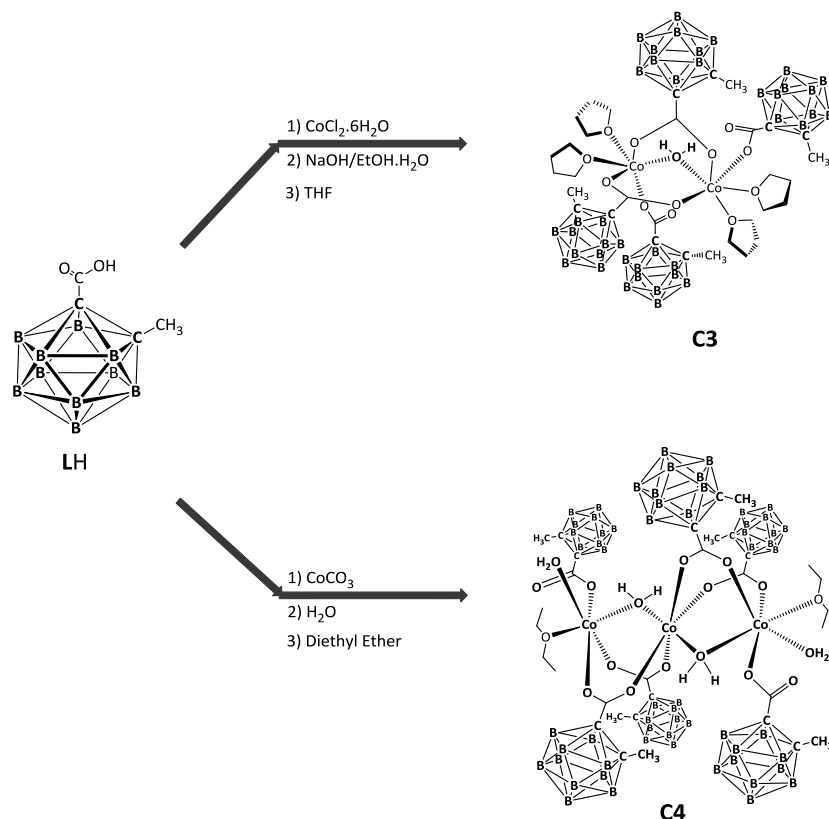
Figure 10. Packing diagram of complex **C1** showing the hexagons formed.

The IR and the $^1\text{H}\{^{11}\text{B}\}$ -, ^{11}B -, $^{11}\text{B}\{^1\text{H}\}$ - and $^{13}\text{C}\{^1\text{H}\}$ -NMR spectra of **C1** were performed and agree with the solid structure confirmed by X-ray crystallography. Moreover, UV-visible spectra of both compounds were performed and three characteristic bands were observed around 350 nm, in the range 479-490 nm and around 555 nm, which were tentatively assigned to LMCT^[8], MLCT^[9] and d-d transitions, ^[10] respectively.

VIII.4. Co(II) complexes

Two different polynuclear cobalt(II) complexes containing the carboranylcarboxylate ligand LH were synthesized and characterized by chemical analysis, spectroscopic and X-Ray diffraction techniques.

It was seen that depending on the cobalt(II) salt used as starting material, the solvent medium and the synthetic strategy utilized, the binuclear compound $[\text{Co}_2(\mu\text{-H}_2\text{O})(\text{L})_4(\text{THF})_4]$, **C3**, or the polymeric compound $[\text{Co}(\mu\text{-H}_2\text{O})(\text{L})_2]_n \cdot (\text{H}_2\text{O})_n$, **C5**, was obtained. It was also seen that polymeric structure of compound **C5** was broken in diethyl ether leading to the trinuclear compound $[\text{Co}_3(\mu\text{-H}_2\text{O})_2(\text{L})_6(\text{H}_2\text{O})_2(\text{C}_4\text{H}_{10}\text{O})_2]$, **C4**. (Scheme 5)



Scheme 5. Synthetic strategy for the preparation of Co(II) complexes.

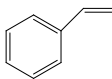
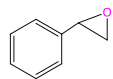
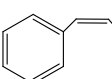
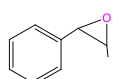
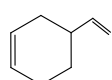
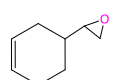
Concerning the X-Ray structures of complexes **C3** and **C4**, it was noticed that, although both compounds displayed different nuclearity, in both structures the cobalt atoms were held together through two carboranylcarboxylate and one aqua ligands. Besides, terminal cobalt

atoms in both complexes presented a monodentate carboranylcarboxylate ligand and two additional oxygen atoms from the solvent medium leading to an octahedral geometry around each cobalt atom. X-Ray structure of compound **C5** was not performed; however, their structure was confirmed by X-ray powder diffraction (XRD).

The IR spectra and the $^1\text{H}\{^{11}\text{B}\}$ -, ^{11}B -, $^{11}\text{B}\{^1\text{H}\}$ - and $^{13}\text{C}\{^1\text{H}\}$ -NMR spectra of these complexes were carried out and agreed with the solid structure confirmed by X-ray crystallography. Besides, UV-visible spectra of compounds **C3** and **C5** were performed and two characteristic bands, one in the range 300-400 nm and another in the range 420-570 nm were observed and assigned to LMCT transitions,^[11] and to the two spin-allowed d-d transitions, $^4\text{T}_1(\text{F})\rightarrow^4\text{A}_2(\text{F})$ and $^4\text{T}_1(\text{F})\rightarrow^4\text{T}_1(\text{P})$.,^[12] respectively.

Finally, catalytic activity of compound **C3** was tested in the epoxidation of alkenes using styrene, *cis*- β -methylstyrene and 4-vinyl-1-cyclohexene as substrates. In general, this complex presented moderate performance and selectivity for all the substrates tested after 4 minutes of reaction, with values that improve in some cases after 30 minutes (see Table 2 for further details).

Table 2. Epoxidation tests performed with cobalt complex **C3**

		C3	
Substrate	Product	Conv. (%)	Select. (%)^a
		21 ^c	56 ^c
		39 ^d	23 ^d
		16 ^c	46 ^c <i>c/t</i> =49% ^b
		42 ^d	45 ^d <i>c/t</i> =62% ^b
		41 ^c	55 ^c
		67 ^d	70 ^d

Conditions (see experimental section for further details): catalyst (2.6 μmol), substrate (260 μmol), CH_2Cl_2 (2.5 mL). Peracetic acid 32% (520 μmol) added at 0 $^\circ\text{C}$, then reaction at RT.

^aCalculated as [epoxide yield/substrate conversion] \times 100. ^b*c/t* represents the percentage of *cis* isomer obtained.

^c Aliquot taken after 4 minutes of reaction. ^d Aliquot taken after 30 minutes of reaction

If we compare the catalytic activity of this compound with manganese complexes it could be concluded that manganese(II) compounds present higher catalytic activity in the epoxidation of alkenes than the cobalt(II) compound **C3**, containing the same kind of ligands.

CHAPTER IX. General conclusions

In this thesis, new compounds containing carboranylcarboxylate ligands with relevant metal ions of the first transition series have been synthesized and characterized and their catalytic activity for different oxidation reactions, such as alkene epoxidation and water oxidation have been tested.

Even though conclusions obtained from this research have been included in each chapter, a summary of the main conclusions are listed below:

1. A series of new mononuclear and carboranylcarboxylate-bridged binuclear copper(II) complexes containing the 1-CH₃-2-CO₂H-1,2-*closo*-C₂B₁₀H₁₀ carborane ligand (LH) have been synthesized.
 - a. Reaction of different copper salts with LH at room temperature, leads to binuclear compounds of general formula [Cu₂(μ-L)₄(L_t)₂] (L_t=THF, **A1**; L_t=H₂O, **A1'**). The reaction of **A1** and **A1'** with different terminal pyridyl ligands gives rise to the formation of a series of structurally analogous complexes by substitution of the terminal ligand THF or H₂O (L_t= py, **A2**; p-CF₃-py, **A3**; p-CH₃-py, **A4** and pz, **A6**), which maintain the structural Cu₂(μ-O₂CR)₄ core in the majority of the cases except for *o*-(CH₃)₂-py, where a mononuclear compound (**A5**) is exclusively obtained and for 4,4'-bpy, where a polymeric compound (**A8**) is seen.
 - b. These compounds have been characterized by elemental analysis, spectroscopic (NMR, IR, UV/vis, ESI-MS) and magnetic techniques. X-Ray structural analysis revealed a *paddle-wheel* structure for the binuclear compounds, with a square pyramidal geometry around each copper ion and the carboranylcarboxylate ions bridging two copper atoms in a syn-syn mode. The mononuclear complex obtained with the *o*-(CH₃)₂-py ligand presents a square planar structure, where the carboranylcarboxylate ligand adopts a monodentate coordination mode. The polymeric compound displays a 1D chain in which each copper ion adopts a distorted octahedral geometry and the carboranylcarboxylate ligand is in a monodentate coordination mode.
 - c. Binuclear compounds are stable in THF and CH₂Cl₂ whereas a partial degradation of the ligand, L, takes place in CH₃OH due to a nucleophilic attack, which leads to the removal of a BH²⁺ from the L ligand that oxidizes to B(OCH₃)₃ reducing the Cu^{II} to Cu⁰ while the *closo* cluster is transformed to *nido*.
 - d. Reactivity of **A1** and **A1'** with py or *p*-CH₃-py leads to the parallel formation of mononuclear compounds together with the binuclear compounds **A2** and **A4**. It was experimentally demonstrated that the electronic effects govern the rupture of the

binuclear structure, a conclusion that has been corroborated by electronic-structure calculations. The calculated Cu-X axial bond energies confirm the stronger interaction of the pyridyl axial ligands with the copper metal centre in comparison with the THF ligand, thus leading in some cases to the de-coordination of the carboranylcarboxylate bridging ligand and the subsequent formation of secondary products with different nuclearities.

e. A correlation between the calculated bond-energy value and the Hammett parameter of the substituents of the pyridine terminal ligands has been also found. Thus, the bond energy is higher for electron-donating groups, like methyl, whereas for electron-withdrawing substituents the bond is weaker.

f. Complex **A1** exhibits irreversible electrochemical redox processes that can be assigned respectively to $\text{Cu}^{\text{II}}/\text{Cu}^{\text{I}}$ and $\text{Cu}^{\text{I}}/\text{Cu}^0$ redox pairs.

g. Reactivity of the analogous μ -acetate copper(II) complexes with regard to the replacement of the apical H_2O or THF ligands by pyridyl ligands follow similar trends to those observed with complexes **A1** and **A1'**, however, the presence of the carboranylcarboxylate groups induces particular electronic and structural properties that establish remarkable differences with the analogous μ -acetate compounds such as their behaviour in nucleophilic solvents or their solubility.

h. The electronic UV-vis spectra of complexes **A1-A6** show two characteristic bands assigned to d-d transitions from the d_{xz} , d_{yz} and d_{xy} orbitals and to LMCT bands from π orbitals of the carboxylate ligands to the empty $d_{x^2-y^2}$ orbitals of the Cu^{II} cations.

i. The magnetic properties of the binuclear compounds **A1**, **A3**, **A4**, and **A6** show a strong antiferromagnetic coupling in all cases (**A1**, $J = -261 \text{ cm}^{-1}$; **A3**, $J = -255 \text{ cm}^{-1}$; **A4**, $J = -241 \text{ cm}^{-1}$; **A6**, $J = -249 \text{ cm}^{-1}$). Computational studies based on hybrid density functional methods have been used to study the magnetic properties of the complexes and also to study their relative stability on the basis of the strength of the bond between each $\text{Cu}(\text{II})$ and the terminal ligand.

2. A new water soluble manganese polymer containing the ligand [1- CH_3 -2- CO_2 -1,2-*closo*- $\text{C}_2\text{B}_{10}\text{H}_{10}$], **L**, has been synthesized and fully characterized: $[\text{Mn}(\mu\text{-H}_2\text{O})(\mu\text{-L})_2]_n \cdot (\text{H}_2\text{O})_n$, **B1**.

a. Polymer **B1** displays an unusual feature in 1-D oligomer $\text{Mn}(\text{II})$ complexes with a nuclearity higher than 2 that is the existence of water molecules bridging each two Mn centres. Each of the $\text{Mn}(\text{II})$ centres possesses a distorted octahedral geometry and the ligands are disposed in a zig-zag fashion through the chain. The bulky nature of the

ligand prevents intermolecular interactions among these lineal arrays. Each Mn(II) atom is coordinated by four carboxylate oxygen atoms and two aqua oxygen atoms, and is bridged to other Mn atoms by two carboranylcarboxylate ligands and by an aqua ligand. Packing diagram revealed two different conformations within adjacent chains (λ and δ) due to the orientation of the methyl groups from the carboranylcarboxylate ligands, thus leading to polymeric chiral chains.

b. The polymeric structure of **B1** is broken in coordinating solvents such as diethyl ether giving rise to the first linear trinuclear Mn(II) compound $[\text{Mn}_3(\text{H}_2\text{O})_4(\text{L})_6(\text{C}_4\text{H}_{10}\text{O})_2]_n$, **B2**, which maintains the precise picture found in **B1** but the terminal Mn ions evidence their origin as a result of fragmenting the polymer.

c. The clean way of fragmentation of the polymer enables a reverse process, allowing the regeneration of the polymer structure. This easy assembling disassembling process is, most probably, what endows **B1** its notorious solubility properties, and its aggregation concentration dependent ability as shown by DLS studies.

d. The reactivity of the polymeric structure of **B1** towards chelating ligands as 2,2'-bpy or 2,2'-bpm leads to the binuclear complex $[\text{Mn}_2(\text{L})_4(\text{bpy})_2]_n$, **B3**, when ligand:complex ratio is 1:2 or to the mononuclear compound $[\text{Mn}(\text{L})_2(\text{bpy})_2]_n$, **B4** when the ratio is 1:1 with 2,2'-bpy. However, the reactivity towards the ligand 2,2'-bpm leads to the formation of a different Mn(II) polymeric structure, $[\text{Mn}(\text{L})_2(\text{bpm})]_n$, **B5**.

e. The X-Ray structure of complex **B3** displays a binuclear compound in which each manganese(II) atom is coordinated by four oxygen atoms from four bridging carboranylcarboxylate ligands and two nitrogen atoms of one 2,2'-bpy ligand displaying a trigonal prismatic geometry. In the mononuclear compound **B4**, the manganese ion is coordinated by four nitrogen atoms from two chelating 2,2'-bipyridine ligands and two oxygen atoms from two monodentate carboranylcarboxylate ligands, both adopting a *cis* configuration around the metal displaying a distorted octahedral structure. Compound **B5** consists of neutral zigzag chains of manganese (II) ions linked by 2,2'-bpm in which, each Mn(II) ion coordinates to two L ligands in a monodentate mode completing the distorted octahedral geometry of the metal centres.

f. Complexes **B1**, **B3** and **B4** exhibit electrochemical oxidation waves corresponding to the oxidation of Mn(II) to Mn(III). Moreover, polymer **B1** presents an increase background water oxidation above 1.4 V and mononuclear compound **B4** exhibits two

anodic peaks assigned to a metal oxidation process together with chemical reactions leading to the formation of binuclear species.

g. It has been corroborated by Cryo-TEM microscopy analysis that the polymeric structure of **B1** exists in solution. Moreover, DLS studies have demonstrated that the self-assembly of polymer in water strongly depends on concentration and the infinite polymeric structure of the sample does not exist in diethyl ether solution because the polymer is cleaved into small particles each less than few nanometres.

h. The magnetic properties of the binuclear compounds **B1**, **B3** and **B5** show a weak antiferromagnetic coupling in all cases (**B1**, $J = -0.91 \text{ cm}^{-1}$; **B3**, $J = -6.58 \text{ cm}^{-1}$ and **B5**, $J = -0.70 \text{ cm}^{-1}$).

i. Complexes **B1** and **B3-B5** have been tested in the epoxidation of representative terminal and internal double bonds of aliphatic and aromatic alkenes, showing good efficiency and selectivity. When *cis*- β -methylstyrene is used as substrate, these complexes showed specificity for the *cis* epoxide, and regiospecificity in the epoxidation of the ring double bond with 4-vinyl-1-cyclohexene. These complexes show good activity in the epoxidation of the aliphatic substrate 1-octene despite the tendency of the latter to be the least reactive olefin in metal-catalysed epoxidation.

j. Catalytic behaviour of the acetate compound $\text{Mn}_3(\text{OAc})_6(\text{bpy})_2$ has been also tested for comparison purposes concluding that the selectivity values for most of the substrates under study are higher for the complexes containing the carboranylcarboxylate ligand than for the trinuclear complex with the acetate.

k. Complex **B1** presents catalytic activity regarding the oxidation of water to molecular oxygen, where the ligand **LH** is stable under the catalytic conditions; it can be concluded that the generated O_2 is not due to the degradation of the *closo* to *nido* cluster.

3. Two new trinuclear mixed-valence iron (II, III) complexes containing the carboranylcarboxylate ligand [1- CH_3 -2- CO_2 -1,2-*closo*- $\text{C}_2\text{B}_{10}\text{H}_{11}$], **LH**, $[\text{Fe}_3(\mu\text{-O})(1\text{-CH}_3\text{-2-CO}_2\text{-1,2-closo-C}_2\text{B}_{10}\text{H}_{10})_6(\text{THF})_3]$, **C1**, and $[\text{Fe}_3(\mu\text{-O})(1\text{-CH}_3\text{-2-CO}_2\text{-1,2-closo-C}_2\text{B}_{10}\text{H}_{10})_6(\text{py})_3]$, **C2**, have been synthesized and characterized by elemental analysis, spectroscopic and X-Ray techniques.

a. Both complexes have been characterized by X-ray diffraction and their structures consist of a planar trigonal Fe_3O core, with six syn,syn bridged carboxylate ligands and three THF, **C1**, or py, **C2**, molecules completing the distorted octahedral sphere around each iron atom. Besides, it has been concluded that the three iron ions in complex **C1**

are crystallographically indistinguishable whereas in **C2** there are two iron (III) and one iron (II).

b. The electronic UV-visible spectra of both complexes exhibit three characteristic bands, one around 350 nm, one in the range 479-490 nm and one around 555 nm, assigned to LMCT, MLCT and d-d transitions, respectively.

4. Two new polynuclear cobalt(II) complexes containing the carboranylcarboxylate ligand **LH**, $[\text{Co}_2(\mu\text{-H}_2\text{O})(1\text{-CH}_3\text{-2-CO}_2\text{-1,2-closo-C}_2\text{B}_{10}\text{H}_{10})_4(\text{THF})_4]$, **C3**, and $[\text{Co}(\mu\text{-H}_2\text{O})(1\text{-CH}_3\text{-2-CO}_2\text{-1,2-closo-C}_2\text{B}_{10}\text{H}_{10})_2]_n\text{-(H}_2\text{O)}_n$, **C5**, have been synthesized and characterized by chemical analysis, spectroscopic and X-Ray diffraction techniques.

a. The polymeric structure of compound **C5** was broken in diethyl ether leading to the trinuclear compound $[\text{Co}_3(\mu\text{-H}_2\text{O})_2(1\text{-CH}_3\text{-2-CO}_2\text{-1,2-closo-C}_2\text{B}_{10}\text{H}_{10})_6(\text{H}_2\text{O})_2(\text{C}_4\text{H}_{10}\text{O})_2]$, **C4**.

b. The X-ray structure of compounds **C3** and **C4** reveal that, although both complexes display different nuclearity, in both structures, cobalt atoms are held together through two carboranylcarboxylate and one aqua ligand and the terminal cobalt atoms present a monodentate carboranylcarboxylate ligand and two additional oxygen atoms from the solvent medium leading to an octahedral geometry around each cobalt atom.

c. The electronic UV-visible spectra of complexes **C3** and **C5** exhibit two characteristic bands, one in the range 300-400 nm and the other in the range 420-570 nm assigned to LMCT transitions and to the two spin-allowed d-d transitions, ${}^4\text{T}_1(\text{F}) \rightarrow {}^4\text{A}_2(\text{F})$ and ${}^4\text{T}_1(\text{F}) \rightarrow {}^4\text{T}_1(\text{P})$, respectively.

d. Compound **C3** has been tested in the epoxidation of styrene, *cis*- β -methylstyrene and 4-vinyl-1-cyclohexene observing that in general this complex presented moderate performance and selectivity for all the substrates tested after 4 minutes of reaction, with values that improve in some cases after 30 minutes.

e. A comparison of the catalytic activity of cobalt and manganese complexes permits to conclude that: compounds containing manganese(II) are more efficient than those containing cobalt(II), however, in both cases the coordination of the carboranylcarboxylate ligand to the metal ion is central for the catalytic activity of our compounds.

5. A series of new mononuclear and carboranylcarboxylate-bridged binuclear copper(II) complexes containing the 1-CO₂H-1,2-closo-C₂B₁₀H₁₀Carborane ligand (**L'H**) have been synthesized.

- a. Reaction of CuSO_4 salt with $\text{L}'\text{H}$ at room temperature, leads to binuclear compound of general formula $[\text{Cu}_2(\mu\text{-L})_4(\text{THF})_2]$, **D1**. The reaction of **D1** with different terminal pyridyl ligands gives rise to the formation of a series of structurally analogous complexes by substitution of the terminal ligand THF by L_t ($\text{L}_t = \text{py}$, **D2**; $p\text{-CF}_3\text{-py}$, **D3**; $p\text{-CH}_3\text{-py}$ and **D4**), which maintain the structural $\text{Cu}_2(\mu\text{-O}_2\text{CR})_4$ core except for the ligand $o\text{-(CH}_3)_2\text{-py}$, where a mononuclear compound (**D5**) is obtained.
- b. These compounds have been characterized through elemental analysis and spectroscopic (RMN, IR, UV/vis) techniques. X-Ray structural analysis revealed a *paddle-wheel* structure for the binuclear compounds, with a square pyramidal geometry around each copper ion and the carboranylcarboxylate ions bridging two copper atoms in a *syn-syn* mode. The mononuclear complex obtained with the $o\text{-(CH}_3)_2\text{-py}$ ligand presents a square planar structure, where the carboranylcarboxylate ligand adopts a monodentate coordination mode.
- c. Reactivity of **D1** with py or $p\text{-CH}_3\text{-py}$ leads to the parallel formation of binuclear compounds of general formula $([\text{Cu}_2(\text{L}')_4(\text{L}_t)_4])$, where $\text{L}_t = \text{py}$ for **D2'** or $p\text{-CH}_3\text{-py}$ for **D4'**, together with compounds **D2** and **D4**. It has been concluded that the existence of dihydrogen bonds $\text{C}_c\text{-H}\cdots\text{H-B}$ between neighbouring carborane ligands in complexes containing the ligand L' are responsible for maintaining the binuclear structures, avoiding the formation of the mononuclear compounds obtained for complexes containing the ligand L . These interactions are responsible for the nuclearity of the secondary products obtained.
- d. It has been observed by $^1\text{H-NMR}$ that the chemical shifts of the proton bonded to the boron atoms in the carboranylcarboxylate ligand for complex **D3** change to higher frequencies when decreasing the temperature, which has been attributed to the existence of intermolecular $\text{B-H}\cdots\text{H-B}$ interactions between several B-H vertexes.
- e. The electronic UV-vis spectra of complexes **D1-D5** show one characteristic band in the range 600-800 nm, assigned to d-d transitions from the d_{xz} , d_{yz} and d_{xy} orbitals.
- f. Complexes **D1-D5** show irreversible electrochemical redox processes that can be assigned respectively to $\text{Cu}^{\text{II}}/\text{Cu}^{\text{I}}$ and $\text{Cu}^{\text{I}}/\text{Cu}^0$ redox pairs. No noticeable shifts in the potential values of compounds **D2-D5** have been observed due to the different electron-withdrawing character of the pyridyl ligands.
6. A new water soluble manganese polymer containing the ligand L' has been synthesized and fully characterized, $[\text{Mn}(\text{H}_2\text{O})(\mu\text{-L}')_2]_n \cdot 2\text{H}_2\text{O}$, **D6**.

- a. X-Ray structure of compound **D6** discloses an unusual 1D manganese(II) polymer in which each of the Mn(II) ions is coordinated by four carboxylate oxygen atoms from two bridging carboranylcarboxylate units, one in a *syn-syn* and another in a *syn-anti* conformation, and one oxygen atom from a terminal aqua ligand displaying a square pyramidal geometry. This conformation has been attributed to the existence of dihydrogen bonds $C_c-H \cdots H-B$ between the carboranylcarboxylate ligands.
- b. The reactivity of the polymeric structure of **D6** towards chelating ligands as 2,2'-bpy leads to the binuclear complex $[Mn_2(L')_4(bpy)_2]$, **D7**, when ligand:complex ratio is 1:2 or to the mononuclear compound $[Mn(L')_2(bpy)_2]$, **D8** when the ratio is 1:1. These complexes display similar X-Ray diffraction structures than analogous ones containing the ligand **L**, **B3** and **B4**; however, their packing diagrams were quite different due to the different arrangement of the substituents in the carboranylcarboxylate ligands.
7. In general, we can conclude that the observed differences in the reactivity of the ligands $[1-CH_3-2-CO_2H-1,2-closo-C_2B_{10}H_{10}]$, **LH**, and $[1-CO_2H-1,2-closo-C_2B_{10}H_{11}]$, **L'H**, with respect Mn(II) and Cu(II) ions are due to the presence of the different substituents on the carbon carboranylcarboxylate ligand, a hydrogen atom for **L'H** or a methyl group for **LH**.

CHAPTER X. References (Chapters I and VIII)

TABLE OF CONTENTS

CHAPTER X. References (Chapters I and VIII)

Chapter I. General Introduction.....	231
Chapter VIII. General results and discussion	238

Chapter I. General Introduction

- [1] a) A. E. Stock, *Hydrides of Boron and Silicon*, Cornell Univ. Press, Ithaca, New York, **1933**, 250; b) A. E. Stock, C. Massanez, *Chem. Ber.*, **1912**, 45, 3539.
- [2] a) H. I. Schlesinger, H. C. Brown, *J. Am. Chem. Soc.*, **1953**, 75, 186; b) H. I. Schlesinger, A. B. Bur, *Chem. Rev.*, **1942**, 31, 1.
- [3] C. S. Herrick, N. Kirk, T. L. Etherington, A. E. Schubert, *Ind. Eng. Chem.*, **1960**, 52, 105.
- [4] W. N. Lipscomb, *Boron Hydrides*, W.A. Benjamin Inc., New York, **1963**, 275.
- [5] http://www.nobelprize.org/nobel_prizes/chemistry/laureates/1976/press.html
- [6] a) M. S. Cohen, E. DeLaney, M. Fein, W. Mitchell, D. J. Mann, Bull. 14th Meeting Joint Army-Navy-Air force Solid Propellant Group, Vol. II, **1958**, May 5-7, p. 49; b) Reaction Motors Division, Report No. RMD 210-S3, Contract No. AF 33(616)-5639, (M. S. Cohen, S. Tannenbaum, W. Mitchell, High Performance Solid Rocket Propellants), October 31, **1959**
- [7] Rohm and Haas Company, Report No. P-59-14, Contract No. DA-01-021-ORD-5135, (R. S. Yost, Quarterly Progress Report on Propellant Research), November 12, **1959**
- [8] OMCC-HEF-111, (R. E. Williams, C. D. Good, Compounds of the Organoborane Series $B_nC_2H_{n+2}$ from Pentaborane(9) and Acetylene: *sym*- Triboradimethyne, $B_3C_2H_5$), February 18, **1958**
- [9] a) R. M. Adams, F. D. Poholsky, *Inorg. Chem.*, **1963**, 2, 640; b) R. Hoffmann, W. N. Lipscomb, *Inorg. Chem.*, **1963**, 2, 231; c) R. Hoffmann, W. N. Lipscomb, *J. Chem. Phys.*, **1962**, 36, 3489; d) I. Shapiro, R. E. Williams, C. D. Good, *J. Am. Chem. Soc.*, **1962**, 84, 3837.
- [10] a) R. N. Grimes, *Carboranes*, Academic Press, New York, **1970**, 54; b) R. E. Williams, *Adv Inorg Chem. Radiochem.*, **1976**, 18, 67; c) *Carboranes, Metallocarboranes and Heterocarboranes* Comprehensive Organometallic Chemistry, **1982**, 1; d) M. F. Hawthorne, *Advances in Boron Chemistry*, The Royal Society of Chemistry, Cornwall, U.K, **1997**.
- [11] a) R. N. Grimes, *Ann. N. Y. Acad. Sci.*, **1974**, 239, 180; b) R. W. Rudolph, *Acc. Chem. Res.*, **1976**, 9, 446; c) R. E. Williams, *Inorg. Chem.*, **1971**, 10, 210; d) K. Wade, *Adv. Inorg. Radiochem.*, **1976**, 18, 1; e) D. M. P. Mingos, *Nature, Phy. Sci.*, **1972**, 236, 99; f) R. W. Rudolph, W. R. Pretzer, *Inorg. Chem.*, **1972**, 11, 1974; g) K. Wade, *Chem. Commun.*, **1971**, 792.
- [12] a) R. N. Grimes, *Angew. Chem., Int. Ed.*, **1993**, 32, 1289; b) J. Plešek, *Chem Rev.*, **1992**, 92, 269; c) W. H. Eberhardt, J. Crawford, W. N. Lipscomb, *Chem. Phys.*, **1954**, 22, 989
- [13] a) F. Teixidor, G. Barberà, A. Vaca, R. Kivekäs, R. Sillanpää, J. Oliva, C. Viñas, *J. Am. Chem. Soc.*, **2005**, 127, 10158; b) R. B. King, *Chem. Rev.*, **2001**, 101, 1119.
- [14] a) H. Kimura, K. Okita, M. Ichitani, T. Sugimoto, S. Kuroki, I. Ando, *Chem. Mater.*, **2003**, 15, 355; b) M. K. Kolel-Veetil, T. M. Keller, *J. Polym. Sci. A*, **2006**, 44, 147; c) A. González-Campo, B. Boury, F. Teixidor, R. Núñez, *Chem. Mater.*, **2006**, 18, 4344; d) E. Hao, B. Fabre, F. R. Fronczek, M. G. H. Vicente, *Chem. Mater.*, **2007**, 19, 6195; e) O. K. Farha, A. M. Spokoyny, K. L. Mulfort, M. F. Hawthorne, C. A. Mirkin, J. T. J. Hupp, *J. Am. Chem. Soc.*, **2007**, 129, 12680.
- [15] a) D. Grafstein, J. Dvork, *Inorg. Chem.*, **1963**, 2, 1128; b) S. Dunn, G. M. Rosair, R. L. Thomas, A. S. Weller, A. J. Welch, *Angew. Chem. Int. Ed. Engl.*, **1997**, 36, 645; c) S. Dunn, A. S. Weller, *Chemical Communications*, **1998**, 0, 1065.
- [16] N. N. Greenwood, A. Earnshaw, *Chemistry of the elements*, Butterworth-Heinemann, Oxford,, **1997**,
- [17] a) F. Teixidor, a. S. O. S. O. C. Viñas Carboranes and Metallocarboranes, *Carboranes and Metallocarboranes, a Science of Synthesis. Organometallics*, ed. D. E. Kaufmann, D. S. Matteson, Stuttgart, **2005**, ; b) V. I. Bregadze, *Chem. Rev.*, **1992**, 92, 209.
- [18] a) H. Schroeder, T. L. Heying, J. L. Reiner, *Inorg. Chem.*, **1963**, 2, 1092; b) J. F. Sieckhaus, N. S. Semenuk, T. A. Knowles, H. Schroeder, *Inorg. Chem.*, **1969**, 8, 2452.
- [19] a) C. Viñas, G. Barberà, J. Oliva, F. Teixidor, A. J. Welch, G. M. Rosair, *Inorg. Chem.*, **2001**, 40, 26 ; b) C. Viñas, G. Barberà, F. Teixidor, *J. Organom. Chem.*, **2002**, 642, 16; c) G. Barberà, C. Viñas, F. Teixidor, G. M. Rosair, A. J. Welch, *J. Chem. Soc. Dalton Trans.*, **2002**, 3647.
- [20] R. A. Wiesboeck, M. F. Hawthorne, *J. Am. Chem. Soc.*, **1964**, 86, 1642.
- [21] J. Bucharan, E. M. J. Hamilton, D. Reed, A. J. Welch, *J. Chem. Soc. Dalton Trans.*, **1990**, 677.

- [22] C. Viñas, J. Pedradas, J. Bertran, F. Teixidor, R. Kivekäs, R. Sillanpää, *Inorg. Chem.*, **1997**, 36, 2482.
- [23] a) R. Nuñez, O. Tutusaus, F. Teixidor, M. E. Light, M. B. Hursthouse, H. R. Ogilvie, *Eur. J. Inorg. Chem.*, **2005**, 11, 5637; b) J. G. Planas, C. Viñas, F. Teixidor, M. E. Light, M. B. Hursthouse, H. R. Ogilvie, *Eur. J. Inorg. Chem.*, **2005**, 4193; c) J. G. Planas, C. Viñas, F. Teixidor, A. Comas-Vives, G. Ujaque, A. Lledós, M. E. Light, M. B. Hursthouse, *J. Am. Chem. Soc.*, **2005**, 127, 15976; d) M. F. Hawthorne, J. I. Zink, J. M. Skelton, M. J. Bayer, C. Liu, E. Livshits, R. Baer, D. Neuhauser, *Science*, **2004**, 303, 1849; e) F. Teixidor, J. Pedrajs, I. Rojo, C. Viñas, R. Kivekäs, R. Sillanpää, I. Sivaev, V. Bregadze, S. Sjöberg, *Organometallics*, **2003**, 22, 3414.
- [24] M. M. Fein, J. Boniski, N. Mayes, N. N. Schawartz, M. S. Cohen, *Inorg. Chem.*, **1963**, 2, 1111.
- [25] C. Viñas, G. Barberà, F. Teixidor, *J. Organomet. Chem.*, **2002**, 642, 16.
- [26] a) W.-C. Kwong, H.-S. Chan, Y. Tang, Z. Xie, *Organometallics*, **2004**, 23, 3098; b) G. F. Zi, H.-W. Li, Z. W. Xie, *Organometallics*, **2002**, 21, 5415; c) G. F. Zi, H.-W. Li, Z. W. Xie, *Organometallics*, **2002**, 21, 3464; d) G. F. Zi, H.-W. Li, Z. W. Xie, *Chem. Commun.*, **2001**, 1110; e) K. Chui, Q. Yang, T. C. W. Mak, W. H. Lam, Z. Lin, Z. Xie, *J. Am. Chem. Soc.*, **2000**, 122, 5758.
- [27] L. Deng, H.-S. Chan, Z. Xie, *Angew. Chem. Int. Ed.*, **2005**, 44, 2.
- [28] a) H. Kimura, K. Okita, M. Ichitani, T. Sugimoto, S. Kuroki, I. Ando, *Chem. Mater.*, **2003**, 15, 355; b) M. K. Kolel-Veetil, T. M. Keller, *J. Polym. Sci. A*, **2006**, 44, 147; c) A. González-Campo, B. Boury, F. Teixidor, R. Nuñez, *Chem. Mater.*, **2006**, 18, 4344; d) E. Hao, B. Fabre, F. R. Fronczek, M. G. H. Vicente, *Chem. Mater.*, **2007**, 19, 6195; e) A. M. Spokoyniy, O. K. Farha, K. L. Mulfort, J. T. Hupp, C. A. Mirkin, *Inorg. Chim. Acta*, **2010**, 364, 266.
- [29] a) F. Teixidor, R. Nuñez, C. Viñas, R. Sillanpää, R. Kivekäs, *Angew. Chem. Int. Ed.*, **2000**, 112, 4460; b) F. Teixidor, R. Nuñez, C. Viñas, R. Sillanpää, R. Kivekäs, *Angew. Chem. Int. Ed.*, **2000**, 39, 4290; c) R. Nuñez, P. Farrás, F. Teixidor, C. Viñas, R. Sillanpää, R. Kivekäs, *Angew. Chem.*, **2006**, 118, 1292; d) R. Nuñez, P. Farrás, F. Teixidor, C. Viñas, R. Sillanpää, R. Kivekäs, *Angew. Chem. Int. Ed.*, **2006**, 45, 1270; e) F. Teixidor, G. Barbera, A. Vaca, R. Kivekäs, R. Sillanpää, *J. Am. Chem. Soc.*, **2005**, 127, 10158.
- [30] a) M. F. Hawthorne, *Angew. Chem.*, **1993**, 105, 997; b) M. F. Hawthorne, *Angew. Chem. Int. Ed. Engl.*, **1993**, 32, 950; c) A. H. Soloway, W. Tjarks, B. A. Barnum, F.-G. Rong, R. F. Barth, I. M. Codogni, J. G. Wilson, *Chem. Rev.*, **1998**, 98, 1515; d) J. F. Valliant, K. J. Guenther, A. S. King, P. Morel, P. Schaffer, O. O. Sogbein, K. A. Stephenson, *Coord. Chem. Rev.*, **2002**, 232, 173; e) I. B. Sivaev, V. Bregadze, S. Sjöberg, *Research and Development in Neutron Capture Therapy*, (Eds.: W. Sauerwein, R. Moss, A. Wittig) Monduzzi Editore, Bologna, **2002**, 19-23; f) P. Cigler, M. Kozisek, P. Rezáčová, J. Brynda, Z. Otwinowski, J. Pokorná, J. Plešek, B. Grüner, L. Dolecková-Maresová, M. Mása, *Proc. Natl. Acad. Sci. USA*, **2005**, 102, 15394; g) R. Julius, O. Farha, J. Chiang, L. Perry, M. F. Hawthorne, *Proc. Natl. Acad. Sci. USA*, **2007**, 104, 4808.
- [31] K. Kokado, Y. Chujo, *Macromolecules*, **2009**, 42, 1418.
- [32] D. A. Brown, H. M. Colquhoun, J. A. Daniels, J. A. H. MacBride, I. R. Stephenson, K. Wade, *Journal of Materials Chemistry*, **1992**, 2, 793.
- [33] a) R. Hamasaki, M. Ito, M. Lamrani, M. Mitsuishi, T. Miyashita, Y. Yamamoto, *J. Mater. Chem.*, **2003**, 13, 21; b) J. Taylor, J. Caruso, A. Newlon, U. Englich, K. Ruhlandt-Senge, J. T. Spencer, *Inorganic Chemistry*, **2001**, 40, 3381; c) M. Lamrani, R. Hamasaki, M. Mitsuishi, T. Miyashita, Y. Yamamoto, *Chem. Comm.*, **2000**, 0, 1595.
- [34] Y. Qin, E. Bakker, *Anal. Chem.*, **2003**, 75, 6002.
- [35] N. Zine, J. Bausells, F. Teixidor, C. Viñas, C. Masalles, J. Smitier, A. Errachid, *Mater. Sci. Eng. C*, **2006**, 26, 399.
- [36] M. Ito, T. X. Wei, P.-L. Chen, H. Akiyama, M. Matsumoto, K. Tamada, Y. Yamamoto, *J. Mater. Chem.*, **2005**, 15, 478.
- [37] a) F. Teixidor, M. A. Flores, C. Viñas, R. Kivekäs, R. Sillanpää, *Angew. Chem., Int. Ed. Engl.*, **1996**, 35, 2251; b) A. Felekidis, M. Goblet-Stachow, J. F. Liegeois, B. Pirrotte, J. Delarge, A. Demonceau, M. Fontaine, A. F. Noels, I. T. Chizhevsky, *J. Organomet. Chem.*, **1997**, 537, 405; c) J. A. Belmont, J. Soto, R. E. King III, A. J. Donaldson, J. D. Hewes, M. F. Hawthorne, *J. Am. Chem. Soc.*, **1989**, 111, 7475.
- [38] a) M. F. Hawthorne, A. Maderna, *Chemical Reviews*, **1999**, 99, 3421; b) J. F. Valliant, K. J. Guenther, A. S. King, P. Moral, P. Schafer, O. O. Sogbein, K. A. Stephenson, *Coord. Chem. Rev.*, **2002**, 232, 173.
- [39] a) T. Li, J. Hamdi, M. F. Hawthorne, *Bioconjugate Chem.*, **2006**, 17, 15; b) E. Hao, M. G. H. Vicente, *Chem. Commun.*, **2005**, 1306.
- [40] R. R. Srivastava, D. K. Hamlin, D. S. Wilbur, *J. Org. Chem.*, **1996**, 61, 9041.
- [41] P. Cigler, M. Kozisek, P. Rezáčová, J. Brynda, Z. Otwinowski, J. Pokorná, J. Plešek, B. Grüner, L. Dolcková-Maresová, M. Mása, J. Sedláček, J. Bodem, H.-G. Kräusslich, V. Král, J. Konvalinka, *Proc. Nat. Acad. Sci.*, **2005**, 102, 15395.

- [42] a) C. Viñas, S. Gómez, J. Bertrán, J. Barron, F. Teixidor, J. F. Dozol, H. Rouquette, R. Kivekäs, R. Sillanpää, *J. Organomet. Chem.*, **1999**, 581, 188; b) C. Viñas, J. Bertrán, S. Gómez, F. Teixidor, J. F. Dozol, H. Rouquette, R. Kivekäs, R. Sillanpää, *J. Chem. Soc, Dalton Trans.*, **1998**, 17, 677; c) C. Viñas, J. Bertrán, S. Gómez, F. Teixidor, J. F. Dozol, H. Rouquette, *J. Chem. Soc, Chem. Commun.*, **1998**, 191; d) J. Rais, M. Kryš, S. Hermanek, *Czech. Patent N^o153 933. 1974; Chem. Abs*, **1975**, 82, 23370c
- [43] F. Teixidor, R. Nuñez, C. Viñas, *Contributions to Science*, **2000**, 1, 435.
- [44] a) F. Teixidor, M. A. Flores, C. Viñas, R. Sillanpää, R. Kivekäs, *Journal of the American Chemical Society*, **2000**, 122, 1963; b) F. Teixidor, M. A. Flores, C. Viñas, R. Kivekäs, R. Sillanpää, *Organometallics*, **1998**, 17, 2278.
- [45] M. F. Hawthorne, *Advances on Boron and the Boranes*, eds. J.F. Liebman, A. G., R.E. Williams, VCH Publishers, New York, **1988**, 10, p.225.
- [46] a) O. Tutusaus, S. Delfosse, A. Demonceau, A. F. Noels, R. Nuñez, C. Viñas, F. Teixidor, *Tetrahedron Lett.*, **2002**, 43, 983; b) A. Demonceau, F. Simal, A. F. Noels, R. Nuñez, C. Viñas, F. Teixidor, *Tetrahedron Lett.*, **1997**, 38, 7879.
- [47] O. Tutusaus, S. Delfosse, F. Simal, A. Demonceau, A. F. Noels, R. Nuñez, C. Viñas, F. Teixidor, *Inorg. Chem. Commun.*, **2002**, 5, 941.
- [48] a) F. Teixidor, C. Viñas, *Sci. Synth.*, **2005**, 6, 1235; b) V. I. Bregadze, *Chem. Rev.*, **1992**, 92, 209
- [49] a) R. B. King, *Chem. Rev.*, **2001**, 101, 1119; b) J. Llop, C. Masalles, C. Viñas, F. Teixidor, R. Sillanpää, R. Kivekäs, *Dalton Trans.*, **2003**, 556; c) H. Yao, M. Sabat, R. N. Grimes, F. F. de Biani, P. Zanello, *Angew. Chem.*, **2003**, 115, 1032; d) H. Yao, M. Sabat, R. N. Grimes, F. F. de Biani, P. Zanello, *Angew. Chem. Int. Ed.*, **2003**, 42, 1002; e) F. Teixidor, C. Viñas, A. Demonceau, R. Nuñez, *Pure Appl. Chem.*, **2003**, 75, 1305; f) A. I. Stoica, C. Viñas, F. Teixidor, *Chem. Commun.*, **2009**, 4988; g) L. Schwartz, L. Eriksson, R. Lomoth, F. Teixidor, C. Viñas, S. Ott, *Dalton Trans.*, **2008**, 2379; h) A. I. Stoica, C. Viñas, F. Teixidor, *Chem. Commun.*, **2008**, 6492
- [50] a) R. N. Grimes, *Angew. Chem.*, **1993**, 105, 1350; b) R. N. Grimes, *Angew. Chem. Int. Ed. Engl.*, **1993**, 32, 1289; c) M. A. Fox, A. K. Hughes, *Coord. Chem. Rev.*, **2004**, 248, 457; d) H. Jude, H. Disteldorf, S. Fischer, T. Wedge, A. M. Hawkrige, A. M. Arif, M. F. Hawthorne, D. C. Muddiman, P. J. Stang, *J. Am. Chem. Soc.*, **2005**, 127, 12131; e) A. V. Puga, F. Teixidor, R. Kivekäs, R. Sillanpää, C. Viñas, *Chem. Eur. J.*, **2009**, 15, 9764
- [51] a) P. A. Kollman, L. C. Allen, *Chem. Rev.*, **1972**, 72, 283; b) C. Ceccarelli, G. A. Jeffrey, R. Taylor, **1981**, 70, 255.
- [52] a) W. W. Cleland, M. M. Kreevoy, *Science* **1994**, 264, 1887; b) P. A. Frey, S. A. Whitt, J. B. Tobin, *Science* **1994**, 264, 1927.
- [53] a) A. M. Beatty, *Coord. Chem. Rev.*, **2003**, 246, 131; b) P. Hubberstey, U. Suksangpanya, *Struct. Bond.*, **2004**, 111, 33.
- [54] a) G. A. Jeffrey, *An Introduction to Hydrogen Bonding*, Oxford University press, Oxford, **1997**; b) T. Steiner, *Angew. Chem. Int. Ed.*, **2002**, 41, 48.
- [55] a) R. Sumathi, A. K. Chandra, *Chem. Phys. Lett.*, **1997**, 271, 287; b) S. J. Grabowski, *Chem. Phys. Lett.*, **2000**, 327, 203.
- [56] a) G. R. Desiraju, *Acc. Chem. Res.*, **1996**, 29, 441; b) J. Gu, T. Kar, S. Scheiner, *J. Am. Chem. Soc.*, **1999**, 121, 9411; c) J. Gu, T. Kar, S. Scheiner, *J. Mol. Struct. (THEOCHEM)* **2000**, 500, 441.
- [57] a) A. K. Chandra, M. T. Nguyen, *J. Chem. Res. Synop.*, **1997**, 216; b) F. H. Allen, V. J. Hoy, J. A. K. Howard, *J. Am. Chem. Soc.*, **1997**, 119, 3477.
- [58] a) S. J. Grabowski, *J. Chem. Res. Synop.*, **1996**, 534; b) P. Ahlberg, O. Davidsson, *J. Am. Chem. Soc.*, **1997**, 119, 1745.
- [59] a) Y. Feng, S. W. Zhao, L. Liu, J. T. Wang, X. S. Li, Q. X. Guo, *J. Phys. Org. Chem.*, **2004**, 17, 1099; b) L. M. Epstein, E. S. Shubina, *Coord. Chem. Rev.*, **2002**, 231, 165; c) R. Custelcean, J. E. Jackson, *Chem. Rev.*, **2001**, 101, 1963; d) C. F. Matta, J. Hernández-Trujillo, T.-H. Tang, R. F. W. Bader, *Chem. Eur. J.*, **2003**, 9, 1940.
- [60] I. Alkorta, I. Rozas, J. Elguero, *Chem. Soc. Rev.*, **1998**, 27, 163.
- [61] a) S. J. Grabowski, A. Pfitzner, M. Zabel, A. T. Dubis, M. Palusiak, *The Journal of Physical Chemistry B*, **2004**, 108, 1831; b) T. Kar, S. Scheiner, *J. Chem. Phys.*, **2003**, 119, 1473.
- [62] G. N. Patwari, T. Ebata, N. J. Mikami, *J. Chem. Phys.*, **2001**, 105, 8642.
- [63] L. M. Epstein, E. S. Shubina, *Inorg. Chem.*, **1998**, 37, 3013.
- [64] D. Braga, F. Grepioni, P. E. M. Lopes, *New J. Chem.*, **1999**, 219.

- [65] a) I. Alkorta, K. Zborowski, J. Elguero, M. Solimannejad, *J. Phys. Chem. A*, **2006**, 110, 10279; b) M. Solimannejad, S. Scheiner, *J. Phys. Chem. A* **2005**, 109, 11933; c) L. Sobczyk, S. J. Grabowski, T. M. Krygowski, *Chem. Rev.*, **2005**, 105, 3513.
- [66] a) C. P. Lau, S. M. Ng, G.-C. Jia, Z.-Y. Lin, *Coord. Chem. Rev.*, **2007**, 251, 2223; b) G.-J. Zhao, K.-L. Han, *J. Chem. Phys.*, **2007**, 127, 024306; c) T. Sagara, E. Ganz, *J. Phys. Chem. C* **2008**, 112, 3515; d) R. H. Crabtree, O. Eisenstein, G. Sini, E. Peris, *J. Org. Chem.*, **1998**, 567, 7; e) C. F. Matta, J. Hernández-Trujillo, T.-H. Tang, R. F. W. Bader, *Chemistry – A European Journal*, **2003**, 9, 1940.
- [67] S. Sabo-Etienne, B. Chaudret, *Chem. Rev.*, **1998**, 98, 2077.
- [68] a) J. A. Ayllon, S. Sabo-Etienne, B. Chaudret, S. Ulrich, H.-H. Limbach, *Inorg. Chim. Acta.*, **1997**, 259, 1; b) Y. Guari, J. A. Ayllon, S. Sabo-Etienne, B. Chaudret, B. Hessen, *Inorg. Chem.*, **1998**, 37, 640.
- [69] a) J. Giner Planas, F. Teixidor, C. Viñas, M. E. Light, M. B. Hursthouse, *Chemistry – A European Journal*, **2007**, 13, 2493; b) E. J. Juárez-Pérez, C. Viñas, F. Teixidor, R. Núñez, *Journal of Organometallic Chemistry*, **2009**, 694, 1764; c) J. G. Planas, C. Viñas, F. Teixidor, A. Comas-Vives, G. Ujaque, A. Lledós, M. E. Light, M. B. Hursthouse, *Journal of the American Chemical Society*, **2005**, 127, 15976.
- [70] M. A. Fox, A. K. Hughes, *Coordination Chemistry Reviews*, **2004**, 248, 457.
- [71] F. Di Salvo, B. Camargo, Y. Garcia, F. Teixidor, C. Vinas, J. G. Planas, M. E. Light, M. B. Hursthouse, *CrystEngComm*, **2011**, 13, 5788.
- [72] E. J. Juárez-Pérez, R. Núñez, C. Viñas, R. Sillanpää, F. Teixidor, *European Journal of Inorganic Chemistry*, **2010**, 2010, 2385.
- [73] a) J. Boonmak, S. Youngme, T. Chotkhun, C. Engkagul, N. Chaichit, J. A. Van Albada, J. Reedijk, *Inorg. Chem. Comm.*, **2008**, 11, 1231; b) C. N. Rao, S. Natarajan, R. Vaidyanathan, *Angew. Chem. Int. Ed.*, **2004**, 43, 1466; c) M. Kato, Y. Muto, *Coord. Chem. Rev.* **92**, **1988**, 45; d) M. Melník, *Coord. Chem. Rev.*, **1982**, 42, 259; e) P. S. Subramanian, P. C. Dave, V. P. Boricha, D. Srinivas, *Polyhedron*, **1998**, 17, 443.
- [74] a) J. Su, Y. Wang, S. Yang, G. Li, F. Liao, J. Lin, *Inorg. Chem.*, **2007**, 46, 8403; b) A. Caneschi, F. Ferraro, D. Gatteschi, M. Ch. Melandri, P. Rey, R. Sessoli, *Angew. Chem. Int. Ed. Engl.*, **1989**, 28, 1365; c) S. Mukhopadhyay, S. K. Mandal, S. Bhaduri, W. H. Armstrong, *Chem. Rev.*, **2004**, 104, 3981; d) M.-H. Zeng, M.-C. Wu, H. Liang, Y.-L. Zhou, X.-M. Chen, S. W. Ng, *Inorg. Chem.*, **2007**, 46, 7241; e) R. D. Cannon, A. J. P. White, *Prog. Inorg. Chem.*, **1988**, 36, 195; f) J. Du Bois, T. J. Mizoguchi, S. J. Lippard, *Coord. Chem. Rev.*, **2000**, 200; g) J. Catterick, M. B. Hursthouse, P. Thornton, A. J. Welch, *J. Chem. Soc., Dalton Trans.*, **1977**, 223; h) J. Hudák, R. Boča, L. Dlháň, J. Kožíšek, J. Moncol, *Polyhedron*, **2011**, 30, 1367.
- [75] a) S. S.-Y. Chui, S. M.-F. Lo, J. P. H. Charmant, A. G. Orpen, I. D. Williams, *Science* **1999**, 283, 1148; b) M. Eddaoudi, J. Kim, N. Rosi, D. Vodak, J. Wachter, M. O. Keeffe, O. M. Yaghi, *Science*, **2002**, 295, 469.
- [76] O. K. Farha, A. M. Spokoyny, K. L. Mulfort, M. F. Hawthorne, C. A. Mirkin, J. T. Hupp, *J. Am. Chem. Soc.*, **2007**, 129, 12680.
- [77] C. Janiak, J. K. Vieth, *New Journal of Chemistry*, **2010**, 34, 2366.
- [78] a) S. Chavan, D. Srinivas, P. Ratnasamy, *Journal of Catalysis*, **2000**, 192, 286; b) S. Youngme, A. Cheansirisomboon, C. Danvirutai, C. Pakawatchai, N. Chaichit, *Inorg. Chem. Comm.*, **2008**, 11, 57; c) J.-J. Wang, Z. Chang, A.-S. Zhang, T.-L. Hu, X.-H. Bu, *Inorganica Chimica Acta.*, **2010**, 363, 1377.
- [79] a) B. Chiari, O. Piovesana, T. Tarantelli, P. F. Zanazzi, *Inorg. Chem.*, **1988**, 27, 3246; b) S. K. Dey, B. Bag, K. M. A. Malik, M. S. El Fallah, J. Ribas, S. Mitra, *Inorg. Chem.*, **2003**, 42, 4029.
- [80] a) R. Baggio, M. T. Garland, J. Manzur, O. Peña, M. Perec, E. Spodine, A. Vega, *Inorg. Chim. Acta* **1999**, 286, 74; b) O. Kahn, *Molecular Magnetism VCH Publ. Inc.*, **1993**; c) M. V. Marinho, M. I. Yoshida, K. J. Guedes, K. K. Krambrock, A. J. Bortoluzzi, M. Hörner, F. C. Machado, W. M. Teles, *Inorg. Chem.*, **2004**, 43, 1539.
- [81] a) R. J. Doedens, *Prog. Inorg. Chem.*, **1976**, 21, 209; b) C. Mehrotra, R. C. Bohra, *Metal carboxylates*, Academic Press, New York, **1983**; c) Y.-H. Chung, H.-H. Wei, G.-H. Lee, Y. Wang, *Inorg. Chim. Acta*, **1999**, 293, 30; d) A. Doyle, J. Felcman, M. T. D. P. Gambardella, C. N. Verani, M. L. B. Tristao, *Polyhedron*, **2000**, 19, 2621; e) Y.-H. Wen, J. K. Cheng, J. Zhang, Z.-J. Li, Y. Kang, Y.-G. Yao, *Inorg. Chem. Commun.*, **2004**, 7, 1120.
- [82] G. A. Timco, S. Carretta, F. Troiani, F. Tuna, R. J. Pritchard, C. A. Muryn, E. J. L. Mblnnes, A. Ghirri, A. Candini, P. Santini, G. Amoretti, M. Affronte, E. P. Winpenny, *Nature Nanotechnology*, **2009**, 4, 173.
- [83] a) F. T. Greenaway, E. Riviere, J. J. Girerd, X. Labouze, G. Morgant, B. Viossat, J. C. Daran, M. Roch-Arveiller, N.-H. Dung, *J. Inorg. Biochem.*, **1999**, 76, 19; b) D. Kovala-Demertzi, A. Theodorou, M. A. Demertzis, C. P. Raptopoulou, A. Terzis, *J. Inorg. Biochem.*, **1997**, 65, 151; c) B. Kozlevcar, I. Leban, I. Turel, P. Segedin, M. Petric, F. Pohleven, A. J. P. White, D. J. Williams, J. Sieler, *Polyhedron*, **1999**, 18, 755; d) M. Vaidyanathan, R. Viswanathan, M.

- Palaniandavar, T. Balasubramanian, P. Prabhakaran, T. P. Muthiah, *Inorg. Chem.*, **1998**, 37, 6418; e) J. E. Weder, T. W. Hambley, B. J. Kennedy, P. A. Lay, D. MacLachlan, R. Bramley, C. D. Delfs, K. S. Murray, B. Moubaraki, B. Warwick, J. R. Biffin, H. L. Regtop, *Inorg. Chem.*, **1999**, 38, 1736.
- [84] a) C. Eicken, F. Zippel, K. Büldt-Karentzopoulos, B. Krebs, *FEBS Lett.*, **1998**, 436, 293; b) T. Klabunde, C. Eicken, J. C. Sachtini, B. Krebs, *Nature Struct. Biol.*, **1998**, 5, 1084; c) B. Meunier, *Biomimetic Oxidations Catalyzed by Transition Metal Complexes*, Imperial College Press, London, **2000**,
- [85] H. S. Mason, W. L. Fowls, E. Peterson, *J. Am. Chem. Soc.*, **1955**, 77, 2914.
- [86] a) K. A. Magnus, C. Ton-That, J. Bonaventura, W. G. J. Bonaventura, *Hol, Proteins Struct. Funct. Genet.*, **1994**, 19, 302; b) K. A. Magnus, C. Ton-That, J. E. Carpenter, *Chem. Rev.*, **1994**, 94, 727.
- [87] R. Raja, P. Ratnasamy, *J. Mol. Catal.*, **1995**, 100, 93.
- [88] a) O. Kahn, *Molecular Magnetism*, VCH, Weinheim, **1993**; b) J. S. Miller, *Inorg. Chem.*, **2000**, 39, 4392; c) O. Kahn, *Acc. Chem. Res.*, **2000**, 33, 647.
- [89] a) H.-Y. Lin, B. Mu, X.-L. Wang, A.-X. Tian, *Journal of Organometallic Chemistry*, **2012**, 702, 36; b) X.-L. Wang, W. Zhao, J.-W. Zhang, Q.-L. Lu, *Journal of Solid State Chemistry*, **2013**, 198, 162; c) S. K. Chawla, M. Arora, K. Nättinen, K. Rissanen, J. V. Yakhmi, *Polyhedron*, **2004**, 23, 3007; d) A. Das, G. Pilet, D. Luneau, M. S. El Fallah, J. Ribas, S. Mitra, *Inorganica Chimica Acta*, **2005**, 358, 4581.
- [90] A. L. Briseno, J. Aizenberg, Y.-J. Han, R. A. Penkala, H. Moon, A. J. Lovinger, C. Kloc, Z. Bao, *J. Am. Chem. Soc.*, **2005**, 127, 12164.
- [91] W. C. Stallings, K. A. Patridge, R. K. Strong, M. L. Ludwig, *Journal of Biological Chemistry*, **1985**, 260, 16424.
- [92] V. L. Pecorare, *Manganese Redox Enzymes*, VCH Publishers, New York **1992**,
- [93] H. Wariishi, L. Akileswaran, M. H. Gold, *Biochemistry*, **1988**, 27, 5365.
- [94] a) V. Yachandra, V. DeRose, M. Latimer, I. Mukerji, K. Sauer, M. Klein, *Science*, **1993**, 260, 675; b) C. W. Hoganson, G. T. Babcock, *Science*, **1997**, 277, 1953; c) J. Limburg, J. S. Vrettos, L. M. Liable-Sands, A. L. Rheingold, R. H. Crabtree, G. W. Brudvig, *Science*, **1999**, 283, 1524.
- [95] Y. Umena, K. Kawakami, J.-R. Shen, N. Kamiya, *Nature*, **2011**, 473, 55.
- [96] a) C. Zhang, C. Janiak, *Zeitschrift für anorganische und allgemeine Chemie*, **2001**, 627, 1972; b) S. G. Baca, Y. Sevryugina, R. Clérac, I. Malaestean, N. Gerbelean, M. A. Petrukhina, *Inorganic Chemistry Communications*, **2005**, 8, 474.
- [97] a) M. A. Kiskin, I. L. Eremenko, *Russ. Chem. Rev.*, **2006**, 75, 559; b) G. Christou, D. Gatteschi, D. N. Hendrickson, R. Sessoli, *MRS Bull.*, **2000**, 25, 66.
- [98] V. A. Ivanov, T. G. Aminov, V. M. Novotortsev, V. T. Kalinnikov, *Russ. Chem. Bull., Int. Ed.*, **2004**, 53, 2357.
- [99] a) C. Boskovic, E. K. Brechin, W. E. Streib, K. Folting, J. C. Bollinger, D. N. Hendrickson, G. Christou, *Journal of the American Chemical Society*, **2002**, 124, 3725; b) M. A. Kiskin, G. G. Aleksandrov, V. N. Ikorskii, V. M. Novotortsev, I. L. Eremenko, *Inorganic Chemistry Communications*, **2007**, 10, 997.
- [100] a) C. Lampropoulos, M. Murugesu, A. G. Harter, W. Wernsdorfer, S. Hill, N. S. Dalal, A. P. Reyes, P. L. Kuhns, K. A. Abboud, G. Christou, *Inorganic Chemistry*, **2013**, 52, 258; b) L. Thomas, F. Lionti, R. Ballou, D. Gatteschi, R. Sessoli, B. Barbara, *Nature*, **1996**, 383, 145; c) T. Kuroda-Sowa, M. Nakano, G. Christou, D. N. Hendrickson, *Polyhedron*, **2001**, 20, 1537.
- [101] a) E. Cremades, J. Cano, E. Ruiz, G. Rajaraman, C. J. Milios, E. K. Brechin, *Inorg. Chem.*, **2009**, 48, 8012; b) S. Naiya, S. Biswas, M. G. B. Drew, C. J. Gómez-García, A. Ghosh, *Inorg. Chem.*, **2012**, 51, 5332; c) C. C. Stoumpos, R. Inglis, O. Roubeau, H. Sartz, A. A. Kitos, C. J. Milios, G. Aromi, A. J. Tasiopoulos, V. Nastopoulos, E. K. Brechin, S. P. Perlepes, *Inorg. Chem.*, **2010**, 49, 4388; d) C. C. Stoumpos, R. Inglis, G. Karotsis, L. F. Jones, A. Collins, S. Parsons, C. J. Milios, G. S. Papaefstathiou, E. K. Brechin, *Cryst. Growth Des.*, **2009**, 9, 24.
- [102] a) G. Maayan, G. Christou, *Inorg. Chem.*, **2011**, 50, 7015; b) P. Mukherjee, P. Kar, S. Ianelli, A. Ghosh, *Inorg. Chim. Acta*, **2011**, 365, 318; c) P. Kar, R. Haldar, C. J. Gómez-García, A. Ghosh, *Inorg. Chem.*, **2012**, 51, 4265.
- [103] a) A. K. Poulsen, A. Rempel, C. J. McKenzie, *Angew. Chem. Int. Ed.*, **2005**, 44, 6916; b) N. S. Venkataramanan, G. Kuppuraj, S. Rajagopal, *Coordination Chemistry Reviews*, **2005**, 249, 1249; c) A. Murphy, G. Dubois, T. D. P. Stack, *J. Am. Chem. Soc.*, **2003**, 125, 5250; d) B. Kang, M. Kim, J. Lee, Y. Do, S. Chang, *The Journal of Organic Chemistry*, **2006**, 71, 6721.
- [104] a) H. G. Seiler, A. Sigel, H. Sigel, *Handbook on Metals in Clinical and Analytical Chemistry*, Marcel Dekker, New York **1994**; b) J. B. Vincent, G. L. Olivier-Lilley, B. A. Averill, *Chemical Reviews*, **1990**, 90, 1447; c) R. R. Crichton, *Inorganic Biochemistry of Iron Metabolism*, Hardvar, New York, **1991**,

- [105] a) R. H. Holm, P. Kennepohl, E. I. Solomon, *Chem. Rev.*, **1996**, 96, 2239; b) E. I. Solomon, T. C. Brunold, M. I. Davis, J. N. Kemsley, S.-K. Lee, N. Lehnert, F. Neese, A. J. Skulan, Y.-S. Yang, J. Zhou, *Chem. Rev.*, **2000**, 100, 235; c) E. Y. Tshuva, S. J. Lippard, *Chem. Rev.*, **2004**, 987; d) Y. Li, C. M. M. Soe, J. J. Wilson, S. L. Tuang, U.-P. Apfel, S. J. Lippard, *Eur. J. Inorg. Chem.*, **2013**, 2011.
- [106] a) S. J. Lippard, *Angew Chem. Int. Ed. Engl.*, **1988**, 27, 344; b) R. L. Rardin, W. B. Tolman, S. J. Lippard, *New J. Chem.*, **1991**, 15, 417; c) Y.-L. Miao, J.-L. Liu, Z.-J. Lin, Y.-C. Ou, J.-D. Leng, M.-L. Tong, *Dalton Transactions*, **2010**, 39, 4893.
- [107] a) J. F. Duncan, C. R. Kanekar, K. F. Mok, *Journal of the Chemical Society a -Inorganic Physical Theoretical*, **1969**, 480; b) G. J. Long, D. L. Bridges, *Abstracts of Papers of the American Chemical Society*, **1972**, 164, 8.
- [108] a) V. Rabe, W. Frey, A. Baro, S. Laschat, M. Bauer, H. Bertagnolli, S. Rajagopalan, T. Asthalter, E. Roduner, H. Dilger, T. Glaser, D. Schnieders, *Eur. J. Inorg. Chem.*, **2009**, 2009, 4660; b) G. Novitchi, L. Helm, C. Anson, A. K. Powell, A. E. Merbach, *Inorganic Chemistry*, **2011**, 50, 10402.
- [109] S. M. Heald, E. A. Stern, B. Bunker, E. M. Holt, S. L. Holt, *J. Am. Chem. Soc.*, **1979**, 101, 67.
- [110] a) S. Ito, K. Inoue, M. Mastumoto, *Journal of the American Chemical Society*, **1982**, 104, 6450; b) E. Ertürk, M. Göllü, A. S. Demir, *Tetrahedron*, **2010**, 66, 2373.
- [111] F. Miccichè, G. J. Long, A. M. Shahin, F. Grandjean, W. Ming, J. van Haveren, R. van der Linde, *Inorganica Chimica Acta*, **2007**, 360, 535.
- [112] a) F. Basolo, R. G. Pearson, *Mechanisms of Inorganic Reactions*, 2nd ed.; Wiley, New York, **1967**; b) M. L. Tobe, J. Burgess, *Inorganic Reaction Mechanisms*, Longman, New York, **1999**; c) J. D. Atwood, *Inorganic and Organometallic Reaction Mechanisms*, Wiley-VCH: Weinheim, Germany, **1997**; d) R. Wilkins, *Kinetics and Mechanism of Reactions of Transition Metal Complexes*, VCH: Weinheim, Germany, **1991**; e) R. B. Jordan, *Reaction Mechanism of Inorganic and Organometallic Systems*, Oxford University Press: Oxford, U. K., **1991**.
- [113] a) H. G. Jang, S. J. Geib, Y. Kaneko, M. Nakano, M. Sorai, A. L. Rheingold, B. Montez, D. N. Hendrickson, *Journal of the American Chemical Society*, **1989**, 111, 173; b) J. Overgaard, E. Rentschler, G. A. Timco, N. V. Gerbeleu, V. Arion, A. Bousseksou, J. P. Tuchagues, F. K. Larsen, *Journal of the Chemical Society, Dalton Transactions*, **2002**, 0, 2981; c) R. Wu, M. Poyraz, F. E. Sowrey, C. E. Anson, S. Wocadlo, A. K. Powell, U. A. Jayasooriya, R. D. Cannon, T. Nakamoto, M. Katada, H. Sano, *Inorg. Chem.*, **1998**, 37, 1913; d) C.-C. Wu, S. A. Hunt, P. K. Gantzel, P. Gütlich, D. N. Hendrickson, *Inorganic Chemistry*, **1997**, 36, 4717.
- [114] a) R. Sessoli, A. K. Powell, *Coord. Chem. Rev.*, **2009**, 253, 2328; b) G. Aromi, E. K. Brechin, *Struct. Bond.*, **2006**, 122, 1; c) Y.-Z. Zheng, M.-L. Tong, W. Xue, W.-X. Zhang, X.-M. Chen, F. Grandjean, G. J. Long, *Angew. Chem. Int. Ed.*, **2007**, 46, 6076; d) E. K. Brechin, J. C. Huffman, G. Christou, J. Yoo, M. Nakano, D. N. Hendrickson, *Chem. Comm.*, **1999**, 0, 783.
- [115] a) R. Bircher, G. Chaboussant, C. Dobe, H. U. Gudel, S. T. Ochsenbein, A. Sieber, O. Waldmann, *Adv. Funct. Mater.*, **2006**, 16, 209; b) E. Coronado, D. Gatteschi, *J. Mater. Chem.*, **2006**, 16(26), 2513; c) C. J. Milios, S. Piligkos, E. K. Brechin, *Dalton Trans.*, **2008**, 14, 1809; d) D. Gatteschi, R. Sessoli, A. Cornia, *Chem. Commun.*, **2000**, 9, 725; e) G. Christou, *Polyhedron*, **2005**, 24, 2065; f) B. Cage, S. E. Russek, R. Shoemaker, A. J. Barker, C. Stoldt, V. Ramachandaran, N. S. Dalal, *Polyhedron*, **2007**, 26, 2413.
- [116] a) V. F. Puentes, D. Zanchet, C. K. Erdonmez, A. P. Alivisatos, *J. Am. Chem. Soc.*, **2002**, 124, 12874; b) V. F. Puentes, K. M. Krishnan, A. P. Alivisatos, *Science*, **2001**, 291, 2115; c) S. M. Ostrovsky, R. Werner, D. A. Brown, W. Haase, *Chemical Physics Letters*, **2002**, 353, 290.
- [117] a) D. Lee, P.-L. Hung, B. Spingler, S. J. Lippard, *Inorg. Chem.*, **2002**, 41, 521; b) Y. Bao-Hui, C. Xiao-Ming, *Chinese Journal of Chemistry*, **2003**, 21, 531; c) C.-S. Liu, J.-J. Wang, L.-F. Yan, Z. Chang, X.-H. Bu, E. C. Sañudo, J. Ribas, *Inorganic Chemistry*, **2007**, 46, 6299; d) J. Hudák, R. Boča, J. Moncol, J. Titiš, *Inorganica Chimica Acta*, **2013**, 394, 401.
- [118] J. A. Larrabee, S.-A. Chyun, A. S. Volwiler, *Inorg. Chem.*, **2008**, 47, 10499.
- [119] a) H. L. Carrell, J. P. Glusker, V. Burger, F. Manfre, D. Tritsch, J.-F. Biellmann, *Proc. Natl. Acad. Sci. USA*, **1989**, 86, 4440; b) A. Lavie, K. N. Allen, G. A. Petsko, D. Ringe, *Biochemistry*, **1994**, 33, 5469; c) K. N. Allen, A. Lavie, G. A. Petsko, D. Ringe, *Biochemistry*, **1995**, 34, 3742; d) T. D. Fenn, D. Ringe, G. A. Petsko, *Biochemistry*, **2004**, 43, 6464; e) D. A. Brown, W. Errington, W. K. Glass, W. Haase, T. J. Kemp, H. Nimir, S. M. Ostrovsky, R. Werner, *Inorg. Chem.*, **2001**, 40, 5962; f) M. H. Sazinsky, M. Merckx, E. Cadieux, S. Tang, S. J. Lippard, *Biochemistry*, **2004**, 43, 16263; g) R. C. Holz, *Coord. Chem. Rev.*, **2002**, 232.
- [120] a) J. Luo, M. Hong, R. Wang, R. Cao, L. Han, D. Yuan, Z. Lin, Y. Zhou, *Inorganic Chemistry*, **2003**, 42, 4486; b) Q. Yang, L. Huang, M. Zhang, Y. Li, H. Zheng, Q. Lu, *Crystal Growth & Design*, **2013**, 13, 440; c) Y.-H. Liu, H.-L. Tsai, Y.-L. Lu, Y.-S. Wen, J.-C. Wang, K.-L. Lu, *Inorg. Chem.*, **2001**, 40, 6426; d) N. Stock, S. Biswas, *Chem. Rev.*, **2012**, 112, 933.

- [121] a) R. A. Sheldon, J. K. Kochi, *Metal Catalyzed Oxidation of Organic Compounds*, Academic Press, New York, **1981**; b) P. Gamez, P. G. Aubel, W. L. Driessen, J. Reedijk, *Chem. Soc. Rev.*, **2001**, 30, 376; c) A. Robert, B. Meunier, *Biomimetic Oxidations Catalyzed by Transition Metal Complexes*, Ed. Meunier, B.; Imperial College Press, **2000**, Ch. 12; d) P. C. A. Bruijninx, G. Van Koten, R. J. M. K. Gebbink, *Chem. Soc. Rev.*, **2008**, 37, 2716.
- [122] R. A. Sheldon, R. A. Van Santen, *Catalytic Oxidation: Principles and Applications*, World Scientific, Singapore, **1995**,
- [123] A. Chauvel, A. Delmon, W. F. Hölderich, **1994**, 115, 173.
- [124] J. M. Bregeault, F. Launay, *Actualite Chimique*, **2002**, 45.
- [125] a) R. A. Sheldon, *CHEMTECH*, **1991**, September, 566; b) R. A. Sheldon, *Stud. Surf. Sci. Catal*, **1990**, 55, 1; c) R. A. Sheldon, *Topics Curr. Chem.*, **1993**, 164, 21.
- [126] S. J. Lippard, J. M. Berg, *Principles of Bioinorganic Chemistry*, University Science Books: Mill Valley, California, **1994**,
- [127] S. Antoniotti, E. Dunach, *Synthesis-Stuttgart*, **2003**, 2753.
- [128] a) K. B. Sharpless, *Angewandte Chemie International Edition*, **2002**, 41, 2024; b) A. H. Hoveyda, D. A. Evans, G. C. Fu, *Chemical Reviews*, **1993**, 93, 1307.
- [129] a) J. E. Bäckvall, *Modern Oxidation Methods*, Wiley-VCH Weinheim, **2004**; b) S. D. H. F. Gagnon, *Encyclopedia of Polymer Science and Engineering*, 2nd ed., Eds. Mark, H. F., Bikales N. M., Overberger C. G., Menges G., Kroschwitz J. I., John Wiley & Sons, New York, **1985**, Vol.6, 273; c) G. de Faveri, G. Ilyashenko, M. Watkinson, *Chem. Soc. Rev.*, **2011**, 40, 1722.
- [130] a) J. G. Smith, *Synthesis and Reactivity in Inorganic, Metal.-Organic and Nano-Metal Chemistry*, **1984**, 629; b) E. N. Jacobsen, *Acc. Chem. Res.*, **2000**, 33, 421; c) E. J. de Vries, D. B. Janssen, *Curr. Opin. Biotechnol.*, **2003**, 14, 414; d) J. Muzart, *Eur. J. Org. Chem.*, **2011**, 4717; e) A. S. Jepsen, M. Roberson, R. G. Hazell, *Chemical Communications*, **1998**, 0, 1599.
- [131] a) C. P. Horwitz, S. E. Creager, R. W. Murray, *Inorganic Chemistry*, **1990**, 29, 1006; b) Q. H. Xia, H. Q. Ge, C. P. Ye, Z. M. Liu, K. X. Su, *Chemical Reviews*, **2005**, 105, 1603; c) A. Martinez, C. Hemmert, C. Loup, G. Barré, B. Meunier, *The Journal of Organic Chemistry*, **2006**, 71, 1449.
- [132] a) E. N. Jacobsen, W. Zhang, M. L. Guler, *Journal of the American Chemical Society*, **1991**, 113, 6703; b) T. Katsuki, *Journal of Molecular Catalysis A: Chemical*, **1996**, 113, 87; c) N. S. Finney, P. J. Pospisil, S. Chang, M. Palucki, R. G. Konsler, K. B. Hansen, E. N. Jacobsen, *Angewandte Chemie International Edition in English*, **1997**, 36, 1720; d) P. Brandt, P.-O. Norrby, A. M. Daly, D. G. Gilheany, *Chemistry – A European Journal*, **2002**, 8, 4299; e) A. M. Daly, D. G. Gilheany, *Tetrahedron: Asymmetry*, **2003**, 14, 127.
- [133] a) A. Murphy, A. Pace, T. D. P. Stack, *Org. Lett.*, **2004**, 6, 3119; b) A. Murphy, T. D. P. Stack, *J. Mol. Catal. A: Chem.*, **2006**, 251, 78.
- [134] a) X. Sala, I. Romero, M. Rodríguez, L. Escriche, A. Llobet, *Angewandte Chemie International Edition*, **2009**, 48, 2842; b) G. C. Dismukes, R. Brimblecombe, G. A. N. Felton, R. S. Pryadun, J. E. Sheats, L. Spiccia, G. F. Swiegers, *Accounts of Chemical Research*, **2009**, 42, 1935.
- [135] N. S. Lewis, D. G. Nocera, *Proc. Natl. Acad. Sci. U.S.A.*, **2007**, 104, 20142.
- [136] M. Freemantle, *Chem. Eng. News* **1998**, 37.
- [137] a) R. M. Navarro, M. A. Pena, J. L. G. Fierro, *Chem. Rev.*, **2007**, 107, 3952; b) D. G. Nocera, *Daedalus (Boston)*, **2006**, 135, 112; c) M. Daniel, D. E. Alessandro, *Int J Hydrogen Energy* **2008**, 33, 3041; d) N. S. Lewis, *Science*, **2007**, 315, 798; e) S. I. Allakhverdiev, J. Casal, T. Nagata, *Photochem Photobiol Sci*, **2009**, 8, 137.
- [138] a) S. Reece, J. Hamel, K. Sung, T. Jarvi, A. Esswein, J. Pijper, D. Nocera, *Science*, **2004**, 334, 645; b) M. W. Kanan, D. G. Nocera, *Science*, **2008**, 321, 1072; c) R. K. Hocking, R. Brimblecombe, L.-Y. Chang, A. Singh, M. H. Cheah, C. Glover, W. H. Casey, L. Spiccia, *Nat Chem*, **2011**, 3, 461; d) S. Y. Reece, J. A. Hamel, K. Sung, T. D. Jarvi, A. J. Esswein, J. J. H. Pijpers, D. G. Nocera, *Science*, **2011**, 334, 645.
- [139] a) J. M. Berg, J. L. Tymoczko, L. Stryer, *Biochemistry*, W. H. Freeman & Co, New York, **2011**; b) P. Atkins, T. Overton, J. Rourke, M. Weller, F. A. Armstrong, *Inorganic Chemistry*, Oxford University Press, Oxford, **2010**; c) L. Taiz, E. Zeiger, *Plant Physiology*, Sinauer Ass, Sunderland, **2010**,
- [140] a) B. Kok, B. Forbush, M. McLooin, *Photochem. Photobiol.*, **1970**, 457, 11; b) J. Yano, J. Kern, K. Sauer, M. J. Latimer, Y. Pushkar, J. Biesiadka, B. Loll, W. Saenger, J. Messinger, A. Zouni, V. K. Yachandra, *Science*, **2006**, 314, 821; c) G. C. Dismukes, R. Brimblecombe, G. A. N. Felton, R. S. Pryadun, J. E. Sheats, L. Spiccia, G. F. Swiegers, *Acc. Chem. Res.*, **2009**, 42, 1935.

- [141] K. Kawakami, Y. Umena, N. Kamiya, J.-R. Shen, *Journal of Photochemistry and Photobiology B: Biology*, **2011**, 104, 9.
- [142] a) T. J. Meyer, *Acc. Chem. Res.*, **1989**, 22, 163; b) S. Romain, L. Vigara, A. Llobet, *Acc. Chem. Res.*, **2009**, 42, 1944; c) H. Dau, C. Limberg, T. Reier, M. Risch, S. Roggan, P. Strasser, *ChemCatChem*, **2010**, 2, 724.
- [143] a) N. D. McDaniel, F. J. Coughlin, L. L. Tinker, S. Bernhard, *J. Am. Chem. Soc.*, **2008**, 130, 210; b) R. Lalrempuia, N. D. McDaniel, H. Müller-Bunz, S. Bernhard, M. Albrecht, *Angew. Chem. Int. Ed.*, **2010**, 49, 9765; c) J. F. Hull, D. Balcells, J. D. Blakemore, C. D. Incarvito, O. Eisenstein, G. W. Brudvig, R. H. Crabtree, *Journal of the American Chemical Society*, **2009**, 131, 8730.
- [144] a) Q. Yin, J. M. Tan, C. Besson, Y. V. Geletii, D. G. Musaev, A. E. Kuznetsov, Z. Luo, K. I. Hardcastle, C. L. Hill, *Science*, **2010**, 328, 342; b) D. K. Dogutan, R. McGuire, D. G. Nocera, *J. Am. Chem. Soc.*, **2011**, 133, 9178; c) D. J. Wasylenko, C. Ganesamoorthy, J. Borau-Garcia, C. P. Berlinguette, *Chem. Commun.*, **2011**, 47, 4249.
- [145] a) W. C. Ellis, N. D. McDaniel, S. Bernhard, T. J. Collins, *J. Am. Chem. Soc.*, **2010**, 132, 10990; b) J. L. Fillol, Z. Codolà, I. Garcia-Bosch, L. Gómez, J. J. Pla, M. Costas, *Nature Chem.*, **2011**, 3, 807.
- [146] C. S. Mullins, V. L. Pecoraro, *Coord. Chem. Rev.*, **2008**, 252, 416.
- [147] a) C. W. Cady, R. H. Crabtree, G. W. Brudvig, *Coord. Chem. Rev.*, **2008**, 252, 444; b) L. Limburg, J. S. Vrettos, H. Y. Chen, J. C. de Paula, R. H. Crabtree, G. W. Brudvig, *J. Am. Chem. Soc.*, **2001**, 123, 423; c) M. M. Najafpour, B. Kozlevcar, V. McKee, Z. Jaglicic, M. Jagodic, *Inorg. Chem. Commun.*, **2011**, 14, 125.
- [148] a) F. E. Mabbs, D. J. Machin, *Magnetism and Transition Metal Complexes*, Chapman and Hall, London, **1973**; b) J. Ribas, *Ed. Química de Coordinación*, Edicions UB - Ediciones Omega S.A., Barcelona, **2000**.
- [149] J. H. Van Vleck, *The Theory of Electric and Magnetic Susceptibilities*, Oxford University Press., Oxford, **1932**.
- [150] a) P. A. Dirac, *Proc. R. Soc. London, Ser. A*, **1926**, 112, 661; b) W. Heisenberg, *Z. Phys.*, **1926**, 38, 411; c) W. Heisenberg, *Z. Phys.*, **1928**, 49, 619; d) B. Bleaney, K. D. Bowers, *Proc. R. Soc. London, Ser. A*, **1952**, 214, 451.
- [151] F. Sapiña, M. Burgos, E. Escrivá, J.-V. Folgado, D. Beltrán, *Inorg. Chim. Acta* **1994**, 216, 185
- [152] a) H. G. Guedel, A. Stebler, A. Furrer, *Inorg. Chem.*, **1979**, 18, 1021; b) M. Yamanaka, H. Uekusa, S. Ohba, Y. Saito, S. Iwata, *Acta Crystallogr. B*, **1991**, 47, 344
- [153] M. Melnik, *Coord. Chem. Rev.*, **1981**, 36, 1.
- [154] a) H.-L. Wu, *Synthesis and Reactivity in Inorganic, Metal-Organic and Nano-Metal Chemistry*, **2007**, 37, 57; b) L. K. Thompson, B. S. Ramanswamy, R. D. Dawe, *Can. J. Chem.*, **1978**, 56, 1311.
- [155] a) C. Chen, H. Zhu, D. Huang, T. Wen, Q. Liu, D. Liao, J. Cui, *Inorganica Chimica Acta*, **2001**, 320, 159; b) D. Huang, W. Wang, X. Zhang, C. Chen, F. Chen, Q. Liu, D. Liao, L. Li, L. Sun, *European Journal of Inorganic Chemistry*, **2004**, 2004, 1454; c) A. Escuer, B. Cordero, X. Solans, M. Font-Bardia, T. Calvet, *European Journal of Inorganic Chemistry*, **2008**, 5082; d) Y. Ma, N. A. G. Bandeira, V. Robert, E.-Q. Gao, *Chemistry – A European Journal*, **2011**, 17, 1988.
- [156] R. L. Rardin, W. B. Tolman, S. J. Lippard, *New J. Chem.*, **1991**, 15, 417.
- [157] a) V. Gómez, M. Corbella, *Eur. J. Inorg. Chem.*, **2009**, 4471; b) V. Gómez, M. Corbella, M. Font-Bardia, T. Calvet, *Dalton Trans.*, **2010**, 39, 11664; c) V. Gómez, M. Corbella, *J. Chem. Crystallogr.*, **2011**, 41, 843.

Chapter VIII. General results and discussion

- [1] K. Kokado, Y. Chujo, *Macromolecules*, **2009**, 42, 1418
- [2] a) M. Eddaoudi, D. B. Moler, H. Li, B. Chen, T. M. Reineke, M. O'Keeffe, O. M. Yaghi, *Acc. Chem. Res.*, **2001**, 34, 319; b) B. Moulton, M. J. Zaworotko, *Curr. Opin. Solid State Mater. Sci.*, **2002**, 6, 117; c) C. Janiak, *J. Chem. Soc., Dalton Trans.*, **2003**, 2781; d) O. M. Yaghi, M. O'Keeffe, N. W. Ockwig, H. K. Chae, M. Eddaoudi, J. Kim, *Nature Chemical Biology*, **2003**, 423, 705; e) U. Mueller, M. Schubert, F. Teich, H. Puetter, K. Schierle-Arndt, J. Pastre, *J. Mater. Chem.*, **2006**, 16, 626; f) M. Andruh, *Chem. Commun.*, **2007**, 2565; g) B. Wang, A. P. Cote, H. Furukawa, M. O'Keeffe, O. M. Yaghi, *Nature Chemical Biology*, **2008**, 453, 207; h) B. Moulton, M. J. Zaworotko, *Chem. Rev.*, **2001**, 101, 1629; i) A. K. Cheetham, C. N. R. Rao, R. K. Feller, *Chem. Commun.*, **2006**, 4780; j) G. A. Timco, S. Carretta, F. Troiani, F. Tuna, R. J. Pritchard, C. A. Muryn, E. J. L. McInnes, A. Ghirri, A. Candini, P. Santini, G. Amoretti, M. Affronte, E. P. Winpenny, *Nat. Nanotechnol.*, **2009**, 4, 173; k) R. D. Cannon, A. J. P. White, *Prog. Inorg. Chem.*, **1988**, 36, 195; l) V. Rabe, W. Frey, A. Baro, S. Laschat, M. Bauer, H. Bertagnolli, S. Rajagopalan, T. Asthalter, E. Roduner, H. Dilger, T. Glaser, D. Schnieders, *Eur. J. Inorg. Chem.*, **2009**, 2009, 4660; m) V. F. Puentes, K. M. Krishnan, A. P. Alivisatos, *Science*, **2001**, 291, 2115; n) S. M. Ostrovsky, R. Werner, D. A. Brown, W. Haase, *Chemical Physics Letters*,

- 2002**, 353, 290; o) V. F. Puentes, D. Zanchet, C. K. Erdonmez, A. P. Alivisatos, *J. Am. Chem. Soc.*, **2002**, 124, 12874; p) J. A. Larrabee, S.-A. Chyun, A. S. Volwiler, *Inorg. Chem.*, **2008**, 47, 10499; q) E. K. Brechin, J. C. Huffman, G. Christou, J. Yoo, M. Nakano, D. N. Hendrickson, *Chem. Comm.*, **1999**, 0, 783; r) G. Aromi, E. K. Brechin, *Struct. Bond.*, **2006**, 122, 1; s) Y.-Z. Zheng, M.-L. Tong, W. Xue, W.-X. Zhang, X.-M. Chen, F. Grandjean, G. J. Long, *Angew. Chem. Int. Ed.*, **2007**, 46, 6076; t) R. Sessoli, A. K. Powell, *Coord. Chem. Rev.*, **2009**, 253, 2328.
- [3] a) S. S.-Y. Chui, S. M.-F. Lo, J. P. H. Charmant, A. G. Orpen, I. D. Williams, *Science* **1999**, 283, 1148 ; b) M. Eddaoudi, J. Kim, N. Rosi, D. Vodak, J. Wachter, M. O. Keffe, O. M. Yaghi, *Science*, **2002**, 295, 469 ; c) H. Jude, H. Disteldorf, S. Fischer, T. Wedge, A. M. Hawkridge, A. M. Arif, M. F. Hawthorne, D. C. Muddiman, P. Stang, *J. Am. Chem. Soc.*, **2005**, 127, 12131; d) R. N. Grimes, *Angew. Chem.*, **1993**, 105, 1350 ; e) M. A. Fox, A. K. Hughes, *Coord. Chem. Rev.*, **2004**, 248, 457 ; f) H. G. Jang, S. J. Geib, Y. Kaneko, M. Nakano, M. Sorai, A. L. Rheingold, B. Montez, D. N. Hendrickson, *Journal of the American Chemical Society*, **1989**, 111, 173; g) C.-C. Wu, S. A. Hunt, P. K. Gantzel, P. Gütlich, D. N. Hendrickson, *Inorganic Chemistry*, **1997**, 36, 4717; h) R. Wu, M. Poyraz, F. E. Sowrey, C. E. Anson, S. Wocadlo, A. K. Powell, U. A. Jayasooriya, R. D. Cannon, T. Nakamoto, M. Katada, H. Sano, *Inorg. Chem.*, **1998**, 37, 1913; i) J. Overgaard, E. Rentschler, G. A. Timco, N. V. Gerbeleu, V. Arion, A. Bousseksou, J. P. Tuchagues, F. K. Larsen, *Journal of the Chemical Society, Dalton Transactions*, **2002**, 0, 2981.
- [4] O. Kriz, A. L. Rheingold, M. Y. Shang, T. P. Fehlner, *Inorganic Chemistry*, **1994**, 33, 3777.
- [5] A. Bernheim-Groswasser, R. Zana, Y. Talmon, *J. Phys. Chem. B*, **2000**, 104, 4005.
- [6] a) M. Palucki, N. S. Finney, P. J. Pospisil, M. L. Güler, T. Ishida, E. N. Jacobsen, *Journal of the American Chemical Society*, **1998**, 120, 948; b) A. Murphy, G. Dubois, T. D. P. Stack, *J. Am. Chem. Soc.*, **2003**, 125, 5250.
- [7] K.-P. Ho, W.-L. Wong, K.-M. Lam, C.-P. Lai, T. H. Chan, K.-Y. Wong, *Chemistry – A European Journal*, **2008**, 14, 7988.
- [8] A. K. Dutta, S. K. Maji, S. Dutta, *Journal of Molecular Structure*, **2012**, 1027, 87.
- [9] V. Paredes-García, D. Venegas-Yazigi, R. O. Latorre, E. Spodine, *Polyhedron*, **2006**, 25, 2026.
- [10] J. S. Pap, J. Kaizer, M. Giorgi, G. Speier, *Inorganic Chemistry Communications*, **2010**, 13, 1069.
- [11] Z. Salman, R. Khalaf, H. D. Ashour, *Iraqi National Journal Of Chemistry*, **2009**, 489.
- [12] a) K. B. Gudasi, S. A. Patil, R. S. Vadavi, R. V. Shenoy, *Transition Metal Chemistry*, **2006**, 31, 586; b) R. V. S. S. N. Ravikumara, K. Ikedaa, A. V. Chandrasekharb, Y. P. Reddy, P. S. Raod, J. Yamauchie, *Journal of Physics and Chemistry of Solids*, **2003**, 64, 2433; c) D. A. Brown, W. K. Glass, N. J. Fitzpatrick, T. J. Kemp, W. Errington, G. J. Clarkson, W. Haase, F. Karsten, A. H. Mahdy, *Inorg. Chim. Acta*, **2004**, 357, 1411; d) A. Karmakar, R. J. Sarma, J. B. Baruah, *Polyhedron*, **2007**, 26, 1347

SUPPORTING INFORMATION

**CHAPTER III. Cu(II) complexes containing the carbora-
nylcarboxylate ligand 1-CH₃-2-CO₂H-1,2-closo-C₂B₁₀H₁₀.
Study of their steric and electronic effects.**

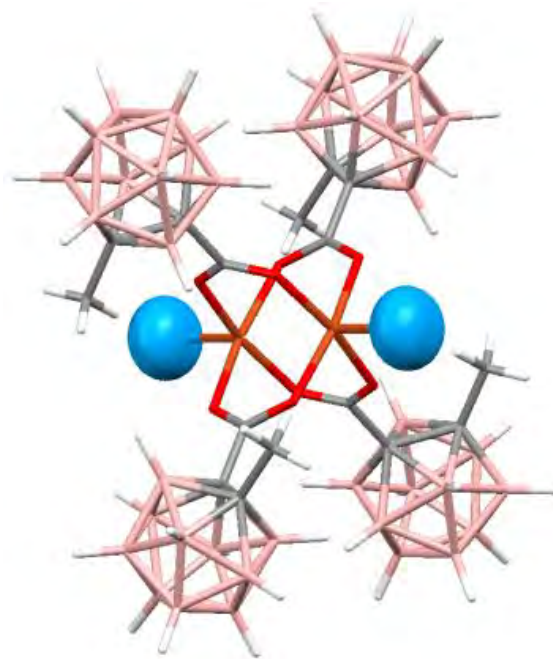


Figure S1. X-ray structures (Ortep-plots with ellipsoids at 40% probability level) and labelling scheme for (a) **A2'** (b) **A4'** and (c) **A4''**.

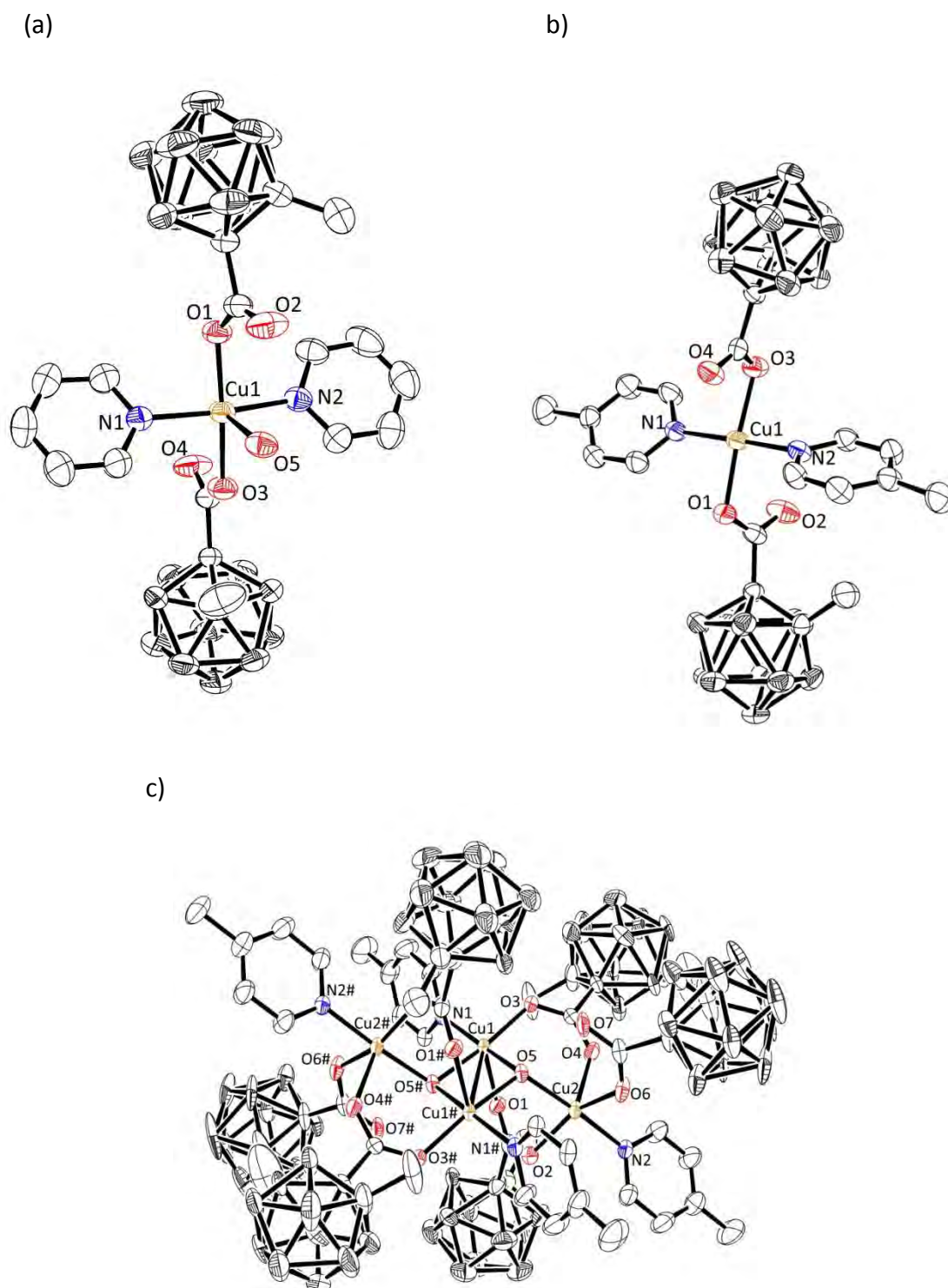
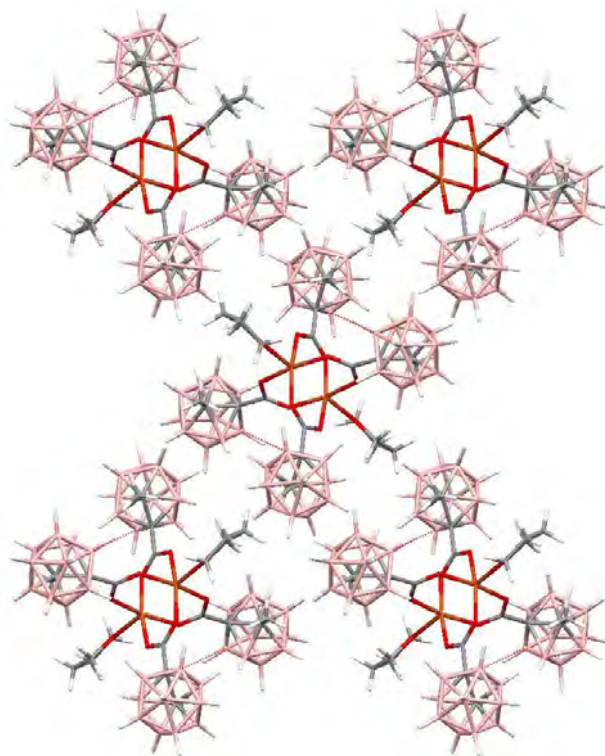
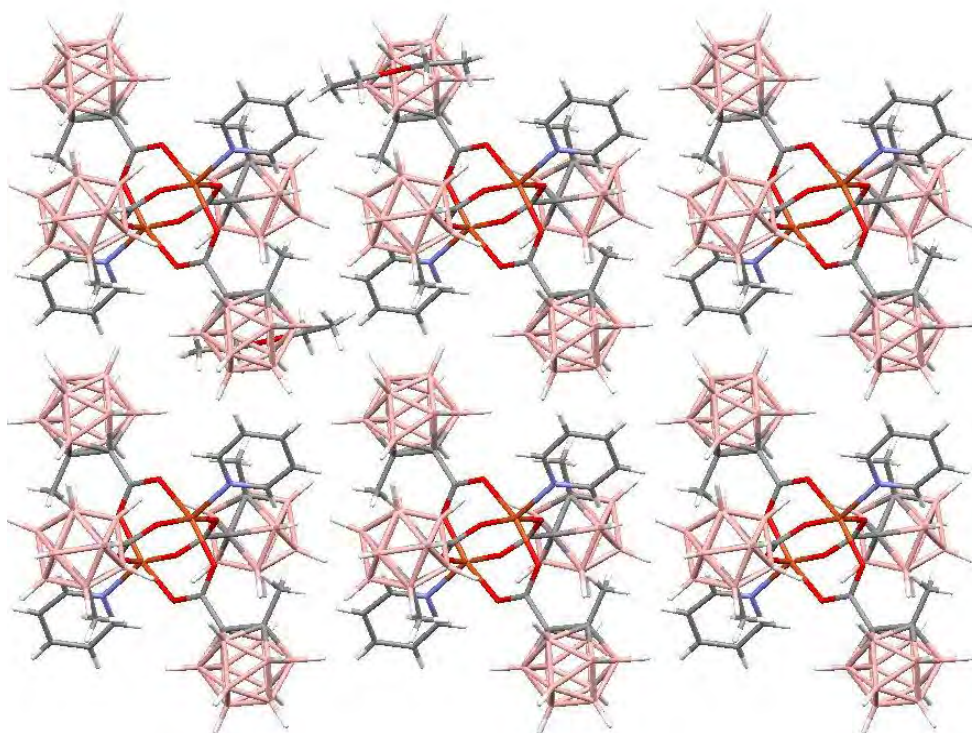


Figure S2. Packing diagram of complexes along the *a* axis (a) **A1**, (b) **A2**, (c) **A3**, (d) **A4**, (e) **A6**, (f) **A2'** and (g) **A8**.

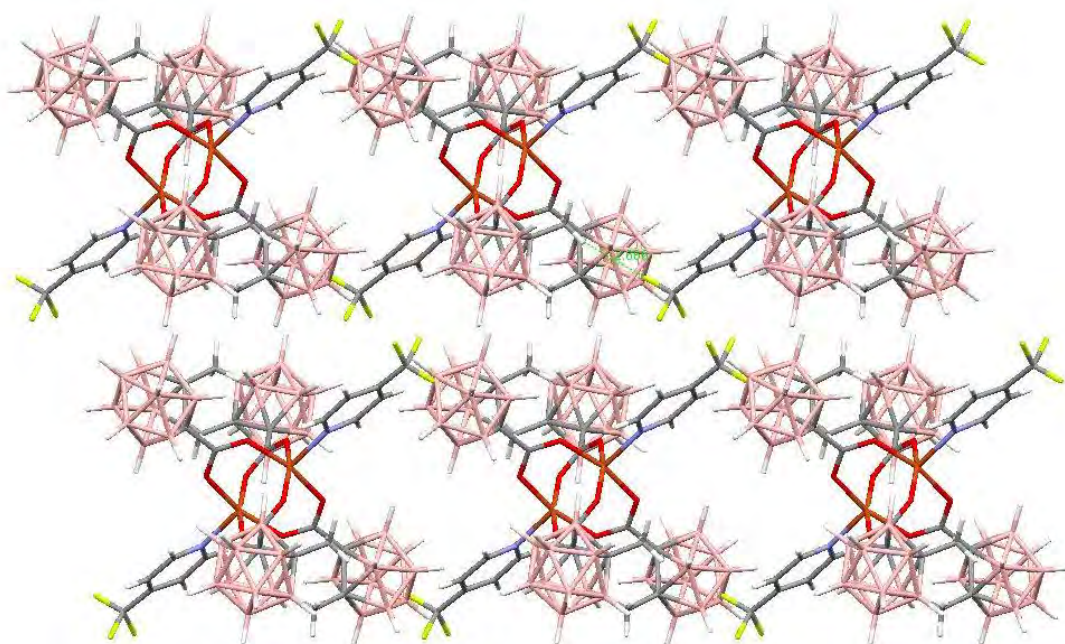
(a)



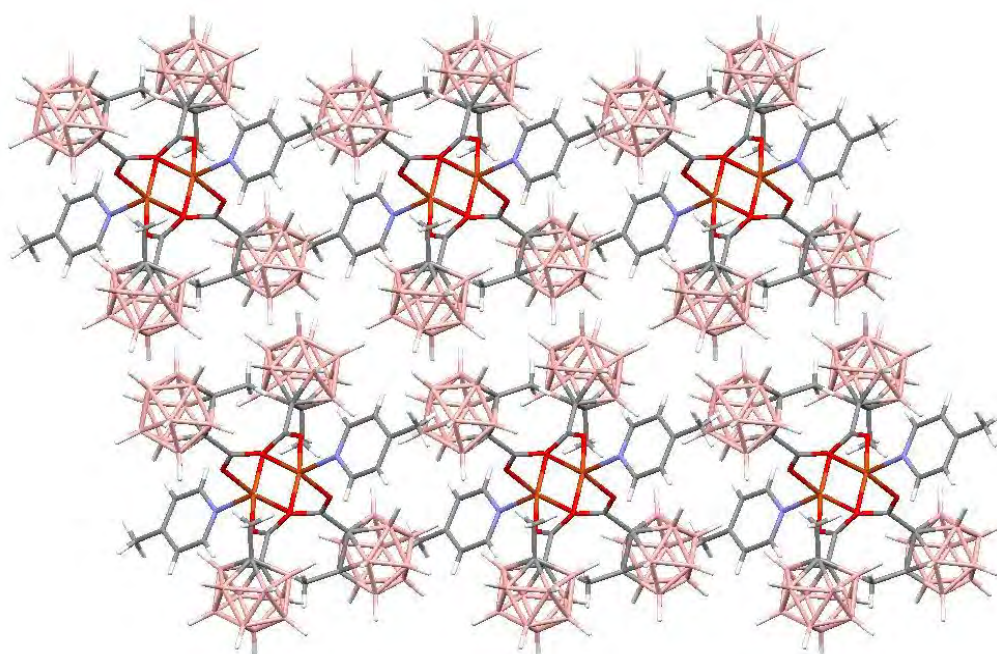
(b)



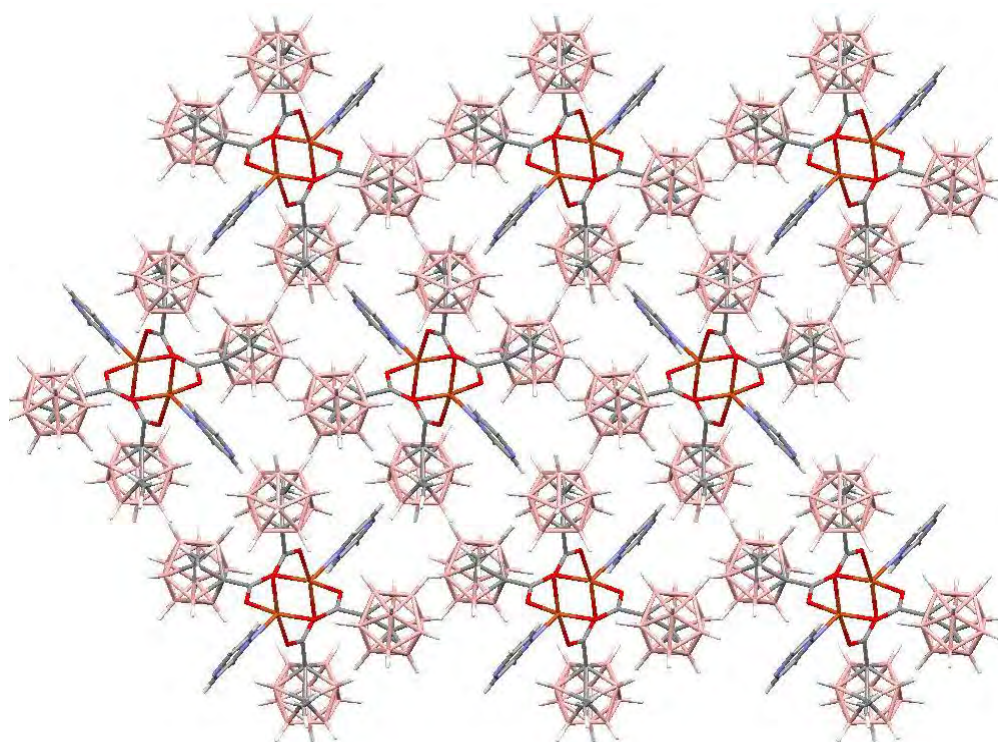
(c)



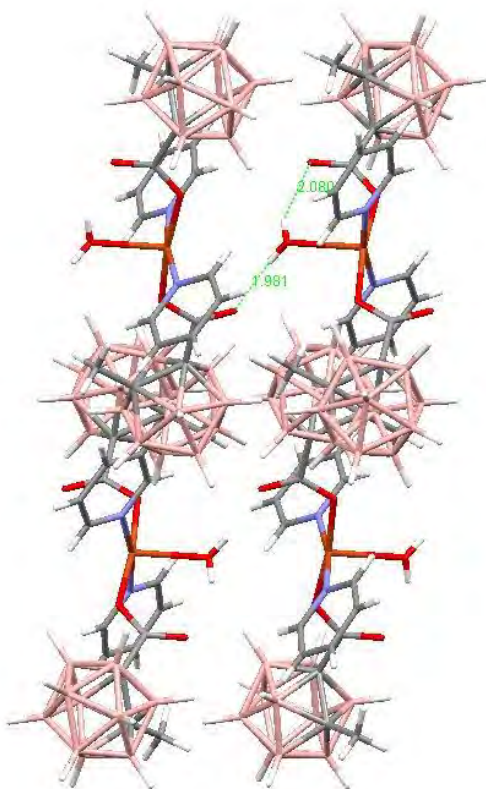
(d)



(e)



(f)



(g)

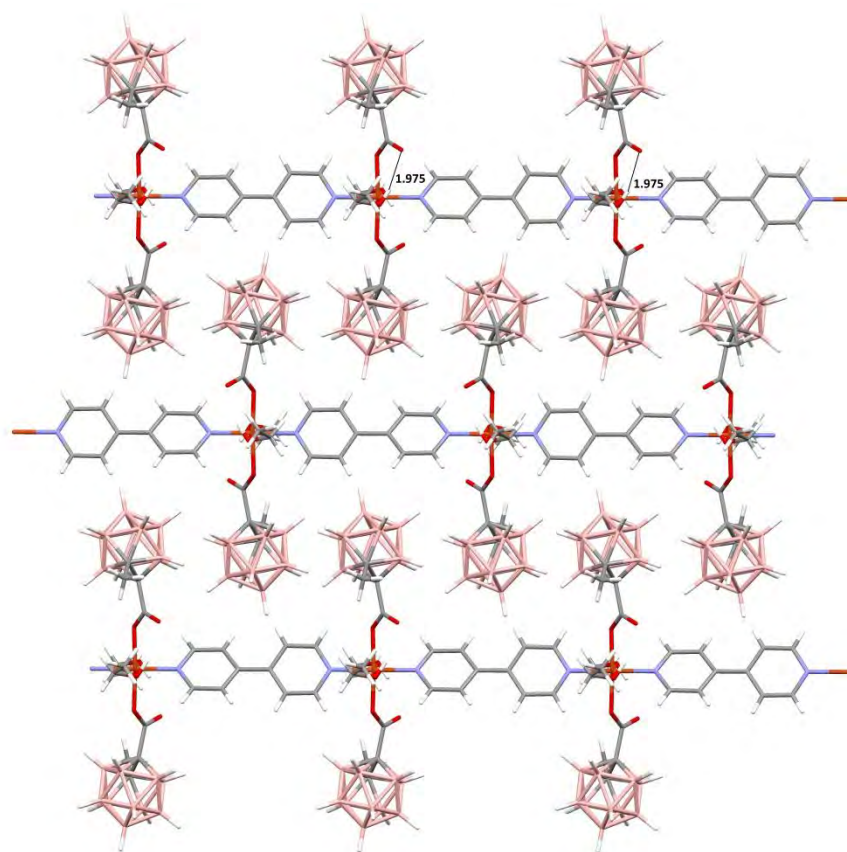


Figure S3. X-ray structure of $[\text{Cu}_2(\mu\text{-CH}_3\text{COO})_4(\text{p-CF}_3\text{-py})_2]$

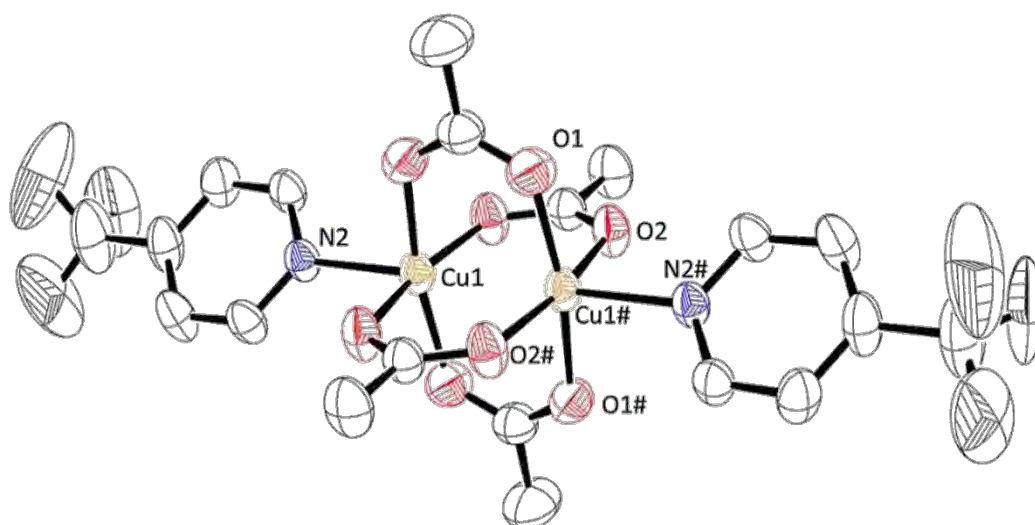


Figure S4. ESI-MS spectrum of a solution of complex **A3** in methanol after 18 hours of preparation

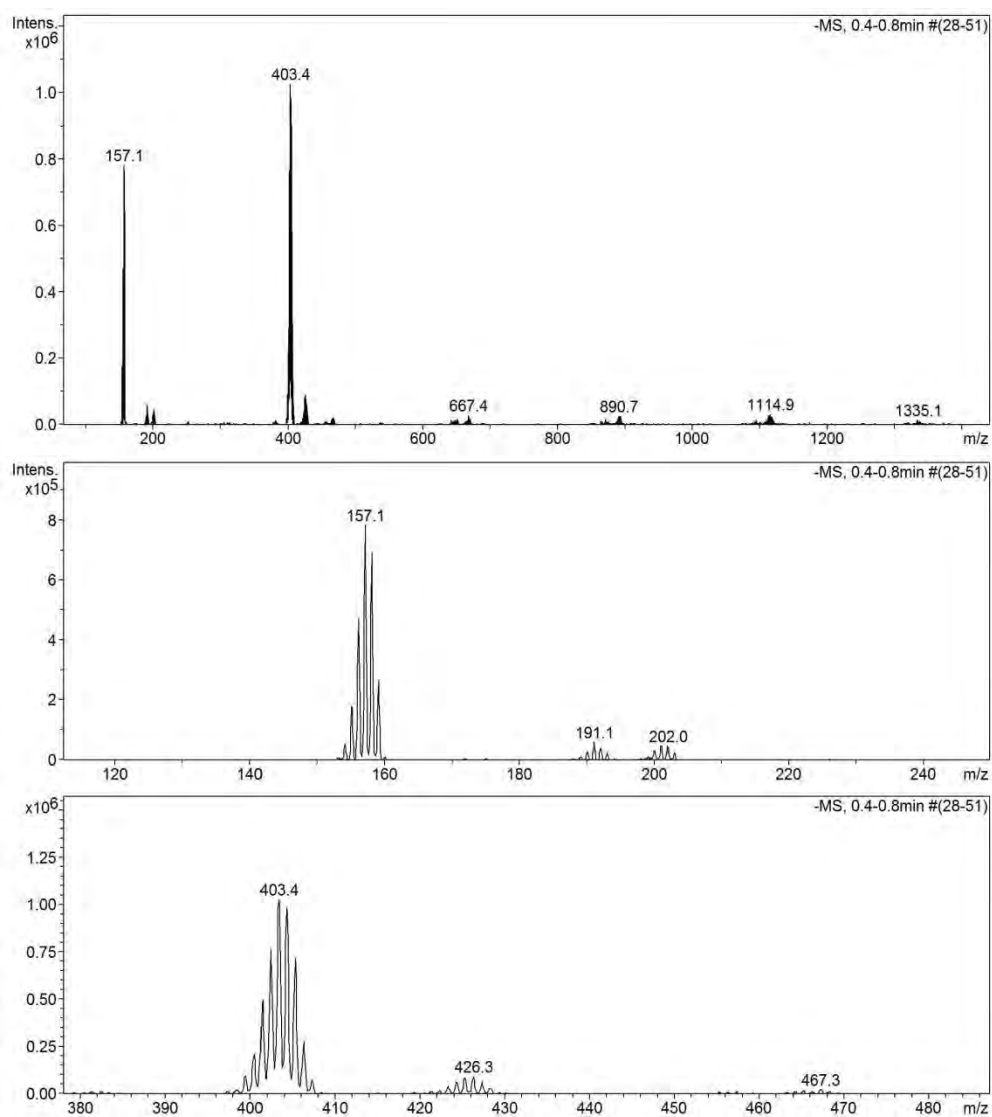


Figure S5. UV-vis spectral changes for complex **A1** obtained by the addition from one to four equivalents of *p*-methylpyridine

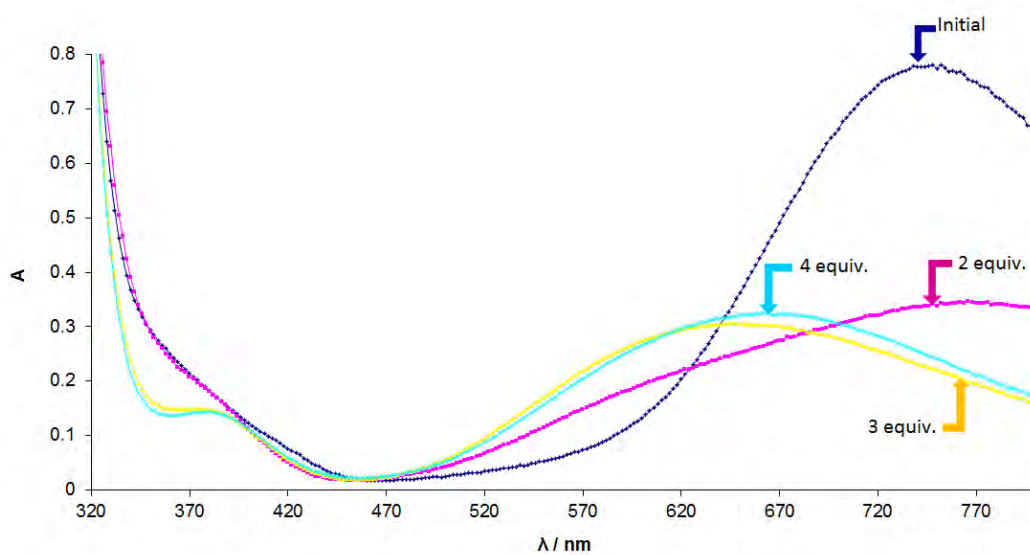
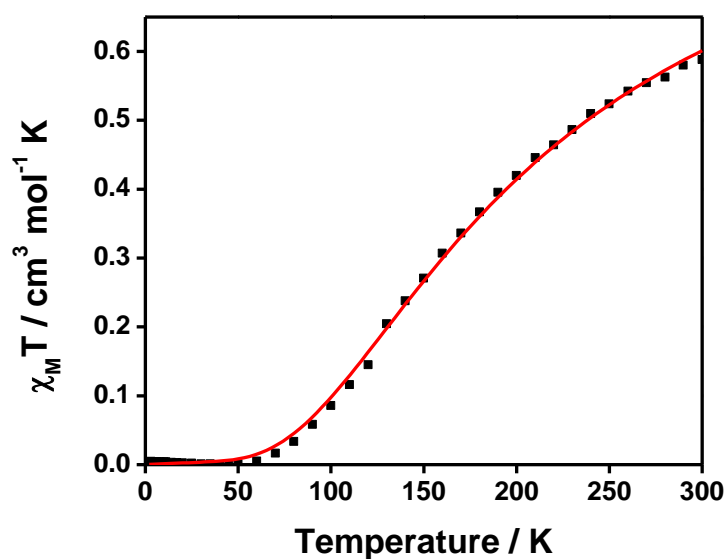
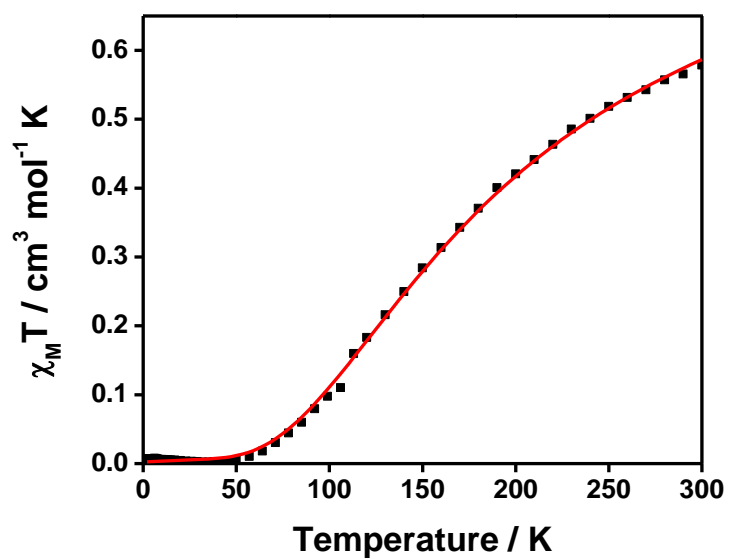


Figure S6. Fitting of the $\chi_M T$ vs T of a) **A3**, b) **A4** and c) **A6** between 2.0 and 300.0 K. The experimental data is shown as black spheres and the red line corresponds to the theoretical values.

a)



b)



c)

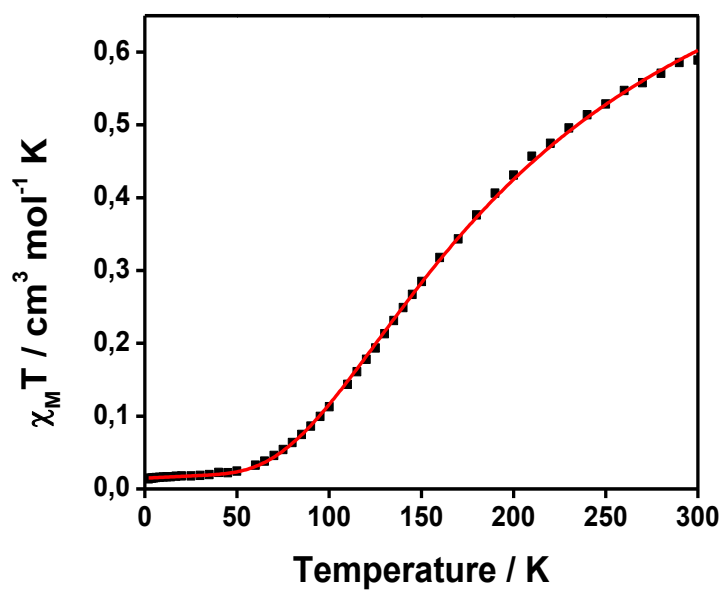
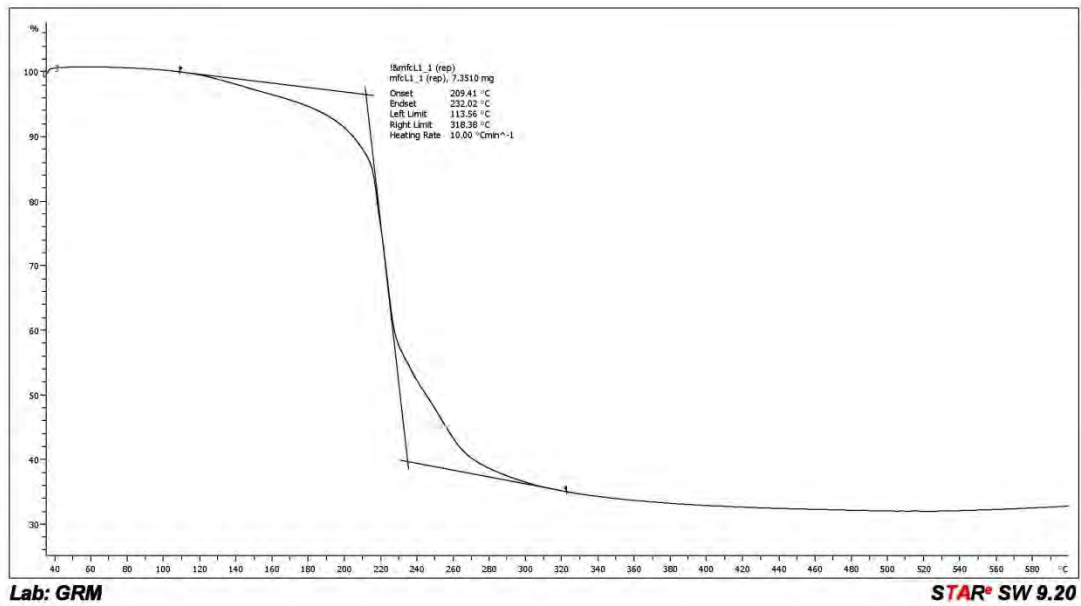
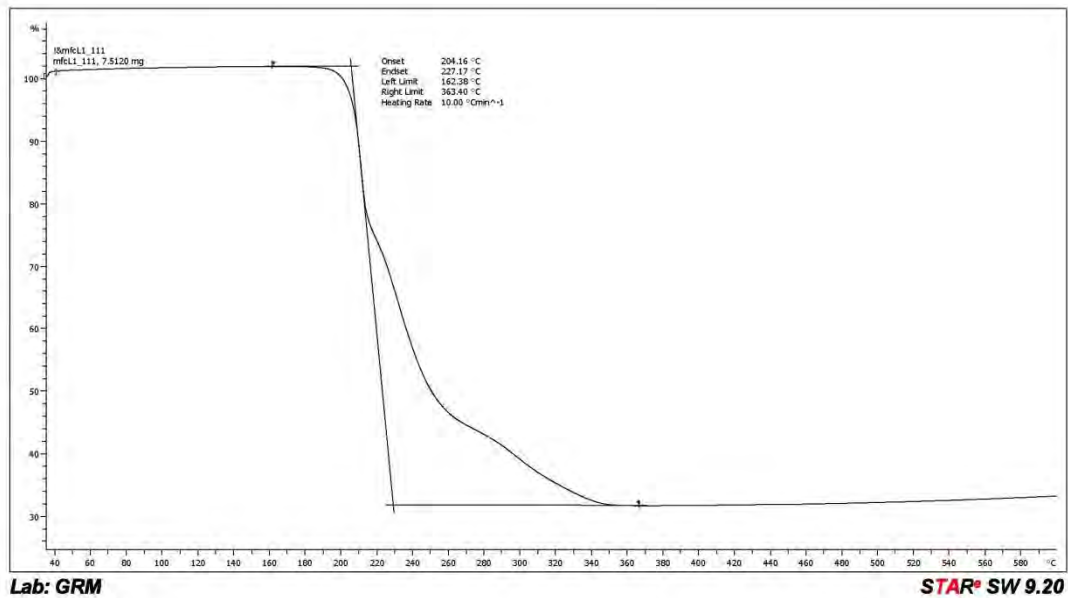


Figure S7. Thermal gravimetric analysis (TGA) of a) **A1**, b) **A3**, c) **A6**, d) **A7**.

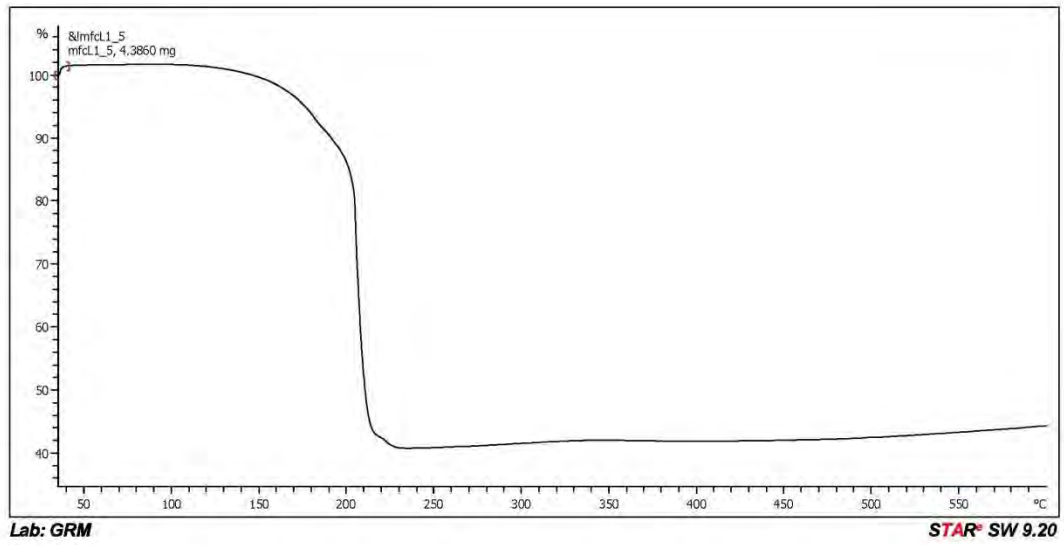
a)



b)



c)



d)

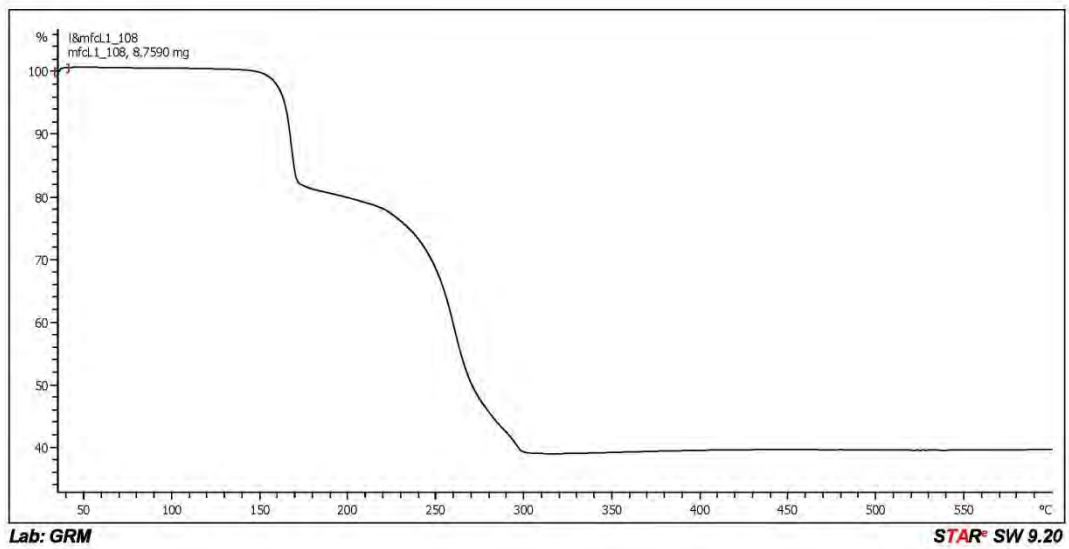
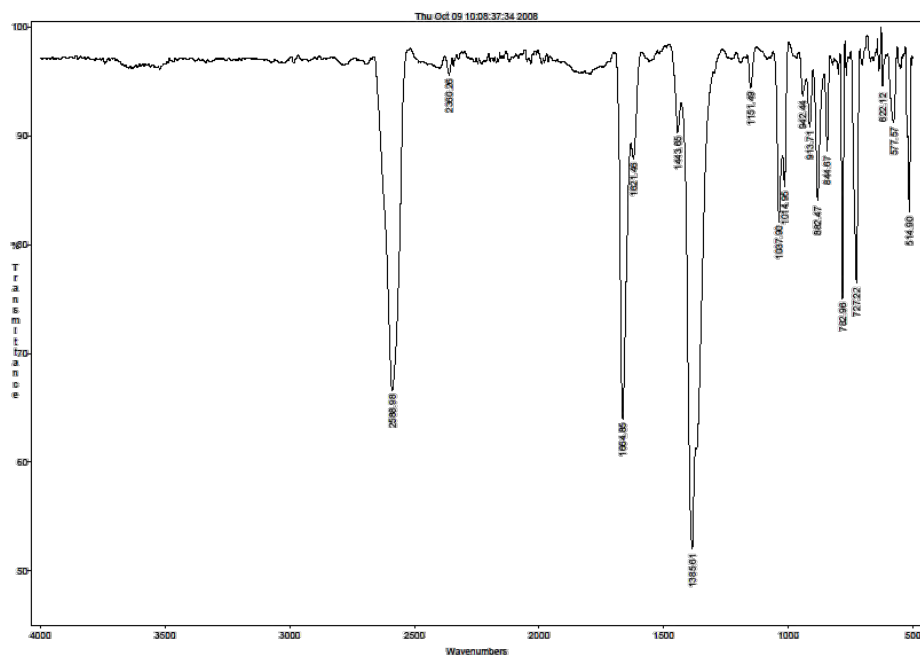
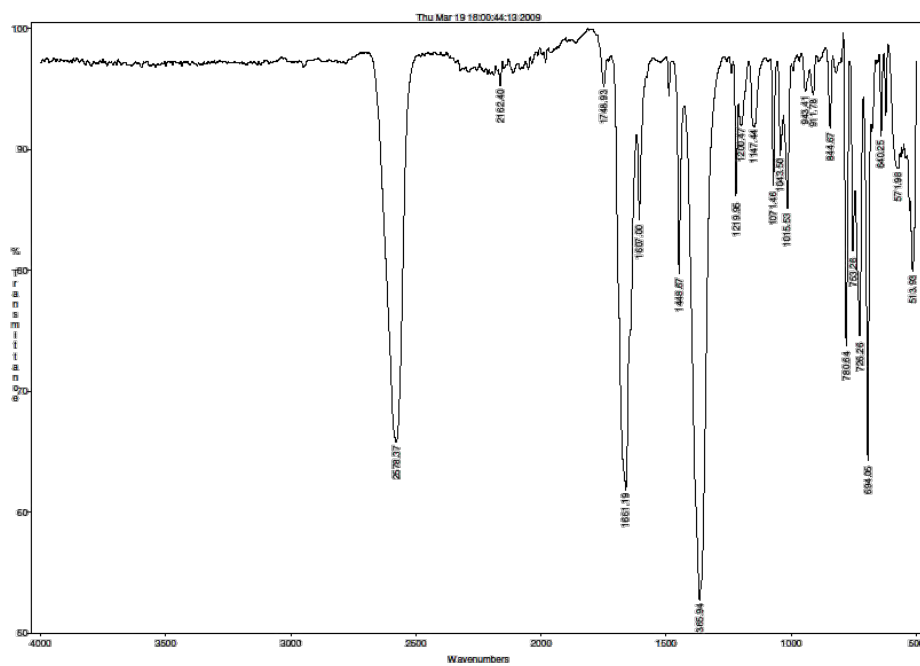


Figure S8. IR spectrum of the compounds a) A1, b) A2, c) A2', d) A3, e) A4, f) A5, g) A6, h) A7, i) A8, j) LH

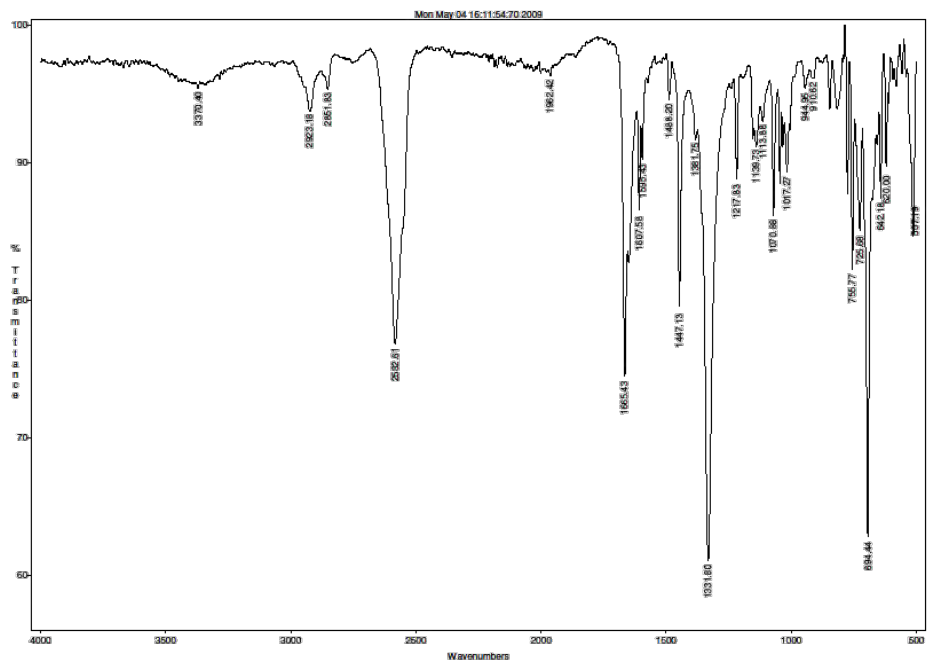
a)



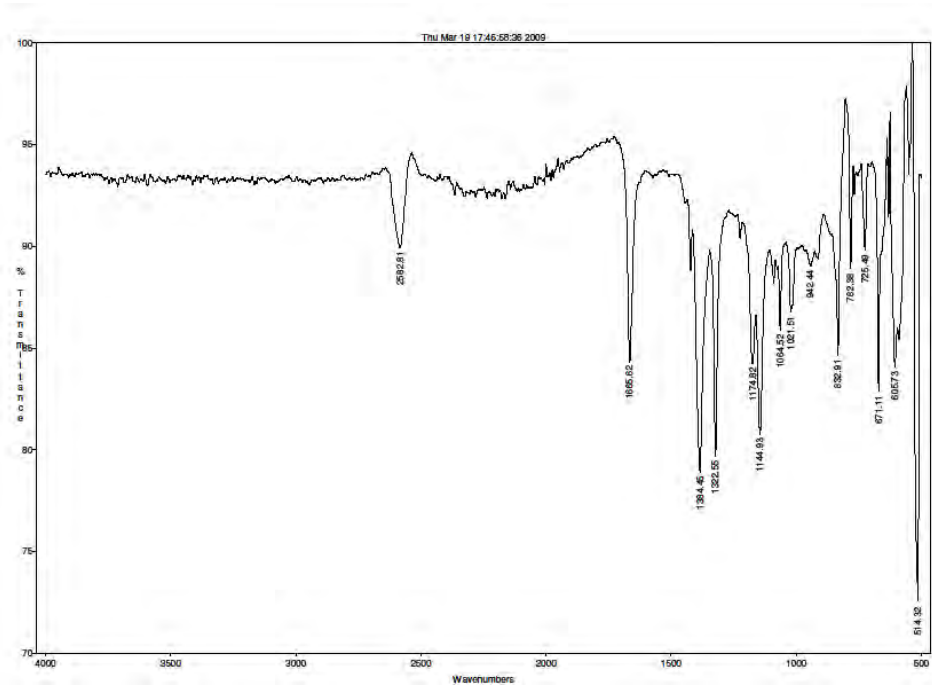
b)



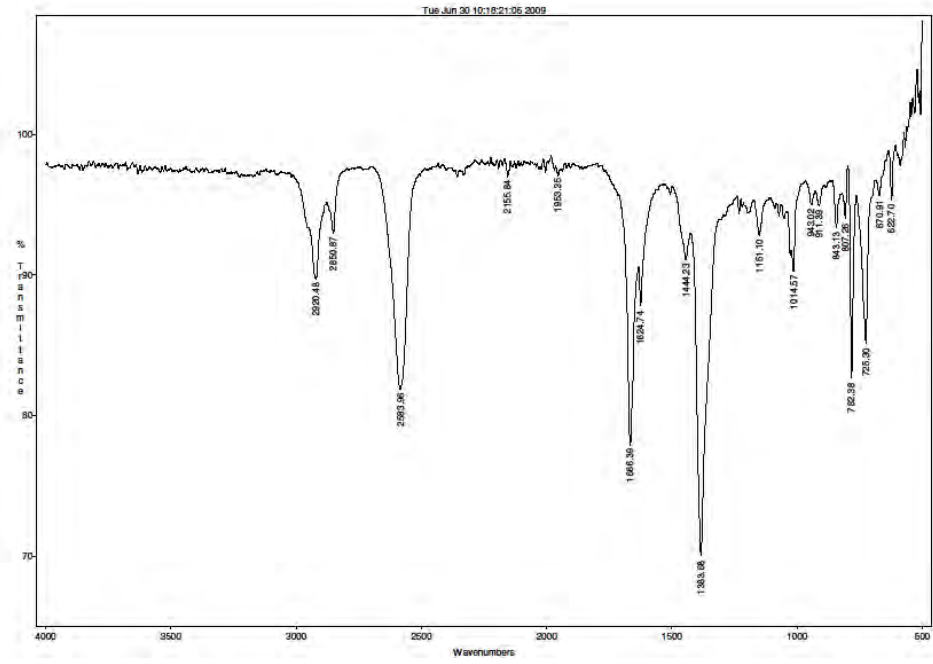
c)



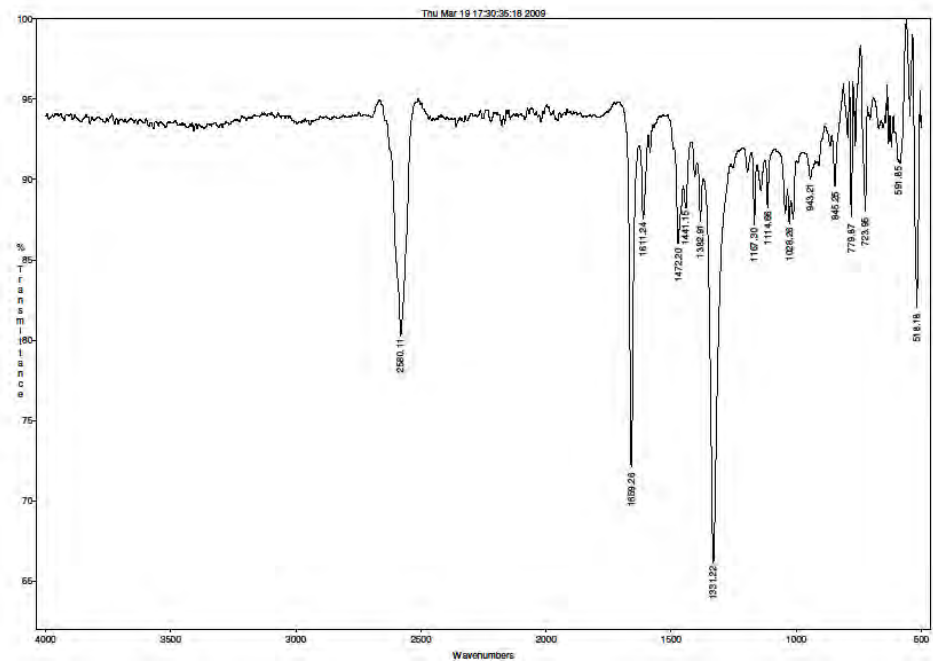
d)



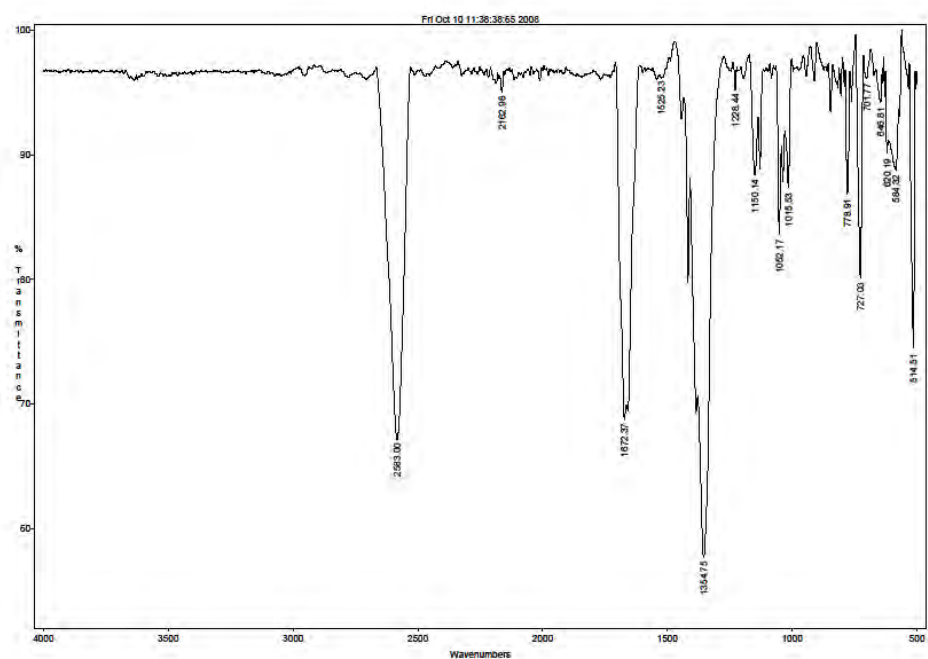
e)



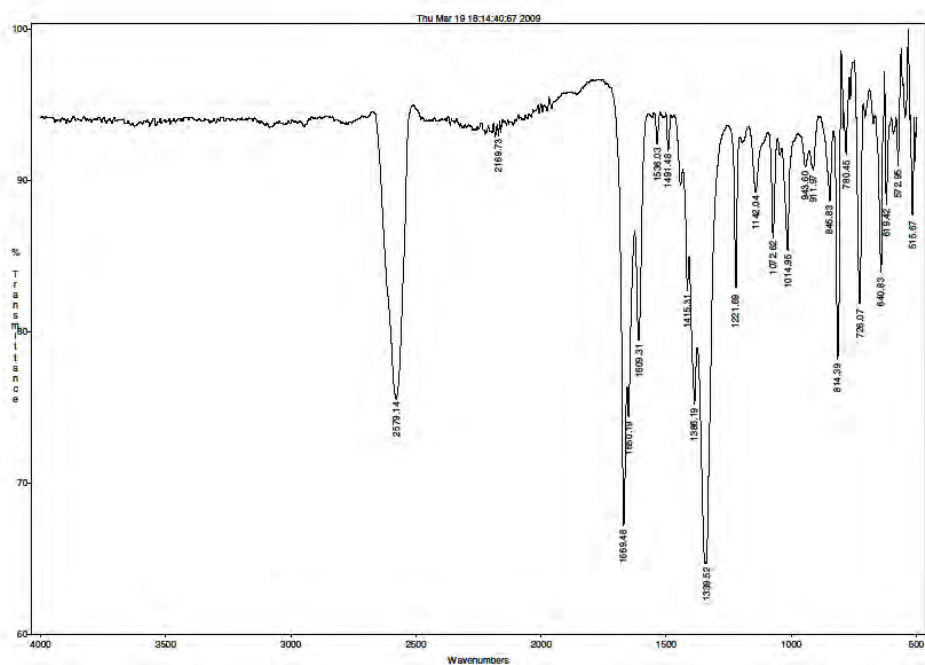
f)



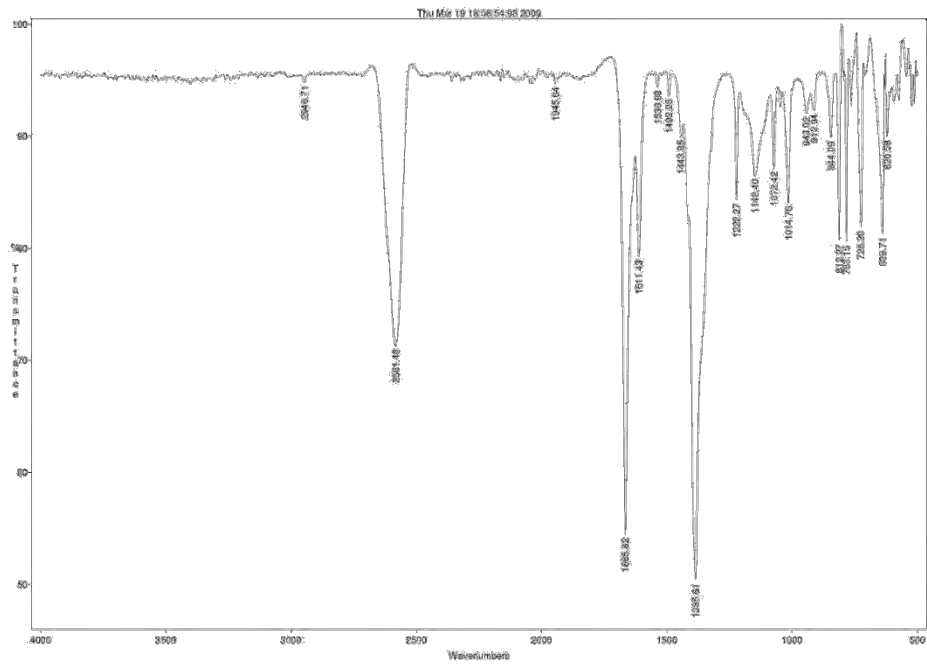
g)



h)



i)



j)

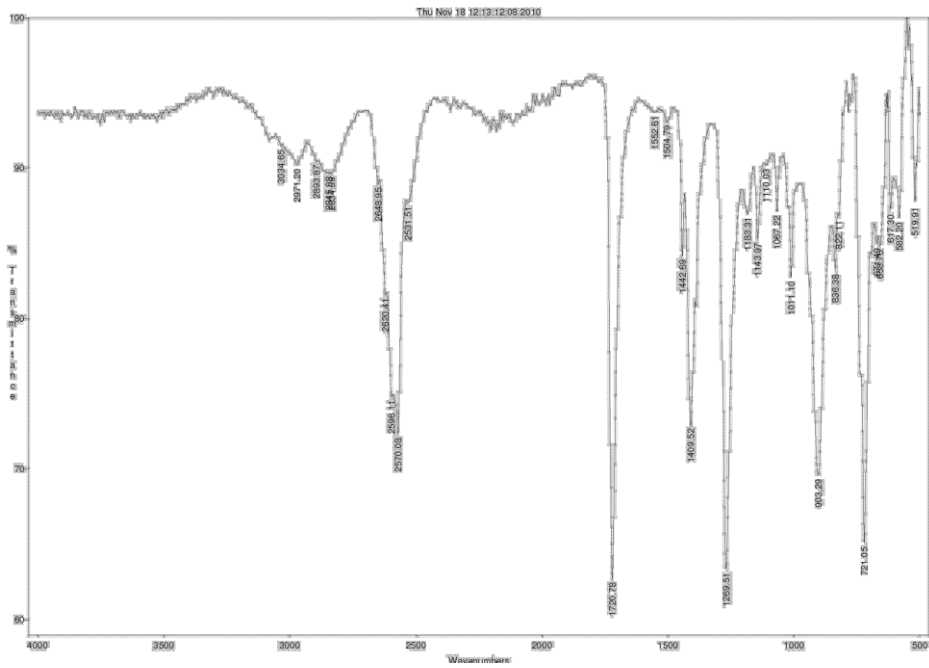
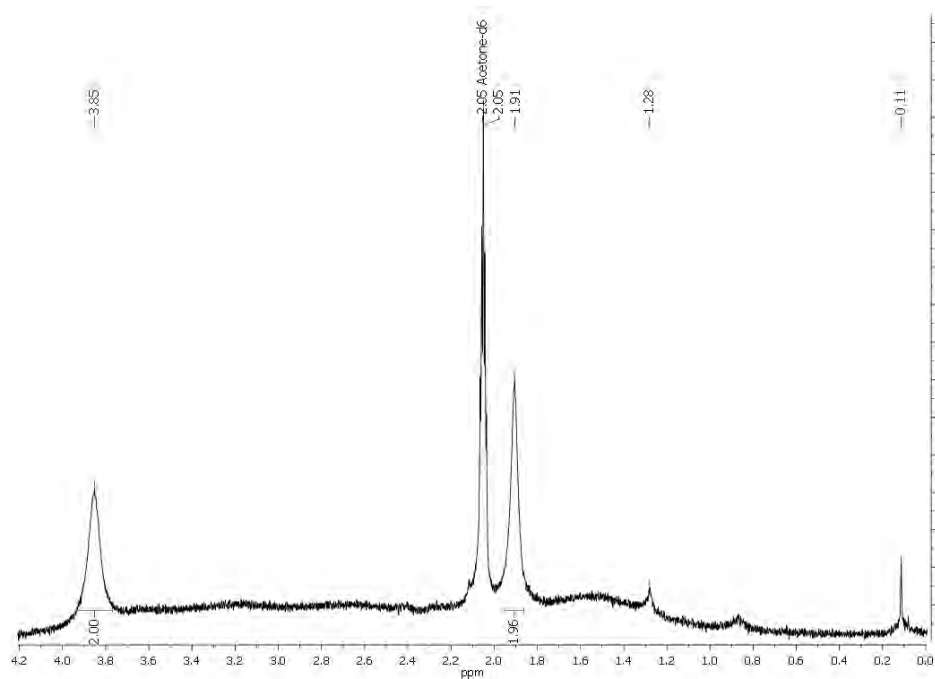


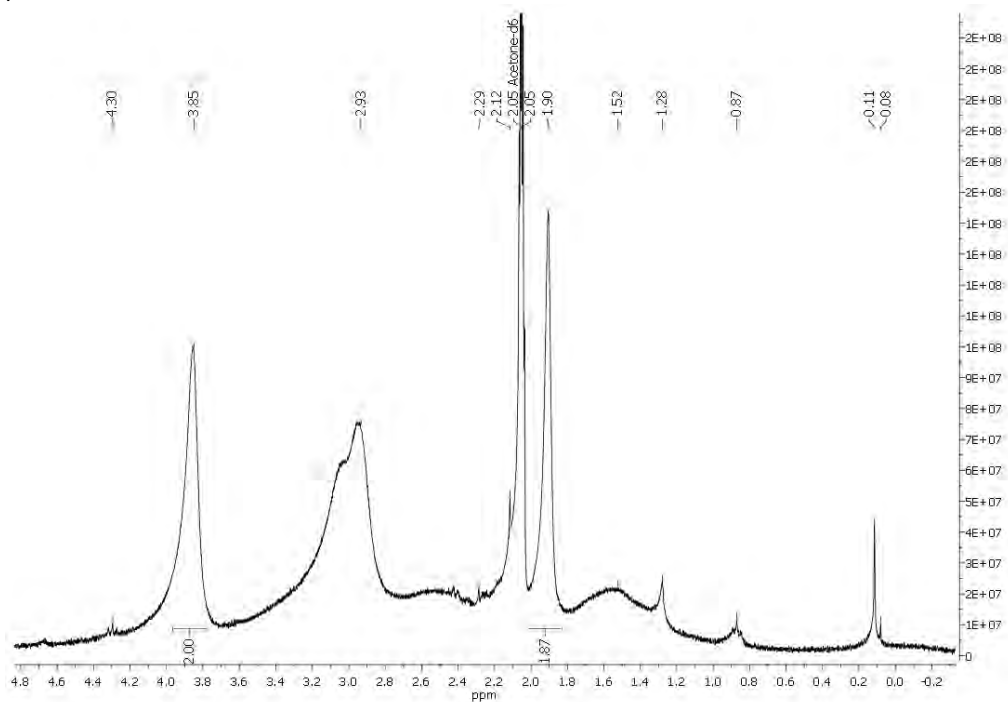
Figure S9. i) ^1H -RMN, ii) $^1\text{H}\{^{11}\text{B}\}$ -RMN, iii) ^{11}B -RMN, iv) $^{11}\text{B}\{^1\text{H}\}$ -RMN, v) ^{13}C -RMN vi) deconvolution of $^{11}\text{B}\{^1\text{H}\}$ spectra of the compounds a) **A1**, b) **A2**, c) **A2'**, d) **A3**, e) **A4**, f) **A6**, g) LH

a)

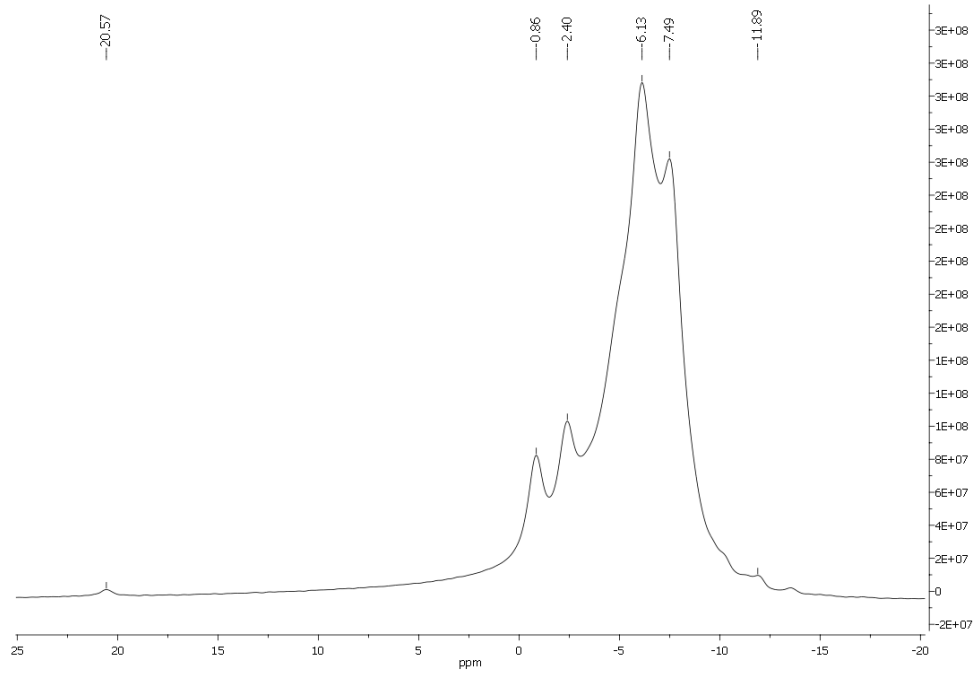
i)



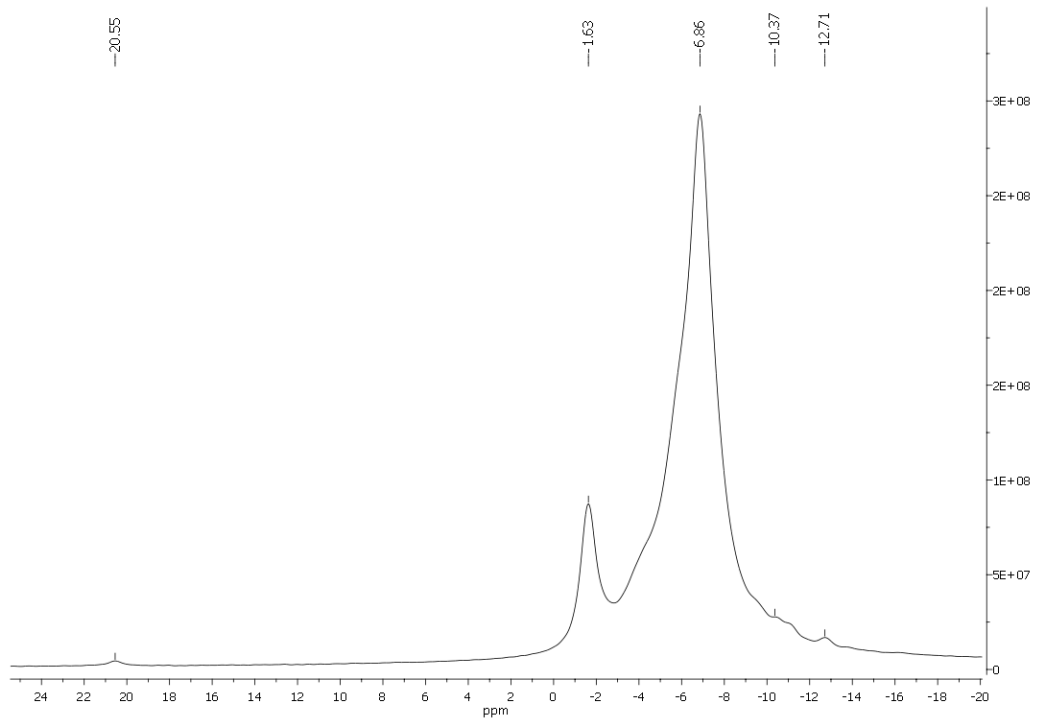
ii)

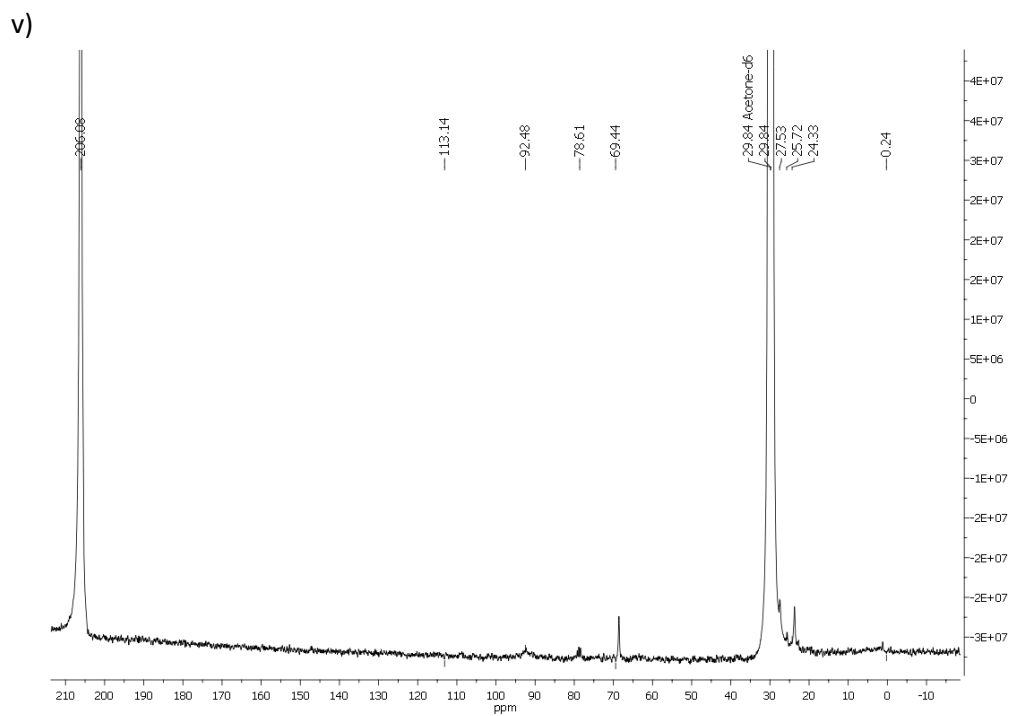


iii)



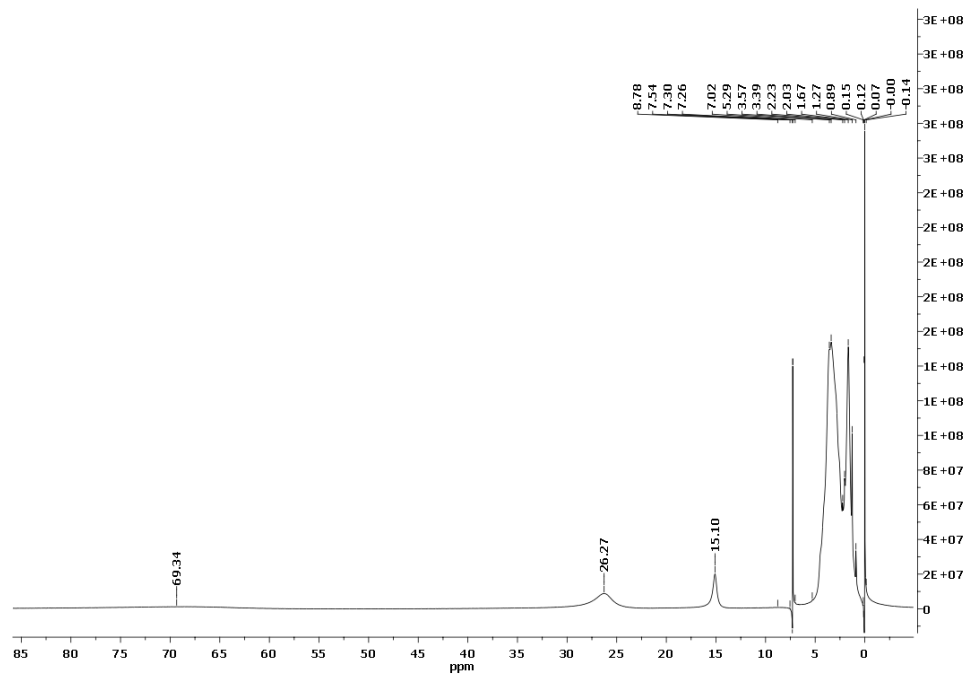
iv)



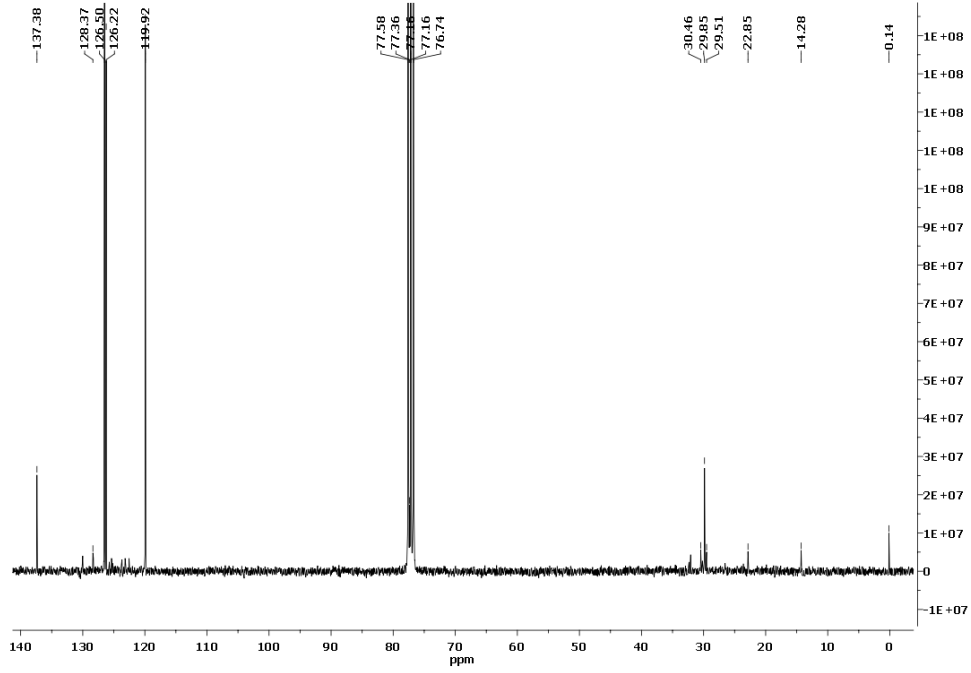


b)

i)

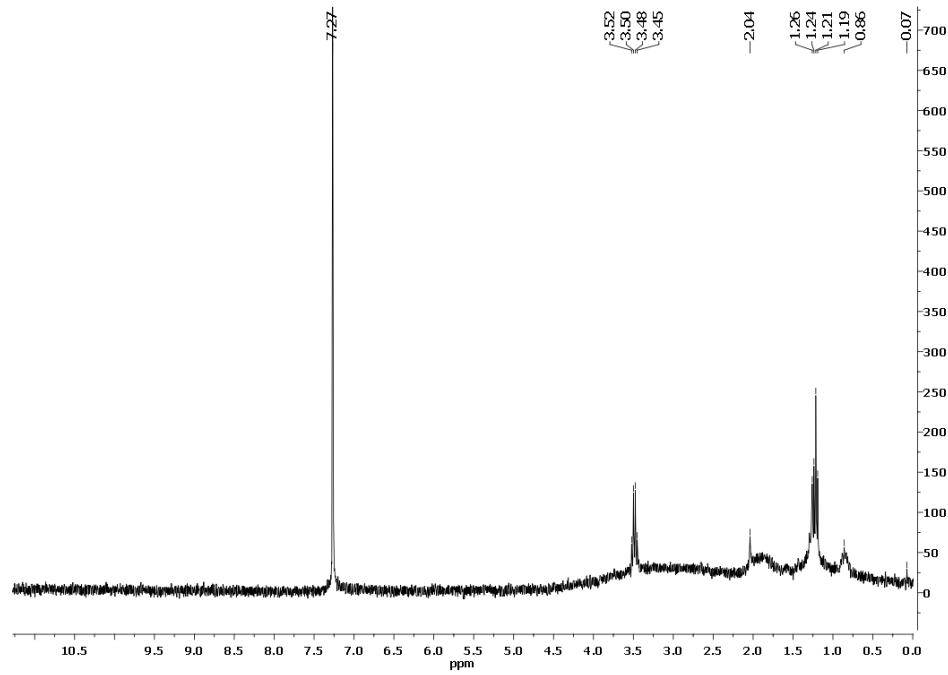


v)

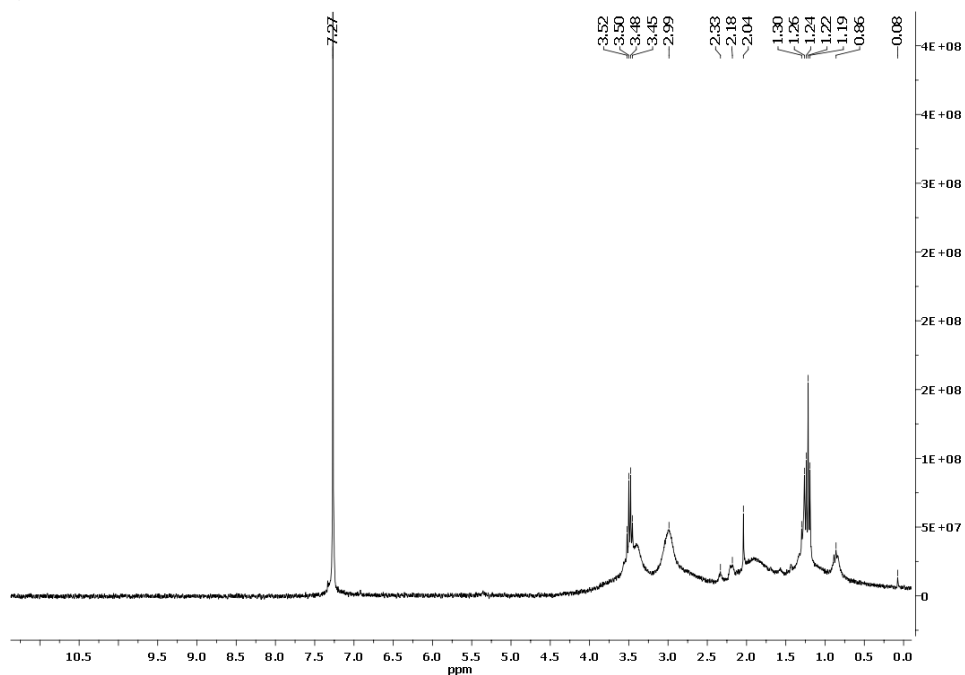


c)

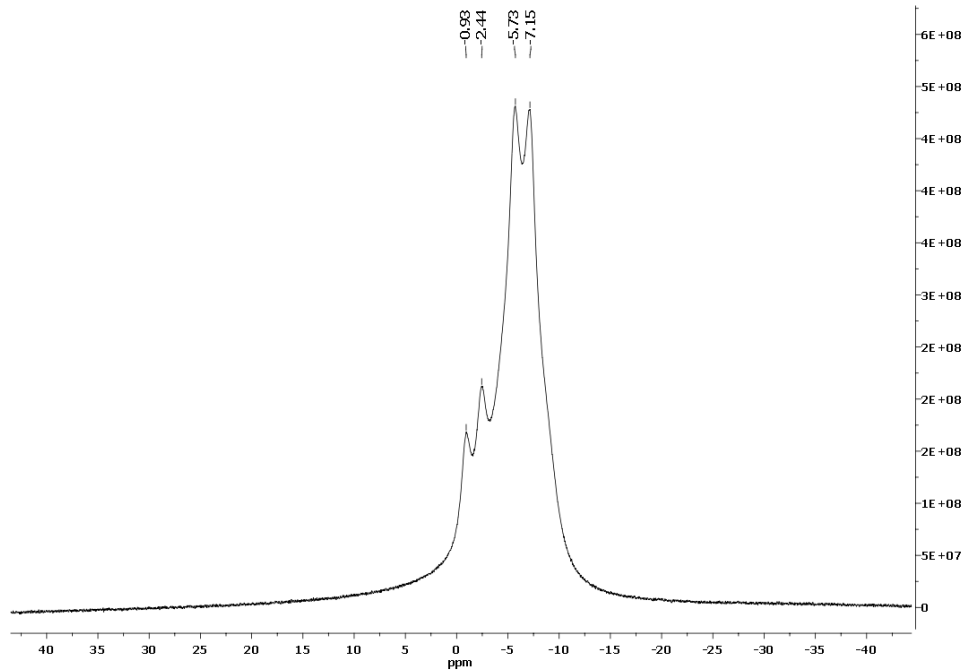
i)



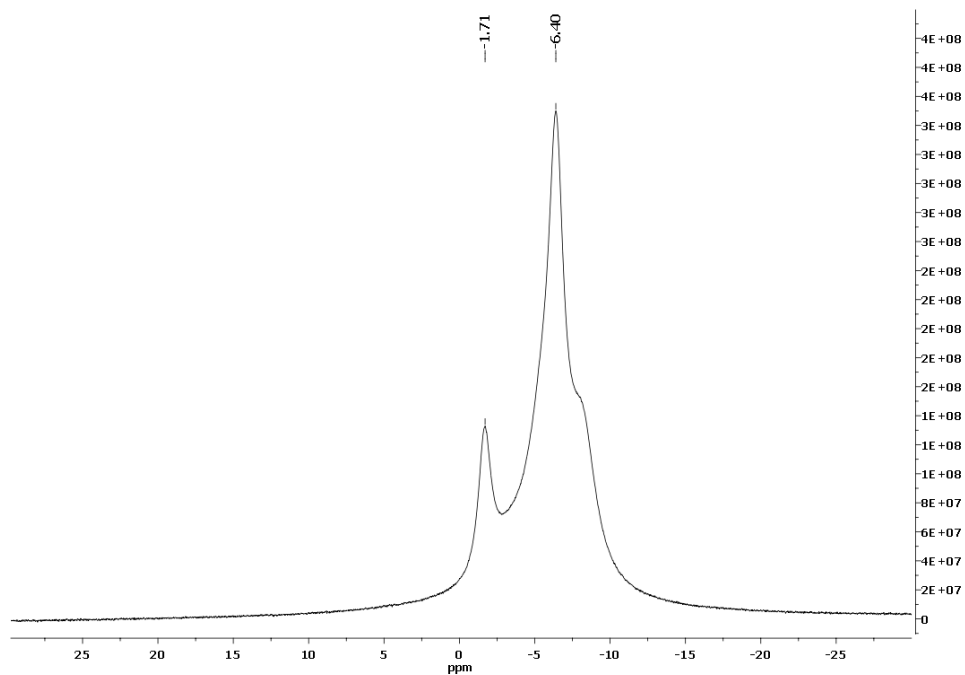
ii)



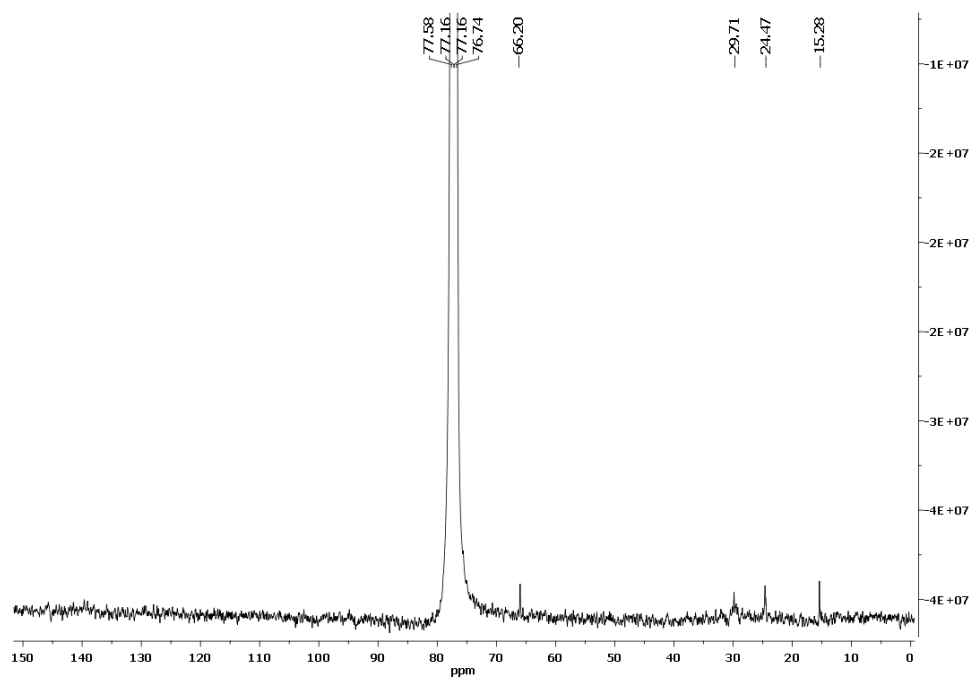
iii)



iv)

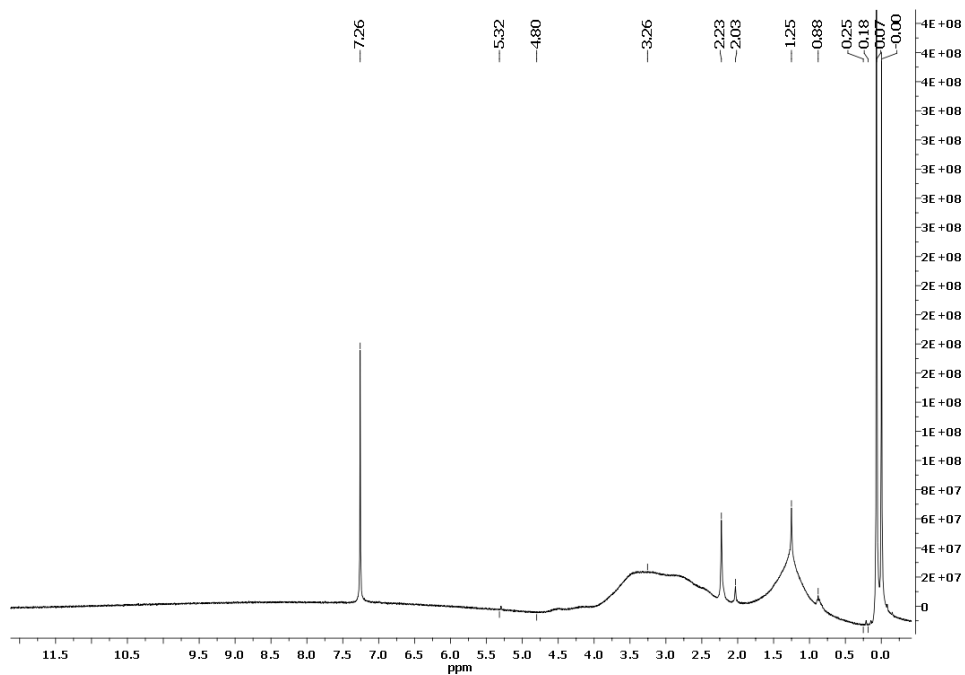


v)

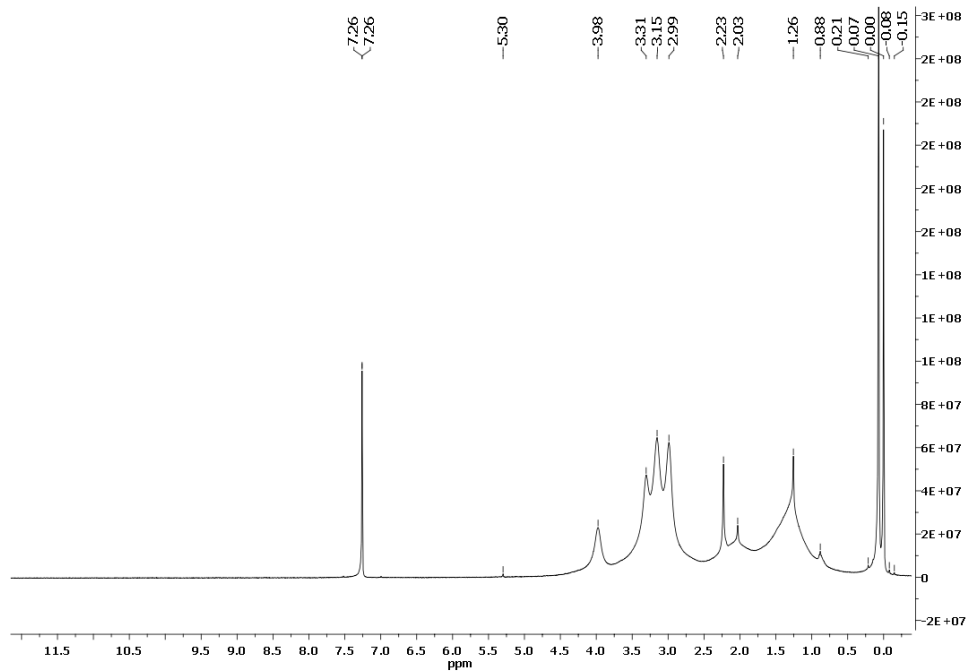


d)

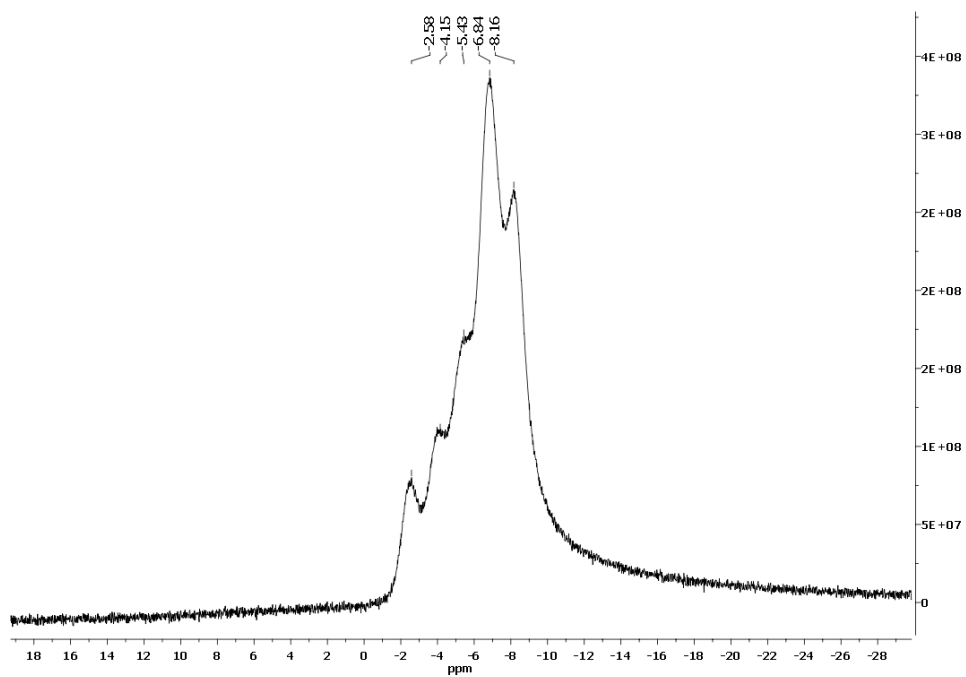
i)



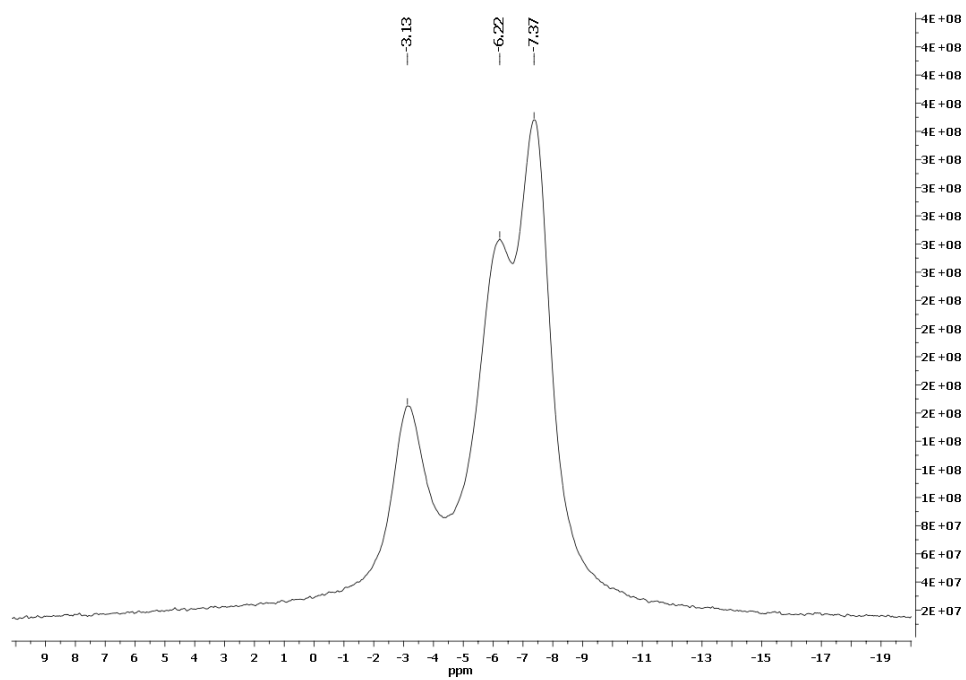
ii)



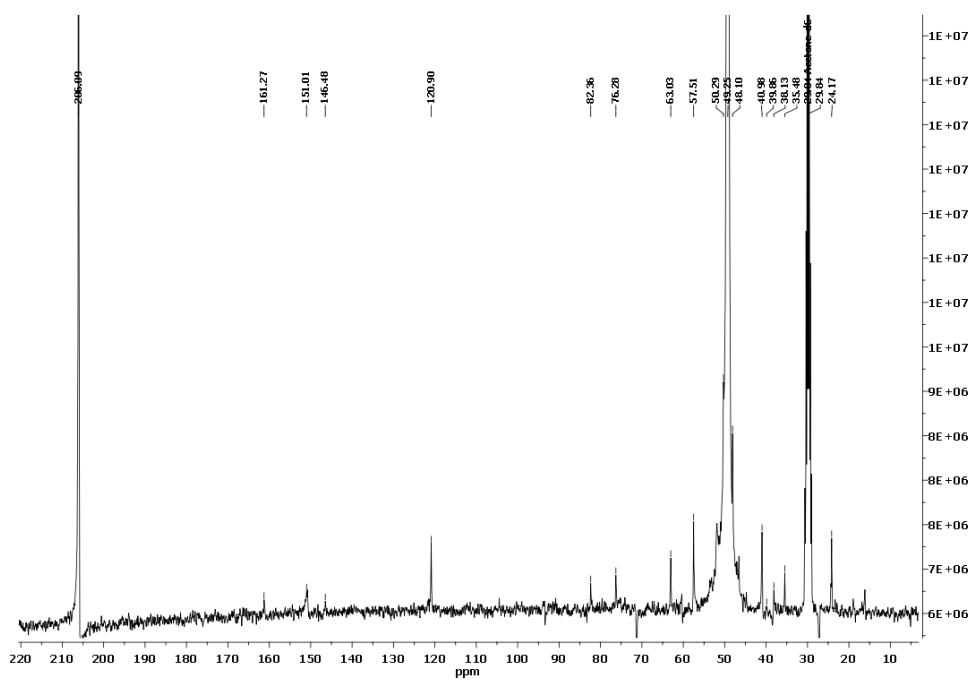
iii)



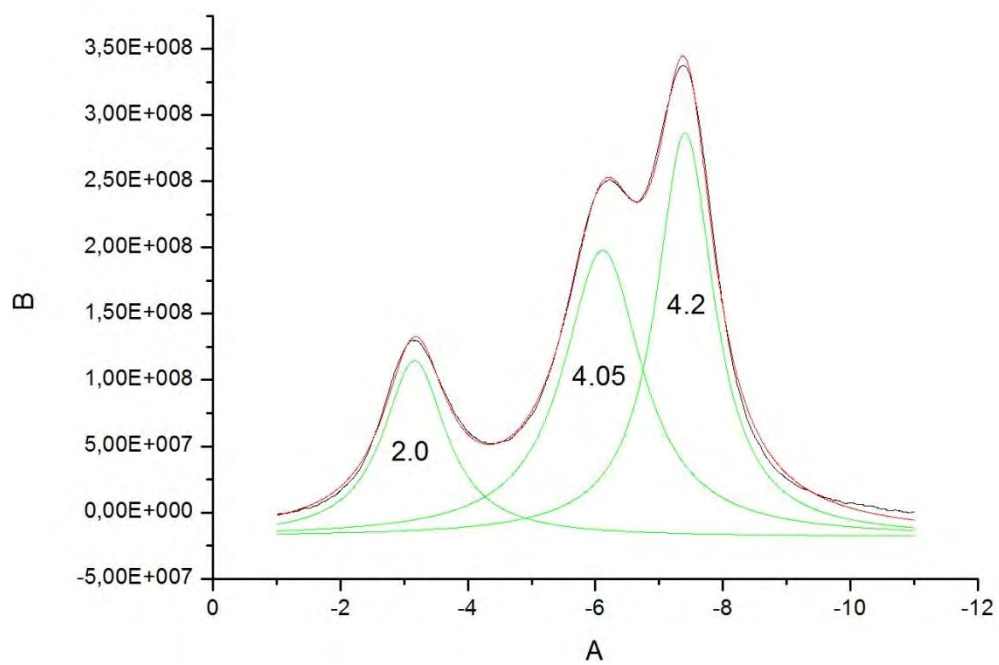
iv)



v)

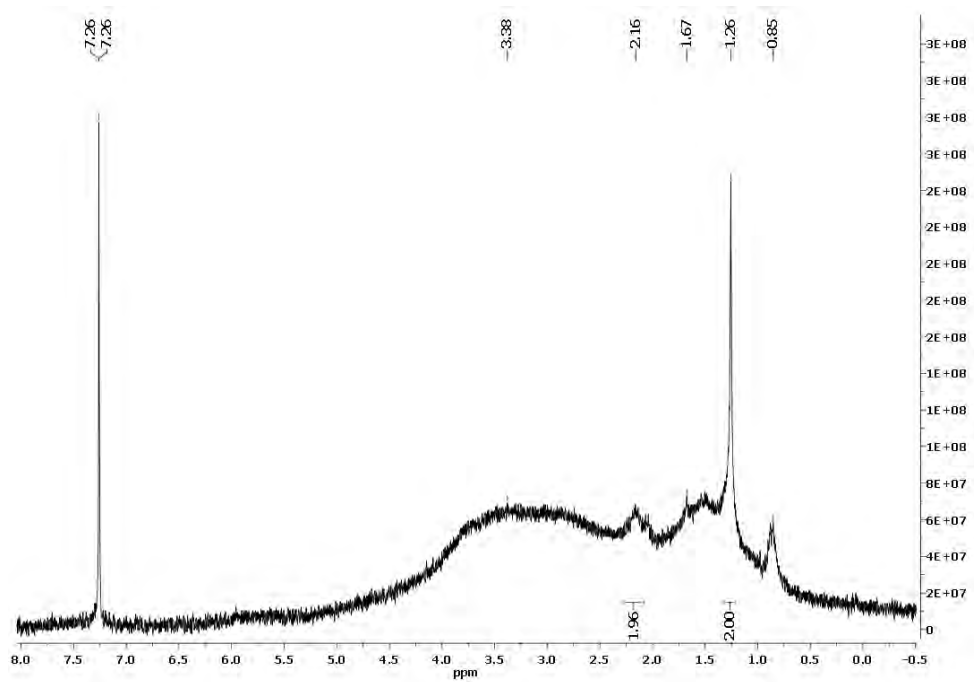


vi)

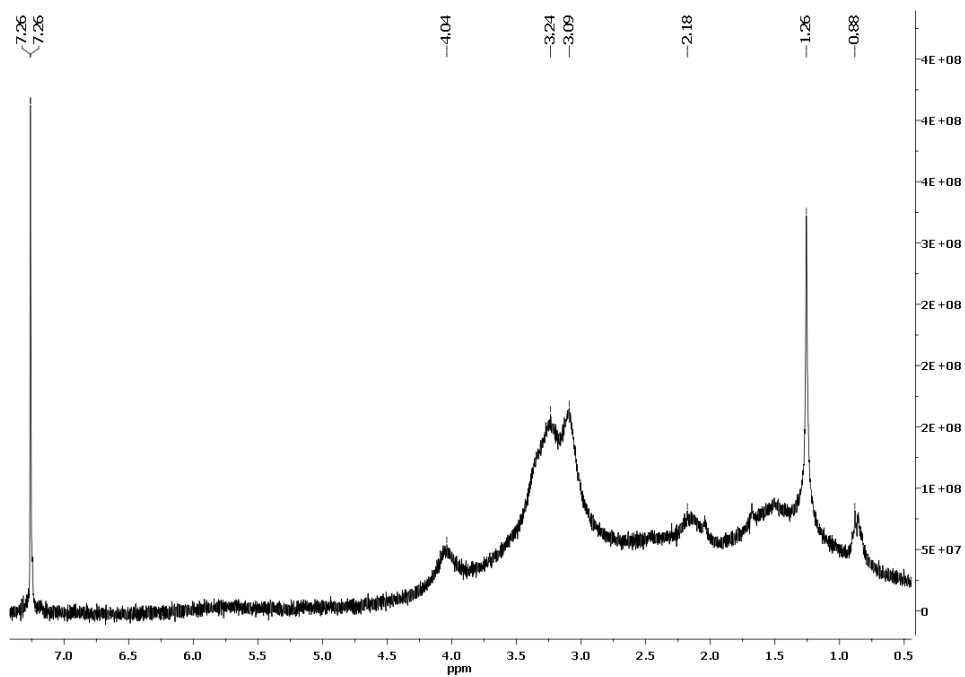


e)

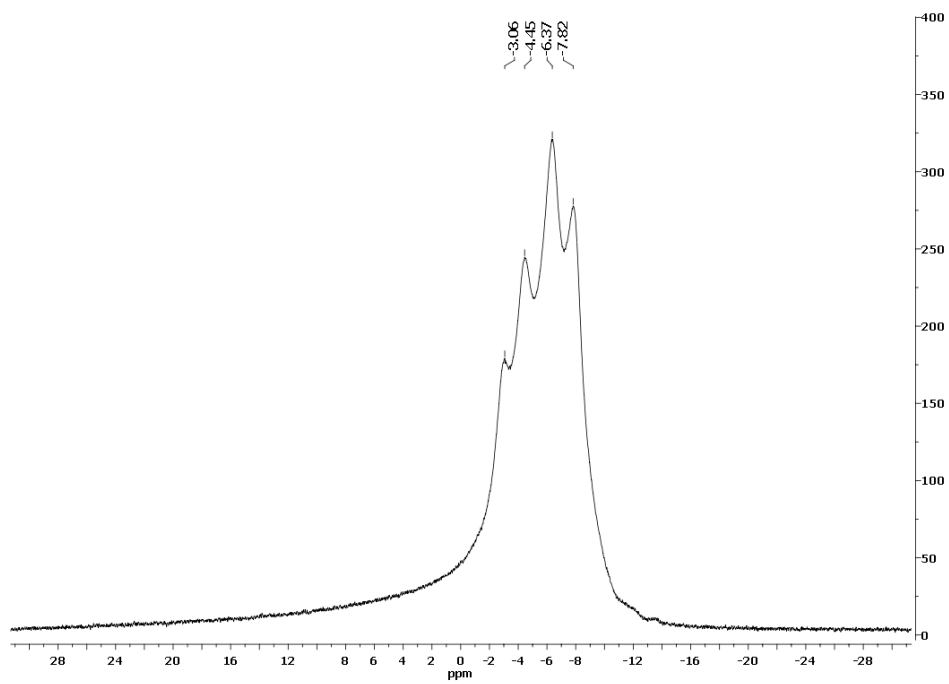
i)



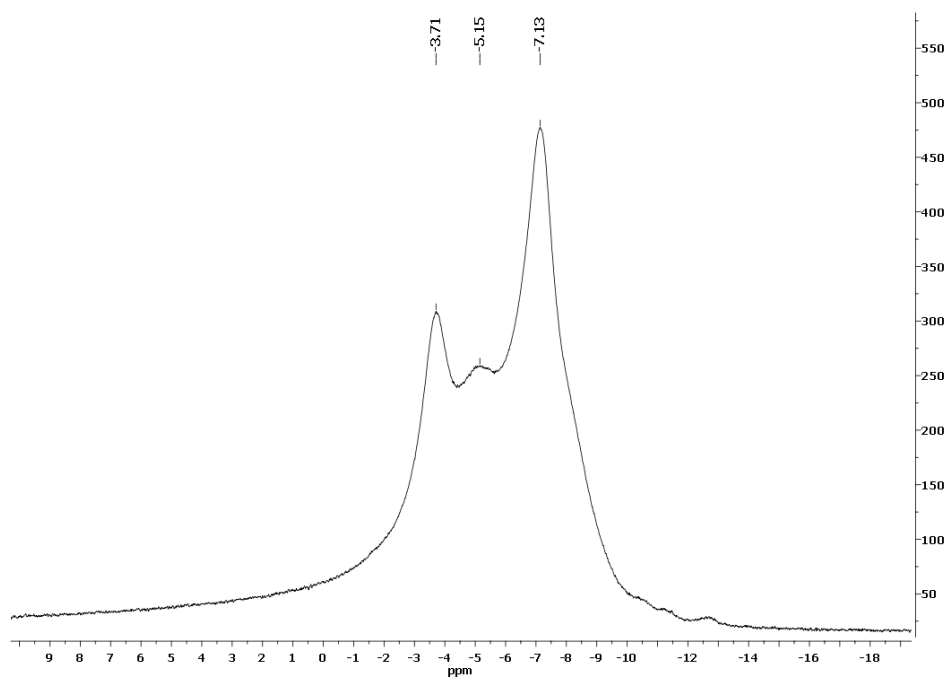
ii)



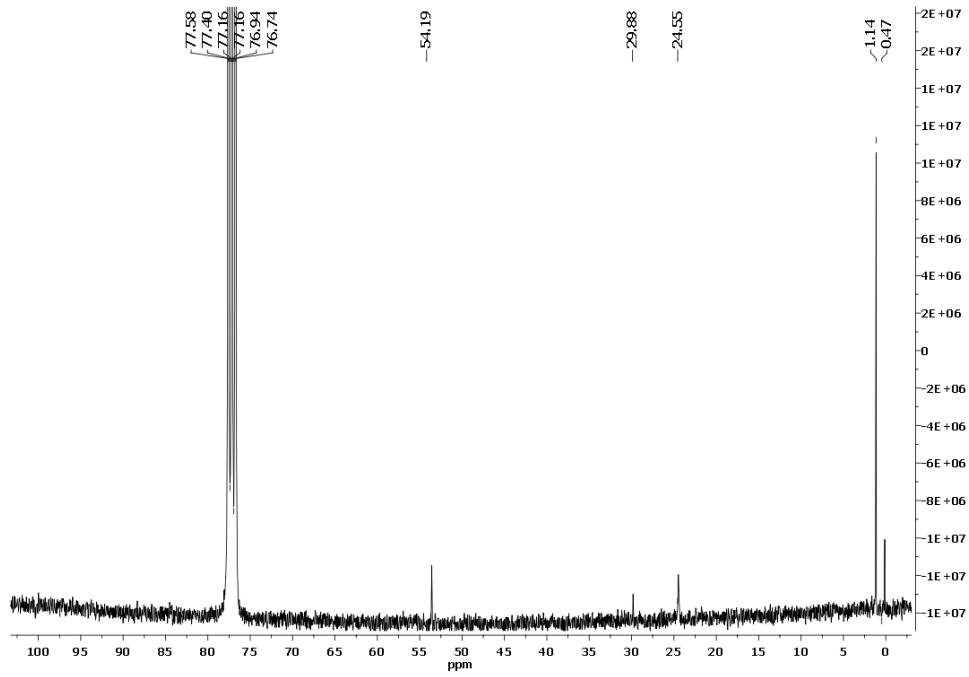
iii)



iv)

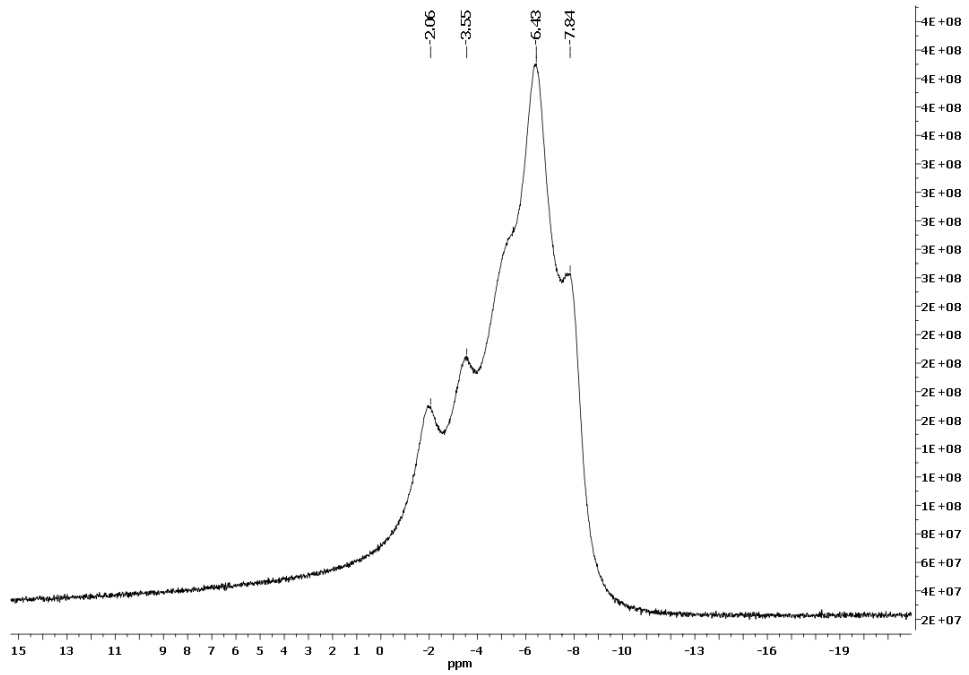


v)

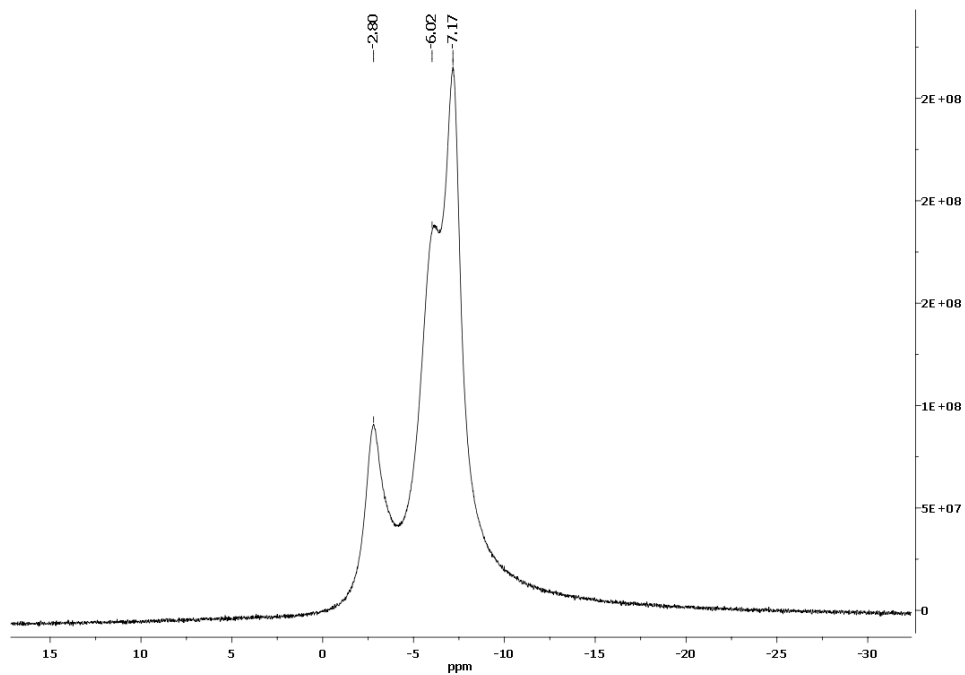


f)

iii)

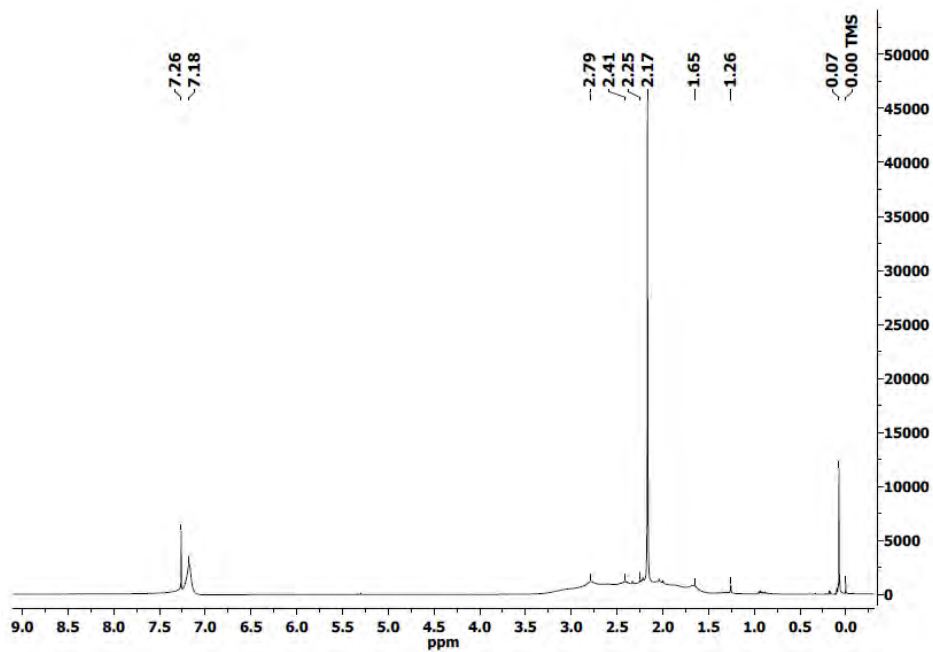


iv)

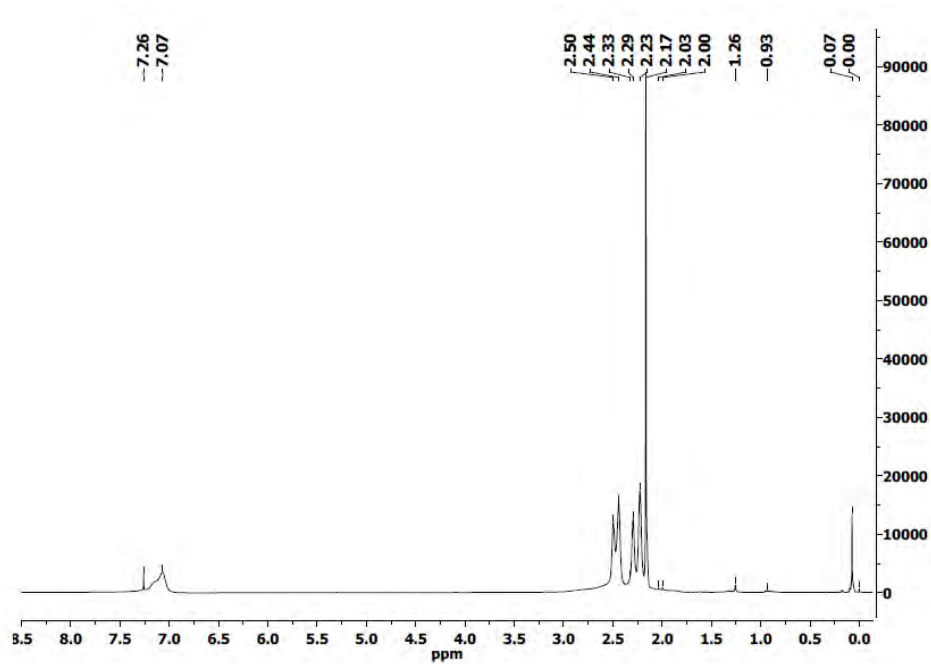


g)

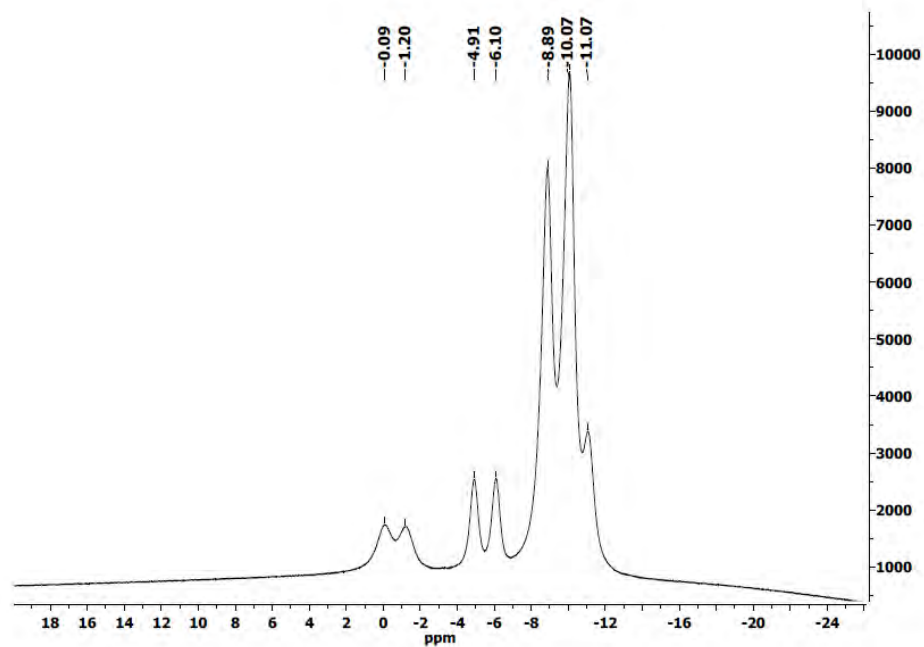
i)



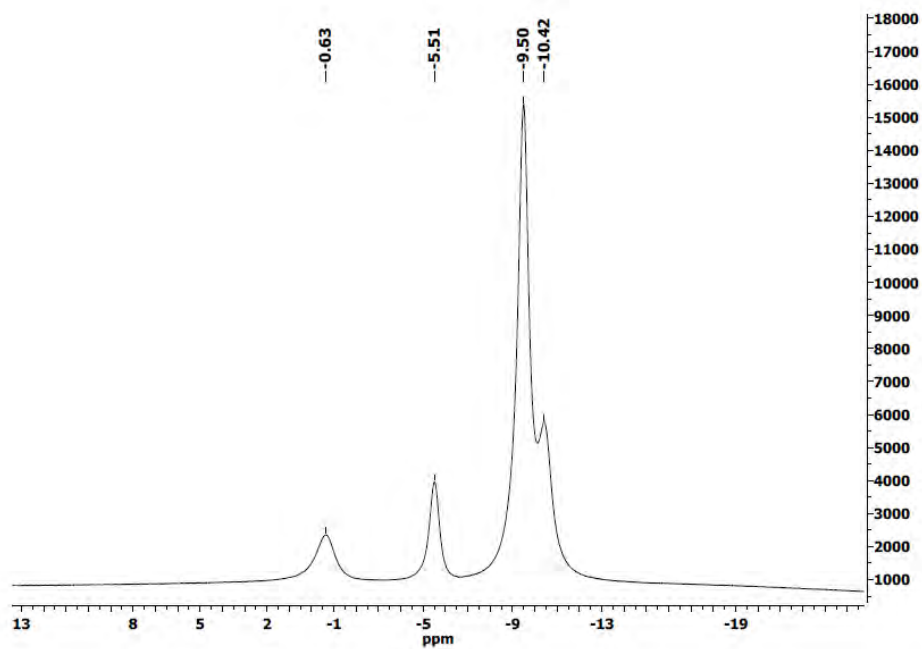
ii)



iii)



iv)



v)

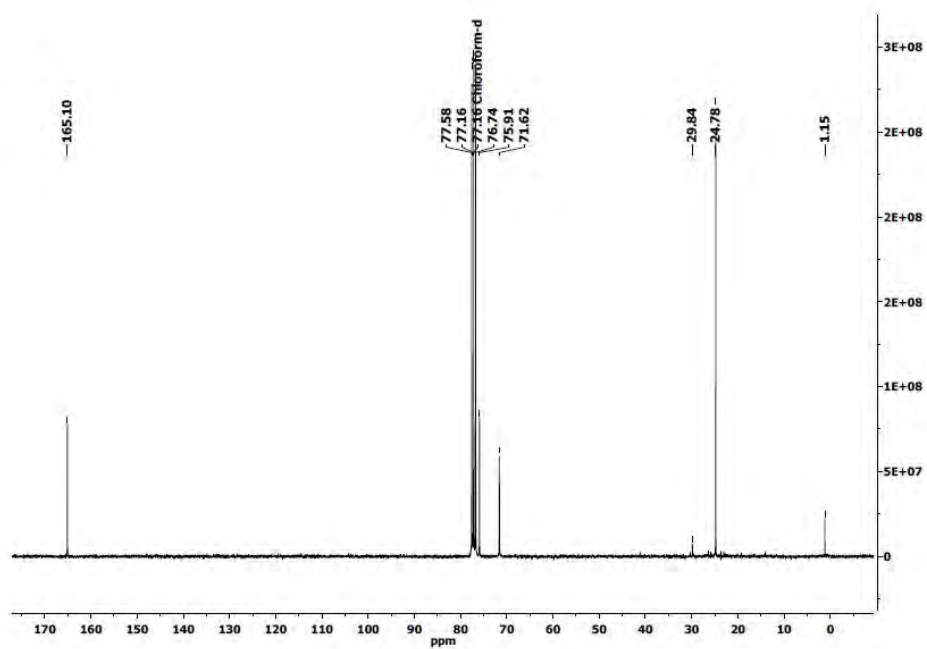


Table S1. Crystal Data for X-ray structures of **A1-A6** and **A8**.

	A1	A2	A3	A4	A5	A6	A8
Empirical formula	C ₂₄ H ₆₈ B ₄₀ O ₁₀ Cu ₂	C ₃₄ H ₈₂ B ₄₀ N ₂ O ₁₀ Cu ₂	C ₂₈ H ₆₀ B ₄₀ F ₆ N ₂ O ₈ Cu ₂	C ₂₈ H ₆₆ B ₄₀ N ₂ O ₈ Cu ₂	C ₂₂ H ₄₄ B ₂₀ N ₂ O ₄ Cu	C ₂₄ H ₆₀ B ₄₀ N ₄ O ₈ Cu ₂	C ₂₂ H ₄₆ B ₂₀ N ₂ O ₆ Cu
Formula weight	1076.26	1238.50	1226.26	1118.31	680.33	1092.24	714.35
Crystal system	Monoclinic	Triclinic	Triclinic	Triclinic	Monoclinic	Monoclinic	Monoclinic
Space group	<i>P</i> 21/ <i>c</i>	<i>P</i> -1	<i>P</i> -1	<i>P</i> -1	<i>P</i> 21/ <i>c</i>	<i>P</i> 21/ <i>n</i>	<i>C</i> 2/ <i>c</i>
a [Å]	10.497(13)	11.589(4)	12.546(9)	10.494(2)	12.623(6)	10.9023(10)	19.182(2)
b [Å]	13.784(17)	12.486(4)	12.619(9)	11.919(3)	11.599(5)	13.1212(12)	11.0983(16)
c [Å]	22.141(19)	13.171(4)	13.329(10)	13.600(2)	14.177(7)	20.1464(19)	18.871(4)
α [°]	90	82.319(5)	68.888(11)	66.308(9)	90	90	90
β [°]	117.29(4)	67.480(5)	65.600(11)	70.011(8)	114.836(7)	90.283(2)	107.964(3)
γ [°]	90	68.329(5)	67.224(11)	72.206(4)	90	90	90
V [Å ³]	2847(6)	1636.0(9)	1721(2)	1435.6(5)	1883.7(15)	2881.9(5)	3821.6(11)
Formula Units/Cell	2	1	1	1	2	2	4
ρ _{calc.} [g cm ⁻³]	1.255	1.257	1.183	1.294	1.199	1.259	1.242
μ [mm ⁻¹]	0.792	0.699	0.674	0.786	0.612	0.783	0.610
R ₁ ^[a] , [I > 2σ(I)]	0.0403	0.0682	0.0756	0.0750	0.0440	0.0577	0.0643
wR ₂ ^[b] [all data]	0.1241	0.1764	0.2136	0.2301	0.1292	0.1489	0.1559

[a] $R_1 = \frac{\sum ||F_o| - |F_c||}{\sum |F_o|}$

[b] $wR_2 = \left[\frac{\sum \{w(F_o^2 - F_c^2)^2\}}{\sum \{w(F_o^2)^2\}} \right]^{1/2}$, where $w = 1/[\sigma^2(F_o^2) + (0.0042P)^2]$ and $P = (F_o^2 + 2F_c^2)/3$

Table S2. Crystal Data for X-ray structures of **A2'**, **A4'** and **A4''**.

	A2'	A4'	A4''
Empirical formula	C ₁₈ H ₃₈ B ₂₀ O ₅ N ₂ Cu	C ₂₀ H ₄₀ B ₂₀ O ₄ N ₂ Cu	C ₅₆ H ₁₂₈ B ₆₀ N ₄ O ₁₆ Cu ₄
Formula weight	642.24	652.28	2016.38
Crystal system	Monoclinic	Monoclinic	Monoclinic
Space group	<i>P</i> 21/ <i>c</i>	<i>P</i> 21/ <i>c</i>	<i>P</i> 21/ <i>c</i>
a [Å]	13.354(3)	13.373(2)	15.552(6)
b [Å]	23.296(5)	22.834(4)	27.087(10)
c [Å]	11.755(2)	11.495(2)	14.463(5)
α [°]	90	90	90
β [°]	92.587(4)	96.417(3)	110.088(6)
γ [°]	90	90	90
V [Å ³]	3653.2(12)	3488.1(10)	5722(4)
Formula Units/Cell	4	4	2
ρ _{calc.} [g cm ⁻³]	1.168	1.242	1.170
μ [mm ⁻¹]	0.629	0.658	0.784
R1 ^[a] , [I > 2σ(I)]	0.0506	0.0651	0.0747
wR2 ^[b] [all data]	0.1441	0.1552	0.2085

[a] $R_1 = \sum ||F_o| - |F_c|| / \sum |F_o|$

[b] $wR_2 = [\sum \{w(F_o^2 - F_c^2)^2\} / \sum \{w(F_o^2)^2\}]^{1/2}$, where $w = 1/[\sigma^2(F_o^2) + (0.0042P)^2]$ and $P = (F_o^2 + 2F_c^2)/3$

Table S3. Selected bond lengths (Å) and angles (°) for complexes **A2'**, **A4'** and **A4''**.

	A2'	A4'		A4''		A4''
Cu(1)-O(1)	1.9514(16)	1.967(3)	Cu(1)-O(1)	2.295(3)	Cu(2)-O(5)	1.972(3)
Cu(1)-O(3)	1.9532(16)	1.985(3)	Cu(1)-O(5)#1	1.981(3)	Cu(2)-O(6)	1.983(3)
Cu(1)-N(2)	2.013(2)	2.005(3)	Cu(1)-O(5)	1.969(3)	Cu(2)-O(2)	1.995(3)
Cu(1)-N(1)	2.019(2)	2.012(3)	Cu(1)-O(3)	1.941(3)	Cu(2)-O(4)	2.206(3)
Cu(1)-O(5)	2.302(2)	2.118(3)	Cu(1)-N(1)	1.986(4)	Cu(2)-N(2)	1.985(4)
O(1)-Cu(1)-O(3)	172.88(7)	175.70(11)	Cu(1)-Cu(1)#1	2.9652(12)	O(5)-Cu(2)-O(6)	95.13(11)
O(1)-Cu(1)-N(2)	89.66(8)	87.27(12)	O(3)-Cu(1)-O(5)#1	169.53(12)	O(5)-Cu(2)-O(2)	88.97(11)
O(3)-Cu(1)-N(2)	90.81(8)	88.58(12)	O(3)-Cu(1)-O(5)	94.30(11)	O(6)-Cu(2)-O(2)	151.18(13)
O(1)-Cu(1)-N(1)	87.96(8)	91.18(12)	O(5)#1-Cu(1)-O(5)	82.72(11)	O(5)-Cu(2)-O(4)	89.66(11)
O(3)-Cu(1)-N(1)	90.28(8)	93.01(12)	O(3)-Cu(1)-O(1)	100.76(12)	O(6)-Cu(2)-O(4)	93.79(13)
N(2)-Cu(1)-N1	169.31(8)	177.43(14)	O(5)#-Cu(1)-O(1)	89.53(11)	O(2)-Cu(2)-O(4)	114.79(12)
O(1)-Cu(1)-O(5)	98.41(8)		O(5)-Cu(1)-O(1)	95.33(11)	N(2)-Cu(2)-O(4)	92.35(13)
O(3)-Cu(1)-O(5)	88.69(8)		O(3)-Cu(1)-N(1)	88.25(13)	N(2)-Cu(2)-O(2)	87.16(14)
N(2)-Cu(1)-O(5)	90.67(8)		O(5)#-Cu(1)-N1	93.05(12)	O(5)-Cu(2)-N(2)	176.11(13)
N(1)-Cu(1)-O(5)	99.99(8)		O(5)-Cu(1)-N1	170.02(13)	O(6)-Cu(2)-N(2)	88.05(14)
			O(1)-Cu(1)-N1	93.66(13)		
			O(3)-Cu(1)-Cu(1)#1	134.97(9)		
			O(5)#-Cu(1)-Cu(1)#1	41.21(7)		
			O(5)-Cu(1)-Cu(1)#1	41.51(7)		
			O(1)-Cu(1)-Cu(1)#1	93.22(8)		
			N(1)-Cu(1)-Cu(1)#1	133.61(10)		

Table S4. Crystal data for the X-ray structure of complex $[\text{Cu}_2(\mu\text{-CH}_3\text{COO})_4(\text{p-CF}_3\text{-py})_2]$

$[\text{Cu}_2(\mu\text{-CH}_3\text{COO})_4(\text{p-CF}_3\text{-py})_2]$	
Empirical formula	$\text{C}_{20}\text{H}_{20}\text{N}_2\text{O}_8\text{F}_6\text{Cu}_2$
Formula weight	657.46
Crystal system	Orthorhombic
Space group	Cccm
a [Å]	14.3204(11)
b [Å]	19.5305(14)
c [Å]	19.6511(14)
α [°]	90
β [°]	90
γ [°]	90
V [Å ³]	5496.1(7)
Formula Units/Cell	8
$\rho_{\text{calc.}}$ [g cm ⁻³]	1.589
μ [mm ⁻¹]	1.632
$R_1^{[a]}$, [I > 2 σ (I)]	0.0377
$wR_2^{[b]}$ [all data]	0.1014

[a] $R_1 = \sum ||F_o| - |F_c|| / \sum |F_o|$

[b] $wR_2 = [\sum \{w(F_o^2 - F_c^2)^2\} / \sum \{w(F_o^2)^2\}]^{1/2}$, where $w = 1 / [\sigma^2(F_o^2) + (0.0042P)^2]$ and $P = (F_o^2 + 2F_c^2) / 3$

CHAPTER IV. Mn(II) complexes containing the carboranylcarboxylate ligand 1-CH₃-2-CO₂H-1,2-closo-C₂B₁₀H₁₀: a water soluble Mn(II) polymer with aqua metal bridges and its derivatives.

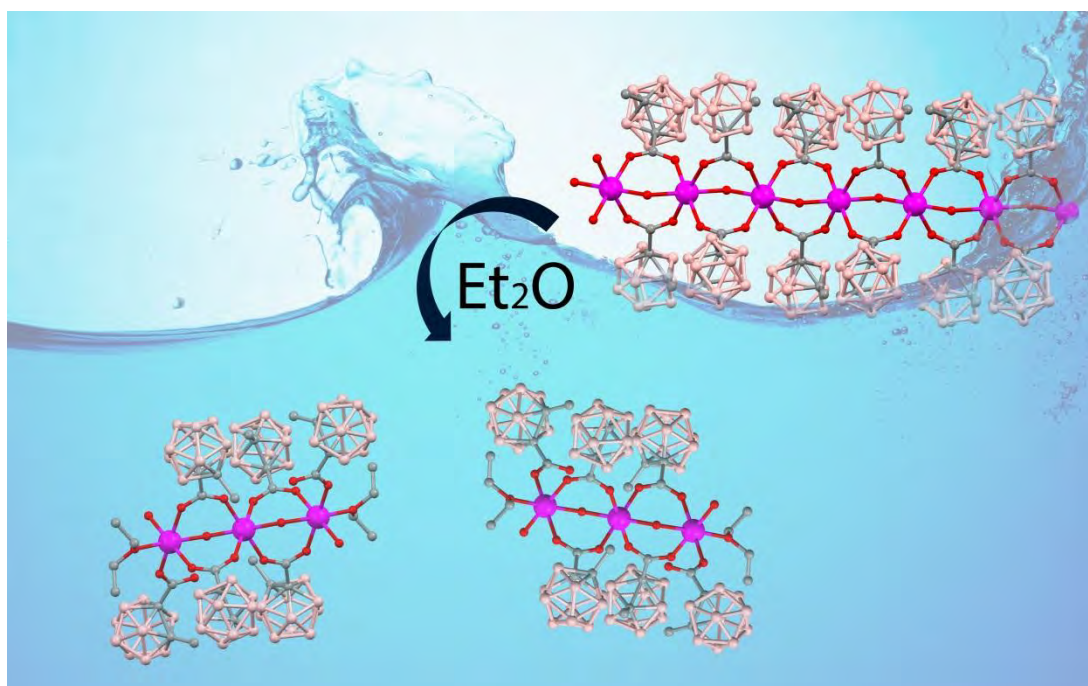


Table S1. Crystal Data for X-ray structures of **B1-B5**

	B1	B2	B3	B4	B5
Empirical formula	C ₈ H ₃₀ B ₂₀ O ₆ Mn	C ₄₈ H ₁₄₆ B ₆₀ O ₂₂ Mn ₃	C ₃₆ H ₆₈ B ₄₀ N ₄ O ₈ Mn ₂	C ₂₈ H ₄₂ B ₂₀ N ₄ O ₄ Mn	C ₁₈ H ₃₈ B ₂₀ N ₄ O ₅ Mn
Formula weight	491.44	1889.07	1227.22	769.80	661.66
Crystal system	Orthorhombic	Triclinic	Triclinic	Triclinic	Triclinic
Space group	Pna21	P-1	P-1	P-1	P-1
a [Å]	13.21(2)	14.5473(14)	11.4996(13)	13.423(2)	10.900(5)
b [Å]	28.04(4)	14.7700(14)	12.4097(13)	15.840(2)	12.004(6)
c [Å]	7.569(12)	15.5876(15)	13.7823(15)	20.982(3)	14.857(7)
α [°]	90	63.6570(10)	67.880(2)	92.319(3)	66.825(7)
β [°]	90	74.414(2)	65.446(2)	103.205(3)	81.032(8)
γ [°]	90	67.632(2)	71.870(2)	105.239(3)	71.370(8)
[Å ³]	2804(8)	2755.4(5)	1629.1(3)	4166.5(10)	1692.4(14)
Formula Units/Cell	4	1	1	4	2
ρ _{calc.} [g cm ⁻³]	1.164	1.138	1.251	1.227	1.298
μ [mm ⁻¹]	0.493	0.392	0.436	0.356	0.428
R1 ^[a] , [I > 2σ(I)]	0.0788	0.0625	0.0630	0.0729	0.0786
wR2 ^[b] [all data]	0.1943	0.1821	0.1996	0.2145	0.2523

$$[a] R_1 = \frac{\sum ||F_o| - |F_c||}{\sum |F_o|}$$

$$[b] wR_2 = \left[\frac{\sum \{w(F_o^2 - F_c^2)^2\}}{\sum \{w(F_o^2)\}} \right]^{1/2}, \text{ where } w = 1/[\sigma^2(F_o^2) + (0.0042P)^2] \text{ and } P = (F_o^2 + 2F_c^2)/3$$

Figure S1. X-ray structure of **B2** showing the intramolecular and intermolecular hydrogen bonds.

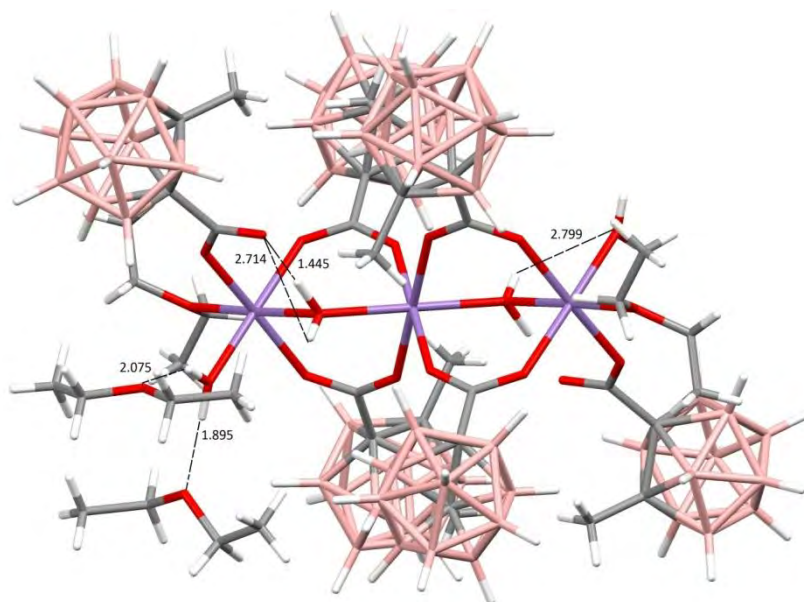
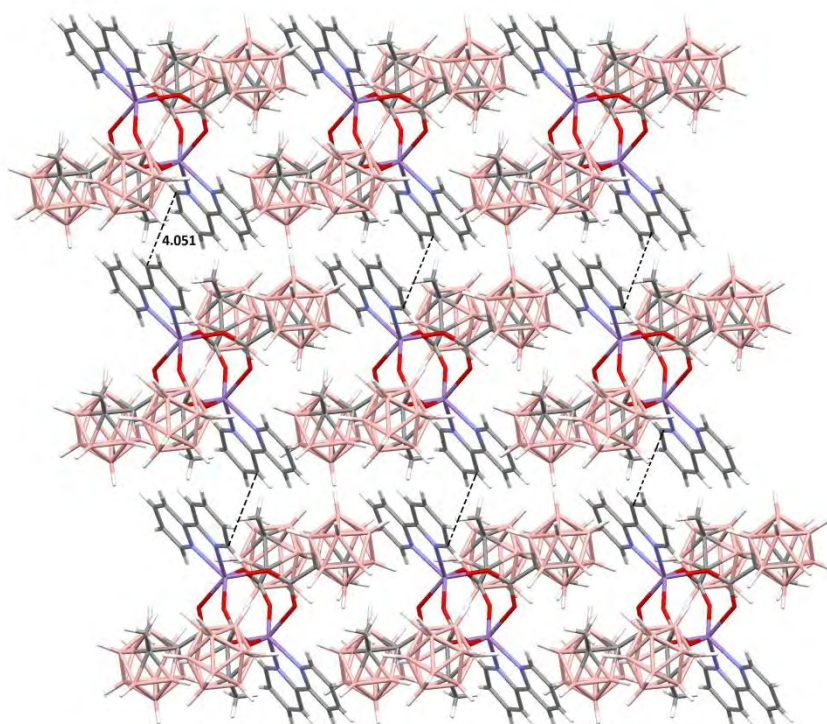


Figure S2. Packing structure of a) **B3** showing the $\pi \cdots \pi$ stacking interactions between the 2,2'-bpy ligands of adjacent molecules b) **B5** along *a* axis.

a)



b)

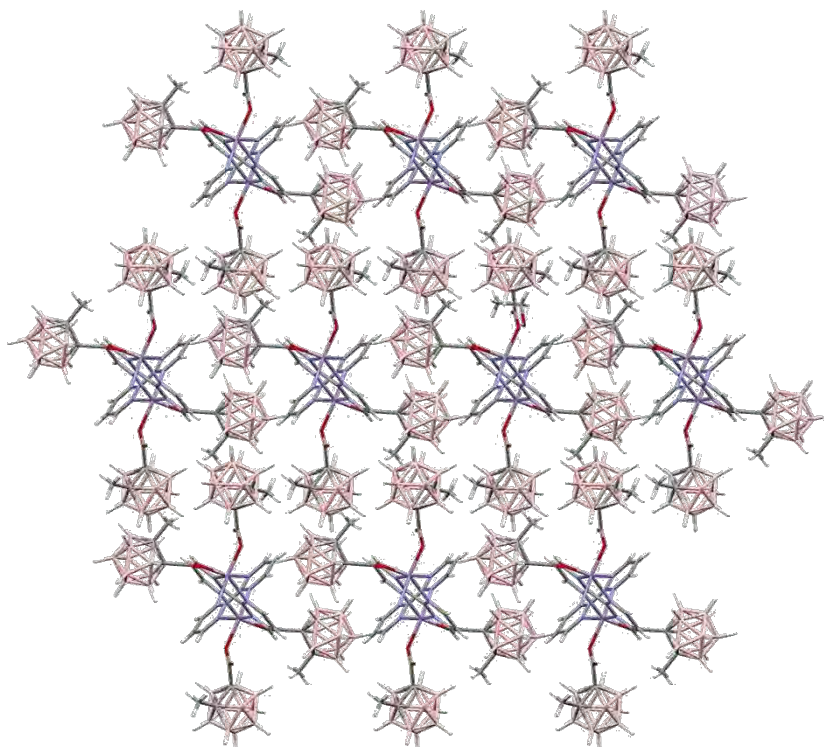


Figure S3. X-ray structure of **B5** showing the hydrogen bond with the ethanol crystallization molecule

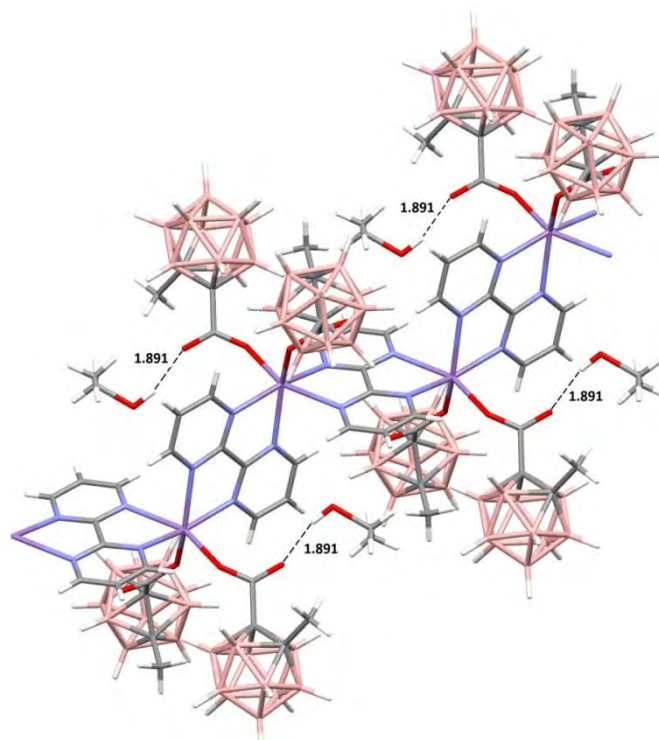
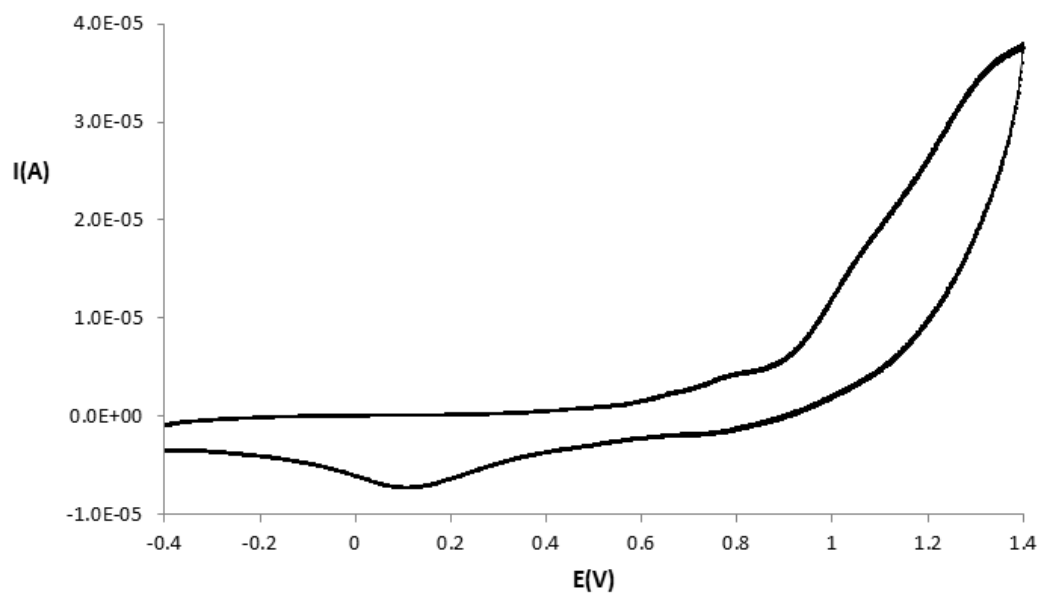


Figure S4. CV of a solution of a) complex **B3** in MeOH +0.1M NH_4ClO_4 , b) **B4** (black) in CH_2Cl_2 + 0.1 M TBAH, at a graphite electrode (2 mm diameter); scan rate:100mV/s.

a)



b)

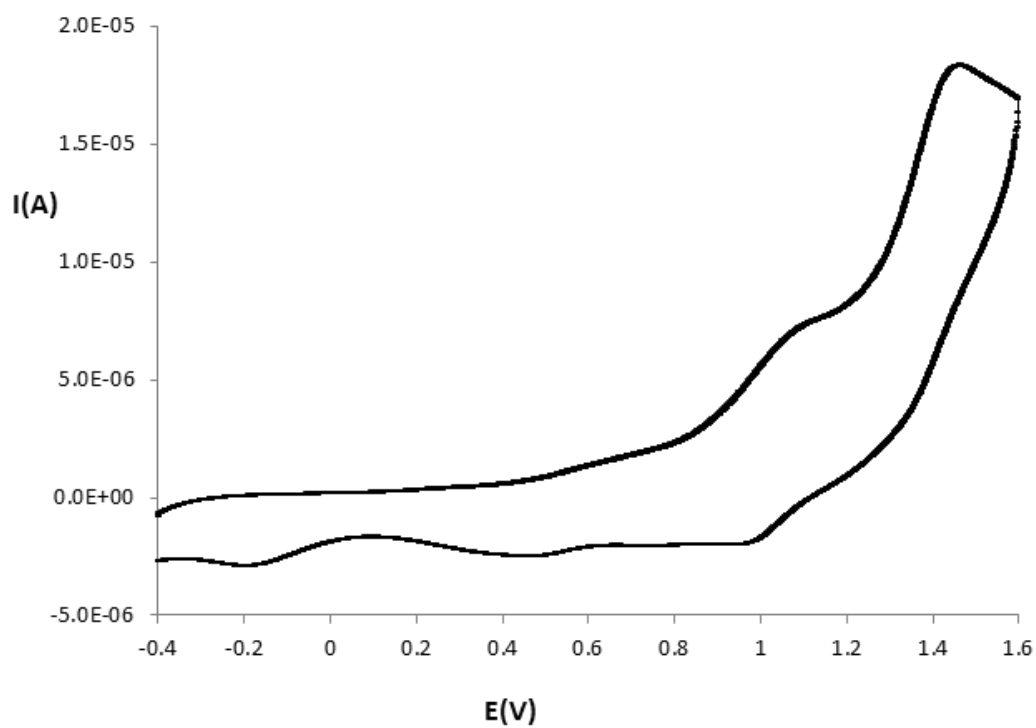
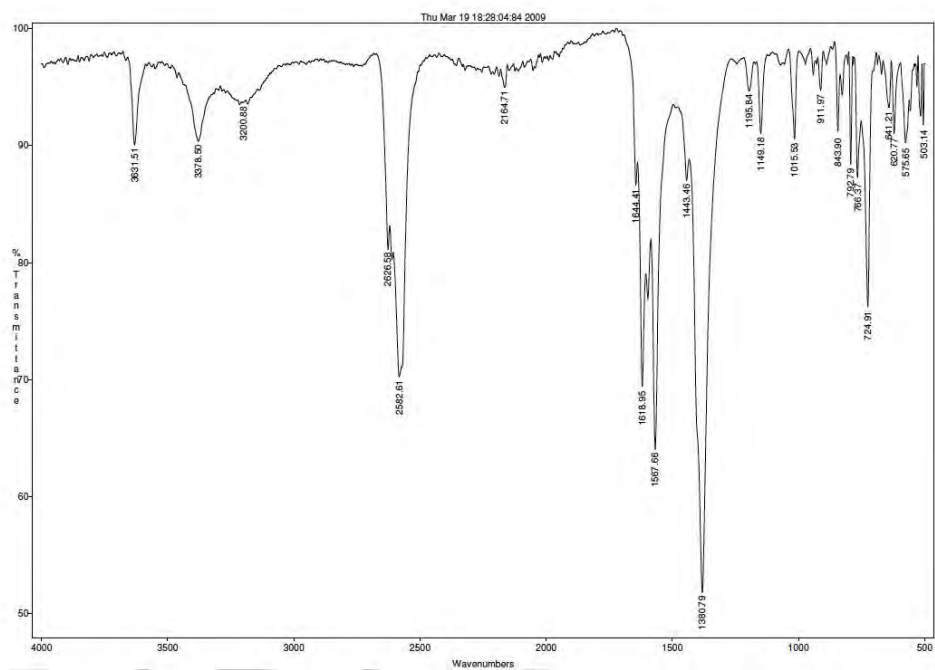
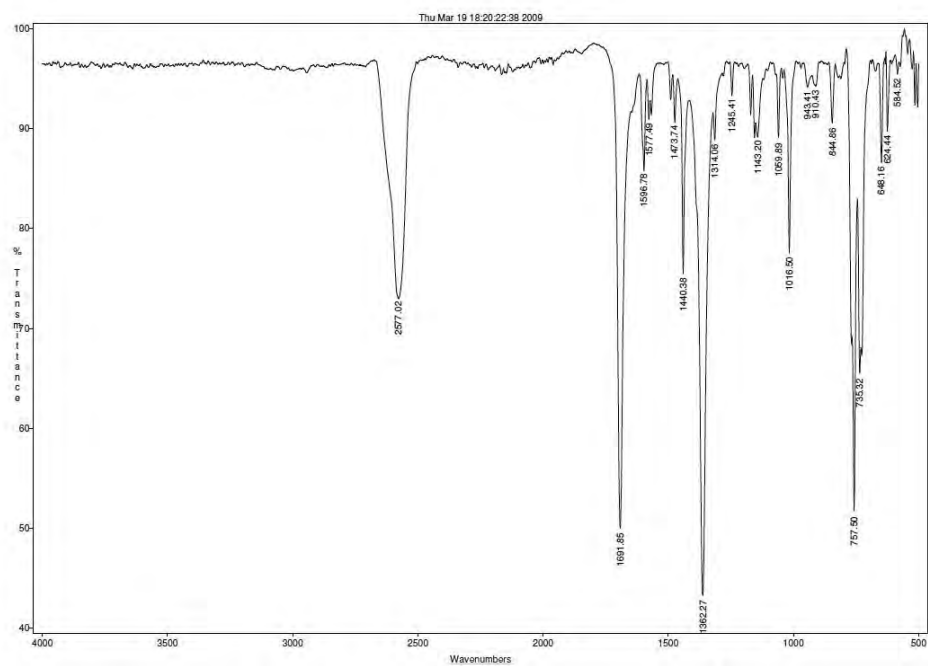


Figure S5. IR spectrum of the compounds a) B1, b) B3, c) B4, d) B5.

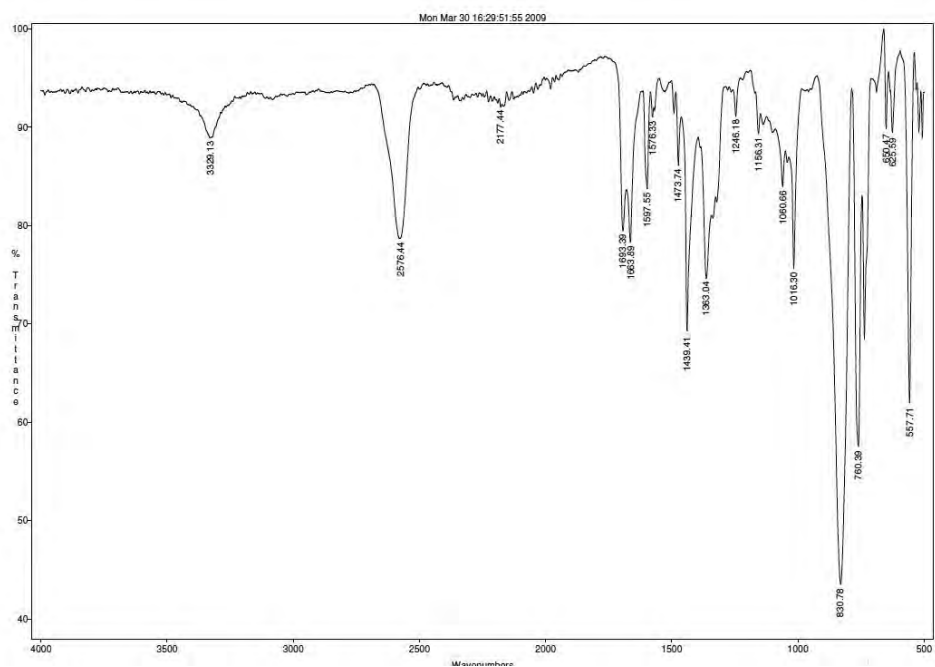
j)



k)



l)



m)

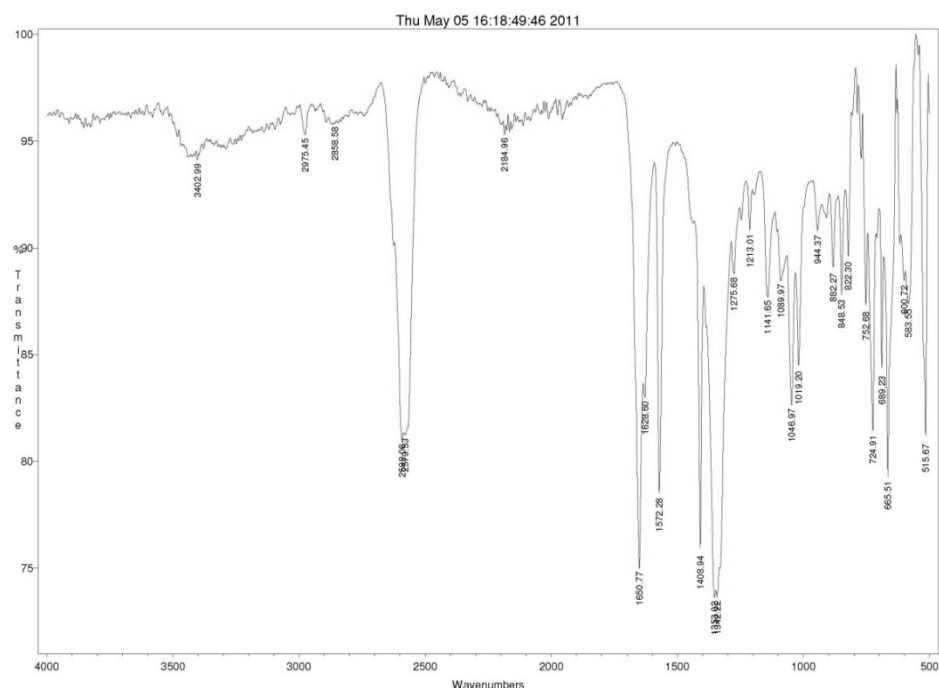
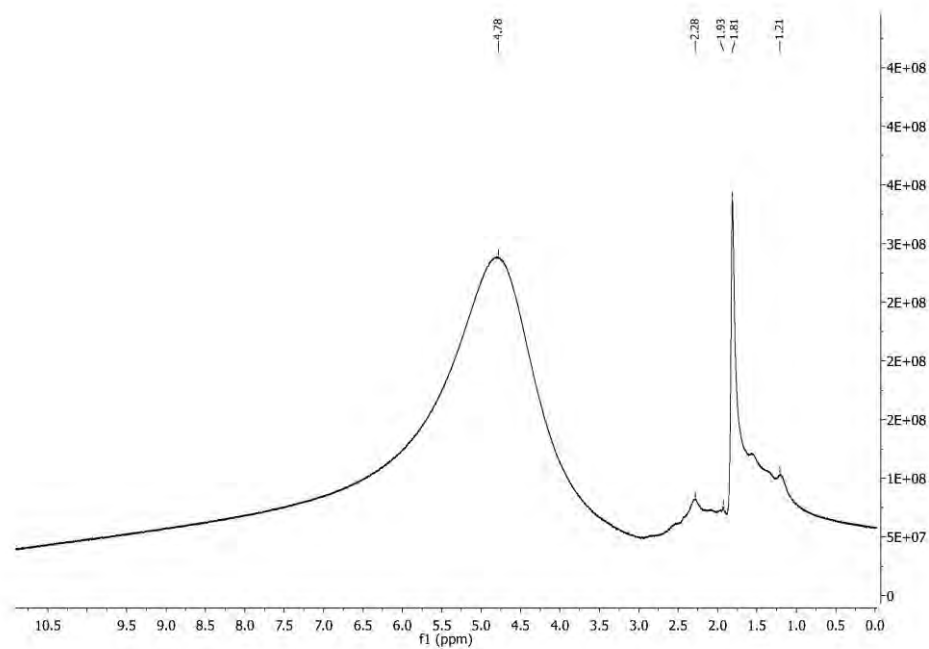


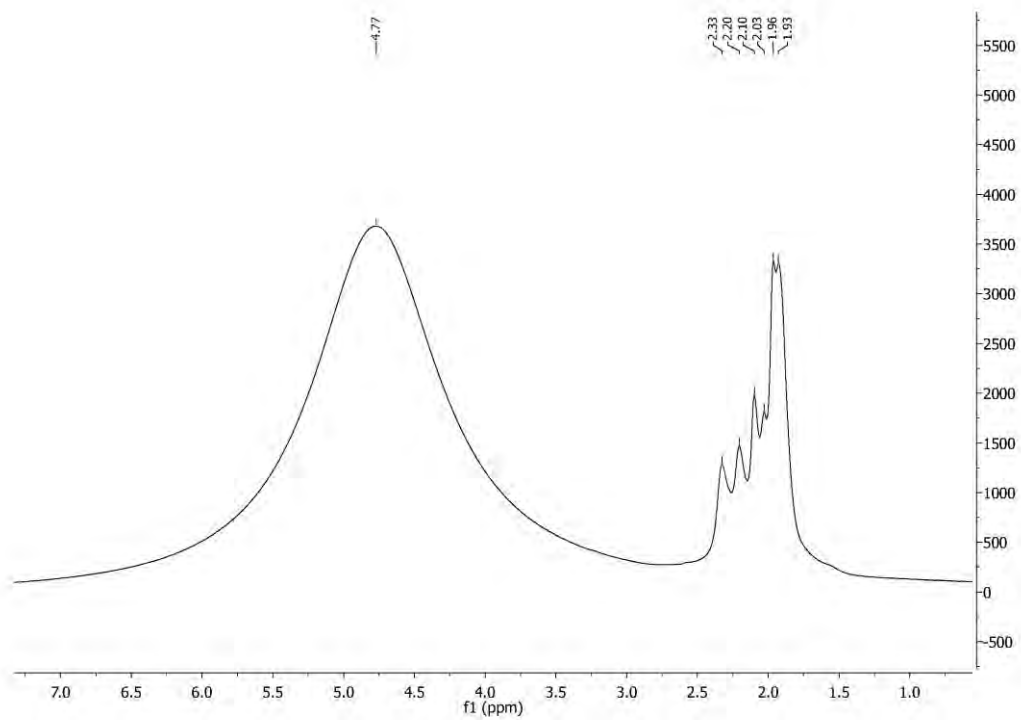
Figure S6. i) ^1H -RMN, ii) $^1\text{H}\{^{11}\text{B}\}$ -RMN, iii) ^{11}B -RMN, iv) $^{11}\text{B}\{^1\text{H}\}$ -RMN spectra of the compounds a) **B1**, b) **B3**.

g)

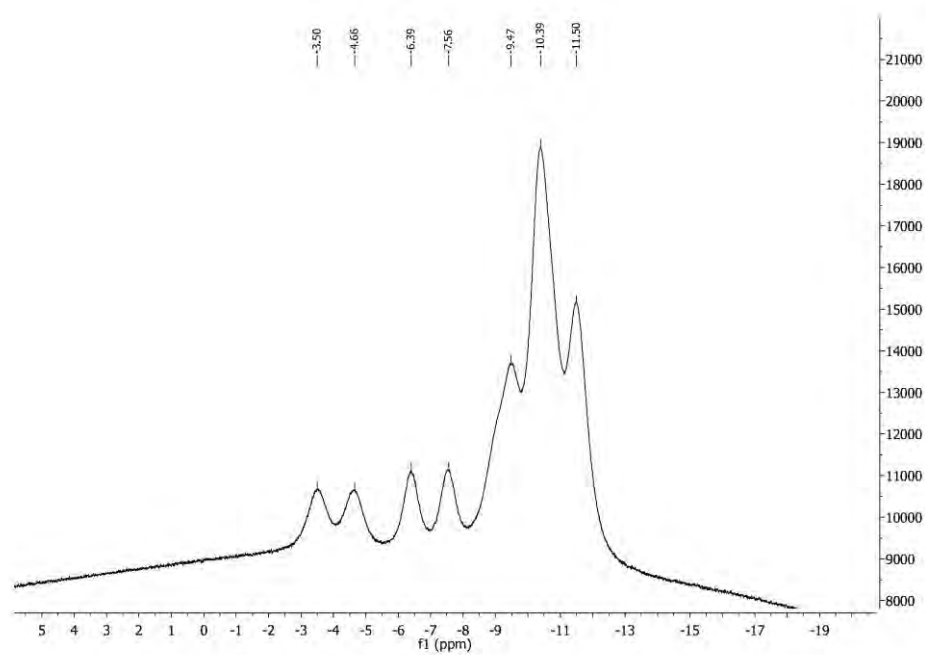
i)



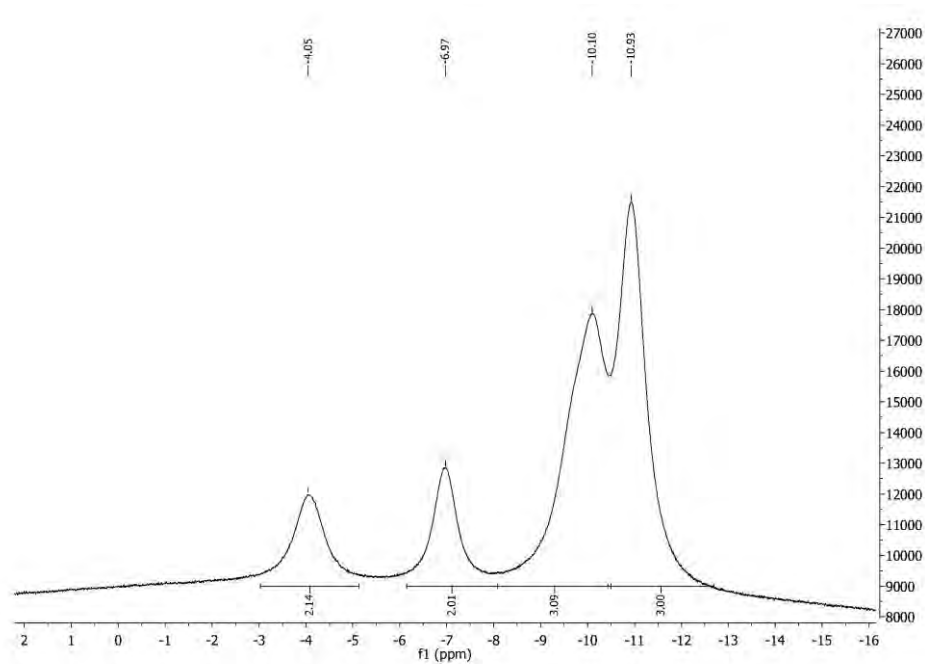
ii)



iii)



iv)



h)
iii)

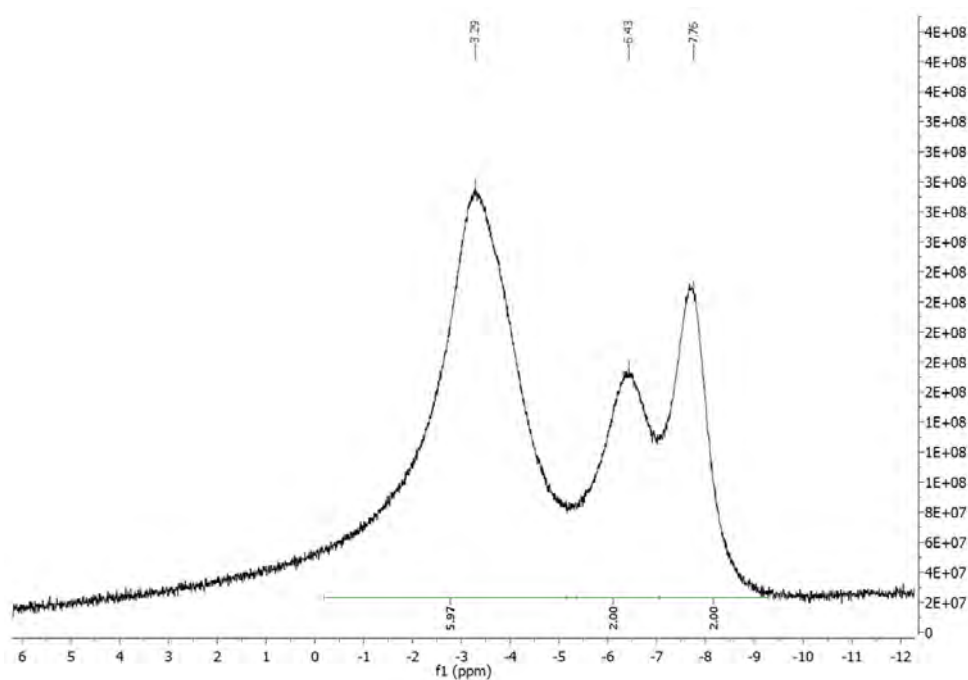
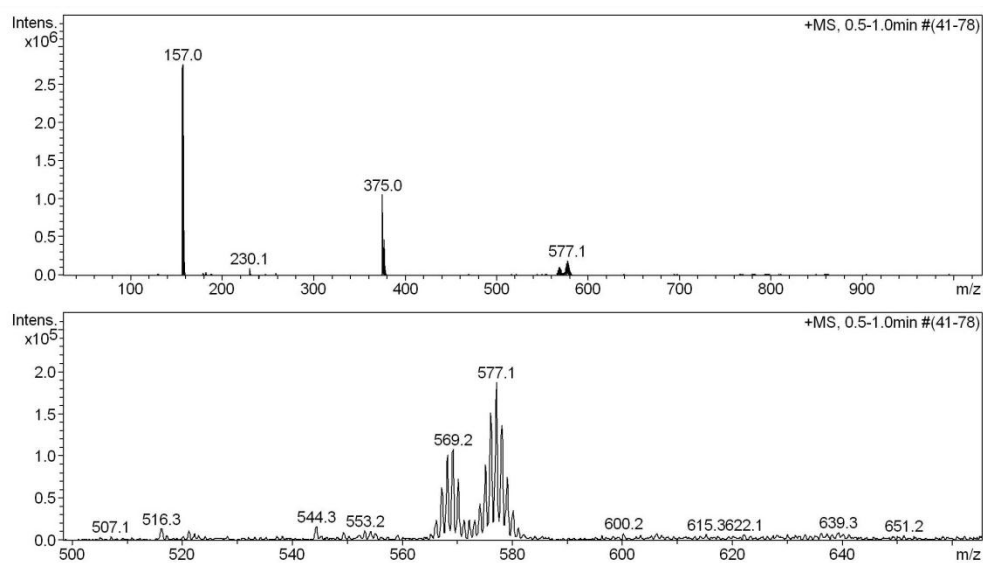
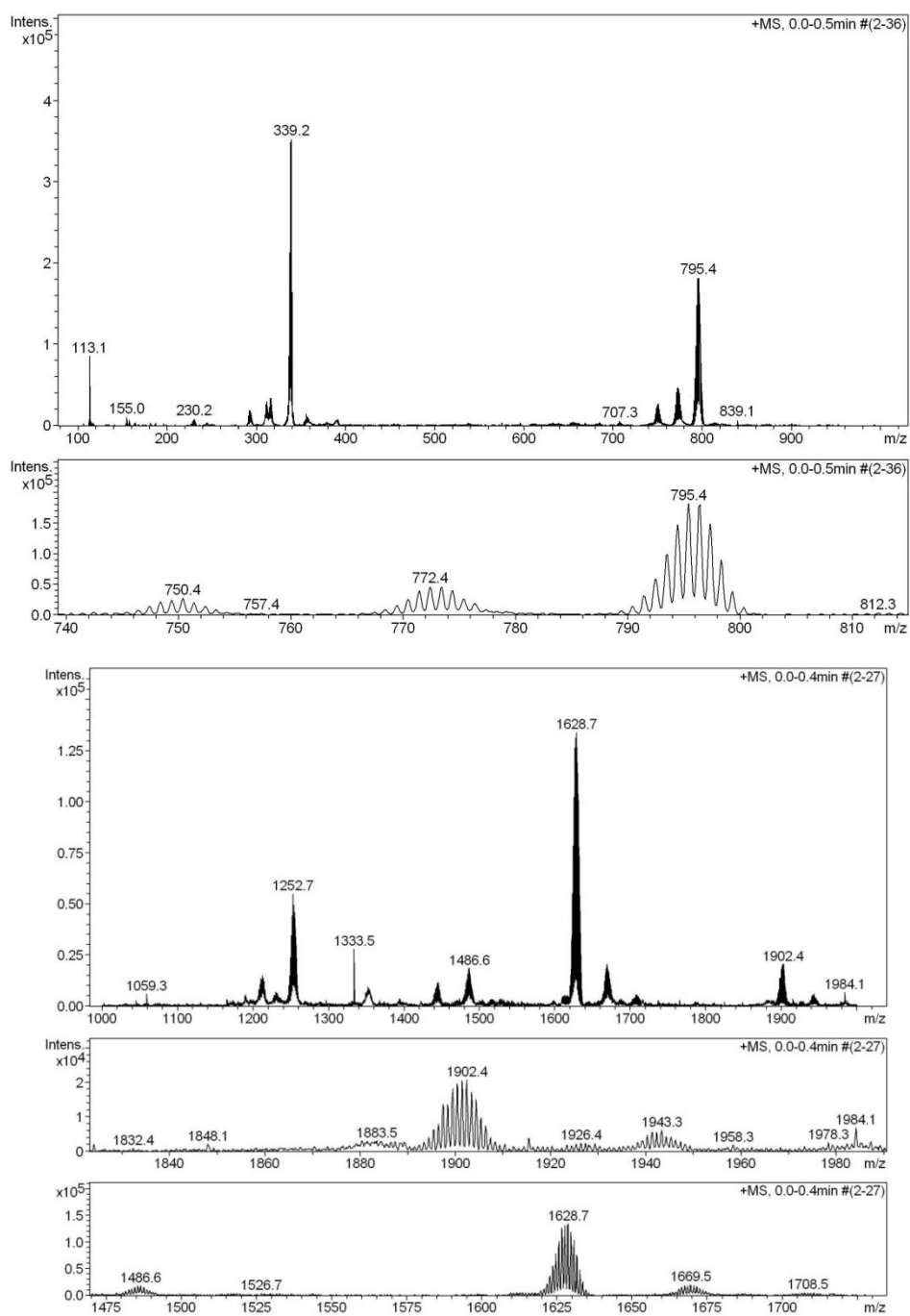


Figure S7. ESI-MS spectrum of a solution of complex a) **B1** in water, b) **B3** in MeOH, c) **B4** in MeOH.

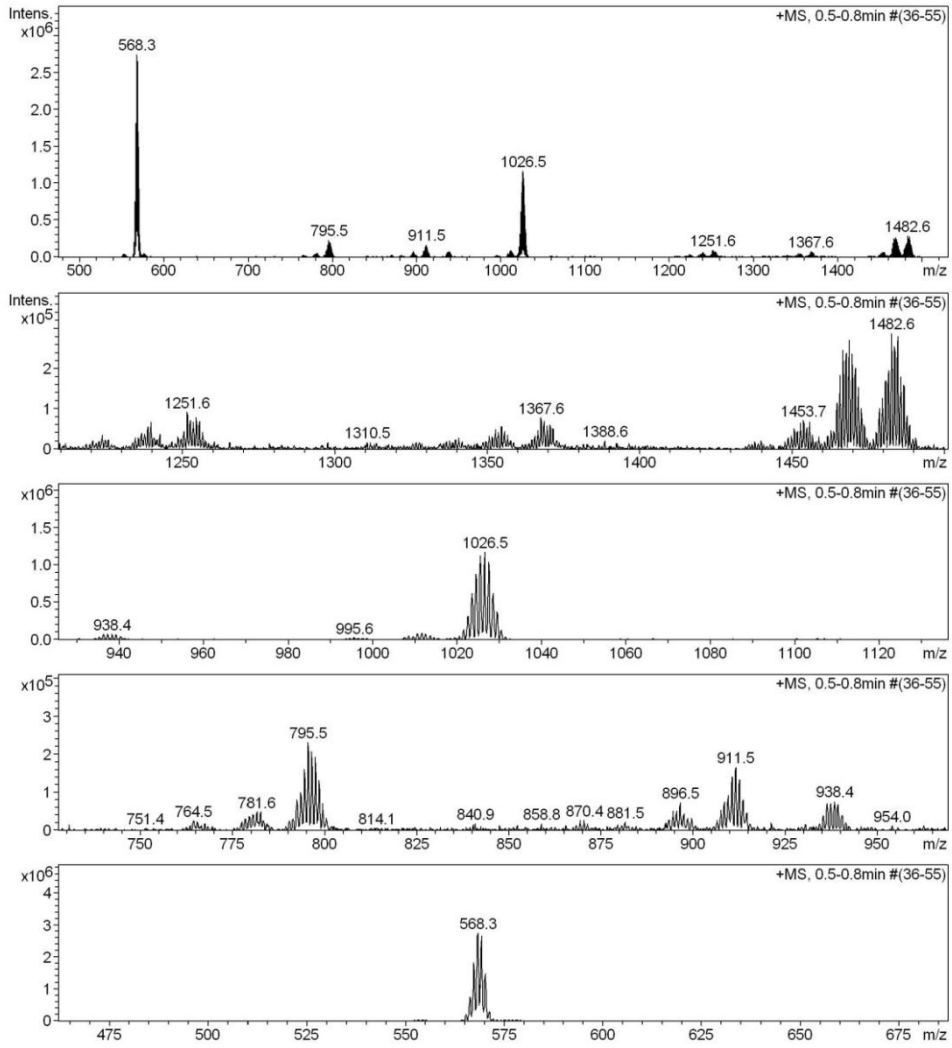
a)



b)



c)



CHAPTER V. Study of the reactivity of the carboranyl-carboxylate ligand 1-CH₃-2-CO₂H-1,2-closo-C₂B₁₀H₁₀ with Fe and Co.

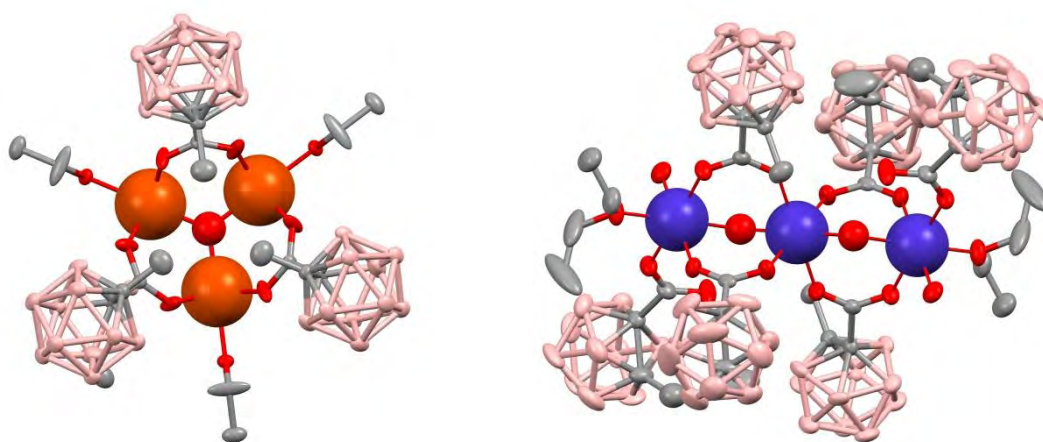


Figure S1. Deviation of the Fe atoms from the equatorial plane of their octahedra formed by the four oxygen atoms of the carboranylcarboxylate ligands Å toward the μ_3 -O atom.

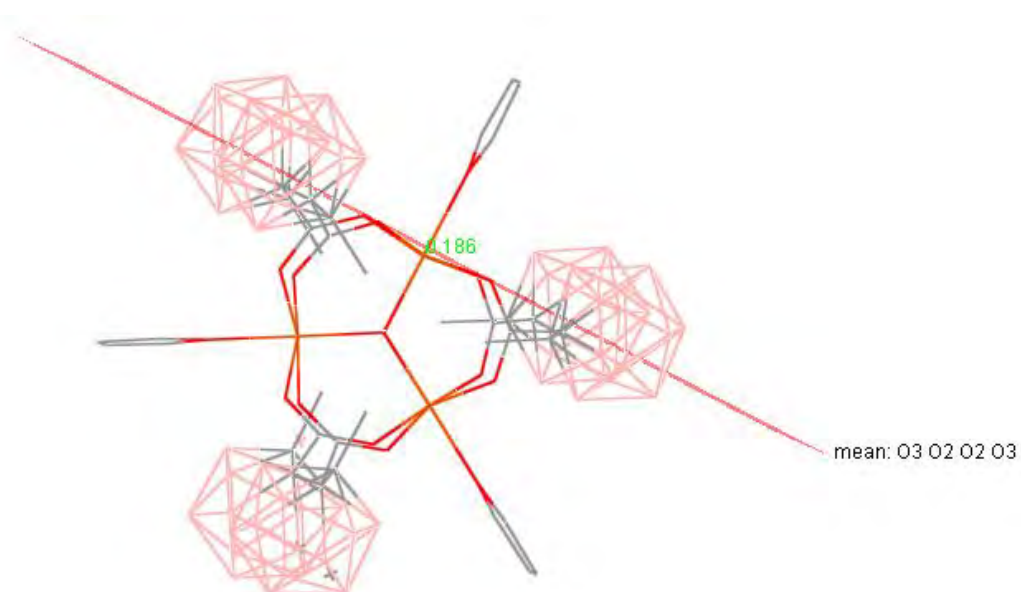
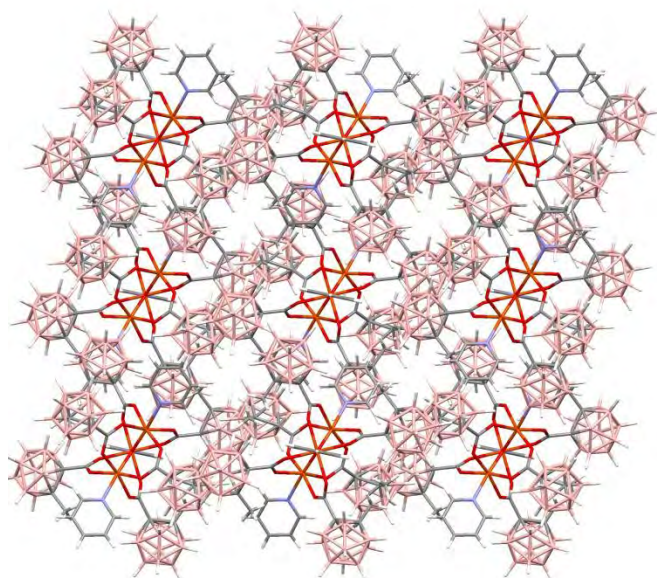


Figure S2. Packing arrangement of **C2** along a) *b* axis, b) *c* axis

a)



b)

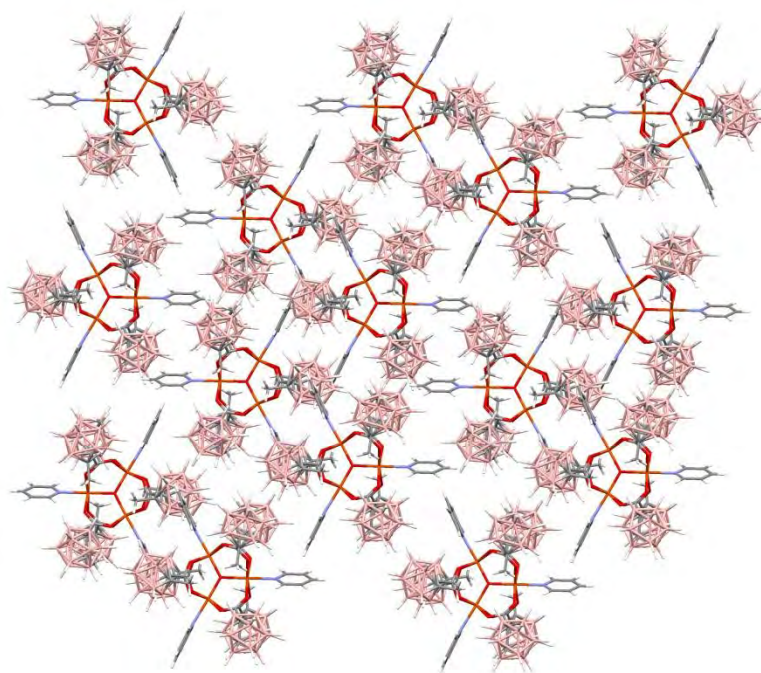
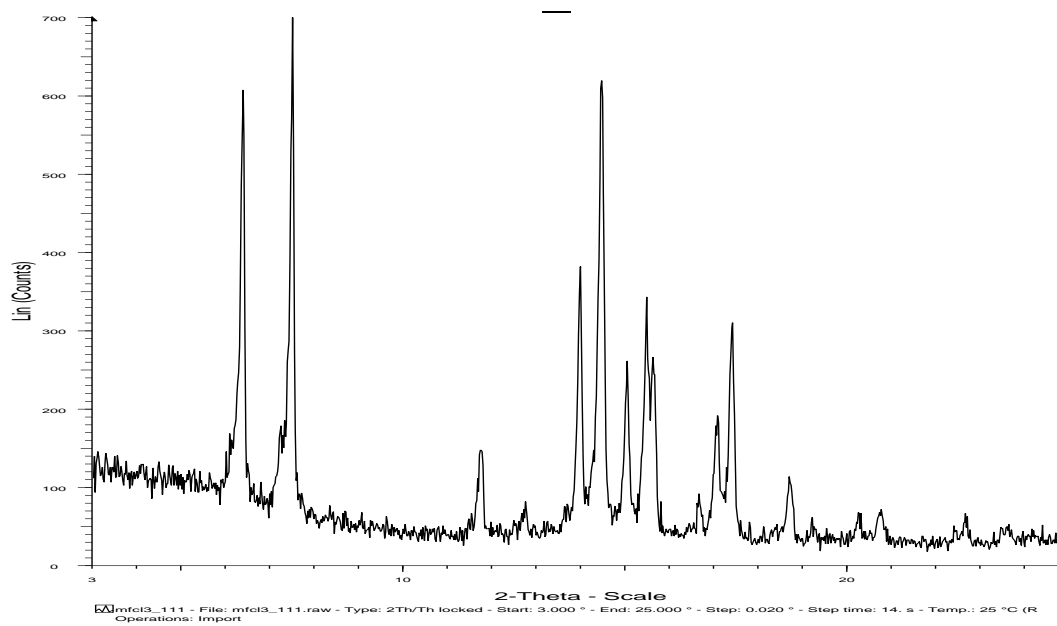


Figure S3. a) X-ray powder diffraction (XRD) of **C5** b) calculated XRD for **C4**.

a)



b)

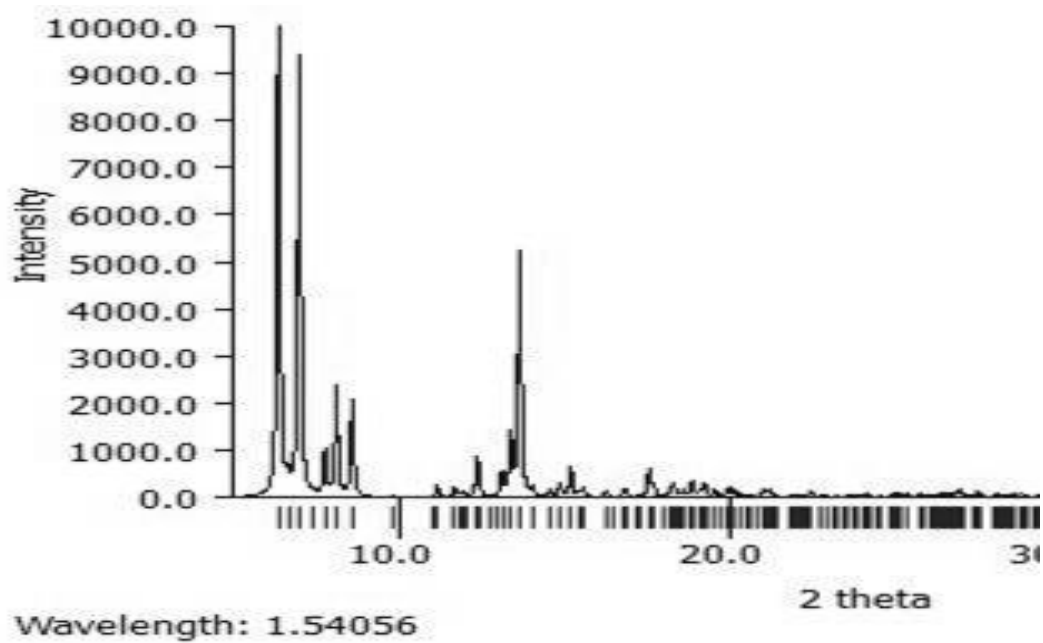
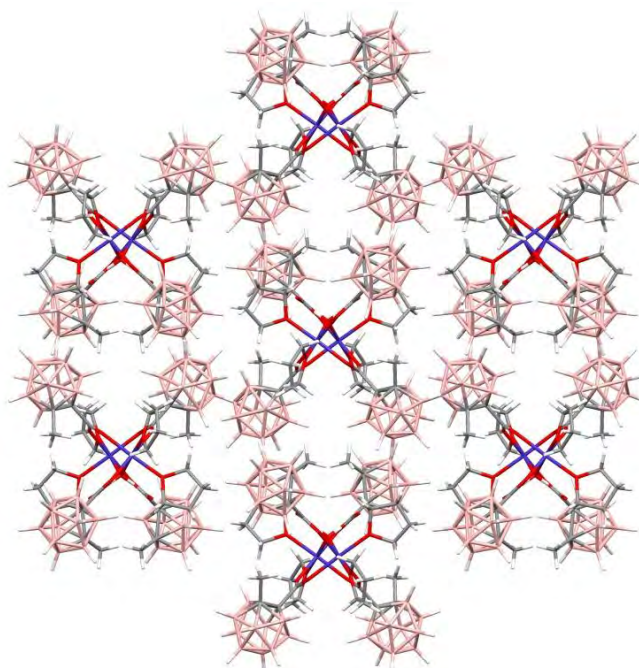


Figure S4. Packing diagram of complexes a) **C3** along the a axis b) **C4** along the c axis

a)



b)

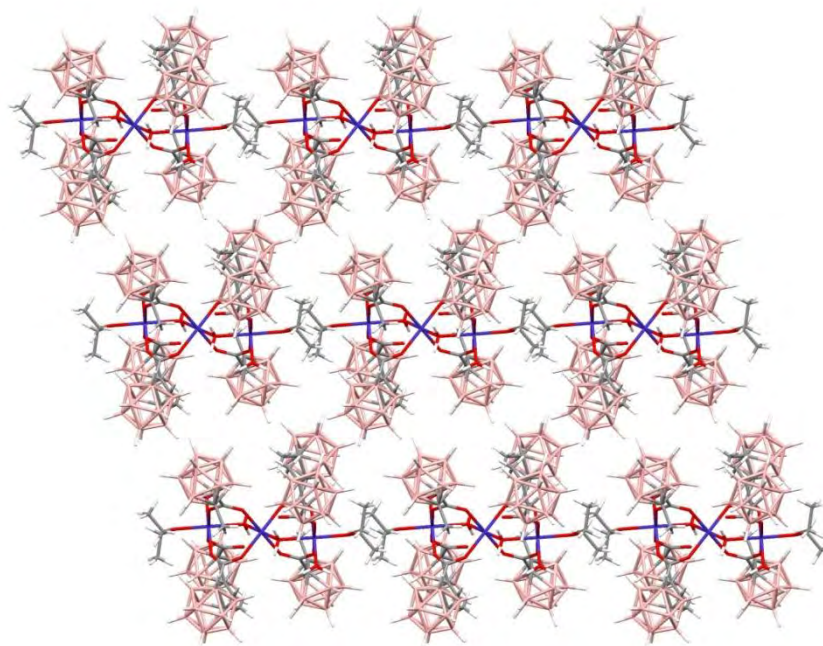
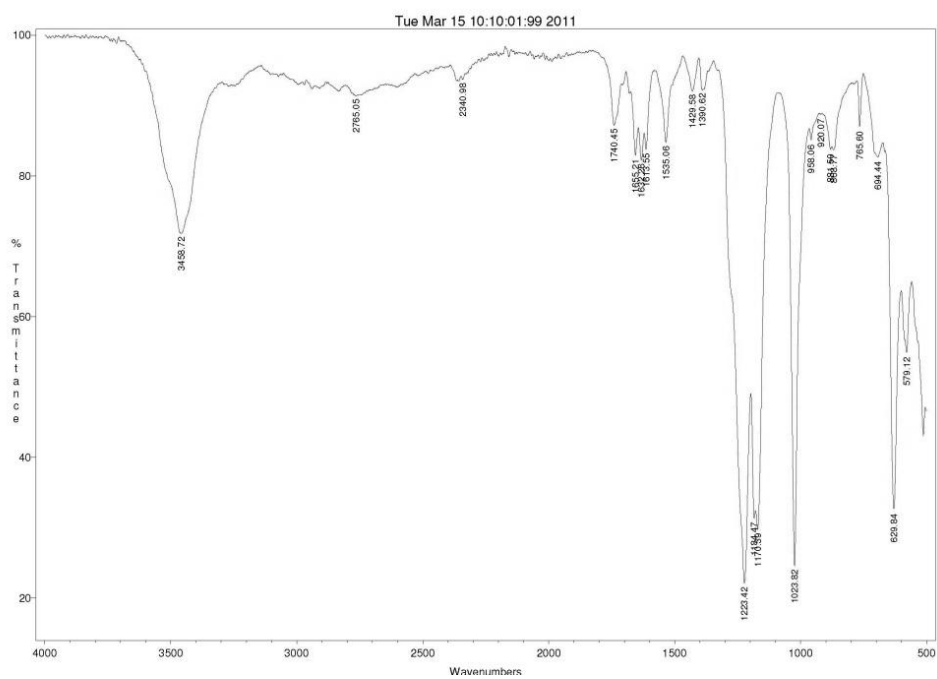
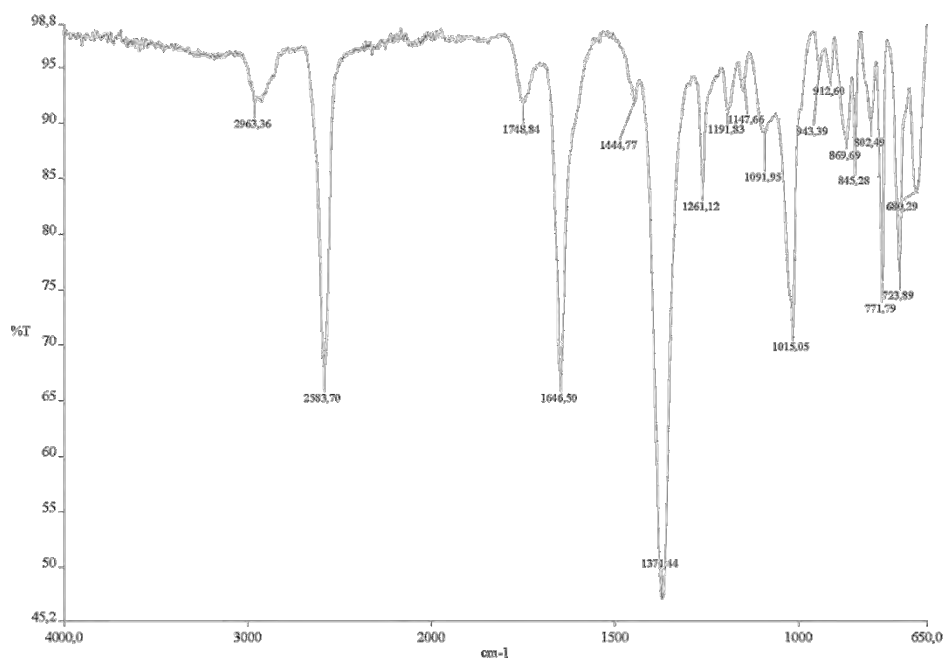


Figure S5. IR spectrum of the compounds a) $[\text{Fe}(\text{CF}_3\text{SO}_3)_2]$, b) **C1**, c) **C2**, d) **C3**, e) **C5**.

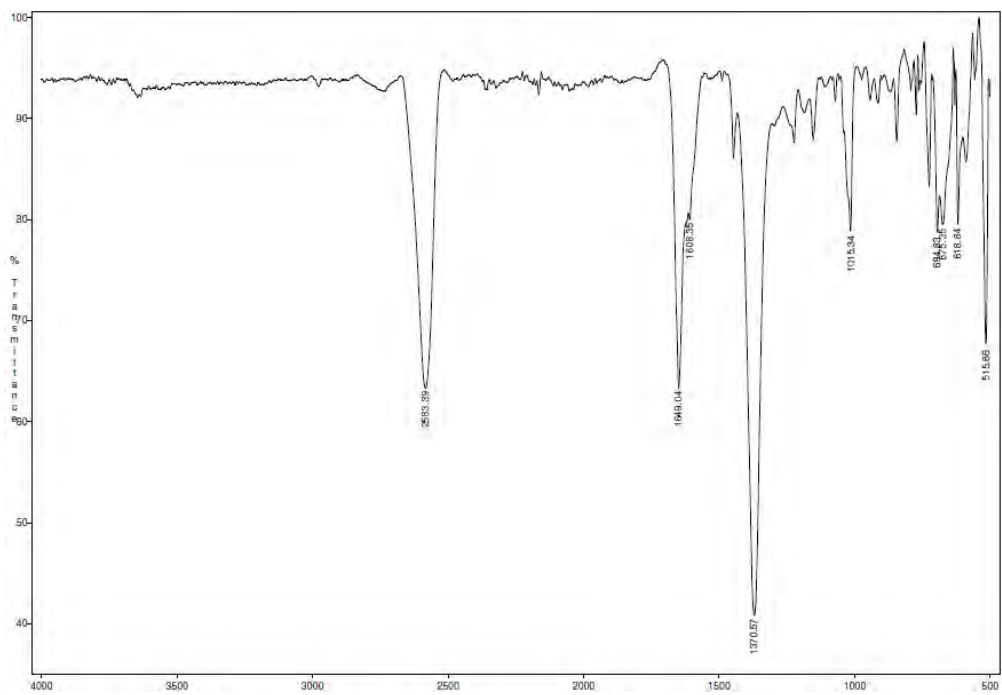
n)



o)

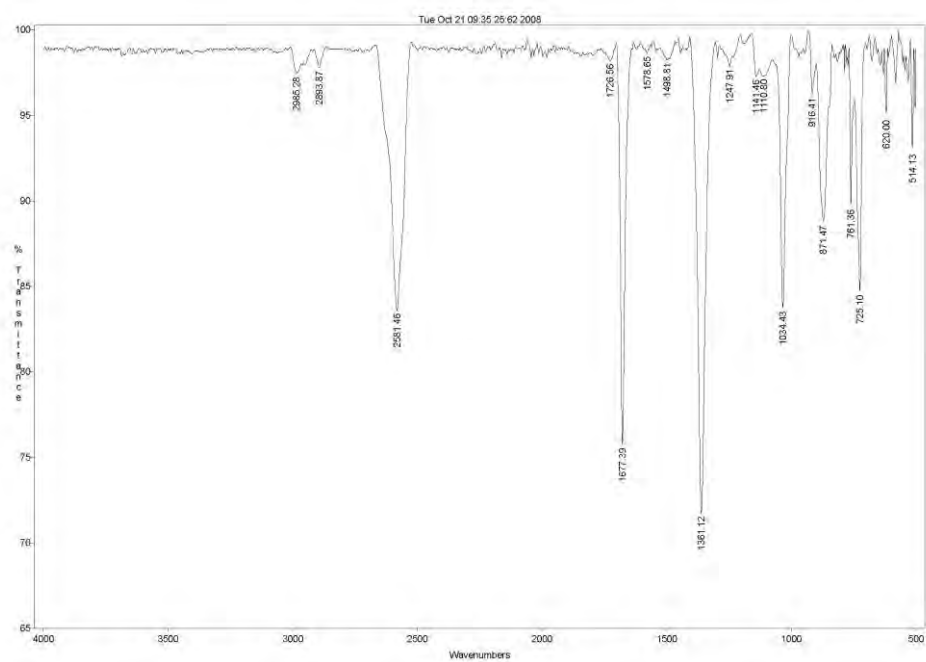


p)



CHAPTER V

q)



e)

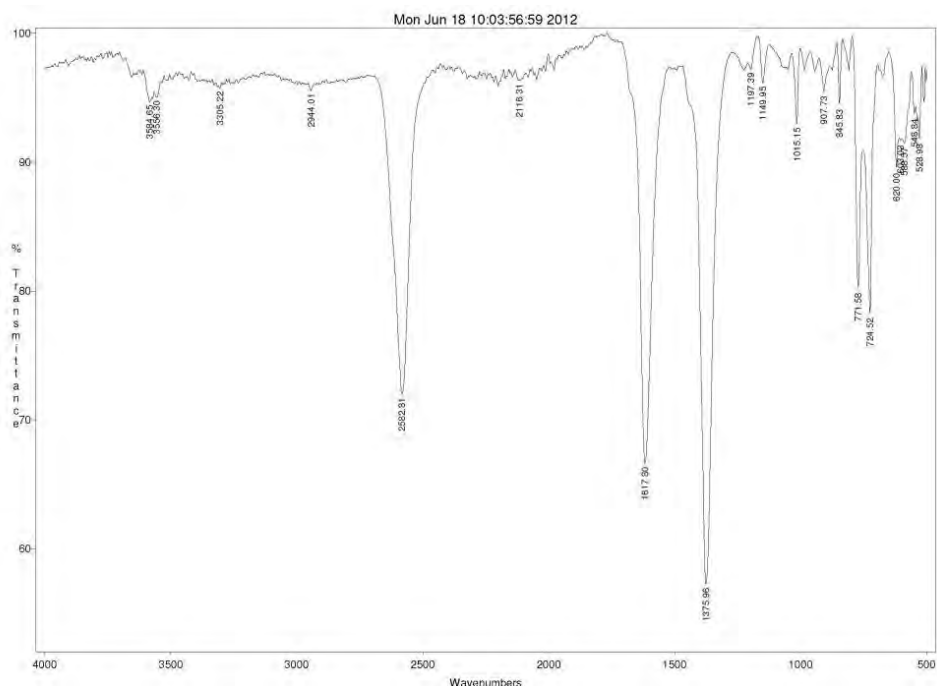
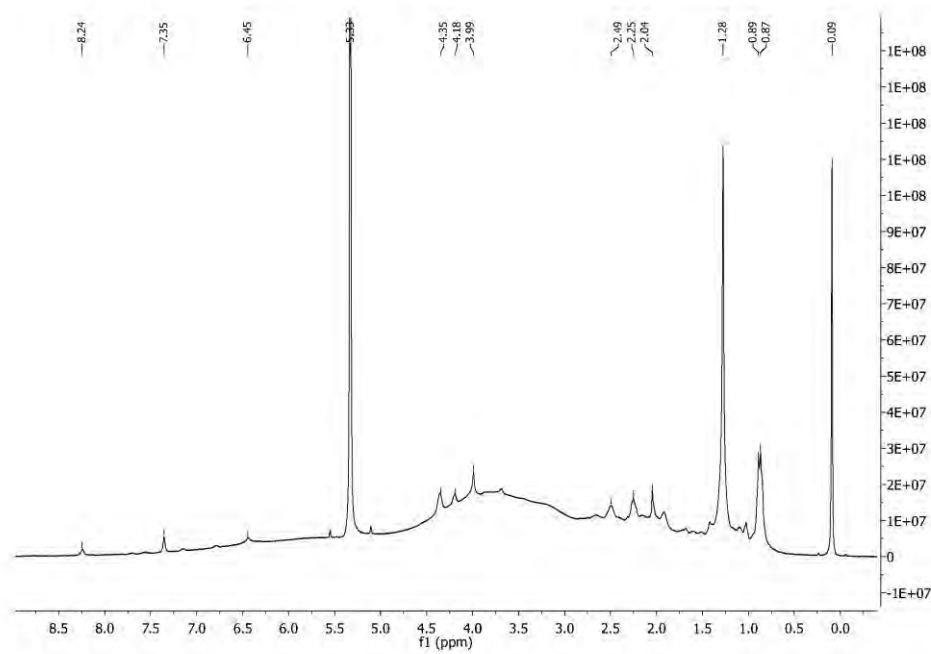


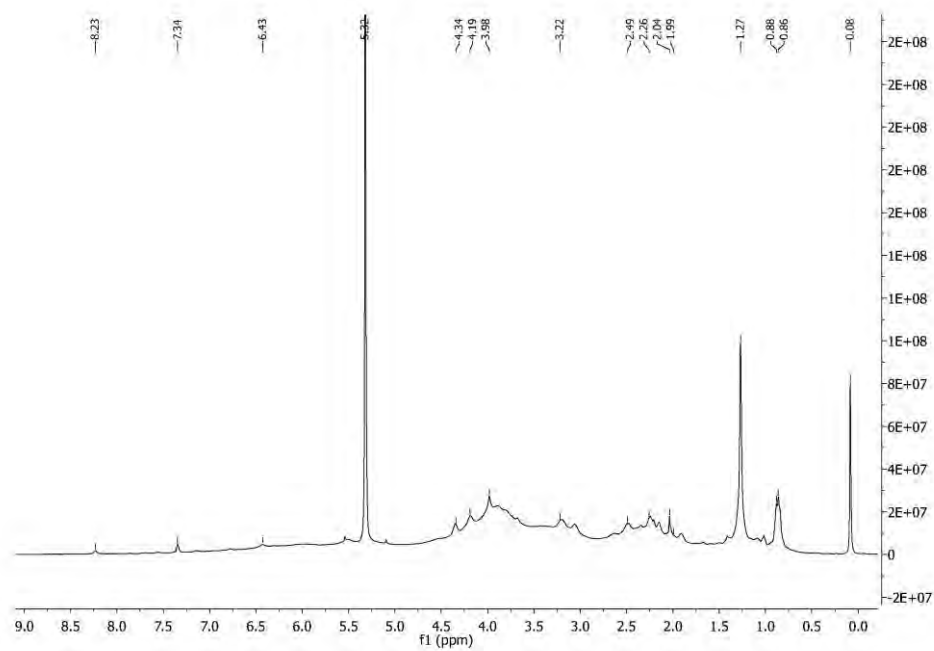
Figure S6. i) ^1H -RMN, ii) $^1\text{H}\{^{11}\text{B}\}$ -RMN, iii) ^{11}B -RMN, iv) $^{11}\text{B}\{^1\text{H}\}$ -RMN, v) ^{13}C -RMN vi) deconvoluted ^{11}B -RMN spectra of compounds a) **C1**, b) **C3**, c) **C5**

i)

i)

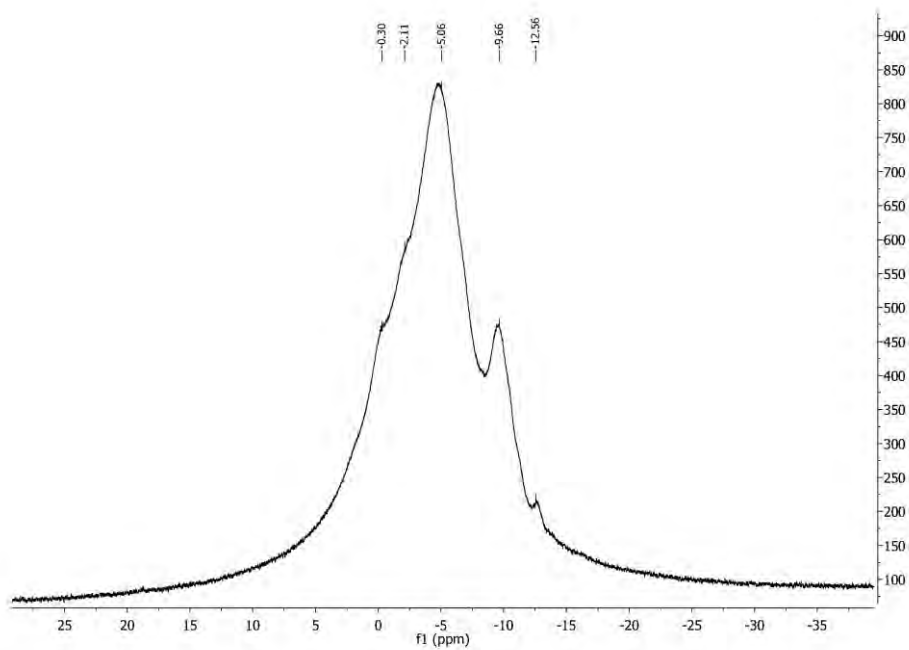


ii)

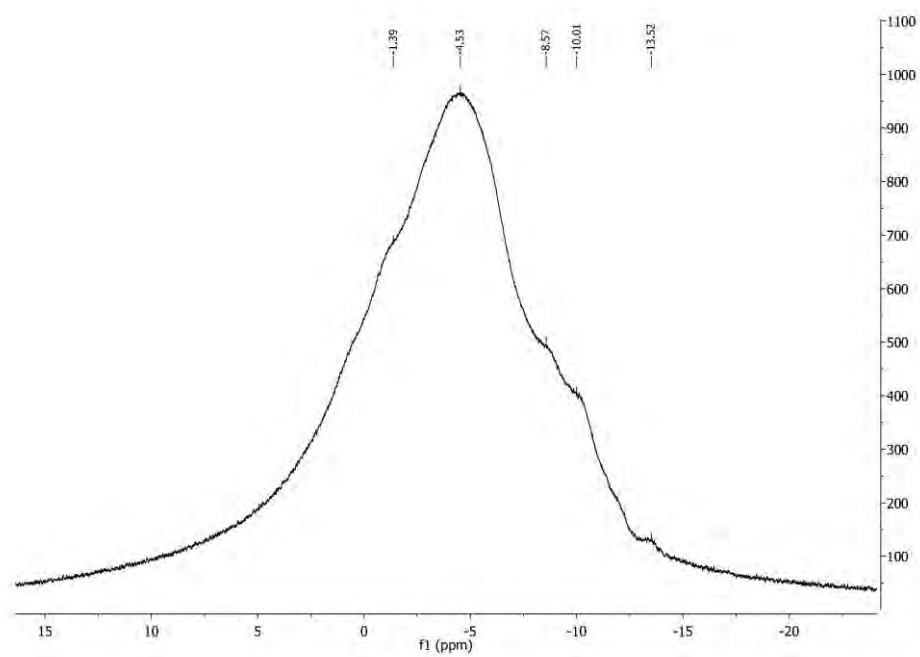


CHAPTER V

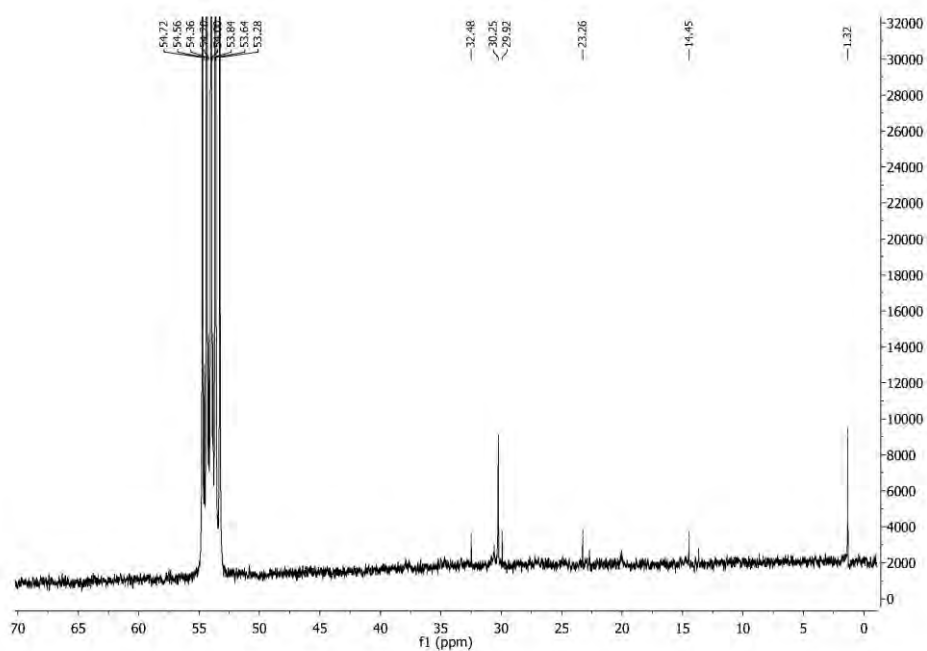
iii)



iv)

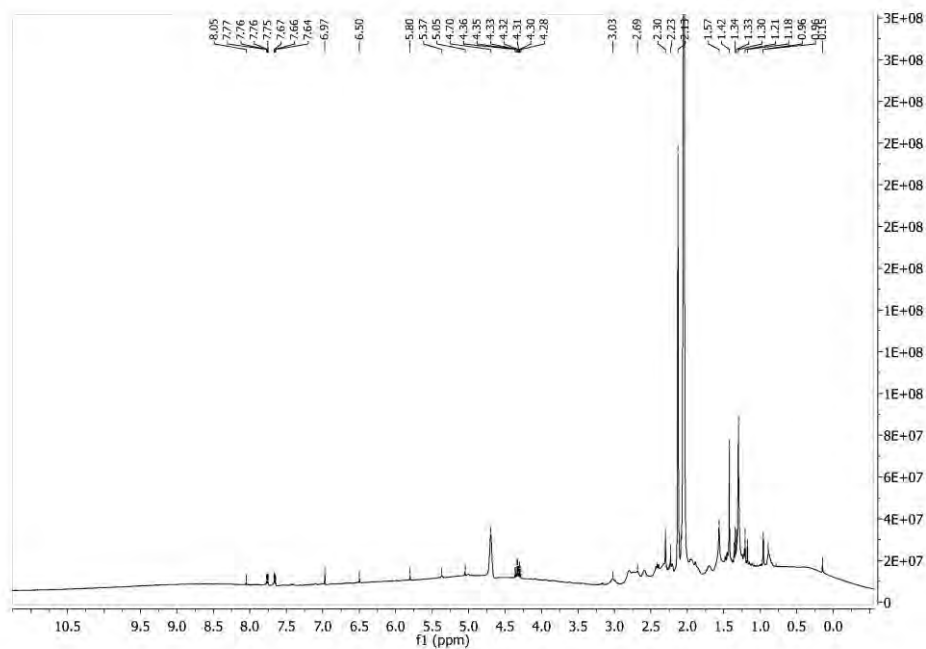


v)



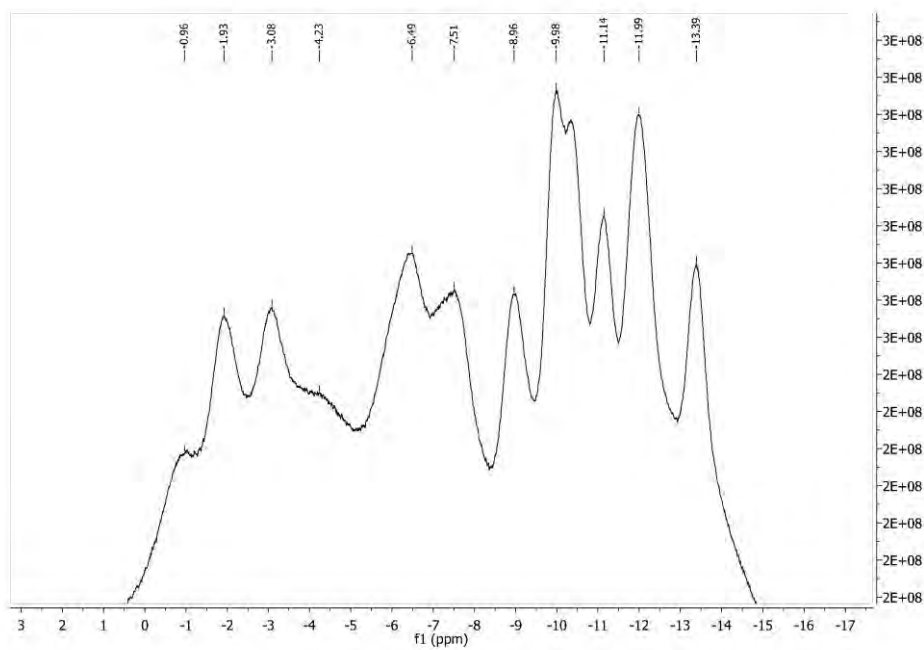
j)

ii)

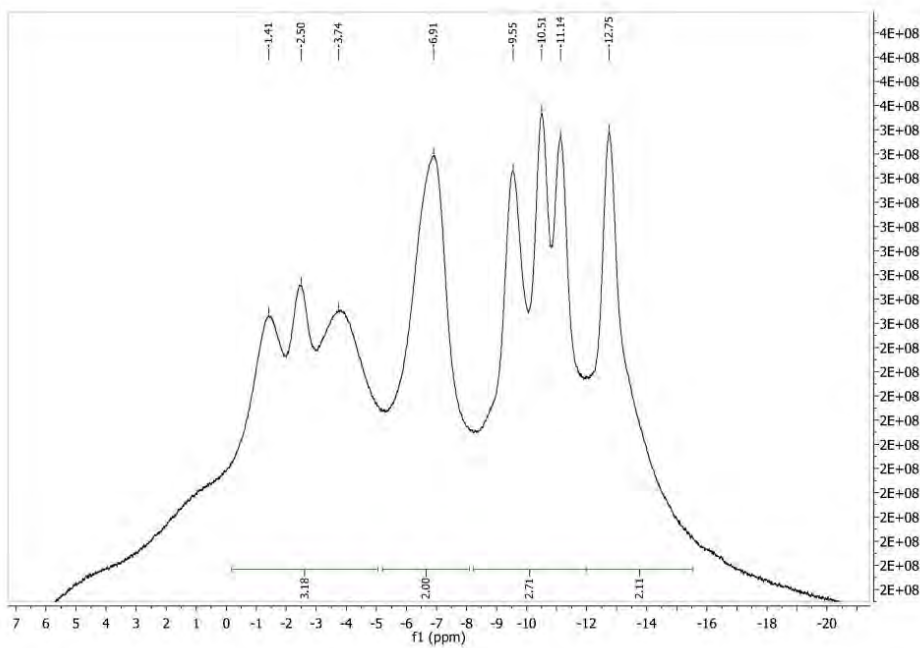


CHAPTER V

iii)

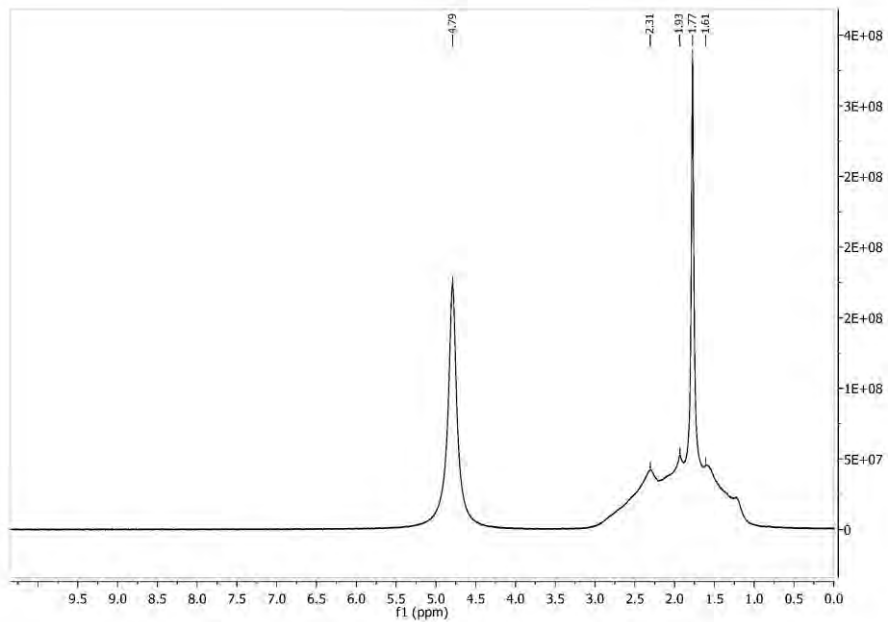


iv)

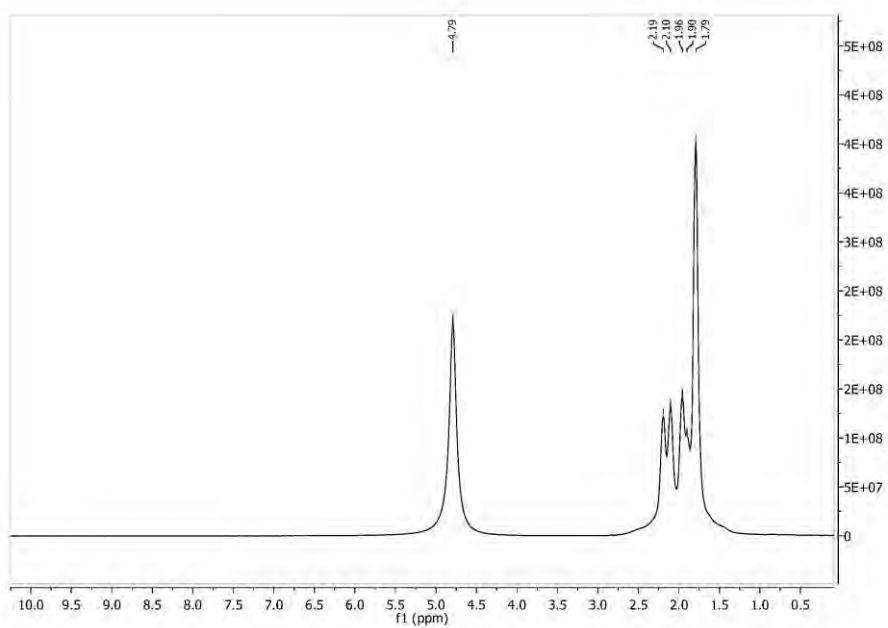


k)

i)

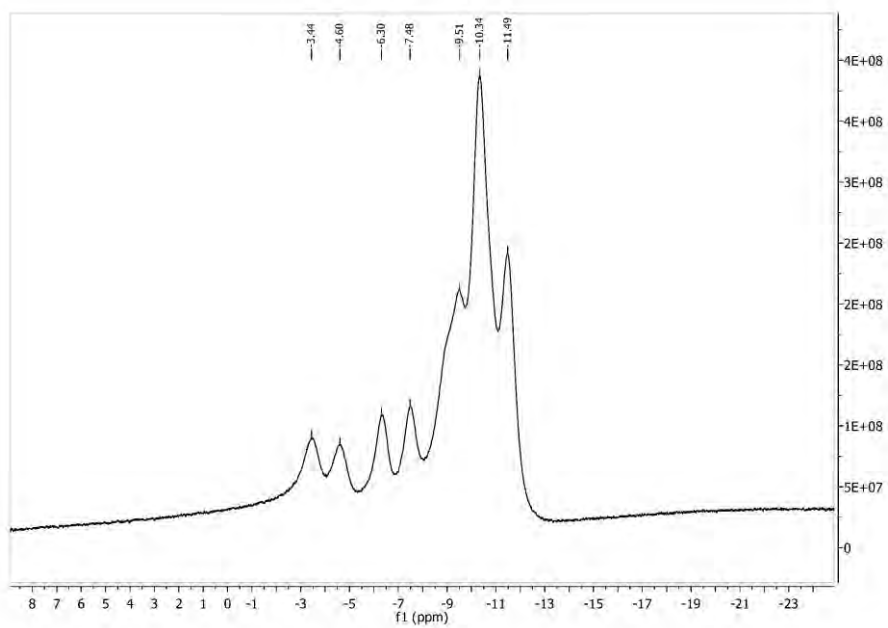


ii)

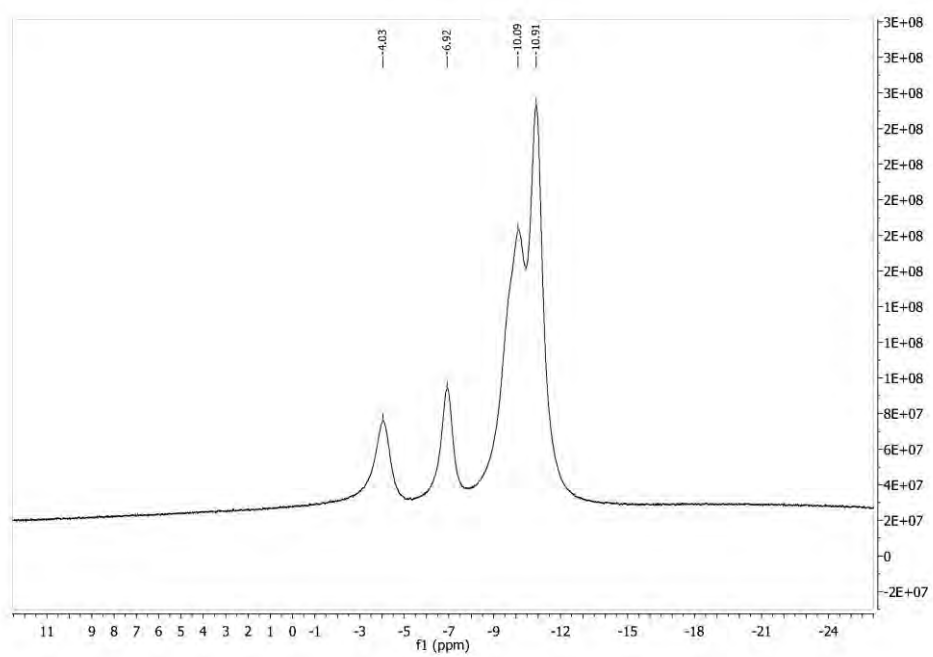


CHAPTER V

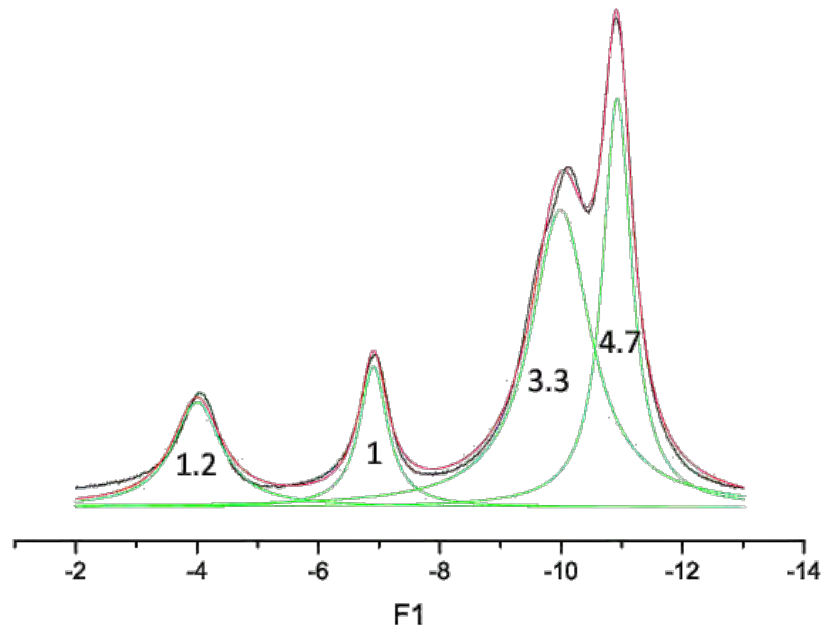
iii)



iv)



vi)



CHAPTER VI. Cu(II) and Mn(II) complexes containing the carboranylcarboxylate ligand 1-CO₂H-1,2-closo-C₂B₁₀H₁₁.

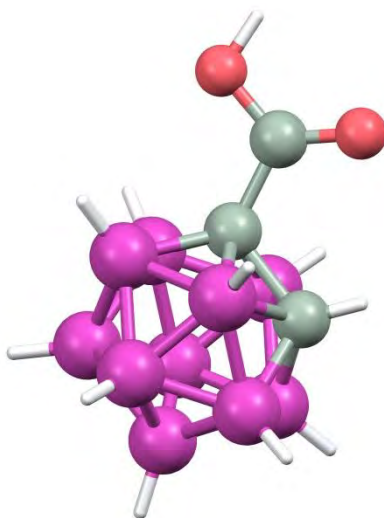
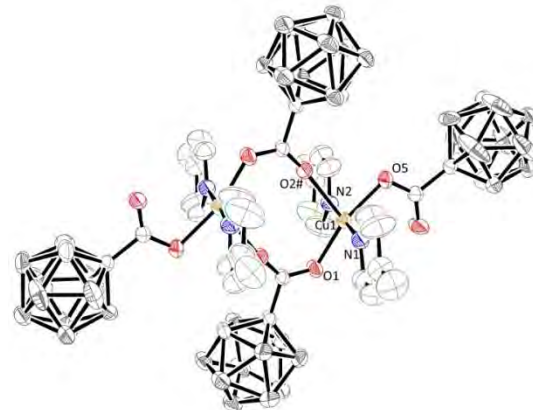


Figure S1. X-ray structures (Ortep-plots with ellipsoids at 30% probability level) and labelling scheme for (a) **D2'** (b) **D4'** and (c) **D5'**.

(a)



(b)



(c)

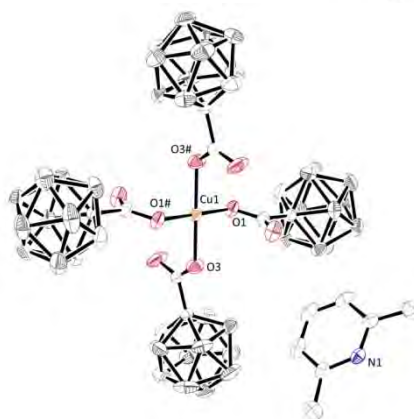


Figure S2. Packing diagram of **D4** along *a* axis. H atoms have been omitted for clarity.

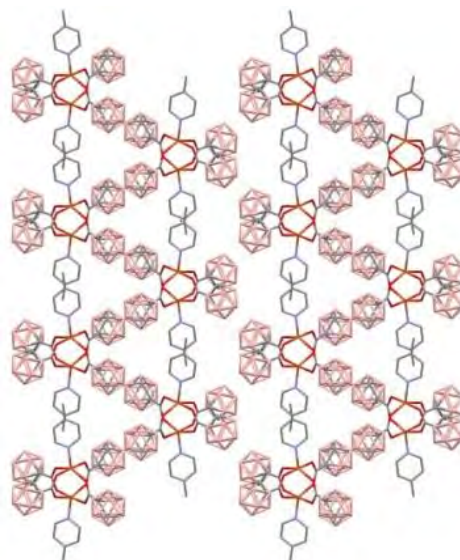


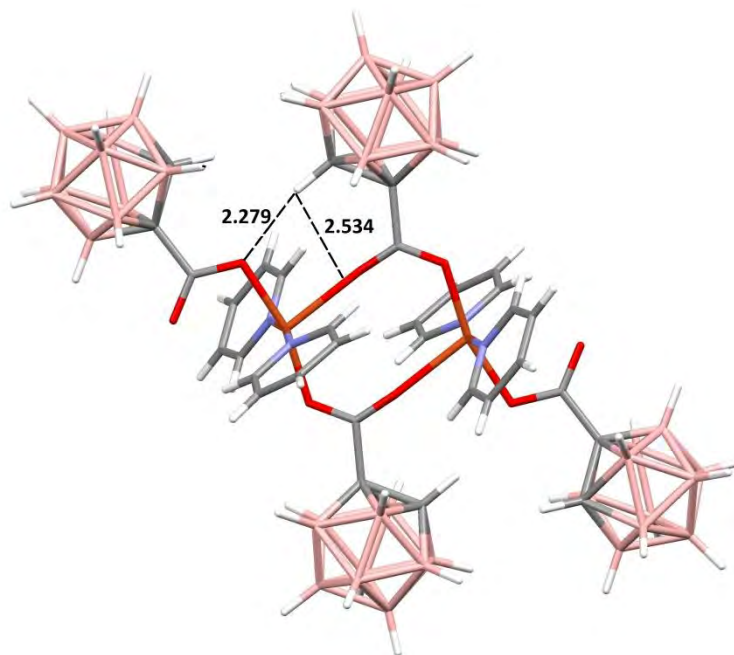
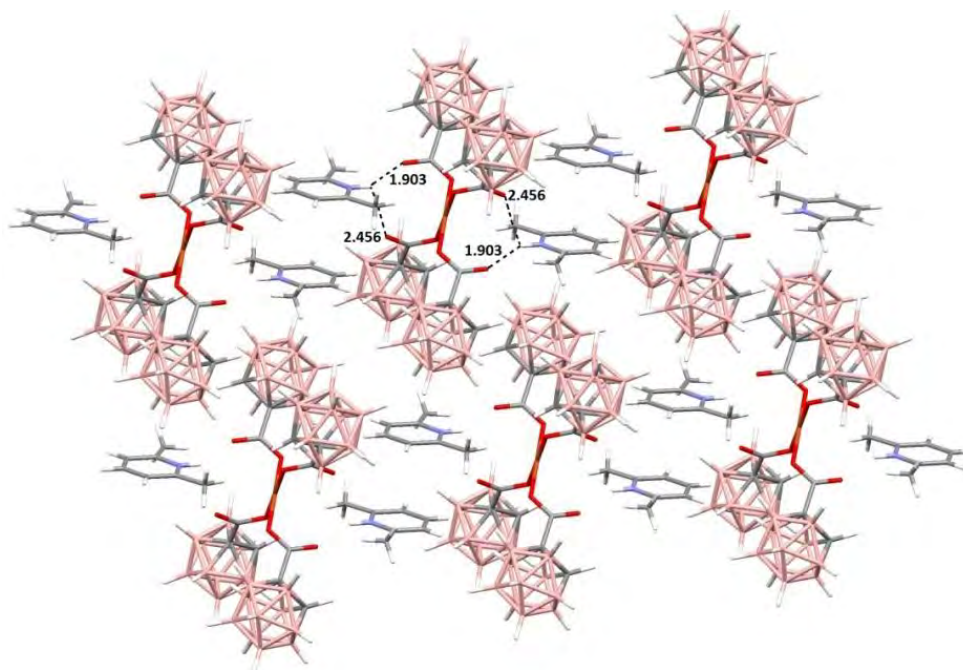
Figure S3. H-bond in complex **D2'****Figure S4.** Packing arrangement of complex **D5'** showing the two intermolecular hydrogen bonds.

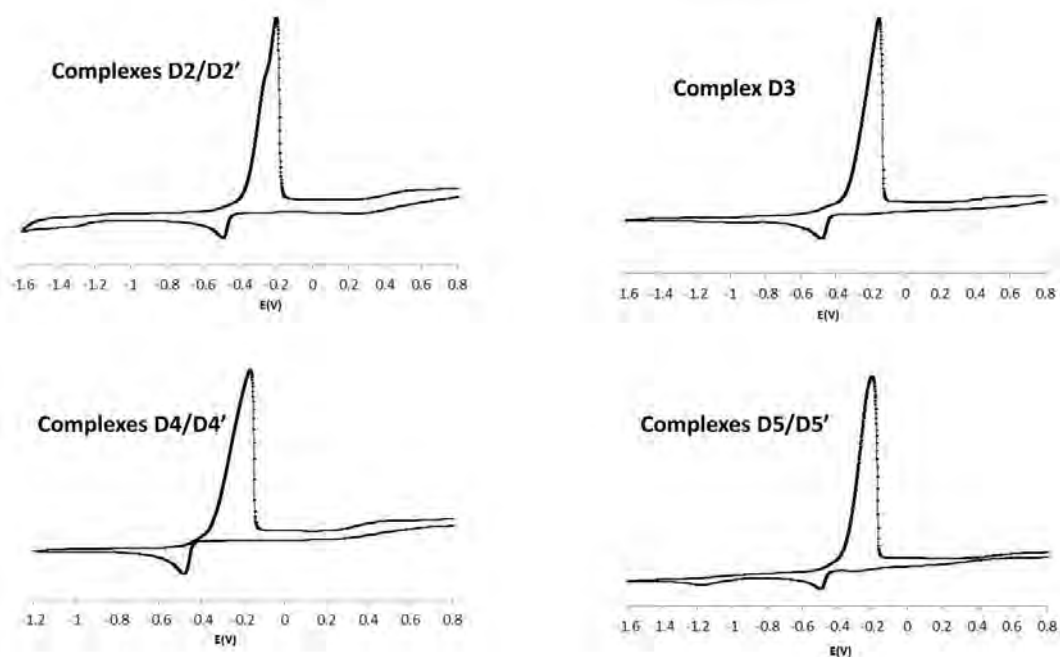
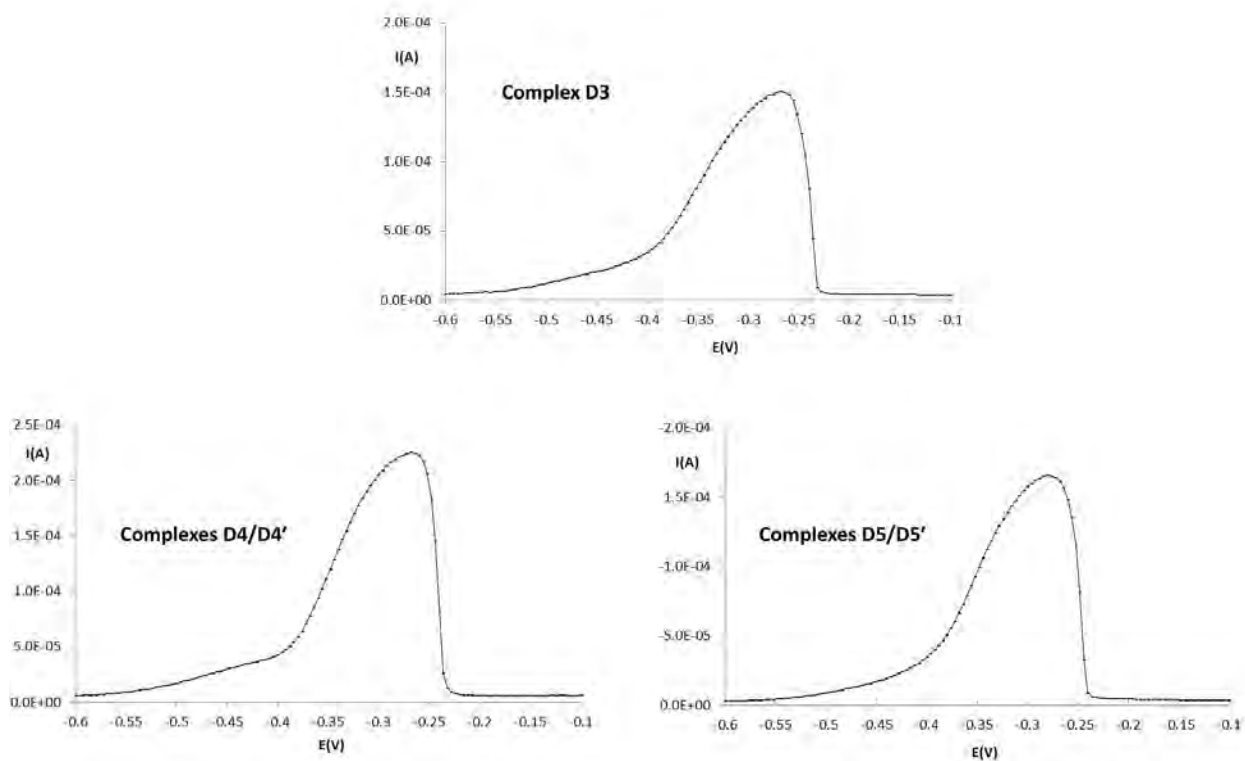
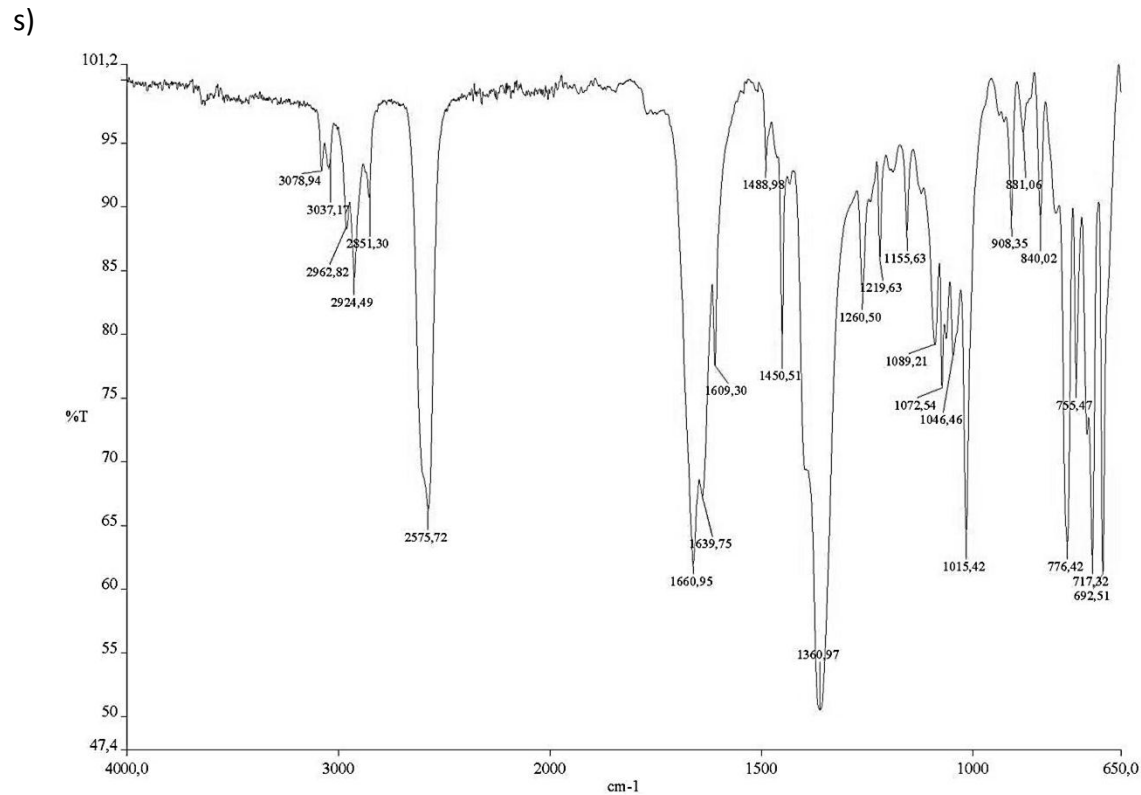
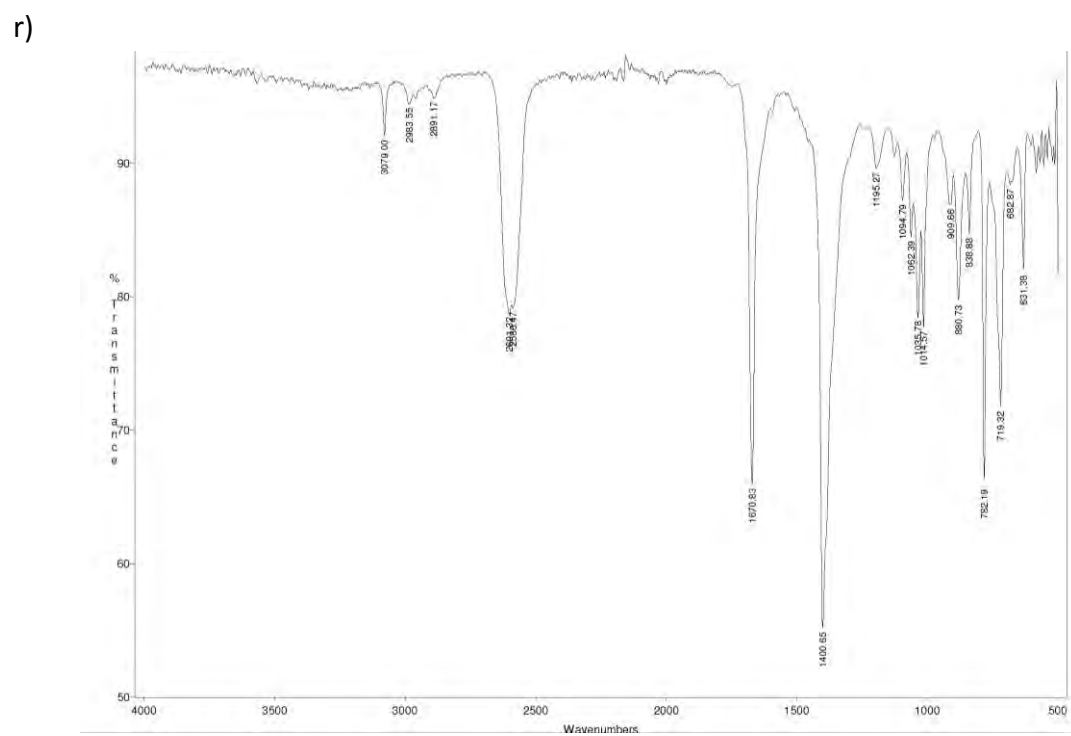
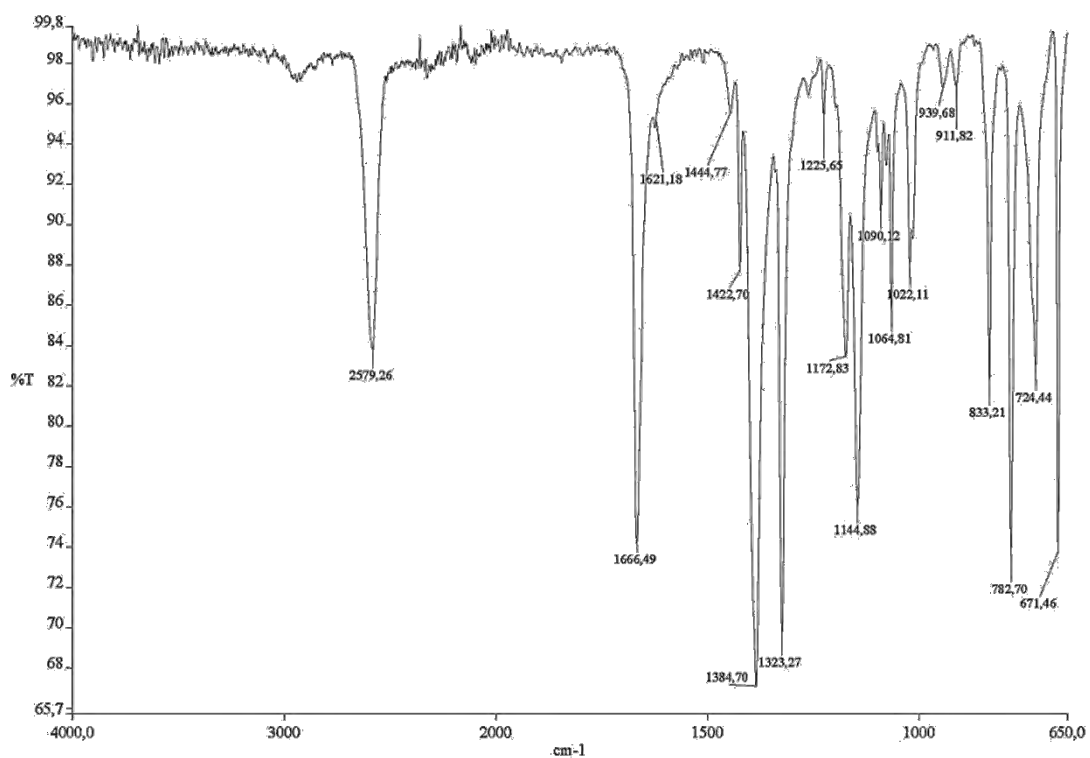
Figure S5. Cyclic voltammograms recorded for complexes **D2-D5** in acetonitrile**Figure S6.** DPV images for complexes **D3-D5** at potential range from -0.6 to -0.1 in acetonitrile (0.1 M TBAH) with pulse amplitude of 0.05 V, pulse width of 0.05 s, sampling width of 0.02 s and pulse period of 0.5 s.

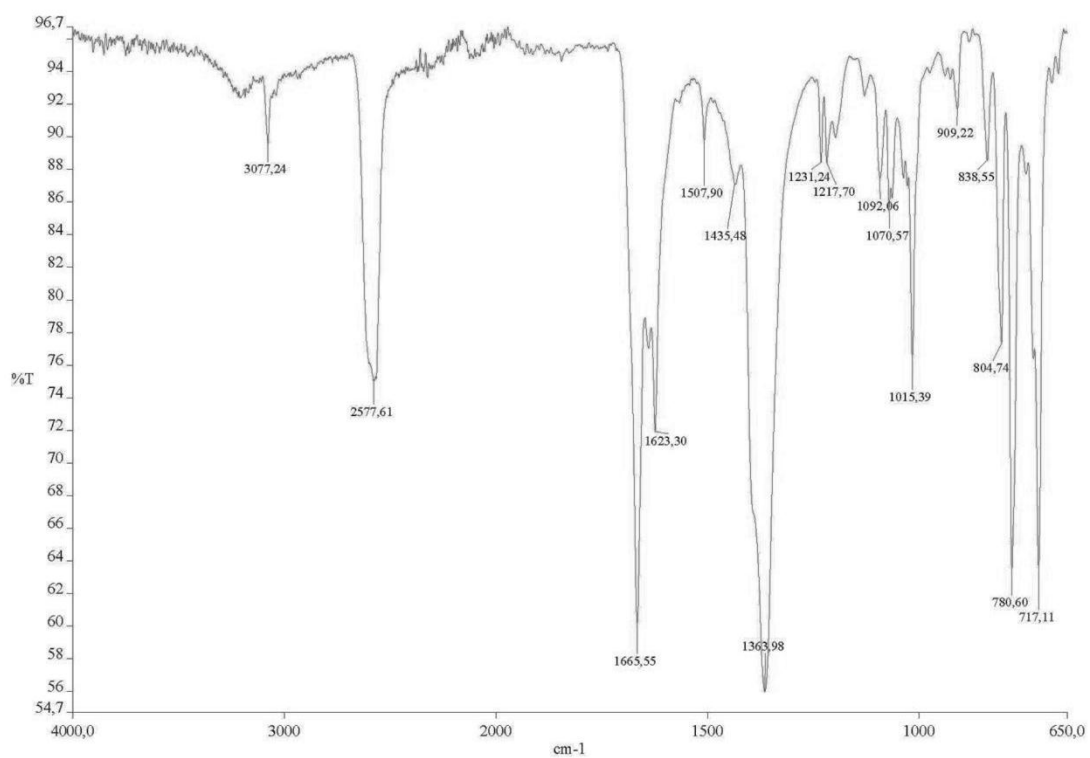
Figure S7. IR spectrum of the compounds a) D1, b) D2/D2', c) D3, d) D4/D4', e) D5/D5', f) D6/D6' g) D7, h) D8 i) L'H.



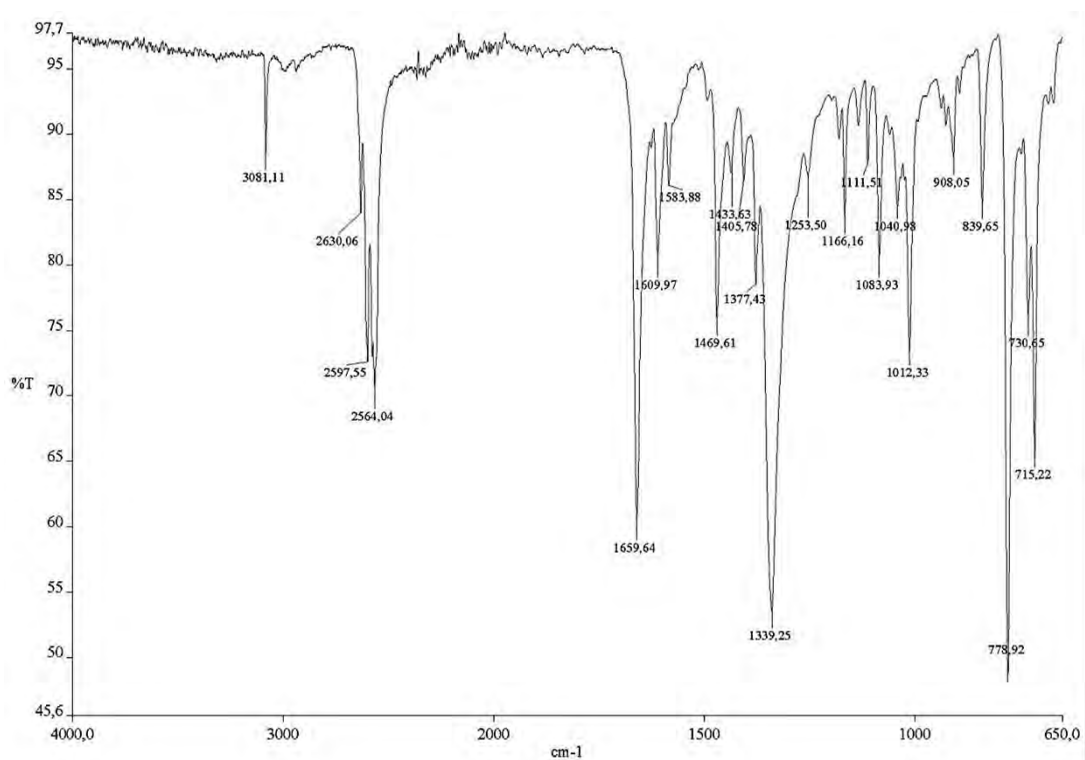
t)



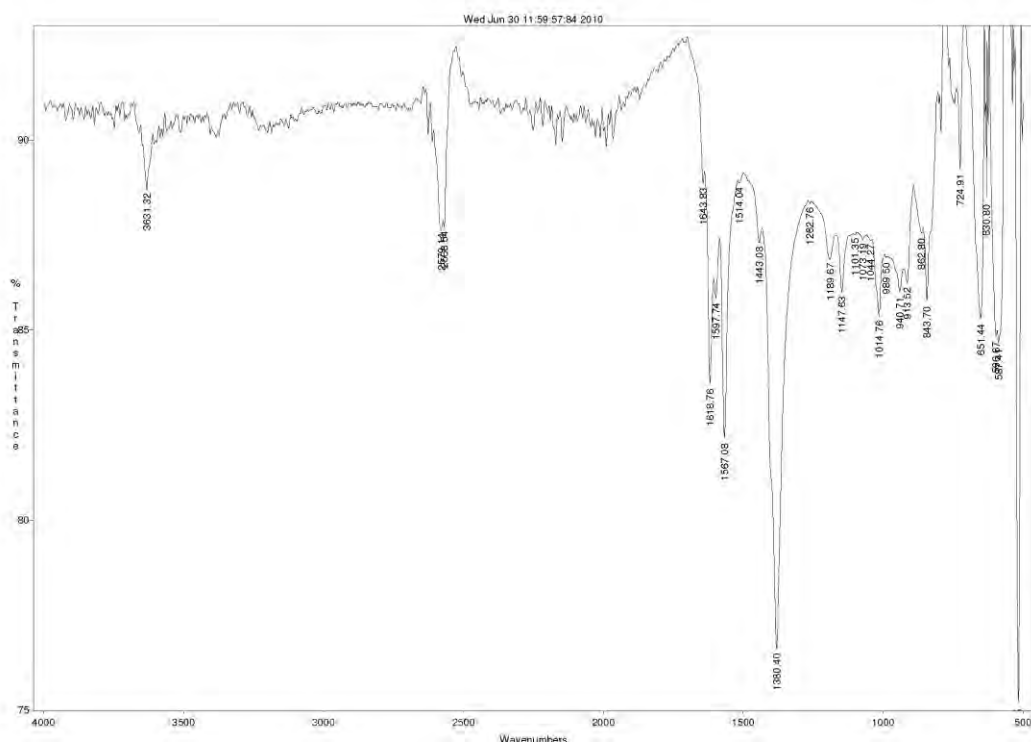
u)



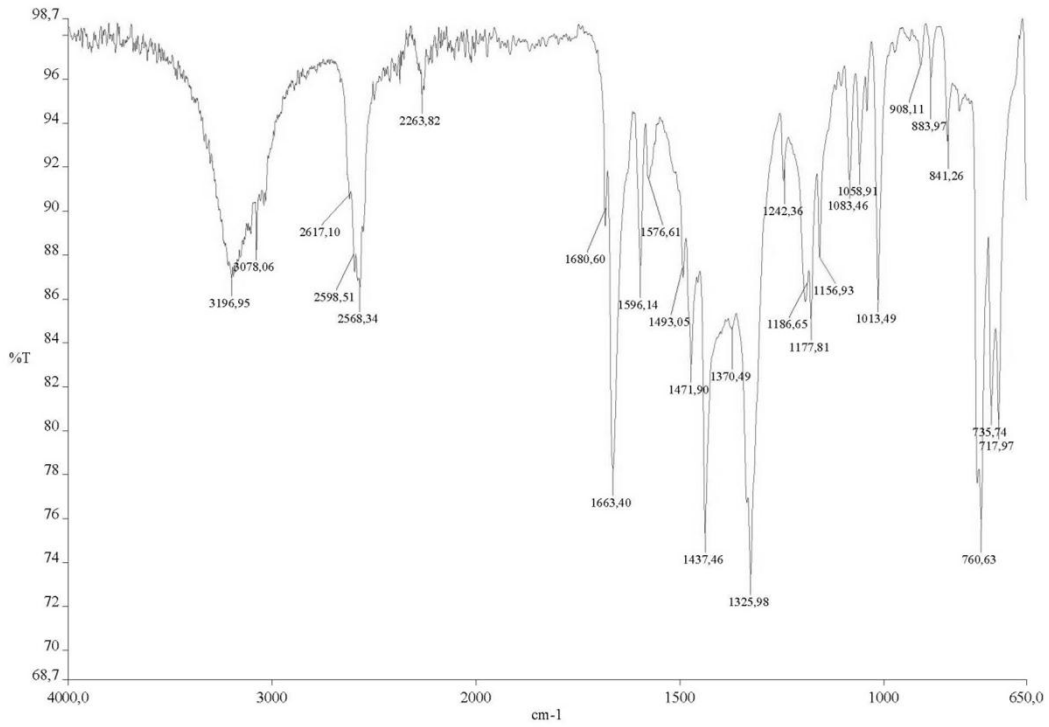
v)



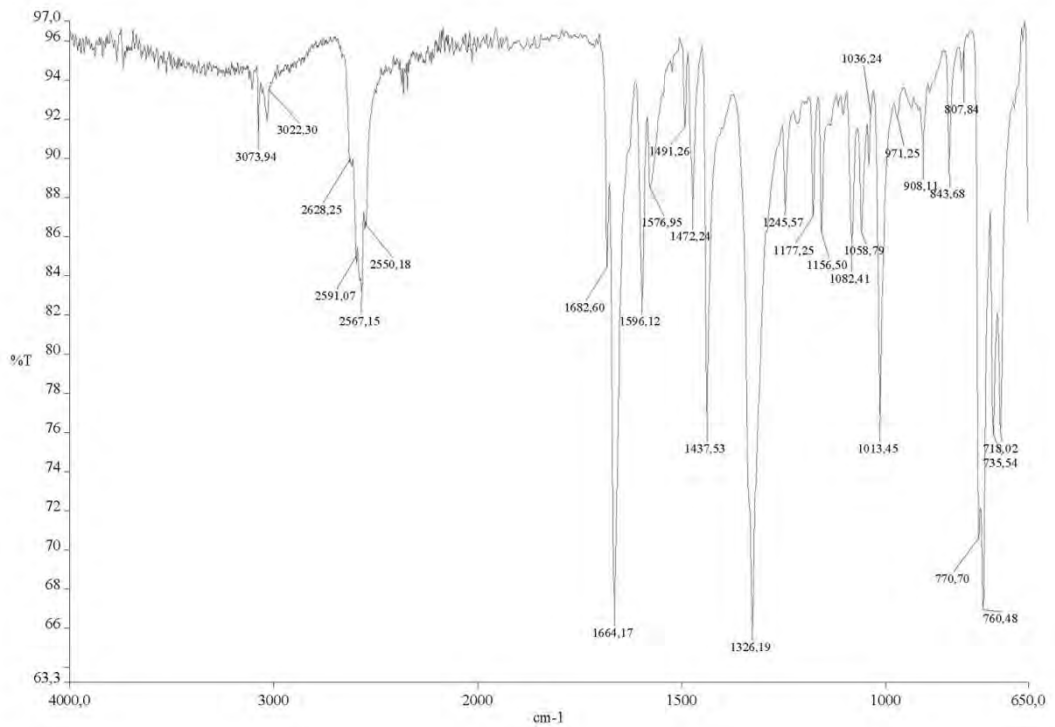
f)



g)



h)



i)

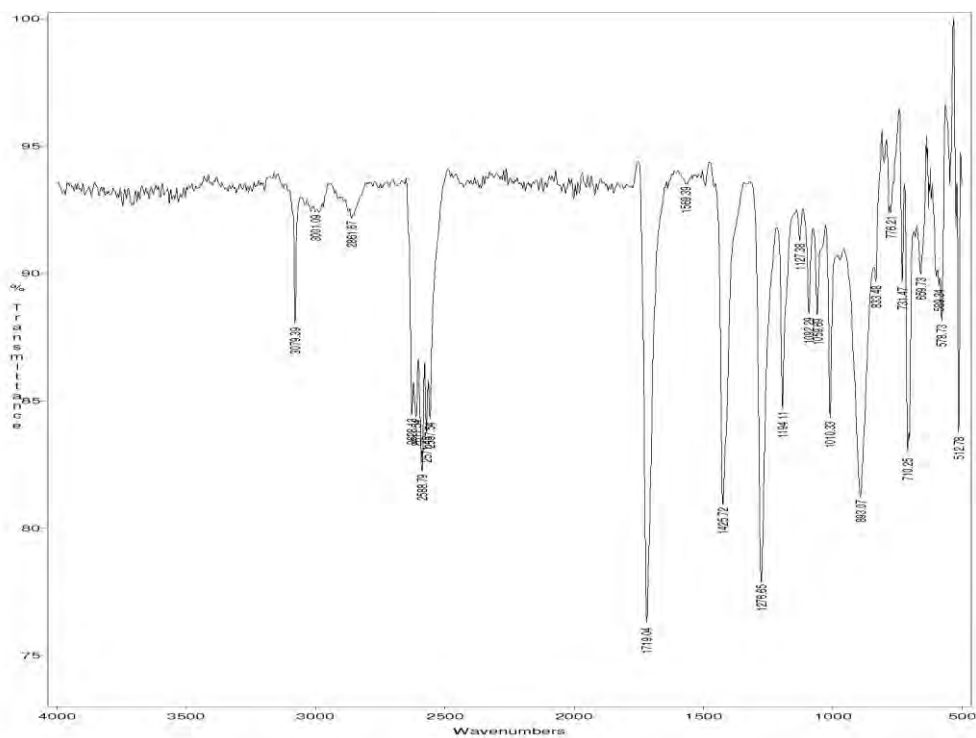
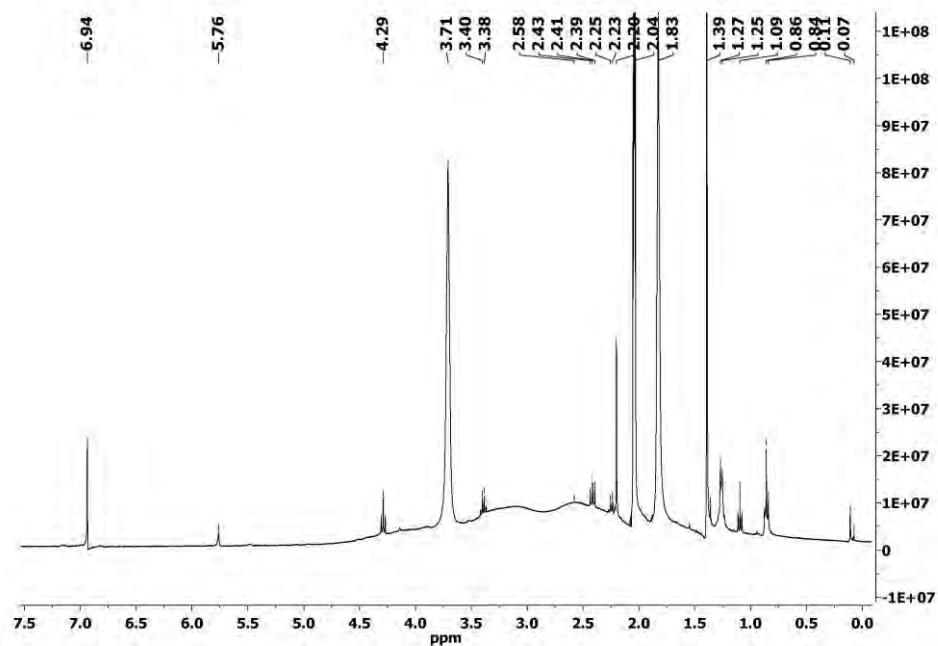


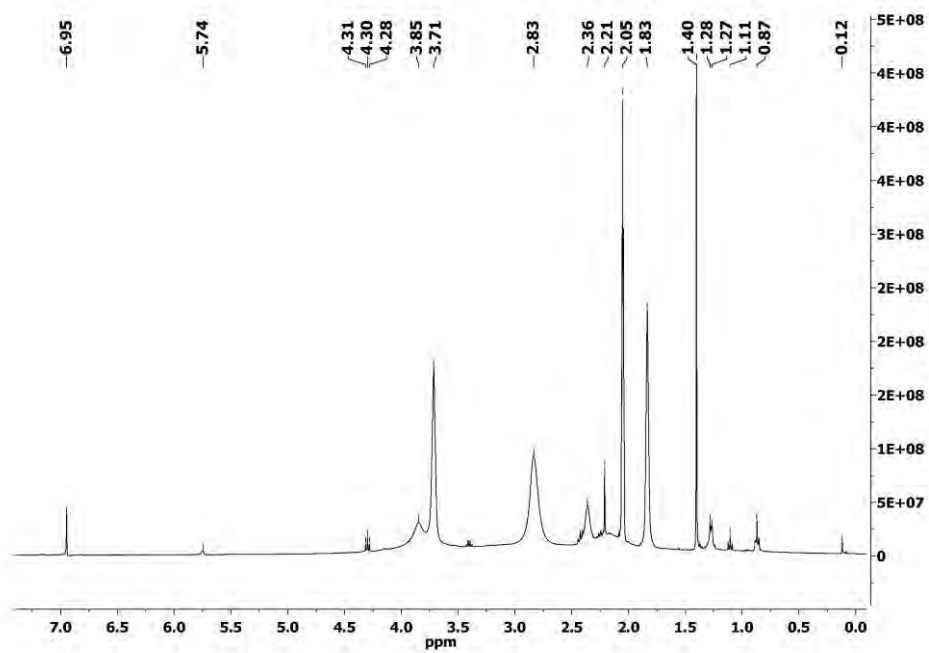
Figure S8. i) ^1H -RMN, ii) $^1\text{H}\{^{11}\text{B}\}$ -RMN, iii) ^{11}B -RMN, iv) $^{11}\text{B}\{^1\text{H}\}$ -RMN, v) ^{13}C -RMN vi) deconvolution of $^{11}\text{B}\{^1\text{H}\}$ spectra of the compounds a) **D1**, b) **D2/D2'**, c) **D3**, d) **D4/D4'**, e) **D5/D5'**, f) **D6** g) **L'H**.

l)

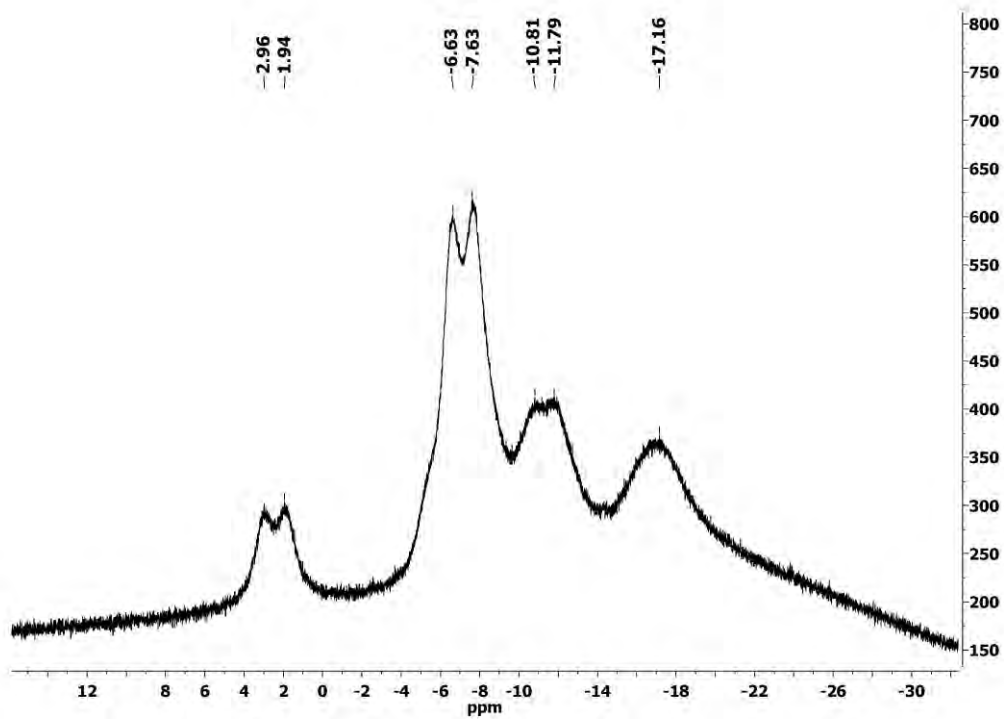
i)



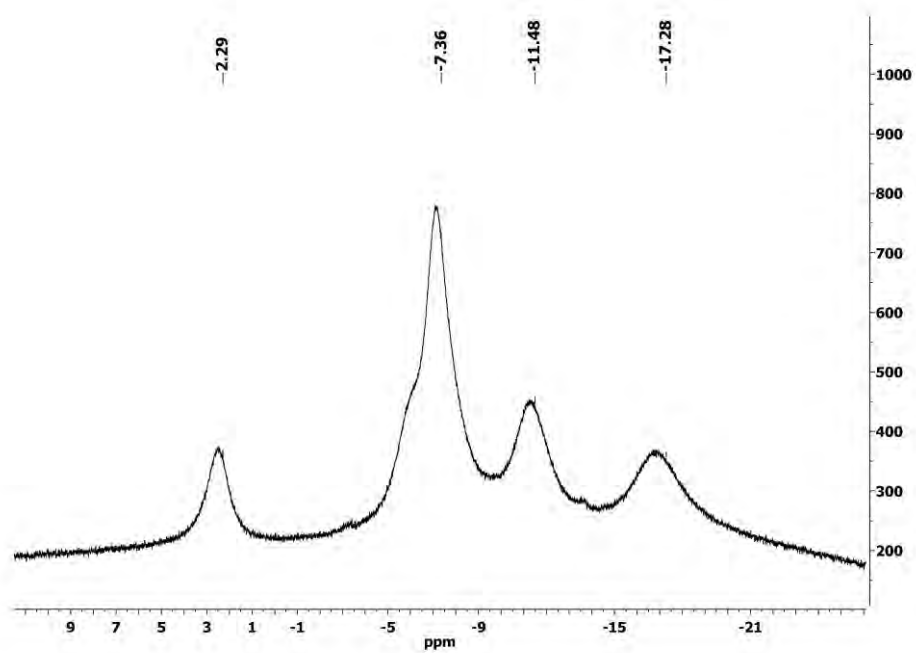
ii)



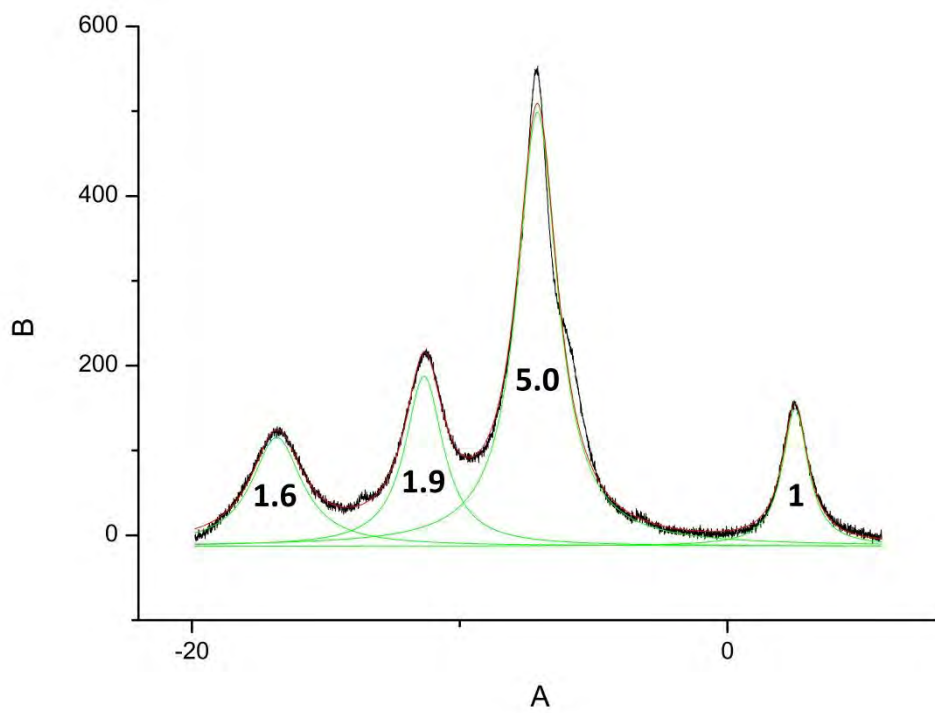
iii)



iv)

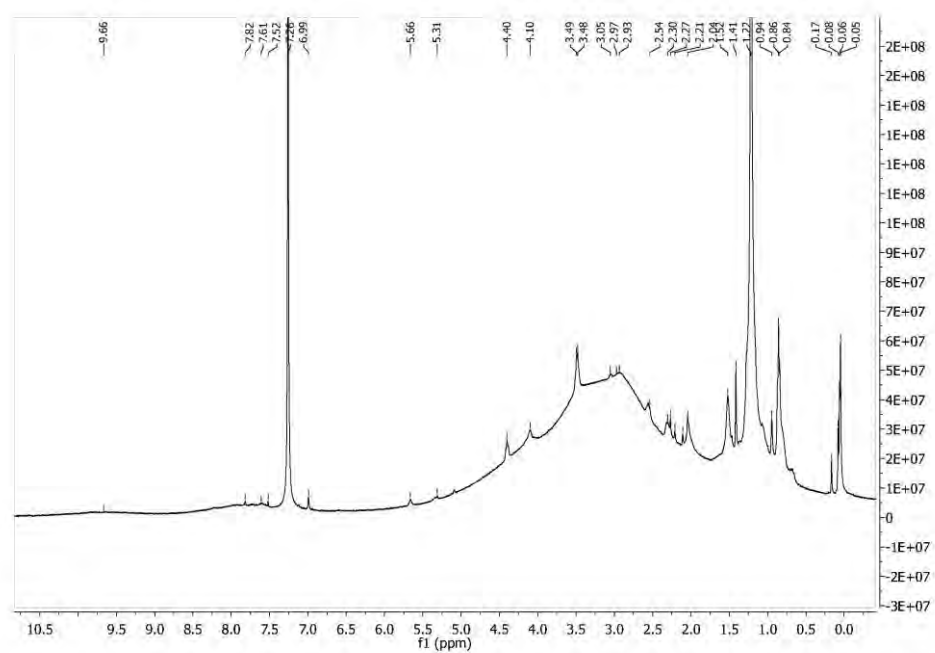


vi)

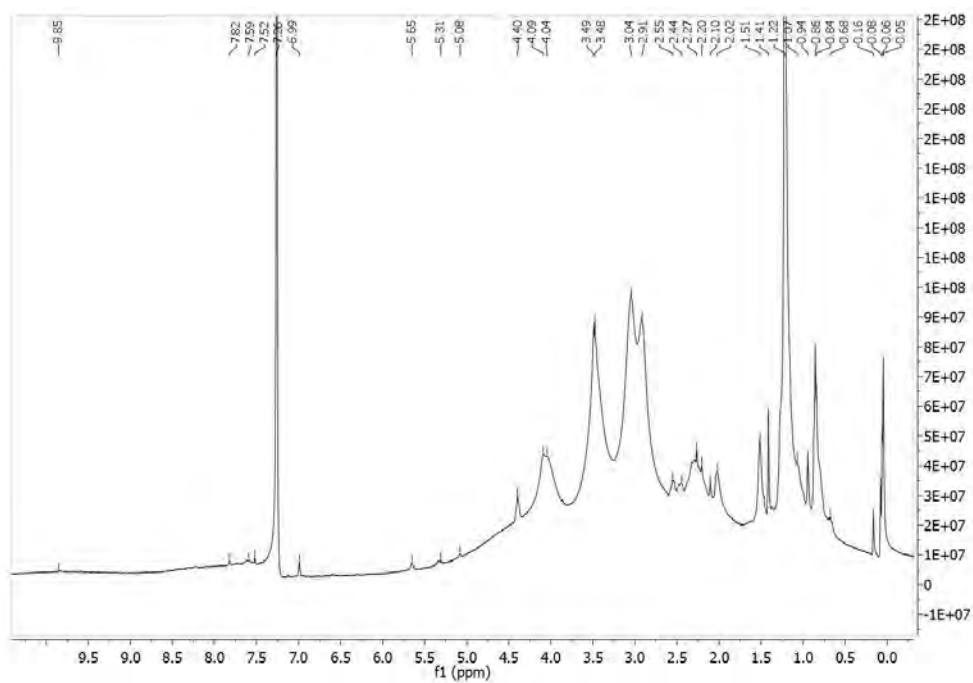


m)

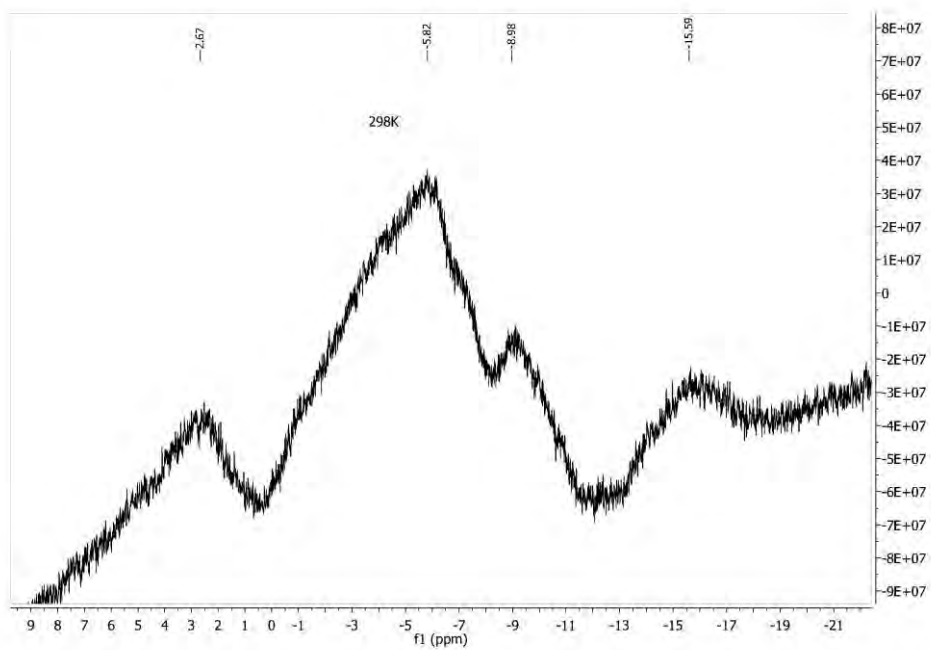
i)



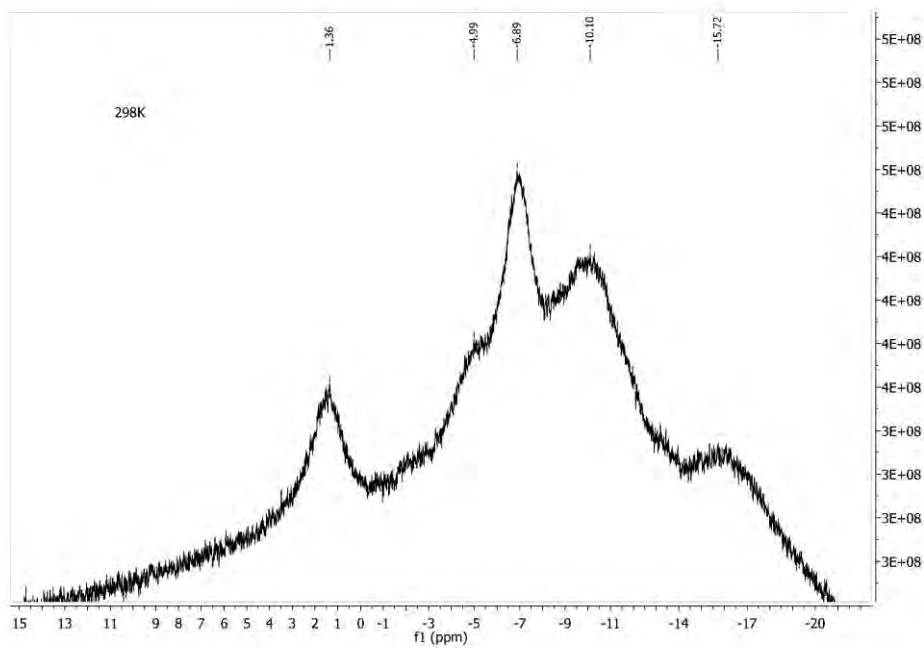
ii)



iii)

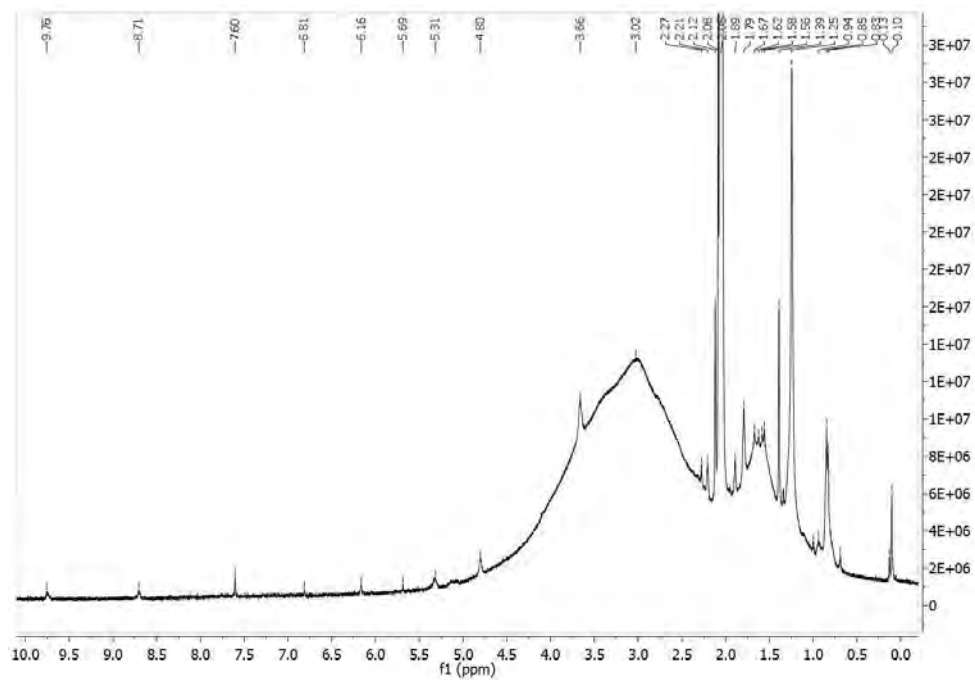


iv)

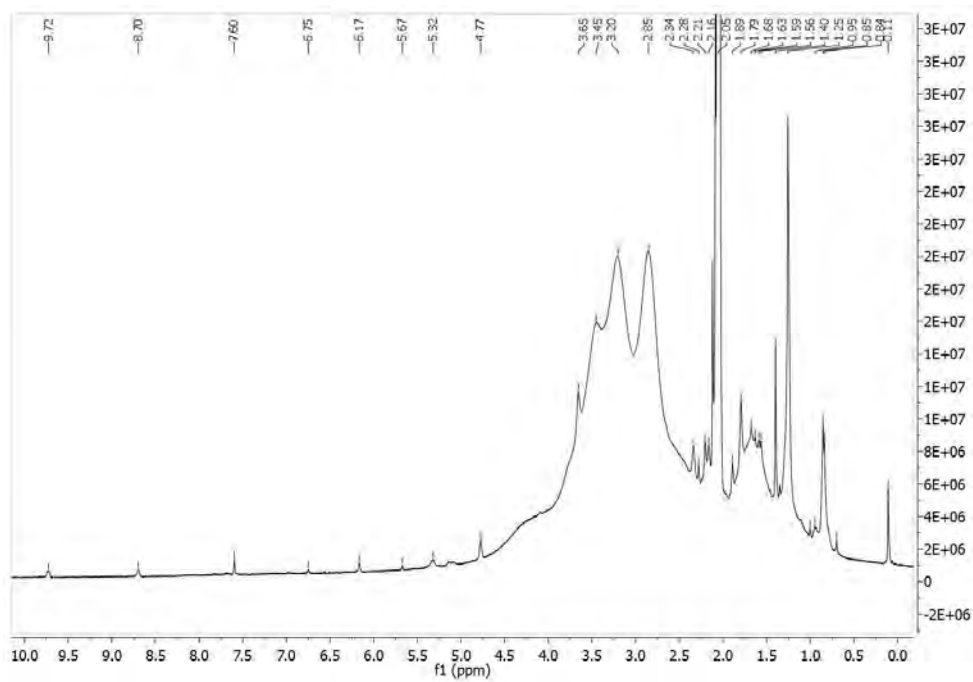


n)

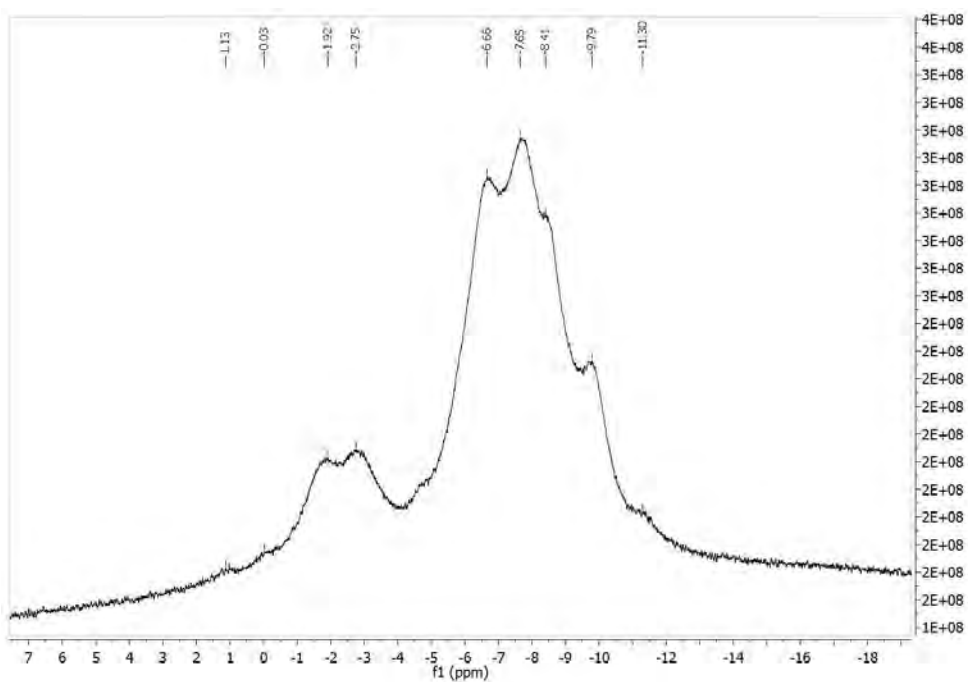
i)



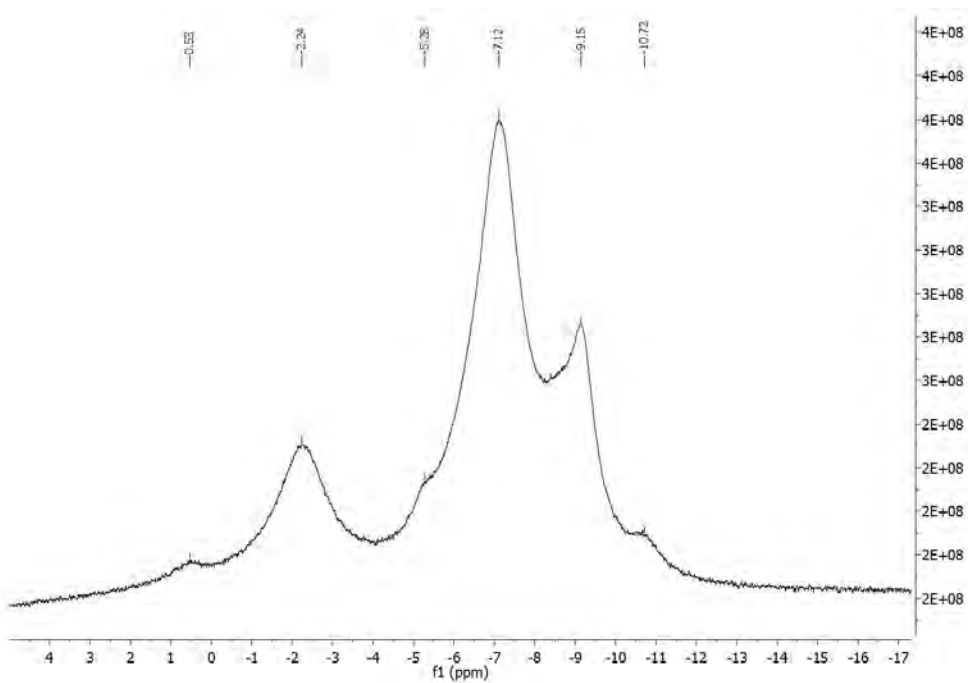
ii)



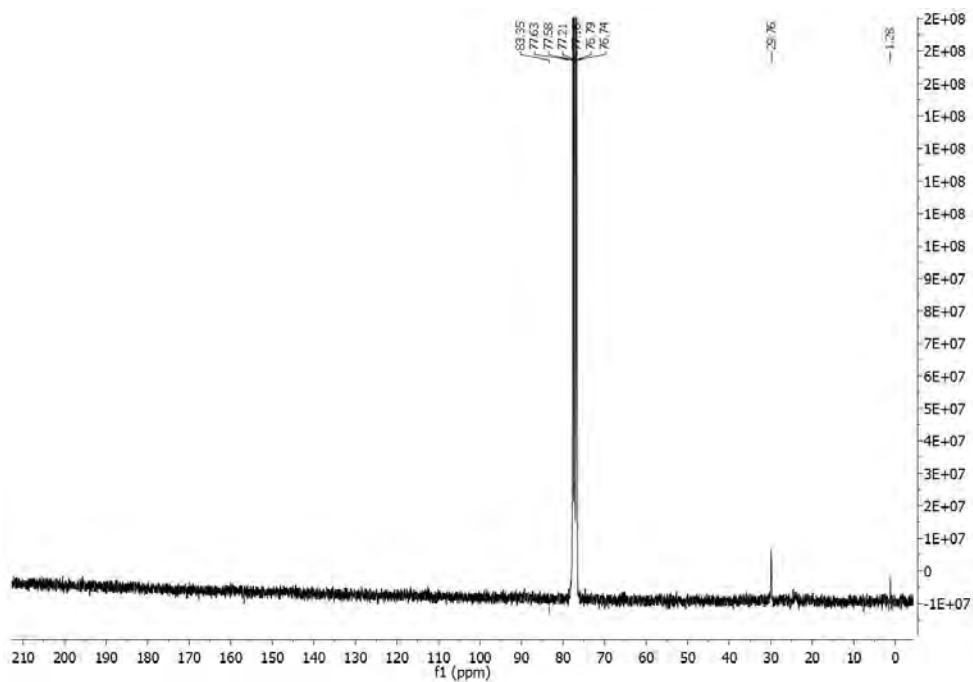
iii)



iv)

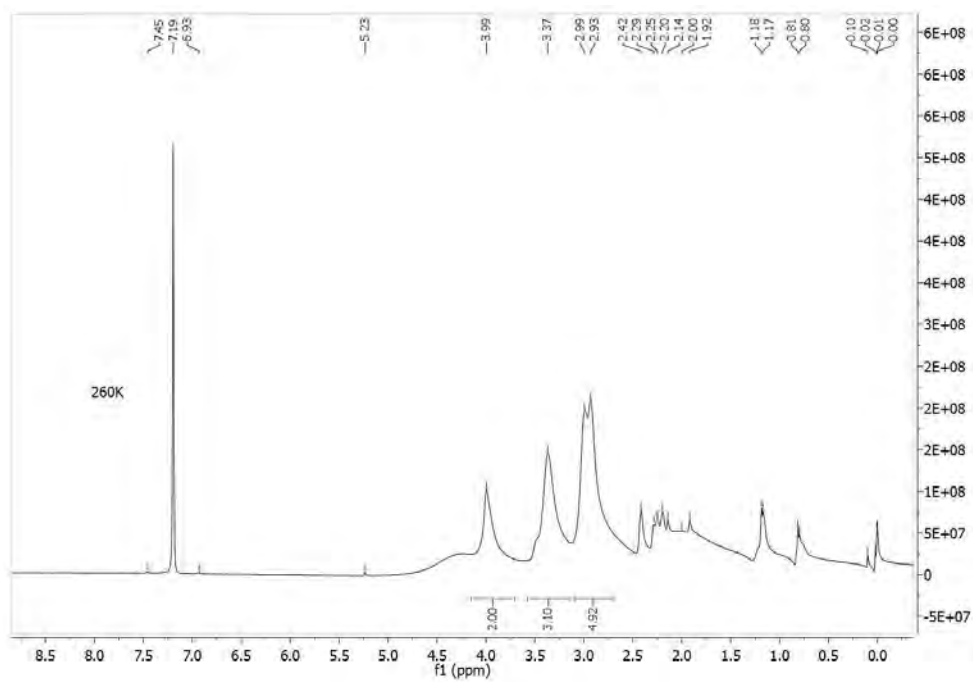


v)

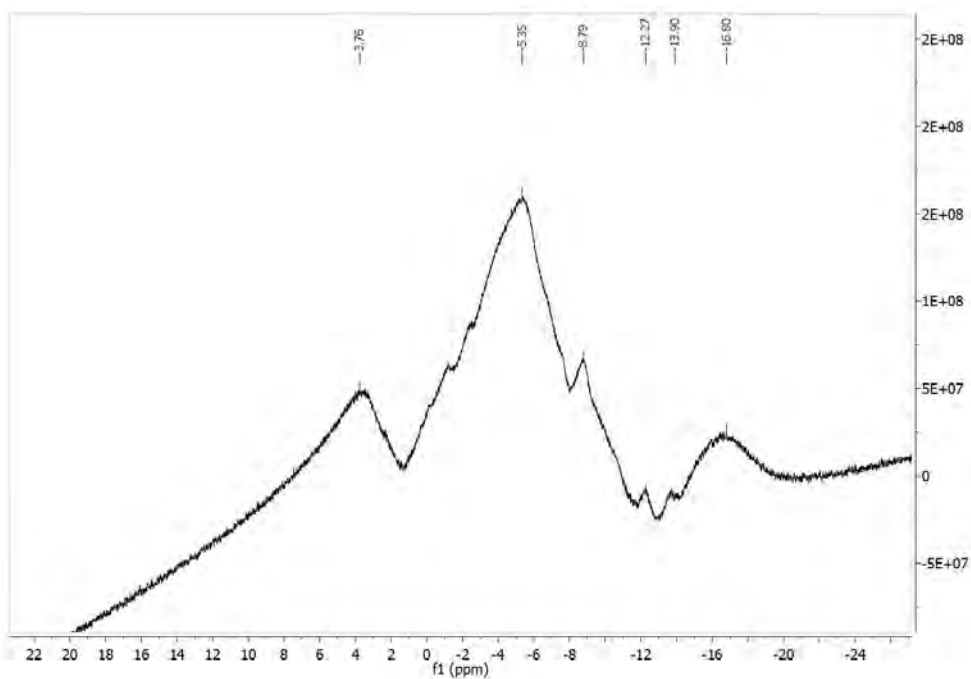


o)

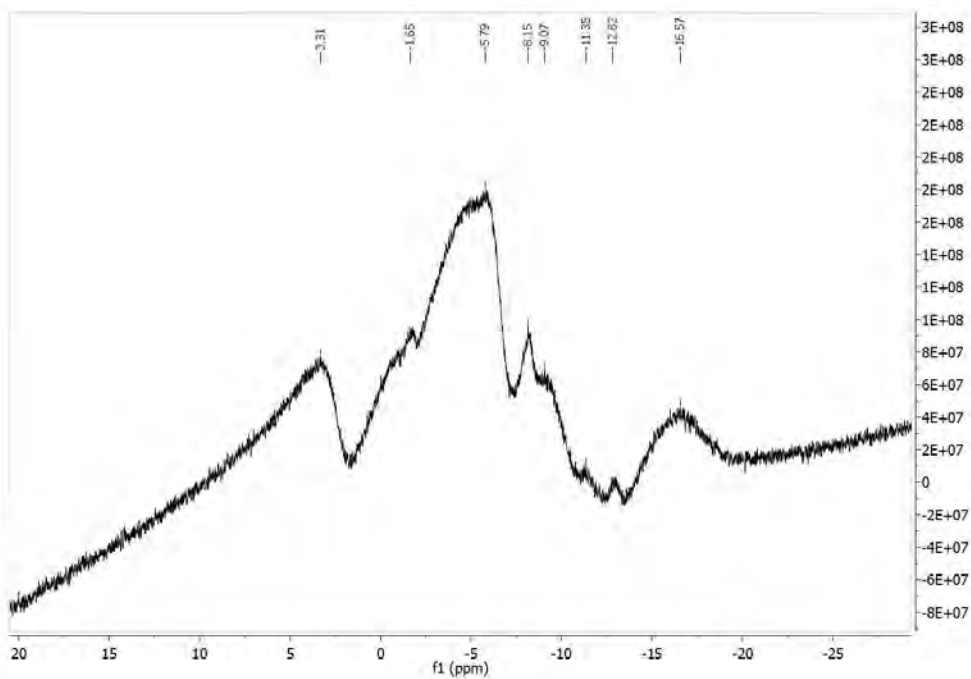
ii)



iii)

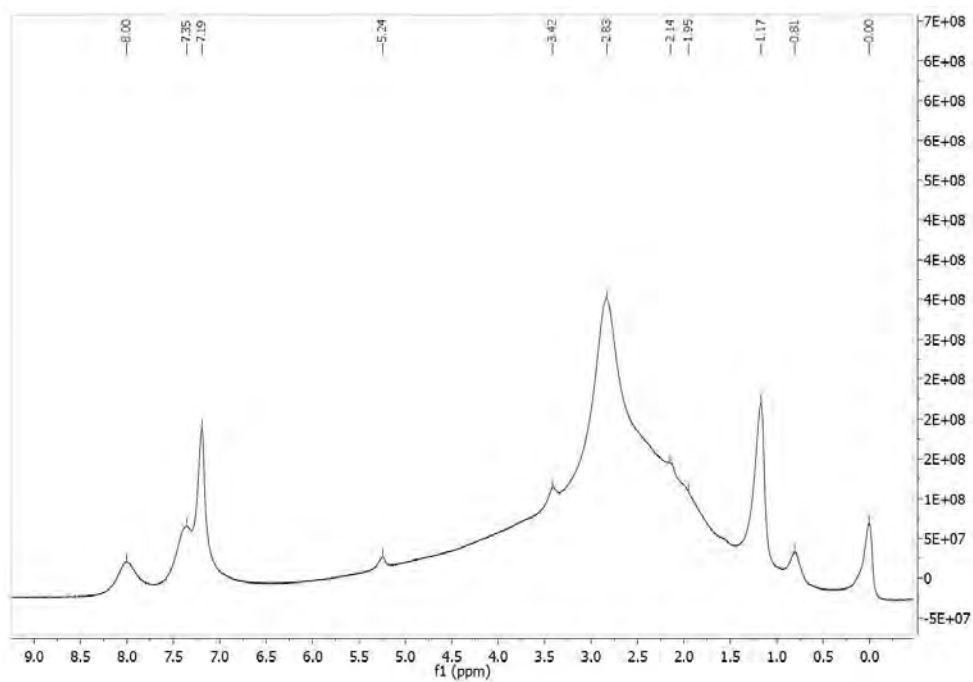


iv)

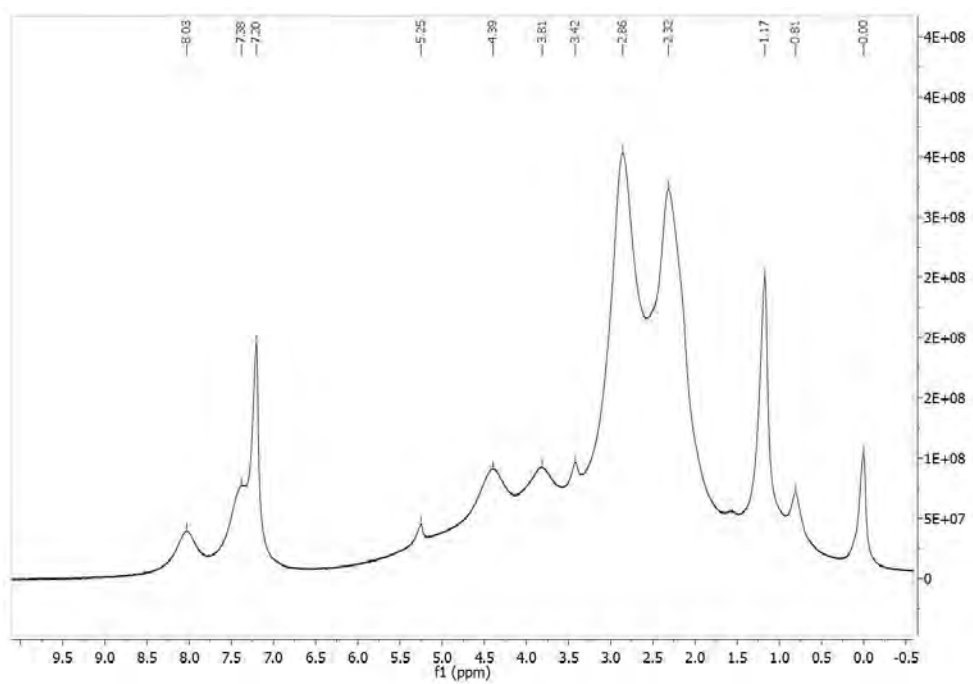


p)

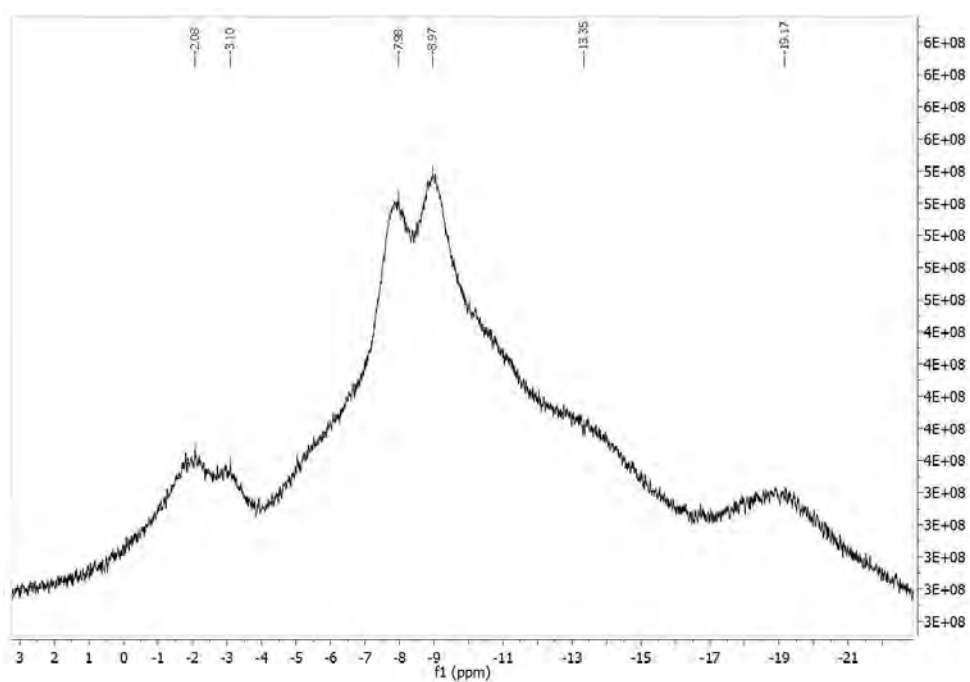
i)



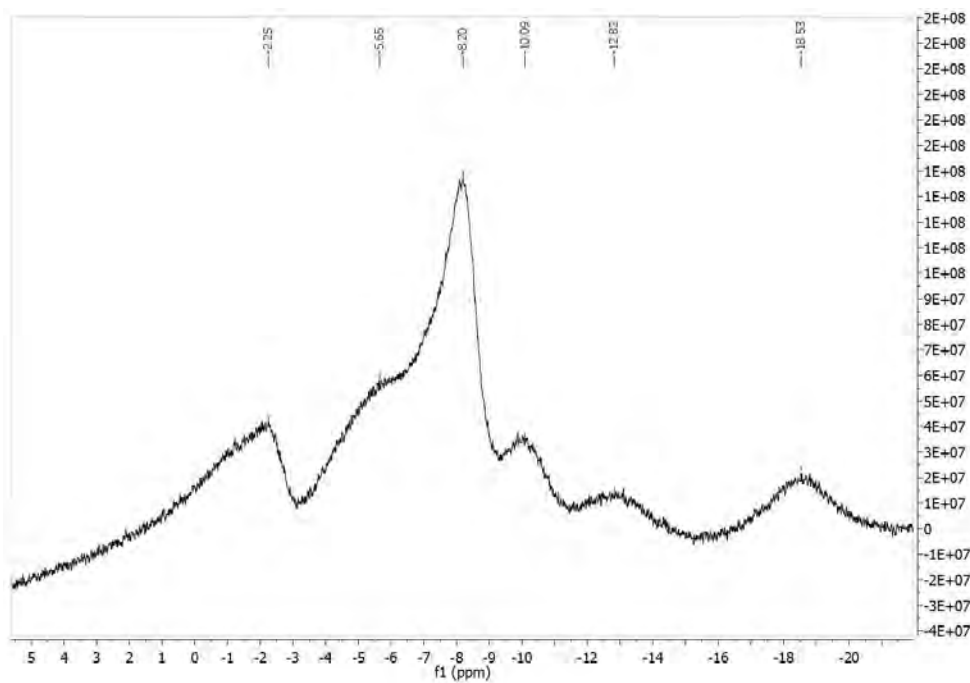
ii)



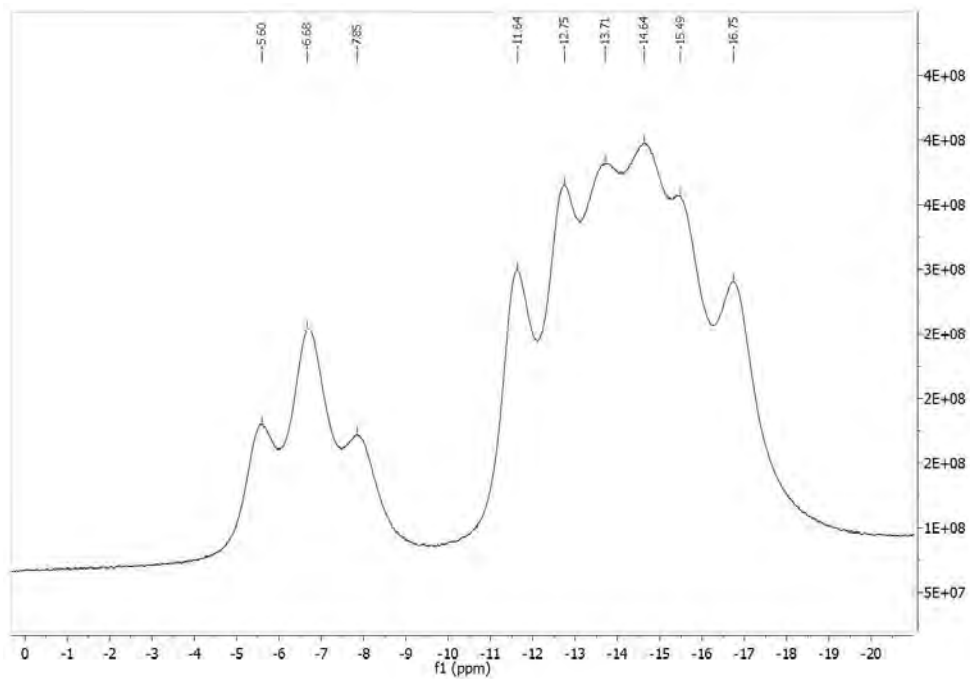
iii)



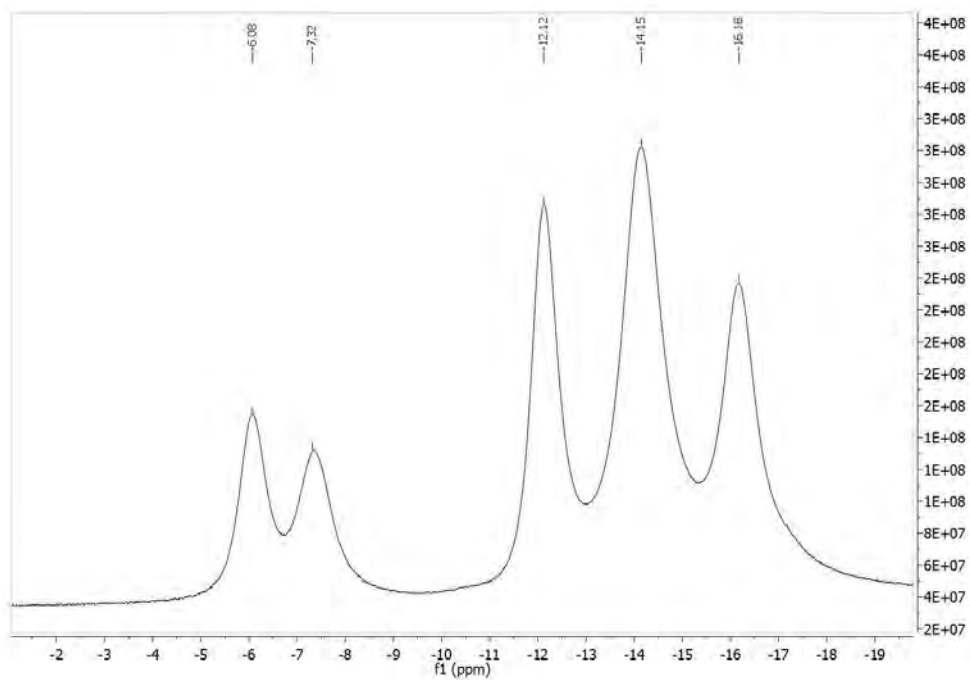
iv)



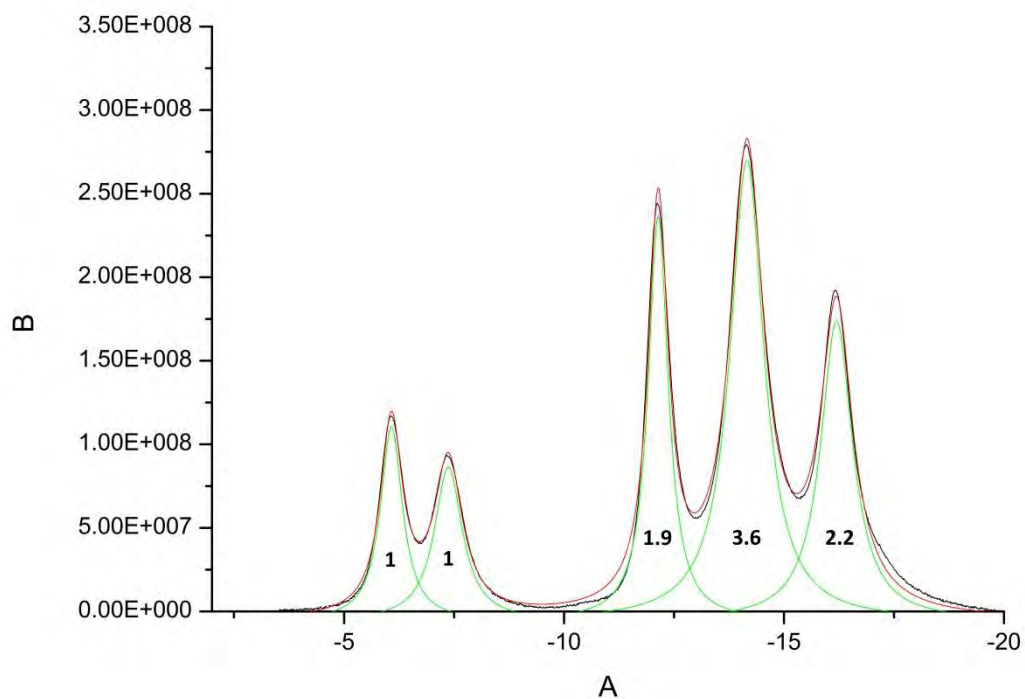
q)
iii)



iv)

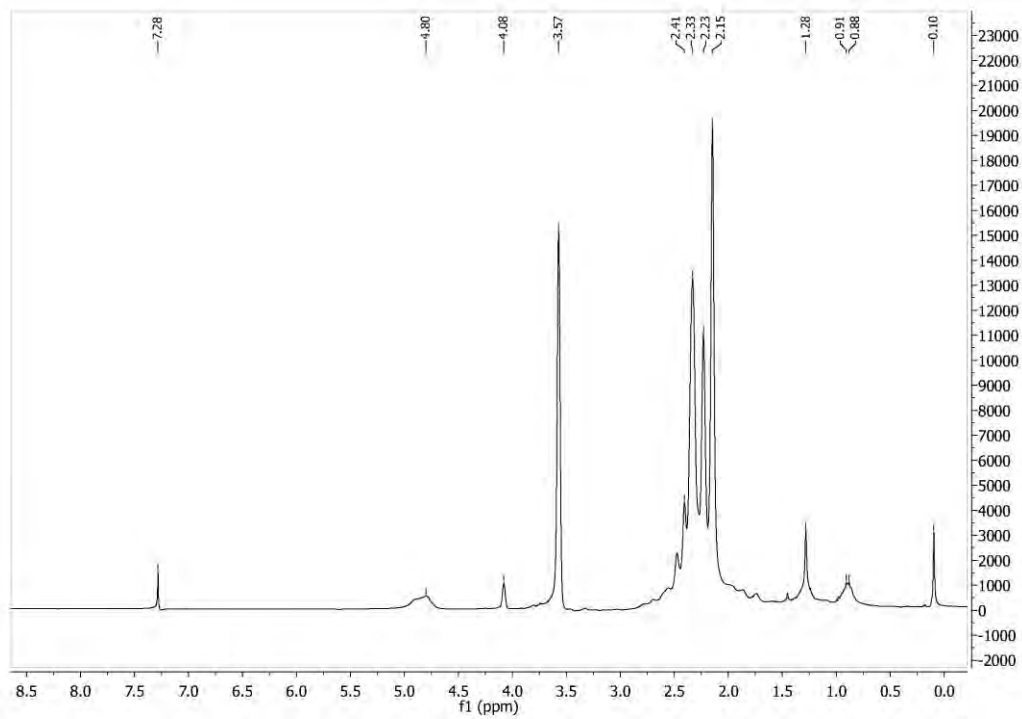


vi)

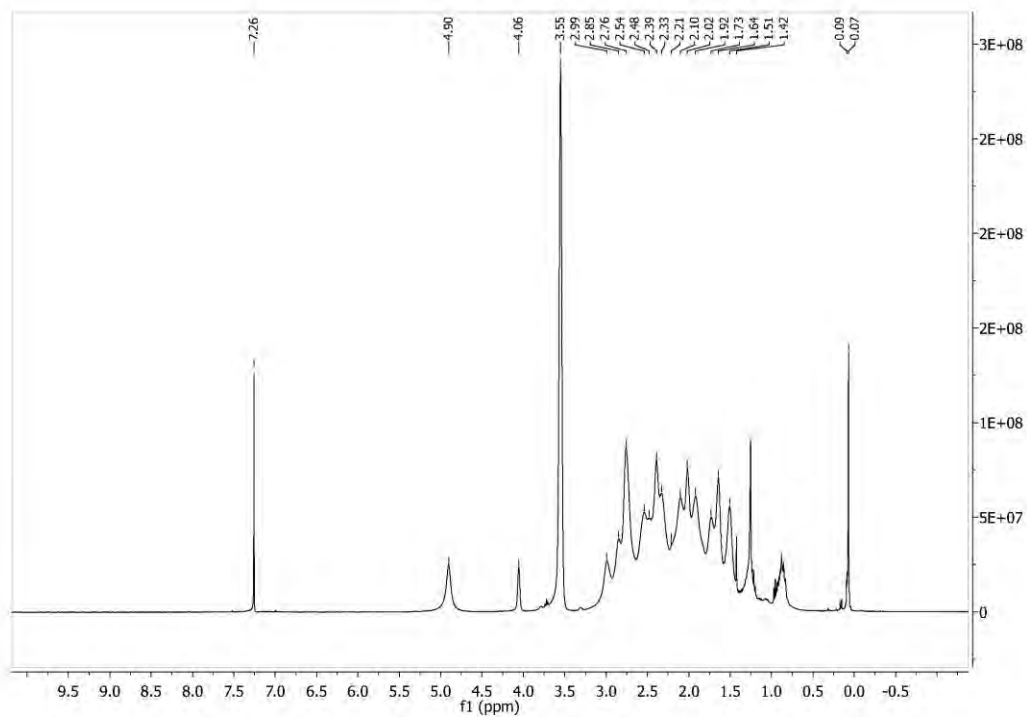


r)

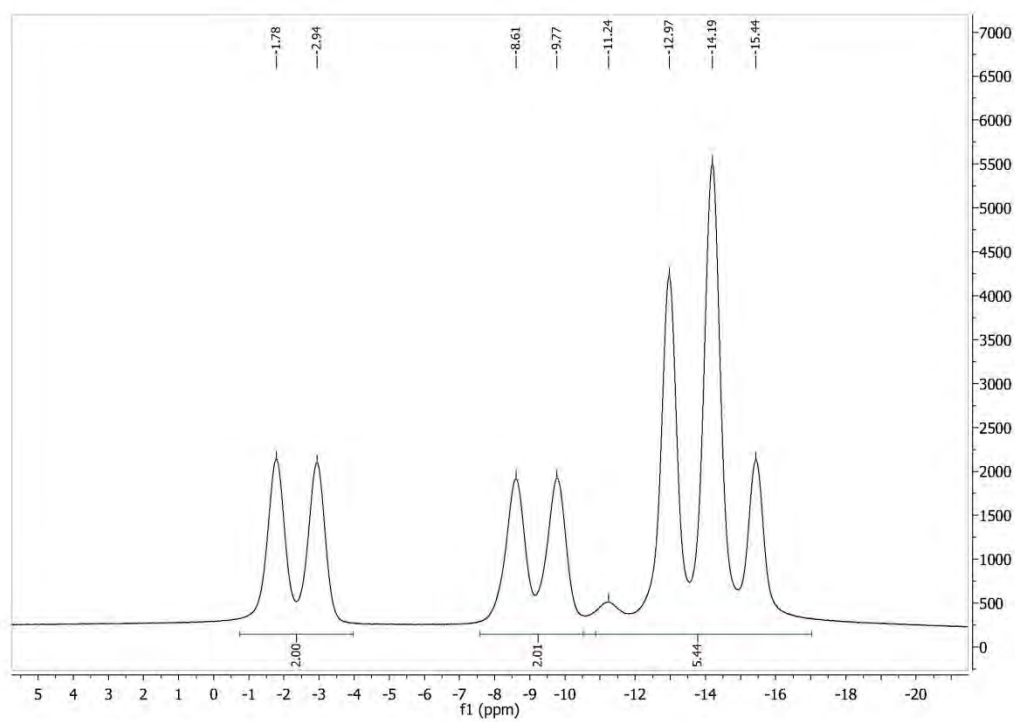
i)



ii)

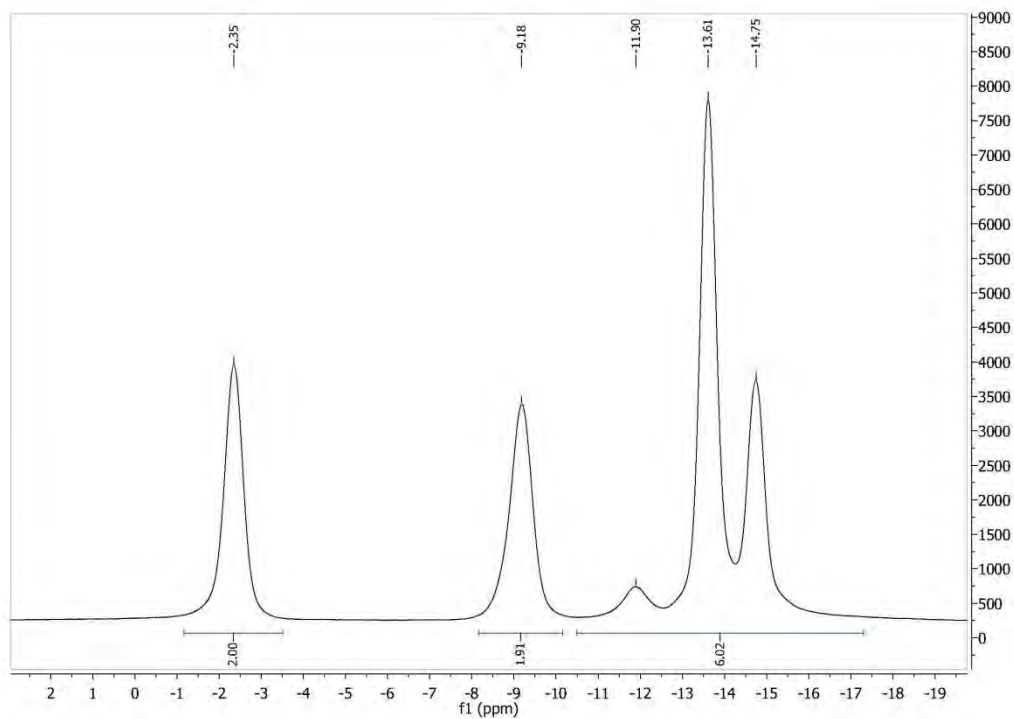


iii)



CHAPTER VI

iv)



v)

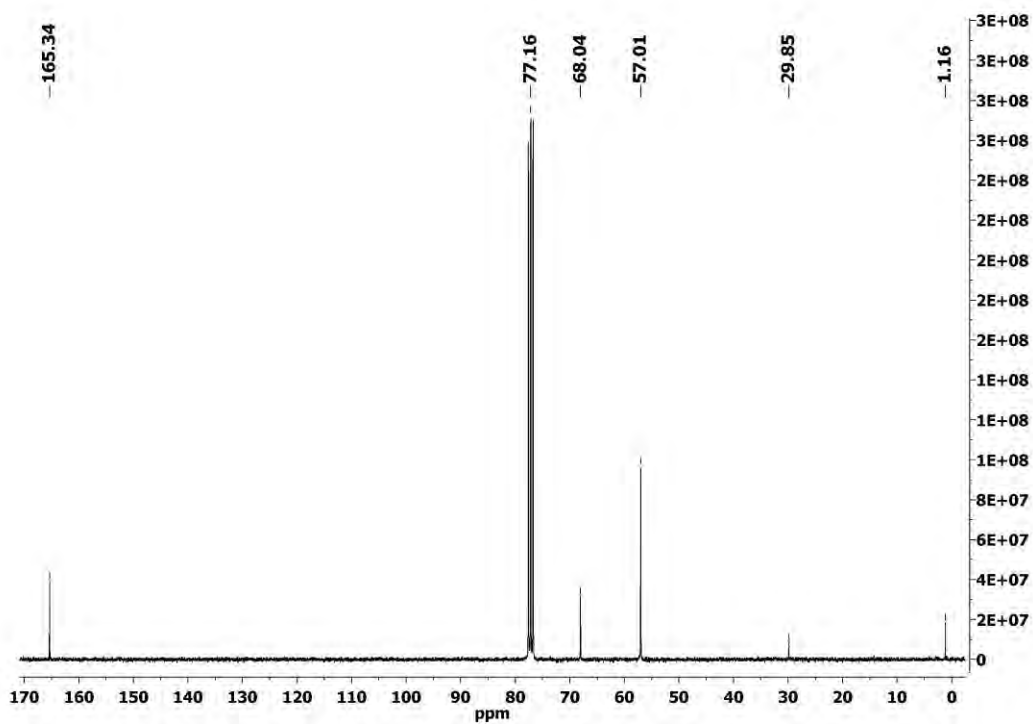
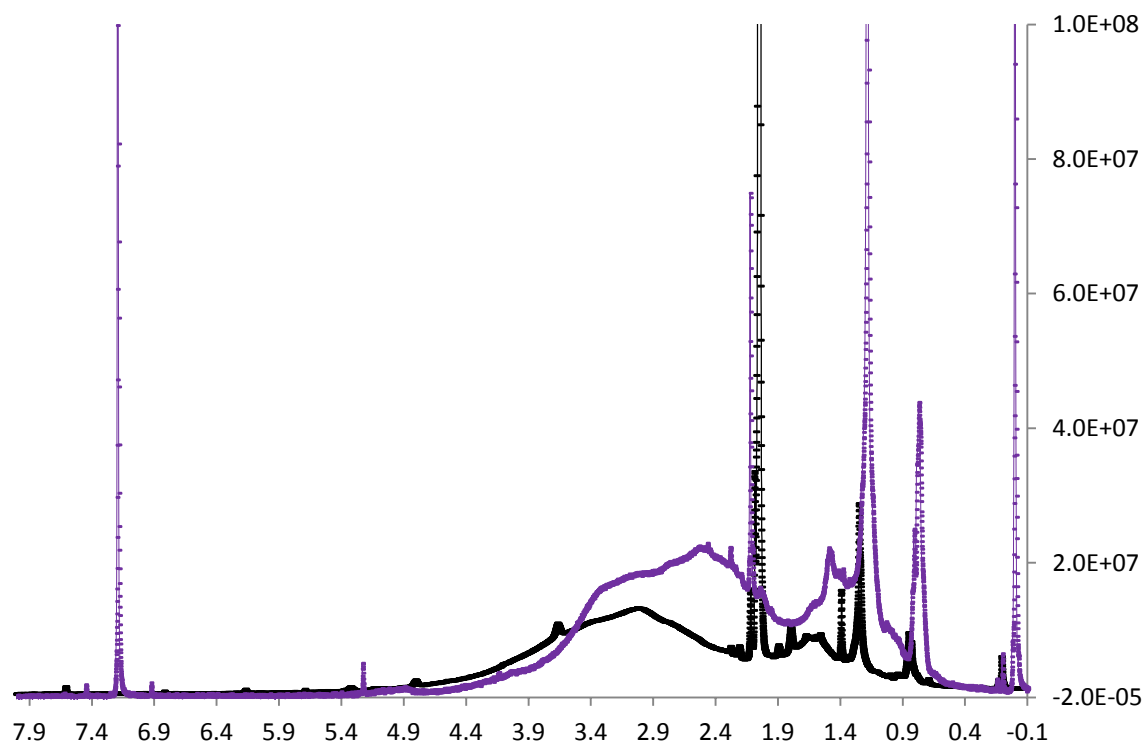


Figure S9. Comparison of a) ^1H -RMN, b) $^1\text{H}\{^{11}\text{B}\}$ -RMN of compound **D3** in chloroform at 298K (purple) and in acetone at 260K (black).

a)



b)

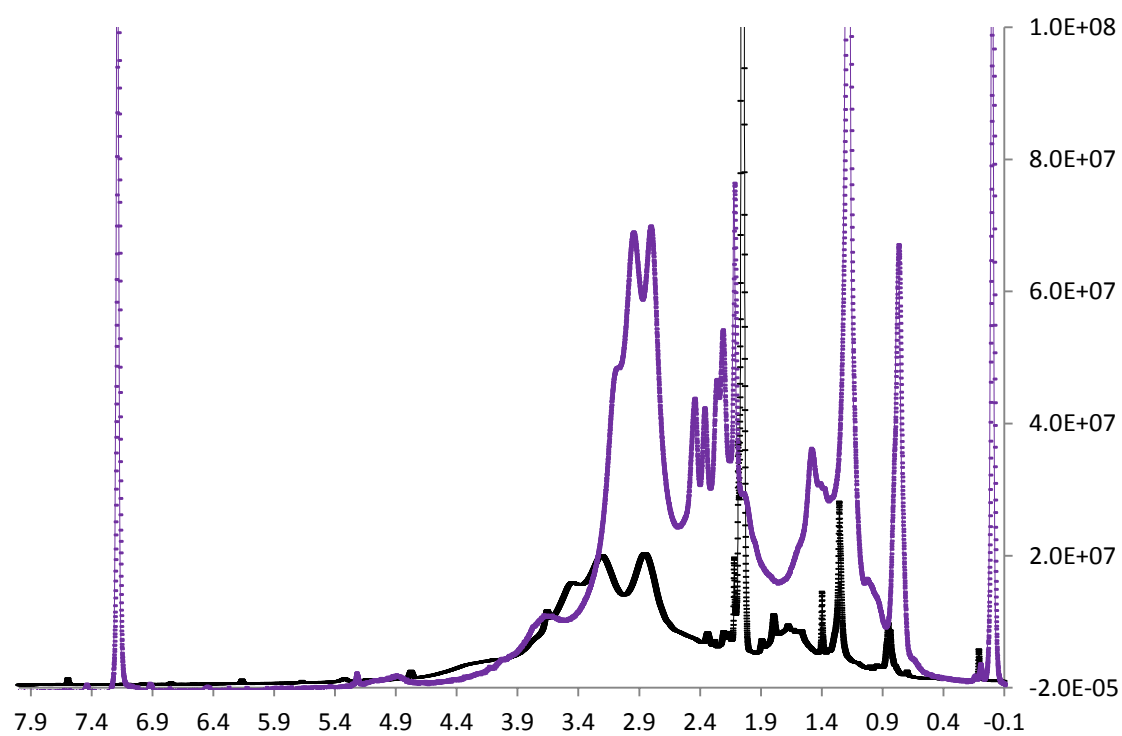


Figure S10. Intermolecular interactions B-H ... H-B in complex **D3**.

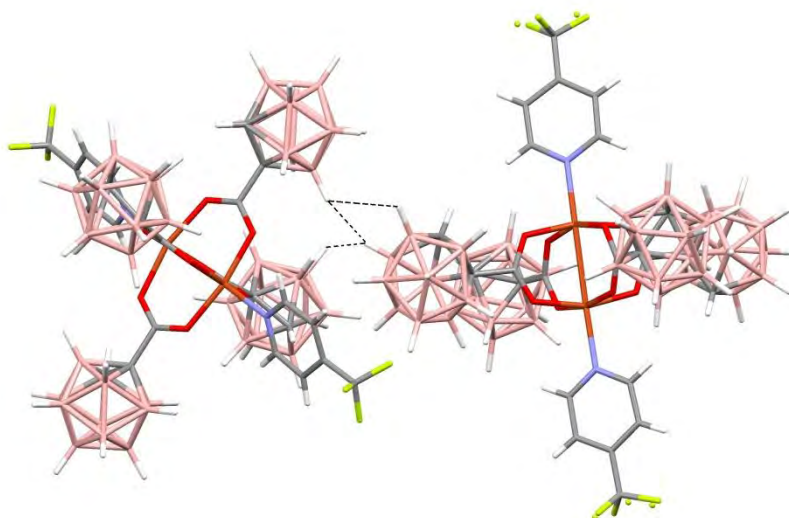


Figure S11. Displacement of the O(2) and O(3) atoms respect the plane form by the adjacent oxygen atom of the same carboxylate ligand and the two joined Mn atoms in compound **D6**.

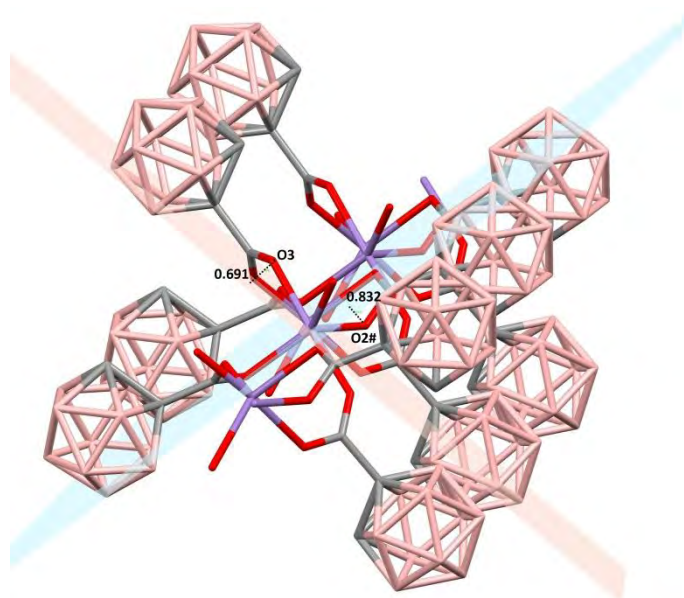
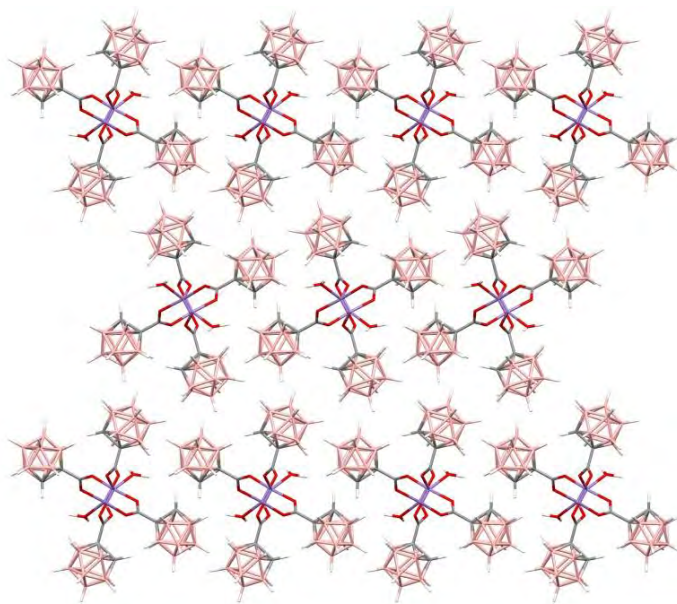
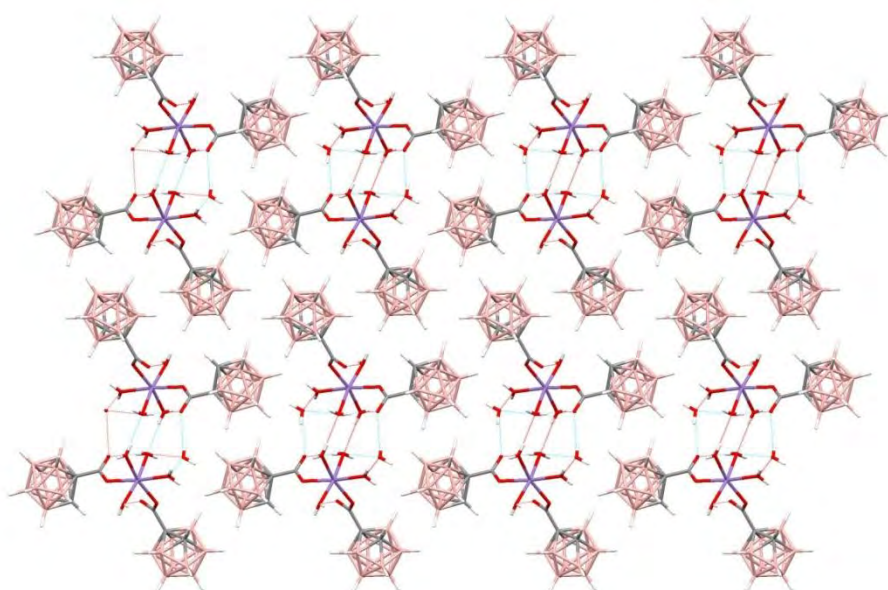


Figure S12. Packing diagram of a) **D6** along *b* axis, b) **D6'** along *a* axis showing the H bonds, c) **D7** showing the $\pi\cdots\pi$ stacking interactions between the 2,2'-bpy ligands of adjacent molecules.

a)



b)



c)

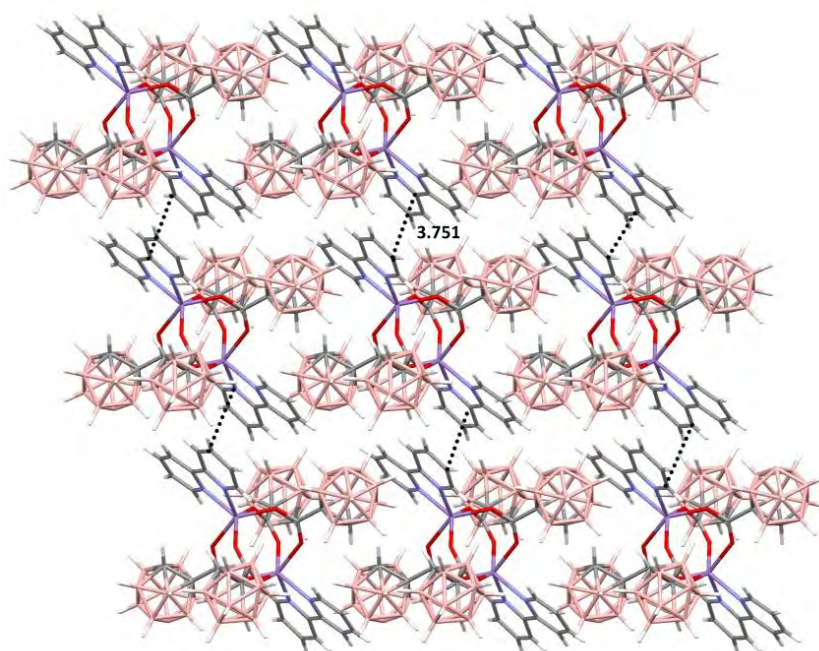
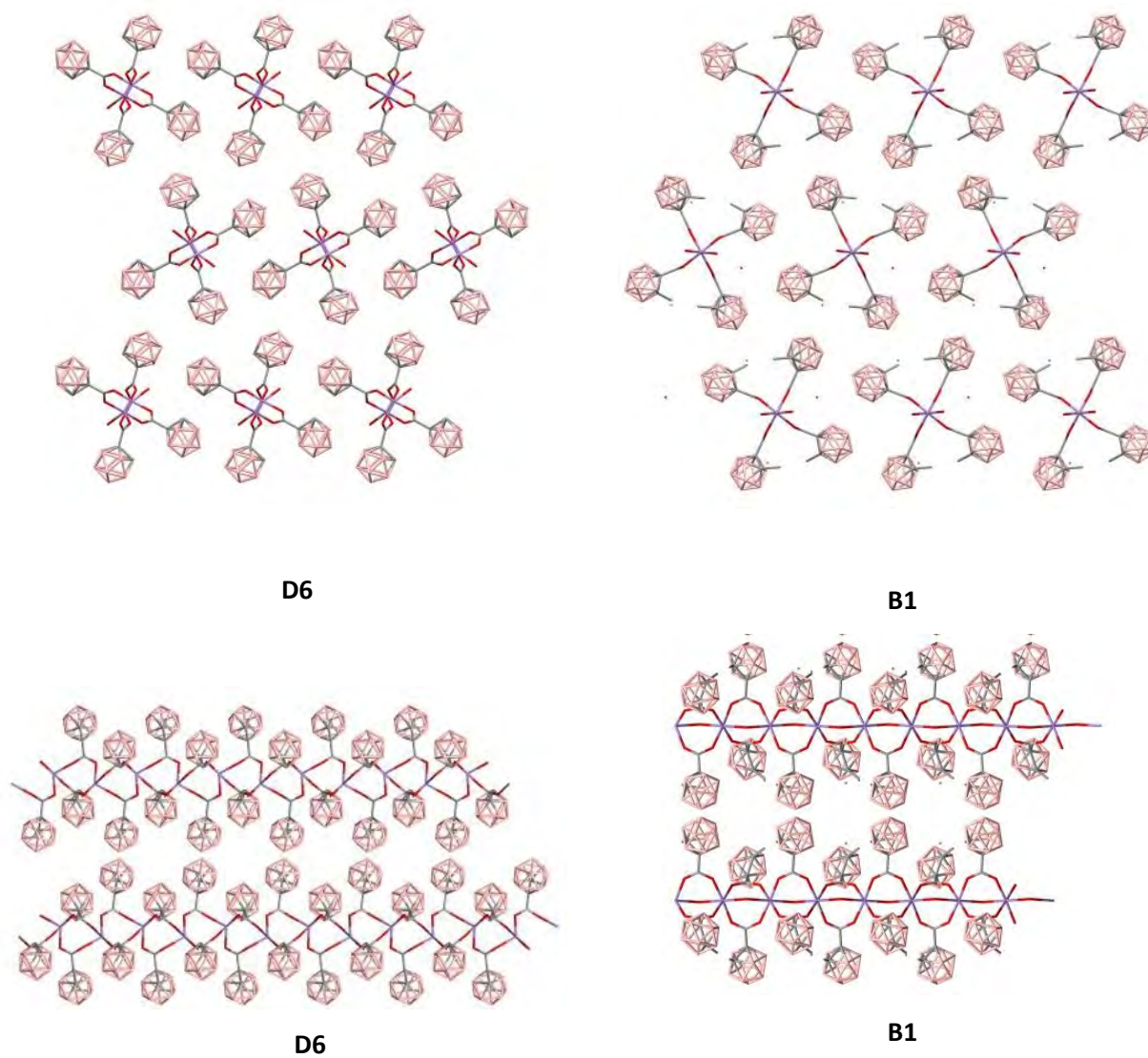


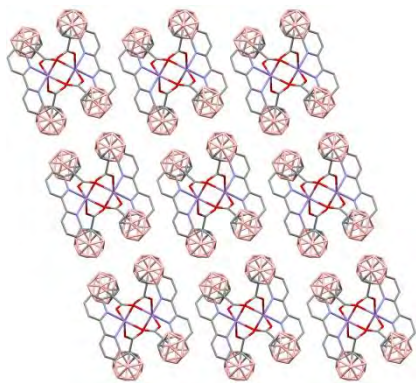
Figure S13. Packing diagram and comparison with the analogous compound synthesized in Chapter IV of a) **D6** and b) **D7** along axis *a* (i), axis *b* (ii) and axis *c* (iii). (H atoms have been omitted for clarity)

a)

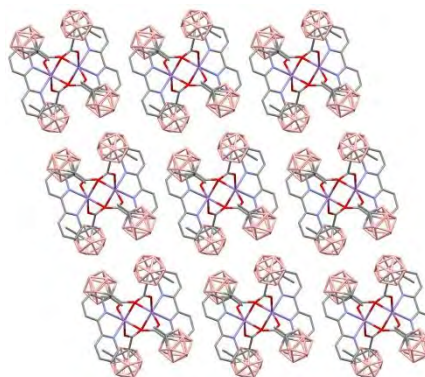


b)

i)

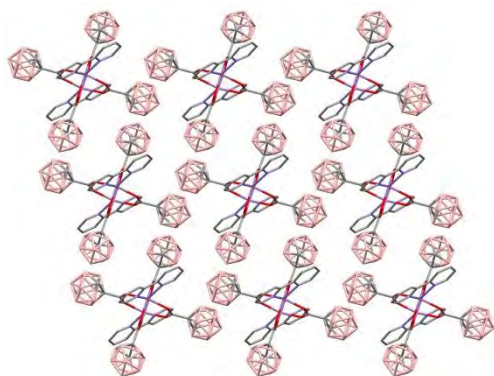


D7

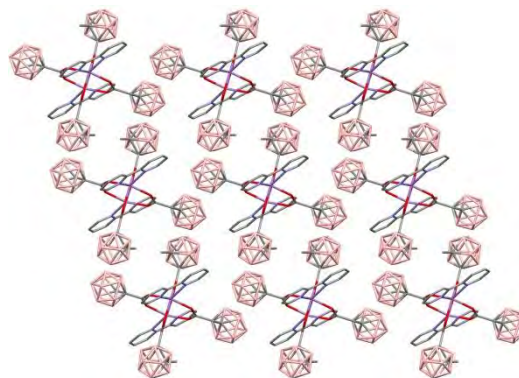


B3

ii)

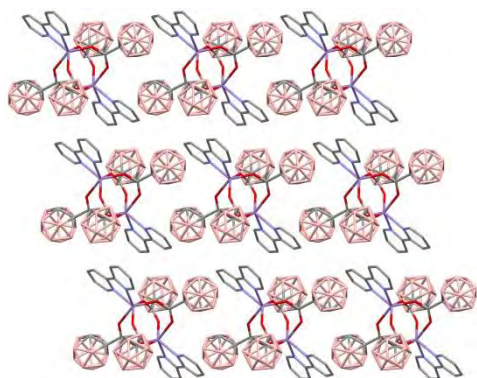


D7

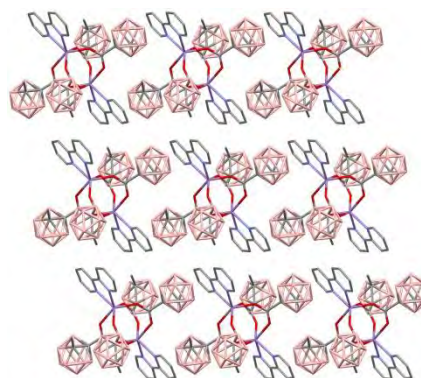


B3

iii)



D7



B3

Table S1. Crystal Data for X-ray structures of **D1-D5**.

	D1	D2	D3	D4	D5
Empirical formula	C ₂₀ H ₆₀ B ₄₀ O ₁₀ Cu ₂	C ₂₂ H ₅₄ B ₄₀ N ₂ O ₈ Cu ₂	C ₂₄ H ₅₂ B ₄₀ F ₆ N ₂ O ₈ Cu ₂	C ₂₄ H ₆₀ B ₄₀ N ₂ O ₉ Cu ₂	C ₂₀ H ₄₀ B ₂₀ N ₂ O ₄ Cu
Formula weight	1020.26	1034.15	1170.16	1080.22	652.28
Crystal system	Monoclinic	Monoclinic	Monoclinic	Monoclinic	Triclinic
Space group	<i>P</i> 21/ <i>c</i>	<i>P</i> -21/ <i>c</i> 1	<i>P</i> -21/ <i>c</i> 1	<i>C</i> 2/ <i>C</i>	<i>P</i> -1
a [Å]	10.318(12)	10.439(18)	22.168(14)	25.36(2)	7.1845(19)
b [Å]	13.473(16)	13.510(2)	12.368(8)	20.832(17)	10.920(3)
c [Å]	22.1272(19)	22.149(3)	22.299(14)	12.538(11)	12.489(3)
α [°]	90	90	90	90	70.332(4)
β [°]	117.26(4)	117.38(6)	101.86(10)	106.308(13)	83.340(4)
γ [°]	90	90	90	90	71.536(4)
V [Å ³]	2734(5)	2773.8(7)	5980.6(7)	6357(9)	875.1(4)
Formula Units/Cell	2	2	4	4	1
ρ _{calc.} [g cm ⁻³]	1.239	1.238	1.300	1.129	1.238
μ [mm ⁻¹]	0.820	0.808	0.772	0.709	0.655
R1 ^[a] , [I > 2σ(I)]	0.0569	0.0920	0.0586	0.0699	0.0424
wR ₂ ^[b] [all data]	0.1799	0.3179	0.1907	0.2408	0.1131

[a] $R_1 = \frac{\sum ||F_o| - |F_c||}{\sum |F_o|}$

[b] $wR_2 = \left[\frac{\sum \{w(F_o^2 - F_c^2)^2\}}{\sum \{w(F_o^2)^2\}} \right]^{1/2}$, where $w = 1/[\sigma^2(F_o^2) + (0.0042P)^2]$ and $P = (F_o^2 + 2F_c^2)/3$

Table S2. Crystal Data for X-ray structures of **D2'**, **D4'** and **D5'**

	D2'	D4'	D5'
Empirical formula	C ₃₂ H ₆₄ B ₄₀ O ₈ N ₄ Cu ₂	C ₃₆ H ₆₈ B ₄₀ O ₈ N ₄ Cu ₂	C ₂₆ H ₆₄ B ₄₀ N ₂ O ₈ Cu
Formula weight	1192.35	1244.42	1028.73
Crystal system	Triclinic	Triclinic	Triclinic
Space group	<i>P</i> -1	<i>P</i> -1	<i>P</i> -1
a [Å]	11.764(3)	13.360(8)	11.365(10)
b [Å]	13.327(3)	13.632(8)	11.485(11)
c [Å]	13.366(3)	24.431(14)	11.589(10)
α [°]	99.539(3)	76.585(10)	79.379(15)
β [°]	115.311(3)	75.857(9)	75.876(14)
γ [°]	112.975(3)	60.941(9)	73.289(14)
V [Å ³]	1598.8(6)	3738(4)	1394(2)
Formula Units/Cell	1	2	1
ρ _{calc.} [g cm ⁻³]	1.238	1.106	1.225
μ [mm ⁻¹]	0.711	0.611	0.436
R1 ^[a] , [I > 2σ(I)]	0.1312	0.0622	0.0614
wR ₂ ^[b] [all data]	0.4576	0.2052	0.1707

$$[a] R_1 = \frac{\sum ||F_o| - |F_c||}{\sum |F_o|}$$

$$[b] wR_2 = \left[\frac{\sum \{w(F_o^2 - F_c^2)^2\}}{\sum \{w(F_o^2)^2\}} \right]^{1/2}, \text{ where } w = 1/[\sigma^2(F_o^2) + (0.0042P)^2] \text{ and } P = (F_o^2 + 2F_c^2)/3$$

Table S3. Selected bond lengths (Å) and angles (°) for complexes **D2'**, **D4'** and **D5'**

	D2'	D4'		D5'
Cu(1)-O(1)	1.954(4)	1.964(19)	Cu(1)-O(1)	1.919(2)
Cu(1)-O(2)#1	2.288(5)	2.382(2)	Cu(1)-O(1)#1	1.919(2)
Cu(1)-O(5)	1.977(5)	1.993(19)	Cu(1)-O(3)	1.926(2)
Cu(1)-N(1)	2.013(8)	2.006(3)	Cu(1)-O(3)#1	1.926(2)
Cu(1)-N(2)	2.017(8)	2.011(3)	O(1)-Cu(1)-O(1)#1	180.00(1)
Cu(1)-Z			O(3)-Cu(1)-O(3)#1	180.00(9)
O(1)-Cu(1)-Y			O(3)-Cu(1)-O(1)#1	90.49(11)
O(1)-Cu(1)-O(5)	164.1(2)	163.89(8)	O(3)#1-Cu(1)-O(1)	90.49(11)
O(1)-Cu(1)-N(1)	88.3(2)	88.57(10)	O(3)-Cu(1)-O(1)	89.51(11)
O(5)-Cu(1)-N(1)	88.1(2)	90.07(10)	O(3)#1-Cu(1)-O(1)#1	89.51(11)
O(1)-Cu(1)-N(2)	89.2(2)	89.57(10)		
O(5)-Cu(1)-N(2)	92.0(2)	90.94(10)		
N(1)-Cu(1)-N(2)	170.7(2)	176.68(9)		
O(1)-Cu(1)-O(2)#1	109.93(19)	115.31(7)		
O(5)-Cu(1)-O(2)#1	85.72(18)	80.73(7)		
N(1)-Cu(1)-O(2)#1	92.8(2)	89.61(9)		
N(2)-Cu(1)-O(2)#1	96.5(2)	93.68(8)		

Table S4. Crystal Data for X-ray structures of **D6**, **D6'**, **D7** and **D8**

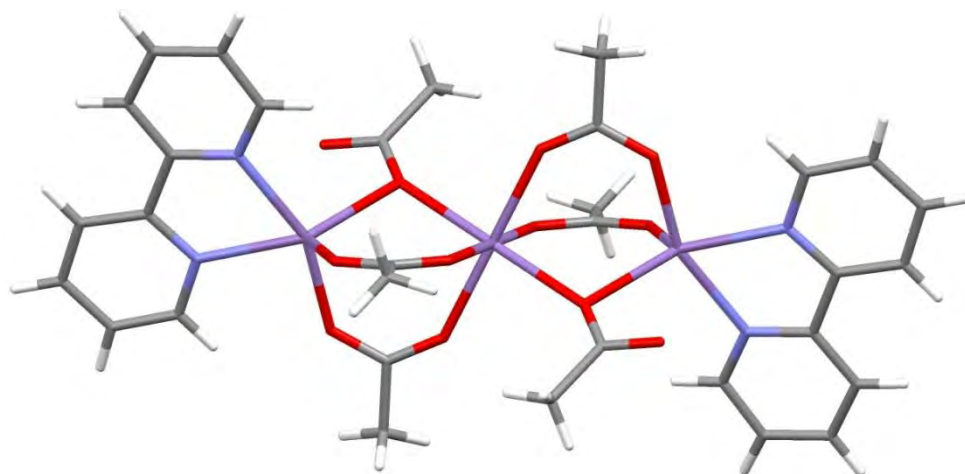
	D6	D6'	D7	D8
Empirical formula	C ₆ H ₃₂ B ₂₀ O ₉ Mn	C ₆ H ₂₄ B ₂₀ O ₅ Mn	C ₃₂ H ₅₈ B ₄₀ N ₄ O ₈ Mn ₂	C ₂₆ H ₃₈ B ₂₀ N ₄ O ₄ Mn
Formula weight	519.46	447.39	1169.10	741.74
Crystal system	Triclinic	Orthorhombic	Triclinic	Monoclinic
Space group	<i>P</i> -1	<i>P</i> -2 ₁ 2 ₁ 2 ₁	<i>P</i> -1	<i>P</i> 2(1)- <i>c</i>
a [Å]	6.7506(7)	7.4659(15)	11.570(5)	13.646(3)
b [Å]	12.3923(13)	11.373(2)	11.858(5)	23.784(5)
c [Å]	16.4761(17)	27.463(6)	13.750(6)	13.452(3)
α [°]	93.074(2)	90	66.996(8)	90
β [°]	101.589(2)	90	68.312(8)	118.672(3)
γ [°]	102.177(2)	90	69.179(8)	90
V [Å ³]	1313.2(2)	2331.8(8)	1563.6(12)	3830.5(13)
Formula Units/Cell	2	4	1	4
ρ _{calc.} [g cm ⁻³]	1.314	1.274	1.242	1.286
μ [mm ⁻¹]	0.538	0.583	0.451	0.385
R1 ^[a] , [I > 2σ(I)]	0.0405	0.0590	0.0859	0.0805
wR2 ^[b] [all data]	0.1292	0.1444	0.2066	0.2313

$$[a] R_1 = \frac{\sum ||F_o| - |F_c||}{\sum |F_o|}$$

$$[b] wR_2 = \left[\frac{\sum \{w(F_o^2 - F_c^2)^2\}}{\sum \{w(F_o^2)^2\}} \right]^{1/2}, \text{ where } w = 1/[\sigma^2(F_o^2) + (0.0042P)^2] \text{ and } P = (F_o^2 + 2F_c^2)/3$$

CHAPTER VII. Catalytic activity of Mn(II) and Co(II) compound containing the carboranylcarboxylate ligand 1-CH₃-2-CO₂H-1,2-closo-C₂B₁₀H₁₀



Figure S1. X-ray structure of $\text{Mn}_3(\text{OAc})_6(\text{bpy})_2$.**Table S1.** Crystal Data for X-ray structures of $\text{Mn}_3(\text{OAc})_6(\text{bpy})_2$.

Empirical formula	$\text{C}_{32}\text{H}_{34}\text{O}_{12}\text{N}_4\text{Mn}_3$
Formula weight	831.45
Crystal system	Triclinic
Space group	P-1
a [Å]	8.142(8)
b [Å]	9.865(10)
c [Å]	12.857(13)
α [°]	106.74(16)
β [°]	96.234(16)
γ [°]	108.456(16)
V [Å ³]	915.1(16)
Formula Units/Cell	1
$\rho_{\text{calc.}}$ [g cm ⁻³]	1.509
μ [mm ⁻¹]	1.084
R_1 ^[a] , [I > 2 σ (I)]	0.0332
wR_2 ^[b] [all data]	0.0983

$$[a] R_1 = \frac{\sum ||F_o| - |F_c||}{\sum |F_o|}$$

$$[b] wR_2 = \left[\frac{\sum \{w(F_o^2 - F_c^2)^2\}}{\sum \{w(F_o^2)^2\}} \right]^{1/2}, \text{ where } w = 1/[\sigma^2(F_o^2) + (0.0042P)^2] \text{ and } P = (F_o^2 + 2F_c^2)/3$$

